Research Report – UCD-ITS-RR-08-49

Investigation of Noise, Durability, Permeability, and Friction Performance Trends for Asphaltic Pavement Surface Types: First- and Second-Year Results

February 2008

Aybike Ongel
John Harvey
Erwin Kohler
Qing Lu
Bruce Steven

Institute of Transportation Studies ◦ University of California, Davis
One Shields Avenue ◦ Davis, California 95616
PHONE (530) 752-6548 ◦ FAX (530) 752-6572
www.its.ucdavis.edu

February 2008
Research Report: UCPRC-RR-2007-03

Investigation of Noise, Durability, Permeability, and Friction Performance Trends for Asphaltic Pavement Surface Types: First- and Second-Year Results

Authors:

Aybike Ongel, John T. Harvey, Erwin Kohler,
Qing Lu, and Bruce D. Steven

Partnered Pavement Research Center Strategic Plan Element No. 4.16: Investigation of Noise, Durability, Permeability, and Friction Performance Trends for Asphaltic Pavement Surface Types

PREPARED FOR:

California Department of Transportation
Division of Research and Innovation
Office of Materials and Infrastructure

PREPARED BY:

University of California
Pavement Research Center
UC Davis, UC Berkeley

DOCUMENT RETRIEVAL PAGE			**Research Report: UCPRC-RR-2007-03**
Title: Investigation of Noise, Durability, Permeability, and Friction Performance Trends for Asphaltic Pavement Surface Types: First- and Second-Year Results			
Authors: Aybike Ongel, John T. Harvey, Erwin Kohler, Qing Lu, and Bruce D. Steven			
Prepared for: Caltrans Division of Research and Innovation	**FHWA No:** CA091200A	**Report Date:** February 2008	**Work Submitted:** June 27, 2008
Contract No.: 65A0172	**Status:** Final Stage 6, approved version May 20, 2009		**Version:** Final

Abstract: The central purpose of the research is to support the California Department of Transportation (Caltrans) Quieter Pavement Research Program, which has as its goals and objectives the identification of quieter, safer asphalt pavement surfaces. The research conforms with Federal Highway Administration (FHWA) guidance provided to state departments of transportation (DOTs) that conduct tire/pavement noise research. Results from this research are intended to identify best practices for selecting asphaltic surfaces based on performance trends identified from field measurements for noise, permeability, friction, and durability.

This report evaluates the first two years of measurements of noise (on-board sound intensity), permeability, skid resistance (friction), roughness, and surface distresses of the most common asphalt pavement surface types in California: open-graded asphalt concrete, which includes conventional mixes (OGAC), rubberized mixes (RAC-O), and F-mixes; rubberized gap-graded asphalt concrete (RAC-G); and dense-graded asphalt concrete (DGAC).

The sample of pavement surfaces in this study includes three age categories, two traffic types, and two rainfall regions. This report presents results for the sections in the factorial experiment in the detailed Work Plan for this project. This report also presents similar results for the Division of Environmental Analysis sections and other special test sections, which are referred to as ES sections. This report presents all results for the factorial sections and ES sections, some of which were presented in previous interim reports.

Conclusions are made regarding the performance of open-graded mixes and RAC-G compared with DGAC; the variables affecting tire/pavement noise; the correlation of laboratory absorption values with field-measured noise levels; and the performance of mix types included in the study in addition to DGAC, OGAC, RAC-O, and RAC-G. Preliminary recommendations are made for practice based on the results, and recommendations are made for future work.

Keywords:
asphalt concrete, decibel (dB), noise, absorption, macrotexture, microtexture, open-graded, gap-graded, dense-graded, onboard sound intensity

Proposals for implementation:
No proposals for implementation are presented in this report.

Related documents:
Work Plan for project 4.16, "Investigation of Noise, Durability, Permeability, and Friction Performance Trends for Asphaltic Pavement Surface Types"

Signatures:

A. Ongel **First Author**	J. Harvey **Technical Review**	D. Spinner **Editor**	J. Harvey **Principal Investigator**	T. Joe Holland **Caltrans Contract Manager**

DISCLAIMER

The contents of this report reflect the views of the authors who are responsible for the facts and accuracy of the data presented herein. The contents do not necessarily reflect the official views or policies of the State of California or the Federal Highway Administration. This report does not constitute a standard, specification, or regulation.

PROJECT OBJECTIVES

The research presented in this report is part of the California Department of Transportation (Caltrans) Quieter Pavement Research (QPR) Work Plan. The central purpose of the research is to support the Caltrans Quieter Pavement Research Program, which has as its goals and objectives the identification of quieter, safer asphalt pavement surfaces. The program Road Map and Work Plan outline the tasks carried out in this research.

The research conforms with Federal Highway Administration (FHWA) guidance provided to state departments of transportation that conduct tire/pavement noise research.

Results from this research are intended to identify best practices for selecting asphaltic surfaces based on performance trends identified from field measurements for noise, permeability, friction, and durability. This work includes the following objectives:

1. Provide a literature survey of U.S. and European practice and research regarding the performance of asphaltic surfaces.
2. Develop an operational capacity at the Partnered Pavement Research Center (PPRC) to measure field on-board sound intensity, laboratory noise impedance, and field surface friction.
3. Develop a database structure for field and laboratory measurements collected in this project.
4. Measure the properties of as-built surfaces (sound intensity, permeability, friction, and distresses) over time, with trends in data summarized annually. Continue data collection as authorized by Caltrans. Measure the same properties for mixes from outside California and summarize data and trends reported from outside California.
5. Perform statistical analyses on measurement results from the field and laboratory and report performance trends and modeling results.
6. Prepare a report summarizing the work related to completion of the first five objectives.

This report presents results from completion of these objectives, including the first two years of field measurements and laboratory test results.

CONVERSION FACTORS

SI* (MODERN METRIC) CONVERSION FACTORS				
APPROXIMATE CONVERSIONS TO SI UNITS				
Symbol	**Convert From**	**Multiply By**	**Convert To**	**Symbol**
LENGTH				
in. ft	inches feet	25.4 0.305	millimeters meters	mm m
AREA				
$in.^2$ ft^2	square inches square feet	645.2 0.093	square millimeters square meters	mm^2 m2
VOLUME				
ft^3	cubic feet	0.028	cubic meters	m^3
MASS				
lb	pounds	0.454	kilograms	kg
TEMPERATURE (exact degrees)				
°F	Fahrenheit	5 (F – 32)/9 or (F – 32)/1.8	Celsius	C
FORCE and PRESSURE or STRESS				
lbf $lbf/in.^2$	poundforce poundforce/square inch	4.45 6.89	newtons kilopascals	N kPa
APPROXIMATE CONVERSIONS FROM SI UNITS				
Symbol	**Convert From**	**Multiply By**	**Convert To**	**Symbol**
LENGTH				
mm m	millimeters meters	0.039 3.28	inches feet	in. ft
AREA				
mm^2 m^2	square millimeters square meters	0.0016 10.764	square inches square feet	$in.^2$ ft^2
VOLUME				
m^3	cubic meters	35.314	cubic feet	ft^3
MASS				
kg	kilograms	2.202	pounds	lb
TEMPERATURE (exact degrees)				
C	Celsius	1.8C + 32	Fahrenheit	F
FORCE and PRESSURE or STRESS				
N kPa	newtons kilopascals	0.225 0.145	poundforce poundforce/square inch	lbf $lbf/in.^2$

*SI is the symbol for the International System of Units. Appropriate rounding should be made to comply with Section 4 of ASTM E 380. (Revised March 2003.)

EXECUTIVE SUMMARY

With traffic noise becoming a growing concern, the public is expecting "quieter pavements" to be constructed to abate traffic noise levels. Quieter pavement, a new concept intended to reduce the impact that tire/pavement noise has on the highway environment, offers new options for minimizing the impact of traffic noise levels on neighborhoods adjacent to highways.

Over the past several years, the concept of using quieter pavement to reduce noise impact has received increasing attention, in California and across the nation. Much of the research on queiter pavements has generally established their short-term benefits; therefore, most of the recent attention has turned to the development of a better understanding of long-term acoustic benefits. The California Department of Transportation (Caltrans) has initiated several studies to evaluate the acoustic properties of pavements and pavement surface characteristics on tire/pavement noise levels. The research presented in this report is part of one of those studies and is part of the Caltrans Quieter Pavement Research (QPR) Work Plan.

The Caltrans QPR Plan is a systematic research proposal intended to examine the impact of quieter pavements on traffic noise levels and to establish which pavement characteristics have the greatest impact on tire/pavement noise. The goal of the QPR program is to evaluate the acoustic properties and performance characteristics of both flexible and rigid pavements and of bridge decks used by the state. This report only covers flexible pavement surfaces. Additionally, the QPR program is intended to identify surface treatments, materials, and construction methods that will result in quieter pavements that are also safe, durable, and cost-effective. The information gathered will be used to develop quieter pavement design features and specifications for noise abatement throughout California.

For the flexible pavement part of the QPR program, Caltrans identified the need for research in the areas of acoustics, friction, and pavement performance of asphalt pavement surfaces for the state highway network. In November 2004, the Caltrans Pavement Standards Team (PST) approved a new research goal for the Partnered Pavement Research Center (PPRC) Strategic Plan; it was numbered Element 4.16 and titled "Investigation of Noise, Durability, Permeability, and Friction Performance Trends for Asphaltic Pavement Surface Types."

The central purpose of this research is to support the Caltrans QPR program Road Map and Work Plan with goals and objectives that address identification of asphalt pavement surfaces that are both quieter and safer. The research conforms with FHWA guidance provided to state departments of transportation that conduct tire/pavement noise research.

The objectives and deliverables from the Work Plan for this project completed with this report are shown in the following table.

Work Plan Section	Objective	Deliverables
1.2.1	1. Literature survey	• Literature survey of U.S. practice, performed by PPRC • Literature survey of European practice performed by Swiss Federal Laboratories for Materials Testing and Research (EMPA)
1.2.2	2. PPRC test capability	PPRC operational capability to measure field sound intensity, lab noise impedance, and field surface friction
1.2.3	3. Database structure	• Database structure • Populated database at completion of data collection objective (Objective 4)
1.2.4	4. Data collection	
	4a. Field sections in California	• Properties of as-built surfaces (sound intensity, permeability, friction, and distresses) over time, with trends in data summarized annually • Continued data collection as authorized by Caltrans.
	4b. Field and lab data from outside California	Database of measurements of outside mixes and report summarizing data collected and trends
1.2.5	5. Performance-trend statistical analysis	Report documenting statistical analysis results from data collection objective (Objective 4), with summary of performance trends and modeling results
1.2.6	6. Two-year summary report	Report summarizing all of the work completed; this document constitutes the report

Results from this research are intended to identify best practices for selecting asphaltic surfaces based on performance trends identified from field measurements for noise, permeability, friction, and durability. This report presents the results from the entire two-year research study involving the pavement noise, permeability, durability, roughness, surface distress, and friction characteristics of the most common asphalt pavement surface types in California: open-graded asphalt concrete, which includes conventional mixes (OGAC), rubberized mixes (RAC-O), and F-mixes; rubberized gap-graded asphalt concrete (RAC-G); and dense-graded asphalt concrete (DGAC). The sample of pavement surfaces in this study includes three age categories, two traffic types, and two rainfall regions.

Age categories consist of the following: less than one year old, one to four years old, and four to eight years old. Traffic types are based on Caltrans 2004 annual average daily traffic (AADT) data for highways and freeways. Traffic was categorized as high if the AADT (two-way) was greater than 32,000 vehicles per day, with lower amounts categorized as low. Rainfall is based on annual average rainfall in California from 1960 to 1990, with amounts greater than 620 mm (24.4 inches) categorized as high and smaller quantities as low.

The pavement sections in the experiment are referred to as QP sections. This experiment design includes 52 QP sections and 10 Stantec sections (identified as 01-N* and 06-N*). The F-mixes were placed only in low-trafficked areas, so traffic levels could not be evaluated for these sections. Similar results for 23 Division of Environmental Analysis pavement sections and other special test sections (referred to as ES sections) are also included in this report.

UCPRC field crews visited each of the test sections twice with Caltrans Maintenance traffic closures — approximately one year apart with a rainy season in between — and collected data on permeability, skid resistance (friction), roughness, noise, and surface distress. Cores were also taken from each 125- or 150-m (410- or 492-ft) section. The cores were used to determine air-void content and were burned in an ignition oven to obtain aggregate gradations.

The measured results and the qualitative and statistical analyses from this testing program are documented in this report. This information is organized in this report as follows:

- Chapter 1 introduces the QPR study, presents the background to the study, the objectives, and the performance parameters for pavement surfaces.
- Chapter 2 provides a summary literature survey covering U.S. and European sources.
- Chapter 3 presents the methodology used for the study.
- Chapter 4 describes the independent variables and abbreviations used in the analysis.
- Chapter 5 presents an analysis of the permeability and air-void content data and an evaluation of clogging.
- Chapter 6 contains an analysis of skid resistance data, including data on microtexture and macrotexture.
- Chapter 7 provides an analysis of ride-quality data in terms of the International Roughness Index (IRI).
- Chapter 8 presents an analysis of the condition survey data.
- Chapter 9 presents an analysis of the on-board sound intensity (OBSI) data collected on the test sections, laboratory sound absorption data from field cores, and the correlation between OBSI and absorption.
- Chapter 10 presents an analysis of the data collected on the ES sections.
- Chapter 11 presents an overall evaluation of the performance models developed in this study, and an assessment of the life spans of the different surface mixes for different conditions and failure criteria based on the models.
- Chapter 12 lists the conclusions from the analyses and includes preliminary recommendations.
- Appendices provide various data corrections used and detailed condition survey information.

The data presented in this report is included in a relational database that will be delivered to Caltrans separately. Specific data in the database includes:

- Microtexture and macrotexture data that affect skid resistance;
- Ride quality in terms of International Roughness Index (IRI);
- On-board sound intensity (OBSI), a measure of tire/pavement noise;
- Sound intensity for different frequencies; and
- Surface distresses, including bleeding, rutting, raveling, transverse cracking, and cracking in the wheelpaths;
- Climate data; and
- Traffic data.

The analyses presented for each performance variable in Chapters 5 through 9 include a summary of the expected trends from the literature, descriptive statistics, and where the data is sufficient, statistical models. Several appendices provide data corrections used and detailed condition survey information. The data presented in this report is included in a relational database that will be delivered to Caltrans separately.

Conclusions

In this report, the performance of open-graded mixes as well as of other asphaltic mixes used in California was evaluated in terms of safety, noise, and durability. Data was collected on the OGAC, RAC-O, RAC-G, and DGAC mixes as well as on some new mixes such as bonded wearing course (BWC), gap-graded asphalt rubber (RUMAC-GG), gap-graded rubber modified asphalt (Type G-MB), and dense-graded rubber modified asphalt (Type D-MB). The objectives of this study were to:

- Evaluate the durability and effectiveness of open-graded mixes in increasing safety and reducing noise compared to other asphalt surfaces
- Determine the pavement characteristics that affect tire/pavement noise
- Correlate sound absorption with tire/pavement noise
- Evaluate the performance of new mixes compared to the asphaltic mixes currently used in California

<u>Performance of Open-Graded Mixes</u>

The results showed that current open-graded mixes reduced tire/pavement noise compared to the dense-graded mixes included in the study by almost 2 dB (A) on average for all sections over the eight-

year range of ages, which according to the literature is near the limit of what the human ear can discern. Twenty-five percent of the open-graded mixes provided noise reduction above 3 dB (A) compared to the average noise level of a DGAC mix, which is 104 dB (A) for the sections tested. Over the entire set of sections including all ages, the open-graded mix noise levels were between 1 dB (A) greater and 4 dB (A) less than the average DGAC noise level. The noise levels of the DGAC mixes in the study were similar across all ages of pavement.

Noise reductions between 2 dB (A) and 6 dB (A) were reported in the literature for open-graded mixes. The results presented in this report are from comparisons between different surfaces of similar ages. Greater noise reductions would be expected when new open-graded surfaces are placed on existing DGAC surfaces that have widespread and severe distresses than when comparing the noise levels of open-graded mixes with those of DGAC surfaces of similar ages as was done in this study.

Also note that noise levels above 1,000 Hz are generally considered more annoying, and that increasing air-void content and increasing macrotexture reduce the noise levels at higher frequencies. Since open-graded mixes have higher air-void content and macrotexture, they may reduce the noise levels at higher frequencies and so may be perceived by the human ear as quieter and the noise as less annoying than dense-graded mixes, even though the overall A-weighted noise levels are not significantly different from each other.

Open-graded mixes have higher permeability and friction than dense-graded and RAC-G mixes; therefore, they can reduce hydroplaning and spray and splash and hence improve safety. Based on the results of the conditions surveys for pavements less than nine years old included in this study, they also may be less prone to transverse cracking. However, although it could not be revealed statistically in this study, it is expected that open-graded mixes would be more prone to raveling since their high permeability would be expected to increase the oxidation rate of the binder, in comparison to the less permeable DGAC and RAC-G mixes.

Open-graded mixes lose their noise-reducing properties with time mainly due to clogging and also due to the presence of distresses on the pavement surface. The work in this study predicts their noise levels to reach those of dense-graded mixes within seven years. Clogging occurs at the top part of the surface layer and reduces its permeability. There is also some indication that thicker mixes, above 50 mm, may be less clogged and hence have higher permeabilities than thinner mixes. The longevity of benefits provided by open-graded mixes varies with mix properties, rainfall, and presence of raveling.

From this small sample of pavements in California, there does not appear to be a major difference in performance between RAC-O and OGAC mixes with respect to noise and permeability benefits across the age ranges. However, the rate of increase in IRI is slower for rubberized mixes. Although the data was not

statistically significant in this study, rubberized mixes tended to have better cracking performance, which would be expected to slow the rate of noise in later years.

Performance of RAC-G Mixes

It appears from the data that RAC-G mixes provide some noise benefit compared to DGAC mixes. Most of the noise benefits from RAC-G appear to come from the fact that they have higher air-void content than DGAC mixes when they are built (compaction of RAC-G is by method specification, where the compaction method is specified and the relative density is not specified, rather than by an end-result specification where the relative density is specified and the contractor chooses the compaction method.). However, they lose their permeability faster than the open-graded mixes, and hence their noise-reducing properties. Based on the descriptive statistics, the noise levels from RAC-G mixes appear to approach those of DGAC within four years. The sound intensity model overpredicts the noise levels of RAC-G mixes; therefore, this model cannot be used to estimate the lifetime of RAC-G mixes in terms of noise reduction.

Variables Affecting Tire/Pavement Noise

The study showed that tire/pavement noise is greatly influenced by pavement surface characteristics such as gradation, macrotexture, age, and presence of distresses. Coarser gradation and increasing air-void content reduce the overall noise levels, and the presence of distresses and increasing macrotexture and age increase the overall noise levels, confirming the previous findings of other researchers. However, this study found that the overall A-weighted noise levels are insensitive to changes in air-void content for open-graded mixes with air-void content above 15 percent. This insensitivity occurs because air-void content above 15 percent is usually associated with higher macrotexture (MPD) values, and for large texture depths, increasing air-void content does not reduce the overall noise levels, and its effects are surpassed by those of increased tire vibrations.

Since California mixes are placed in thin layers (around 30 mm), thickness was not found to affect the noise levels of the sections studied. However, there is some indication that increasing thickness may lower the noise levels for thicknesses above 50 mm (2 inches).

The pavement temperature was not found to significantly affect the noise levels.

The use of rubber asphalt binders was also not found to significantly affect the noise levels, although the noise levels of RAC-O mixes were somewhat less than those of OGAC mixes.

The low frequencies of tire/pavement noise were found to be governed by tire vibrations due to high macrotexture, and the higher frequencies were found to be governed by air-pumping mechanisms that can be reduced by the presence of air voids on the pavement surface, confirming the findings of previous researchers on the noise-generation mechanisms. However, increasing air-void content was found to

increase the noise levels at a given macrotexture at lower frequencies, probably due to increased tire vibrations.

At frequencies around 800 to 1,000 Hz, where the tire/pavement noise is highest, the air-pumping cannot be reduced by increasing air-void content above 15 percent, and tire vibrations govern the noise generation for mixes with high air-void content and high macrotexture values. This trend can also be seen in the overall noise levels.

At frequencies above 1,000 Hz, higher air-void content and higher macrotexture values reduce the air-pumping noise. Therefore, open-graded mixes have significantly lower noise levels at frequencies above 1,000 Hz.

Correlation of Absorption Values with Noise Levels

The noise levels of dense- and gap-graded mixes decrease with increasing absorption. However, no correlation was found between the overall A-weighted sound intensity and absorption for open-graded mixes. Correlations between sound intensity (noise) measured in the field and laboratory absorption values depended on frequency. Noise levels around 500 Hz are governed by tire vibrations; therefore, absorption has no effect on the noise levels for any mix type. At frequencies above 630 Hz, absorption reduces the noise levels caused by air pumping for dense- and gap-graded mixes, and there are clear trends relating noise to absorption.

Tire vibrations may cause significant noise levels for open-graded mixes with high macrotexture values at lower frequencies (less than 1,000 Hz), and there is no trend between noise and absorption. The noise-reducing effect of absorption can be seen at 1,000 Hz for open-graded mixes, if macrotexture is also considered. The noise-reducing effects of absorption can be clearly seen at frequencies above 1,000 Hz for open-graded mixes. Air-pumping noise governs noise generation at frequencies above 1,000 Hz, confirming the earlier findings, as increasing absorption reduces the noise levels regardless of the macrotexture values. This trend is stronger for higher frequencies, which are considered more annoying to humans.

Performance of New Mixes

The bituminous wearing course (BWC) mix placed on the LA 138 sections has lower permeability and friction, higher noise levels, and almost the same distress development as current Caltrans open-graded mixes in the LA 138 section study.

Based on the Fresno 33 (Firebaugh) sections, the RUMAC-GG and Type G-MB mixes did not perform as well the RAC-G mix when placed in thin lifts (45 mm); the RUMAC-GG and Type G-MB mixes have higher noise levels and are more susceptible to bleeding. However, RUMAC-GG was more

crack resistant when placed in thick layers (90 mm). Type D-MB, which may be a candidate as an alternative to dense-graded mixes after further investigation, has performance characteristics very similar to those of DGAC mixes, and it may provide better crack resistance; however, it was more susceptible to bleeding.

The European gap-graded (EU-GG) mix placed on LA 19 has performance characteristics very similar to those of gap-graded mixes (RAC-G) used in California.

F-mixes have been used only in a wet environment on the north coast. Indications are that they do not perform as well as OGAC and RAC-O with regard to noise, probably because of their large NMAS values and raveling.

Other Conclusions

Note that the conclusions presented here are valid within the range of the air-void content, thickness, age, and gradation properties of the mixes used in this study and under California climate and traffic conditions. The OBSI measurements were conducted using an Aquatread 3 tire and a passenger car. The conclusions may differ for trucks and vehicles with different tires as noise-generation mechanisms are highly dependent on the vehicle and tire type. Also note that the OBSI method is a near-source measurement; therefore, it captures only the tire/pavement noise. Since the noise levels next to highways are also affected by noise propagation and noise absorption under propagation, the greater absorption values measured as part of this project may indicate that the open-graded mixes provide higher levels of noise reduction at the side of the highway than these results may show.

The comparison of pass-by measurements made by Volpe (unverified by UCPRC with regard to wind speeds and other factors) with OBSI measurements indicated that absorption may provide additional noise reduction next to highways since 75-mm OGAC shows higher noise reduction than dense-graded mixes when measured using the pass-by method. However, the pass-by measurements found no additional noise reduction for the 30-mm OGAC and RAC-O sections.

The effects of NMAS and thickness could not be fully evaluated as these variables have different specifications for different mix types. Open-graded mixes have NMAS values of 9.5 and 12.5 mm, and dense- and gap-graded mixes have NMAS values of 12.5 and 19 mm. F-mixes are the only open-graded mixes with an NMAS value of 19 mm. Open-graded mixes are placed in thin layers, while RAC-G and DGAC mixes are usually placed in a thicker lift. RAC-G mixes are usually placed at half the thickness of DGAC mixes as the rubber content allows for reduced thickness, providing structural and reflection crack retardation equivalency. Therefore, NMAS and thickness effects were identified only within each mix type. Also, rubberized mixes are usually overlays of pavements with more extensive cracking than the

pavements on which DGAC mixes are placed. Therefore, the effects of rubber on crack retardation could not be fully evaluated.

The effects of stiffness on noise levels were evaluated by comparing the noise levels of rubberized and nonrubberized mixes as well as by comparing shear modulus values with noise levels. The study's preliminary conclusion is that stiffness does not play a major role in determining noise levels for mixes of the types included in this study.

Recommendations

Based on the findings, none of the other asphalt mix types evaluated in this study can provide an alternative to current Caltrans open-graded mixes in terms of noise reduction and safety. However, durability of open-graded mixes compared to other mix types depends on the climatic conditions and traffic.

The results indicate that the current recommendation for the best approach to noise reduction is to use thin layers of open-graded mixes with nominal maximum aggregate sizes of 12.5 or 9.5 mm. The smaller aggregate sizes will somewhat reduce air-void content and permeability; however, open-graded mixes with smaller aggregate sizes will likely have greater durability because of their lower air-void content and will likely cost less than open-graded mixes with larger aggregate sizes because they can be constructed as thinner lifts. The results indicated that the desired air-void content for open-graded mixes for noise reduction could be limited to a maximum of 15 percent since higher air-void content does not provide any additional noise reduction and reduces durability. Mixes with lower air-void content would also be more resistant to clogging.

There do not appear to be noise-reduction benefits from increasing the thickness of open-graded mixes for thicknesses less than 50 mm. However, the results gave some indication that thicknesses greater than 50 mm (2 inches) reduce noise. Placing open-graded mixes in thicker lifts would also help reduce the IRI value and increase cracking resistance for overlays of PCC. The results also gave some indication that thicker lifts may be less susceptible to clogging.

Open-graded mixes have longer lives in terms of noise and permeability with low levels of truck traffic and rainfall. High truck traffic increases clogging, and mixes under low rainfall are also more susceptible to clogging, although they are less likely to show raveling and polishing. When placing open-graded mixes, the air-void content and thickness will need to be balanced with the permeability requirements needed to reduce hydroplaning for a given site.

Overall preliminary recommendations for open-graded mix design based on the results of this study are shown in the table below. These recommendations are also the basis for recommendations for further

work to improve the performance of open-graded mixes, discussed in the next section of this report (Section 12.3).

Table Preliminary Recommendation for Open-Graded Mix and Thickness Design to Achieve Performance Goals

	Performance Criteria (relevant section of report)				
Mix and Thickness Design Variables	**Noise (Sections 9.1.4 and 9.2.3)**	**Permeability (Section 5.4)**	**Durability** (Section 8.6)***	**Ride Quality (Section 7.3)**	**Friction (Section 6.7)**
Air-Void Content	15 percent or greater	Maximize*	Minimize		Maximize
Nominal Max Aggregate Size	Minimize	12.5 mm instead of 9.5 mm			Maximize
Gradation	Greater fineness modulus (coarser gradation)	Greater fineness modulus (coarser gradation)			Greater fineness modulus (coarser gradation)
Binder Type			Rubberized	Rubberized	
Overlay Thickness	Greater than 50 mm may help				

* Permeability recommendations should be based on expected rainfall events for a particular project location. Development of these criteria are outside the scope of this project.
** Durability is defined as resistance to distress development.
*** Few sections had significant distresses, and results were not statistically significant. Recommendations regarding durability are based on judgment as well as the results of this study.

Recommendations for Further Work

In this study, pavement characteristics and noise were observed for two years. However, two years is a short time to observe any trends. Therefore, permeability, friction, IRI, and sound intensity measurements and condition surveys should be conducted on the given sections for at least two or three years to develop better time histories and see more sections reach failure.

Open-graded mixes have lower noise levels than dense- and gap-graded mixes at higher frequency levels, which may be a benefit that A-weighted measurement does not capture well in terms of annoyance rather than audibility. Since the human ear is most sensitive at frequencies between 1,000 and 4,000 Hz, the open-graded mixes may be perceived as quieter than dense-graded mixes with the same overall noise levels. The noise levels should be correlated with the human perception of annoyance to better evaluate noise-mitigation strategies.

Since the reason for placing open-graded mixes is to reduce the noise levels next to highways, the way-side measurements should be better correlated with OBSI levels than was possible in this study to understand the actual noise reduction provided by open-graded mixes.

At 500 Hz, increasing air-void content was found to increase noise levels along with macrotexture; however, the noise-generation mechanism is unknown. The further effects of air-void content on noise levels at lower frequencies should be evaluated. In addition, a new parameter that correlates better with the sound intensity levels should be developed. This parameter can be a combination of MPD, RMS, and air-void content as well as a new measure of macrotexture.

The results gave some indication that open-graded mixes with finer gradations (lower fineness modulus) may provide lower noise levels, particularly at higher frequencies of noise. In this study, only a few open-graded mixes had fine gradations. The effects of fineness modulus on the noise levels should be further evaluated, particularly for mixes with the same NMAS.

This study could not fully evaluate the effects of NMAS and thickness on pavement performance. Therefore, a laboratory study should be performed to consider the durability, sound absorption (correlated with high-frequency noise), and permeability for a full factorial experiment considering these variables. Some optimization of the mixes based on initial results should also be performed. Since the presence of polymer-modified binders could not be identified for the OGAC sections in this study because of a lack of reliable as-built records for many sections, polymer and conventional binders, as well as rubberized binders used by Caltrans, should also be included in the factorial. Macrotexture should also be measured, since the results indicate that absorption and macrotexture provide an indication of noise at 1,000 Hz.

The results of the laboratory study will provide a basis for designing a factorial for field-test sections to verify the laboratory results regarding the effects of thickness, NMAS, fineness modulus, and binder type on clogging, cracking, and noise levels. Permeability and noise measurements as well as condition surveys should be conducted on these test sections. The air-void content should also be measured using CT scans with a higher resolution than used in this study. A resolution around 15 microns (based on the results of this study) would be enough to see fine particles clogging the mix. The effects of pavement temperature on noise levels were evaluated measuring nine sections at three temperatures. No correlation was found between pavement temperatures and noise levels. A larger data set, with open-, gap-, and dense-graded mixes, should be obtained, and measurements should be conducted using a wider range of pavement temperatures. It would be useful to analyze the effects of pavement temperature on noise levels separately for each mix type.

TABLE OF CONTENTS

PROJECT OBJECTIVES ..... **iii**
CONVERSION FACTORS ..... **iv**
EXECUTIVE SUMMARY ..... **v**
LIST OF TABLES ..... **xxiii**
LIST OF FIGURES ..... **xxv**
LIST OF ABBREVIATIONS ..... **xxxi**
1 INTRODUCTION **1**
1.1 Background 1
1.2 Quieter Pavement Research Objectives Addressed in This Report 2
1.3 Traffic Noise 3
1.4 Desired Properties of Open-Graded Mixes 6
1.4.1 Performance of Open-Graded Mixes 7
1.4.1.1 Permeability 7
1.4.1.2 Skid Resistance (Friction) 7
1.4.1.3 Roughness 8
1.4.1.4 Durability 8
1.4.1.5 Noise Reduction 8
1.5 Contents of This Report 9
2 LITERATURE SURVEY **11**
2.1 Permeability 11
2.2 Skid Resistance (Friction) 14
2.3 Roughness (Unevenness) and Ride Quality 18
2.4 Pavement Distresses 20
2.4.1 Bleeding 20
2.4.2 Rutting 20
2.4.3 Transverse Cracking 21
2.4.3.1 Transverse Cracking Caused by Thermal Stresses 21
2.4.3.2 Transverse Cracking Caused by Reflection Cracking 22
2.4.4 Raveling 22
2.4.5 Fatigue Cracking 23
2.5 Highway Noise 24
2.5.1 Pavement Variables Affecting Noise 27
2.5.1.1 Texture 27

2.5.1.2 Roughness (Unevenness) 29
2.5.1.3 Air-Void Content (Porosity) 29
2.5.1.4 Stiffness 32
2.5.1.5 Age 32
2.5.1.6 Temperature 33
3 METHODOLOGY 35
3.1 Site Selection 35
3.1.1 Experimental Design of the Test Sections 35
3.2 Data Collection 51
3.2.1 Coring 53
3.2.2 Condition Survey 55
3.2.3 Permeability 55
3.2.4 Friction 56
3.2.5 Air Temperature and Pavement Temperature 57
3.2.6 On-Board Sound Intensity 57
3.2.7 International Roughness Index (IRI) 58
3.2.8 Macrotexture 59
3.2.9 Air-Void Content 60
3.2.10 Aggregate Gradation 61
3.2.11 Extent of Clogging 61
3.2.12 Acoustical Absorption 62
4 ANALYSIS OF INDEPENDENT VARIABLES 65
4.1 Variable Definitions 65
5 EVALUATION OF PERMEABILITY AND AIR-VOID CONTENT OF ASPHALT CONCRETE MIXES 77
5.1 Permeability Analysis 78
5.1.1 Descriptive Analysis 78
5.1.2 Regression Analysis 81
5.2 Air-Void Content Analysis 85
5.2.1 Descriptive Analysis 85
5.2.2 Air-Void Content Determination by CT Scan 89
5.3 Evaluation of Clogging 91
5.3.1 Field Permeability Measurements 91
5.3.2 CT Scan 97

5.4 Summary of Findings 101
6 EVALUATION OF SKID RESISTANCE (FRICTION) OF ASPHALT CONCRETE MIXES 105
6.1 Microtexture 105
6.2 Descriptive Analysis 106
6.3 Correction of British Pendulum Numbers for Temperature 110
6.4 Statistical Modeling of Microtexture 111
6.5 Macrotexture 116
6.5.1 Descriptive Analysis 117
6.5.2 Statistical Modeling of Macrotexture 120
6.6 International Friction Index (IFI) 123
6.7 Figure 66: Comparison of F_{60} values for different mix types at different ages 125
6.7 126
6.8 Summary of Findings 126
7 EVALUATION OF ROUGHNESS OF ASPHALT CONCRETE MIXES 129
7.1 Descriptive Analysis 129
7.2 Regression Analysis 132
7.3 Summary of Findings 137
8 PAVEMENT DISTRESS EVALUATION 139
8.1 Bleeding 139
8.2 Rutting 140
8.3 Transverse and Reflection Cracking 142
8.3.1 Descriptive Analysis 142
8.3.2 Regression Analysis 144
8.4 Raveling 146
8.4.1 Descriptive Analysis 146
8.4.2 Regression Analysis 148
8.5 Wheelpath Crack Initiation 150
8.5.1 Descriptive Analysis 150
8.5.2 Survival Analysis 151
8.6 Summary of Findings 154
9 ANALYSIS OF ACOUSTICAL PROPERTIES OF ASPHALT MIXES 157
9.1 On-Board Sound Intensity Levels 157
9.1.1 Descriptive Analysis 157

9.1.2 Single-Variable Regression Analysis 163
9.1.3 Principal Components Regression 177
9.1.4 Summary of Findings 183
9.2 One-Third Octave Band Analysis of Sound Intensity Levels 185
9.2.1 Evaluation of Pavement Surface Effects on the Spectral Content of Sound Intensity Levels 186
9.2.2 Evaluation of Pavement Temperature Effects on the Frequency Content of Sound Intensity Levels 207
9.2.3 Summary of Findings 213
9.3 Evaluation of Acoustical Absorption Values 215
9.3.1 Descriptive Analysis 215
9.3.2 Correlation of Acoustical Absorption Values with Air-Void Content and Surface Thickness 217
9.3.3 Correlation of Absorption Values with A-Weighted Sound Intensity Levels 219
9.3.4 Correlation of Sound Absorption Values with One-Third Octave Band Frequency Sound Intensity Levels 222
9.3.4.1 Sound Intensity Levels for 500-Hz One-Third Octave Band 222
9.3.4.2 Sound Intensity Levels for 630-Hz One-Third Octave Band 224
9.3.4.3 Sound Intensity Levels for 800-Hz One-Third Octave Band 225
9.3.4.4 Sound Intensity Levels for 1,000-Hz One-Third Octave Band 227
9.3.4.5 Sound Intensity Levels for 1,250-Hz One-Third Octave Band 230
9.3.4.6 Sound Intensity Levels for 1,600-Hz One-Third Octave Band 231
9.3.5 Summary of Findings 233
10 ANALYSIS OF ENVIRONMENTAL NOISE MONITORING SITE SECTIONS 235
10.1 Fresno 33 Sections 235
10.2 Sacramento 5 and San Mateo 280 Sections 242
10.3 LA 138 Sections 251
10.4 LA 19 Section 261
10.5 Yolo 80 Section 265
10.6 Summary of Environmental Noise Monitoring Site Sections Analysis 269
11 EVALUATION OF PERFORMANCE MODELS AND PREDICTION OF LIFETIME FOR DIFFERENT ASPHALT MIX TYPES 273
11.1 Evaluation of Permeability and Clogging Models 273
11.2 Evaluation of Microtexture Models 275

11.3 Evaluation of Roughness Models 278
11.4 Evaluation of On-Board Sound Intensity Model 280
11.5 Prediction of Lifetime for Different Asphalt Mix Types 281
12 CONCLUSIONS, RECOMMENDATIONS, AND RECOMMENDATIONS FOR FURTHER WORK 285
12.1 Conclusions 285
12.1.1 Performance of Open-Graded Mixes 285
12.1.2 Performance of RAC-G Mixes 286
12.1.3 Variables Affecting Tire/Pavement Noise 287
12.1.4 Correlation of Absorption Values with Noise Levels 287
12.1.5 Performance of New Mixes 288
12.1.6 Other Conclusions 288
12.2 Recommendations 289
12.3 Recommendations for Further Work 291
REFERENCES 293
APPENDIX A: Correction of OBSI Values for Speed (from 35 mph to 60 mph) 304
APPENDIX B: Air-Density Correction 305
APPENDIX C: Regression Analysis for Each Frequency Level 306
APPENDIX D: Condition Survey of Environmental Noise Monitoring Site Sections for Two Years 317

LIST OF TABLES

Table 1: Summary of Objectives and Deliverables in Work Plan 2
Table 2: FHWA Noise Abatement Criteria (NAC) in dB (A) (hourly A-weighted sound level) 5
Table 3: Road Noise Level Regulations in Europe in dB (A) 6
Table 4: Experimental Design of the Selected Test Sections 40
Table 5: Caltrans Environmental Noise Monitoring Site (ES) Sections* 49
Table 6: Climatic Information for ES Test Sections* 50
Table 7: Traffic Volume and Truck Traffic for ES Test Sections* 50
Table 8: Data Collection in the Field During Traffic Closures 52
Table 9: Data Collection at Highway Speed 52
Table 10: Laboratory Measurements and Tests on Cores Collected in the Field 53
Table 11: Descriptive Statistics for the Independent Variables 70
Table 12: Regression Analysis of Permeability 82
Table 13: Comparison of Air-Void Content by CT Scan and CoreLok Methods 90
Table 14: Regression Analysis of Clogging 93
Table 15: Weighted Least Squares Regression Analysis of Clogging 93
Table 16: Regression Analysis of Clogging for the Center of the Lane 95
Table 17: Weighted Least Squares Regression Analysis of Clogging for the Center of the Lane 95
Table 18: Regression Analysis of Clogging in Wheelpath 96
Table 19: Weighted Least Squares Regression Analysis of Clogging in Wheelpath 97
Table 20: Regression Analysis of Microtexture 112
Table 21: Wheelpath BPN Difference 116
Table 22: Regression Analysis of Macrotexture 120
Table 23: Regression Analysis of Difference in Macrotexture Between Two Years 123
Table 24: Regression Analysis of IRI Values 133
Table 25: Regression Analysis of Difference in IRI Values Between Two Years 137
Table 26: Sections Showing Rutting in the Second Year 141
Table 27: Regression Analysis of Presence of Transverse Cracking 145
Table 28: Regression Analysis of Presence of Raveling 149
Table 29: Number of Previously and Currently Cracked Sections 151
Table 30: Single-Variable Cox Regression Model for Wheelpath Crack Initiation 153
Table 31: Regression Analysis of Single-Variable Models for Sound Intensity Levels 164
Table 32: Comparison of Shear Modulus and A-Weighted Sound Intensity Levels for Selected Cores 173

Table 33: Regression Analysis of Change in Sound Intensity Levels 177
Table 34: Correlation Matrix of Significant Variables 179
Table 35: Pattern Matrix Extracted by Principal Components Analysis 181
Table 36: Structure Matrix Extracted by Principal Components Analysis 181
Table 37: Pattern Matrix Extracted by Principal Axis Factoring 182
Table 38: Structure Matrix Extracted by Principal Axis Factoring 182
Table 39: Pavement Characteristics Affecting Noise Levels at Different Frequencies 188
Table 40: Absorption Values and Noise Reduction of LA 138 Open-Graded and BWC Sections 259
Table 41: Predicted Lifetime of Different Mix Types for BPN Values 277
Table 42: Predicted Lifetime of Different Asphalt Mix Types with Respect to Performance Variables 283
Table 43: Preliminary Recommendation for Open-Graded Mix and Thickness Design to Achieve Performance Goals 291

LIST OF FIGURES

Figure 1: Addition of two sound sources. 4
Figure 2: Mastic distribution of the open-graded mixes through the thickness (31). 13
Figure 3: Positive texture. 15
Figure 4: Negative texture. 15
Figure 5: IRI roughness scale (WAPA [54] from Sayers, 1986 [55]). 19
Figure 6: Noise-generation mechanisms (14). 26
Figure 7: Pavement texture and roughness (unevenness). 28
Figure 8: Noise reflection on reflective surface. 31
Figure 9: Noise reflection on porous surface. 32
Figure 10: Map of the test sections. 35
Figure 11: Dense-graded asphalt concrete (DGAC). 45
Figure 12: Open-graded asphalt concrete (OGAC). 45
Figure 13: Rubberized open-graded asphalt concrete (RAC-O). 46
Figure 14: Rubberized open-graded asphalt concrete F-mix (RAC-O F-mix). 46
Figure 15: Rubberized gap-graded asphalt concrete (RAC-G). 47
Figure 16: Typical aggregate gradations for different mix types from ignition oven, with 12.5-mm NMAS. 47
Figure 17: Typical aggregate gradations for different mix types from ignition oven, with 19-mm NMAS. 48
Figure 18: Typical field sampling layout. (Note: Core locations in the second year are within 1 m upstream of the first-year locations and core locations 1 and 2, 5 and 6, and 9 and 10.) 54
Figure 19: Falling-head permeameter. 56
Figure 20: British Pendulum skid-resistance tester. 57
Figure 21: On-board sound intensity (OBSI) microphone setup. 58
Figure 22: Laser profilometer beam. 59
Figure 23: MPD calculations (ASTM E 1845). 60
Figure 24: CoreLok seal of specimen. 60
Figure 25: Computed Tomography scanner (106). 62
Figure 26: Impedance tube system. 63
Figure 27: Distribution of average annual rainfall. 71
Figure 28: Distribution of average annual minimum daily temperature of the coldest month (°C). 72
Figure 29: Distribution of average annual maximum daily temperature of the hottest month (°C). 72
Figure 30: Distribution of annual ESALs in the coring lane. 73

Figure 31: Distribution of annual freeze-thaw cycles. 73
Figure 32: Pairwise comparison of surface and mix properties. 74
Figure 33: Pairwise comparison of climate variables. 75
Figure 34: Pairwise comparison of cold temperature variables and temperature differences..... 75
Figure 35: Pairwise comparison of traffic data. 76
Figure 36: Box plot of permeability values for different mix types..... 78
Figure 37: Box plot of permeability values for different mix types at different ages (Note: Age category 0 is less than one year old, category 1 is one to four years old, and category 2 is greater than four years old)..... 79
Figure 38: Comparison of permeability values for different mix types at different ages for first and second years..... 80
Figure 39: Comparison of permeability differences between first-year and second-year measurements for different mix types at different ages (positive value indicates a reduction in permeability). 81
Figure 40: Permeability (cm/sec) versus air-void content for different mix types. 83
Figure 41: Permeability variation for open-graded mixes with different NMAS values. 85
Figure 42: Box plot of air-void content for different mix types (dots show the mean values). 86
Figure 43: Box plot of air-void content for different mix types at different ages. 87
Figure 44: Box plot of fineness modulus for different mix types at different ages. 87
Figure 45: Comparison of air-void content for different mix types at different ages for first and second years. 88
Figure 46: Difference in air-void content between first-year and second-year measurements for different mix types at different ages (positive values indicate a reduction in air-void content)..... 89
Figure 47: Permeability difference between the center and the right wheelpath for different mix types (positive value indicates greater permeability in the center of the lane than in the wheelpath). 91
Figure 48: CT scan image of an open-graded mix (top view). 98
Figure 49: Air-void distribution of open-graded mixes and EU gap-graded mix through the thickness of the surface layer. 99
Figure 50: Air-void distribution of dense-graded mixes and BWC mix through the thickness of the surface layer. 100
Figure 51: Air-void content trend for open-graded mixes and EU gap-graded mix through the thickness of the surface layer. 101
Figure 52: Box plot of BPNs for different mix types including all ages. 107
Figure 53: Box plot of BPNs for different mix types at different ages. 108
Figure 54: Comparison of BPNs for different mix types at different ages for first and second years. 109

Figure 55: Difference in BPNs between first-year and second-year measurements for different mix types at different ages (positive values indicate reduction in friction). 110
Figure 56: Scatter plot of BPN versus AADT. 113
Figure 57: Box plot of BPNs at the center and the right wheelpath. 115
Figure 58: Box plot of MPD values for different mix types with F-mixes separated. 117
Figure 59: Box plot of MPD values for different mix types at different ages. 118
Figure 60: Comparison of MPD values for different mix types at different ages for first and second years. 119
Figure 61: Difference in MPD values between first-year and second-year measurements for different mix types at different ages (positive values indicate increase in MPD values). 119
Figure 62: MPD values for different NMAS values and for open-graded and dense- and gap-graded mixes. 121
Figure 63: Comparison of F_{60} values for different mix types. 124
Figure 64: Comparison of S_p values for different mix types. 124
Figure 65: Comparison of F_{60} values for different mix types, F-mixes separated. 125
Figure 66: Comparison of F60 values for different mix types at different ages. 125
Figure 67: Variation in IRI values for different mix types. 130
Figure 68: Variation in IRI values for different mix types at different ages. 130
Figure 69: Comparison of IRI values for different mix types at different ages for first and second years. 131
Figure 70: Difference in IRI values for different mix types at different ages (positive values indicate an increase in IRI). 132
Figure 71: Number of sections with and without bleeding categorized by mix type. (Note: Year 1 refers to the first year of measurement and Year 2 to the second year of measurement.) 140
Figure 72: Sections with and without rutting. 142
Figure 73: Number of sections with and without transverse cracking for different mix types. 143
Figure 74: Number of sections with and without transverse cracking for rubberized and nonrubberized mixes. (Note: 1st Year refers to the first year of measurement and 2nd Year to the second year of measurement.) 144
Figure 75: Number of sections with and without raveling for different mix types. (Note: Year 1 refers to the first year of measurement and Year 2 to the second year of measurement.) 147
Figure 76: Number of sections with and without raveling for rubberized and nonrubberized mixes. (Note: Year 1 refers to the first year of measurement and Year 2 to the second year of measurement.) 148

Figure 77: A-weighted sound intensity levels for different mix types. 158
Figure 78: A-weighted sound intensity levels for different mix types with F-mixes separated. 159
Figure 79: A-weighted sound intensity levels for different mix types at different ages. 160
Figure 80: Cumulative distribution function of noise reduction of OGAC, RAC-O, and RAC-G mixes across an eight-year range of ages (positive value indicates a reduction in noise). 161
Figure 81: Comparison of A-weighted sound intensity levels for different mix types at different ages for first and second years. 162
Figure 82: Difference in A-weighted sound intensity levels between first and second years for different mix types at different ages (positive value indicates an increase in noise). 163
Figure 83: Scatter plot with a best-fit line of A-weighted sound intensity levels versus NMAS (mm). 165
Figure 84: Scatter plot of A-weighted sound intensity levels versus NMAS (mm) without QP-48. 166
Figure 85: Scatter plot of sound intensity levels versus MPD for different mix types. 167
Figure 86: Scatter plot of A-weighted sound intensity levels versus air-void content for different mix types. 168
Figure 87: Scatter plot of A-weighted sound intensity levels versus log (permeability) for different mix types. 168
Figure 88: Scatter plot of A-weighted sound intensity levels versus fineness modulus for different mix types. 169
Figure 89: Scatter plot of A-weighted sound intensity levels versus surface layer thickness for different mix types. 170
Figure 90: Scatter plot of air-void content versus surface thickness for different mix types. 171
Figure 91: Scatter plot of sound intensity levels for rubberized and nonrubberized mixes. 172
Figure 92: Relationship between A-weighted sound intensity levels and surface temperatures (ºC). 174
Figure 93: Scatter plot of A-weighted sound intensity levels versus log (permeability) for different mix types and for different MPD categories. 176
Figure 94: Scree plot for principal components analysis. 180
Figure 95: Example of one-third octave band spectrum of OBSI. 186
Figure 96: 500-Hz band sound intensity levels versus MPD. 192
Figure 97: 500-Hz band sound intensity levels versus air-void content. 192
Figure 98: Sound intensity levels at 630-Hz band versus age. 193
Figure 99: Sound intensity levels for 800 Hz versus air-void content for different mix types. 194
Figure 100: Sound intensity levels for 800 Hz versus MPD values for different mix types. 195
Figure 101: Air-void content versus fineness modulus for different mix types. 197
Figure 102: Sound intensity levels for 1,000-Hz band versus air-void content for different mix types. 198

Figure 103: Sound intensity levels for 1,000-Hz band versus MPD values for different mix types. 198
Figure 104: 1,250-Hz band sound intensity levels versus MPD for different mix types 201
Figure 105: 4,000-Hz band sound intensity levels versus air-void content for different mix types. 205
Figure 106. 4,000-Hz band sound intensity levels versus MPD for different mix types. 205
Figure 107: Relationship between sound intensity at 500 Hz and surface temperatures (ºC). 207
Figure 108: Relationship between sound intensity at 630 Hz and surface temperatures (ºC). 208
Figure 109: Relationship between sound intensity at 800 Hz and surface temperatures (ºC). 208
Figure 110: Relationship between sound intensity at 1,000 Hz and surface temperatures (ºC). 209
Figure 111: Relationship between sound intensity at 1,250 Hz and surface temperatures (ºC). 209
Figure 112: Relationship between sound intensity at 1,600 Hz and surface temperatures (ºC). 210
Figure 113: Relationship between sound intensity at 2,000 Hz and surface temperatures (ºC). 210
Figure 114: Relationship between sound intensity at 2,500 Hz and surface temperatures (ºC). 211
Figure 115: Relationship between sound intensity at 3,150 Hz and surface temperatures (ºC). 211
Figure 116: Relationship between sound intensity at 4,000 Hz and surface temperatures (ºC). 212
Figure 117: Relationship between sound intensity at 5,000 Hz and surface temperatures (ºC). 212
Figure 118: Example of one-third octave band sound intensity levels for different mix types at different ages. 213
Figure 119: Box plots of absorption values for different mix types. 216
Figure 120: Comparison of wheelpath absorption values for different mix types at different ages. 217
Figure 121: Correlation of absorption values with air-void content for all mixes pooled together. 218
Figure 122: Correlation of absorption values with surface layer thickness for different mix types. 219
Figure 123: A-weighted sound intensity levels versus absorption values for different mix types. 220
Figure 124: Correlation of sound intensity levels with wheelpath absorption for dense- and gap-graded mixes. 221
Figure 125: Correlation of sound intensity levels with wheelpath absorption for open-graded mixes..... 221
Figure 126: Sound intensity levels for 500-Hz band versus absorption values. 223
Figure 127: Sound intensity levels for 630-Hz band versus absorption values. 224
Figure 128: Sound intensity levels for 800-Hz band versus absorption values. 226
Figure 129: Sound intensity levels for 1,000-Hz band versus absorption values. 228
Figure 130: Sound intensity levels for 1,000-Hz band versus absorption values for different mix types and different macrotexture values. 229
Figure 131: Sound intensity levels for 1,250-Hz band versus absorption values. 230
Figure 132: Sound intensity levels for 1,600-Hz band versus absorption values. 232
Figure 133: Layout of Fresno 33 sections. 237

Figure 134: First-year and second-year air-void content for Fresno 33 sections. 238
Figure 135: First-year and second-year permeability values for Fresno 33 sections. (Note: The scale for permeability was selected for comparison of permeability values across different ES sections). 239
Figure 136: First-year and second-year MPD values for Fresno 33 section. 240
Figure 137: First-year and second-year sound intensity levels for Fresno 33 sections. 241
Figure 138: Bleeding for 45-mm Type G-MB mix 242
Figure 139: First-year and second-year air-void content for Sacramento 5 sections. 244
Figure 140: First-year and second-year permeability values for Sacramento 5 sections. 244
Figure 141: First-year and second-year air-void content for San Mateo 280 section. 245
Figure 142: First-year and second-year permeability values for San Mateo 280 section. 245
Figure 143: First-year and second-year IRI values for Sacramento 5 sections. 246
Figure 144: First-year and second-year IRI values for San Mateo 280 section. 247
Figure 145: First-year and second-year MPD values for Sacramento 5 sections. 248
Figure 146: First-year and second-year MPD values for San Mateo 280 section. 248
Figure 147: First-year and second-year sound intensity levels for Sacramento 5 sections. 249
Figure 148: First-year and second-year sound intensity levels for San Mateo 280 section. 250
Figure 149: Layout of the test sections. 252
Figure 150: Comparison of first-year and second-year air-void content for LA 138 sections. 253
Figure 151: Comparison of first-year and second-year permeability values for LA 138 sections. 253
Figure 152: First-year and second-year IRI values for LA 138 sections. 254
Figure 153: First-year and second-year MPD values for LA 138 sections. 255
Figure 154: Comparison of sound intensity levels for LA 138 sections. 256
Figure 155: Noise reduction from pass-by measurements by Volpe National Transportation Systems Center for LA 138 mixes. 257
Figure 156: Comparison of gradation of LA 19 section with RAC-G gradation. 262
Figure 157: First-year and second-year air-void content for LA 19 section. 262
Figure 158: Comparison of first-year and second-year permeability values for LA 19 section. 263
Figure 159: First-year and second-year MPD values for LA 19 section. 264
Figure 160: First-year and second-year sound intensity levels for LA 19 section. 265
Figure 161: First-year and second-year air-void content for Yolo 80 section. 266
Figure 162: First- year and second-year permeability values for Yolo 80 section. 267
Figure 163: First-year and second-year MPD values for Yolo 80 section. 268
Figure 164: First-year and second-year sound intensity levels for Yolo 80 section. 269

LIST OF ABBREVIATIONS

AADT	average annual daily traffic
AADTCL	average annual daily traffic in the coring lane
AADTT	average annual daily truck traffic
AC	asphalt concrete
ADT	average daily traffic
ADTT	average daily truck traffic
AV	air-void content
BWC	bonded wearing course
BPN	British Pendulum Number
BS	British Standard
Caltrans	California Department of Transportation
Caltrans PCS	Caltrans Pavement Condition Survey
CDIM	Climate Database for Integrated Model
CTM	Circular Texture Meter
CT scan	Computed Tomography scan
DEA	Division of Environmental Analysis
DFT	Dynamic Friction Tester
DGAC	dense-graded asphalt concrete
DMI	Distance Measuring Instrument
EB	eastbound (used for pavement traffic direction)
EMPA	Swiss Federal Laboratories for Materials Testing and Research
ESAL	equivalent single-axle load
ES sections	environmental noise monitoring site sections
ETD	estimated texture depth
EU-GG	European gap-graded asphalt concrete
FHWA	Federal Highway Administration
F-mixes	open-graded gradation mixes with 19 mm NMAS (originally developed by the Oregon DOT)
Fre 33	Fresno 33
G_{bulk}	bulk specific gravity
G_{mm}	maximum specific gravity
IFI	International Friction Index
IRI	International Roughness Index
IQR	interquartile range
LA 138	Los Angeles 138
LA 19	Los Angeles 19
LTTP	Long-Term Pavement Performance
MPD	mean profile depth
MTD	mean texture depth
NAC	noise abatement criteria
NB	northbound (used for pavement traffic direction)
NCAT	National Center for Asphalt Technology
NMAS	nominal maximum aggregate size
OBSI	on-board sound intensity
OGAC	open-graded asphalt concrete
OLS regression models	ordinary least squares regression models
PCC	portland cement concrete
PCR	principal components regression
PCS	Pavement Condition Survey
PMS	Pavement Management System

QP sections	quiet pavement experimental design sections
RAC-G	rubberized gap-graded asphalt concrete
RAC-O	rubberized open-graded asphalt concrete
RMS	root mean square
RUMAC-GG	rubber-modified asphalt concrete (dry process, a local-government specification)
Sac 5	Sacramento 5
SB	southbound (used for pavement traffic direction)
SM 280	San Mateo 280
SMA	stone mastic asphalt
Type D-MB	dense-graded mix with binder meeting MB specification
Type G-MB	gap-graded mix with binder meeting MB specification
UCPRC	University of California Pavement Research Center
VMA	voids in the mineral aggregate
WIM	weigh in motion

1 INTRODUCTION

1.1 Background

With traffic noise becoming a growing concern, the public is expecting *quieter pavements* to be constructed to abate traffic noise levels. Quieter pavements may offer new options for minimizing the impact of traffic noise levels on neighborhoods adjacent to highways.

Quieter pavement is a new concept intended to reduce the impact that tire/pavement noise has on the highway environment. The concept of using quieter pavements to reduce noise has received increasing attention in California and nationwide over the past several years. With the short-term benefits of quieter pavements somewhat documented, most of the new attention has focused on developing a better understanding of the long-term acoustic benefits of quieter pavements. In response to public expectations, the California Department of Transportation (Caltrans) has initiated several studies to evaluate the acoustic properties of pavements and the role of pavement surface characteristics on tire/pavement noise levels. The research presented in this report is part of one of these studies and is part of the Caltrans Quieter Pavements Research (QPR) Work Plan (1)

The Caltrans QPR plan is a systematic research proposal intended to examine the impact of quieter pavements on traffic noise levels and to establish which pavement characteristics have the greatest impact on tire/pavement noise. The goal of the QPR study is to evaluate the acoustic properties and performance characteristics of both flexible and rigid pavements and of bridge decks used by the state. Additionally, the QPR study is intended to identify surface treatments, materials, and construction methods that will result in quieter pavements that are also safe, durable, and cost effective. The information gathered in the study will be used to develop quieter-pavement design features and specifications for noise abatement throughout the state. (1)

For the flexible pavement part of the QPR study, Caltrans identified a need for research in the areas of acoustics, friction, and pavement performance of asphalt pavement surfaces for the state highway network. In November 2004, the Caltrans Pavement Standards Team (PST) approved a new research goal for the Partnered Pavement Research Center (PPRC) Strategic Plan; it was numbered Element 4.16 and titled "Investigation of Noise, Durability, Permeability, and Friction Performance Trends for Asphaltic Pavement Surface Types."

The goals of this research as described in the Work Plan (2) approved by the PST are to:

1. Develop a database for lifetime performance trends to identify best practices. Trends will be determined for California open-graded (including mixes with and without rubberized asphalt binder), rubberized gap-graded asphalt concrete (RAC-G). and dense-graded asphalt concrete

(DGAC) mixes with regard to sound intensity, durability (raveling, rutting, and cracking), friction, and permeability. Performance trends will be analyzed as a function of gradation, binder type, traffic [speed, average daily traffic (ADT), average daily truck traffic (ADTT), and equivalent single-axle load (ESAL)], climate (rainfall, temperature, and freezing), and roughness [International Roughness Index (IRI)].

2. Gather and summarize information on laboratory tests that are correlated with these performance measures (sound intensity, durability, friction, and permeability), gather information on mix design methods, and identify best practices that can potentially be brought to California.

3. Survey practice and research in other states and in Europe on the lifetime performance of their open-graded mix types with respect to sound intensity, durability, friction, and permeability. Gather and summarize performance data and identify promising mixes that can be brought to California.

4. Determine whether a relationship exists between a laboratory noise absorption test, the impedance tube, and field sound intensity measurements using field cores.

1.2 Quieter Pavement Research Objectives Addressed in This Report

The objectives in the Work Plan for PPRC Strategic Plan Element 4.16 (PPRC SPE 4.16) are shown in Table 1 (2).

Table 1: Summary of Objectives and Deliverables in Work Plan

Work Plan Section	Objective	Deliverables
1.2.1	1. Literature survey	• Literature survey of U.S. practice, performed by PPRC • Literature survey of European practice performed by Swiss Federal Laboratories for Materials Testing and Research (EMPA)
1.2.2	2. PPRC test capability	PPRC operational capability to measure field sound intensity, lab noise impedance, and field surface friction
1.2.3	3. Database structure	• Database structure • Populated database at completion of data collection objective (Objective 4)
1.2.4	4. Data collection	
	4a. Field sections in California	• Properties of as-built surfaces (sound intensity, permeability, friction, and distresses) over time, with trends in data summarized annually • Continued data collection as authorized by Caltrans.
	4b. Field and lab data from outside California	Database of measurements of outside mixes and report summarizing data collected and trends
1.2.5	5. Performance-trend statistical analysis	Report documenting statistical analysis results from data collection objective (Objective 4), with summary of performance trends and modeling results
1.2.6	6. Two-year summary report	Report summarizing all of the work completed; this document constitutes the report

This report completes Objective 6. The results presented in this report complete Objectives 4a and 5.

A summary of the results of Objective 1, the literature survey completed earlier, have been included in this report, and it includes information regarding performance properties. A separate technical memorandum summarizes a literature survey completed in 2006 regarding open-graded mix design practices and specifications. The data and analysis presented for Objectives 4a and 5 are for the first two years of data collection on the quiet pavement sections (QP sections) in the experimental factorial in the PPRC SPE 4.16 Work Plan, and for the Division of Environmental Analysis (DEA) sections and other special test sections, which are collectively referred to as ES sections. Among the DEA sections are sections that DEA has monitored for noise properties for a number of years, as well as other test sections placed by Caltrans over the past five years that are outside the main factorial for this project. The data collected on all sections over the first two years of the study has been entered into the project database that will be submitted separately. Data was not available to complete Objective 4b, however. Caltrans, its consultants, and UCPRC have been working with other states and other consultants to develop common noise measurement protocols so that data can be compared in the future. This report constitutes completion of Objective 6.

1.3 Traffic Noise

Noise is defined as unwanted or unpleasant sound. Like all other sounds, noise is produced by vibrating objects and transmitted by pressure waves in a compressible medium such as air. As pressure waves travel through a medium, they produce sound. Sound waves are characterized by three parameters.

- Wavelength: The distance of the crest of one wave to the crest of the one following.
- Frequency: The number of waves that pass a particular point each second
- Amplitude: The measure of the energy present in a sound wave; the greater the amplitude of the sound energy, the louder the sound

Sound pressure or sound intensity levels are used to quantify the loudness of an ambient sound. The frequencies of sounds audible to humans range from 20 to 20,000 Hz, and sound pressures range from 20 micropascals (μPa), the threshold of hearing, to 120 pascals (Pa), the threshold of pain (3). Since it is hard to work with such a broad range of sound pressure, the linear sound pressure, p, is converted to a logarithmic sound pressure level, SPL, which compresses the scale of numbers into a manageable range. The conversion from linear sound pressure to logarithmic scale is given in Equation (1):

$$SPL = 10 \times \log (p/p_{ref}) \quad \textbf{(1)}$$

where p_{ref} is an international standardized reference sound pressure of 2×10^{-5} Pa. The unit of SPL is called the decibel (dB).

Noise levels can also be expressed in terms of sound intensity, which is a measure of energy flow through a unit area. Sound intensity is converted to a logarithmic sound intensity level, L_I, according to Equation (2):

$$L_I = 10 \times \log (I/I_{ref}) \quad \textbf{(2)}$$

where I_{ref} is 10^{-12} W/m^2.

I_{ref} is chosen to obtain the same reading in decibels regardless of whether SPL or L_I is used to define the sound wave, and irrespective of whether pressure or intensity in an acoustic free field is measured. The unit of L_I is also the decibel (dB).

The human ear is not equally sensitive to all sound frequencies; the ear can hear high-frequency noise better than low-frequency noise that has the same sound pressure (dB). Therefore, noise measurement readings can be adjusted to incorporate this difference in sensitivity. The adjustment of sound measurements according to human sensitivity is called A-weighting, and adjusted noise levels are written as dB (A).

Since the decibel scale is nonlinear, resultant noise levels from two different sound sources that emit two incoherent sounds with the same sound pressure would increase the noise level by 3 dB (70 dB + 70 dB = 73 dB, not 140 dB). The formula used to add together multiple sources of sound is given in Equation (3). The effect of two incoherent sound levels is shown in Figure 1.

$$dB(A)_{Total} = 10 \log_{10} \sum_{i=soundsources} 10^{\frac{dB(A)_i}{10}} \quad \textbf{(3)}$$

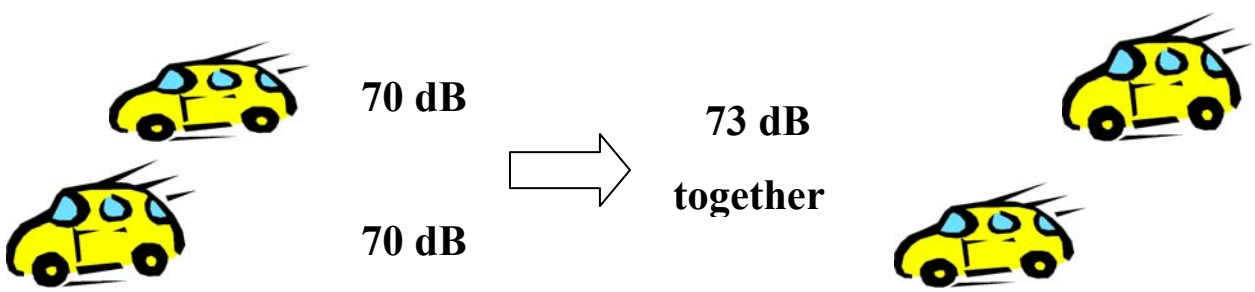

Figure 1: Addition of two sound sources.

Noise levels are mainly affected by the distance from the source. As sound waves travel through a medium, they spread out over a spherical or circular surface; hence, their energy is distributed over a greater surface area. Since the energy of waves is conserved and the area through which the waves travel increases, sound intensity decreases. Intensity variation is proportional to the square of the distance from the source. If the distance from the source is doubled, the sound intensity level is decreased by a factor of four.

The measurement of noise is adjusted to reflect the sensitivity of human hearing because noise disturbance can affect the quality of human lives. In recent decades, noise pollution has become a major concern in the United States and the world. Noise pollution can impair hearing, cause sleep disturbances, have cardiovascular effects, interfere with social behavior (aggressiveness, protest, and helpfulness) and verbal communication, and cause annoyance (4). The economic consequences of these health impairments include loss of property value in areas subject to noise, reduced work performance by those affected by noise (5) and medical costs for improving the health of those affected by noise (6). Among all environmental noises (construction, rail, road, and airplane noise), road noise has been identified as the most annoying (7). Road noise mostly affects people in residences and businesses next to highways and people in road vehicles.

Because of increases in motorization and the number of highways, the problem of traffic noise has begun receiving a lot of attention. The adverse effects of traffic noise on health and the economy have forced communities to seek solutions to improve quality of life by reducing this noise. Most industrialized countries have introduced noise emission regulations. The Federal Highway Administration (FHWA) specifies noise levels for different types of land zoning where noise abatement should be considered. FHWA Noise Abatement Criteria (8) are given in Table 2.

Table 2: FHWA Noise Abatement Criteria (NAC) in dB (A) (hourly A-weighted sound level)

Activity Category	NAC, $L_{eq}(h)$*	Description of Activity Category
A	57 (exterior)	Lands on which serenity and quiet are of extraordinary significance and serve an important public need and where the preservation of those qualities is essential if the area is to continue to serve its intended purpose
B	67 (exterior)	Picnic areas, recreation areas, playgrounds, active-sports areas, parks, residences, motels, hotels, schools, churches, libraries, and hospitals
C	72 (exterior)	Developed lands, properties, or activities not included in Category A or B
D	-	Undeveloped lands
E	52 (interior)	Residences, motels, hotels, public meeting rooms, schools, churches libraries, hospitals, and auditoriums

* $L_{eq}(h)$ is the sound pressure averaged over one hour.

European countries have also imposed regulations regarding noise levels, given in Table 3 (9). Additionally, the European Union specifies noise emission limits for new tires for passenger cars and for heavy and light trucks (10). The EU has created a project called Coordination of European Research for Advanced Transport Noise Mitigation (CALM) that supports research and development of new technologies to reduce all transport-related noise (11).

Table 3: Road Noise Level Regulations in Europe in dB (A)

Country	Planning Value L_{eq} *	Maximum Limit L_{eq} *	Remarks
Austria	55	-	-
Switzerland	Day 50 Night 40	Day 55 Night 45	-
France	Day 60 Night 55	65	Average for day from 8 a.m. to 8 p.m. Average for night from 10 p.m. to 6 a.m.
Denmark	55	-	-
UK	Day 55 Night 45	Day 72 Night 66	Average for day from 7 a.m. to 11 p.m.
Netherlands	Day 55 Night 45	Day 58 Night 48	35 dB (A) inside 25 dB (A) inside at night
Sweden	55	-	30 dB (A) inside

* L_{eq} sound pressures are averaged over 24 hours unless otherwise indicated in Remarks column.

Highway noise arises from automobiles, buses, trucks, and motorcycles in motion. Vehicle noise has three components: aerodynamic noise, power-unit noise, and tire/pavement noise. At lower speeds, the power train and its ancillaries generate the major component of traffic noise, while at higher speeds—approximately above 50 km/h for passenger cars and 70 km/h for heavy vehicles—tire/pavement interaction noise dominates the other mechanisms (12, 13). Tire/pavement noise depends on pavement surface characteristics, vehicle speed, environmental conditions, type of tire, and the dynamics of the rolling process (14). The tire/pavement noise level increases logarithmically with increasing speed (13).

1.4 Desired Properties of Open-Graded Mixes

For open-graded mixes to be accepted as a noise mitigation tool, they should have good performance and lower life-cycle costs than competing alternatives such as gap- and dense-graded mixes. Rubberized gap-graded asphalt concrete (RAC-G) mixes have been proposed as an alternative to open-graded mixes with respect to noise reduction, while both dense-graded asphalt concrete (DGAC) and RAC-G mixes can be alternatives to open-graded mixes with respect to durability and ride quality. Neither RAC-G nor DGAC can be considered an alternative to open-graded mixes with respect to permeability. However, RAC-O and open-graded asphalt concrete (OGAC) mixes are the competing

alternatives for improved permeability. The following section explains the expected behavior of open-graded mixes in terms of performance factors.

1.4.1 Performance of Open-Graded Mixes

1.4.1.1 Permeability

Permeability is the most important performance variable for open-graded mixes as they are primarily placed to improve wet-weather surface friction. Open-graded mixes have higher air-void content, and hence higher permeability, than conventional asphalt mixes, which enables them to remove standing water. Open-graded mixes can reduce hydroplaning and water spray and splash by draining the water into the mix and hence enhance wet-weather safety.

Hydroplaning is the loss of directional control when a vehicle is moving fast enough that the tires lose contact with the surface and ride up on the water film present on the pavement surface. Splash is the mechanical impact of tires that forces the water out of the tire/pavement contact area. Splash results in reduced visibility. Hydroplaning and splash are affected by the water depth on the surface.

Open-graded mixes are susceptible to clogging at least at the surface. When the surface air voids are clogged with fine materials, air-void content and hence permeability decreases, and the benefits of open-graded mixes diminish. Therefore, the performance of open-graded mixes is governed mainly by the length of time that they maintain their permeability.

1.4.1.2 Skid Resistance (Friction)

Skid resistance is the force required to prevent a vehicle tire from sliding along the pavement surface. It is important for safety because inadequate skid resistance can result in loss of control and longer stopping distances, and hence skid-related accidents. Higher friction or skid numbers mean safer pavements. Skid resistance depends on the pavement surface's microtexture and macrotexture. Microtexture refers to small-scale irregularities of the pavement aggregate, and macrotexture refers to large-scale irregularities of the pavement surface that are affected by aggregate orientation. Macrotexture can be measured by the sand patch method as well as by laser measurements; microtexture can be measured by British Pendulum Tester or Dynamic Friction Tester (DFT) values. A British Pendulum Number (BPN) above 45 indicates a satisfactory surface according to a Caltrans (15) research document believed to be from the 1960s. This value is used as a criterion for discussion and comparison of different test sections in this research study, but it is not a Caltrans standard and should not be construed as an official standard. The performance of open-graded mixes can be evaluated by the length of time that they provide satisfactory friction and by comparison of their friction values to those of alternative mixes.

1.4.1.3 Roughness

Roughness refers to surface irregularities with wavelengths greater than 0.5 m. It is associated with ride quality. Ride quality is an indication of the comfort level of the ride over a pavement surface. Road users judge a road condition mainly based on its ride quality.

On a rough pavement, the vehicle vertical movements are high. The roughness of the pavement surface is related to the vibration of the vehicle, tire wear, operating speed, and vehicle operating costs. Roughness is currently typically measured by a standardized scale called the International Roughness Index (IRI). IRI is obtained by performing a quarter-car simulation on a longitudinal profile in the wheelpath. According to the FHWA, pavements with an IRI value greater than 95 inches per mile and less than or equal to 170 inches per mile are classified as acceptable, and pavements with an IRI value less than or equal to 95 inches per mile are classified as good (16). The performance of open-graded mixes can be evaluated by the length of time that they provide at least acceptable ride and by comparison of their roughness progression to that of alternative mixes.

1.4.1.4 Durability

Durability is the capacity of a pavement to keep its functionality over time. It can be evaluated in terms of distress development. Surface distresses can be in the form of cracks; deformation such as rutting, corrugation, bleeding, or shoving; or disintegration such as raveling, stripping, and spalling. When cracks are present on the pavement surface, water may enter the pavement structure. Since the base, subbase, and subgrade lose their load-carrying capacities when they are wet, the water entering through the cracks may lead to more severe pavement failures. Presence of distresses on the pavement surface may lead to rougher pavements and hence poor ride quality. Additionally, the presence of bleeding on the pavement surface may reduce friction.

Common distresses of open-graded mixes that have been observed or reported in the literature are rutting, transverse cracking, reflection cracking, bleeding, raveling, and fatigue cracking, most of which are also identified in the Caltrans Maintenance Technical Advisory Guide (17). The performance of open-graded mixes can be evaluated in terms of how long the mixes take to develop distresses and how the distresses progress compared to distresses in alternative mixes.

1.4.1.5 Noise Reduction

Open-graded mixes may provide noise reduction due to their higher air-void content. However, they may lose their noise-reducing properties with time due to clogging, raveling and cracking. When the surface air voids are clogged, not only is the permeability reduced but so is noise reduction. Open-graded mixes should lower the traffic noise at least 3 dB (A) compared to conventional road surfaces without

jeopardizing pavement safety and durability (10). A reduction of 3 dB (A) has the same effect as reducing the traffic volume by half. A 3 dB (A) change is just noticeable to the human ear. The performance of open-graded mixes can be evaluated in terms of the amount of noise reduction they can provide compared to alternative mixes and the length of time that they can maintain their noise-reducing properties.

1.5 Contents of This Report

Chapter 1 presents an introduction and background information about asphalt mix types and noise and summarizes the objectives and scope of this report. Chapter 2 presents a review of the literature pertinent to permeability, skid resistance (friction), roughness/ride quality, pavement distresses, and highway noise and pavement characteristics affecting noise levels. Chapter 3 describes the selection of the test sections and equipment and test methods used in the study. Chapter 4 describes the variables used in the study and presents the descriptive statistics for the independent variables. Chapter 5 evaluates the permeability and air-void content variable of different mix types and presents the analysis of variables affecting permeability and clogging. Chapter 6 presents the frictional properties of different mix types and the variables affecting friction. Chapter 7 describes the roughness of different mix types and the variables affecting roughness. Chapter 8 evaluates pavement distresses, including bleeding, rutting, raveling, transverse and reflection cracking, and fatigue cracking. Chapter 9 evaluates the acoustical properties of pavements, including sound intensity levels and acoustical absorption properties. Chapter 10 compares the performance of rubber-modified asphalt concrete (RUMAC-GG), gap-graded mix with modified binder (Type G-MB), and dense-graded mix with modified binder (Type D-MB) asphalt mixes with the mixes currently used and evaluates the effects of thickness and age on pavement performance for California Department of Transportation (DOT) environmental noise monitoring site (ES) sections. It also compares pass-by noise measurements using the on-board sound intensity (OBSI) method. Chapter 11 evaluates the performance models and predicts the lifetime for different types of mixes. Chapter 12 summarizes the findings, makes recommendations for open-graded mix design, and suggests future research.

2 LITERATURE SURVEY

2.1 Permeability

Permeability is the most important functional performance criterion for open-graded asphalt concrete mixes, as was discussed in Section 1.4.1. Open-graded pavements let water drain into the surface mix through the air voids rather than keeping it on the surface of the pavement, which results in reduced hydroplaning, water splash, and spray, and hence improved safety. Also, glare from the road surface is reduced and visibility is improved (18). Open-graded mixes have been used primarily to improve wet-weather skid resistance by removing stagnant water from the pavement surface. However, open-graded mixes can lose their permeability and hence their noise-reducing properties over time due to clogging.

Various factors that affect permeability have been reported in the literature. Air-void content has been shown to be the most important factor affecting permeability of asphalt pavements (Kanitpong, 2001; Brown, 2004; Mallick et al., 2003). As air-void content increases, permeability increases. However, a study by Huang (1999) indicated that the interconnectivity of air voids is more important in determining permeability than the total volume of the air voids.

Aggregate gradation and size also affect permeability. Mixes with coarser gradations were shown to have higher permeability values than those with finer gradations (19; 20; 21; 22). Coarse-graded mixes have larger voids, and hence greater potential for connected air voids, which results in greater permeability. The nominal maximum aggregate size (NMAS) has also been found to affect the field permeability of asphalt mixes (21, 23). Pore size increases as NMAS increases; hence the possibility of connected air voids increases. Therefore, mixes with larger NMAS values are expected to be more permeable at a given air-void content than mixes with smaller NMAS values.

Another factor that may affect permeability of DGAC and RAC-G, which are intended to be impermeable, is lift thickness. Although the Florida DOT (22) and Mallick (21) concluded that increased lift thicknesses could lead to better pavement compaction and hence lower permeability, the Wisconsin DOT (24) could not find any relationship between lift thickness and permeability. There have also been studies looking at the effects of the thickness-to-NMAS (t/NMAS) ratio on permeability (20, 24). The Wisconsin DOT (24) found that permeability increased for smaller t/NMAS ratios for a mix with limestone aggregate; however, no trend was observed for a gravel-aggregate mix. Brown (20) concluded that higher t/NMAS ratios provide lower air-void content, which may result in lower permeability values.

Because open-graded mixes have higher air-void content, and hence higher permeability than conventional asphalt mixes, they are susceptible to clogging. Clogging is the blockage of air voids with fine particles generated by vehicles and deposited from elsewhere by wind and vehicles. When air voids

are clogged with fine materials, air-void content, and hence permeability, decreases, and the benefits of open-graded mixes diminish.

A minimum permeability value of from 0.01 to 0.4 cm/sec is specified for open-graded mixes by European standards for porous asphalt (25). The requirement for in-situ permeability of open-graded mixes in Switzerland is 0.11 cm/sec (15 l/min) (26). No permeability requirements for open-graded mixes could be found in the literature from the United States.

According to Sandberg et al. (10), traffic and rainfall are the most important factors affecting in-service permeability of open-graded mixes. Fine particles that lodge in the voids of the surface layer can be suctioned out by the hydraulic action of traffic. This cleaning effect is more pronounced under heavy rainfall and fast traffic. Due to the suction effect of traffic, wheel tracks were found to remain more permeable than road shoulders (10, 27). However, lower air-void content of open-graded mixes in the wheelpaths may also be caused by densification of the mix under traffic loading, which has been observed in Arizona (28).

However, according to Bendsten (29), the most important factors affecting the in-service permeability of open-graded mixes are the age of the pavement, maximum aggregate size, air-void content and distribution, speed of vehicles, and shape of aggregates. Another study, conducted in Denmark (30), evaluated the air-void content of open-graded mixes in horizontal planes taken through the thickness using Computed Tomography (CT) scan technology, and no significant difference was found between the air-void content of the wheelpath and shoulder. The bottom part of these older open-graded mixes was found to have at least twice the air-void content of the top part, which suggests that fine particles accumulate only in the top part of the surface layer (the top 20 to 25 mm) which was typically 50 mm thick. Figure 2 shows the mastic (composed of asphalt binder, sand, and dirt) distribution of open-graded asphalt cores that are six years old from another study in Denmark (31). The trend lines shown in the figure indicate that mastic content decreases from top to bottom. The mastic content in the top 20 mm of the surface layer is higher than that in the lower part. The higher mastic content in the upper part of the pavement surface was explained by the clogging of air voids by fine particles. However, note that the mixes shown in the figure are two-layer porous asphalt, where the top layer is 20 to 25 mm thick and has smaller-size aggregate, and the bottom layer is thicker and has larger-size aggregate.

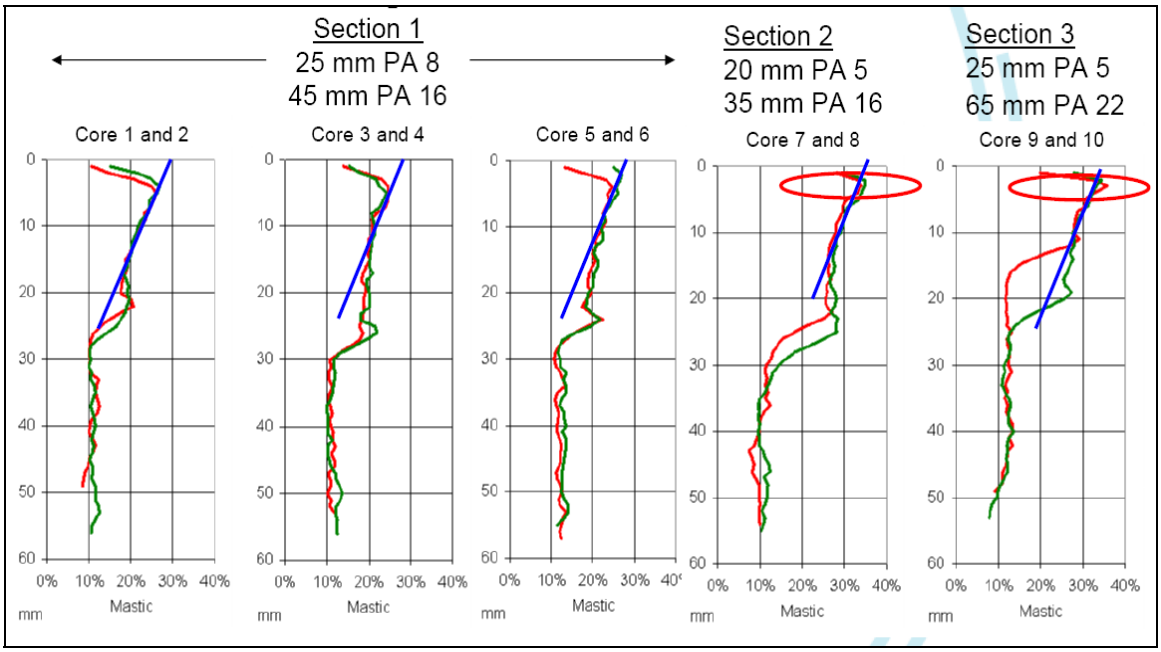

Figure 2: Mastic distribution of the open-graded mixes through the thickness (31).

In the United Kingdom, a study found that open-graded mixes using larger maximum aggregate size keep their porosity longer compared to mixes with smaller aggregate size (32). On the basis of this result, the United Kingdom specifies 20-mm maximum aggregate size for its open-graded mixes.

Sandberg et al. (10) suggested that binder type may affect clogging. There is some evidence that dirt does not stick to polymer-modified asphalt binder as much as it sticks to unmodified asphalt binder (10). This effect may be due to the higher softening point of polymer-modified binder. However, this effect was identified as needing further investigation. If the softening point at high temperatures affects the dirt accumulation in the voids, the temperatures experienced by the pavement may also affect clogging.

The location of the pavement, defined as urban or rural, has also been found to affect the clogging of open-graded mixes (10, 33, 29). Rural roads were found to be more likely to get clogged by mud and sand carried by agricultural trucks.

All the research on clogging was conducted in Europe. Therefore, the results are limited to asphalt-mix designs and traffic levels and climatic conditions in Europe, which are different from those in the United States. Factors affecting clogging of California open-graded mixes, which experience different traffic and climate conditions than those in Europe, still need to be identified.

Earlier studies have shown the effects of air-void content and gradation on permeability. However, research is still needed to clarify the effect of thickness on the permeability of different asphalt mix types and the changes in permeability of different mixes over time. Permeability is controlled not

only by total air-void content, but also by interconnectivity of the air-void system and by distribution of air voids within the layer.

2.2 Skid Resistance (Friction)

Skid resistance is the force required to prevent a vehicle tire from sliding along the pavement surface. It is important in terms of safety because inadequate skid resistance may result in skid-related accidents. Skid resistance is generally quantified in terms of friction measurements such as friction or skid numbers. A skid number is actually the coefficient of friction. Skid resistance can be measured by locked-wheel tests, spin-up tests, and surface-texture measurements.

Skid numbers above 30 are acceptable for low-volume roads, and skid numbers above 35 are acceptable for heavily traveled roads (34). Higher friction or skid numbers result in shorter stopping distances. Skid resistance is controlled by the microtexture and macrotexture of the surface as well as the geometrical design of the road.

Microtexture is the deviation of a pavement surface from a true planar surface with a maximum dimension of 0.5 mm (35). It is associated with microscopic properties of the surface and controlled by the individual aggregate surface properties, such as shape and harshness. Microtexture controls the adhesion component of friction between the tire and the road surface. Therefore, it is important for providing a good grip, and hence skid resistance between the tire and the pavement surface, at low speeds and under dry road conditions; although microtexture contributes to skid resistance at all speeds, it has the most influence at speeds less than 30 mph.

Macrotexture is the deviation of a pavement surface from a true planar surface with a dimension between 0.5 and 50 mm (35). The visible irregularities of a pavement surface caused by large aggregate particles control the texture wavelength. Macrotexture facilitates water drainage by providing water channels on the pavement surface, preventing a film of water from developing between the pavement and the tire and loss of contact between the pavement and the tire (hydroplaning). Macrotexture also contributes to friction of the pavement surface and controls skid resistance at higher speeds.

Macrotexture can be reported as mean profile depth (MPD) or mean texture depth (MTD). MPD is a two-dimensional estimate of three-dimensional MTD. Laser measurements give the MPD, and sand-patch measurements give the MTD. In addition to the MPD, laser measurements provide the root mean square (RMS), which is a statistical value showing how much the measured profile (actual data) deviates from a modeled profile of the data.

Surface texture can be positive or negative depending on the aggregate orientation. Negative texture has voids on the surface without exposed aggregates, while positive texture has exposed aggregates protruding from the pavement surface. Negative textured surfaces have lower noise levels than

neutral or positive textured surfaces (36). Figure 3 shows a surface with a positive texture, and Figure 4 shows a surface with a negative texture. Two surfaces can be considered mirror images of each other and hence have the same peak height. They would have the same RMS value, but the positive textured surface would have a much higher MPD value than the negative textured surface. For example, chip seal provides positive texture, while grooved portland cement concrete provides negative texture (37).

A texture orientation calculation method was proposed by McGhee et al. (37). Surfaces for which the MPD was 5 percent or more than the RMS value were considered to be positively textured, and surfaces for which the RMS value was 5 percent or more than the MPD value were considered to be negatively textured. For sections with RMS and MPD values approximately equal, the surfaces were categorized as neutral in texture.

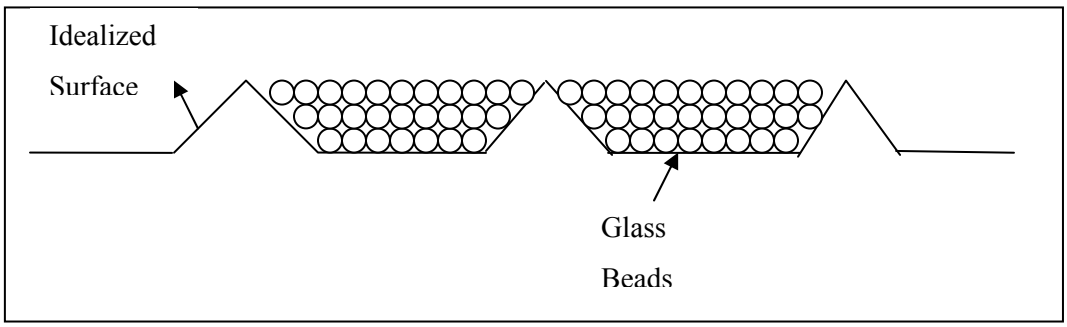

Figure 3: Positive texture.

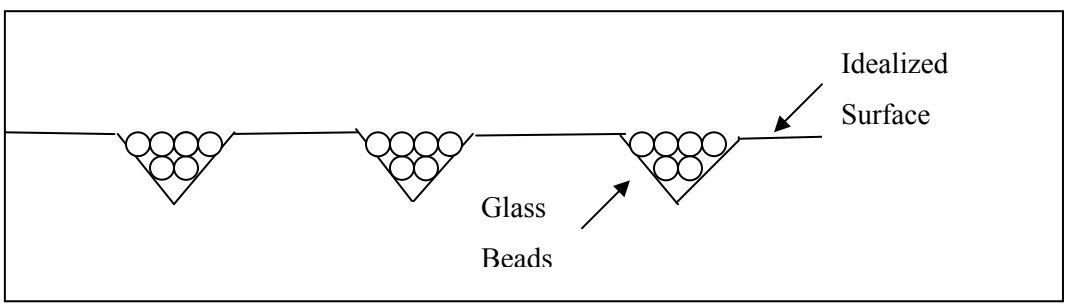

Figure 4: Negative texture.

The World Road Association (PIARC) proposed an International Friction Index (IFI) for use in pavement friction surveys to harmonize friction and texture measurement devices. IFI is a universal, two-parametric index with a coefficient of friction at 60 kilometers per hour, which is related to the microtexture of the surface (F_{60}), and the slip speed or velocity of sliding friction, which is related to the macrotexture of the surface (S_p) (38). F_{60} and S_p can be calculated for different measurement devices, and therefore IFI allows comparison of friction values measured by different devices.

Skid resistance is influenced by many factors: tire-related properties such as rubber compound, tread design and condition, inflation pressure, and operating temperature; pavement-surface properties

such as mix type, microtexture and macrotexture, and surface temperature; and intervening-substance-related factors such as quantity of water, presence of loose particulate matter, and oil contaminants on the pavement surface (39). Skid resistance is usually measured on wet surfaces. The water film on the pavement surface acts as a lubricant and reduces the contact between the aggregates and the tire (34). Therefore, wet pavement surfaces exhibit lower friction than dry surfaces.

The skid resistance of asphalt pavements changes over time. Typically, it increases in the first few years after construction as the asphalt binder on surface aggregates is worn away by traffic and the aggregate surfaces become more exposed, and then it decreases over the remaining life of the pavement as aggregates become more polished under additional traffic (40). Polishing of aggregates results in smoother and rounder aggregates and therefore reduces friction. Hill et al. (41), Skerritt (42), Crouch et al. (43), and Smith et al. (44) also found a significant reduction in the microtexture and macrotexture of pavement surfaces due to traffic.

Skid resistance has also been shown to vary seasonally. It is typically lower in the spring and summer and higher in the fall and winter if there is no ice on the pavement surface (40, 41, 45). The seasonal variations are mainly caused by environmental factors such as temperature and rainfall. Croney et al. (46) attributed the seasonal changes of skid numbers in Britain to rainfall effects. This study hypothesized that runoff water removes lubricating agents and surface contaminants and increases skid resistance. Therefore, in spring and summer when rainfall in the United Kingdom is low, runoff would be low, resulting in deposition of contaminants on the road surface; skid resistance decreases as deposition of contaminants increases. It was also shown that skid numbers decrease and reach a minimum level after seven days of dry weather, and that the skid numbers increase after rainfall (47).

The seasonal variation in skid resistance can also be attributed to temperature. Oliver (48) studied the effects of seasonal variation on pavement friction in Australia. This study included laboratory-prepared surfaces similar to pavement surfaces with surface texture depth between 0 and 1.5 mm. The friction measurements were conducted using the British Pendulum Tester at temperatures between 7 and 59°C. The study found a good correlation between the friction values and the pavement temperature, given in Equation (4).

$$SRV_t/SRV_{20} = 1 - 0.00525 \times (t - 20) \quad \textbf{(4)}$$

where

t = prepared pavement surface temperature (°C),

SRV_t = the skid resistance value obtained at temperature t (°C), and

SRV_{20} = the skid resistance value obtained at 20°C.

Bazlamit et al. (45) also evaluated the temperature effects on the friction values. Friction measurements were conducted at 10 sites throughout the state of Ohio using the British Pendulum Tester at five temperatures: 0, 10, 20, 30, and 40°C. This study also found strong correlations between the pavement temperature and friction values, shown in Equation (5).

$$BPN_T = 125.2508 - 0.232T \quad \textbf{(5)}$$

where T is the temperature in Kelvin, and BPN_T is the value of British Pendulum Number at temperature T.

Luo (39) also showed a reduction in skid resistance with increasing temperature. This study explained that the reason for the reduction in skid resistance was the reduction in microtexture. At higher temperatures, asphalt binder is softer and may cover more of the aggregate, reducing the microtexture.

The lower friction values found during spring and summer by researchers previously cited may also be due to higher temperatures. However, the effects of rainfall and of temperature on the seasonal skid resistance variation cannot be distinguished from each other.

The presence of surface distresses may also affect the friction values. Bleeding of asphalt and rutting due to traffic compaction would further embed the aggregates in the asphalt and prevent them from contacting the vehicle tire, hence reducing the microtexture and the skid resistance.

Aggregate gradation is also important for the skid resistance of pavements. It may affect microtexture and macrotexture differently. Fwa (49) investigated the effects of aggregate gap (spacing) on the frictional properties of laboratory-prepared specimens using the British Pendulum Tester. The gaps between aggregates ranged between 2 and 10 mm in the study. The 2-mm gap represented that of a dense-graded mix, and the 10-mm gap represented a porous (open-graded) asphalt mix. The study concluded that the larger the spacing between aggregates, the lower the friction value. This finding indicates that open-graded mixes would have lower friction values than dense-graded ones. Some studies conducted in Europe also found that open-graded mixes have lower microtexture (friction numbers) compared to most conventional mixes used in each country (50, 51). However, increasing the aggregate spacing would increase the macrotexture.

Stroup-Gardiner (52) evaluated the effects of aggregate gradation on macrotexture. The estimated texture depth (ETD), which is an estimate of mean texture depth, was obtained using the MPD values from the ROSAN laser measurement. This study found a good correlation between the ETD and the maximum size of the aggregate, the percentage passing the 4.75-mm sieve, the coefficient of curvature (C_c), and the coefficient of uniformity (C_u). Increasing the maximum aggregate size and C_u increased the texture value, while increasing the percentage passing the 4.75-mm sieve (finer gradation) and C_c values reduced the texture value. Flintsch (53) measured the MPD of different wearing courses, including stone

mastic asphalt (SMA), Superpave mixtures, and open-graded friction courses, in Virginia with a laser inertial road profiler. The MPD was found to be strongly correlated with NMAS and the voids in the mineral aggregate (VMA). An increase in the NMAS or VMA value increased the macrotexture (MPD) value.

Earlier studies have shown that the microtexture is affected by climate and traffic, and that the macrotexture is affected by traffic and gradation properties. However, research is still needed to identify the effects of surface distresses and mix type and the interaction of mix type with traffic and climatic variables on the microtexture as well as the effects of distresses and climatic factors on the macrotexture.

2.3 Roughness (Unevenness) and Ride Quality

Roughness (unevenness) is the deviation of a road surface from a true planar surface with dimensions between 0.5 and 50 m. It is usually regarded as the most important component of pavement performance because it directly affects the comfort of road users and therefore is the most evident performance measure to the user. Roughness is related to ride quality and safety and is measured by a standardized scaled parameter called the International Roughness Index (IRI). IRI is a worldwide accepted measurement of pavement roughness.

IRI is calculated from a mathematical model that simulates the response of a vehicle's suspension to roughness. The model is called a quarter-car simulation as it represents the roughness response of one wheel of a typical passenger vehicle to the longitudinal profile. IRI is the measured vehicle chassis' vertical movements per distance traveled in the simulation of the quarter-car on the pavement and is reported in inches per mile or millimeters per meter. On a rough pavement, the vehicle's vertical movements would be high. IRI is calculated from pavement profile measurements. According to the FHWA, pavements with an IRI less than or equal to 170 inches per mile (2.65 m/km) are classified as acceptable, and pavements with an IRI less than or equal to 95 inches per mile (1.28 m/km) are classified as good (16). Caltrans takes action when the IRI of the pavement exceeds 224 inches per mile (3.6 m/km) for asphalt-surfaced roads. A roughness scale based on age and use of pavements is shown in Figure 5.

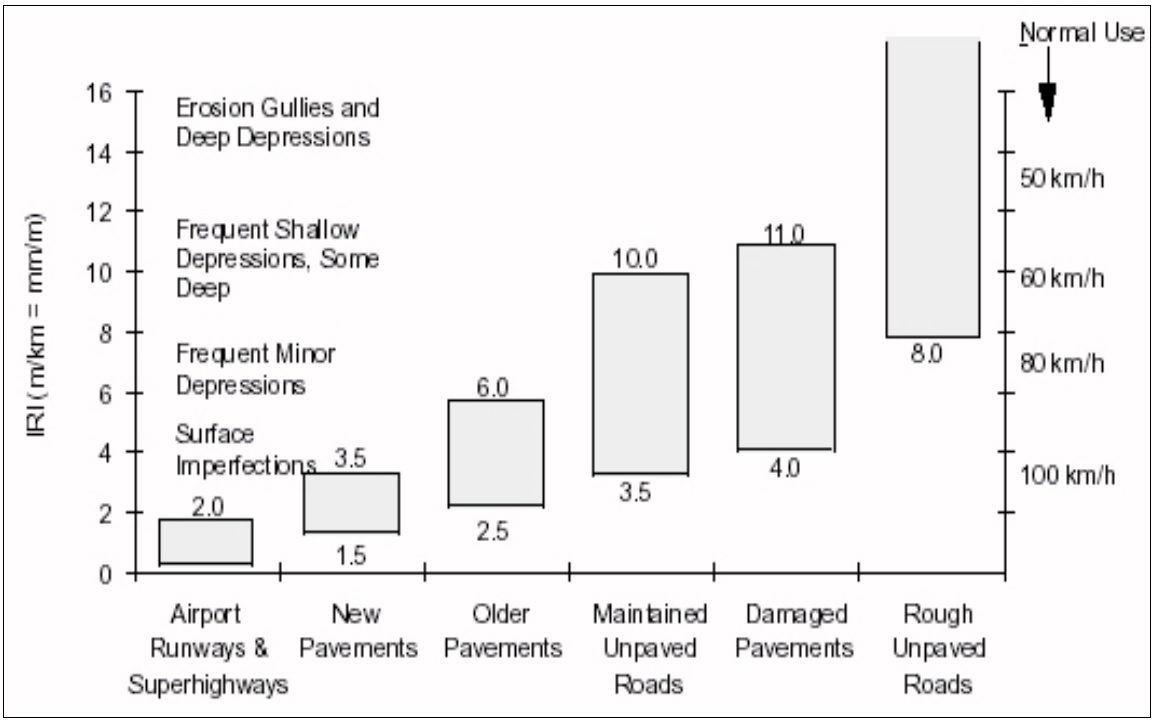

Figure 5: IRI roughness scale (WAPA [54] from Sayers, 1986 [55]).

IRI is affected by traffic, climate, and pavement characteristics. Also, surface distresses affect the pavement roughness (the more cracks or disintegration, the rougher the pavement will be).

Lee et al. (56) investigated the factors affecting as-built roughness of asphalt pavements. It was found that IRI increases with decreasing pavement thickness and the length of pavement (lane-km) included in the construction project, while the pavement base type under the asphalt overlay—old asphalt concrete (AC), old portland cement concrete (PCC), pulverized, rubblized, or other type—does not affect as-built IRI. It is not clear why as-built IRI would increase with increasing project length, yet not be affected by the base type. It was also found that the contractor's prior history of constructing smooth or rough pavements was a significant factor.

The FHWA Long-Term Pavement Performance (LTTP) study (57) investigated the factors affecting the increase in IRI of asphalt overlays (AC on AC and AC on PCC). For AC overlays on AC pavements, this study found that the sections that had higher IRI prior to placement of the overlay generally showed a higher rate of increase in IRI. An overlay placed on a pavement with a higher structural number was found to show a lower rate of increase in IRI. Sections with low AC bulk specific gravities, low air-void content, and a high number of freeze-thaw cycles showed a higher rate of increase in IRI. The mean air temperature was not found to affect the IRI change, while the occurrence of rutting was found to lead to a greater increase in roughness. Sections with greater cumulative traffic, a higher

moisture content of the subgrade, a higher percentage of the material passing the No. 200 sieve in the subgrade, and a higher plasticity index of the subgrade were found to show a greater increase in IRI.

For AC overlays placed on PCC pavements, the same study found that change in the IRI was not affected by the IRI before overlay placement or by the environmental parameters. The factors that influence the roughness development of PCC pavement were found to control the roughness development in the AC overlay.

In another study using the LTTP data for flexible and rigid pavements, Mantravadi (58) concluded that an increased number of days per year with temperatures above 32°C decreased the IRI values. The amount of traffic loading was also found to contribute to the roughness of flexible pavement (59, 60, 61).

Earlier studies have shown that the change in IRI is affected by traffic, climatic conditions, constructed project length, subgrade properties, surface layer thickness, and distresses on the pavement surface. However, none of the studies compared the IRI progression for open-graded versus dense-graded mixes and rubberized versus nonrubberized mixes. Therefore, the IRI development should be evaluated for different mix types.

2.4 Pavement Distresses

The evaluation of distresses is important in determining how long different mixes last for use when performing life-cycle cost analysis comparisons. Common distresses of open-graded mixes that have been observed or reported in the literature are bleeding, rutting, raveling, transverse cracking, fatigue cracking, and reflection cracking (17).

2.4.1 Bleeding

Bleeding occurs when asphalt fills the air voids in the mix during hot weather and then expands onto the surface of the pavement, creating a shiny reflective surface. Bleeding is caused by excessive asphalt binder in a mix and/or excessive densification of the mix under traffic. The presence of bleeding on the pavement surface may reduce friction by causing loss of contact of aggregates with the tire when wet.

2.4.2 Rutting

There are two types of rutting: asphalt mix rutting and rutting of soil layers. Asphalt mix rutting is a longitudinal surface depression in the wheelpath due to the shear deformation and densification of the pavement under load. It generally develops at high temperatures when the asphalt binder is softer and under heavy load and high tire pressures. The causes of rutting of the asphalt layers are excessive asphalt

content, excessive fine aggregate content, and high percentages of natural, rounded aggregate particles. Rutting of soil layers occurs as a result of inadequate pavement structure. In the case of rutting of soil layers, the asphalt mix does not show rutting; however, the underlying soil shows wheelpath depressions due to traffic load (18).

Rutting of the asphalt mix is greatly affected by the asphalt binder type. A study by Gokhale et al. (62) found that modified (SBS) mixes are less likely to show rutting compared to unmodified mixes. Note that polymer-modified and conventional asphalt binders in open-graded and dense-graded mixes could not be separated based on construction records or field core examination for this study because either a large proportion of the field records do not contain this information or field personnel indicated that the information in the records was not reliable.

2.4.3 Transverse Cracking

Transverse cracks appear at right angles to the centerline of the road and generally at regular intervals. They primarily result from the reflection of cracks or joints from the underlying pavement or the contraction and shrinkage of the surface layer due to cold temperatures and aging of the asphalt binder.

The presence of transverse cracks on the pavement may result in rough ride, increased noise levels, and stripping in the cracking zones. Cracks on the surface may allow water into the pavement structure, which may result in reduced subbase/subgrade strength, pumping of unbound fines from the underlying material, and increased rate of stripping in the asphalt concrete. As the cracks propagate, they may create an uneven surface and cause a bumpy and noisy ride.

2.4.3.1 Transverse Cracking Caused by Thermal Stresses

Fromm and Phang (63) investigated the effects of mix properties on the transverse cracking performance of 33 pavement sections in Ontario, Canada. Thermal cracking increases as the viscosity ratio (the ratio of viscosity at 15.6°C to viscosity at 135°C), freezing index, critical temperature (temperature at which the viscous flow under creep loading in one hour equals the temperature shrinkage in one hour), and stripping rate increase. Fromm and Phang believe that at temperatures higher than the critical temperature, the viscous flow of the material will be high and would therefore relieve the stresses developed due to thermal contraction. The stripping rate was used as an indicator of the bond strength between the asphalt and aggregate, which in part governs the tensile strength of the asphalt mix, where low stripping would correspond to high tensile strength. Increasing air-void content, recovered asphalt penetration [in decimillimeters (dmm); 1 dmm = 0.1 mm] at 25°C, asphalt percentage by weight,

percentage passing a 0.075-mm sieve for granular base, and percentage passing a 0.075-mm sieve for asphalt concrete were found to reduce the transverse cracking.

Haas et al. (63) conducted a similar study investigating the pavement characteristics affecting the spacing of transverse cracking. Data was collected for 26 airport pavements throughout Canada. The study found that transverse crack spacing increases as asphalt concrete thickness, minimum temperature experienced by the pavement, and penetration of the asphalt increases; and the spacing decreases as the coefficient of thermal contraction increases.

A study conducted by Rauhut (60) found that transverse cracking increases with age for thin overlays (less than 60 mm), but no effect of age was found for thick overlays. Thicker pavements were also found to be more resistant to transverse cracking than were thinner ones. Lytton et al. (65) found that as the asphalt thickness increases, the transverse cracking becomes more dependent on the binder and mix design properties and less dependent on age and thickness. Pavement age was found to be the strongest contributor to the occurrence of transverse cracking (59), which contradicts the findings of Rauhut for mixes with thicknesses over 60 mm.

2.4.3.2 Transverse Cracking Caused by Reflection Cracking

Reflection cracking is the cracking of asphalt concrete overlay when a crack or joint that is already present in the underlying pavement (asphalt or portland cement concrete) is reflected in the new pavement surface. When the overlay is fully bonded with the underlying layer, any movement in the underlying layer due to temperature or traffic induces concentrated tensile stresses directly above the crack or joint, resulting in cracks reflected through the new layer. Reflection cracking is more common when a rigid pavement is overlaid with a flexible layer, due to the presence of joints. The open-graded and gap-graded mixes used in California are usually placed as rehabilitation or maintenance overlays on distressed pavements. Since all mixes included in this study were placed as overlays, reflection cracking of transverse cracks is a major distress consideration for these mixes.

2.4.4 Raveling

Raveling is the roughening of the asphalt surface texture due to the wearing away of aggregates from the pavement surface. The bond between the aggregate particles and asphalt is lost, and the asphalt wearing course disintegrates from the top downward. Possible causes of raveling are oxidation and hardening of the binder, thin asphalt binder film or reduction of effective asphalt content as a result of the presence of absorptive aggregates, and high air-void content. Additionally, the presence of water in asphalt when under traffic may result in hydrostatic pressure, which may cause debonding of aggregates from the binder (66).

2.4.5 Fatigue Cracking

In California, fatigue cracking is recognized as the most important distress in asphalt concrete pavements on major state highways (67). Fatigue cracking is primarily caused by repeated wheel loadings over time. Extensive models, both empirical and mechanistic-empirical, have been developed to predict and characterize fatigue cracking in asphalt concrete mixes.

Nearly all the research on fatigue of asphalt layers has focused on DGAC and RAC-G mixes, and very little work has been done on open-graded mixes.

The major factors affecting fatigue cracking of DGAC and RAC-G are asphalt mix properties, traffic loading, and climatic factors. Finn and Epps (68) found that possible causes of fatigue cracking are structural deficiency, excessive air voids, changes in properties of the asphalt over time, aggregate gradation, stripping, and drainage. Among many others, Pell et al. (69), Lister et al. (1987), and Harvey et al. (67) showed that the air-void content and asphalt content have significant effects on the fatigue performance of asphalt concrete. They found that increased asphalt content resulted in increased fatigue life, while increased air-void content reduced fatigue life.

Traffic and temperature indirectly affect fatigue life by controlling the strain and the stiffness of the asphalt layer. Tangella et al. (71) observed several pavement sections and concluded that higher temperatures reduce fatigue life for thick asphalt pavements and increase fatigue life of thin pavements. In general, in terms of fatigue behavior, thick pavements are those thicker than 50 to 125 mm, depending on the subgrade support, truck and traffic load, and tire pressure, according to Tangella. Von Quintus (72) found that age, freezing index, and precipitation are the most important factors affecting fatigue performance using the FHWA LTTP data. Fatigue cracking increases as pavement ages. Pavement sections in a climate with less precipitation but higher freeze indices were found to have more fatigue cracking.

Using pavement condition data from 1983 to 1999 from the Washington State Pavement Management System (PMS), Madanat (73) conducted a study of fatigue initiation in thin asphalt overlays of asphalt pavements. A Cox Model was used to analyze the data. The factors affecting the number of cumulative equivalent single-axle loads (ESALs) to failure, where failure is defined as 5 percent of the wheelpath with any combination of alligator cracking and longitudinal cracking, were evaluated. Existing alligator or longitudinal cracking underneath the surface layer and the interaction of precipitation and freeze-thaw cycles were found to reduce the number of ESALs to cracking. Increasing the thickness of the underlying asphalt concrete pavement layers, thickness of the untreated base, thickness of asphalt concrete-treated base, thickness of portland cement–treated base, average monthly maximum temperature of the hottest month, and average monthly minimum temperature of the coldest month increases the ESALs to cracking.

Wang et al. (74) conducted a similar study on asphalt pavements using the LTTP pavement condition data. Failure was defined as 3.5 percent of the pavement surface cracked, and data was analyzed using a parametric accelerated failure time model. The study found that the expected fatigue failure time increases with increasing thickness of asphalt and concrete bases and decreases with increasing traffic, freeze-thaw cycles, and precipitation.

The variables affecting rutting, bleeding, raveling, and transverse and fatigue cracking have been documented in the literature. However, most studies to date have focused on the mechanisms of transverse and fatigue cracking in gap- and dense-graded mixes. Therefore, the mechanisms that contribute to the initiation and progression of transverse and fatigue cracking in open-graded mixes should be evaluated. The initiation and progression of raveling, rutting, and bleeding should also be evaluated for different mix types under different traffic and climatic conditions.

2.5 Highway Noise

Highway noise arises from vehicles in motion. Primary sources of vehicle noise are as follows:

1. Aerodynamic noise: The noise from turbulent airflow around the vehicle caused by the movement of the vehicle;

2. Power-unit noise: The noise from the engine, exhaust, power train, and cooling system; and

3. Tire/pavement noise: The noise emitted from a rolling tire due to the interaction of the tire with the pavement. Tire/pavement noise is affected by pavement surface characteristics such as texture, roughness, air-void content, thickness, stiffness, and age. It can therefore be influenced by pavement design. Tire/pavement noise is generated through the following mechanisms (12):

a. Impacts and shocks resulting from the contact between the tire tread and road surface. This component of tire noise results from vibrations generated by impcts and deflections when the tread elements first contact and then later break contact with the pavement surface as the tire rotates. As the tread element makes contact with the pavement surface, vibrations are driven radially into the tire. Similarly, as the blocks leave the contact patch at the trailing edge, the tire is released from tension and returns to its undeflected rolling radius. This phenomenon is known as block snap-out and excites both radial and tangential vibration modes in the tire (Bergmann, 1980, as cited in 12). The changing radial deflections when the tire flattens in the contact patch generate additional tangential forces between the tire and the pavement surface. These tangential forces are resisted by the frictional forces between the tire tread and the road surface. When the sliding forces exceed the frictional forces, there is some movement of the tread blocks relative to the pavement surface, which also excites the tangential vibrations.

The generation of vibrations on a rolling tire is dependent on the design of the tire tread, macrotexture, and frictional adhesion between the tire and the pavement surface (75; Kropp, 1992 as cited

in 75; 76). Additionally, Sandberg et al. (75) suggested that stiffer pavements may generate more noise, with bituminous pavements being quieter than concrete pavements. However, Beckenbauer [(2001) as cited in 76] revealed that this was not the case. The noise generated due to the vibrations of the tire tends to occur at frequencies of less than 1,000 Hz (12, 32; 78). This phenomenon occurs because the tire acts as a low-frequency band-pass filter, attenuating the noise radiation at higher frequencies.

b. Aerodynamic processes between the tire and the road surface. Noise is generated by various mechanisms, caused by the movement of air in the cavities of the tread pattern that occurs in the contact patch area. Air pumping is the most important aerodynamic process contributing to tire noise. It is the sudden expelling of air that is trapped in the tread grooves or pavement texture due to the reduced groove volume when the tire makes contact with the road surface, and the sudden suction of air when the tire leaves the contact patch (79). The air-pumping mechanism may cause significant levels of noise in the frequency range above 1,000 Hz when the surface is nonporous and smooth (75, Petersson, 1988, as cited in 12; Kropp, 1992, as cited in 76). The higher texture depth in the pavement also helps dissipate the air trapped in the grooves; therefore, open-graded mixes with higher air-void content and macrotexture would largely prevent air pumping (75).

c. Adhesion mechanisms. These mechanisms are caused by tire vibrations associated with the frictional forces that develop at the contact patch between the tire and the pavement surface (12). The tire flattens at the contact path, causing tangential forces due to the changing radial deflections. These forces are resisted by the friction between the pavement surface and the stiffness of the tire, and the remaining forces are dissipated by the slip of the tread over the pavement surface. Friction between the tread and the pavement has two components: adhesion and hysteresis.

The adhesion component is governed by small roughness characteristics or microtexture of the surface, and the hysteresis component is largely controlled by macrotexture. During relative sliding between the tire and the pavement surface, the adhesion bonds formed between them break apart, with the result that contact is lost and the tire is free to slip across the surface. The noise generated is a combination of the slip of the tread elements as adhesion is lost at the contact patch followed by the development of the hysteresis component of friction as the tread is deformed. This process, known as slip/stick, occurs at the contact patch and excites the tire vibration. Reduction of local friction and higher surface flexibility may help reduce the vibrations generated by slip/stick.

Noise-generation mechanisms are shown in Figure 6.

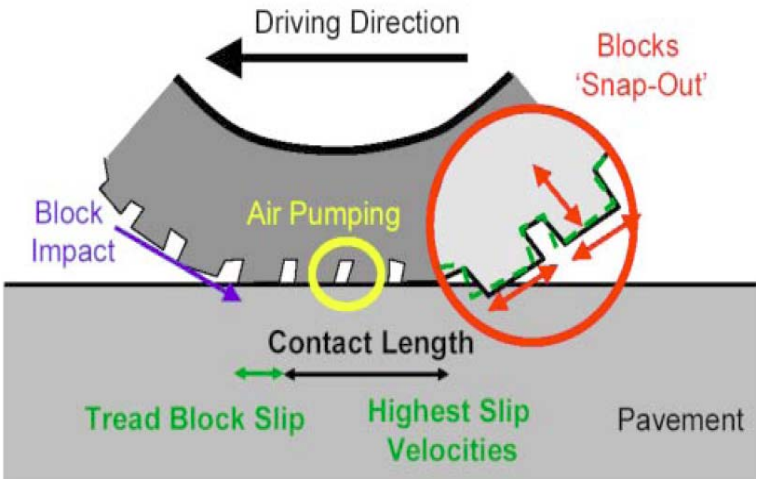

Figure 6: Noise-generation mechanisms (14).

As indicated here, a number of studies have modeled the tire/pavement noise. However, the tire/pavement noise-generation mechanisms depend on the tire and pavement properties and the speed of the vehicle in a complicated way. None of the proposed models were able to explain the noise-generation mechanisms completely; therefore, some parts of the models are based on assumptions. Most of these tire/pavement noise models are theoretical and based on nonporous surfaces. There has been little or no validation of the theoretical models. Since all the research on tire/pavement noise has been conducted in Europe, the models should be validated with experimental data not only for different surfaces but also for the tires and vehicles in the United States, although the basic principles are applicable.

Sound levels are usually given in one-third octave band or octave band frequencies to explain the sources of noise better. The noise at each octave or one-third octave band frequency is summed to give the overall A-weighted noise level. Therefore, a pavement characteristic may not be found to significantly affect the overall A-weighted sound intensity level even though it influences certain one-third octave band frequency levels.

Knowledge of the frequency content of a sound is important because it has been found that people exposed to noise with tonal components are more annoyed than people exposed to other noise (80). Additionally, the absence of an expected tone can decrease the perceived quality of noise (81). The human ear is most sensitive in the frequency range between 1,000 and 3,000 Hz (82). A study by Ishiyama (83) found that annoyance increased as the high-frequency (above 1,000 Hz) component of the noise increased, even though A-weighted equivalent sound exposure levels were the same. Therefore, noise mitigation strategies should focus on attenuating noise levels above 1,000 Hz.

An example of the importance of the frequency content of noise in regard to annoyance can be seen on a freeway segment of Route 85 in Santa Clara (SCl-85) in California. The road was first constructed as PCC using Caltrans standard longitudinal tining. However, due to public complaints about high traffic noise after the opening of the freeway, a short segment of the freeway was grooved and grinded as an experimental test section. The aim of the test section was to evaluate the effect of pavement surface modification on the noise levels. After the surface was subjected to grooving and grinding, the reaction from the community was quite favorable.

To quantify the favorable effect of the surface modification, sound intensity measurements were made comparing the ground pavement to that of the original tining. The overall difference in the noise levels of the two surfaces was only slightly more than 2 dB (A). When the frequency content of the noise levels was evaluated, the largest reductions, more than 4 dB (A), were found in bands around 1,600 Hz. Although there was not a significant improvement in the overall noise levels, the public considered the change positive. Since a 2-dB difference in sound level is barely heard, the noise reduction perceived by the public was attributed to the noise reduction at 1,600 Hz. The frequencies around 1,600 Hz may be responsible for a "sizzle" sound that can be noticeable in the community (84).

Since annoyance is related to the frequency levels rather than the overall A-weighted sound levels, it is also important to know the pavement parameters affecting the sound intensity levels at different frequencies.

2.5.1 Pavement Variables Affecting Noise

As mentioned earlier, the pavement surface has a great influence on traffic noise. Pavement characteristics affecting tire/road noise are explained in this section.

2.5.1.1 Texture

Texture is the deviation of a road surface from a true planar surface with a maximum dimension (wavelength) of 0.5 m (35). Texture can be controlled by aggregate size, aggregate shape, and aggregate gradation. Pavement texture and roughness are shown in Figure 7.

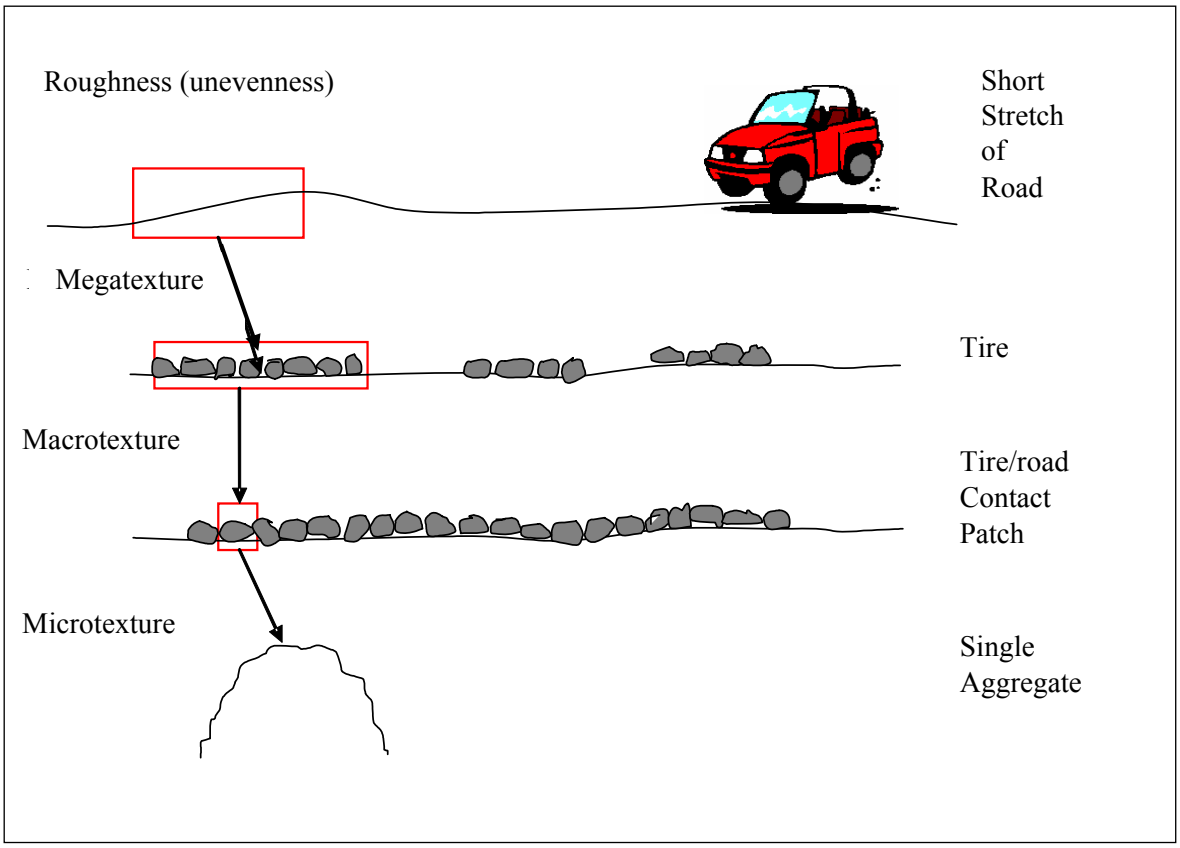

Figure 7: Pavement texture and roughness (unevenness).

Texture is divided into three types:

1. Microtexture: The deviation of a pavement surface from a true planar surface with a maximum dimension of 0.5 mm (35). Microtexture is related to the aggregate properties. Studies conducted on the effect of microtexture on tire/road noise levels have failed to detect any correlation (10, 85).

2. Macrotexture: The deviation of a pavement surface from a true planar surface with a dimension between 0.5 and 50 mm (35). Macrotexture has wavelengths on the order of tread elements. Macrotexture can have both beneficial and adverse effects on the tire/pavement noise. According to Descornet et al. (86), sound pressure levels at low frequencies increase with increasing texture amplitudes for texture wavelengths from 10 to 50 mm, while at high frequencies sound pressure levels decrease with increasing texture amplitudes for texture wavelengths between 0.5 and 10 mm. Based on this finding, quieter pavement surfaces can be created by designing high macrotexture amplitudes in the 0.5- to 10-mm wavelength range and low macrotexture amplitudes in the 10- to 50-mm wavelength range.

3. Megatexture: The deviation of a pavement surface from a true planar surface with a dimension between 50 and 500 mm (10). Megatexture is an unwanted characteristic that is a result of surface deteriorations such as alligator cracking, plucking, or spalling (87).

Megatexture is a major contributor to tire/pavement noise. Increasing megatexture (presence of distresses on the pavement surface) increases the tire/pavement noise; therefore, megatexture should be removed to reduce noise levels (32, 86). This can be achieved by designing and building pavements that are smooth and that remain smooth for long periods after construction, and by maintenance practices that maintain smoothness.

2.5.1.2 Roughness (Unevenness)

Roughness (unevenness) is the deviation of a road surface from a true planar surface with dimensions between 0.5 and 50 m (10). Higher roughness at lower-texture wavelengths (0.5 to 0.8 m) has been found to increase tire/pavement noise (88).

2.5.1.3 Air-Void Content (Porosity)

Mixes with high air-void content (porosity) reduce the generated noise levels. There are two noise reduction mechanisms in pavements with open-graded (porous) surfaces: noise absorption and noise propagation.

1. Noise absorption: The presence of air voids in the surface layer helps dissipate trapped air in the tire's tread grooves. This results in reduced air pumping and therefore reduces noise emission (89). Porosity also gives the pavement surface acoustical absorption properties in which sound waves are dissipated into heat within the voids of the surface layer (10). The acoustical absorption not only reduces the tire noise but also the power-unit noise.

Acoustical properties of porous structures are characterized using either phenomenological or microstructural models. Microstructural models consider that sound propagation occurs in straight air voids and then account for tortuosity of the air voids using shape factors. Phenomenological models consider the porous medium to be a globally compressible fluid where dissipation occurs (90). Microstructural models use the specific air-flow resistance (R_s), porosity, tortuosity or shape factor, and viscous and thermal shape factors, while phenomenological models use only the specific air-flow resistance, porosity, and tortuosity to characterize the porous medium. Berengier (91) showed that phenomenological models are in close agreement with microstructural models for the case of porous pavements. Therefore, phenomenological models were found to provide a simpler description using the specific air-flow resistance, porosity, and tortuosity to predict the acoustical absorption properties of pavements (90).

Specific air-flow resistance is the frictional resistance to flow through the air voids. Increasing specific air-flow resistance reduces the maximum absorption coefficient and tends to flatten the absorption curves.

Thickness has an effect both on the shape of the absorption curve and the frequencies at which the maxima occur. Increasing thickness increases the absorption coefficient and lowers the frequencies where the maxima occur. However, after a certain thickness, called superthickness, is reached, increasing thickness further has no effect on the absorption coefficient. The superthickness depends on other parameters such as porosity, specific air-flow resistance, and shape factor. Berengier et al. (91) reported that for a porous medium with a porosity of 25 percent, shape factor of 3.5, and specific air-flow resistance of 20 rayl/cm, superthickness would be 47 cm. A rayl is one of two units of acoustic impedance. When sound waves pass through any physical substance, the pressure of the waves causes the particles of the substance to move. The sound impedance is the ratio of the sound pressure to the particle velocity it produces. The impedance is one rayl if unit pressure produces unit velocity. In International System (SI) base units, a rayl is kg/(s m^2).

Porosity or air-void content is the ratio of the volume of connected air voids to the total volume of the asphalt mix. For low values of $R_s \times e/2\rho c$ (where ρc is the acoustic impedance), the porosity has no effect on the maximum absorption values and no effect on the frequencies at which the maxima occur. However, higher porosity increases the absorption values between the maximum values. For very large $R_s \times e/2\rho c$ values or at superthicknesses, increasing porosity increases the maximum absorption values, where:

R_s = specific air-flow resistance,

ρc = characteristic air impedance,

c = speed of sound,

ρ = density of air, and

e = thickness (m) of the pavement surface layer.

The shape factor, or tortuosity, takes into account the air paths not following the normal direction. For not-too-high values of $R_s \times e/2\rho c$, the shape factor has almost no influence on the maximum values. An increase in the shape factor narrows the width of the curves and decreases the minimum values of absorption (90).

2. Noise propagation: Noise propagating from a sound source into a free surface attenuates as it travels farther from the source, and the rate of attenuation depends on the shape of the wave front (89).

Road surfaces have a great effect on noise propagation. Figure 8 shows the simple geometry of a source and a receiver above a reflective (dense) flat surface. If the source and receiver are close to the ground, there will be sound reflections from the ground plane coming from an image source located below the surface of the ground. Sound waves emitted from the vehicle will be reflected from the ground,

resulting in an interaction of the reflected wave and the direct wave. For a highly reflective (high-density) surface, the path difference between the reflected and the direct wave would be small, resulting in destructive interference only at higher frequencies, typically greater than 8 kHz (32). However, at lower frequencies, in the range where the human ear is more sensitive, these two waves, direct and reflected, are additive, therefore increasing sound levels at the receiver (89).

Figure 9 shows the noise propagation mechanism when the surface is porous. In this case, the sound waves will be reflected in a different way: some waves will be reflected at the road surface, and some waves will propagate through the porous layer and will be reflected from the underlying impervious surface. With this mechanism, reflected and direct waves may become out of phase, and the phase difference between the direct and reflected rays will often be greater compared to that of dense surfaces (89). The phase difference results in destructive interferences at lower frequencies, typically between 800 and 1,000 Hz, which is the range where most of the acoustic energy generation from traffic is located (32).

Using data collected in Denmark, Sweden, and Belgium, Sandberg et al. (10) conducted a study on the effects on noise reduction of the equivalent thickness of air, defined as the product of the air-void content and the thickness of the surface layer. The study found that the equivalent thickness of the air of the surface layer was able to explain 75 percent of the total variation in noise reduction.

Higher porosity usually means better noise-reducing properties. However, high porosity may cause poor mechanical strength and durability.

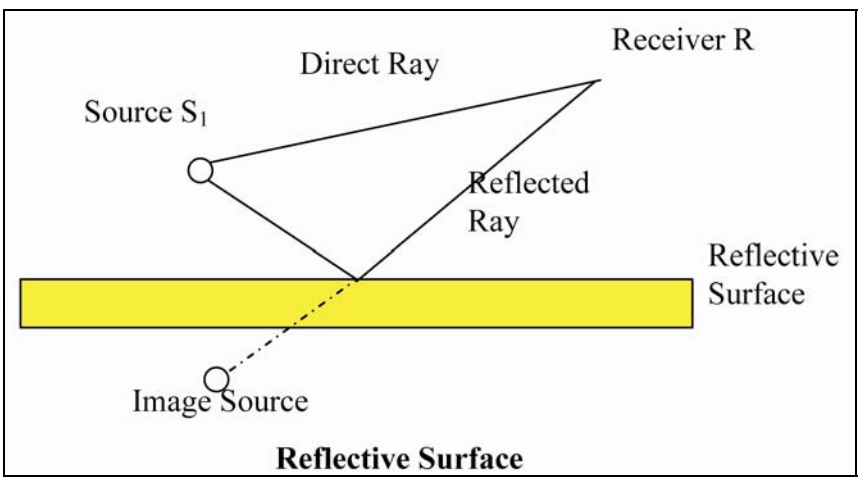

Figure 8: Noise reflection on reflective surface.

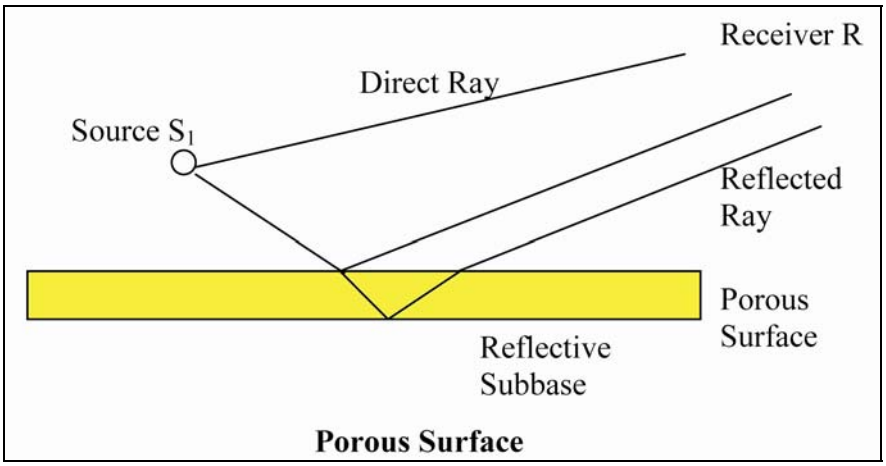

Figure 9: Noise reflection on porous surface.

2.5.1.4 Stiffness

Stiffness is the relationship between stress and strain for asphalt-aggregate mixes. It varies widely and is controlled by the mix, duration of loading (or frequency), and temperature.

Until now, no studies have focused on the effects of stiffness of open-graded mixes on tire/road noise. An experimental type of mix being tested in Japan is a porous elastic surface that uses granulate rubber as its aggregates, to increase elasticity (reduce stiffness). This mix is reported to reduce noise levels by 4 to 5 dB (A) compared to conventional open-graded mixes (92, 93). This finding suggests that the high elasticity (lower stiffness) may reduce tire/road noise levels, which may be measurable for California mixes since the Caltrans rubberized gap-graded mix (RAC-G) typically has a stiffness of 4,000 megapascals (MPa) at 20°C, while dense-graded mix has a stiffness of about 7,500 MPa at the same temperature and air-void content. However, these porous elastic surfaces have air-void content of 35 to 40 percent, with grain size ranging from 1 to 10 mm, while conventional open-graded mixes have an air-void content of 20 percent with a maximum aggregate size of 9 to 13 mm. Since aggregate size and air-void content, which are known to affect noise, were not controlled, the noise reduction of the mixes cannot be explained based on stiffness alone. Further research is needed on the effects of stiffness on tire/noise levels.

2.5.1.5 Age

Noise levels of a pavement change over its service life. The rate of change of noise with time is different for different pavements (10). Age effects are mainly caused by texture and air-void changes and by cracks formed on the surface due to traffic loads and climate effects (10).

Studies have shown that asphalt concrete pavement noise levels increase with increasing age (27, 29, 94, 95). Bendtsen (29) monitored the noise-reduction properties of different types of open-graded

mixes over six years and found that the noise levels increased by 3 to 6 dB (A); one of the mixes lost all noise-reduction properties, resulting in higher noise levels compared to dense-graded asphalt. The loss of noise-reducing properties can be explained by permeability decrease or air-void content reduction at the top part of the surface layer over time as a result of clogging (30, 95).

2.5.1.6 Temperature

Pavement and air temperatures affect noise levels. Studies have found that increasing pavement temperatures decreases noise levels (96, 97). This decrease in noise is due to the reduction in stiffness of tires and pavement with increasing temperature, and hence the reduction of contact stresses. The effect of pavement temperature on tire/pavement noise is less for pavements with high air-void content than for dense-graded ones.

Kuijpers (98) showed that pavement temperature change has a moderate effect on low-frequency sound (below 500 Hz) and a greater influence on higher frequency ranges (500 to 5,000 Hz) for air temperatures between 5 and 35°C (pavement temperatures of approximately 5 and 50°C). Anfosso-Le´de´e (97), however, found that temperature has a great influence on noise levels at frequency ranges below 500 and a low effect at frequency ranges between 500 and 1,250 Hz for pavement temperatures between 5 and 50°C, which contradicts the findings of Kuijpers (98); the findings regarding the effect of pavement temperature on noise levels at higher frequencies were inconclusive in that study.

Sandberg et al. (99) concluded that the only frequencies that are not generally affected by temperature are those at which the spectral peak occurs. The friction coefficient of the pavement surface decreases as the temperatures increases, which can cause a reduction in high-frequency noise levels by affecting the stick/slip mechanisms.

Many studies have looked at pavement surface characteristics as they affect the overall tire/pavement noise levels as well as the frequency content of tire/pavement noise. The studies showed that pavement texture, tire stiffness, and air-void content affect the noise levels, but findings regarding the pavement temperature and stiffness effects were inconclusive. These studies did not provide any information on the other surface characteristics such as IRI, age, distresses, and gradation properties. Additionally, the earlier studies had small sample sizes and measured the correlation of a single parameter with noise levels. The relative influence and interactions of various pavement characteristics on tire/pavement noise has not been well established in the literature. Therefore, studies are needed to evaluate all pavement surface characteristics and their possible effects on overall noise levels as well as one-third octave band frequency noise levels.

Air-void content was shown to be one of the variables that determines the acoustical absorption coefficient. Air-void content was also shown to affect the noise levels.

3 METHODOLOGY

3.1 Site Selection

In this research, field data was collected from two sets of test sections. The first set was drawn from an experiment designed to test the effects of age, traffic, and climate on the asphalt mix types commonly used in California, and the second set consists of the Caltrans environmental noise monitoring sites placed to compare some new mixes with the asphaltic mixes commonly used in California. All the test sections are shown in Figure 10.

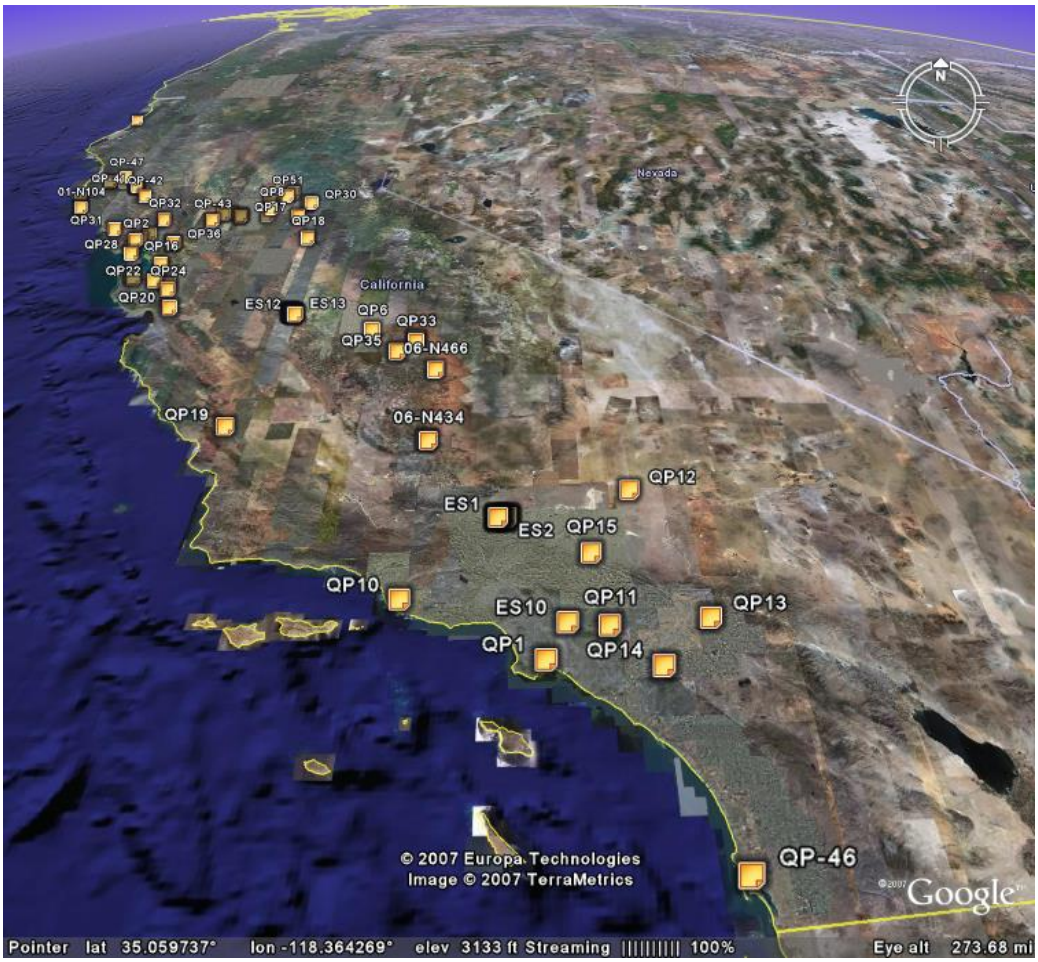

Figure 10: Map of the test sections.

3.1.1 Experimental Design of the Test Sections

The experimental design of the first set of field sections is a full factorial including three asphalt pavement mix types, three age categories, two traffic types, and two rainfall regions. There are some replicates in the factorial. The three mix types include:

- Open-graded asphalt concrete:
    - With conventional and polymer modified binders (OGAC)
    - With rubberized binder (RAC-O), and
    - F-mixes with a conventional or rubberized binder;
- Rubberized gap-graded asphalt concrete (RAC-G); and
- Dense-graded asphalt concrete with conventional and polymer modified binders (DGAC).

The difference between the F-mixes and the OGAC and RAC-O mixes is the nominal maximum aggregate size (NMAS). F-mixes use an NMAS of 19 mm, and OGAC and RAC-O mixes use an NMAS of 9.5 or 12.5 mm.

Age categories are as follows: less than a year old, one to four years old, and four to eight years old.

In reading the rest of this report, remember that a fundamental assumption of the experimental design is that pavements in different sections with different ages can be pooled together to obtain an indication of the effects of time and traffic on their performance properties. This assumption is clearly not completely valid because differences in construction, mix components, underlying structure, and other variables influence performance. However, this project was initiated and completed to obtain preliminary information for Caltrans using this assumption. These results were obtained at far less expense than would be required to build the number of test sections included in this study in one or two years, and they were obtained in a few years as opposed to the eight years that would be needed to monitor specially built sections.

Traffic type, based on Caltrans 2004 annual average daily traffic (AADT) data for highways and freeways (100), is categorized as high if the AADT (two way) is greater than 32,000 vehicles per day and as low otherwise. Traffic speed was considered in the original planning for the experimental design, but investigation showed that traffic speed was generally highway speeds for most sections, but highly variable depending on the time of day for other sections. Several potential variables combining traffic volume and traffic speed distributions were considered but were ultimately not used in the final experimental design because of their complexity and because of uncertainty as to their actual values considering the wide variability of traffic speeds.

Rainfall is based on annual average rainfall in California from 1960 to 1990, obtained from the Climate Database for Integrated Model (CDIM) software (101). The rainfall is categorized as high if average annual rainfall is greater than 620 mm (24.4 inches) and as low otherwise.

The selected test sections and their locations, IDs, ages, average annual daily traffic in the coring lane (AADTCL), and average annual rainfall are given in Table 4. More detailed information for all

sections is included in databases available from UCPRC. The AADT and average annual rainfall were calculated as the average over the lifetime of each individual overlay. The initial selection of each test section was based on annual rainfall over 30 years (1960 to 1990). Therefore, in some cases the rainfall data for an overlay from the time of construction falls somewhat outside the original selection categories. This is all right because rainfall was not used as a class variable, and the original selection categories were intended to obtain as balanced a factorial as possible.

The F-mixes were placed only in low-trafficked areas so traffic levels could not be evaluated for these sections. In addition, the ages of some sections do not fit the cell in the factorial they were intended to fill, because of the difference between the actual construction date and the as-built construction date available in documents when the experiment was designed. The ages of the sections were confirmed by checking the maintenance history in the Caltrans Pavement Management System (PMS) data. In the analysis, the environmental test sections were evaluated with the experimental design sections where they fit the cell in the factorial.

The mixes evaluated in this study—open-graded asphalt concrete (OGAC and RAC-O), gap-graded rubberized asphalt concrete (RAC-G), and dense-graded asphalt concrete (DGAC) mixes—are the most common three materials used for overlays in California. Open-, gap-, and dense-graded mix types are also used in other states as well as in Europe. However, the mix designs of these mixes vary for each state and each country. Rubber inclusion is not as common in other states and in other countries as it is in California. On average, $45,390 per lane-mile was spent on maintenance applications of rubberized (RAC-O and RAC-G) asphalt mixes annually between 2000 and 2004; this amount was $35,320 per lane-mile for OGAC mixes and $32,560 per lane-mile for DGAC mixes. The total maintenance treatment applied between 2000 and 2004 was 511 lane-miles for OGAC mixes, 123 lane-miles for rubberized (RAC-O and RAC-G) mixes, and 601 lane-miles for DGAC mixes. Most of the mixes evaluated in this study are thin maintenance overlays that do not provide any additional structural support.

Dense-graded mixtures (DGAC) have continuous aggregate gradations sized from the largest to the smallest aggregate in the system. Normally, AR-4000 and 8000 grades are used as binders; however, performance-based polymer-modified asphalt (PBA-6) can also be used if thermal cracking is expected to occur. In this study, dense-graded mixes with polymer-modified binder could not be distinguished from those mixes with conventional binders because the mix designs used in each test section were not available. Therefore, modified and unmodified DGAC mixes were evaluated together. Asphalt rubber has not usually been used in dense-graded mixes because it was originally developed as a thin overlay material for reflective cracking, and gap-graded mixes allow higher binder contents, which aids reflective cracking resistance. DGAC mixes have an NMAS of 12.5 or 19 mm. A new (less than one year old) DGAC mix is shown in Figure 11.

Open-graded mix is a wearing course that includes aggregate with relatively uniform grading. It is normally used as a sacrificial course over DGAC pavement in areas with heavy traffic volumes and moderate to heavy rainfall. However, in some projects rubberized open-graded mixes (RAC-O) were placed in a relatively thin layer on top of portland cement concrete (PCC) pavements. Open-graded mixes are used to extract water as well as to renew functional performance, such as ride quality and friction, of the existing pavement surfaces. Modified binders such as asphalt rubber (RAC-O) or PBA-6a or PBA-6b may be used to address different environmental and traffic conditions. Since the mix designs of selected open-graded mixes could not be obtained because they were not available or because field personnel indicated that there may have been changes in binder type during construction that were not included in the as-built records, all polymer mixes (PBA binder) were evaluated as conventional open-graded mixes (OGAC). Open-graded mixes are considered to add little or no structural benefit to the pavement. Usually, they have an NMAS of 12.5 mm and are placed in thin layers of about 30 mm (0.1 foot). For lower thicknesses, the 9.5-mm NMAS mix is specified. The design air-void content of open-graded mixes ranges from 18 to 20 percent. A five-year-old OGAC mix is shown in Figure 12, and a five-year-old RAC-O mix is shown in Figure 13.

In areas where the 12.5-mm NMAS open-graded mix is prone to clogging, a special mix called F-mix with a 25-mm maximum aggregate size has been used experimentally. This material follows the Oregon DOT F-mix specification and is used on the north coast of California, which has a climate similar to that of Oregon. Some of the F-mix sections placed in California have rubberized asphalt binder, which was not used in Oregon with the same gradations. F-mix placed in California has a minimum lift thickness of 50 mm (0.17 foot) and a maximum lift thickness of 75 mm (0.25 foot). A new (less than one year old) RAC-O F-mix is shown in Figure 14.

RAC-G mix is the most commonly used asphalt rubber product in California. The gap (missing fraction) in the mix is used to accommodate the asphalt rubber binder, which increases the stone-to-stone contact. RAC-G mixes are used to increase resistance to reflective cracking and rutting, and the mixes provide good surface friction due to the gapped aggregate grading. RAC-G overlays may also be used as a structural layer in the pavement. The thickness of RAC-G overlays depends on the structural requirements. For designs intended to resist cracking, the thickness of the RAC-G overlay is usually half the thickness that would have been required if a DGAC mix were used instead. RAC-G is placed in a minimum lift thickness of 30 mm and a maximum lift thickness of 60 mm with an NMAS of 12.5 or 19 mm. A five-year-old RAC-G mix is shown in Figure 15.

Figure 16 and Figure 17 show the aggregate gradations of different mix types with NMAS values of 12.5 and 19 mm, respectively. Figure 17 shows the gradations for RAC-G and DGAC mixes as there are no open-graded mixes with an NMAS of 19 mm. The sieve sizes are shown in logarithmic scale, and

the percent passing rate shows the average of maximum and minimum specifications for each sieve size. The data shows that dense-graded mixes are well graded with aggregates from all sizes, gap-graded mixes lack midsize aggregates, and open-graded mixes have only a small percentage of small-size aggregate particles.

Table 4: Experimental Design of the Selected Test Sections

Mix Type	Age	Rainfall Category	Traffic Volume (AADT)	DIST/CTY/RTE/PM	Site ID	Actual Age	AADT on the Coring Lane	Rainfall Since Construction (mm)
Open-Graded Asphalt Concrete (OGAC) (conventional and polymer modified)	Less than 1 year old	High	High	03-PLA-80-1.4/2.6	QP-44	<1	19,250	1,002
			Low	No sections found to fit this cell		-	-	-
		Low	High	03-Yol-80-0.0/0.4	QP-45	<1	20,833	867
			Low	05-SCR-152-7.6/8.0	QP-20	<1	3,050	1,214
	1–4 years old	High	High	04-Mrn-101-0.0/2.5	QP-28	4	13,625	758
			Low	04-Son-121-3.4/7.3	QP-4	4	8,230	760
		Low	High	04-SCl-237-R3.8/7.10	QP-23	5	15,639	407
			Low	08-SBd-38-S0.0/R5.0	QP-13	5	4,733	253
	5–8 years old	High	High	04-Mrn-37-12.1/14.4	QP-3	5	8,482	436
			Low	01-MEN-1-0.1/15.2	01-N103, 01-N104, 01-N105	5	1,450	968
		Low	High	04-SCl-237-R1.0/2.3	QP-22	8	15,148	414
			Low	03-Sac-16-6.9/20.7	QP-29	8	6,367	483

* Note: More detailed information for all test sections is included in the UCPRC database for this project, available on request.

Table 4: Experimental Design of the Selected Test Sections *(continued)*

Mix Type	Age	Rainfall Category	Traffic Volume (AADT)	DIST/CTY/RTE/PM	Site ID	Actual Age	AADT on the Coring Lane	Rainfall Since Construction (mm)
Rubberized Open-Graded Asphalt Concrete (RAC-O)	Less than 1 year old	High	High	03-Pla-80-14.3/33.3	QP-51	<1	14,167	834
			Low	01-MEN-20-R37.9/43.0	QP-41	<1	5,200	2,099
				01-LAK-29-R37.3/R37.6	QP-42	<1	5,850	1,093
		Low	High	06-TUL-99-42.0/47.0	QP-35	<1	10,400	402
			Low	06-TUL-63-19.8/R30.1	QP-34	<1	3,325	442
	1–4 years old	High	High	03-Sac-50-16.10/17.30	QP-8	5	17,694	523
			Low	10-Ama-49-14.7/17.6	QP-17	3	4,060	876
		Low	High	07-LA-710-6.8/9.7	QP-1	3	19,208	417
				04-CC-680-23.9/24.9	QP-36	3	17,107	507
			Low	06-Tul-65-21/29	06-N466, 06-N467, 06-N468	3	4,919	293
	5–8 years old	High	High	No sections found to fit this cell	-	-	-	-
			Low	04-Nap-128-5.1/7.4	QP-32	8	1,353	886
		Low	High	04-SCl-85-1.9/4.7	QP-24	8	16,986	496
			Low	08-SBD-58-R0.0/5.3	QP-12	5	6,497	183

Table 4: Experimental Design of the Selected Test Sections *(continued)*

Mix Type	Age	Rainfall Category	Traffic Volume (AADT)	DIST/CTY/RTE/PM	Site ID	Actual Age	AADT on the Coring Lane	Rainfall Since Construction (mm)
Rubberized Gap-Graded Asphalt Concrete (RAC-G)	Less than 1 year old	High	High	No sections found to fit this cell	-	-	-	-
			Low	01-MEN-20-R37.9/43.0	QP-39	<1	5,200	2,105
		Low	High	04-SCl-280-R0.0/R2.7	QP-26	<1	25,667	582
			Low	06-TUL-63-19.8/R30.1	QP-33	<1	4,800	442
	1–4 years old	High	High	04-Mrn-101-18.9/23.1	QP-2	4	2,100	535
			Low	04-Son-1-0.0/8.4	QP-31	5	2,250	956
		Low	High	08-Riv-15-33.8/38.4	QP-14	5	19,528	252
			Low	05-SLO-46-R10.8/R22.0	QP-19	4.5	3,233	405
	5–8 years old	High	High	04-Mrn-101-2.5/8.5	QP-5	9	20,925	270
			Low	10-Cal-4-0/18.8	QP-18	6	2,211	880
		Low	High	11-SD-8-0.8/1.9	QP-46	6	26,607	321
			Low	07-Ven-34-4.3/6.3	QP-10	5	8,007	395

Table 4: Experimental Design of the Selected Test Sections *(continued)*

Mix Type	Age	Rainfall Category	Traffic Volume (AADT)	DIST/CTY/RTE/PM	Site ID	Actual Age	AADT on the Coring Lane	Rainfall Since Construction (mm)
Dense-Graded Asphalt Concrete (DGAC)	Less than 1 year old	High	High	03-Pla-80-14.3/33.3	QP-27	<1	8,333	298
			Low	01-MEN-20-R37.9/43.0	QP-40	<1	5,200	2,105
		Low	High	06-FRE-99-10.7/15.9	QP-6	<1	15,500	493
			Low	07-LA-138-60.2/61.6	QP-15	<1	7,750	247
	1–4 years old	High	High	03-ED-50-17.3/18.3	QP-21	3	12,969	1,431
			Low	03-ED-50-18.5/20.3	QP-30	4	6,385	1,137
		Low	High	06-KER-99 29.5/31.0	QP-7	5	10,417	158
			Low	04-SOL-113-0.1/18.0	QP-43	1	2,750	513
	5–8 years old	High	High	04-SM-280-9.6/10.8	QP-9	5	10,986	531
			Low	01-Men-1-20.8/38.7	01-N114	7	813	954
					01-N121	7	581	954
		Low	High	04-Ala-92-6.6/8.8	QP-16	14	6,744	437
			Low	06-KER-65-R0.0/2.9	06-N434	6	3,107	144
					06-N436	6	4,950	144
				07-LA-60 R25.4/R30.5	QP-11	7	29,818	371
				04-CC-680-23.9/24.9	QP-25	8	18,071	308

Table 4: Experimental Design of the Selected Test Sections *(continued)*

Mix Type		Age	Rainfall Category	Traffic Volume (AADT)	DIST/CTY/RTE/ PM	Site ID	Actual Age	AADT on the Coring Lane	Rainfall Since Construction (mm)
F-mixes	RAC Binder	Less than 1 year old	High	Low	01-Men-101-37.4/38.8	QP-52	1	4,000	1,679
		1–4 years old	High	Low	01-Men-101-50.8/ 51.5	QP-47	3	5,081	1,426
					01-HUM-101-111.1/111.5	QP-50	4	2,130	1,183
	Conventional Binder	58 years old	High	Low	01-Men-20-21.19/21.69	QP-48	8	1,289	1,187
					01-Men-20-22.18 /22.68	QP-49	8	1,289	1,187

Figure 11: Dense-graded asphalt concrete (DGAC).

Figure 12: Open-graded asphalt concrete (OGAC).

Figure 13: Rubberized open-graded asphalt concrete (RAC-O).

Figure 14: Rubberized open-graded asphalt concrete F-mix (RAC-O F-mix).

Figure 15: Rubberized gap-graded asphalt concrete (RAC-G).

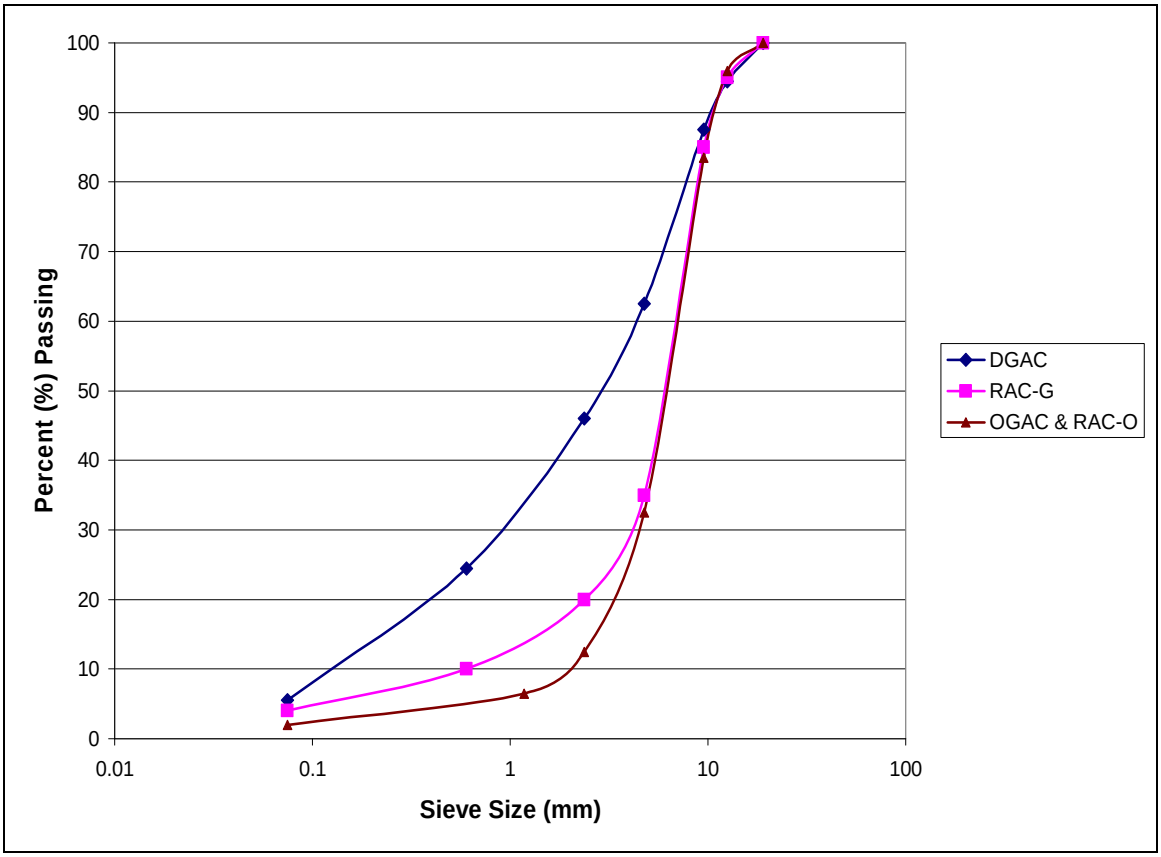

Figure 16: Typical aggregate gradations for different mix types from ignition oven, with 12.5-mm NMAS.

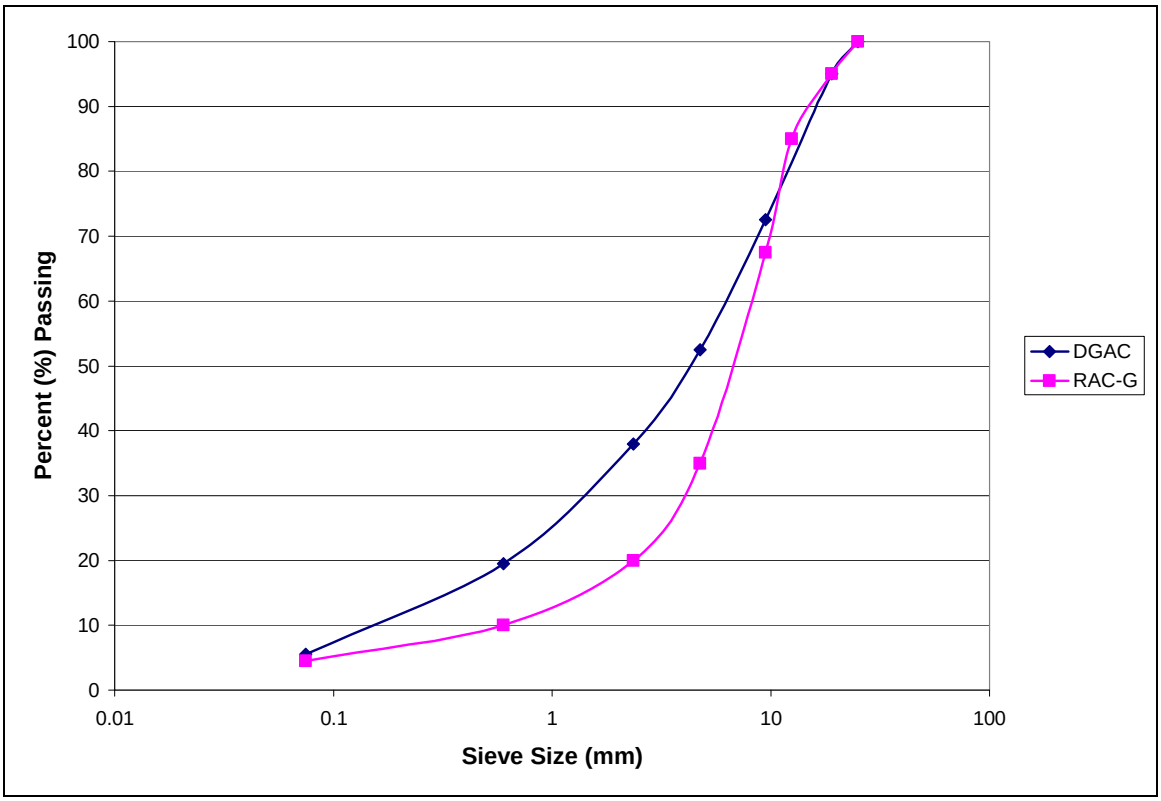

Figure 17: Typical aggregate gradations for different mix types from ignition oven, with 19-mm NMAS.

The second set of sections consists of the California DOT environmental noise monitoring site (ES) sections, where different mix surface types were placed and have been monitored in terms of noise and performance every year. These sections were built to compare the performance of new mixes such as bonded wearing course (BWC), rubber modified asphalt concrete ([RUMAC-GG], dry process, a local-government specification), gap-graded mix with modified binder (Type G-MB), and dense-graded mix with modified binder (Type-D-MB), with the commonly used mixes and evaluate the effect of thickness on pavement performance. The environmental noise monitoring sites are listed in Table 5.

Table 5: Caltrans Environmental Noise Monitoring Site (ES) Sections*

Site Name	Site Location	Mix Types, Design Thicknesses	Construction Date
Los Angeles 138 (LA 138)	07-LA-138/PM 16.0-21.0	OGAC, 75 mm OGAC, 30 mm RAC-O, 30 mm BWC, 30 mm DGAC, 30 mm	Spring 2002
Los Angeles 19 (LA 19)	07-LA-19/ PM 3.4	European gap-graded, 30 mm	May 2005
Yolo 80	03-Yolo-80/PM 2.9-5.8	OGAC, 20 mm	Summer 1998
Fresno 33 (Fre 33)	06-Fre-33/PM 70.9-75.08	RAC-G, 45 mm RAC-G, 90 mm RUMAC-GG, 45 mm RUMAC-GG, 90 mm Type G-MB, 45 mm Type G-MB, 90 mm Type D-MB, 45 mm Type D-MB, 90 mm DGAC, 90 mm	Summer 2004
San Mateo 280 (SM 280)	04-SM-280/PM R0.0-R5.6	RAC-O, 45 mm	Fall 2002
Sacramento 5 (Sac 5)	03-Sac-5/PM 17.2-17.9	OGAC, 30 mm	Summer 2004

* Note: More detailed information for all test sections is included in the UCPRC database for this project, available on request.

- OGAC: Open-graded asphalt concrete
- RAC-O: Rubberized open-graded asphalt concrete
- BWC: Bonded wearing course
- RAC-G: Rubberized gap-graded asphalt concrete (wet process)
- RUMAC-GG: Rubber modified asphalt concrete (dry process, a local-government specification)
- Type D-MB: Dense-graded rubberized asphalt concrete (terminal blend)
- Type G-MB: Gap-graded rubberized asphalt concrete (terminal blend)
- DGAC: Dense-graded asphalt concrete

Since climatic and traffic factors affect pavement performance, data on these was also collected for the environmental test sections. Climate data includes average annual rainfall and temperature, freezing index, freeze-thaw cycles, and degree-days above 30ºC, as shown in Table 6. Traffic data includes average annual daily traffic (AADT) and average annual daily truck traffic (AADTT), as shown in Table 7.

Table 6: Climatic Information for ES Test Sections*

Section Name	Average Annual Temperature(°C)	Number of Freeze-Thaw Cycles	Freezing Index	Total Yearly Precipitation (mm)	Degree-Days Above 30°C
Yolo 80	15.6	7	0	481	194.8
Sacramento 5	16.1	3	0	446	202.1
LA 138	16.2	35	4	197	191.2
Fresno 33	17.7	10	0	210	218.7
San Mateo 280	14.8	12	0	754	182.6
LA 19	18.3	0	0	520	277.8

*Note: More detailed information for all test sections is included in the UCPRC database for this project, available on request.

Table 7: Traffic Volume and Truck Traffic for ES Test Sections*

Section Name	Location	AADT**	AADTT***	Speed Limit (mph)
Yolo 80	03-Yolo-80/PM 2.9-5.8	134,000	8,991	65
Sacramento 5	03-Sac-5/PM 17.2-17.9	122,000	16,116	65
LA 138	07-LA-138/PM 16.0-21.0	4,300	606	55**
Fresno 33	06-Fre-33/PM 70.9-75.08	7,575	1,439	55**
San Mateo 280	04-SM-280/PM R0.0-R5.6	110,000	2,552	65
LA 19	07-LA-19/ PM 3.4	36,500	1,861	45

*Note: More detailed information for all test sections is included in the UCPRC database for this project, available on request.
** AADT is based on the 2005 counts. AADTT is based on the 2004 truck percentage of the AADT.
*** Actual typical speed is higher than the posted limit.

The LA 138 site contains five sections with four different surfacings. All the LA 138 mixes have an NMAS of 12.5 mm. It has OGAC surfacing with different thicknesses to allow observation of the effects of thickness on noise levels and pavement performance. It has section a RAC-O surfacing that has the same thickness as 30-mm OGAC, which allows comparison of performance of RAC-O and OGAC mixes for same thickness. The fifth section is a 30-mm thick bonded wearing course (BWC), which is a gap-graded hot-mix asphalt mix with polymer-modified binder applied over a thick polymer modified asphalt emulsion membrane. BWC is being evaluated as an alternative to open-graded mixes to reduce hydroplaning and spray and splash.

A 30-mm thick DGAC mix was used as a control. OGAC, RAC-O, and BWC mixes were placed on both the eastbound and westbound lanes, and DGAC was place only on the westbound lanes. Data was collected for both the eastbound and westbound lances. Since these test sections are under the same traffic and climate, they allow direct comparison of performance of different mix types and different thicknesses.

All the mixes have an NMAS of 12.5 mm. The LA 138 noise levels were also measured using the pass-by method, used to measure the noise levels next to the highway; this allows comparison of the noise levels measured by the OBSI method and the pass-by method.

The LA 19 section has a mix called a European gap-graded (EU-GG) asphalt mix, which was placed at a 30-mm thickness. This mix is a product of the Colas company and has been used in France. It has air-void content of 12 percent, close to that of open-graded mixes used in California, and an NMAS of 12.5 mm.

The Yolo 80 section has a 20-mm OGAC mix with an NMAS of 9.5 mm as a wearing surface. It is the oldest section among all the environmental noise monitoring sites.

The Fresno 33 test sections include rubberized asphalt concrete sections with three different rubber processes—RAC-G (wet process), rubber modified asphalt concrete (RUMAC-GG, dry process), and gap-graded mix with modified binder (Type G-MB, terminal blend) and dense-graded mix with modified binder (Type D-MB, terminal blend)—with DGAC as a control section. The wet process blends the crumb rubber with the asphalt cement at the plant just before the binder is mixed with the aggregate. The terminal blend is a form of wet process in which the crumb rubber is blended with asphalt binder at an asphalt cement supply terminal. Terminal blend also contains polymers in addition to rubber. The dry process blends the crumb rubber with the aggregate before the binder is incorporated into the mix.

The 19-mm NMAS DGAC control section is 90 mm thick. The 19-mm NMAS rubberized asphalt concrete sections were placed in 45- and 90-mm thicknesses. The objective in placing these test sections was to evaluate the performance of dry- and terminal-process rubber, to compare their performance with wet-process asphalt rubber and dense-graded asphalt concrete under actual field conditions, and to check the effect of the increased thickness of RAC pavements on remedying reflection cracking.

The San Mateo 280 section has a RAC-O mix placed over a PCC pavement. The mix is 45 mm thick with an NMAS of 12.5 mm.

The Sacramento 5 section has RAC-O mix placed over a PCC pavement. This mix was placed in both the northbound and southbound lanes. The mix is 30 mm thick with an NMAS of 12.5 mm.

3.2 Data Collection

The same data collection procedure was to be used on both sets of sections annually over a two-year period. However, in the second year of data collection, no replicates were used in the factorial (one section per cell was chosen from Table 4). Therefore, fewer sections were evaluated in the second year.

The data collection process for each section occurred in two phases: the first during traffic closures and the second at highway speed after the closures. Data types and the specific tests performed

during closures are shown in Table 8. Data collected at highway speed is listed in Table 9. Laboratory tests were conducted on the cores collected from the field; the laboratory tests are listed in Table 10.

Table 8: Data Collection in the Field During Traffic Closures

Type of Data	Specific Test/Sampling	Data Collection Schedule
Condition survey	Caltrans Office of Flexible Pavement Manual of Condition Survey	Annually
Permeability	Developed by NCAT	Annually
Friction (microtexture)	British Pendulum, ASTM E 303	Annually
Cores	100-mm and 150-mm diameter cores	Annually
Air temperature	Thermocouple	During friction testing
Pavement surface temperature	Thermocouple	During friction testing

Table 9: Data Collection at Highway Speed

Type of Data	Specific Test/Sampling	Data Collection Schedule
On-board sound intensity; pavement-tire noise	OBSI	Annually
International Roughness Index (IRI)	Laser Profilometer, ASTM E 1926	Annually
Macrotexture	Laser Profilometer, ASTM E 1845	Annually
Air temperature	Thermocouple	Before and after sound intensity measurements
Pavement surface temperature	Thermocouple	Before and after sound intensity measurements

Table 10: Laboratory Measurements and Tests on Cores Collected in the Field

Type of Data	Specific Test	Data Collection Time
Noise absorption	Impedance Tube (ASTM E 1050-98)	Once (first phase only)
Extent of clogging	Computed Tomography (CT) scan	Once (first phase only)
Thickness of layers of cores	Visual inspection	Annually
Bulk specific gravity	CoreLok®	Annually
Maximum specific gravity (G_{mm})	Caltrans Test Method CT 309	Annually
Air-void content	Using bulk specific gravity and G_{mm}	Annually
Removal of aggregate from binder	Ignition Oven	Once (first phase only)
Aggregate gradation	CT 202	Once (first phase only)

The following sections describe the test methods and sampling procedures used in this project.

3.2.1 Coring

In the first year of this study, 12 cores were taken from each section. Four of these cores were 100 mm in diameter, and the other 8 were 150 mm; 6 of the 12 cores were taken from the wheelpaths, and 6 were taken from between the wheelpaths, which is assumed to be a nontrafficked area. Coring and all other field operations took place within a 150-m segment of road, with 25-m subsegments, as shown in Figure 18. If the section had a thin surface layer, one more core (a thirteenth core) was collected on the wheelpath to provide enough material to obtain the aggregate gradation. One full-depth core was obtained to try to identify all pavement layers. The other cores were not full depth but were taken in such a way as to obtain the first layer (one or more lifts) and about 50 mm of the second layer.

Sound absorption tests, aggregate gradations from the ignition oven, and CT scan measurements were conducted only on cores taken during the first year. The cores collected in the second year were used to obtain air-void content. Therefore, only 6 cores—cores 1 and 2, 5 and 6, and 9 and 10—were taken from each section in the second year. The number of cores taken from each section in the second year was reduced because the maximum theoretical density was determined in the first year; the number also was reduced to reduce the number of people needed (due to cost) and shorten the exposure time to traffic.

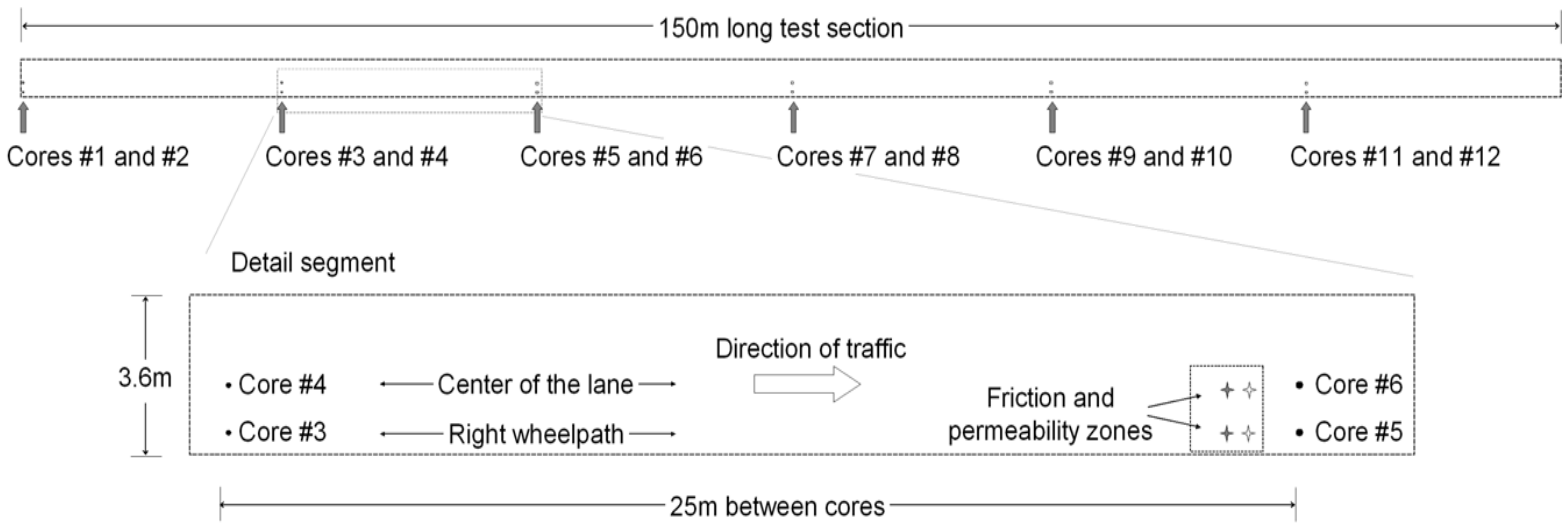

1. Cores 1 through 4 are 100 mm (4 in.); cores 5 through 12 are 50 mm (6 in.).
2. Core thickness includes the upper layer plus about 50 mm of the second layer. One core is full depth.
3. Friction and permeability readings are taken next to each core and numbered according to core label.
4. Condition surveys begin at the first core and extend for 150 m.

Figure 18: Typical field sampling layout. (Note: Core locations in the second year are within 1 m upstream of the first-year locations and core locations 1 and 2, 5 and 6, and 9 and 10.)

3.2.2 Condition Survey

A visual inspection of the pavement surface was performed following the procedures and using the forms described in the *Caltrans Guide to the Investigation and Remediation of Distress in Flexible Pavements* (102), and the results were summarized and mapped to the distress type, severity, and extent definitions in the *Caltrans Pavement Evaluation Manual* used by the Caltrans Pavement Management System (103). The type, severity, and extent of the distresses were recorded in 25-m intervals. Condition surveys were conducted on the entire length of the 150-m section.

3.2.3 Permeability

Permeability was measured using a falling-head permeameter (see Figure 19), a device developed at the National Center for Asphalt Technology (NCAT) (104). The falling-head method measures the amount of water head loss (height of water) through a given sample over time. In this study, permeability measurements in all sections were conducted next to each core, so that 12 permeability readings were obtained in the first year and 6 measurements were obtained in the second year. In some cases, when the permeability was found to be immeasurably low, fewer points were checked within the section. Equation (6) is used to calculate the coefficient of permeability, which represents the rate at which the pavement allows water to pass through it:

$$k = (a \times L/A \times t) \times \ln(h_1/h_2) \qquad \textbf{(6)}$$

where

k = coefficient of permeability,

a = cross-sectional area of stand pipe,

L = estimated effective thickness of sample,

A = cross-sectional area of sample,

t = time elapsed during head loss,

h_1 = water level at upper mark, and

h_2 = water level at lower mark.

Figure 19: Falling-head permeameter.

3.2.4 Friction

Pavement friction was measured with a British Pendulum skid-resistance tester (Figure 20). The British Pendulum is used for laboratory or on-site testing of skid resistance on surfaces, and it measures the skid resistance at low speed (slower than most vehicles using the facility) based on the energy lost due to kinetic friction. The device consists of a small rubber pad at the end of a spring-loaded pendulum. The tester measures frictional resistance between the rubber pad and the point of contact with the pavement. The British Pendulum measurements were taken against traffic and on wet surfaces. They were conducted next to each core (12 measurements in the first phase and 6 measurements in the second phase for each section), the same as in the permeability tests. British Pendulum Number (BPN) measurement at each location consisted of five repetitions.

A minimum BPN of 45 was considered to be acceptable friction based on a criterion discussed in a Caltrans research document believed to have been written in the 1960s (15), which was the only comparison found relating California Test Method 342 (CT Method 342) to other test methods. This criterion is not an official specification of Caltrans and was used only for comparison purposes in this study. Other research is being conducted by UCPRC and others relating the BPN to the Dynamic Friction Tester (DFT), Circular Texture Meter (CTM), and CT Method 342 measures. The BPN was used for this

study because of delays in obtaining DFT and CTM devices at the start of the project, and it continued to be used to maintain consistency across the entire two-year study. It is not the intention of this study to advocate the use of the BPN.

Figure 20: British Pendulum skid-resistance tester.

3.2.5 Air Temperature and Pavement Temperature

Temperatures were measured with thermocouples during British Pendulum testing and before and after the sound intensity testing to correct friction and sound intensity values for temperatures as these values are temperature dependent.

3.2.6 On-Board Sound Intensity

The on-board sound intensity (OBSI) method (105) is a two-channel measurement procedure to evaluate sound intensity levels near the tire and pavement interface. The approach is currently commonly referred to as the OBSI-California method. An OBSI test setup is shown in Figure 21, in which the components can be seen mounted on a passenger vehicle referred to in this report as the sound intensity car.

The sound intensity probe consists of two 25-mm microphones spaced 16 mm apart and preamplifiers in a side-by-side configuration. A foam windscreen is placed over the microphones to reduce wind noise. The probe is positioned 100 mm away from the lane of the tire sidewall and 75 mm above the pavement surface. Signals from the microphones are input to a two-channel, real-time analyzer. The OBSI method requires measurement of sound intensity at two locations of the tire-pavement contact patch (where the tire meets the pavement): one at the tire's leading edge and one at its trailing edge. Three passes of the sound intensity car over the same pavement section are conducted with the probe in each position next to the tire; then the measured results are averaged to obtain the sound intensity for a given pavement. The OBSI test results are obtained for individual frequencies in one-third octave bands (spectral content) to evaluate the sources of sound. Sound intensity measurements are conducted over a five-second recording time, which at 60 mph covers approximately 134 m of the 150-m test section.

Figure 21: On-board sound intensity (OBSI) microphone setup.

3.2.7 International Roughness Index (IRI)

IRI is measured with an inertial laser profilometer mounted on the sound intensity car (Figure 22) according to ASTM E 1926. Two lasers and two accelerometers are housed in an aluminum beam on the rear of the car, and each laser and accelerometer combination measures the road profile in each wheelpath. IRI is automatically calculated by the profilometer from the pavement elevations obtained over the 150-m test section. IRI is reported every 25 m in meters per kilometer (m/km).

Figure 22: Laser profilometer beam.

3.2.8 Macrotexture

The macrotexture parameter is also measured with the laser profilometer, using a 78-kHz laser on the right wheelpath. Macrotexture results are reported in terms of the mean profile depth (MPD) and root mean square (RMS) of the profile; results are reported every 25 m over the 150-m test section.

ASTM and the International Standards Organization (ISO) both describe the MPD calculation as follows (ASTM E 1845; ISO 13473-1):

> The measured profile is divided into segments having a length of 100 mm (4 in.). The slope of each segment is suppressed by subtracting a linear regression of the segment. This also provides a zero mean profile, i.e., the area above the reference height is equal to the area below it. The segment is then divided in half and the height of the highest peak in each half segment is determined. The average of these two peak heights is the mean segment depth. The average value of the mean segment depths for all segments making up the measured profile is reported as the MPD.

A graphical representation of the MPD calculation is presented in Figure 23.

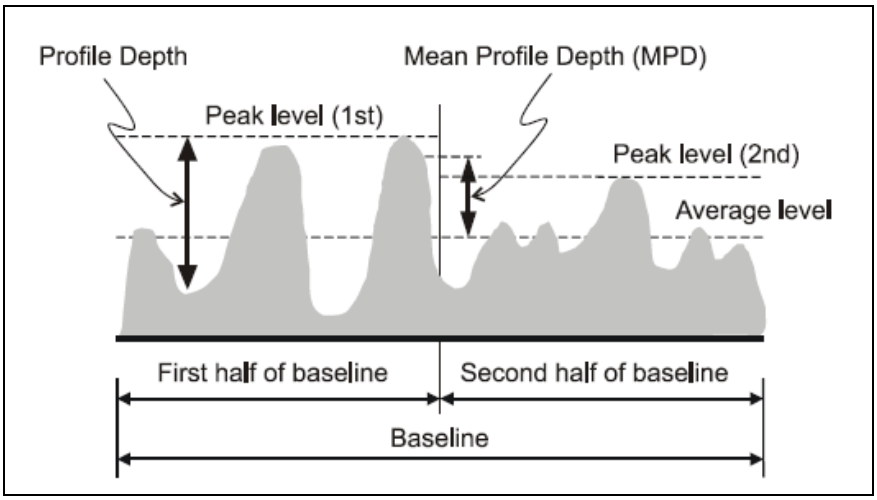

Figure 23: MPD calculations (ASTM E 1845).

3.2.9 Air-Void Content

Air-void content is calculated using the bulk specific gravity value (G_{bulk}) and the theoretical maximum specific gravity value (G_{mm}) obtained from the core samples, according to the formula in Equation (7):

$$\text{Air-void (\% by volume)} = [(G_{mm} - G_{bulk}) \times 100]/G_{mm} \quad \textbf{(7)}$$

The bulk specific gravity of each specimen was measured by the CoreLok method. The G_{mm} was determined for each mix in accordance with the weight-in-water procedure of ASTM D 2041, using the same materials broken from cores that are used to measure bulk specific gravity (Figure 24).

Figure 24: CoreLok seal of specimen.

3.2.10 Aggregate Gradation

Aggregate gradation was obtained by sieve analysis according to ASTM C 136 and ASTM C 117 after the asphalt was removed from the samples by burning in the ignition oven (ASTM D 4125).

3.2.11 Extent of Clogging

The extent of clogging was measured using a Computed Tomography (CT) scan. A CT scan is a nondestructive method of testing for morphological studies that uses X-rays to image the object. This technique can also be used to investigate and evaluate the structure of asphalt concrete cores. It allows comparison of the air-void content distribution within a mix and between different types of asphalt mixes.

X-ray tomography is composed of an X-ray source, an array of detectors, collimators, and an object between the X-ray source and the detector. During tomography, X-rays are produced from an X-ray source, pass through the sample under investigation, and reach an array of detectors as shown in Figure 25. The thickness and shape of the X-rays can be controlled by the collimator. The object under investigation sits on a turntable that can be raised, lowered, or rotated to adjust the sample to the position where an image is required.

This technique is based on the principle that X-rays passing through the material are absorbed based on the material's mass absorption and physical density. CT images of an asphalt sample are the mapping of the attenuation coefficient of its constituents. After the X-ray beams pass through the sample, the intensities of the beams reaching the detector are converted to electronic signals, processed by a computer, and represented by digital images. The materials with higher attenuation coefficients appear brighter in the images. Thus, in an asphalt concrete sample, aggregates, which have higher attenuation coefficients, appear brighter than binder and air voids.

CT scans were performed using cores from sections in the experiment. The testing was performed by A. Ongel at the Swiss Federal Laboratories for Materials Testing and Research (EMPA). Because CT scanning is a time-consuming process, only 20 cores—2 cores each from 10 sections—were analyzed by this method. Asphalt concrete specimens with a 100-mm diameter were scanned. An image size of 600 by 600 mm was used. The resolution of the pictures was 0.2 mm; thus, constituents smaller than 0.4 mm could not be detected. The beam thickness was 0.35 mm, and the spacing between adjacent slices was 0.3 mm, so that there was a 0.05-mm overlap between adjacent slices.

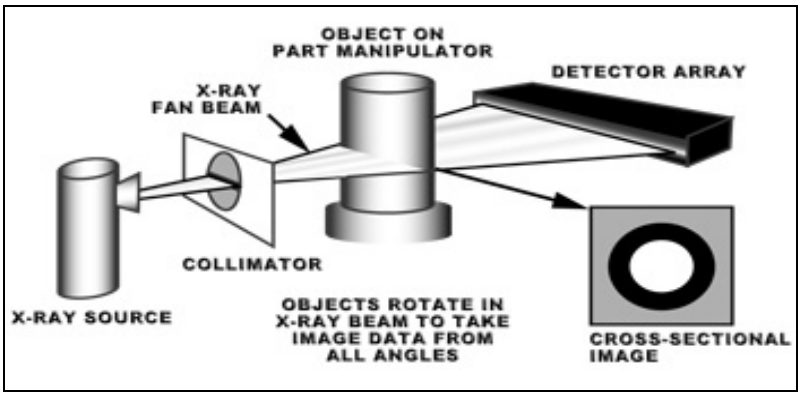

Figure 25: Computed Tomography scanner (106).

3.2.12 Acoustical Absorption

Acoustical absorption measurements were conducted using a Bruel & Kjaer Type 4206A impedance tube with two Bruel & Kjaer Type 4187 one-quarter-inch condenser microphones and Bruel & Kjaer Type 2670 preamplifiers. The impedance tube has a 100-mm internal diameter and an acoustic driver and microphones and a 63.5-mm sample holder. To test the pavement cores, the Bruel & Kjaer 100-mm diameter impedance tube was fitted with custom sample holders ranging in diameter from 101.5 to 104.5 mm to accommodate cores of different diameters and long cores with a wavy vertical profile.

A surgical lubricant (referred to here as acoustic gel) was employed to fill the annulus between the core and the sample holder wall. The surgical gel was employed rather than an oil-based grease, Vaseline petroleum jelly, or cold cream, because the gel could be easily washed off without leaving a residue or dissolving the asphalt, thus preserving the core for further testing. The bottom sections of the cores were considered to be impervious, so the piston seal was not employed for testing. However, the rear surfaces of the cores were sealed with the gel as an added precaution.

The test was conducted according to ASTM E 1050-98 for measuring acoustical absorption with an impedance tube using the two-microphone method. Transfer functions were measured with a Larson Davis Model 2900 analyzer, and data was transferred to a desktop computer with Larson Davis' software. The comma-separated values (CSV) files containing the transfer functions were imported into Excel spreadsheets, from which the transfer functions were copied and pasted into a custom spreadsheet for computation of absorption spectra. Figure 26 shows the impedance tube, microphones, analyzer, and speaker.

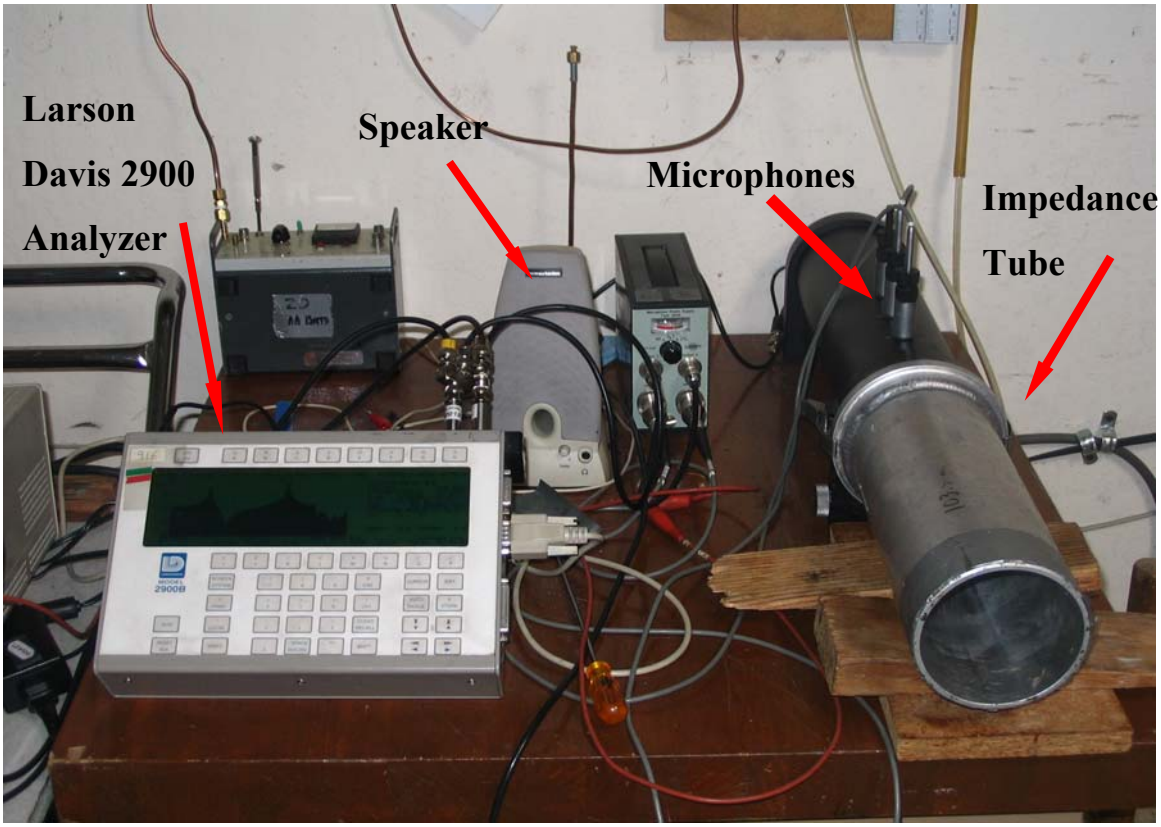

Figure 26: Impedance tube system.

Two transfer functions were obtained for each core: one for the forward microphone orientation and the other for the reverse microphone orientation. These functions were then used to self-calibrate each test result, with the forward transfer function used as the main data sample. Thus, temperature and barometric conditions were consistent during each test, and some minor improvement was obtained for the test results. The impedance tube is accurate only at frequencies below 1,700 Hz due to radial modes that may be present at frequencies above 1,700 Hz. The tube can measure acoustical absorption as low as 200 Hz; frequencies below 200 Hz have phase errors due to the spacing between the two microphones.

4 ANALYSIS OF INDEPENDENT VARIABLES

This chapter describes the independent variables and abbreviations used in the analysis. It also presents the descriptive statistics of the variables and the correlation between independent variables. Skewness and multicollinearity (high degree of linear correlation) between independent variables are two important factors that may affect the inferences in regression analysis. The descriptive statistics help identify the presence of skewness in the data, and the matrix plots help identify the multicollinearity between the independent variables.

4.1 Variable Definitions

Values for variables presented in the section of the report are for the OGAC (including F-mixes), RAC-O (including F-mixes), RAC-G, and DGAC sections. The values do not include the ES sections with other mix types. Values for all sections are included in the database for this project available from the UCPRC on request.

AADTCL: Average annual daily traffic for the coring lane. It is the total volume of traffic divided by the number of lanes.

AADTTCL: Average annual daily truck traffic for the coring lane. It is the total number of trucks multiplied by the lane factor. Lane factors were obtained from a previous UCPRC study of Caltrans weigh-in-motion (WIM) data (Lu, 2002). Since the distribution of AADTTCL is highly skewed, AADTTCL is categorized as high and low. The average AADTTCL for the outer (slow) lane of California highways with WIM stations is 1,750 based on 2004 traffic volumes. In the analysis, high AADTTCL is coded as 1 for sections with truck volumes above 1,750, and low AADTTCL is coded as 0 for sections with truck volumes less than the 1,750.

A.A.Prec: Average annual precipitation (mm). The average annual precipitation (rainfall) is shown in Figure 27 for the different mix types.

ΔPrec: Amount of precipitation between first-year coring and second-year coring.

A.A.Wet Days: Average annual number of wet days.

ΔWet Days: Number of wet days between first-year coring and second-year coring.

A.A.T.C.M.: Average annual minimum temperature (°C) of the coldest month since the construction of the pavement. The distribution of the annual temperature of the coldest month is given in Figure 28.

A.A.T.H.M.: Average annual maximum temperature (°C) of the hottest month (July) since the construction of the pavement. The distribution for each of the four major mix types is shown in Figure 29.

A.A. Max D.T.: Average annual maximum daily temperature (°C).

ΔA.Max D.T.: Average maximum daily temperature (°C) between first-year coring and second-year coring.

A.A.Min D.T.: Average annual minimum daily temperature (°C).

ΔA.Min D.T.: Average minimum daily temperature (°C) between first-year coring and second-year coring.

A.D.D > 30: Annual degree-days above 30°C.

ΔA.D.D > 30: Degree-days above 30°C between first-year coring and second-year coring.

Age: Number of years since construction of the pavement surface at the time of coring by UCPRC.

Age * A.A.Prec: Total amount of precipitation since the construction of the pavement section.

Age * A.A.Wet Days: Total number of wet days since the construction of the section.

Age * A.D.D > 30: Degree-days above 30°C since the construction of the pavement.

Age * N.D. Prec. > 10 mm: Number of days that the precipitation was above 10 mm since the construction of the pavement section.

Age * N.D. T > 25: Number of days that the temperature was above 25°C since the construction of the pavement.

Age * N.D. Prec. > 20 mm: Number of days that the precipitation was above 20 mm since the construction of the pavement section.

Age * N.D. T > 30: Number of days that the temperature was above 30°C since the construction of the pavement.

AV: Air-void content (%). Bulk specific gravity of the cores was measured using the CoreLok method, and the theoretical maximum specific gravity was determined in accordance with ASTM D 2041.

Avg. Daily Temp Diff.: Average daily temperature difference. This is the difference between the maximum and minimum daily temperatures averaged over the age of the pavement (in °C).

BPN: British Pendulum Number (ASTM E 303).

C_c: Coefficient of curvature. $C_c = D_{30}/D_{10} * D_{60}$, where D_{10} is the sieve size through which 10 percent of the aggregate passes (mm), D_{30} is the sieve size through which 30 percent of the aggregate passes (mm), and D_{60} is the sieve size through which 60 percent of the material passes (mm). C_c has not been used as an independent variable. However, it is used with C_u (see the next variable) to determine whether the aggregates are well or poorly graded.

C_u: Coefficient of uniformity. $C_u = D_{60}/ D_{10}$.

ESAL: Annual equivalent single axle load for the coring lane. It converts passes of axles with different loads to passes of a standard 80 kN (18,000 lb) single-axle load in terms of equivalent damage, with damage calculated based on the ratio of the loads raised to an exponent of 4.2 (standard Caltrans

assumption). The distribution of ESALs is given in Figure 30. The figure shows that the majority of the sections have ESALs between 0 and 800,000. Since the distribution is highly skewed, ESALs are categorized as high or low. In the analysis, high ESALs are coded as 1, for sections with annual ESALs above 800,000; and low ESALs are coded as 0, for sections with annual ESALs less than 800,000. ESALs between the first-year and second-year coring were not evaluated because the distribution of ESALs was highly skewed and most ESALs were less than 800,000; this result occurred because the time difference between the data collection was less than one year for some sections.

F.M.: Fineness modulus, a measure of the uniformity of the aggregate gradation. The higher the fineness modulus, the coarser the asphalt mix (a higher percentage of coarse material) and the more uniform the gradation.

F.M. = (∑ percent material retained on each sieve)/100.

F.T.: Annual freeze-thaw cycles. The distribution of the freeze-thaw cycles is shown in Figure 31. Since the distribution of freeze-thaw cycles is highly skewed, it was discretized. Based on California weather data from 1960 to 1990 for the entire state (not just the test sections as shown in the figure), obtained from CDIM software (100), the average annual number of freeze-thaw cycles was 31. The sections with more than 31 freeze-thaw cycles were categorized as high (coded as 1), and those with fewer than 31 cycles were categorized as low (coded as 0).

IRI: International Roughness Index (m/km) (ASTM E 1926).

MPD: Mean profile depth (microns) (ASTM E 1845).

Max. Daily Temp Diff.: Maximum daily temperature difference. This is the maximum difference between the maximum and minimum temperatures experienced since the construction of the pavement section (°C).

Min T: Minimum temperature experienced by the pavement section during its lifetime (°C).

ΔMin T: Minimum temperature experienced by the pavement section between the first-year coring and second-year coring.

N.D. Prec. > 10 mm: Number of days in a year that the precipitation is above 10 mm.

ΔN.D. Prec. > 10 mm: Number of days that the precipitation is above 10 mm between the first-year coring and second-year coring.

N.D. Prec. > 20 mm: Number of days in a year that the precipitation is above 20 mm.

N.D T < 0: Number of days that the temperature is below 0°C.

ΔN.D T < 0: Number of days that the temperature is below 0°C between the first-year coring and second-year coring.

N.D T < 5: Number of days that the temperature is below 5°C.

N.D. T > 25: Number of days that the temperature is above 25°C in a year.

ΔN.D. T > 25: Number of days that the temperature is above 25°C between the first-year coring and second-year coring.

N.D. T > 30: Number of days that the temperature is above 30°C in a year.

Δ N.D. T > 30: Number of days that the temperature is above 30°C between the first-year coring and second-year coring.

NMAS: Nominal maximum aggregate size (mm). The NMAS values for the test sections are 9.5 mm, 12.5 mm, and 19 mm.

Mix Type: Binary variable. It was coded as 1 if the section is open-graded, OGAC, or RAC-O; and 0 if the section is dense-graded (DGAC) or gap-graded (RAC-G).

PCC Below: Categorical variable. It was coded as 1 if the underlying layers contain portland cement concrete (PCC), and it was coded as 0 if the underlying layers contain asphalt concrete (AC).

Presence of Fatigue Cracking Below: Categorical variable. It was coded as 1 if there was fatigue cracking on the surface before the overlay was placed, and it was coded as 0 otherwise.

RMS: Root mean square (ASTM E 1845).

Rubber Inclusion: Binary variable. It was coded as 1 if the binder is rubberized, RAC-G or RAC-O; and it was coded as 0 otherwise.

S.A.: Surface area (m^2/kg).

$$\text{S.A.} = 2 + \sum_{\boldsymbol{No}.4} \%\ passing * 0.02 + \sum_{\boldsymbol{No}.8} \%\ passing * 0.04 + \sum_{\boldsymbol{No}.16} \%\ passing * 0.08 +$$

$$\sum_{\boldsymbol{No}.30} \%\ passing * 0.14 + \sum_{\boldsymbol{No}.50} \%\ passing * 0.30 + \sum_{\boldsymbol{No}.100} \%\ passing * 0.60 + \sum_{\boldsymbol{No}.200} \%\ passing * 1.6$$

Surf Thick: Thickness of the surface layer (mm).

Tot Thick: Thickness of the total pavement section (mm).

Underlying Layer Thickness: Thickness of the pavement layers excluding the surface layer (mm).

Well-Gradedness: Assessed from the coefficient of uniformity, C_u, and the coefficient of curvature, C_c. In the Unified Soil Classification System (USCS), gravels must have a C_u value greater than 4, and a C_c value from 1 to 3 to be considered well graded. Well-gradedness is coded as a binary variable; it is coded as 1 if the soil is well graded, and it is coded as 0 otherwise.

Table 11 shows the mean, standard deviation, minimum, and maximum of the continuous independent variables used in the analysis. IRI, MPD, and BPN were also used as dependent variables. The descriptive statistics presented in this chapter include OGAC, RAC-O, OGAC and RAC-O F-mixes, RAC-G, and DGAC sections along with the environmental test sections that fit the factorial design. The

regression analyses shown in the following chapters are valid only within the range (maximum and minimum) of the values shown for the independent variables.

Table 11: Descriptive Statistics for the Independent Variables

Variable	Mean	Standard Deviation	Minimum	Maximum	Number of Sections
IRI (m/km)	1.5	0.7	0.7	3.8	71
Air-Void Content (%)	12.4	5.0	4.1	21.6	71
Mean Profile Depth (MPD) (microns)	975	328	406	1807	71
Root Mean Square (RMS)	651.4	196.1	282.3	1,121.6	71
British Pendulum Number (BPN)	57.0	7.8	41	75	72
Surface Area (m^2/kg)	23.9	8.0	10.8	45.6	70
Fineness Modulus	5.0	0.5	3.8	5.9	70
Coefficient of Curvature (C_c)	3.4	1.9	1.0	8.0	70
Coefficient of Uniformity (C_u)	21.1	14.9	2.9	58.0	70
Age (years)	3.8	2.7	0.0	13.6	71
AADTCL	9,315	7,418	1289	29,818	71
AADTTCL	1,215	1,534	6	6,454	71
ESALs (annual)	521,890	794,199	1,000	3,481,320	71
A.A.Prec (mm)	632.0	480.5	144.5	2,105.2	71
ΔPrec (mm)	488.1	384.3	37.1	1396.2	64
Age * A.A.Prec (mm)	2,127.0	2,090.0	2.0	9,773.0	71
A.A.Wet Days	80	56.4	0.0	335.0	71
ΔWet Days	98	66.4	24	265	64
Age * A.A.Wet Days	267.4	235.4	0.0	1,007.0	71
N.D.Prec. > 10mm	65	66.9	0.0	310	71
ΔN.D. Prec. > 10 mm	12	11	0.0	43	64
Age * N.D.Prec. > 10mm	18	14.1	0.0	58	71
N.D.Prec. > 20mm	31	36.4	0.0	179	71
Age * N.D.Prec. > 20mm	9	8.8	0.0	35	71
A.A. Max D.T. (°C)	23.0	2.6	15.8	28.9	71
ΔA.Max D.T. (°C)	22.9	2.3	14.3	27.6	64
A.A. Min D.T. (°C)	8.7	2.2	4.2	13.9	71
ΔA.Min D.T. (°C)	8.2	1.8	3.9	11.9	64
N.D. T > 25°C	137	56.5	1	237	71
ΔN.D. T > 25°C	127	50	0	204	64
Age * N.D. T > 25°C	502	389.4	2	1,356	71
N.D. T > 30°C	77	51.7	0	156	71
ΔN.D. T > 30°C	71	45	0	204	64
Age * N.D. T > 30°C	285	254.0	0	877	71
A.D.D > 30°C	2,672.0	1,835.0	0.0	5,422.0	71
ΔA.D.D > 30°C	321.3	223.7	0.0	666.5	64
Age * A.D.D > 30°C	9,832.0	8,882.0	0.0	30,005.0	71
A.A.T.H.M. (°C)	31.8	4.8	18.1	38.5	71
A.A.T.C.M. (°C)	3.6	2.4	–0.4	13.9	71
Average Annual Freeze-	14	14	0	50	72

Variable	Mean	Standard Deviation	Minimum	Maximum	Number of Sections
Thaw Cycles					
Min T (°C)	–3.59	3.36	–8.9	13.9	71
ΔMin T (°C)	–4.71	3.01	–12.8	0.0	64
Average Daily Temp Difference (°C)	14.19	1.79	8.62	17.78	71
Maximum Daily Temp Difference (°C)	26.25	3.58	15.50	32.20	71
N.D. T < 0°C	7	3.60	0	14	71
ΔN.D T < 0°C	23	17	0	63	64
N.D. T < 5°C	16	4.49	0	23	71
Surface Layer Thickness (mm)	43.8	22.1	10.4	112.5	71
Total Pavement Thickness (mm)	225.8	74.9	71.6	438.0	71
Underlying Layer Thickness (mm)	181.4	63.6	54.0	409.8	71

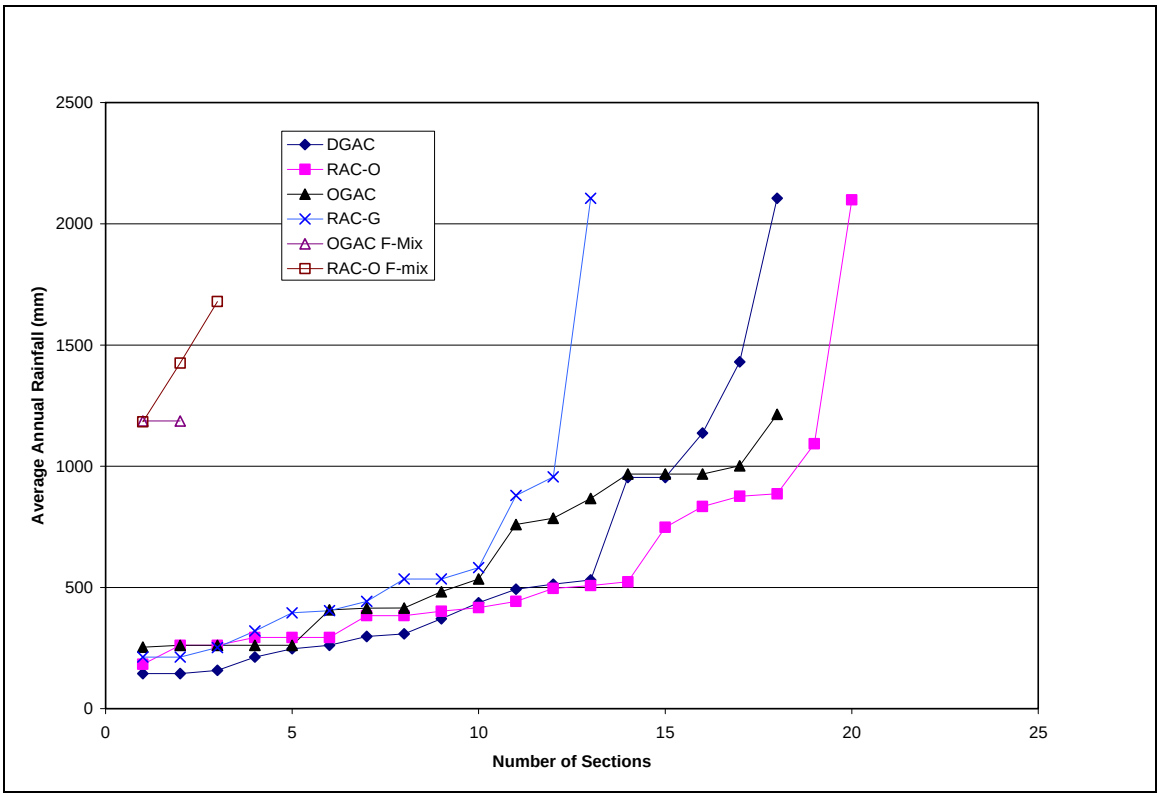

Figure 27: Distribution of average annual rainfall.

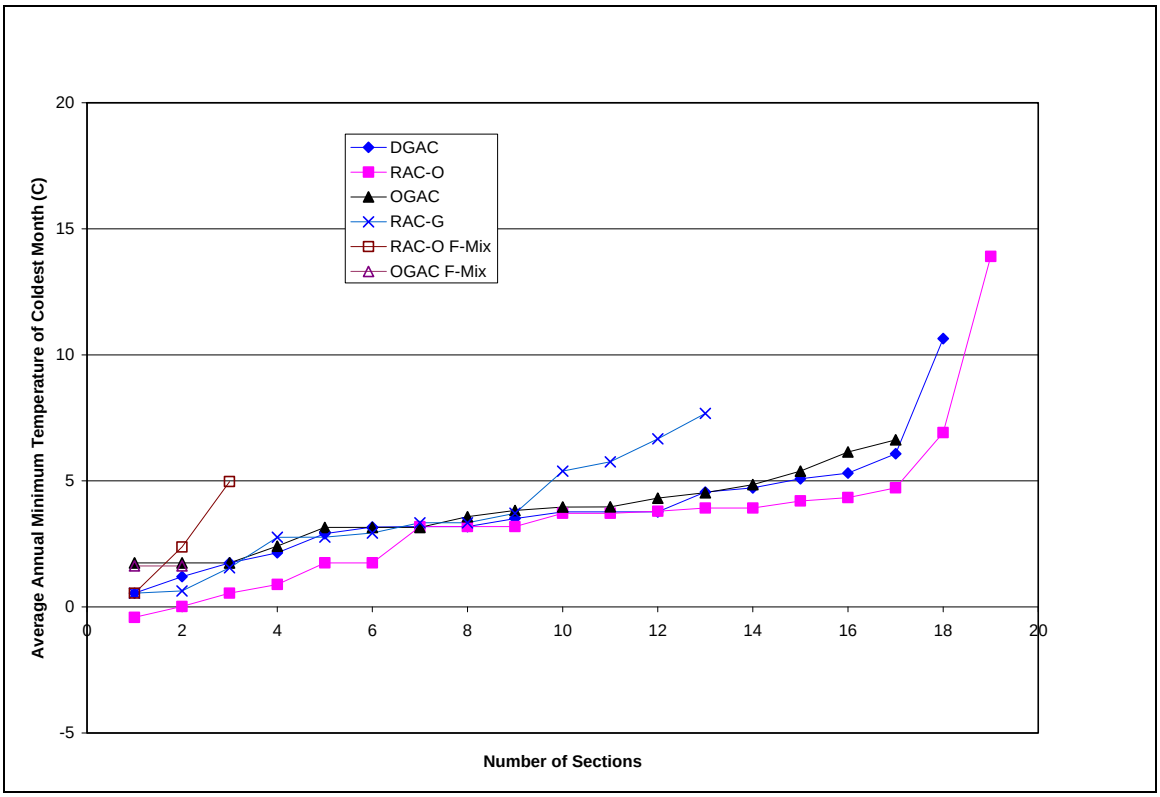

Figure 28: Distribution of average annual minimum daily temperature of the coldest month (°C).

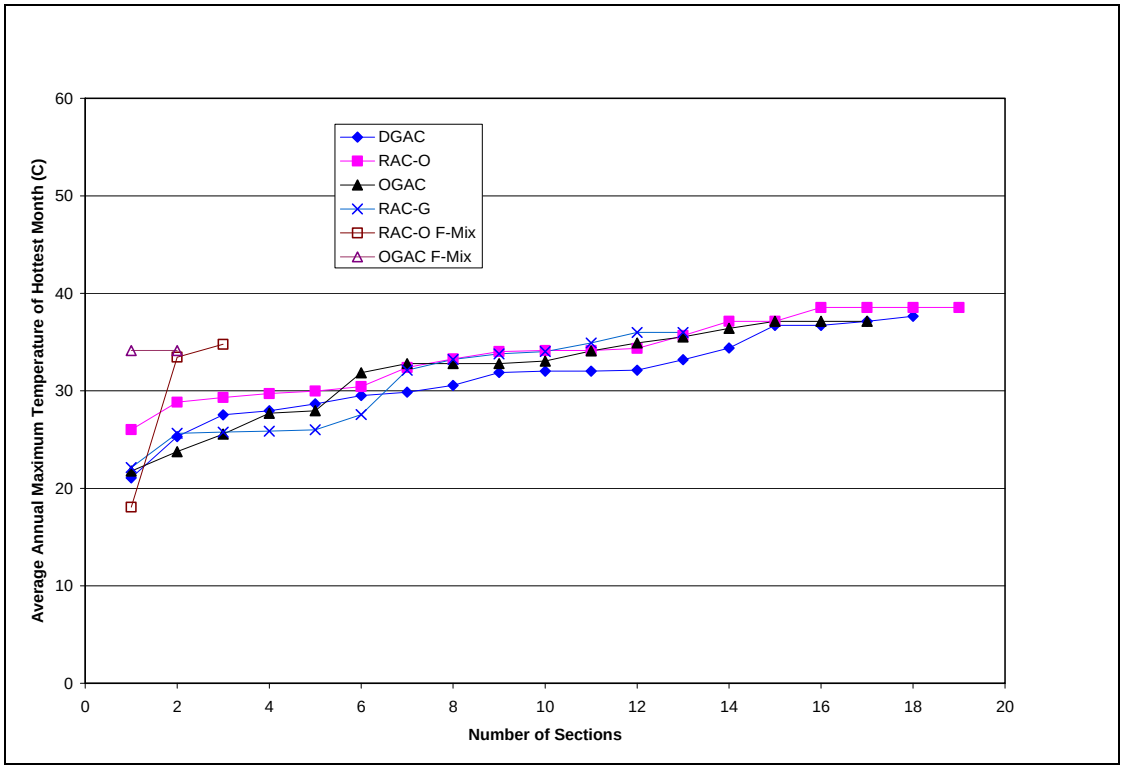

Figure 29: Distribution of average annual maximum daily temperature of the hottest month (°C).

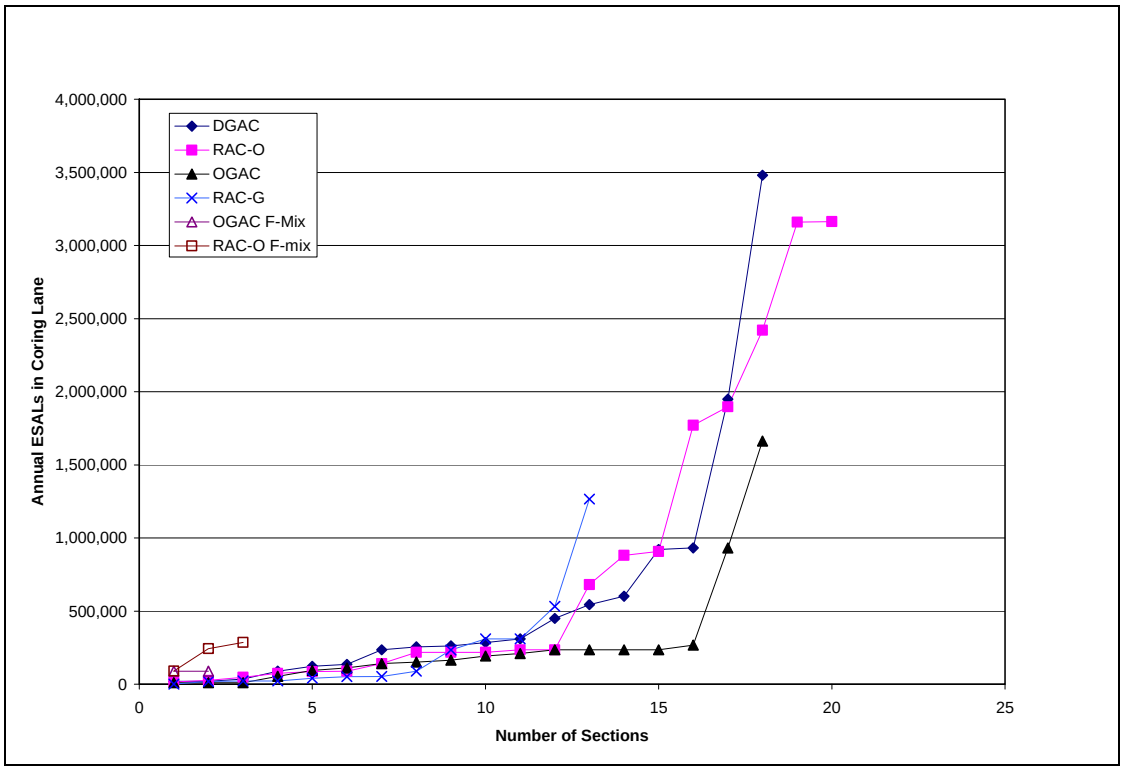

Figure 30: Distribution of annual ESALs in the coring lane.

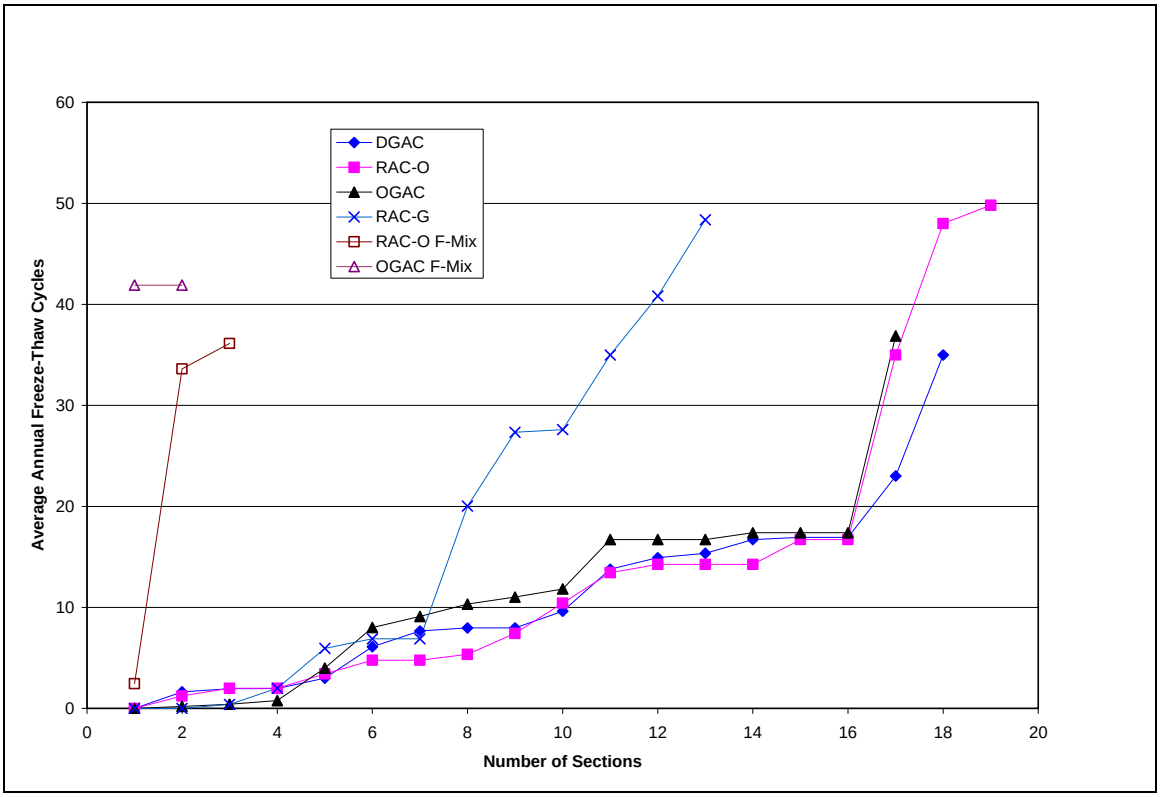

Figure 31: Distribution of annual freeze-thaw cycles.

Figure 32 shows the pairwise correlation of the mix variables: IRI, RMS, MPD, AV, NMAS, S.A., F.M., C_u, and mix type, using a matrix plot. A matrix plot includes all the pairwise scatter plots of the variables on a single plot in a matrix format. That is, if there are k variables $X_1, X_2,...,X_k$, the matrix plot will have k rows and k columns; the ith row and j^{th} column of this matrix will show the relationship between X_i and X_j. The figure shows that the MPD and RMS values have a highly correlated linear relationship. The figure also shows that AV, S.A., MPD, RMS, F.M., C_u, and mix type are correlated with each other.

Figure 33 shows the pairwise correlation of the climate variables: average annual precipitation, annual number of wet days, average annual maximum daily temperature, number of days with temperatures above 25°C, number of days with temperatures above 30°C, annual degree-days above 30°C, annual freeze-thaw cycles, and average annual temperature of the hottest month. The figure shows that the temperature variables are strongly correlated with each other.

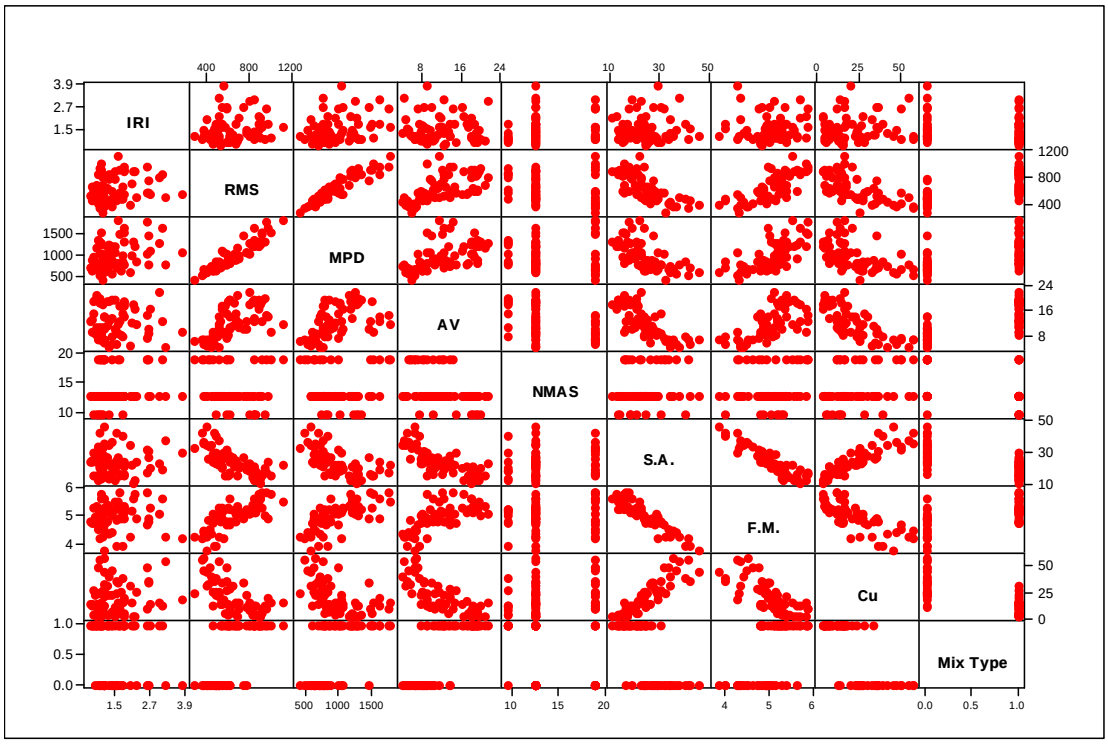

Figure 32: Pairwise comparison of surface and mix properties.

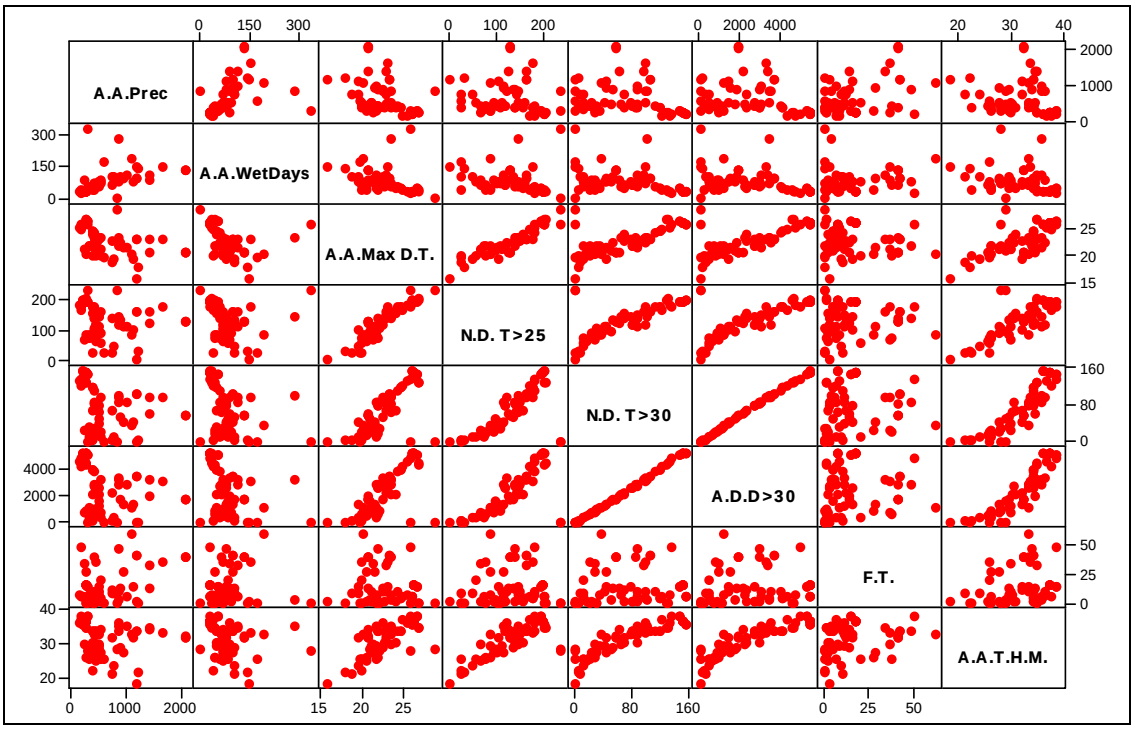

Figure 33: Pairwise comparison of climate variables.

Figure 34 shows the pairwise comparison of cold temperature variables and temperature differences. The figure shows that all the variables are highly correlated with each other.

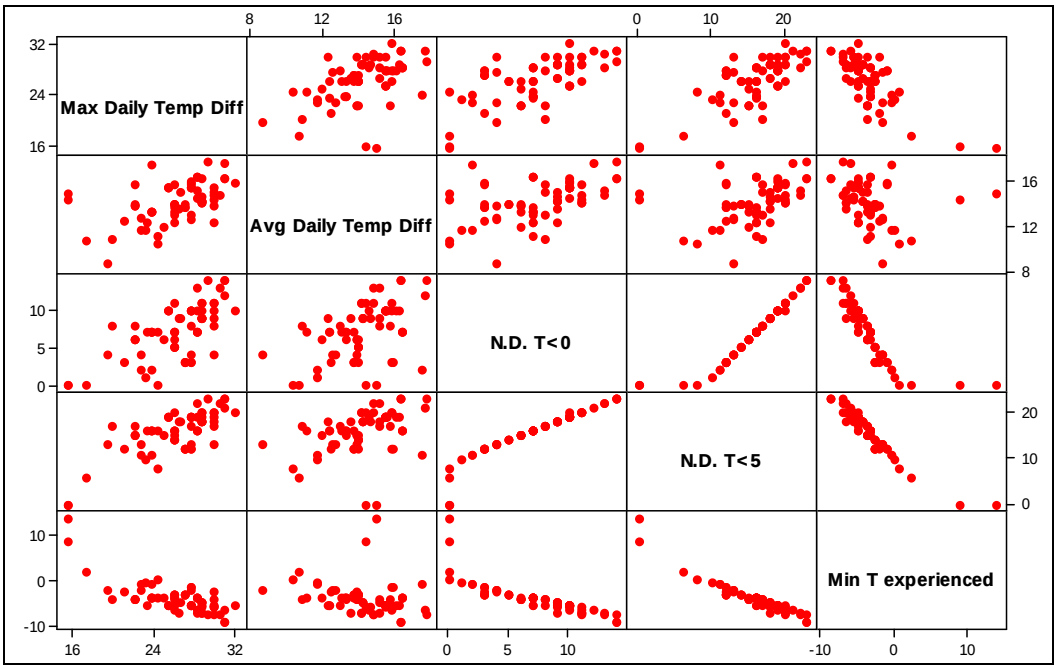

Figure 34: Pairwise comparison of cold temperature variables and temperature differences.

Figure 35 shows the pairwise correlation of AADT, AADTT, and ESALs. The figure shows that AADTT and ESALs are highly correlated, as expected.

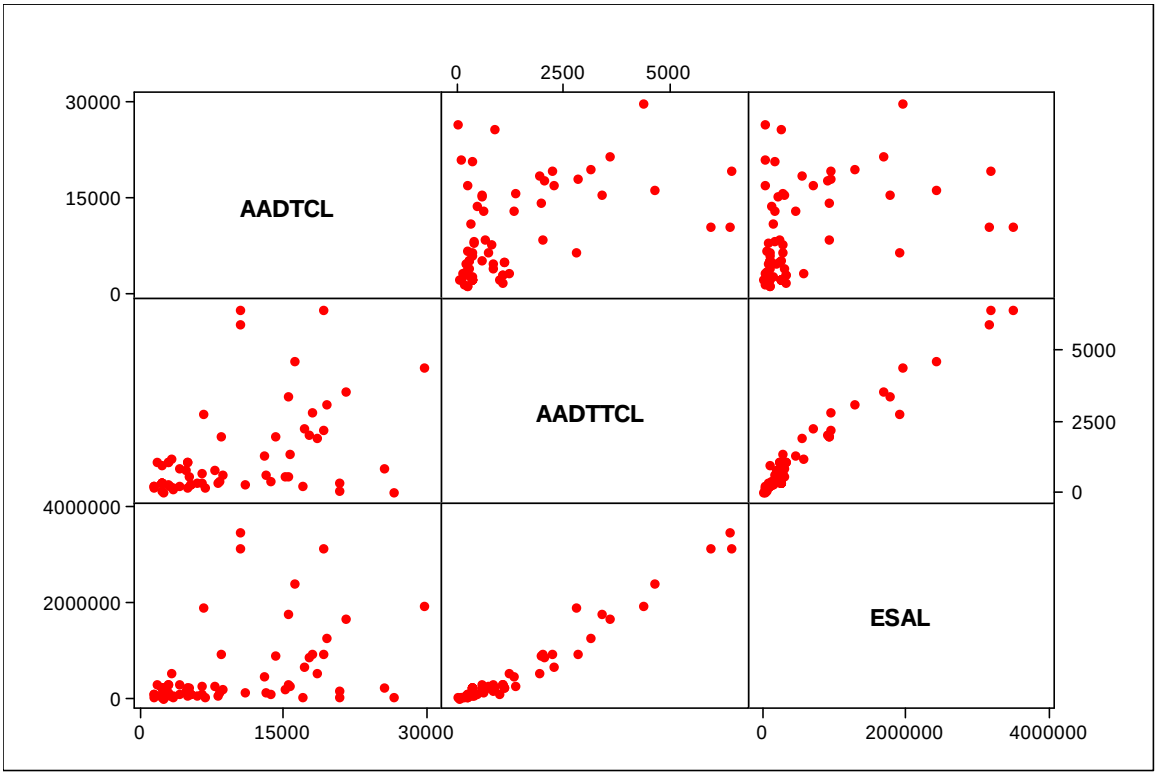

Figure 35: Pairwise comparison of traffic data.

The study showed that the independent variables in each category, namely mix, climate, and traffic, are highly correlated with others within the same category. When multicollinearity is present in a regression equation, it is extremely difficult to evaluate the relative influence of independent variables on the dependent variable without running the risk of making faulty inferences. Therefore, it is important to identify the variables that are highly correlated with each other before they are used in a regression model.

5 EVALUATION OF PERMEABILITY AND AIR-VOID CONTENT OF ASPHALT CONCRETE MIXES

Permeability for each section was obtained by averaging the 12 measurements in the first year and 6 measurements in the second year. It was evaluated using descriptive analysis and regression analysis. Descriptive analysis included the first-year results and comparison of the first- and second-year results. Only the sections where the data was collected for both the first and second year of this study were used in the comparative analysis. Permeability was modeled using the data from first-year measurements.

Air-void content is an important factor affecting both permeability and noise levels. Air-void content of the field cores was measured using two methods: the CoreLok method and CT scanning. A CT scan gives the air-void content at every 0.3 mm of the asphalt surface layer throughout its thickness. Since a CT scan is a time-consuming process, only one core from the wheelpath and one core from the center were tested for 10 sections, while all the sections were measured using the CoreLok method.

Clogging is the blockage of air voids with fine particles generated by vehicles and deposited from elsewhere by the wind. Clogging of air voids by fine particles may reduce drainage capacity, hence diminishing the benefits from open-graded mixes. Clogging was evaluated in two ways: with CT scanning and field permeability measurements. Clogging was first analyzed by comparing the air-void content within a mix using the results from the CT scan. Then it was evaluated as the difference in permeability between the center (between the wheelpaths) and the wheelpath, and then as the permeability difference between the first year and second year.

This chapter answers these questions:

- Can open-graded and gap-graded mixes retain their permeabilites over eight years? Open-graded mixes are intended to retain high permeability, while gap-graded mixes are intended to be as impermeable as dense-graded mixes.
- Do open-graded mixes clog less in the wheelpath than between the wheelpaths? The answer to this question is important because it indicates the overall permeability of the pavement and whether traffic has a cleaning effect in the wheelpaths.
- Where does clogging occur in open-graded mixes: only at the immediate surface or to some depth below the surface?
- How does clogging change with pavement characteristics and with traffic and climatic conditions?
- How does permeability change with pavement characteristics?

5.1 Permeability Analysis

5.1.1 Descriptive Analysis

The variation in permeability by mix type is shown by box plots in Figure 36. In each box plot, the bottom of the box shows the first quartile, and the top of the box shows the third quartile. The line in the middle of the box represents the median, and the dot represents the mean of all the observations. The distance between the first quartile and the third quartile is called the interquartile range (IQR). Each of the whiskers (lines that extend above and below the box) has a length of 1.5 times the IQR. Each data point outside the whisker is an observation that is greater than 1.5 times the IQR; these points are potential outliers and are marked by asterisks. The figure shows the values for cores obtained from the right wheelpath (R) and center of the lane (C). The figure shows that open-graded mixes have higher permeabilities than do dense- and gap-graded mixes. There is no significant difference in permeability between OGAC and RAC-O mixes. Since RAC-G and DGAC mixes have permeabilities close to zero, the variation in permeability values for these mixes is lower than for open-graded mixes.

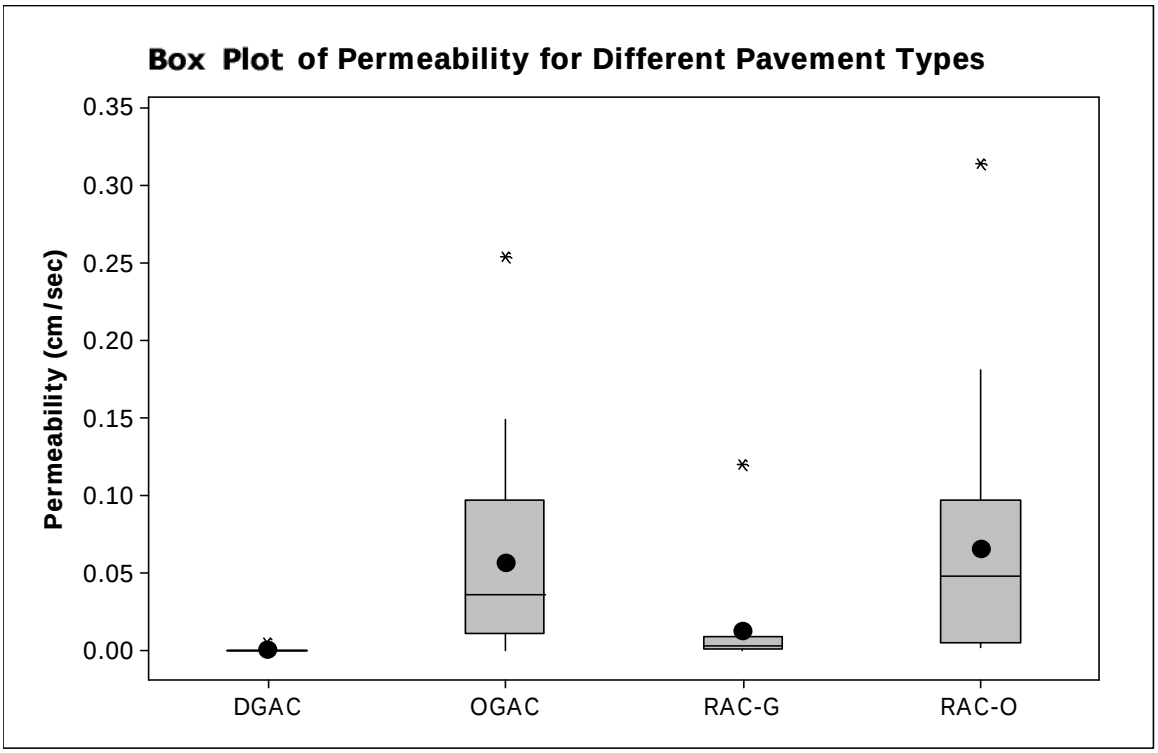

Figure 36: Box plot of permeability values for different mix types.

Figure 37 shows the variation in permeability by mix type and age. The figure shows that permeability decreases with age for RAC-G and RAC-O mixes. For DGAC mixes, the permeability is low for all ages, as it is intended to be. For OGAC mixes, permeability generally decreases with age;

however, the group of mixes that are one to four years old generally have lower permeability than the mixes that are older than four years. As discussed later, this trend occurs at least partly because the OGAC mixes in the one-to-four-year age group have a smaller NMAS than those in the group of mixes older than four years.

RAC-G mixes have higher permeabilities (close to those of open-graded mixes) in their first year; however, they lose their permeability with time, and they have permeabilities close to those of dense-graded mixes as they get older. The open-graded mixes were compared with the only two official criteria that could be found in the literature. Almost all the open-graded mixes satisfy the European minimum permeability requirement of 0.01 cm/sec at the time of construction; and only half of the new open-graded mixes satisfy the Swiss minimum permeability requirement of 0.11 cm/sec, and nearly all the older open-graded mixes have lower permeabilities than the Swiss criterion.

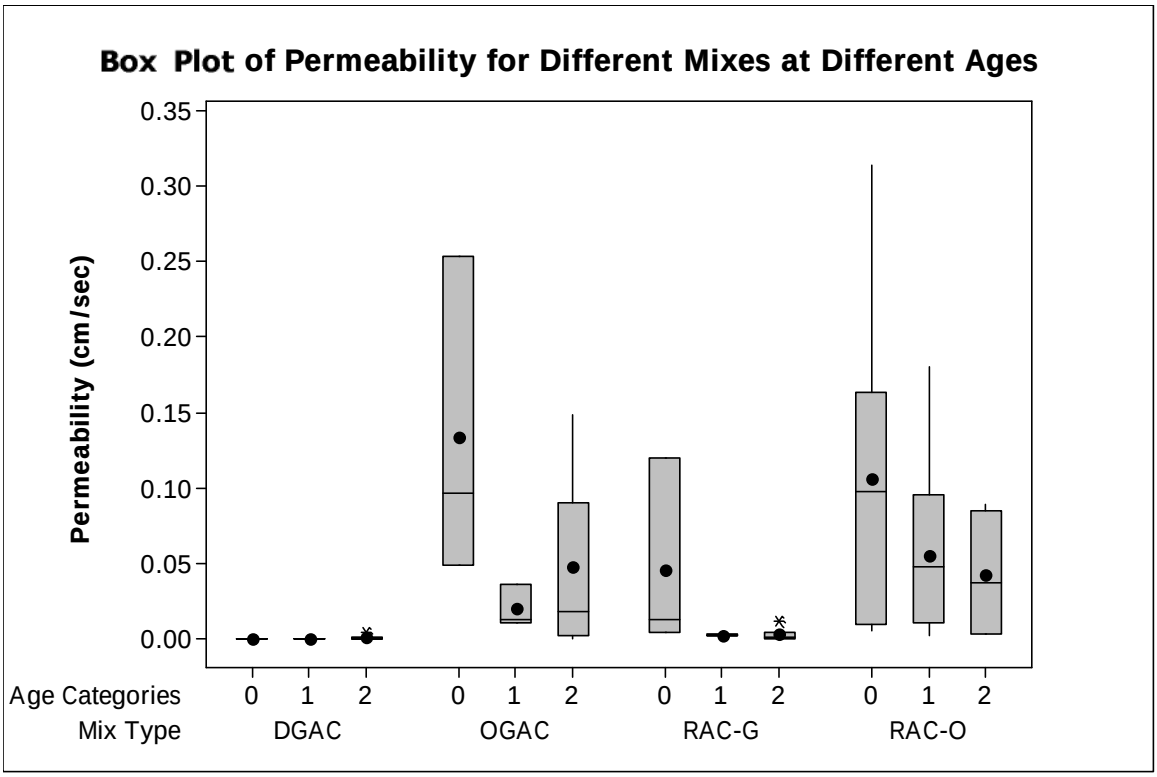

Figure 37: Box plot of permeability values for different mix types at different ages (Note: Age category 0 is less than one year old, category 1 is one to four years old, and category 2 is greater than four years old).

Figure 38 shows a comparison of permeability values for the first year and second year for different mixes at different ages. Note that the age categories from the first year were retained in the second year to allow comparison of the same mixes, so sections that were less than one year old in the first year are included in the same age group for the second year. The figure shows that OGAC, RAC-O,

and RAC-G mixes have lower permeabilities in the second-year measurement. The new RAC-G mixes have high permeabilities—close to those of older open-graded mixes; however, RAC-G mixes lose their permeability with time, and therefore older RAC-G mixes have permeability values close to those of dense-graded mixes, which are close to zero. OGAC mixes that are older than four years have higher permeabilities than OGAC mixes that are in the one-to-four-year age group, because of the presence of OGAC F-mixes in that age group. The F-mixes have higher air-void content than do the conventional OGAC mixes.

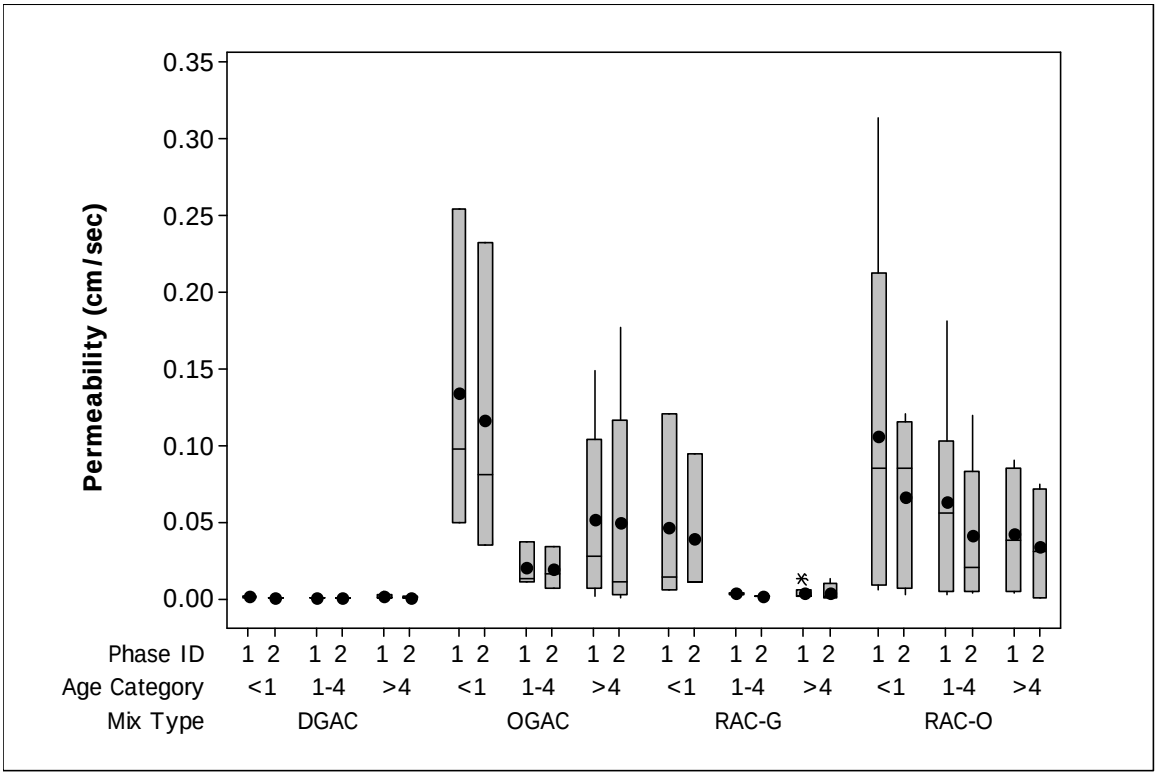

Figure 38: Comparison of permeability values for different mix types at different ages for first and second years.

Figure 39 shows the difference in permeability values between first-year and second-year measurements (permeability in the first year and permeability in the second year) for different mixes at different ages. The figure shows that open- and gap-graded mixes that are less than one year old have greater variability of change between the two years of the study than do older mixes. The figure also shows that reduction in permeability decreases as age increases, probably because older mixes are already clogged and hence show less change in their permeability values.

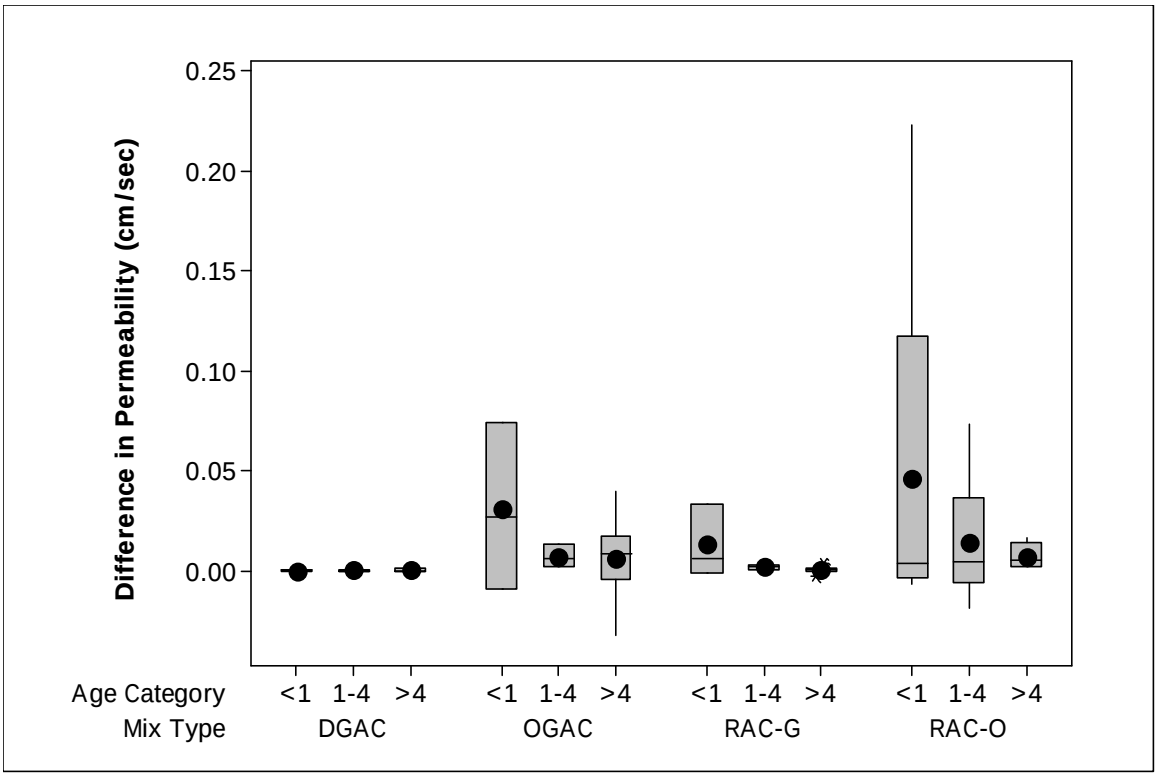

Figure 39: Comparison of permeability differences between first-year and second-year measurements for different mix types at different ages (positive value indicates a reduction in permeability).

5.1.2 Regression Analysis

Regression analysis was performed to determine the significant variables affecting permeability. The single regression analysis revealed that the error terms have unequal variances and are not normally distributed. Since the skewness and variability of the distribution of the error terms increases with the mean response, a log transformation was applied on the Y (dependent) variable, permeability. Then the regression model was fitted to transformed Y data, $Y' = \log_{10}Y$.

Because of the smallness of the data set, one variable was evaluated at a time. The coefficient of the explanatory variable and the constant term along with their p-values and the coefficient of determination (R^2) for each model are given in Table 12. The dependent variable is the logarithm of permeability. A significance level of 5 percent is used in all the analyses in this research. In the table, p-values less than 0.05 are shown in bold.

Table 12: Regression Analysis of Permeability

Model Number	Explanatory Variable			Constant Term	R^2 (%)
	Name	Coefficient	p-value		
1	Air-void content (%)	0.16	**0.00**	–4.27	53.9
2	NMAS (mm)	–0.07	0.10	–1.21	3.9
3	Surface area (kg^2/m)	–0.10	**0.00**	0.25	51.0
4	Fineness modulus	1.57	**0.00**	–10.0	44.7
5	Well graded or not	–0.37	0.17	–2.03	2.8
6	Age (years)	–0.15	**0.00**	–1.66	12.7
7	Mix type	1.63	**0.00**	–3.22	49.5
8	Rubber inclusion	0.74	**0.00**	–2.64	10.6
9	Thickness (mm)	–0.01	0.13	–1.79	3.1

Regression analysis revealed that air-void content, surface area, fineness modulus, age, mix type, and rubber inclusion were significant variables affecting permeability. Mix type, rubber code, and well-gradedness were used as categorical variables in the regression. Mix type was coded as 1 for open-graded mixes and as 0 for dense- and gap-graded mixes. Rubber inclusion was coded as 1 for rubberized mixes and as 0 for nonrubberized mixes. Well-gradedness was coded as 1 for well-graded mixes and 0 for poorly graded mixes based on the criterion given in Chapter 4.

Increasing the air-void content and fineness modulus increases permeability, and increasing the surface area (finer gradations) reduces permeability. Permeability decreases as the mix ages. Open-graded mixes have higher permeability values. Permeability was also found to be higher for rubberized mixes because of the high first-year permeabilities of RAC-G mixes. There is no significant difference overall in permeability between RAC-O and OGAC mixes. Therefore, the study concluded that there is no causal relationship between permeability and rubber inclusion.

Multiple regression models were applied using the significant variables as shown in Equation 8. The age, mix type, air-void content, and fineness modulus were included in the model as independent variables. The variability of the permeability explained using these variables is 72.1 percent. The air-void content and mix type were used in the same equation, and both have low p-values, although they are correlated. The significance of both variables in the same equation suggests that the effect of mix type on permeability is not only due to air-void content.

Figure 40 shows permeability values versus air-void content for open-graded (shown as squares) and dense- and gap-graded (shown as dots) mixes. The figure shows that at a given air-void content, the permeability of open-graded mixes is higher than that of dense- and gap-graded mixes. This distinction may occur because open-graded mixes have more interconnected air voids at a given air-void content, resulting in higher permeability.

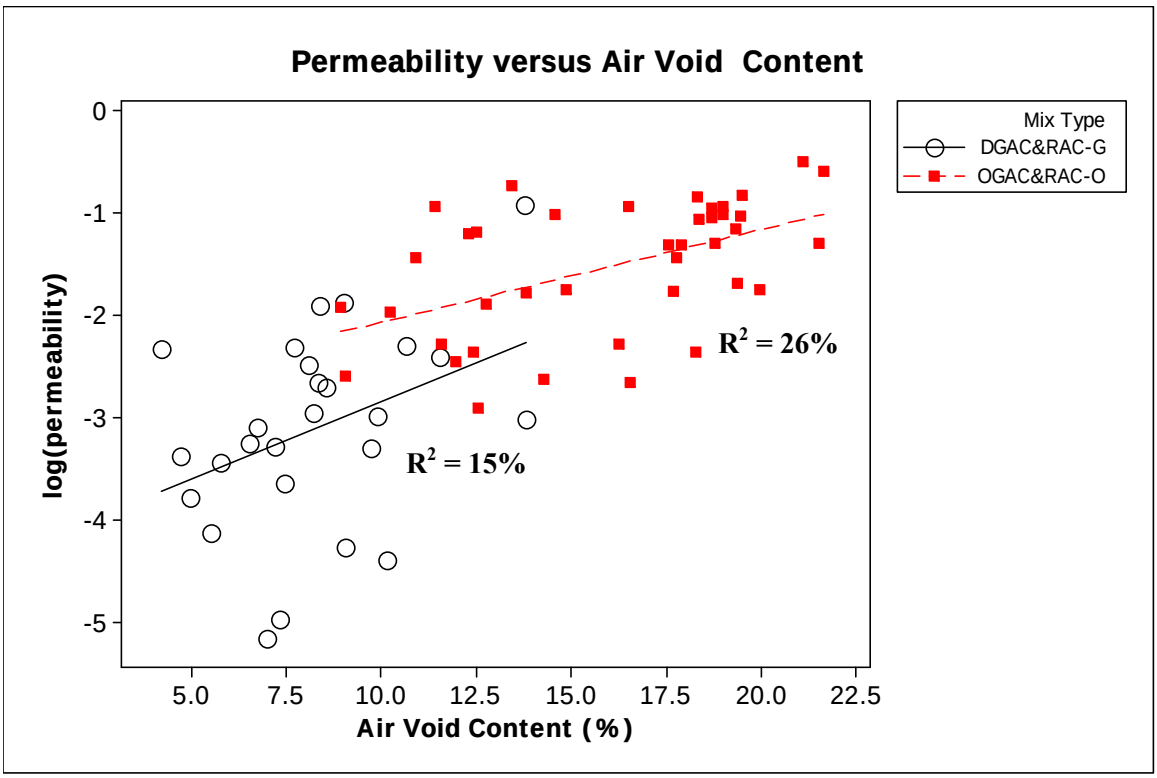

Figure 40: Permeability (cm/sec) versus air-void content for different mix types.

Permeability Model

The regression equation, Equation (8), is

log (permeability) = –6.49 – 0.118 × Age + 0.552 × Mix type + 0.0804 × Air-void content + 0.682 × Fineness modulus **(8)**

Predictor	Coef	SE Coef	T	P
Constant	–6.4932	0.9509	–6.83	0.000
Age	–0.11777	0.02778	–4.24	0.000
Mix type	0.5524	0.2461	2.24	0.028
Air-void content	0.08036	0.02496	3.22	0.002
Fineness modulus	0.6821	0.2086	3.27	0.002

S = 0.607917 R-Sq = 72.1% R-Sq(adj) = 70.2%

Analysis of Variance

Source	DF	SS	MS	F	P
Regression	4	57.173	14.293	38.68	0.000
Residual error	60	22.174	0.370		
Total	64	79.346			

A total of 65 sections were used in the model. The ages of the sections used in the models shown here range from 0.003 to 14 years, the air-void content of these sections ranges from 4.2 to 22 percent, and the fineness modulus ranges from 3.8 to 5.8.

The earlier studies showed that NMAS is a significant variable affecting the permeability values; however, NMAS was not found to be significant in the regression analysis. Open-graded mixes use NMAS values of 9.5 and 12.5 mm, dense- and gap-graded mixes use values of 12.5 and 19 mm, and F-mixes use a value of 19 mm. Since NMAS is correlated with mix type, the NMAS effect on permeability may not have been revealed in the regression analysis. Therefore, NMAS effects on permeability were further evaluated for open-graded mixes; NMAS effects were not further evaluated for dense- and gap-graded mixes as these mixes have permeabilities close to zero.

Figure 41 compares the permeability values for open-graded mixes with different NMAS values. The 19-mm NMAS sections are the F-mixes. There are only five F-mixes among the test sections, and two of them are older than eight years, resulting in greater average age compared to other mix types. The

figure shows that the 12.5-mm NMAS mixes have higher permeability values than the 9.5-mm NMAS mixes, indicating that increasing NMAS may increase the permeability. Mixes with 19-mm NMAS (F-mixes) have lower permeabilities than the 12.5-mm NMAS mixes, probably because they are older; however, they still have higher permeabilities than 9.5-mm NMAS mixes. It thus can be concluded that 12.5-mm NMAS mixes provide greater permeability than do 9.5-mm NMAS mixes for the Caltrans mixes included in the study.

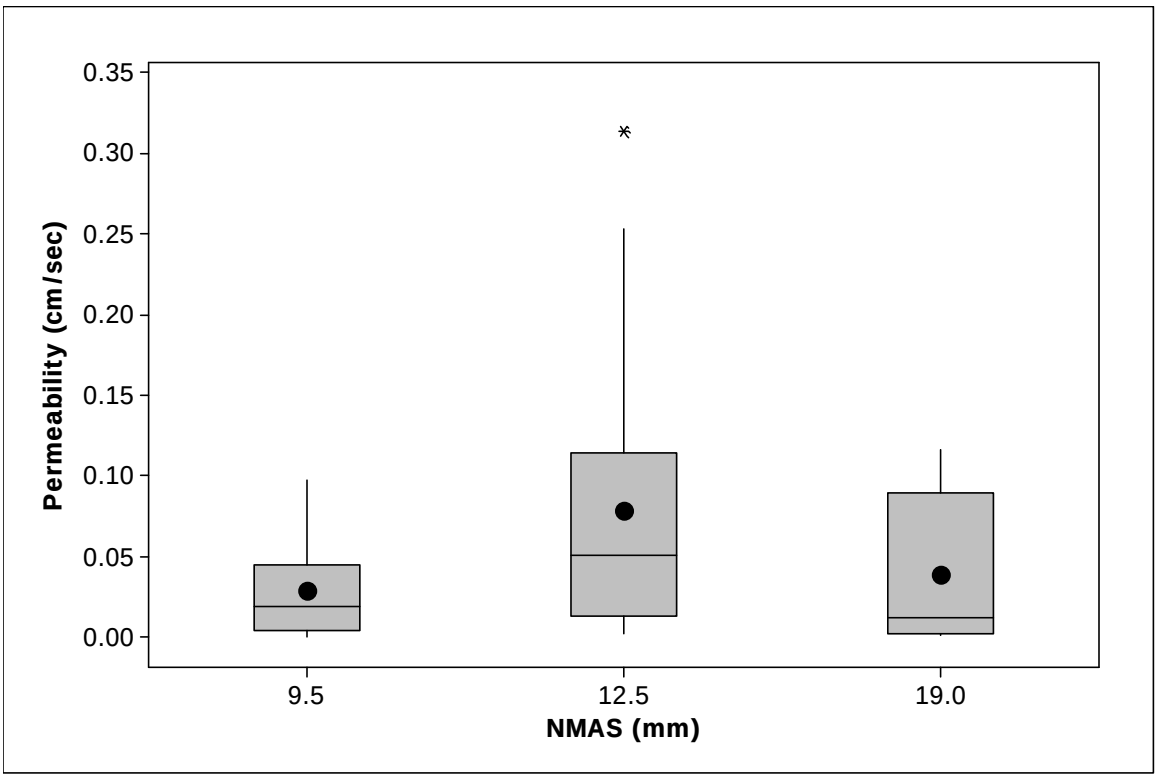

Figure 41: Permeability variation for open-graded mixes with different NMAS values.

5.2 Air-Void Content Analysis

5.2.1 Descriptive Analysis

Figure 42 shows the variation in the air-void content of different mix types, with mean values displayed next to the box plots. The figure shows that OGAC and RAC-O mixes have very similar air-void content, ranging from 8 to 22 percent. RAC-G mixes have an average air-void content of 9.9 percent, and DGAC mixes have an average air-void content of 6.5 percent.

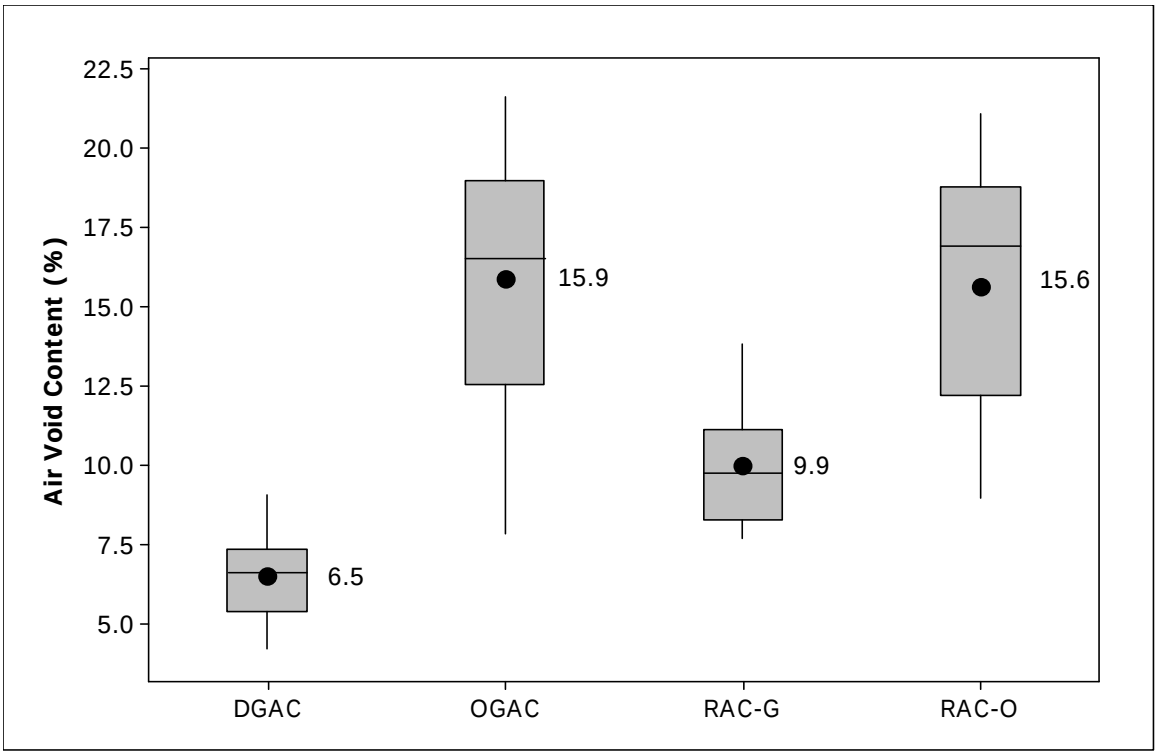

Figure 42: Box plot of air-void content for different mix types (dots show the mean values).

Figure 43 shows the variation in air-void content for different mix types at different ages. According to the figure, the air-void content of OGAC mixes varies largely by age. The new OGAC mixes have air-void content of approximately 20 percent; however, this value is lower in the older age categories, particularly the category of OGAC mixes one to four years old compared to the other age categories of OGAC.

Figure 44 shows the fineness modulus of different mix types at different ages. The figure shows that the OGAC, RAC-O, and RAC-G mixes that are one to four years old also have the smallest fineness modulus. The sections selected for that age group have finer gradations compared to the gradations for the other age groups, by coincidence. The lower air-void content of mixes that are one to four years old is due to the lower fineness modulus of that age group.

In general, open-graded mixes satisfy the Caltrans specification of 18 percent air-void content (107). Further, the permeability plot (refer to Figure 37) and the air-void plot (refer to Figure 43) show the same trends.

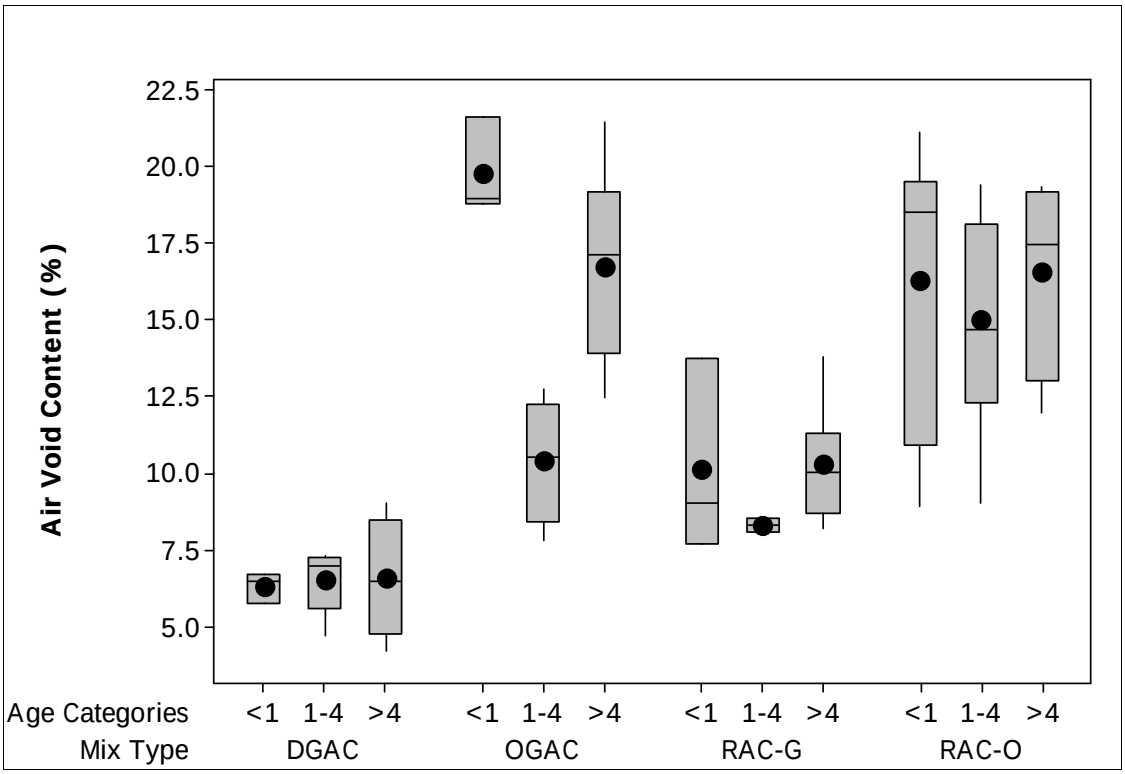

Figure 43: Box plot of air-void content for different mix types at different ages.

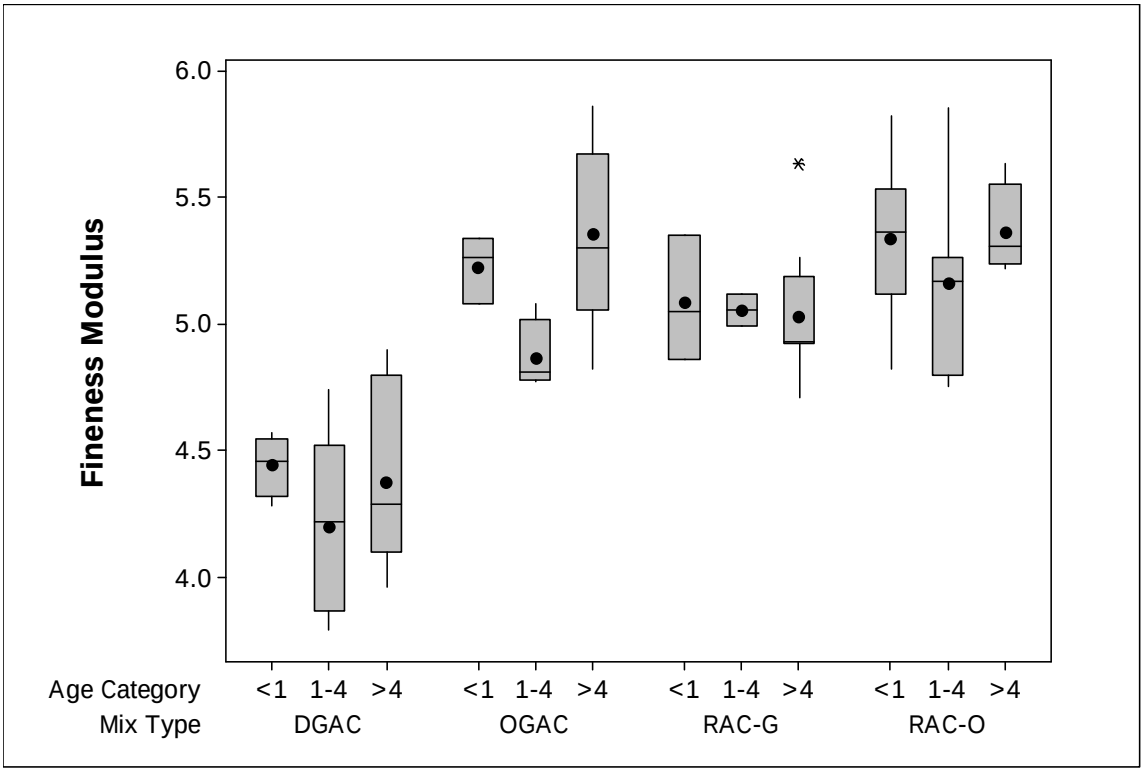

Figure 44: Box plot of fineness modulus for different mix types at different ages.

Figure 45 compares the air-void content values for different mixes at different ages for both the first and second years. According to the figure, there is reduction in the air-void content over one year, probably due to compaction under traffic; however, this reduction is usually very small.

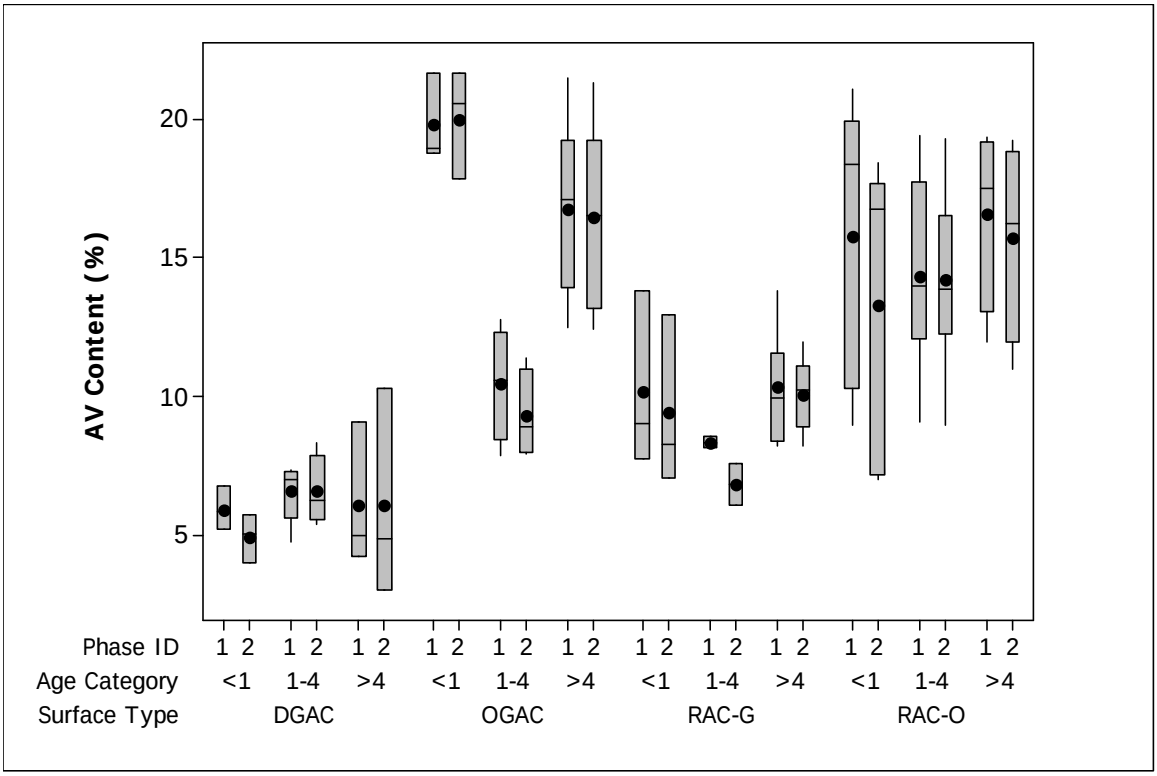

Figure 45: Comparison of air-void content for different mix types at different ages for first and second years.

Figure 46 shows the difference in air-void content between the first and second years. The figure shows that the average difference is usually small: approximately zero. RAC-O mixes that are less than one year old have the greatest difference because one section in that category was cored before it was opened to traffic; because it was compacted under traffic, reduction in the air-void content is higher for that section. The OGAC mixes less than one year old have negative values, indicating an increase in air-void content. This result occurs because one section has high air-void content in one of the measurements in the second year, which could be due to measurement error as well as to variation of air-void content within the section. Because of the extreme values in these two sections, the OGAC and RAC-O mixes less than one year old have greater variation than the mixes in other categories.

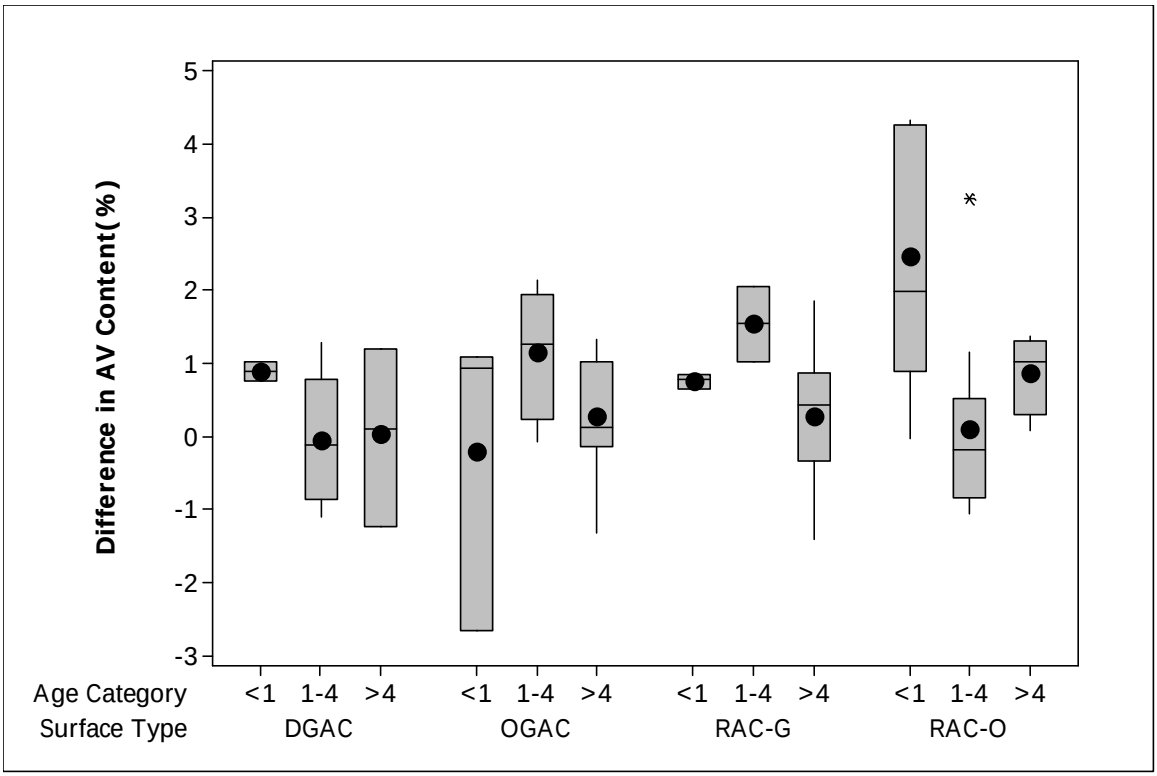

Figure 46: Difference in air-void content between first-year and second-year measurements for different mix types at different ages (positive values indicate a reduction in air-void content).

5.2.2 Air-Void Content Determination by CT Scan

CT scan measurements were conducted on the 100-mm diameter cores taken from 10 sections, from both environmental and experimental design sections. Two cores from each section were analyzed. Table 13 compares the air-void content of the surface layer as determined by two methods: CT scanning and CoreLok. For open-graded mixes, the two methods generally gave similar results, although a few sections show large differences. However, for dense-graded and BWC mixes, the differences between the CT scan and CoreLok air-void content results are nearly always large. The results for open-graded mixes may be more similar because the air voids present in open-graded mixes are greater than 0.4 mm in diameter, which the CT scan is able to detect. The large differences between the air-void content measured by the two methods for the dense- and gap-graded mixes may occur because these mix types contain primarily voids with smaller diameters that are not revealed by CT scanning.

Table 13: Comparison of Air-Void Content by CT Scan and CoreLok Methods

Core Number	AC Type	Age	Measurement Method	Air-Void Content
01-N114C	Dense-graded AC	5	CT Scans	1.26
			CoreLok	8.51
01-N114RW	Dense-graded AC	5	CT Scans	1.11
			CoreLok	8.27
06-N434C	Dense-graded AC	6	CT Scans	2.45
			CoreLok	4.10
06-N434RW	Dense-graded AC	6	CT Scans	1.46
			CoreLok	Not tested
ES-7C	BWC	3.5	CT Scans	0.54
			CoreLok	6.95
ES-7RW	BWC	3.5	CT Scans	3.56
			CoreLok	5.95
01-N104C	OGAC	5	CT Scans	11.19
			CoreLok	17.61
01-N104RW	OGAC	5	CT Scans	13.63
			CoreLok	15.46
01-N105C	OGAC	5	CT Scans	23.65
			CoreLok	21.81
01-N105RW	OGAC	5	CT Scans	24.27
			CoreLok	21.16
06-N467C	RAC-O	3	CT Scans	14.28
			CoreLok	17.10
06-N468RW	RAC-O	3	CT Scans	14.95
			CoreLok	21.65
ES-1C	OGAC	3.5	CT Scans	11.01
			CoreLok	12.40
ES-1RW	OGAC	3.5	CT Scans	9.52
			CoreLok	9.40
ES-3C	OGAC	3.5	CT Scans	9.79
			CoreLok	15.20
ES-3RW	OGAC	3.5	CT Scans	9.88
			CoreLok	10.32
ES-5C	RAC-O	3.5	CT Scans	9.62
			CoreLok	11.81
ES-5RW	RAC-O	3.5	CT Scans	8.15
			CoreLok	13.00
ES-10C	EU-GG	0.5	CT Scans	17.99
			CoreLok	11.92
ES-10RW	EU-GG	0.5	CT Scans	15.93
			CoreLok	11.61

5.3 Evaluation of Clogging

5.3.1 Field Permeability Measurements

Clogging was evaluated from field measurements by examining the difference in permeability values between the center of the lane and the right wheelpath and also by examining the difference in permeability between the first-year and second-year measurements of the center-of-the-lane permeabilities. Clogging was defined as a reduction in permeability between the wheelpath and the centerline of the lane, or between one year and the next at the centerline of the lane. Figure 47 shows the clogging variation of different mix types. As the figure shows, the difference between the center and right wheelpath values for RAC-G and DGAC mixes is very close to zero. Therefore, clogging analysis was conducted only on the OGAC and RAC-O mixes.

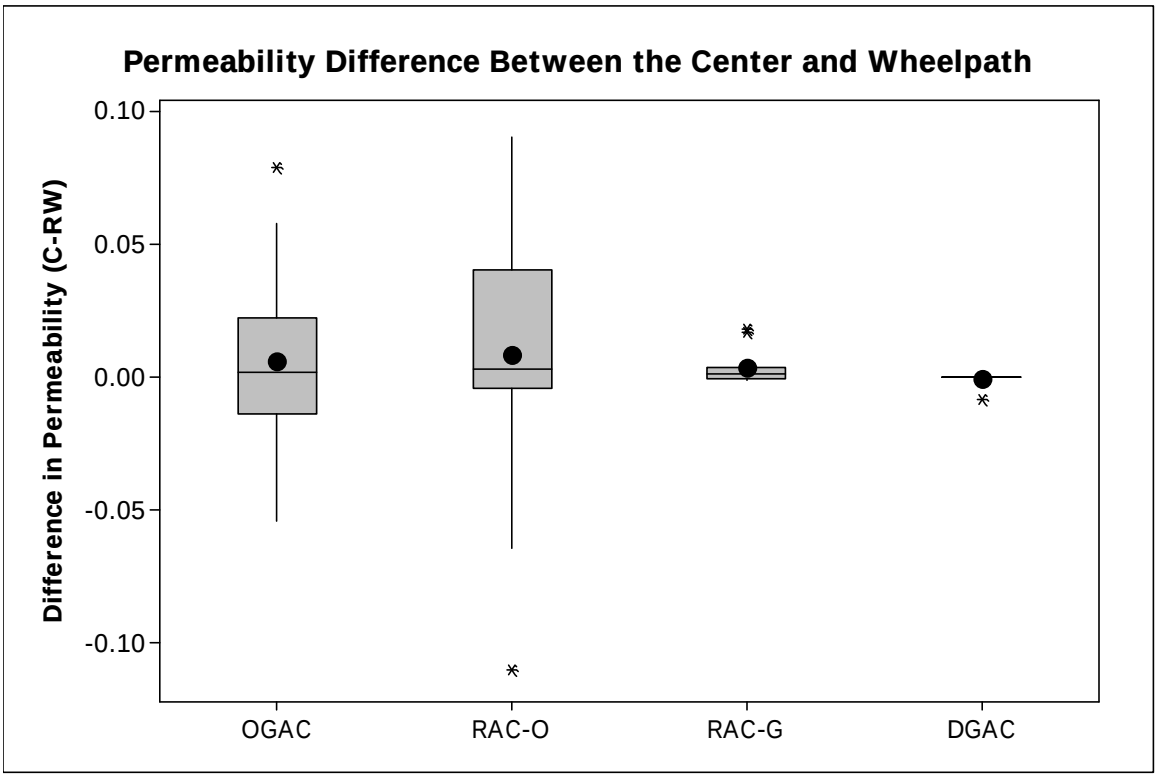

Figure 47: Permeability difference between the center and the right wheelpath for different mix types (positive value indicates greater permeability in the center of the lane than in the wheelpath).

QP-51 was not included in the clogging analysis since the difference in permeability may be due to the compaction difference between the two lanes in which measurements were made rather than to traffic. When QP-51 was cored, Lane 2 was placed the day before the coring and Lane 3 was placed the same day. Sand was placed on the lanes so the permeability measurements were conducted on the only nonsanded areas available: the wheelpaths of Lane 2 and Lane 3. Lane 2 measurements were evaluated as

wheelpath measurements since Lane 2 was under traffic for one day, and Lane 3 measurements were evaluated as center measurements.

Because of the small data set, one variable was evaluated at a time. Table 14 shows the ordinary least squares (OLS) regression models. The coefficient of the explanatory variable and the constant term along with and their p-values and the coefficient of determination (R^2) for each model are given in the table. The dependent variable is the permeability difference between the center and the right wheelpath. A log transformation was applied to cumulative rainfall variables since the variance of error terms was not constant. The p-values less than 0.05 are shown in bold.

The regression analysis revealed that the variances of the error terms of the temperature and AADT variables are not constant and cannot be corrected by transformations. To correct the unequal variance of error terms, weighted least squares regression was applied. Table 15 shows the coefficients and the p-values of explanatory variables. Since the weighted least squares regression is performed through the origin, there is no constant term. The Minitab software does not provide R-squared values for models without an intercept. For regression through the origin, R-squared analysis measures the proportion of the variability in the dependent variable about the origin explained by regression. Therefore, R-squared values for models without intercepts cannot be compared with R-squared values for models with intercepts.

Speed effects could not be evaluated since most of the sections are on highways with speed limits of 60 to 65 mph (97 to 105 km/h), and fast traffic. ESALs were not included as independent variables since there are few open-graded sections with high ESALs.

Table 14: Regression Analysis of Clogging

Model Number	Explanatory Variable			Constant Term	R^2 (%)
	Name	Coefficient	p-value		
1	Air-Void Content (%)	0.0034	**0.04**	–0.047	10.3
2	Air-Void Difference between C and RW	0.0055	**0.04**	0.00099	10.1
3	Age	–0.0043	0.07	0.024	7.9
4	Rubber Inclusion	0.0019	0.87	0.0061	0.1
5	Fineness Modulus	–0.0018	0.92	0.016	0.0
6	C_u	–0.00042	0.63	0.012	0.6
7	NMAS (mm)	–0.0022	0.32	0.036	2.7
8	Average Annual Rainfall (mm)	–0.000008	0.53	0.013	1.0
9	log (Age × Average Annual Rainfall)	–0.038	**0.01**	0.129	15.4
10	Average Annual Wet Days	–0.000046	0.69	0.011	0.4
11	log (Age × Average Annual Wet Days)	–0.039	**0.01**	0.098	15.0
12	N.D. > 10 mm	–0.00030	0.52	0.013	1.1
13	log (Age × N.D. Prec). > 10 mm	–0.030	**0.03**	0.058	11.5
14	N.D. > 20 mm	–0.0004	0.52	0.011	1.1
15	log (Age × N.D. Prec.) > 20 mm	–0.028	**0.02**	0.046	12.4
16	AADTT	0.030	**0.03**	0.00049	11.5
17	Presence of Bleeding	–0.008	0.51	0.0088	1.1

Table 15: Weighted Least Squares Regression Analysis of Clogging

Model Number	Explanatory Variable			Constant Term	R^2 (%)
	Name	Coefficient	p-value		
18	Average Annual Maximum Daily Air Temp (°C)	0.000472	0.81	-	-
19	Annual Number of Days > 25°C	0.0000115	0.93	-	-
20	Age × Annual Number of Days > 25°C	–0.000015	0.15		-
21	Annual Number of Days > 30°C	0.000186	0.17	-	-
22	Age × Annual Number of Days > 30°C	–0.000022	0.21	-	-
23	Annual Degree-Days > 30°C	0.0000025	0.43	-	-
24	Age × Annual Degree-Days > 30°C	0.0000009	0.07	-	-
25	AADT	0.00000004	0.96	-	-

Regression analysis revealed that the air-void content, air-void content difference between the wheelpath and the center, cumulative rainfall, cumulative number of days with rainfall, cumulative number of days with rainfall above 10 mm, and cumulative number of days with rainfall above 20 mm, and AADTT were significant variables affecting the clogging of open-graded mixes. The greater the air-void content, the greater the clogging since there are more voids to be filled. As the air-void content difference between the center and the right wheelpath increases, the clogging increases. This increase may be due to densification in the wheelpath under traffic. Densification in the wheelpath would result in less air-void content, and hence lower permeability values. The cumulative rainfall (since construction) of the pavement reduces the clogging. The rainfall may keep the air voids open and prevent clogging. Higher truck volumes (greater than 1,750) were found to increase clogging. This increase may be due to densification of the wheelpath under heavy truck traffic, resulting in less air-void content and permeability.

It was expected that the sections that show bleeding would have less air-void content in the wheelpath, and hence lower permeability and more clogging; however, observed bleeding was not found to have any effect on clogging. This result may have been obtained because only 5 sections out of 69 show bleeding. No correlation was found between clogging and air temperatures either.

Clogging was also evaluated as the difference in the permeability values between the first year and the second year. Wheelpath permeability differences and center permeability differences between the two years were evaluated separately.

Because of the small data set, one variable was evaluated at a time. Table 16 shows the ordinary least squares (OLS) regression models. The coefficient of the explanatory variable and the constant term along with their p-values and the coefficient of determination (R^2) for each model are given in the table. The dependent variable is the center permeability difference between the first year and the second year. However, no variable was found to significantly affect the difference in center permeability.

Table 16: Regression Analysis of Clogging for the Center of the Lane

Model Number	Explanatory Variable			Constant Term	R^2 (%)
	Name	Coefficient	p-value		
1	Air-Void Content Difference in Center	0.0021	0.34	0.013	2.6
2	Age (first-year coring)	–0.043	0.22	0.052	4.2
3	Rubber Inclusion	0.008	0.30	0.008	3.1
4	Fineness Modulus	0.006	0.63	–0.019	0.7
5	C_u	0.0001	0.85	0.010	0.1
6	NMAS	0.0013	0.37	–0.0044	2.3
7	Amount of Rainfall Since Phase I Coring (mm)	–0.000016	0.14	0.0203	6.2
8	Number of Wet Days Since Phase I Coring	0.0000039	0.95	0.011	0.0
9	N.D. > 10 mm since Phase I Coring	–0.00066	0.08	0.02	8.5

To correct the unequal variance of error terms, weighted least squares regression was conducted for the temperature and AADT independent variables. Table 17 shows the coefficient and the p-values of those explanatory variables. The dependent variable is the center permeability difference between the first year and the second year. The significant variables are shown in bold. The study found that as the number of days with temperatures above 25°C increases, the permeability difference decreases. The lower permeability difference means less clogging; therefore, the regression results suggest that sections experiencing higher temperatures are less susceptible to clogging. However, it was expected that at high temperatures more particles would stick to the asphalt and the mix would tend to densify more, hence increasing the clogging. No explanation can be given regarding why the observed relationship does not match the expected relationship.

Table 17: Weighted Least Squares Regression Analysis of Clogging for the Center of the Lane

Model Number	Explanatory Variable			Constant Term	R^2 (%)
	Name	Coefficient	p-value		
10	Average Annual Maximum Daily Air Temp (°C)	–0.0020	0.18	-	-
11	Annual Number of Days > 25°C	–0.00017	0.02	-	-
12	Annual Degree-Days > 30°C	–0.000028	0.09	-	-
13	AADT	0.0000017	0.12	-	-

Clogging was also evaluated as the difference between first-year and second-year wheelpath permeability measurements. Table 18 shows the ordinary least squares (OLS) regression models. The

coefficient of the explanatory variable and the constant term along with their p-values and the coefficient of determination (R^2) for each model are given in the table. The dependent variable is the wheelpath permeability difference between the first year and the second year. No variable was found to be significant.

Table 18: Regression Analysis of Clogging in Wheelpath

Model Number	Explanatory Variable			Constant Term	R^2 (%)
	Name	Coefficient	p-value		
1	Air-Void Content Difference in WP	0.0-016	0.73	0.0032	0.3
2	Age	–0.0037	0.94	0.0075	0.0
3	Rubber Inclusion	–0.0000001	1.00	0.0041	0.0
4	Fineness Modulus	0.0022	0.89	–0.0077	0.1
5	C_u	0.00071	0.34	–0.0044	2.7
6	NMAS	0.0027	0.16	–0.030	5.7
7	Amount of Rainfall Since Phase I Coring (mm)	–0.0000085	0.56	0.00847	1.0
8	Number of Wet Days Since Phase I Coring	0.000083	0.32	–0.0046	2.9
9	N.D. > 10 mm Since Phase I Coring	–0.00051	0.32	0.0109	2.8
10	AADTT	–0.0049	0.71	0.0052	0.4

Because of the unequal variance of error terms, weighted least squares regression was performed for the temperature and AADT independent variables. Table 19 shows the coefficient and the p-value of explanatory variables. The dependent variable is the wheelpath permeability difference between the first year and the second year. The significant variables are shown in bold. The study found that as the number of days with temperatures above 25°C and degree-days above 30°C increases, the permeability difference decreases. Again, no explanation can be given for the finding that clogging decreased with increasing temperatures.

Table 19: Weighted Least Squares Regression Analysis of Clogging in Wheelpath

Model Number	Explanatory Variable			Constant Term	R^2 (%)
	Name	Coefficient	p-value		
11	Average Annual Maximum Daily Air Temp (°C)	–0.00019	0.08	-	-
12	Annual Number of Days > 25°C	–0.00055	**0.00**	-	-
13	Annual Degree-Days > 30°C	–0.00010	0.00	-	-
14	AADT	0.0020	0.82	-	-

5.3.2 CT Scan

CT scan measurements were conducted at the Swiss Federal Roads Laboratory (EMPA) in Zurich on the 100-mm diameter cores taken from 10 sections. Figure 48 shows an example of the CT scan images taken from an open-graded mix (01-N105). The dark areas are the air-void content, and the lighter areas are the aggregate and the binder. Air-void content was calculated as the ratio of the dark volume to the total volume of the asphalt core. The scan measurements were taken starting from the interface and moving to the surface for every 0.3 mm throughout the thickness. However, since the thickness of the surface layer was not the same everywhere, the interface was not parallel to the surface. Therefore, the distance of the layers from the surface shown in the scan tests may be different than the actual distances from the surface.

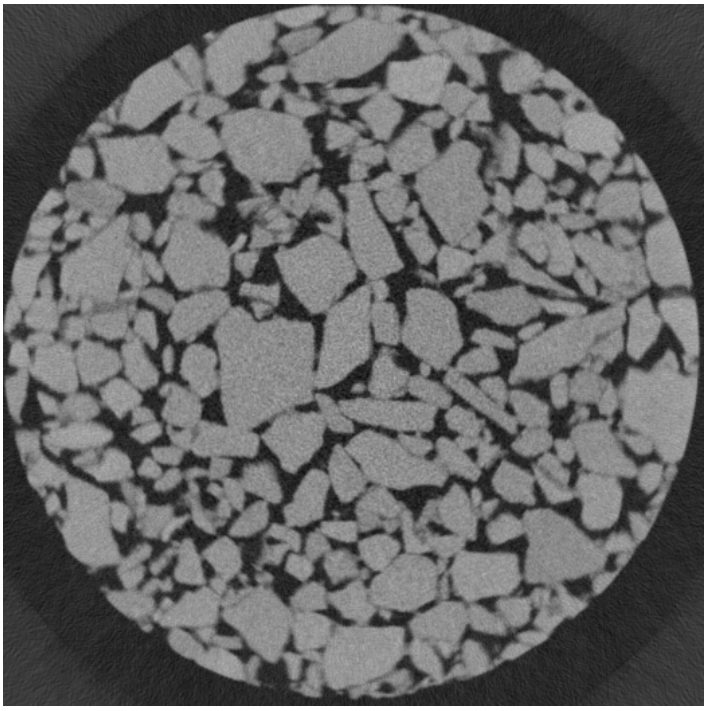

Figure 48: CT scan image of an open-graded mix (top view).

Figure 49 shows the air-void content distribution (for voids with diameters larger than 0.4 mm) throughout the surface layer of OGAC and RAC-O mixes and the European gap-graded ES section mix (EU-GG), and Figure 50 shows the distribution for DGAC mixes. The figures show that the air-void content generally increases moving from top to bottom for open-graded mixes but does not vary much for dense-graded mixes.

Figure 51 shows the air-void content distribution trend for the open-graded and EU-GG mix through the thickness of the surface layer. All the sections subjected to CT scanning except ES-1 and ES-3 show higher air-void content at the bottom of the layer than at the top. The lower air-void content at the top part of the surface layer that is seen for the rest of the mixes suggests that there is accumulation of sand and fine particles at the top part of the surface layer, which supports the results of Bendtsen (30). The higher air-void content seen at the top section of the cores of the ES-1 and ES-3 sections may be due to the thickness effect (these sections are about twice as thick as the other sections), since these mixes have the same gradation and properties as other open-graded mixes. Thicker mixes may be less clogged, or fine particles may accumulate further down from the surface. The effect of thickness on clogging could not be evaluated in this study as the majority of open-graded mixes have thicknesses less than 30 mm. Therefore, a sample of open-graded mixes with different thicknesses is needed to fully evaluate the effects of thickness on the clogging.

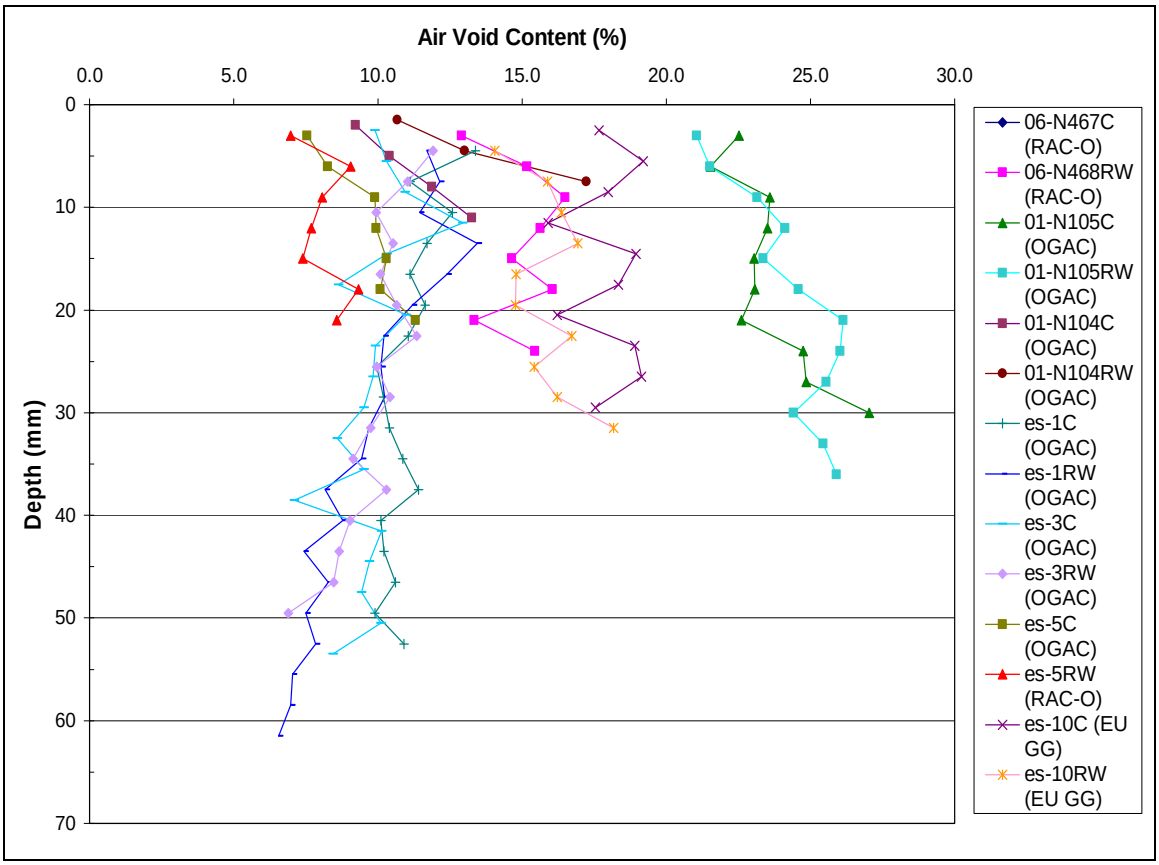

Figure 49: Air-void distribution of open-graded mixes and EU gap-graded mix through the thickness of the surface layer.

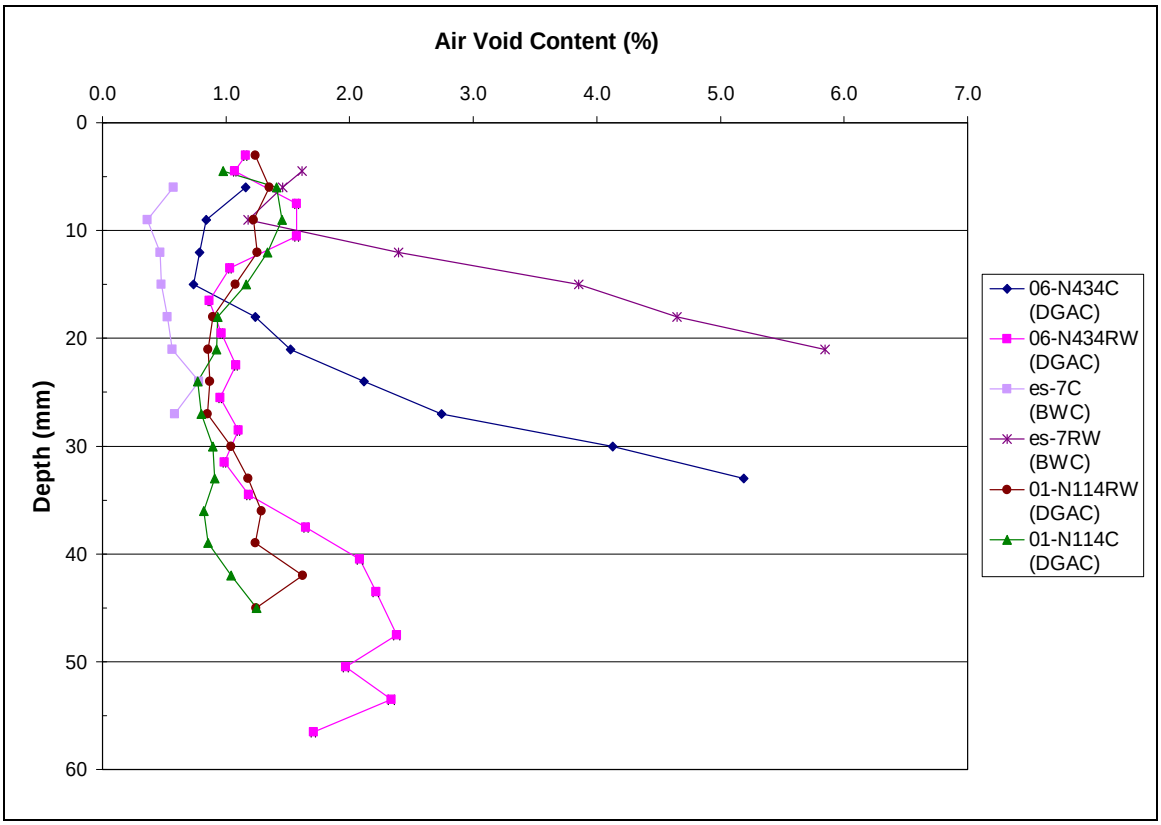

Figure 50: Air-void distribution of dense-graded mixes and BWC mix through the thickness of the surface layer.

There is no clear trend showing that clogging takes place at the top 20 to 25 mm of the surface layer of open-graded mixes. This lack of a discernable trend may be because the thickness of open-graded mixes is usually approximately 30 mm. However, there is some indication that clogging takes place at the top part of the surface layer for thin layers since the air-void content tends to increase moving from top to bottom.

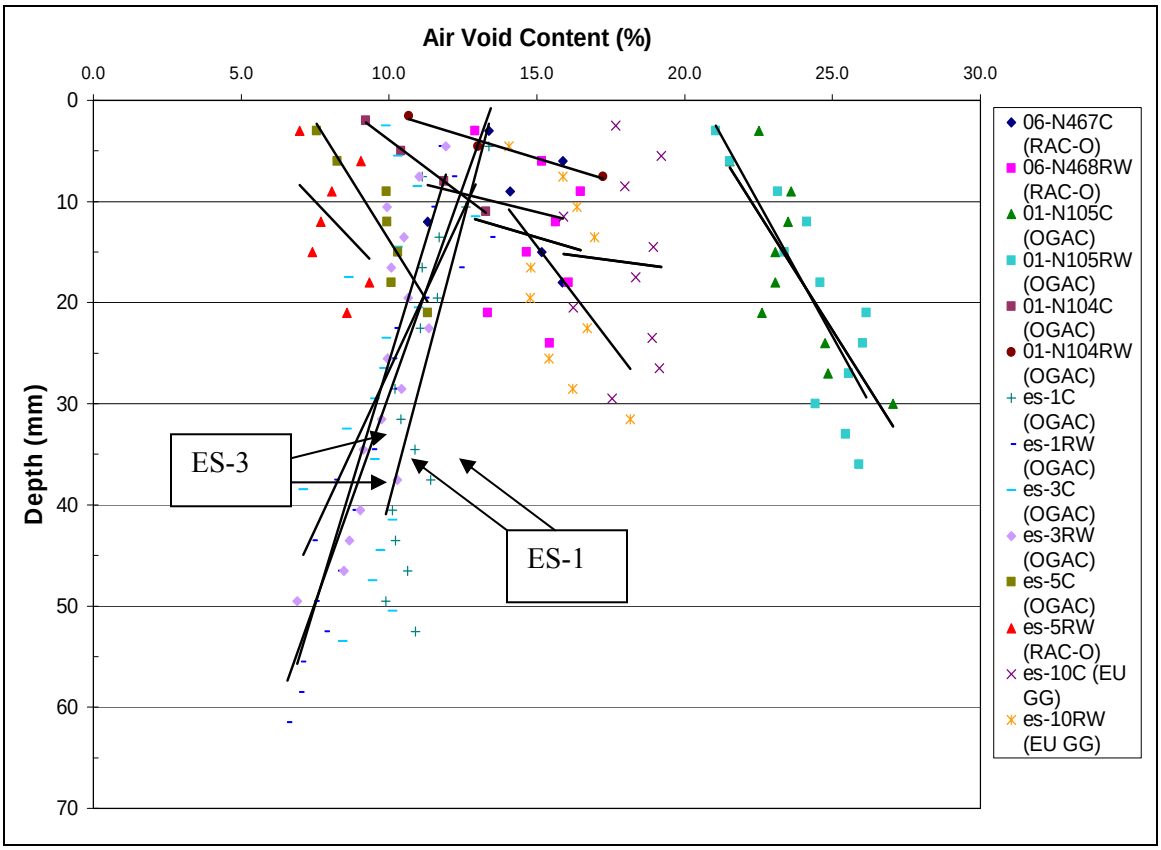

Figure 51: Air-void content trend for open-graded mixes and EU gap-graded mix through the thickness of the surface layer.

5.4 Summary of Findings

- Open-graded mixes have permeabilities greater than those of dense- and gap-graded mixes.
- OGAC and RAC-O mixes have similar permeability values.
- Open-graded mixes lose their permeability with time. However, even after eight years, they still have permeability values greater than those of gap- and dense-graded mixes.
- RAC-G mixes in the first year after construction have permeability values close to those of older open-graded mixes; however, the RAC-G permeability values become similar to those of DGAC within three to four years after construction.
- The permeability difference between the wheelpath and the centerline (between the wheelpaths) and the permeability difference between two years of measurements were compared as to assess clogging due to traffic and outside material. Contrary to the findings of Sandberg (10), the center of the lane was found to be more permeable than the wheelpath. Therefore, traffic was not found to help keep the air voids open. This effect may result from reduction in the air-void content in the wheelpath due to densification under traffic rather than from clogging of the air voids with

fine particles. The European experience cited by Sandberg found that fine particles clog the center of the lane, and suction caused by high-speed traffic when the pavement is wet cleans the particles in the wheelpaths. The preliminary finding in California is that traffic does not appear to reduce clogging in the wheelpaths.

- Analysis of CT scans of a small sample of cores showed that air-void content increases moving from top to bottom for thin open-graded mixes. All the open-graded sections scanned except ES-1 and ES-3 have higher air-void content at the bottom of the layer than at the top, indicating some clogging at the upper part of the surface, which may be due to compaction. The four cores from two sections, ES-1 and ES-3, which show an opposite trend are at least twice as thick as the other cores. The ES-1 and ES-3 sections are the OGAC mixes at the LA 138 site. They have the same NMAS, traffic, and climate as the RAC-O section of the LA 138 site (ES-5) and similar air-void content. The only differences between the ES-1 and ES-3 sections and the ES-5 section are in the mix type (OGAC versus RAC-O) and thickness. The ES-1 and ES-3 sections also have mix design properties similar to those of other OGAC mixes tested for clogging. However, reduction in air-void content with depth was not observed for any of the other OGAC mixes. Therefore, a weak preliminary conclusion of the study is that thicker mixes may be less clogged, or less clogged at the upper part of the surface layer, compared to thinner mixes.
- Clogging was evaluated as the permeability difference between the wheelpath and the centerline. Regression analysis results were extremely weak, with high p-values and low R^2 values. Clogging, evaluated as the difference from year to year in the wheelpath, did have a low p-value for sections that experience higher temperatures, indicating statistical significance. However, this relationship may not be causal.
- The NMAS and binder type were not found to affect clogging in the regression analysis, although the findings of Morgan et al. suggested that the mixes with larger aggregate sizes would be less prone to clogging. The reason that the NMAS was not found to be significant may be because most of the open-graded mixes have an NMAS of 12.5 mm.
- Regression analysis of permeability showed that permeability decreases with age and increasing surface area, and it increases with increasing air-void content and coarser gradation, confirming the results of the earlier studies. Additionally, open-graded mixes have higher permeability values than dense- and gap-graded mixes at a given air-void content and age. This greater permeability may be due to the greater interconnection of the air voids in open-graded mixes than in DGAC and RAC-G mixes with the same air-void content. NMAS and thickness were not found to affect the permeability values when all the mix types were pooled together, which contradicts the results found in the literature. The study showed that open-graded mixes with an NMAS of 12.5 mm

have higher permeability values than those with an NMAS of 9.5 mm, while open-graded mixes with an NMAS of 19 mm, which are the F-mixes, have lower permeability values than mixes with an NMAS of 12.5 mm. This difference may occur because all the F-mixes are older, whereas the other open-graded mixes include younger sections, although this conclusion is speculative. The F-mixes are also all in high-rainfall areas, while the other open-graded mix sections are distributed across different rainfall areas. Since NMAS and thickness specifications are different for different mix types, the thickness and NMAS effects may be different within each mix type.

- Almost all the open-graded mixes satisfy the European minimum permeability requirement of 0.01 cm/sec. However, only half of the open-graded mixes that are less than a year old satisfy the minimum permeability requirement of 0.11 cm/sec set by Switzerland. The literature survey indicated that not much information is available regarding the minimum permeabilities required for good performance of open-graded mixes. As Ferguson states, "Some sort of [hydrologic] modeling is almost inescapable in the design of porous pavements that must meet quantitative hydrologic performance criteria." Ferguson also states that there is a great deal of argument over the infiltration capabilities required of pavement surfaces for different rainfall events. The permeability and thickness required of open-graded mixes for near-complete drainage of the pavement surface has not been determined for typical critical storm events in different climate regions of California.

6 EVALUATION OF SKID RESISTANCE (FRICTION) OF ASPHALT CONCRETE MIXES

This chapter compares the skid resistance (friction) of different mix types and investigates the factors affecting skid resistance. Friction is evaluated in terms of microtexture (BPN), macrotexture (MPD), and International Friction Index (IFI).

This chapter answers these questions:

- Do open-graded mixes have lower friction values than dense-graded and gap-graded mixes?
- Do all asphaltic mixes provide satisfactory BPN?
- What are the pavement characteristics that affect microtexture (BPN)?
- How do traffic and climate affect microtexture?
- Do open-graded mixes in California have negative or positive texture?
- What are the pavement characteristics that affect macrotexture (MPD)?
- How do traffic and climate affect macrotexture?

6.1 Microtexture

As noted in Section 3.2.4 of this report, a minimum British Pendulum Number (BPN) of 45 was considered to be acceptable friction based on a criterion discussed in a Caltrans research document believed to have been written in the 1960s (15), which was the only comparison found relating California Test Method 342 (CT Method 342) to other test methods. It must be emphasized that this criterion is not an official specification of Caltrans and was used only for comparison purposes in this study. Other research is being conducted by UCPRC and others relating the BPN to the Dynamic Friction Tester (DFR), Circular Texture Meter (CTM), and CT Method 342. The BPN was used for this study because of delays in obtaining DFT and CTM devices at the start of the project, and it continued to be used to maintain consistency across the entire two-year study. It is not the intention of this study to advocate the use of BPN.

In every test section, microtexture was measured in the first year using the British Pendulum Tester next to each of the 12 cores taken: 6 in the wheelpath and 6 between the wheelpaths. The number of tests in each section was reduced in the second year to 6: 3 in the wheelpath and 3 between the wheelpaths. Each measurement consisted of five repetitions. In the analysis, the last four measurements were averaged to obtain an average BPN for each core location. The standard deviation of BPN at each core location ranges from 0.0003 to 8.8. According to British Standard (BS) 7976, a maximum standard deviation of 3 BPN is recommended for each test location.

The BPN values in this study were corrected for temperature based on research conducted for this project, as is discussed later. The study regarding temperature correction was performed because it was found that the temperature correction in the standard method, BS 7976, is inadequate and incorrect. The new correction results in much more readily repeatable results.

The evaluation of microtexture includes a descriptive analysis of BPN values, modeling of the BPN, and modeling of the difference in BPN values between the first-year and second-year measurements.

6.2 Descriptive Analysis

Figure 52 shows the wheelpath BPNs for OGAC, RAC-O, RAC-G, DGAC, OGAC F-mixes, and RAC-O F-mixes across all age groups. The figure shows no significant difference between the friction values of the different mix types other than the OGAC F-mixes. The figure shows that OGAC F-mixes have the lowest friction values, probably because both OGAC F-mixes are eight years old, older than the average age of the other mix types.

Except for four sections, two DGAC and two OGAC F-mixes, all mixes satisfy the minimum BPN criterion of 45 used for comparison purposes for this project. The four mixes that do not meet the requirements all are older than five years. The BPNs for these sections may be lower because the aggregates are polished under traffic over time or because less polish-resistant aggregates are used; the aggregate sources of the mixes were not identified in this study, however; therefore, their polish resistance is unknown.

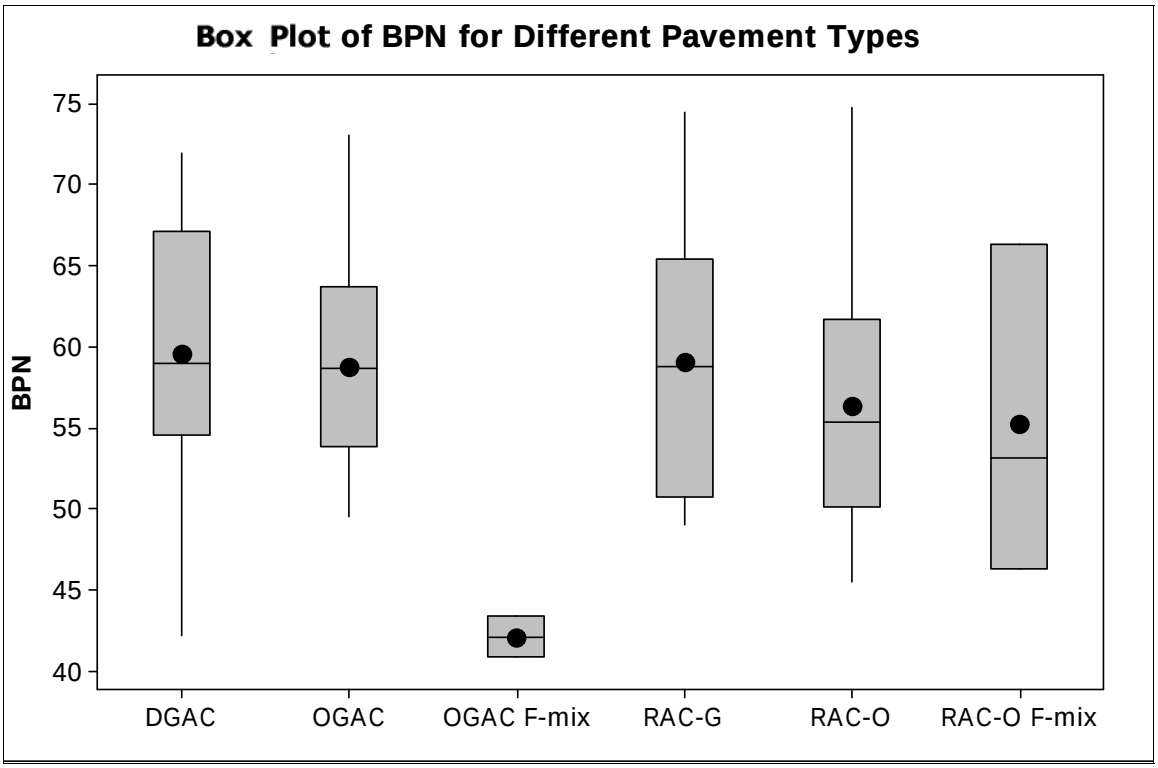

Figure 52: Box plot of BPNs for different mix types including all ages.

Figure 53 shows the wheelpath BPNs for different mix types at different ages without the F-mixes. The figure shows that friction is lower for the DGAC mixes in the greater-than-four-years-old group, however, note that the mixes in different age categories are from different sections, and mixes in that group may have had lower as-built friction values. Generally, all mix types have friction values better than satisfactory in their first years; even most of the older sections satisfy the minimum criterion.

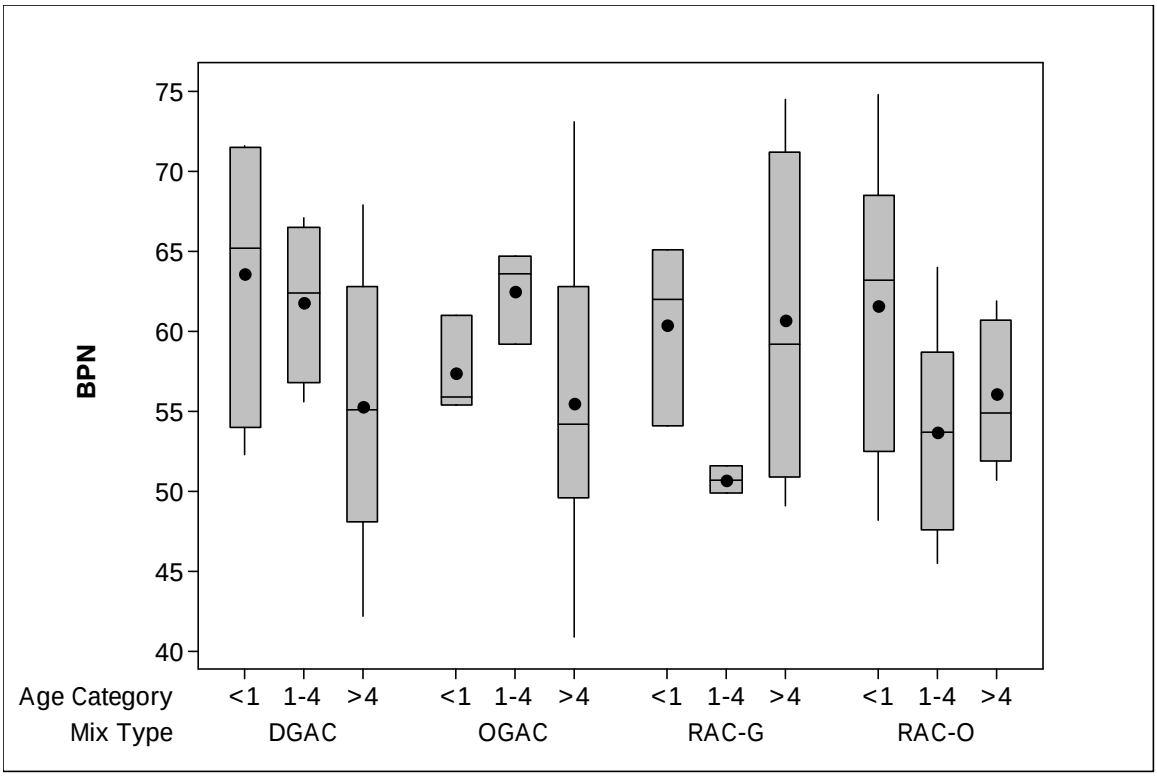

Figure 53: Box plot of BPNs for different mix types at different ages.

Figure 54 compares the wheelpath BPN values for the first year and the second year. Only the sections where BPN measurements were conducted for both the first and second years are shown in the figure. The figure shows that the BPN values of DGAC and RAC-G mixes did not change in a year. The BPN values of OGAC mixes less than one year old decreased, and the BPN values of older OGAC mixes increased in a year. The BPN values of RAC-O mixes increased slightly in one year. Except for one section in the RAC-O age category of one to four years, all the mixes that are less than five years old have BPN values above 45, indicating sufficient friction. Figure 55 shows the difference in BPN values for different mixes at different ages. The figure shows that the average difference is very close to zero, except for OGAC mixes less than a year old, which have an average reduction in BPN of 6 in a year.

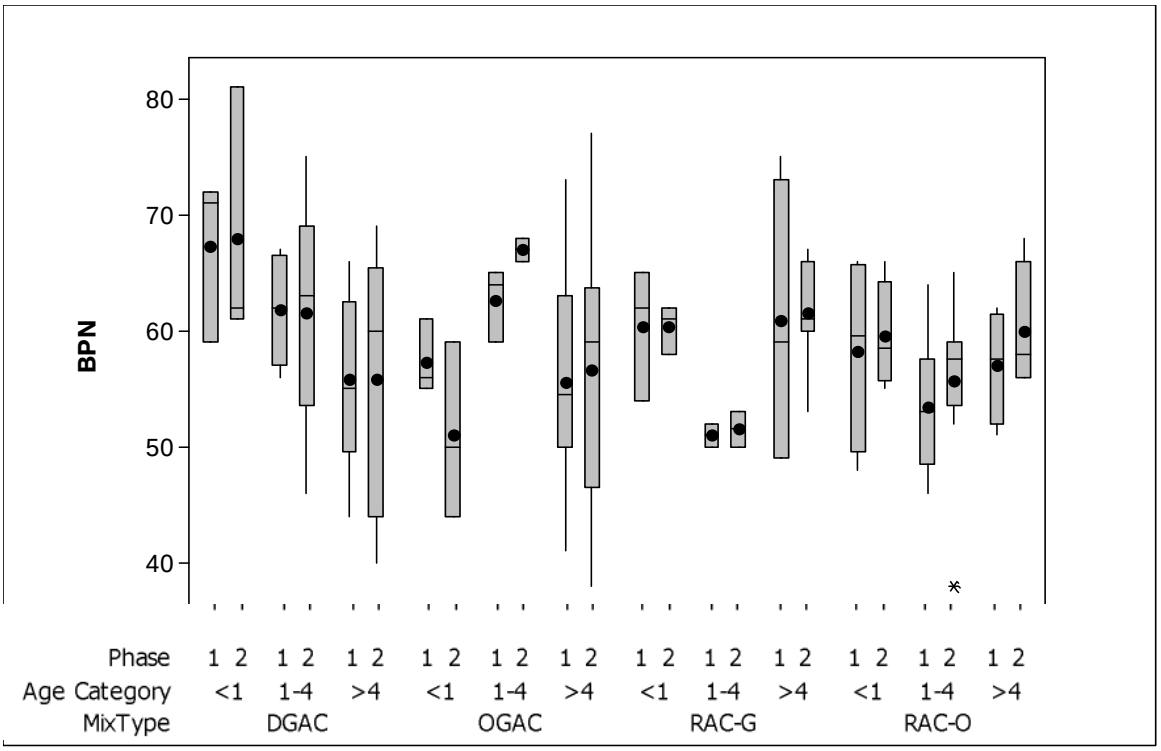

Figure 54: Comparison of BPNs for different mix types at different ages for first and second years.

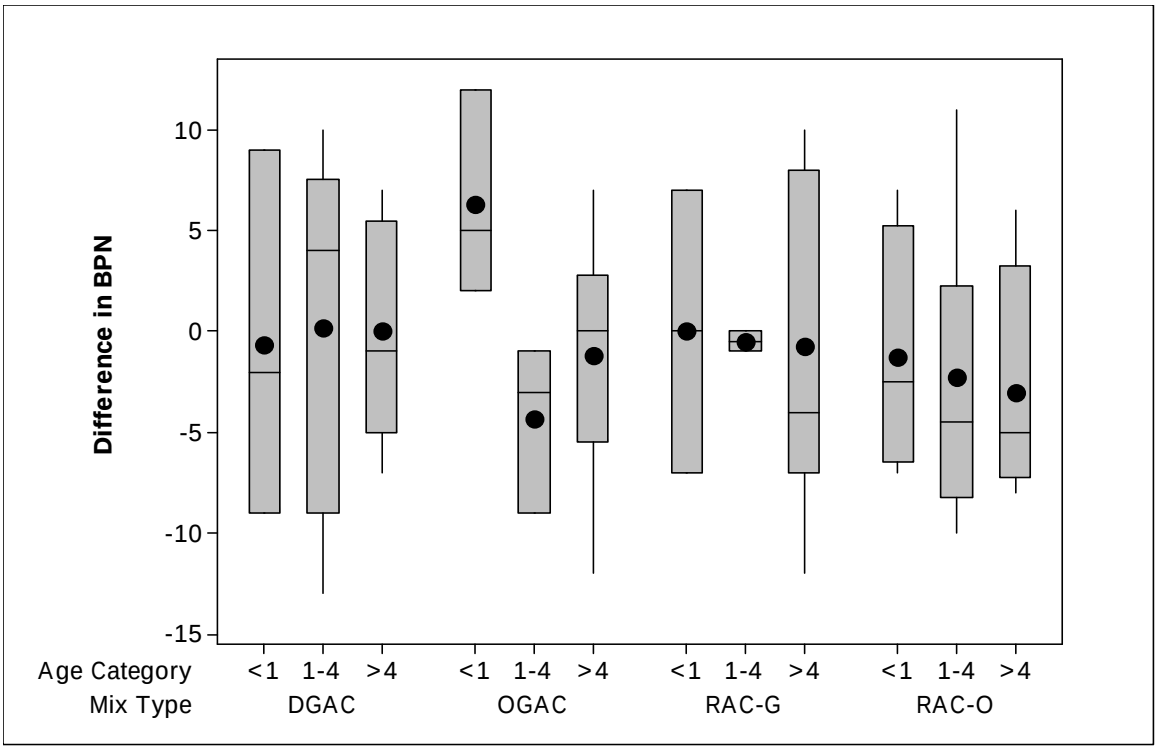

Figure 55: Difference in BPNs between first-year and second-year measurements for different mix types at different ages (positive values indicate reduction in friction).

6.3 Correction of British Pendulum Numbers for Temperature

BPNs are sensitive to pavement and air temperatures. The British Standard method (BS 7976) specifies corrections to adjust the friction values to 20°C. However, BS 7976 provides corrections for pavement temperatures only up to 35°C, and pavement temperatures in California commonly exceed 35°C during the summer. Therefore, a new temperature correction equation was developed by UCPRC (108). British Pendulum tests were conducted at five parking lot pavements at pavement temperatures of 13, 17, 20, 25, 32, 37, 42, and 47°C. The temperature effect on the BPN values from Steven (108) is given in Equation (9).

$$\Delta BPN = 0.466(T - 20) \quad \textbf{(9)}$$

From Equation 9, and assuming that the BPN measured at 20°C is correct, the form of the relationship suggested by Oliver (48) was applied to the UCPRC data as shown in Equation (10).

$$BPN_{20} = \frac{BPN_T}{1 - \alpha(T - 20)} \quad \textbf{(10)}$$

The value of α was determined for each of the five sets of data and then averaged to give a value of 0.00662. The resulting equation is given in Equation (11).

$$BPN_{20} = \frac{BPN_T}{1 - 0.00662(T - 20)} \quad \textbf{(11)}$$

The α values ranged from 0.00454 to 0.00803, a range that spans the value of 0.00525 provided by Oliver (48). Given the wider range of BPNs and temperatures from the study by Oliver (48), a weighted average of the UCPRC and Oliver numbers, using weighting factors of 0.67 and 0.33 respectively, was calculated and found to be 0.0062.

The final model developed to adjust the BPNs to 20°C is presented in Equation (12).

$$BPN_{20} = \frac{BPN_T}{1 - 0.0062(T - 20)} \quad \textbf{(12)}$$

R^2 = 83%; standard error = 2.3

where T is the pavement temperature in °C.

6.4 Statistical Modeling of Microtexture

Regression analysis was conducted to determine the climate, traffic, and asphalt mix effects on microtexture. Because of the small data set, one variable was evaluated at a time. The coefficient of the explanatory variable and the constant term along with their p-values and the coefficient of determination (R^2) for each model are given in Table 20. The dependent variable is the BPN. The p-values less than 0.05 are shown in bold.

In analyzing traffic effects on microtexture, QP-51 was not included since the section was one day old and did not experience traffic prior to coring.

Table 20: Regression Analysis of Microtexture

Model Number	Explanatory Variable			Constant Term	R^2 (%)
	Name	Coefficient	p-value		
1	Air-Void Content (%)	–0.18	0.33	60.23	1.3
2	Age (years)	–0.70	**0.04**	60.5	5.4
3	Mix Type	–2.82	0.14	59.39	3.0
4	Rubber Inclusion	–1.04	0.58	58.32	0.4
5	NMAS (mm)	–0.53	0.10	65.34	4.0
6	Fineness Modulus	–2.57	0.21	70.94	2.3
7	C_u	0.04	0.45	57.02	0.9
8	Average Annual Rainfall (mm)	0.003	0.15	55.92	2.9
9	Age × Average Annual Rainfall	–0.0007	0.09	59.46	3.8
10	Average Annual Wet Days	0.006	0.72	57.29	0.2
11	Age × Average Annual Wet Days	–0.006	0.11	59.62	3.5
12	Average Annual Maximum Daily Air Temp (°C)	–0.50	0.18	69.27	2.5
13	Annual Number of Days > 25°C	–0.021	0.22	60.75	2.1
14	Age × Annual Number of Days > 25°C	–0.006	**0.01**	61.07	9.0
15	Annual Number of Days > 30°C	–0.04	**0.04**	60.83	5.8
16	Age × Annual Number of Days > 30°C	–0.01	**0.01**	60.74	9.6
17	Annual Degree-Days > 30°C	–0.001	**0.04**	60.77	5.9
18	Age × Annual-Degree-Days > 30°C	–0.0003	**0.01**	60.68	9.5
19	Annual FT Cycles	0.54	0.77	57.30	0.1
20	log AADT	–0.63	0.78	59.97	0.1
21	AADTT	–5.61	**0.01**	58.74	8.3
22	ESAL	–5.05	**0.04**	58.48	6.0

Mix type, rubber inclusion, and ESALs and AADTT on the coring lane were used as categorical variables, as explained in Chapter 4. Age, number of days above 25°C since the construction of the pavement, number of days above 30°C since the construction of the pavement (Age × Annual number of days > 25°C), annual number of days above 30°C (Age × Annual number of days > 30°C), annual degree-days above 30°C, and total degree-days above 30°C (Age × Annual degree-days > 30°C) experienced by the pavement, AADTT, and ESALs on the coring lane were found to be the significant variables affecting the microtexture. All these variables have negative effects on the microtexture. An increase in age, number of days above 25°C since the construction of the pavement, number of days above 30°C since the

construction of the pavement, total degree-days above 30°C, and ESALs results in a reduction in microtexture. Sections with truck traffic (AADTT on the coring lane) above 1,750 and with ESALs above 800,000 have significantly lower microtexture compared to the sections with lower truck traffic volumes.

Aging effects can be attributed to the effects of climate, primarily exposure to heat and air, as well as the cumulative effects of traffic and climate. The sections that experienced high temperatures over their lifetimes were found to have lower friction values, although the change in BPN over just two years was not apparent, as shown in Figure 54. These lower values may be the result of the embedding of the aggregates under truck traffic loads in the soft binder at high temperatures, reducing contact with the tire. Truck traffic may also be reducing friction by polishing the aggregates.

Figure 56 shows the BPN values versus the log of AADT for different mixes. The red square points represent the open-graded mixes, and the black round points represent the dense-graded mixes. Note that there is no trend between BPN and AADT for either open-graded or dense-graded mixes.

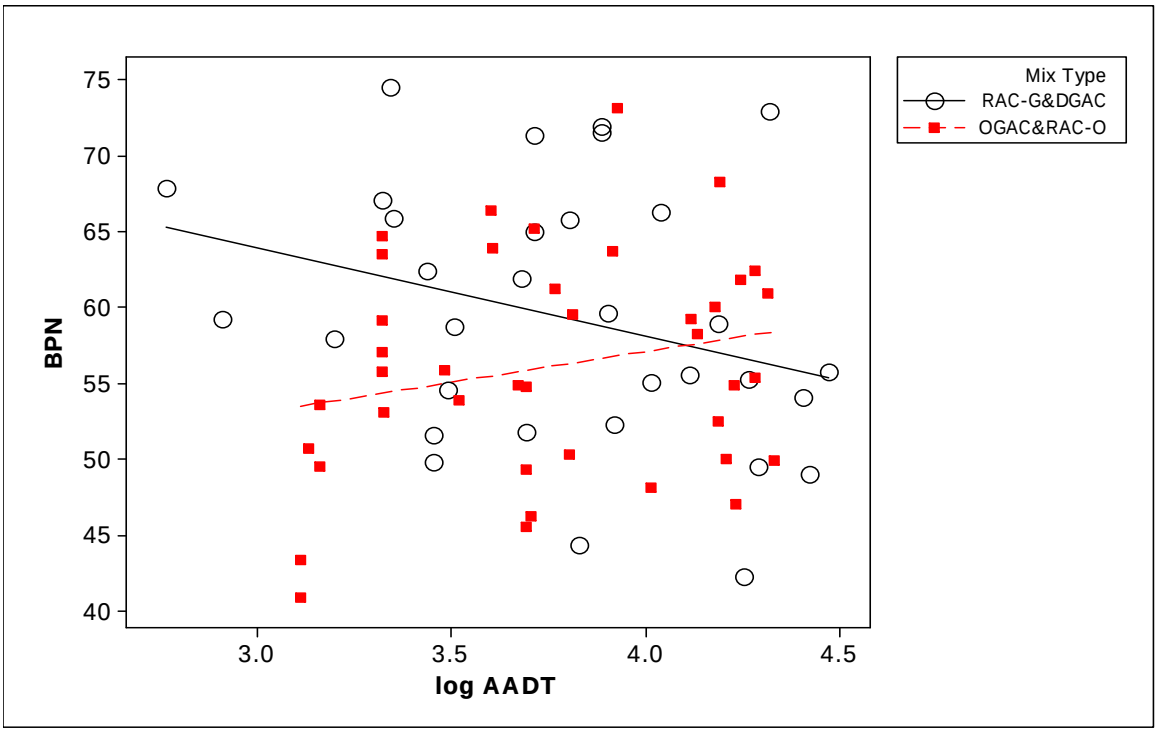

Figure 56: Scatter plot of BPN versus AADT.

The multiple linear regression model using the number of days above 25°C since the construction of the pavement and AADTT as explanatory variables is given in Equation (13). Because of nonconstant residuals, a log transformation was applied to the dependent variable (BPN), and a square-root transformation was applied to the independent variable (number of days above 25°C since the construction of the pavement). The number of days above 25°C since the construction of the pavement

was retained in the multiple regression with a significance level of 0.06 because of the small sample size (meaning a lower ability to estimate effects with precision) and the conceptual relevance of this variable. Only 12.3 percent of the variation in microtexture was explained by the model, perhaps because the model does not distinguish mixes with different aggregate types because the data was not available, although it is well known that aggregate type affects pavement microtexture.

Model for BPN

The regression equation is

$$\log BPN = 1.79 - 0.0398\ AADTT - 0.00140\ (Age \times N.D.\ T > 25)^{0.5} \qquad \textbf{(13)}$$

Predictor	Coef	SE Coef	T	P
Constant	1.79256	0.01715	104.53	0.000
AADTT	–0.03980	0.01660	–2.40	0.019
$(Age \times N.D.\ T > 25)^{0.5}$	–0.0013988	0.0007283	–1.92	0.059

S = 0.0571025 R-Sq = 12.3% R-Sq(adj) = 9.7%

Analysis of Variance

Source	DF	SS	MS	F	P
Regression	2	0.031018	0.015509	4.76	0.012
Residual error	68	0.221727	0.003261		
Total	70	0.252745			

A total of 72 sections were used in the model shown here. The AADTT on the coring lane is either 0 or 1 in the model. The age ranges between 0.003 and 14, and the number of days above 25°C ranges between 1 and 237.

The traffic effects were further evaluated comparing the BPN values at the center and in the right wheelpath of the lane. Both the center and the wheelpath experience the same environmental conditions and have the same mix properties. However, the wheelpath is exposed to traffic, while the center is not. Figure 57 shows the variation in BPN values for the center and the right wheelpath. The difference is most likely caused by polishing of wheelpath aggregates under traffic and embedment of larger aggregates. The difference is not very large, indicating that polishing of aggregates is not a major problem for the sections in the data set.

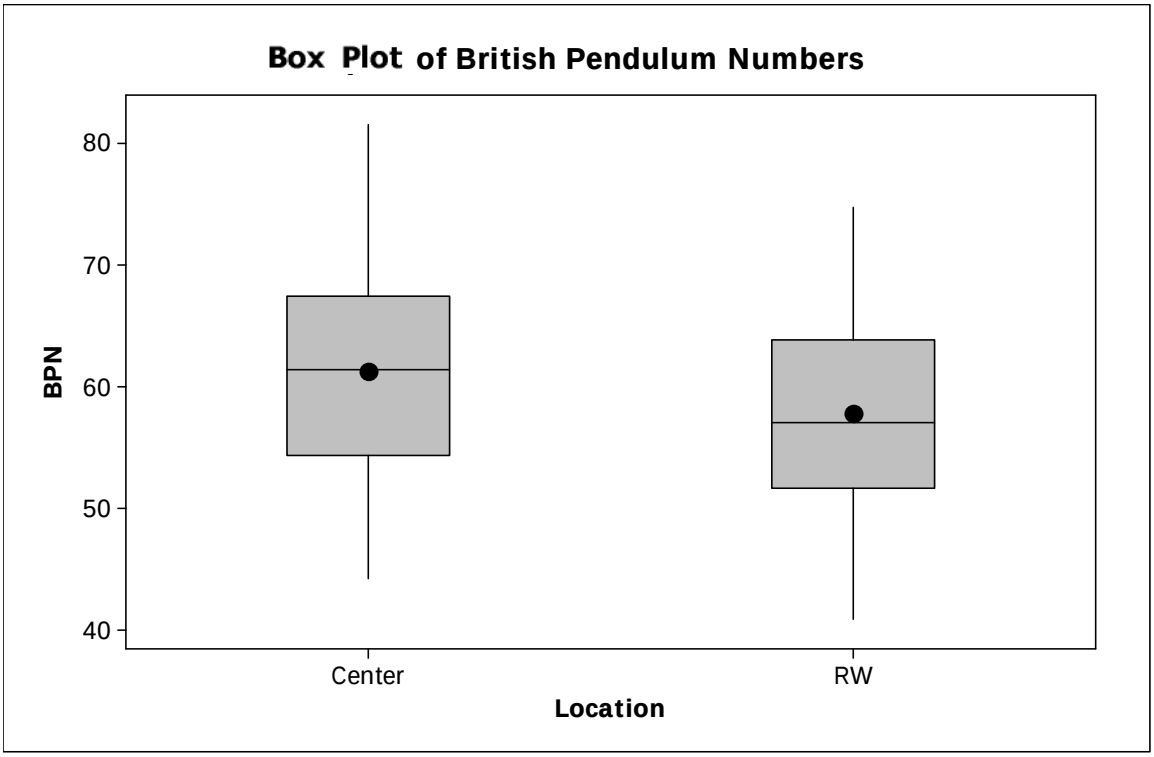

Figure 57: Box plot of BPNs at the center and the right wheelpath.

Further analysis was conducted on the effects of pavement properties, climate, and traffic on the microtexture change. Because of the small data set, one variable was evaluated at a time. The coefficient of the explanatory variable and the constant term along with their p-values and the coefficient of determination (R^2) for each model are given in Table 21. The dependent variable is the difference in BPN between the first year and the second year. A significance level of 0.05 was used in the analysis, and significant variables are shown in bold.

Table 21: Wheelpath BPN Difference

Model Number	Explanatory Variable			Constant Term	R^2
	Name	Coefficient	p-value		
1	Age (first-year coring)	0.015	0.96	–0.93	0.0
2	Age Difference	15.14	**0.02**	–14.65	8.8
3	Mix Type	–1.07	0.52	–0.24	0.7
4	Rubber Inclusion	–1.25	0.44	–0.26	1.0
5	NMAS	0.13	0.64	–2.63	0.4
6	Fineness Modulus	–0.12	0.94	–0.27	0.0
7	C_u	–0.0036	0.95	–0.80	0.0
8	Amount of Rainfall Since Phase 1 Coring	0.0067	**0.00**	–4.50	15.4
9	Number of Wet Days Since Phase I Coring	0.036	**0.00**	–4.85	13.1
10	Average Annual Maximum Daily Air Temp (°C)	–0.377	0.26	7.27	1.8
11	Number of Days > 25°C Since Phase I Coring	–0.005	0.76	–0.81	0.1
12	Number of Days > 30°C Since Phase I Coring	–0.014	0.39	–0.32	1.1
13	Degree-Days > 30°C Since Phase I Coring	–0.004	0.27	0.34	2.0
14	Annual FT Cycles	0.003	0.94	–1.54	0.0
15	log AADT	–0.13	0.91	–0.90	0.0
16	AADTT	–2.81	0.06	–0.19	5.0

Regression analysis revealed that the difference in BPN values between the first year and the second year increases as the age difference (time between the first-year and second-year measurements), amount of rainfall, and number of wet days increase between the two measurements. It can be concluded that higher amounts of rainfall polish the surface and reduce friction.

6.5 Macrotexture

Macrotexture was measured by UCPRC using a profilometer, which has a high-frequency (78 kHz) sampling laser on the right wheelpath, and was reported in terms of mean profile depth (MPD) and root mean square of profile deviations (RMS).

The MPD and RMS values of the test surfaces were evaluated to find out whether the surface has negative, positive, or neutral texture based on the calculation method proposed by McGhee et al. (37). The study found that California mixes all have positive texture.

6.5.1 Descriptive Analysis

Figure 58 shows the variation of macrotexture values for OGAC, RAC-O, RAC-G, and DGAC mixes, with the F-mixes separated from the other RAC-O and OGAC mixes. The figure shows that the RAC-G mixes have higher MPD values than the dense-graded mixes, and that the open-graded mixes have higher MPD values than the gap- and dense-graded mixes. RAC-O mixes have lower MPD values than do the OGAC mixes in the data set. F-mixes have the highest MPD values, regardless of the binder type, most likely due to the higher NMAS of the F-mixes.

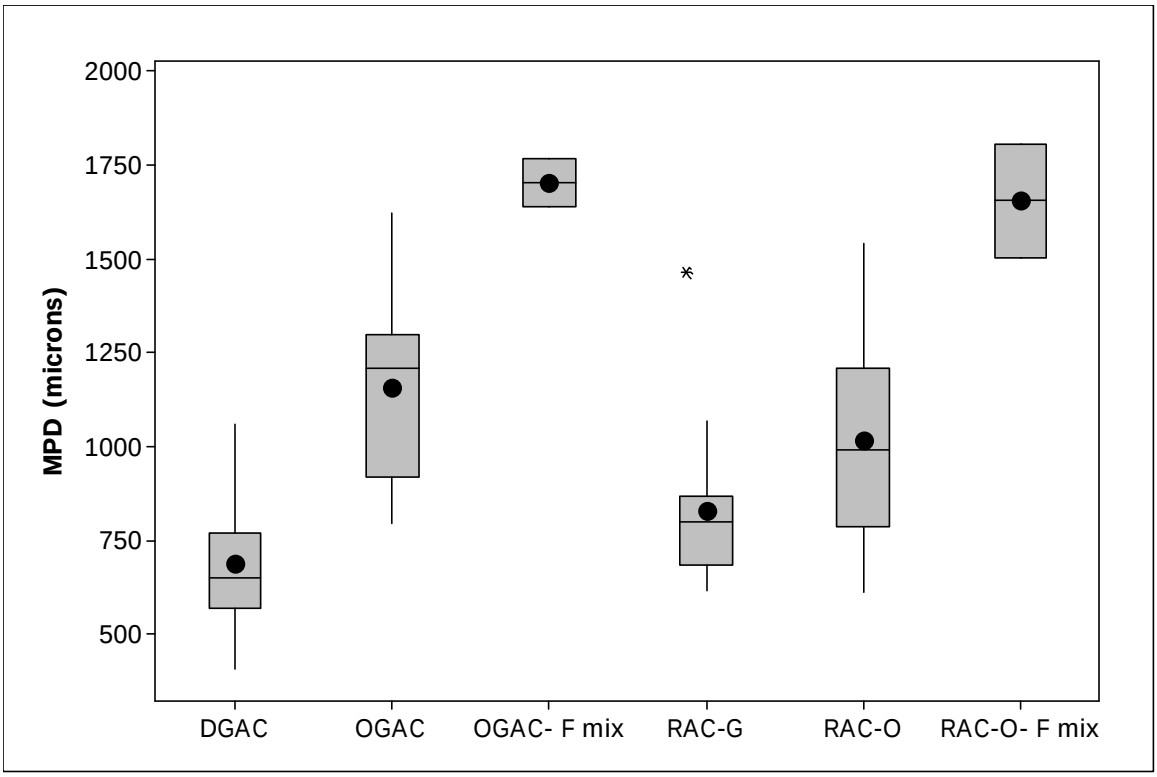

Figure 58: Box plot of MPD values for different mix types with F-mixes separated.

Figure 59 shows the variation in MPD values for different mix types at different ages. According to the plot, the MPD values are generally higher for the older DGAC mixes. The lowest MPD values are those for OGAC, RAC-O, and RAC-G mixes that are one to four years old, due to the lower air-void content and fineness modulus of those mixes as shown earlier in Figure 43 and Figure 44, respectively. Figure 59 shows that the MPD variation has the same pattern as the air-void content variation in Figure 43.

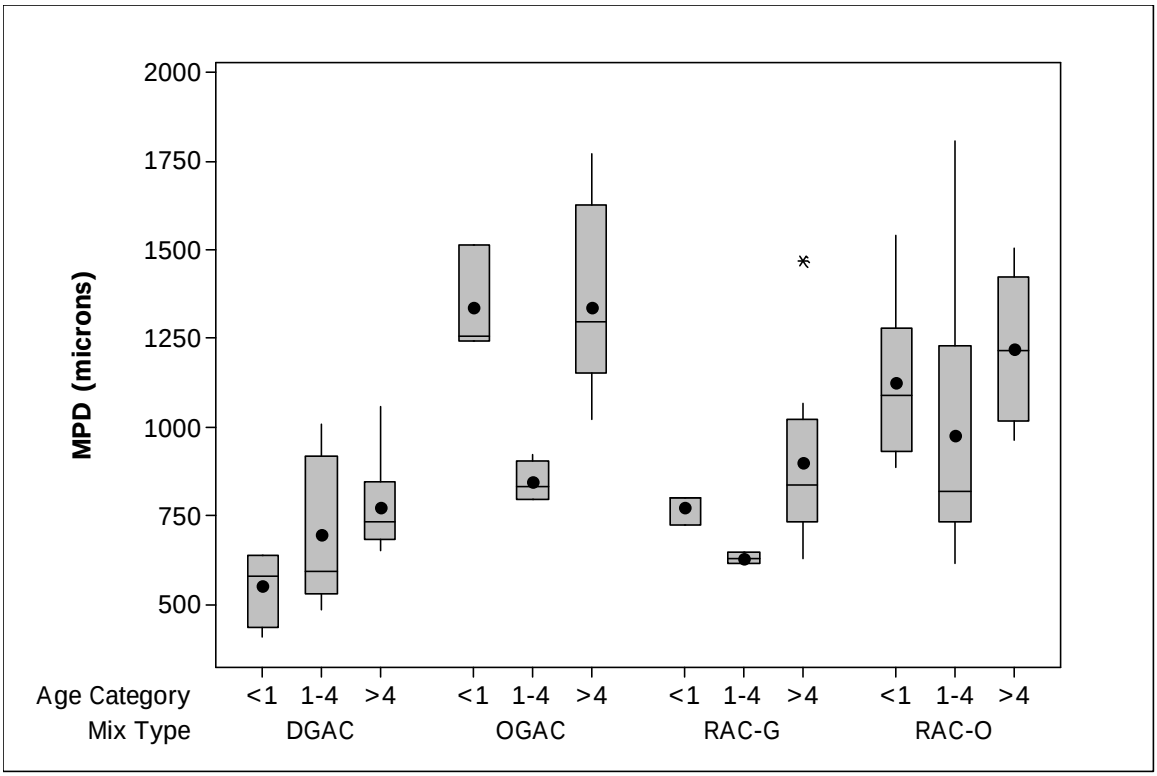

Figure 59: Box plot of MPD values for different mix types at different ages.

Figure 60 compares the MPD values in the first and second years. The figure shows that the MPD values of all the mixes increase in the second year. These increases are most likely due to surface deterioration due to the process of developing raveling: loss of fines between the larger aggregates.

Figure 61 shows the difference in MPD values (MPD second year – MPD first year) in one year. The figure shows that the oldest OGAC mixes have the greatest variability. This greater variability is due to the greater increase in MPD values for OGAC F-mixes.

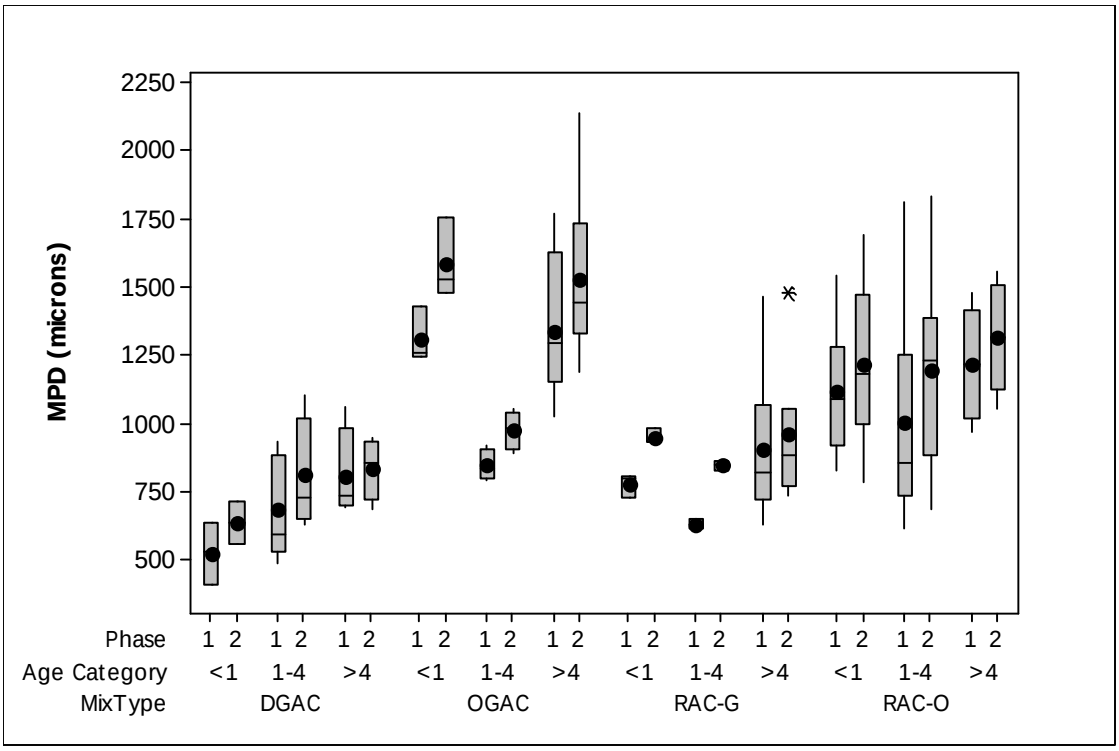

Figure 60: Comparison of MPD values for different mix types at different ages for first and second years.

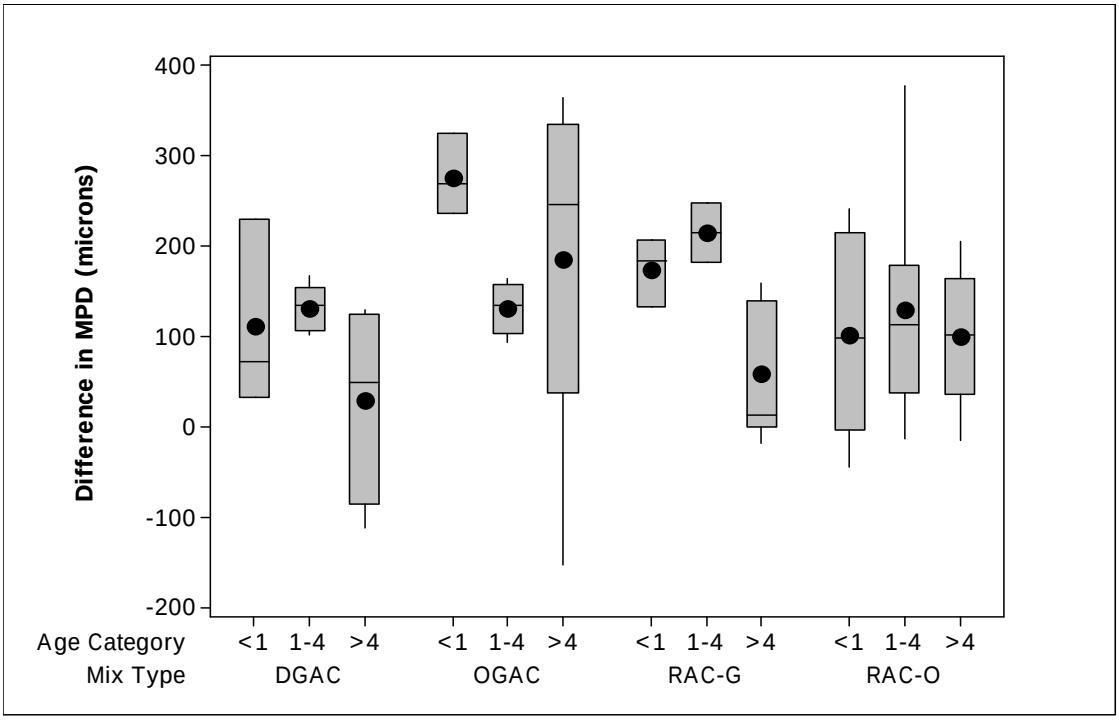

Figure 61: Difference in MPD values between first-year and second-year measurements for different mix types at different ages (positive values indicate increase in MPD values).

6.5.2 Statistical Modeling of Macrotexture

Regression analysis was conducted to determine the climate, traffic, and asphalt mix effects on macrotexture. The coefficient of the explanatory variable and the constant term along with their p-values and the coefficient of determination (R^2) for each model are given in Table 22. A log transformation was applied to the dependent variable (macrotexture) to stabilize the variance of the residuals. The p-values less than 0.05 are shown in bold.

Table 22: Regression Analysis of Macrotexture

Model Number	Explanatory Variable			Constant Term	R^2 (%)
	Name	Coefficient	p-value		
1	Air-Void Content (%)	0.017	**0.00**	2.74	37.6
2	NMAS (mm)	–0.005	0.39	3.03	1.1
4	Fineness Modulus	0.213	**0.00**	1.89	48.7
5	C_u	–0.005	**0.00**	3.08	35.6
6	Age (years)	0.016	**0.01**	2.90	9.4
7	Mix Type	0.170	**0.00**	2.86	37.6
8	Rubber Inclusion	0.010	0.65	2.95	0.3
9	Average Annual Rainfall (mm)	0.000089	**0.01**	2.90	8.8
10	Age × Average Annual Rainfall (mm)	0.00003	**0.00**	2.89	24.2
11	Average Annual Maximum Daily Air Temp (°C)	–0.013	0.06	3.26	5.6
12	Annual FT Cycles	0.093	**0.03**	2.94	6.6
13	NMAS × Mix type	0.014	**0.00**	2.85	45.8

Air-void content, age, fineness modulus, C_u, age, mix type, average annual rainfall, cumulative rainfall (Age × Average annual rainfall), annual freeze-thaw cycles, and interaction of NMAS and mix type were found to be significant variables. Figure 62 shows the NMAS effect on MPD values. The open-graded mixes are shown as red squares, and the dense-graded mixes are shown as black circles.

According to the plot, macrotexture values increase with increasing NMAS for open-graded mixes, and they decrease with increasing NMAS for dense- and gap-graded mixes. NMAS was not found to be statistically significant by itself in explaining MPD. However, the interaction of NMAS with mix type was found to significantly affect macrotexture values.

According to the models shown in Table 22, increasing air-void content and fineness modulus increase macrotexture, and increasing C_u reduces macrotexture. Also, the open-graded mixes have higher macrotexture than the gap- and dense-graded mixes. Based on the models, it can be concluded that higher air-void content, coarser gradation, and gap and open gradations increase the MPD values. A higher amount of rainfall and higher annual number of freeze-thaw cycles (above 31) also result in higher

macrotexture values. Increasing NMAS increases the macrotexture of open-graded mixes. Climate increases the macrotexture due to deterioration of the surface.

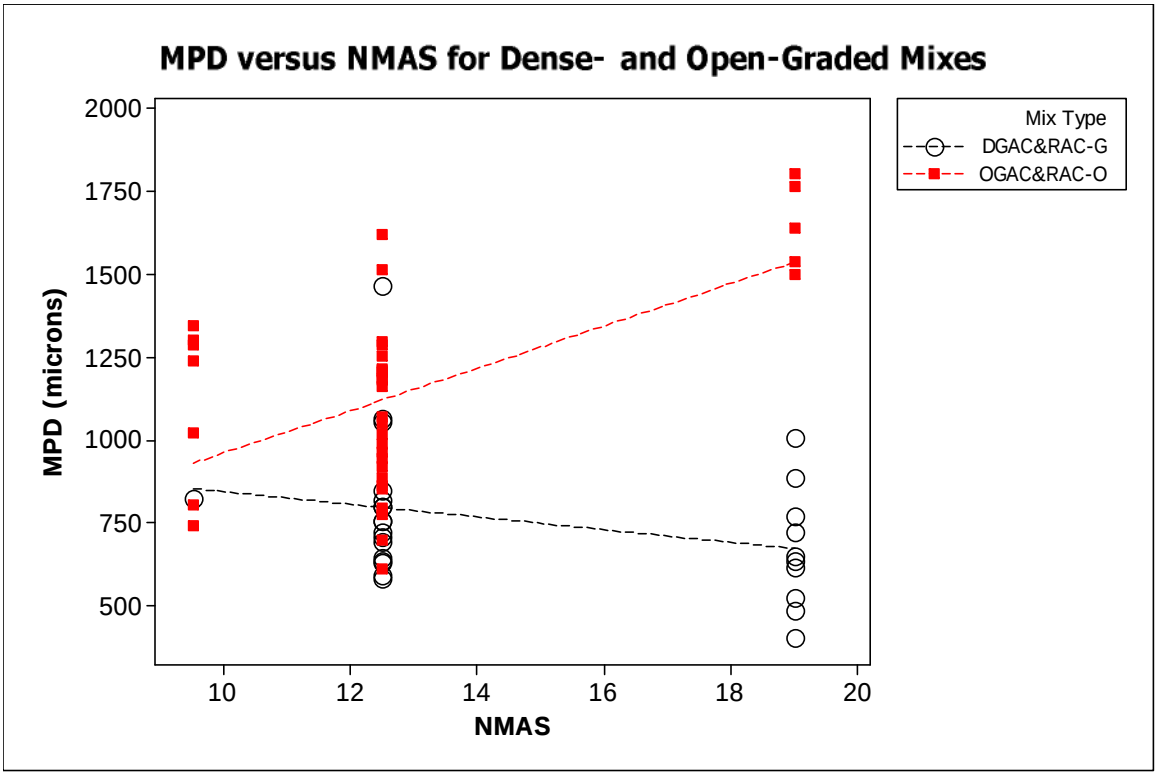

Figure 62: MPD values for different NMAS values and for open-graded and dense- and gap-graded mixes.

The final regression model explaining the macrotexture is presented here. Log-transformed MPD values were used as the dependent variable. Fineness modulus, air-void content, cumulative rainfall (Age × Average annual rainfall), and the interaction of NMAS with mix type were used as independent variables. These variables were able to account for 69 percent of the variation in macrotexture.

Model for MPD

The regression equation, Equation (14), is

log MPD = 2.39 + 0.0768 Fineness modulus + 0.00846 Air-void content + 0.000025 Age × Average annual precipitation + 0.00509 NMAS × Mix type **(14)**

Predictor	Coef	SE Coef	T	P
Constant	2.3865	0.1429	16.70	0.000
Fineness modulus	0.07678	0.03284	2.34	0.023
AV content	0.008459	0.003046	2.78	0.007
Age × Average annual rainfall	0.00002501	0.00000534	4.68	0.000
NMAS × Mix type	0.005094	0.002283	2.23	0.029

S = 0.0835794 R-Sq = 69.0% R-Sq(adj) = 67.0%

Analysis of Variance

Source	DF	SS	MS	F	P
Regression	4	0.94923	0.23731	33.97	0.000
Residual error	61	0.42612	0.00699		
Total	65	1.37535			

A total of 66 sections were used in the model. The air-void content of the mixes used in the model ranges between 4 and 22 percent, the fineness modulus ranges between 3.8 and 5.86, the NMAS value ranges between 9.5 and 19 mm, the age ranges between 0.003 and 14 years, and the average annual rainfall ranges between 145 and 2,145 mm.

To determine the effects of climate, traffic, and asphalt mix on the change in macrotexture between the first and second years, regression analysis was performed. The coefficient of the explanatory variable and the constant term along with their p-values and the coefficient of determination (R^2) for each model are given in Table 23. The difference in the MPD between the first year and the second year is the dependent variable. A significance level of 0.05 was used, and the significant variables are shown in bold.

Regression analysis revealed that mixes with higher air-void content and higher fineness modulus have higher MPD values in the second year (Phase 2 in the figures). It can be concluded that MPD values increase each year, and they increase with increasing air-void content and fineness modulus. This increase

may occur because mixes with high air-void content are more prone to raveling, which may increase the MPD values.

Table 23: Regression Analysis of Difference in Macrotexture Between Two Years

Model Number	Explanatory Variable			Constant Term	R^2 (%)
	Name	Coefficient	p-value		
1	Air-Void Content Difference (%)	5.05	0.68	–133.19	0.3
2	AV (first year) (%)	–6.96	**0.02**	–42.47	8.7
3	NMAS (mm)	–2.57	0.62	–94.93	0.4
4	Fineness Modulus	–61.15	0.04	176.9	6.7
5	C_u	1.66	0.10	–163.35	4.6
6	Age Difference	–67.6	0.58	–68.4	0.5
7	Mix Type	–44.54	0.15	–102.86	3.7
8	Rubber Inclusion	38.73	0.20	–148.97	2.9
9	Total Rainfall Since Coring (mm)	–0.062	0.17	–102.28	3.2
10	Average Annual Maximum Daily Air Temp (ºC)	–2.63	0.67	–68.8	0.3
11	Annual FT Cycles	–1.13	0.18	–103.63	3.1
12	AADT	–0.00010	0.96	–128.95	0.0
13	AADTT	–49.56	0.19	–119.64	3.1

6.6 International Friction Index (IFI)

IFI values were calculated based on ASTM E 1960 using the BPN and MPD values. IFI values are reported in terms of F_{60}, which is wet friction at 60 km/h, and S_p, which is the speed constant of wet-pavement friction. Figure 63 shows the F_{60} values and Figure 64 shows the S_p values for different mixes. The figures show that open-graded mixes have higher F_{60} and S_p values than dense- and gap-graded mixes. RAC-G mixes have higher F_{60} and S_p values than dense-graded mixes.

Figure 65 shows the friction values for different mixes including F-mixes. The figure shows that the RAC-O F-mixes have the highest friction values, a result of their higher NMAS and hence higher MPD values. OGAC F-mixes have the lowest friction values among all open- and gap-graded mixes, because these mixes are older and hence have lower microtexture as measured by the BPN values. No newer F-mix sections exist in the state.

Figure 66 shows the friction values for different mixes at different ages. The figure shows that for open- and gap-graded mixes, the sections that are one to four years old have the smallest friction values compared to the other age categories; DGAC mixes that are one to four years old have the highest friction values compared to the other age categories for that mix type. These findings probably reflect the fact that

the friction values show a trend similar to MPD and air-void content variation, which shows the lowest values for open- and gap-graded mixes that are one to four years old.

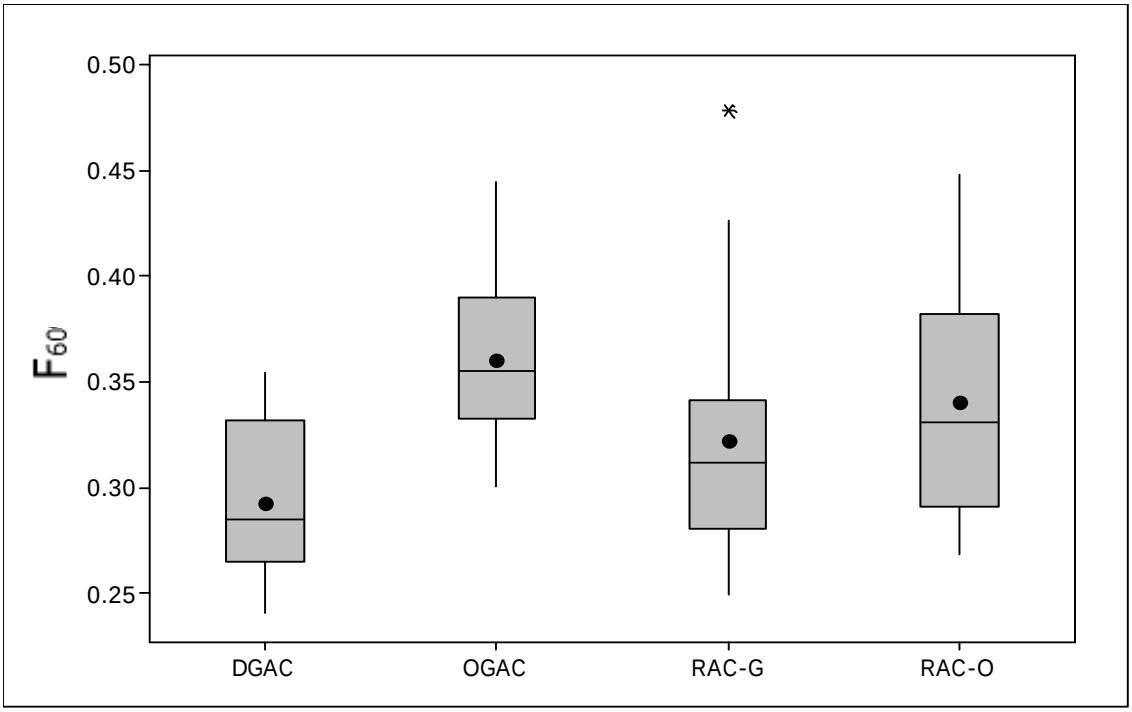

Figure 63: Comparison of F_{60} values for different mix types.

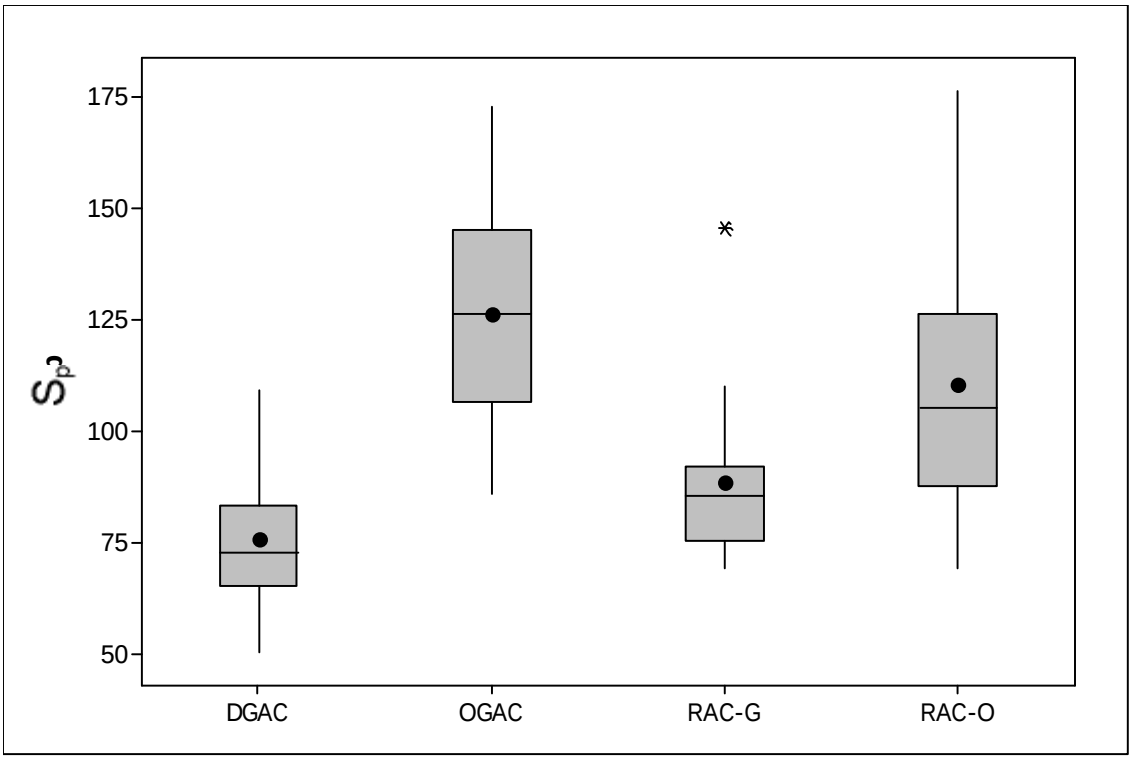

Figure 64: Comparison of S_p values for different mix types.

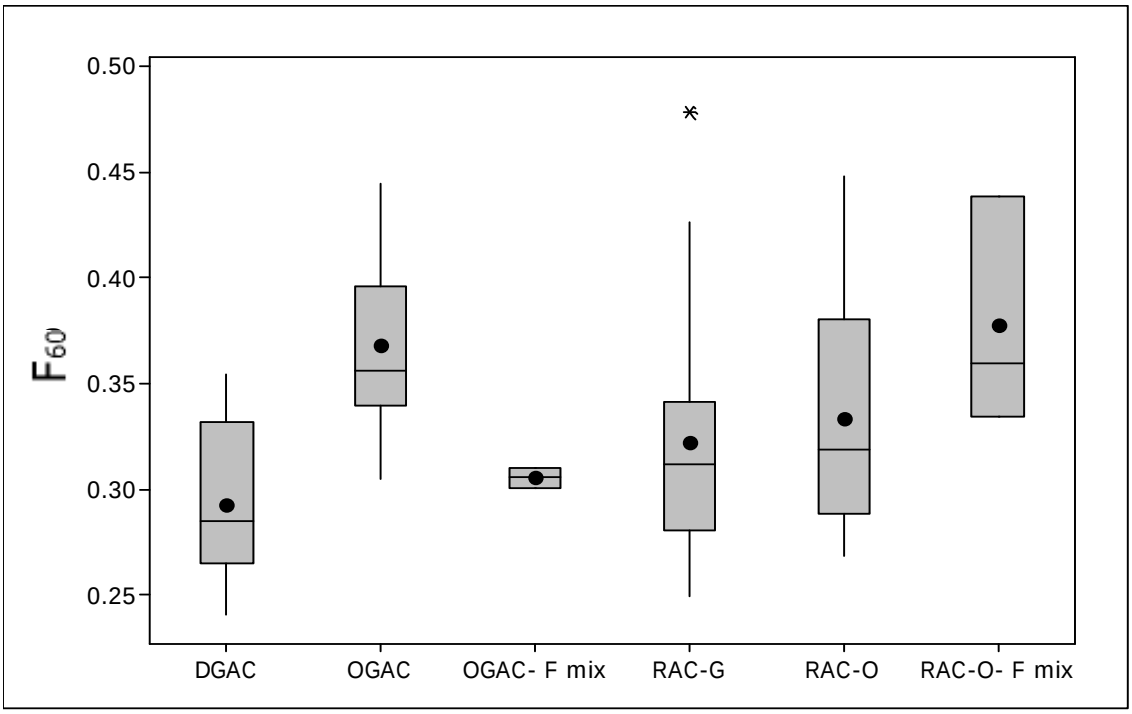

Figure 65: Comparison of F_{60} values for different mix types, F-mixes separated.

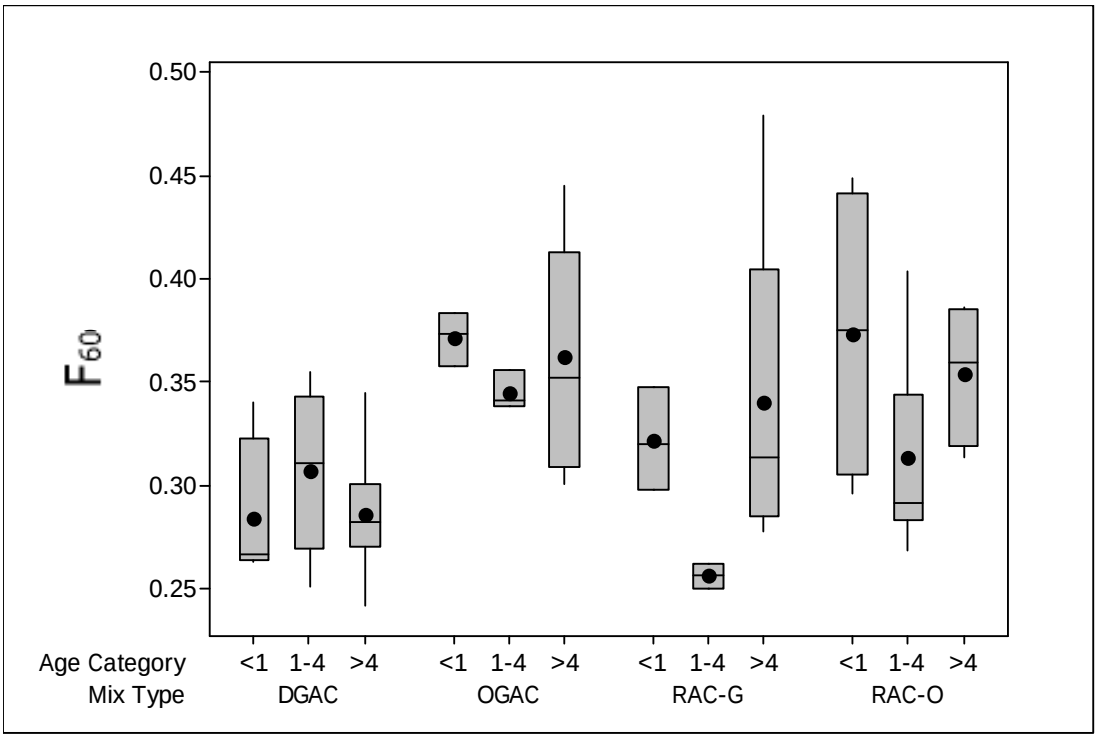

Figure 66: Comparison of F60 values for different mix types at different ages.

6.7 Summary of Findings

- IFI calculations showed that open-graded mixes provide higher friction values compared to dense- and gap-graded mixes, because open-graded mixes have higher macrotexture compared to dense- and gap-graded mixes.
- Except for four sections that are older than five years, all test sections met the criterion used for comparison purposes in this project of a minimum BPN of 45. Therefore, mixes that are less than eight years old generally provide satisfactory friction.
- Regression analysis on the BPN showed that BPN decreases with increasing age and increasing number of high temperatures that the pavement experiences over its lifetime, which supports the results from the earlier studies. These variables were statistically significant; however, their ability to predict BPN values is very low as indicated by the R^2 value of the regression model.
- Sections with higher truck traffic as well as higher ESALs (correlated with truck volume) have lower microtexture values. Microtexture is sensitive to individual aggregate properties and seasonal changes. It is not affected by binder type and gradation properties. Therefore, there is no significant difference in microtexture values for different mix types. Regression analysis on the difference in BPN values from year to year showed that sections with higher rainfall tend to polish faster.
- Open-graded mixes in California have positive texture.
- Open-graded mixes have higher macrotexture values compared to dense- and gap-graded mixes. Gap-graded mixes have higher macrotexture values than dense-graded mixes. The macrotexture value increases with time.
- Regression analysis on the MPD values confirmed the findings of Stroup-Gardiner (52) that the higher the air-void content and the coarser the gradation, the higher the macrotexture value. The macrotexture value increases with increasing age, likely due to some loss of fine particles from the surface (beginnings of raveling). Sections subjected to more rainfall had higher macrotexture values. Macrotexture values are also higher for the sections with more annual freeze-thaw cycles. These two climate factors also likely increase the rate of raveling. NMAS does not affect the macrotexture of dense-graded and gap-graded mixes. However, increasing NMAS increases the macrotexture value for open-graded mixes.
- F-mixes have higher macrotexture values than the other open-graded mixes, because of the higher nominal NMAS of the F-mixes. Increasing NMAS increases the macrotexture of open-graded mixes.

- The increase in macrotexture value over time is greater for sections with higher air-void content and coarser gradation, probably because these sections are more likely to ravel.
- The temperature correction in the literature for the British Pendulum test does not cover the range of temperatures often encountered when testing in California and does not provide a good correction. UCPRC has developed a new temperature correction equation has been developed for this test that provides much better results.

7 EVALUATION OF ROUGHNESS OF ASPHALT CONCRETE MIXES

The IRI measurements were collected in both the left and right wheelpaths. The average of the two wheelpath measurements was used in the analysis.

The manufacturer's recommended procedure was used to check the laser, accelerometers, and the Distance Measuring Instrument (DMI) every month, starting before testing was begun, and continuing through the study. For verification, the profilometer was also checked on one site (one mile long) every month.

The UCPRC profilometer was also compared with the Dynatest Consulting profilometer based in Ventura, California, and used for commercial testing, and with one of the new Caltrans profilometers. The results have been comparable.

The profilometer was not working properly on sections 01-N103, 01-N104, 01-N105, 01-N114, and 01-N121, which had large measurement errors. These sections are excluded from the analysis. The problems on these sections were traced to a problem with the DMI when those sections were tested.

The analysis of the roughness/ride quality answers these questions:

- Do all the mixes evaluated provide "acceptable" ride qualities?
- What pavement characteristics affect the IRI?
  - Is the initial IRI and IRI progression different for rubberized and nonrubberized mixes?
  - Is the initial IRI and IRI progression different for open-graded and dense-graded mixes?
- How do traffic and climate affect the IRI?

7.1 Descriptive Analysis

Figure 67 shows the variation in IRI values for different mix types. According to the plot, the average IRI values of different mixes are close to each other, and most of the sections have acceptable IRI values based on FHWA criteria as discussed in Chapter 2.

Figure 68 shows the IRI values for different mix types for three age categories. According to the plot, the IRI values increase with increasing age for RAC-O and DGAC mixes. This trend is not clear for OGAC and RAC-G mixes. Except for OGAC mixes, all the new mixes have similar IRI values that are less than 1.5 m/km. The high IRI values of OGAC mixes are due to the QP-20 section. The high IRI value of this section may be due to compaction problems during the construction because this section is located on a steep hill.

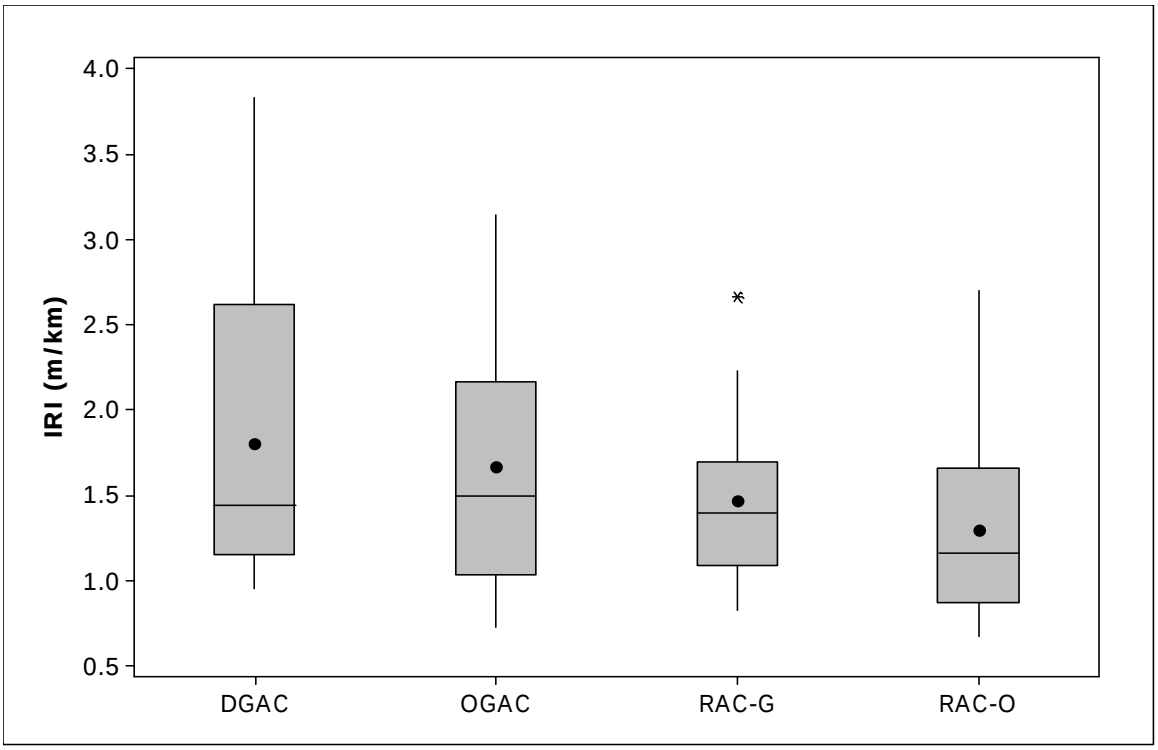

Figure 67: Variation in IRI values for different mix types.

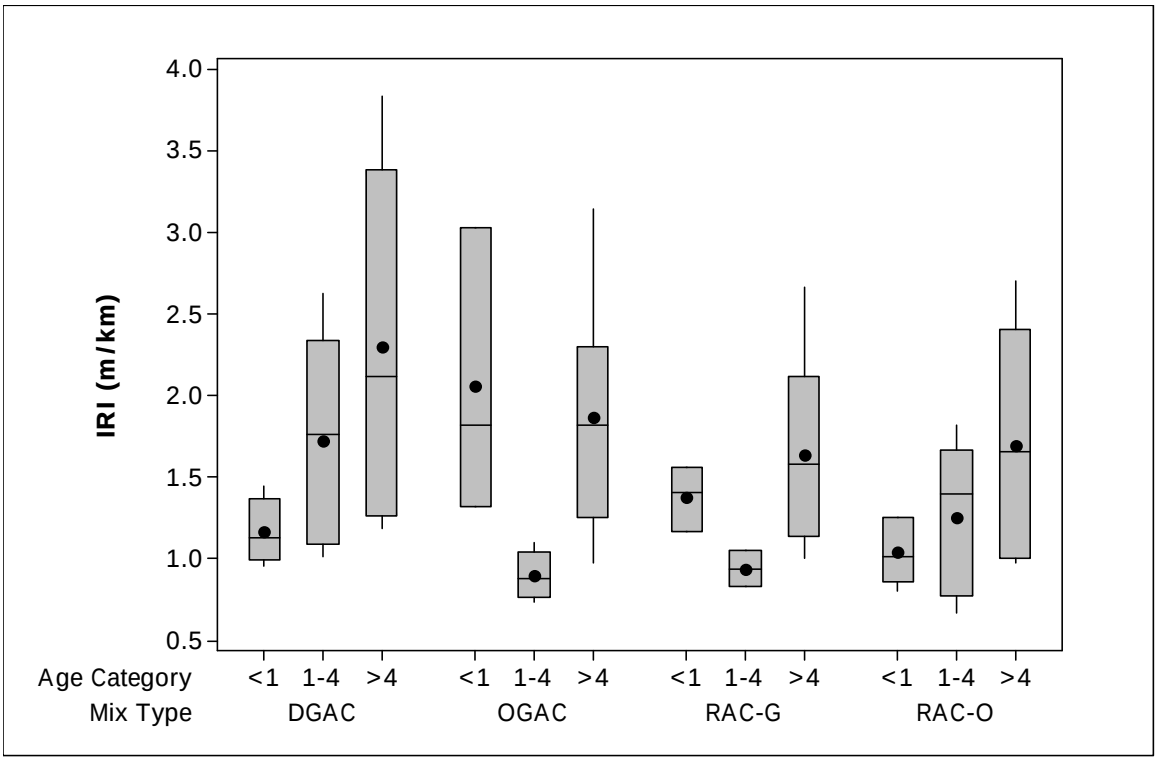

Figure 68: Variation in IRI values for different mix types at different ages.

Figure 69 compares the IRI values in the first and second years. The comparative analysis includes only the sections that were measured in both years. As the figure shows, there is generally an increase in IRI values in the second-year measurements. Except for OGAC mixes, the new DGAC, RAC-G, and RAC-O sections have less variation in IRI values than do the older ones, because older mixes are more likely to have distresses, which increase the IRI values, and the distress propagation would be different for each section since distresses are also affected by underlying pavement structure, climate, and traffic. The greater variation for OGAC mixes that are less than one year old is due to section QP-20, which has a high IRI value. The new RAC-G mixes also show greater variation in their second year of measurement, which also is due to the QP-26 section, which has a high increase in IRI. However, the reason for the IRI increase is not known since the section is still in good condition, without distresses, and there is no measurement error.

Figure 70 shows the difference in IRI values between the first and second years (IRI second year – IRI first year). Since IRI is expected to increase with time, the first-year values are subtracted from the second-year values. The figure shows that the increase in IRI in one year is small since the average differences are close to zero. The greater variation of RAC-G mixes that are less than one year old is due to section QP-26, which has a high increase in IRI.

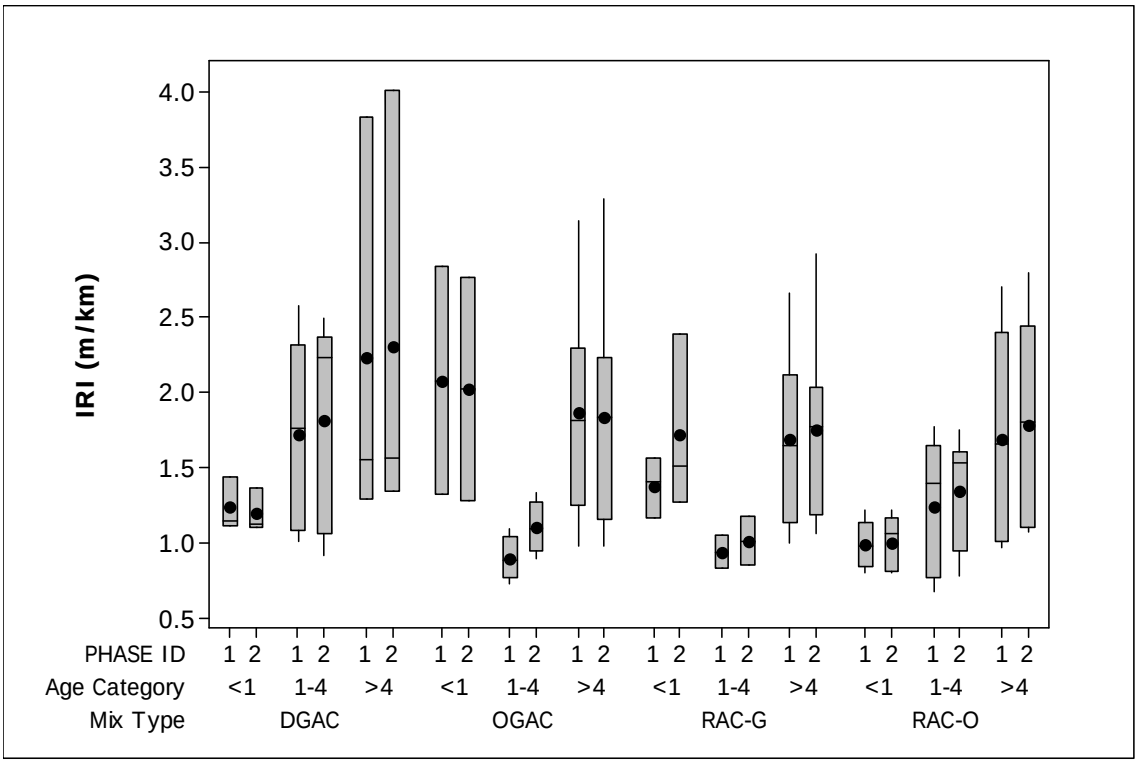

Figure 69: Comparison of IRI values for different mix types at different ages for first and second years.

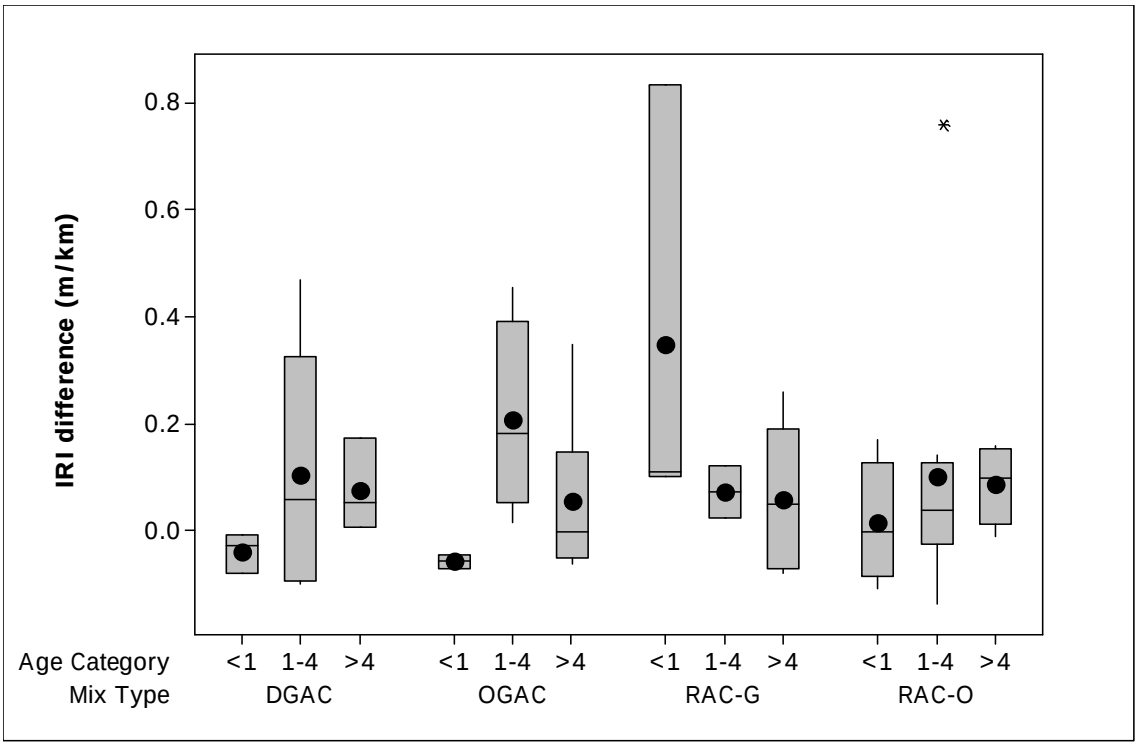

Figure 70: Difference in IRI values for different mix types at different ages (positive values indicate an increase in IRI).

7.2 Regression Analysis

Regression analysis was performed to evaluate the effects of traffic, climate, distresses, and pavement materials on the IRI values, Because the data set is small, one variable is used in each model. The coefficient of the explanatory variable and the constant term along with their p-values and the coefficient of determination (R^2) for each model are given in Table 24. Since the variance of IRI increases with its mean and the error terms are not normally distributed, a reciprocal square-root transformation was applied to the dependent variable, IRI. The p-values less than 0.05 are shown in bold.

Table 24: Regression Analysis of IRI Values

Model Number	Explanatory Variable			Constant Term	R^2 (%)
	Name	Coefficient	p-value		
1	Air-Void Content (%)	0.002	0.59	0.83	0.4
2	Age (years)	–0.02	**0.00**	0.95	15.9
3	Mix Type	0.05	0.18	0.82	2.6
4	Rubber Inclusion	0.08	**0.04**	0.81	5.9
5	Presence of Fatigue Cracking	–0.12	**0.03**	0.85	7.2
6	Presence of Raveling	–0.16	**0.00**	0.87	15.9
7	Presence of Rutting	–0.21	**0.00**	0.86	16.0
8	Number of Transverse Cracks	–0.004	0.08	0.86	4.9
9	Presence of Transverse Cracks	–0.03	0.46	0.85	0.9
10	Average Annual Rainfall (mm)	–0.00007	0.09	0.90	4.4
11	Age × Average Annual Rainfall	–0.00004	**0.00**	0.95	30.4
12	Average Annual Wet Days	–0.0003	0.33	0.88	1.4
13	Age × Average Annual Wet Days	–0.0003	**0.00**	0.95	24.6
14	Average Annual Maximum Daily Air Temp (ºC)	0.03	**0.00**	0.14	23.3
15	Annual Number of Days > 30 ºC	0.0014	**0.00**	0.75	18.6
16	Annual Degree-Days > 30 ºC	0.00004	**0.00**	0.75	19.2
17	Annual FT Cycles	–0.006	0.90	0.86	0.0
18	log AADT	–0.07	0.15	1.15	3.1
19	AADTT	–0.007	0.87	0.86	0.0
20	ESAL	0.008	0.86	0.85	0.0

Mix type, rubber inclusion, presence of cracking, presence of raveling, presence of rutting, and AADTT for the coring lane were used as categorical variables, as explained in Chapter 4. Age, rubber inclusion, presence of fatigue cracking, presence of raveling, presence of rutting, amount of rainfall for the lifetime of the pavement (Age × Average annual rainfall), number of wet days for the lifetime of the pavement, average annual maximum daily temperature (°C), annual number of days above 30°C, and annual degree-days above 30°C are found to be the significant variables affecting the IRI values.

Increasing age and presence of distresses increase the IRI values. Rubberized mixes (RAC-O and RAC-G) have lower IRI values than the nonrubberized (OGAC and DGAC) mixes. As the total amount of rainfall and the number of rainy days for the lifetime of each section increases, the IRI values increase. The moisture in the pavement weakens the underlying layers and results in less support to the asphalt layer, which may result in more cracking. Hotter climates reduce the IRI values. The temperature effect

may be related to cracking or to spalling of the cracks once they occur. However, high temperatures would increase rutting, which may eventually increase IRI.

Unexpectedly, the traffic variables were found to have no effect on the IRI values. This finding could be due in part to the RAC-G and DGAC overlay designs' being particularly dependent on the expected traffic load. The initial IRI of these sections at the time of construction is not known, and some correlation between the initial IRI and the traffic level that cancels any effect of traffic on IRI may be expected.

Since the climate variables are related to distresses, two models were proposed to explain the IRI values. Model 1 contains the climate and rubber inclusion variables, and Model 2 contains the distress variables and age. Due to the nonconstant variance of the error terms, a reciprocal square-root transformation was applied to the dependent variable, IRI, in Model 1 ($Y' = 1/\sqrt{IRI}$). The presence of fatigue cracking is not included in Model 2, since it was correlated with other variables.

Model 1 for IRI

The regression equation, Equation (15), is

$1/\sqrt{IRI}$ = 0.815 + 0.0700 × Rubber inclusion – 0.000038 Age × Average annual rainfall + 0.00115 × Number of temperatures > 30°C **(15)**

Predictor	Coef	SE Coef	T	P
Constant	0.81500	0.04004	20.36	0.000
Rubber inclusion	0.07003	0.03147	2.23	0.030
Age × Average annual rainfall	–0.00003798	0.00000771	–4.93	0.000
Number of temperatures > 30C	0.0011544	0.0003103	3.72	0.000

S = 0.127898 R-Sq = 45.9% R-Sq(adj) = 43.4%

Analysis of Variance

Source	DF	SS	MS	F	P
Regression	3	0.87594	0.29198	17.85	0.000
Residual error	63	1.03055	0.01636		
Total	66	1.90649			

Model 2 for IRI

The regression equation, Equation (16), is

IRI = 1.14 + 0.072 × Age + 0.662 × Presence of rutting + 0.540 × Presence of raveling **(16)**

Predictor	Coef	SE Coef	T	P
Constant	1.1361	0.1202	9.45	0.000
Age	0.0719	0.0280	2.57	0.013
Presence of rutting	0.6616	0.2599	2.55	0.014
Presence of raveling	0.5405	0.1832	2.95	0.005

S = 0.552499 R-Sq = 39.7% R-Sq(adj) = 36.5%

Analysis of Variance

Source	DF	SS	MS	F	P
Regression	3	11.6405	3.8802	12.71	0.000
Residual error	58	17.7048	0.3053		
Total	61	29.3453			

In the second model, the reciprocal square-root transformation was not applied to the dependent variable since the error terms had constant variance. The inclusion of binary variables together with the age variable may have resulted in error terms with constant variance.

The age of the sections used in the models ranges between 0.003 and 14 years, the average annual rainfall ranges between 145 and 2,105 mm, and the annual number of days with temperatures above 30°C ranges between 0 and 156.

The change in IRI values from the first to the second year was also evaluated using regression analysis. Because the data set is small, one variable is used in each model. The coefficient of the explanatory variable and the constant term along with their p-values and the coefficient of determination (R^2) for each model are given in Table 25. The dependent variable is the difference in IRI values between the second year and the first year.

The table shows that none of the variables were found to affect the change in IRI significantly, perhaps because one year is a short term to observe the effects of climate, traffic, and mix type on the change in IRI values.

The effect of distress progression on the IRI change could not be evaluated since only a few sections showed distresses in the second year but not in the first year.

Table 25: Regression Analysis of Difference in IRI Values Between Two Years

Model Number	Explanatory Variable			Constant Term	R^2 (%)
	Name	Coefficient	p-value		
1	Air-Void Content Difference (%)	–0.04	0.08	0.08	5.2
2	Age Difference (years)	0.16	0.50	–0.08	0.8
3	Mix Type	0.006	0.92	0.06	0.0
4	Rubber Inclusion	–0.07	0.22	0.027	2.6
10	Rainfall Since Phase I (mm)	0.00004	0.69	0.048	6.5
11	Number of Wet Days Since Phase I	–0.00013	0.77	0.078	0.2
12	Annual Maximum Daily Air Temp (ºC)	0.0026	0.83	0.004	0.1
13	Number of Days > 25ºC	–0.00032	0.59	0.02	0.5
14	Number of Days > 30ºC	–0.0005	0.44	0.029	1.0
15	Degree-Days > 30ºC	0.00011	0.38	0.03	1.4
16	Number of FT Cycles	0.0007	0.66	0.047	0.3
17	log AADT	–0.116	0.13	0.50	4.0
18	AADTT	–0.088	0.22	0.079	2.6

7.3 Summary of Findings

- All the sections are smoother than the Caltrans Pavement Management System IRI trigger criterion of 3.6 m/km (224 in./mi). Most of the sections have acceptable ride quality according to the FHWA criterion of 2.65 m/km (170 in./mi).
- Rubberized mixes, both open graded and gap graded, have lower IRI values than do nonrubberized mixes.
- IRI values of open-graded mixes and dense- and gap-graded mixes are not significantly different. Therefore, mix type does not affect the IRI values.
- Regression analysis on the IRI values confirmed that IRI increases with age and with the presence of distresses on the pavement surface. Increasing rainfall and colder temperatures increase the IRI values, supporting the results of earlier studies. As-built IRI values are unknown for the sections and are expected to have a very large influence on later IRI values. Traffic variables were not found to be significant in explaining roughness.
- None of the pavement, climate, or traffic variables were found to affect the IRI values from one year to the next, perhaps because one year is a short term for IRI progression.

8 PAVEMENT DISTRESS EVALUATION

The evaluation of distresses is needed to estimate the lives of the different mixes and to perform life-cycle cost-analysis comparisons. Bleeding, rutting, raveling, transverse cracking, and wheelpath cracking of the test sections are evaluated in this study. The evaluation of distresses answers these questions:

- Do the initiation and progression of distresses differ for different mixes: for example, open-graded mixes versus gap- and dense-graded mixes, and rubberized mixes versus nonrubberized mixes?
- How do traffic and climate affect distress initiation and progression?

8.1 Bleeding

In the Caltrans Pavement Condition Survey (PCS) 2000 (102), bleeding is reported in terms of severity—low, medium, and high—and extent, expressed as the percentage of the total area with bleeding. In the analysis for this study, 3 percent of the test section area with bleeding was selected as the threshold for the start of bleeding. The condition survey was conducted on the full 125- or 150-m length of the test section pavement surface for two years. Therefore, 3 percent of the area constitutes 13.5 m^2 when the length of the section surveyed is 125 m, and 16.2 m^2 when the length of the section surveyed is 150 m. This area constitutes approximately 15 percent of the total wheelpath area. A total of 69 sections were evaluated, and with the threshold of 3 percent of the total area, five sections showed bleeding in the first year and nine sections showed bleeding in the second year.

The number of sections with and without bleeding in the first and second years is shown in Figure 71. The figure shows that the number of sections with bleeding increased for all mixes except DGAC. No regression analysis was performed on the bleeding data, since the number of sections with bleeding is small.

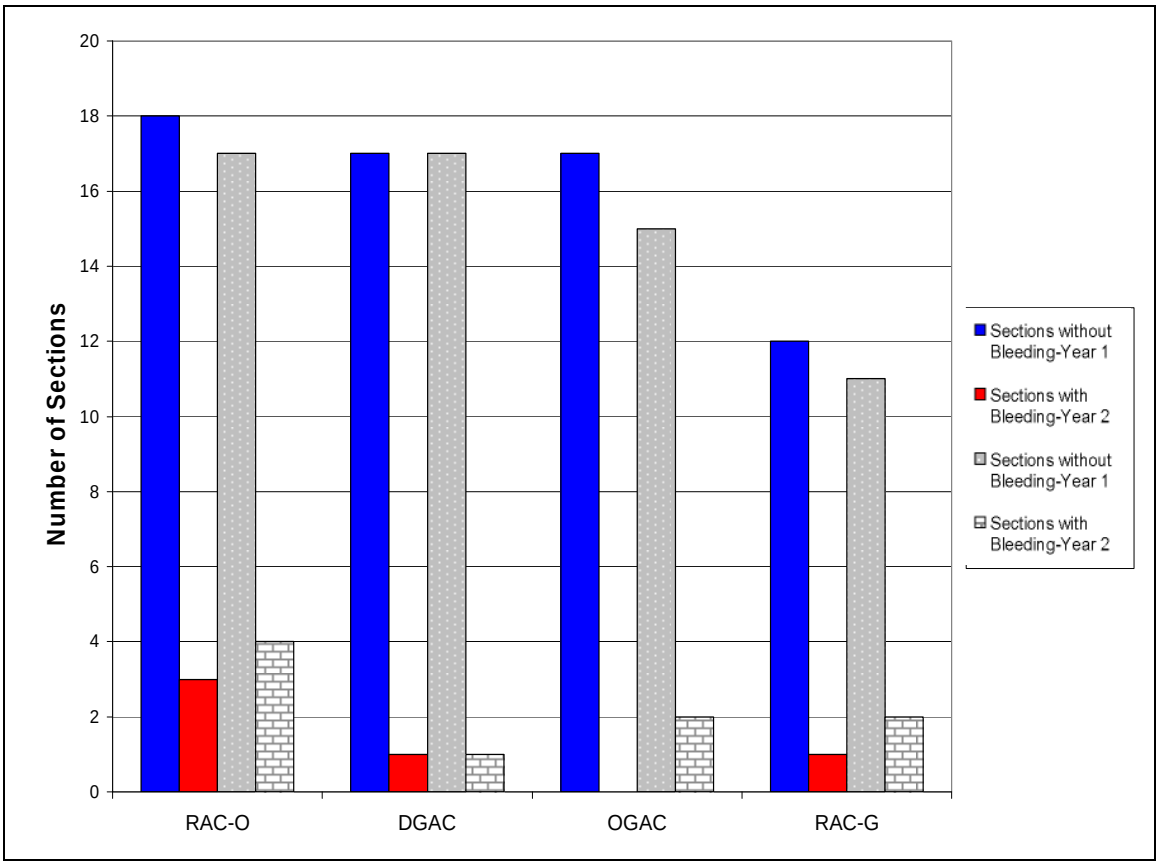

Figure 71: Number of sections with and without bleeding categorized by mix type. (Note: Year 1 refers to the first year of measurement and Year 2 to the second year of measurement.)

8.2 Rutting

The maximum rut depth at every 25 m of the test section was recorded in millimeters following the 2000 PCS. Rut depth was measured across the wheelpaths with a straight-edge ruler. In the analysis, a maximum of a 3-mm rut present on at least 25 m of the total section (125 or 150 m) was assumed as the threshold for analysis of rutting. According to this assumption, only 6 out of 69 sections showed rutting in the first year, and 9 sections showed rutting in the second year.

Table 26 shows the mix type and age of the sections that show rutting. The table shows that the majority of mixes with rutting are more than five years old.

Table 26: Sections Showing Rutting in the Second Year

Mix Type	Section ID	Age
DGAC	QP-16	14
DGAC	QP-25	6
DGAC	QP-30	4
OGAC	QP-22	8
OGAC	QP-23	6
OGAC	QP-29	9
RAC-G	QP-14	5
RAC-G	QP-18	7
RAC-O	QP-32	8

Figure 72 shows the number of sections with and without rutting in the first and second years. The figure shows that the number of RAC-O and DGAC sections rutting stayed the same, and the number of OGAC and RAC-G sections with rutting increased. DGAC has the highest number of sections with rutting. No regression analysis was performed since the number of sections showing rutting is small.

At the end of the second year, only four of the nine sections showing rutting also showed bleeding. Of the four, two were OGAC, one was RAC-G, and one was DGAC.

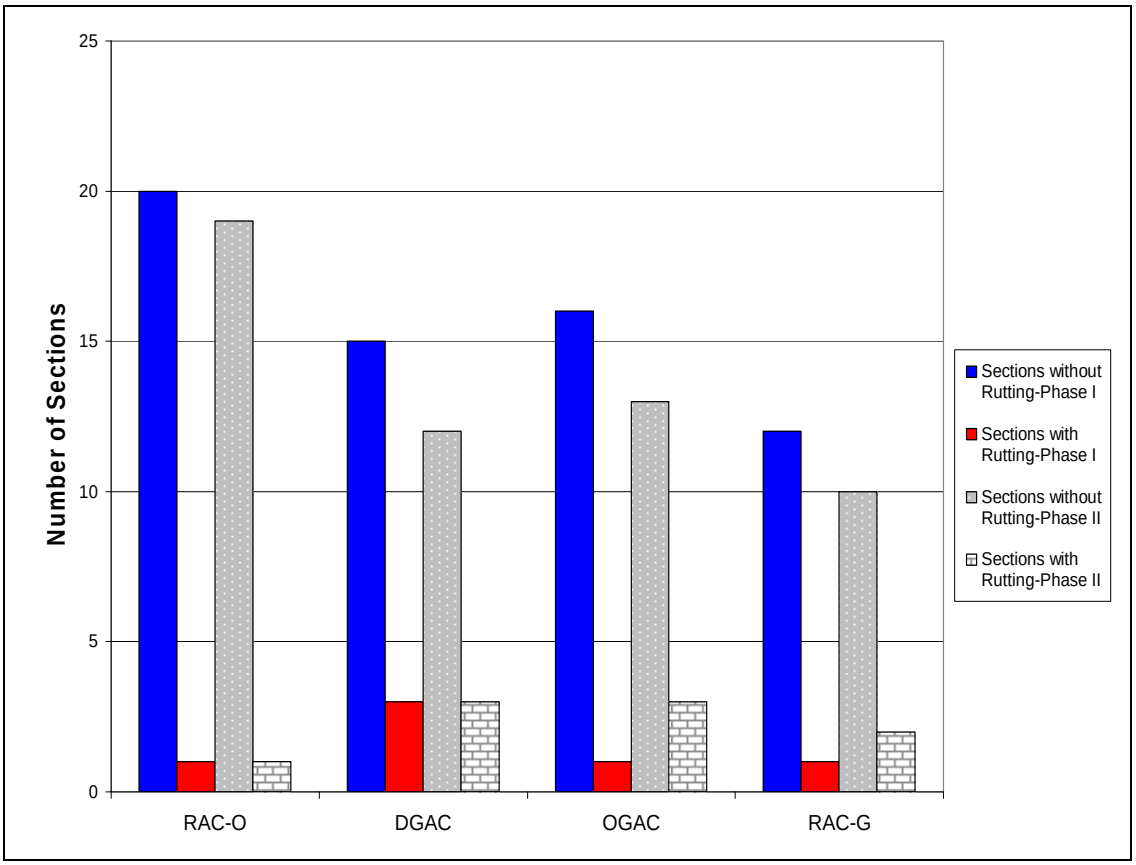

Figure 72: Sections with and without rutting.

8.3 Transverse and Reflection Cracking

All the sections investigated in this study are overlays of AC or PCC. Therefore, many of the transverse cracks observed are probably reflections of underlying transverse cracks or PCC joints. Some of the transverse cracks may be top-down thermal cracks, but it is nearly impossible to distinguish the cracking mechanism. Transverse cracks analyzed in this study include both thermal cracks and reflection cracks.

8.3.1 Descriptive Analysis

In the condition survey, the number, length, and severity of the transverse cracks were recorded for each 25-m subsection. The cracks were categorized as low severity if the crack width was less than 6 mm and as high severity if the crack width was greater than 6 mm. The 2000 PCS (102) rates only the cracks that extend across more than 50 percent of the lane width. However, in this study all the transverse cracks, regardless of length, were recorded in the condition survey.

A 5-m total transverse crack length out of 125 or 150 m was assumed as the threshold of transverse cracking. Using the 5-m threshold, out of 64 sections, 16 in the first year and 25 in the second year showed transverse or reflected transverse cracking. Out of 37 of the open-graded sections, 5 in the first year and 13 in the second year showed transverse cracking, and out of 28 dense- and gap-graded sections, 11 in the first year and 12 in the second year showed transverse cracking.

Figure 73 shows the number of sections with and without transverse cracking for two years, subdivided by mix types (no F-mixes were included). The figure shows that the number of sections with transverse cracking increased for open-graded mixes and stayed roughly the same for dense- and gap-graded mixes. This difference may occur because the progression of cracking is faster for mixes with higher air-void content.

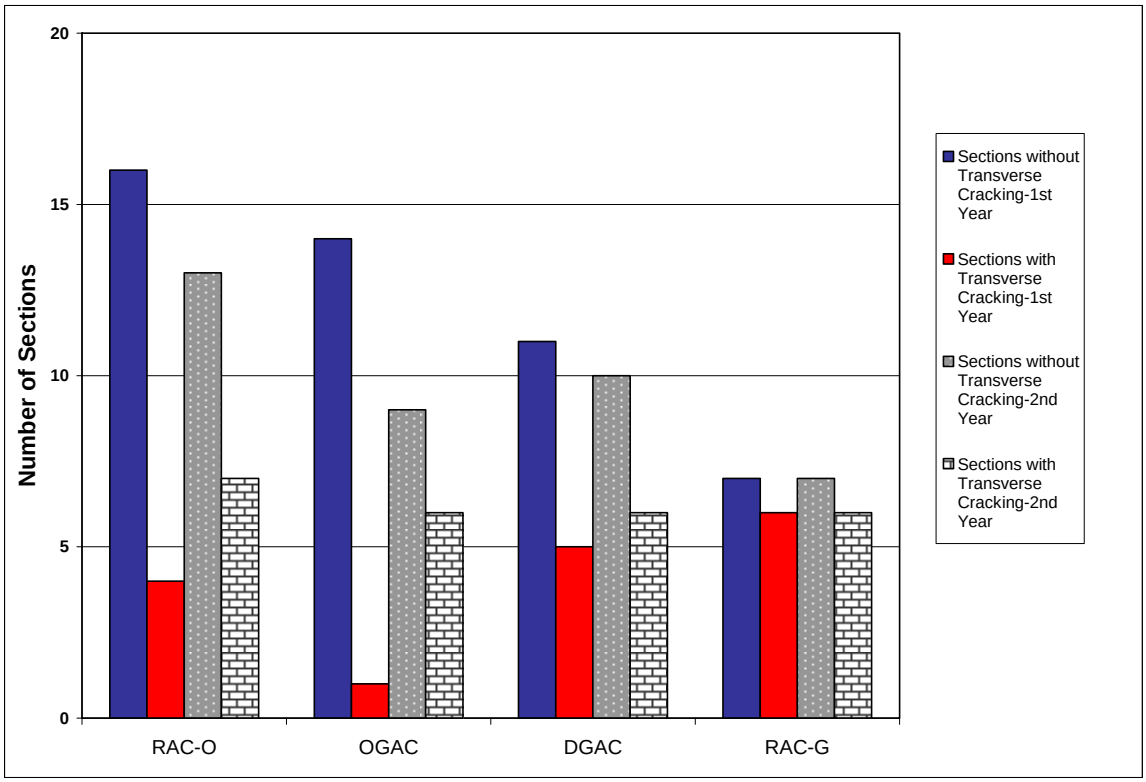

Figure 73: Number of sections with and without transverse cracking for different mix types.

Figure 74 shows the number of sections with and without transverse cracking for rubberized and nonrubberized mixes. The figure shows that rubberized mixes have more sections with transverse cracking. However, the increase in the number of sections with transverse cracking is greater for the nonrubberized mixes over the two years of survey. Based on the observations for two years, it might be concluded that inclusion of rubber does not help prevent cracking. However, evidence from another study (109) indicates that RAC-G and RAC-O mixes tend to be placed on pavements that have a greater extent

of cracking than those on which DGAC and OGAC overlays are placed. Therefore, the increased cracking in the rubber mixes may be biased by the condition of the pavements on which they are placed.

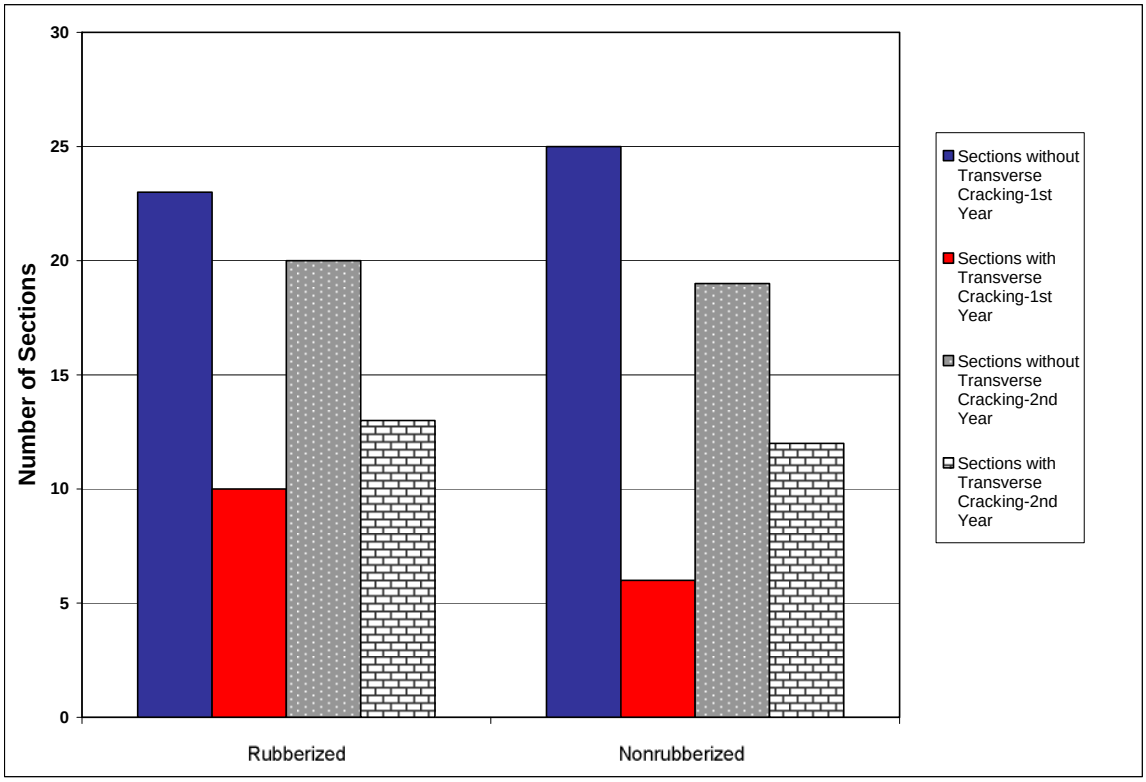

Figure 74: Number of sections with and without transverse cracking for rubberized and nonrubberized mixes. (Note: 1st Year refers to the first year of measurement and 2nd Year to the second year of measurement.)

8.3.2 Regression Analysis

Binary logistic regression, where the dependent variable is dichotomous, was conducted on the first-year data. Binary logistic regression does not impose any restrictions on the independent variables. When the crack length is greater than or equal to 5 m, the dependent variable was given the value 1; otherwise, the dependent variable was given the value 0. The coefficient of the explanatory variable and the constant term along with their p-values are shown in the Table 27. The final column of the table shows the p-values of the Hosmer-Lemeshow test, which is a goodness-of-fit test for the logistic regression. A p-value greater than 0.05 for the Hosmer-Lemeshow test indicates an acceptable fit for the data. The p-values less than 0.05 are shown in bold for explanatory variables.

Table 27: Regression Analysis of Presence of Transverse Cracking

Model Number	Explanatory Variable			Constant Term	Hosmer-Lemeshow p-value
	Name	Coefficient	p-value		
1	Air-Void Content (%)	–0.11	0.06	0.32	0.84
2	NMAS (mm)	–0.08	0.41	0.03	-
3	Fineness Modulus	–1.36	**0.03**	5.68	0.12
4	C_u	0.02	0.21	–1.58	0.32
5	Age (years)	0.24	**0.02**	–2.20	0.11
6	Mix Type	–1.36	**0.02**	–0.49	-
7	Rubber Inclusion	0.59	0.31	–1.46	-
8	Average Annual Rainfall (mm)	–0.002	**0.02**	0.19	0.48
9	Average Annual Number of Wet Days	–0.02	**0.01**	0.82	0.88
10	Average Annual Maximum Daily Air Temp (°C)	0.14	0.21	–4.49	0.69
11	Number of Days > 30°C (yearly)	0.006	0.31	–1.61	0.46
12	Annual Degree-Days > 30°C	0.00017	0.32	–1.58	0.47
13	Annual FT Cycles	–1.55	0.15	–0.92	-
14	A.A.T.H.M.	0.01	0.85	–1.51	0.93
15	A.A.T.C.M.	0.09	0.44	–1.48	0.81
16	Min T Exp.	–0.036	0.69	–1.27	0.381
17	Average Daily Temp Diff (°C)	–0.217	0.17	1.903	0.09
18	Max Daily Temp Diff. (°C)	–0.008	0.91	–0.92	0.22
19	PCC below	2.24	**0.00**	–1.54	-
21	Surface Thickness (mm)	0.014	0.25	–1.75	0.11
22	AADT	0.00006	0.09	–1.76	0.31
23	AADTT	0.5978	0.35	–1.29	-
24	ESALs	0.869	0.19	–1.339	-

In the regression analysis, mix type, rubber inclusion, presence of PCC below, annual freeze-thaw cycles, and ESALs and AADTT for the coring lane were used as categorical variables as explained in Chapter 4. Therefore, the Hosmer-Lemeshow test results could not be obtained for those variables. Age, fineness modulus, mix type (open graded or not), average annual rainfall, average annual number of wet days, and type of underlying layers (presence of PCC below overlay) were found to be the significant variables. The p-values from Hosmer-Lemeshow indicate an acceptable fit for the variables age, fineness modulus, average annual rainfall, and average annual number of wet days.

In the analysis, none of the low-temperature or thermal difference variables were found to be significant. However, most of the sections in this study do not experience very cold temperatures or large

daily temperature differences; cold temperature and temperature difference effects may have been observed if the data set contained extreme values.

As was expected, older pavements are more likely to show transverse cracking. This cracking is due to the stiffening of binder as it ages and to the accumulation of traffic and temperature cycles. The first-year data indicated that open-graded mixes are less likely to show transverse cracking. Open-graded mixes were found to be insensitive to temperatures due to their nature by Luo (39). However, the second-year data, not included in this regression model, showed a large increase in the number of cracked open-graded sections, particularly those without rubberized binders.

Higher fineness modulus was also found to be significant in the first-year data; however, this is probably because fineness modulus is highly correlated with the mix type (open-graded mixes have a higher fineness modulus). The study also found that the sections with low rainfall were more likely to have transverse cracking. However, this may be due to a correlation of low rainfall with colder temperatures. However, there was no causal relationship between the rainfall and transverse cracking unless there is moisture damage. None of the surface mixes from the cores taken in this study showed signs of moisture damage, so the high correlation may be because the sections with high rainfall generally do not experience high temperature differences or very low temperatures. When the section is a composite pavement, AC on top of PCC, it is more likely to show transverse cracking.

Since the Caltrans PMS data does not include transverse cracking data after 1997, the effect of the presence of transverse cracking in the underlying layers on the transverse cracking on the pavement surface could not be evaluated.

8.4 Raveling

8.4.1 Descriptive Analysis

In the condition survey, the extent and severity of raveling were recorded at 25-m intervals. Extent was evaluated as the percentage of the area raveled. Severity was categorized as coarse when the wearing away of the pavement surface resulted in a very rough surface texture due to dislodged coarse aggregates and loss of binder, and it was categorized as fine when the surface texture was moderately roughened due to wearing away of fine aggregate and asphalt binder.

The presence of raveling on 5 percent or more of the total area of the section was selected as the threshold for the start of raveling for this analysis. If the section had 5 percent or more raveling, it was assumed that the section shows raveling. The condition survey was conducted on the 125- or 150-m length of the pavement surface. Therefore, 5 percent of the total area constitutes 27 m^2 when the length of the section surveyed is 125 m, and it constitutes 22.5 m^2 when the length of the section surveyed is 150

m. With the threshold of 5 percent of surface area, only 12 sections out of 69 showed raveling in the first year, and 20 sections showed raveling in the second year.

Figure 75 shows the number of sections with and without raveling for OGAC, RAC-O, RAC-G, and DGAC mixes. The figure shows that none of the RAC-G sections raveled in the first year. The number of sections with raveling increased over time for all types of mixes in the second year of the survey.

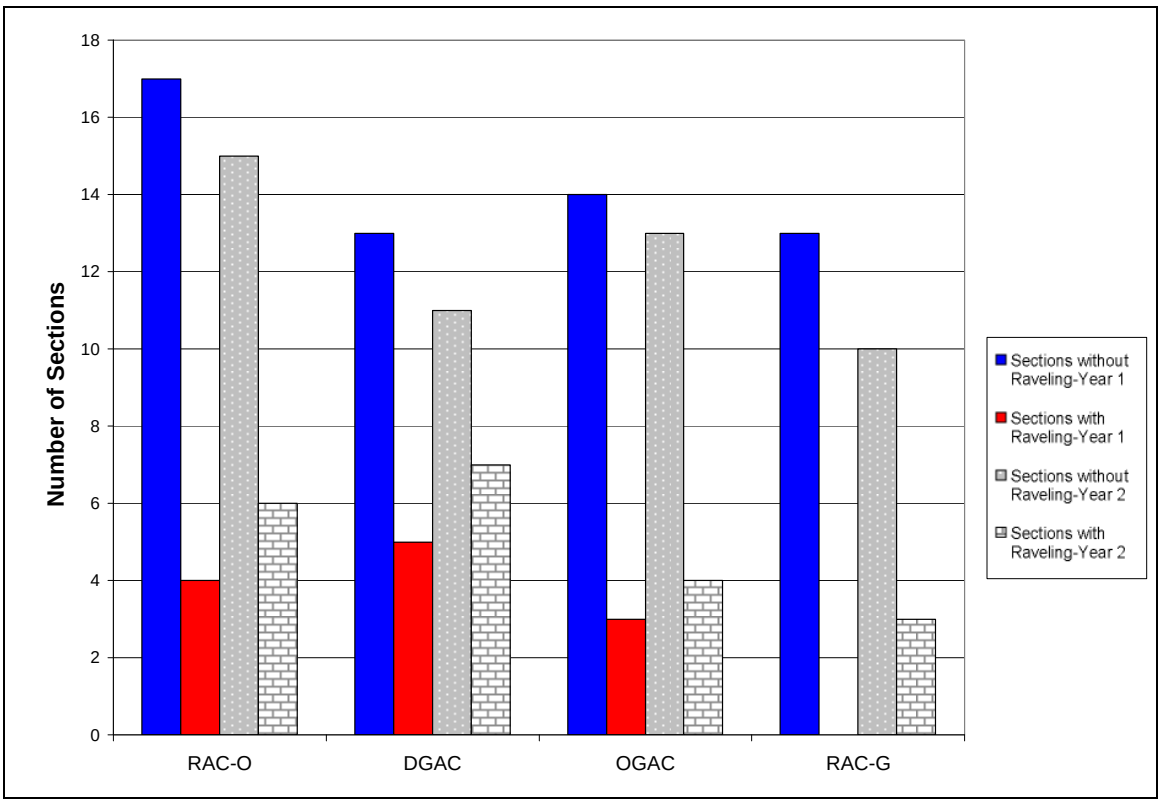

Figure 75: Number of sections with and without raveling for different mix types. (Note: Year 1 refers to the first year of measurement and Year 2 to the second year of measurement.)

Figure 76 shows the sections with and without raveling. The figure shows that fewer sections show raveling for rubberized mixes. The number of sections that show raveling increased both for rubberized and nonrubberized mixes in the second year.

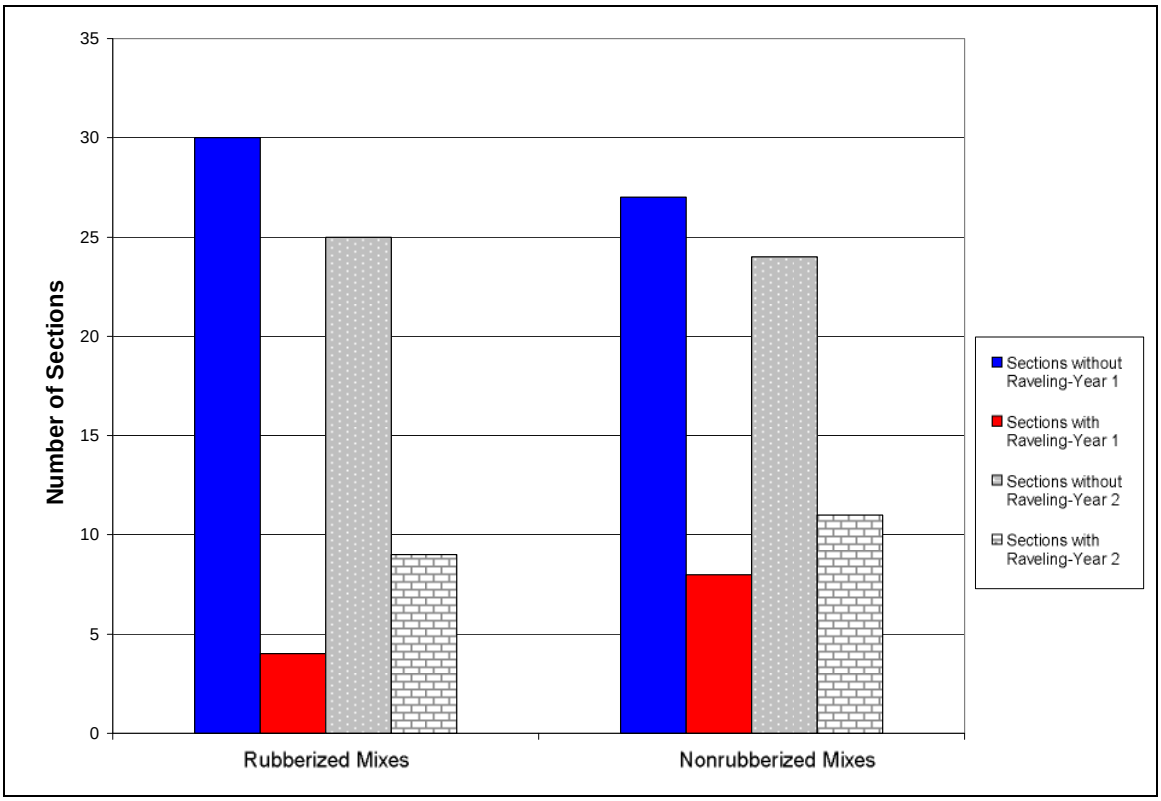

Figure 76: Number of sections with and without raveling for rubberized and nonrubberized mixes. (Note: Year 1 refers to the first year of measurement and Year 2 to the second year of measurement.)

8.4.2 Regression Analysis

Binary logistic regression was conducted on the data. When the percentage of the area raveled was greater than or equal to 5 percent, the dependent variable was given the value 1; otherwise, the dependent variable was given the value 0. The coefficient of the explanatory variable and the constant term along with their p-values and the p-values of Hosmer-Lemeshow tests are shown in the Table 28. The p-values less than 0.05 for explanatory variables are shown in bold.

In the regression analysis, mix type, rubber inclusion, annual freeze-thaw cycles, and AADTT and ESALs for the coring lane were used as categorical variables as explained in Chapter 4. The amount of rainfall and number of wet days over the pavement life, ESALs, the age (without QP-16), and the interaction of age, rainfall, and traffic were found to be the significant variables affecting the presence of raveling.

Table 28: Regression Analysis of Presence of Raveling

Model Number	Explanatory Variable				Constant Term	Hosmer-Lemeshow p-value
	Name		Coefficient	p-value		
1	Air-Void Content (%)		–0.05	0.37	–0.72	0.44
2	NMAS (mm)		0.15	0.11	–3.62	-
3	Fineness Modulus		–0.09	0.88	–0.98	0.54
4	C_u		0.01	0.57	–1.72	0.11
5	Age (years)	With QP-16	0.194	0.09	–2.41	0.02
		Without QP-16	0.28	**0.04**	–2.79	0.10
6	Mix Type		0.16	0.80	–1.64	-
7	Rubber Inclusion		–0.79	0.23	–1.21	-
8	Average Annual Rainfall (mm)		0.0005	0.33	–1.97	0.49
9	Age × Average Annual Rainfall		0.00031	**0.02**	–2.46	0.15
10	Average Annual Wet Days		–0.002	0.71	–1.36	0.00
11	Age × Average Annual Wet Days		0.0025	**0.04**	–2.39	0.30
12	A.A.T.C.M. (°C)		–0.085	0.58	–1.26	0.01
13	Annual FT Cycles		0.44	0.55	–1.65	-
14	Min T Exp. (°C)		–0.26	0.10	–2.69	0.15
15	Average Daily Temp Diff (°C)		0.065	0.72	–2.49	0.92
16	Max Daily Temp Diff (°C)		0.150	0.17	–5.59	0.65
17	N.D T < 0°C		0.12	0.19	–2.53	0.27
18	N.D T < 5°C		0.11	0.19	–3.55	0.34
19	AADT		0.00004	0.27	–1.98	0.06
20	AADTT		1.21	0.07	–1.90	-
21	ESAL		1.47	**0.03**	–1.94	-
22	Age × Average Annual Rainfall × AADT		3×10^{-8}	**0.04**	–2.17	0.07

As pavement ages, its binder gets stiffer, increasing the likelihood that aggregate will separate from the asphalt as traffic repetitions accumulate. The effects of rainfall are cumulative over time. As the amount of rainfall experienced by the pavement increases, the probability of raveling increases. The pavement is also more likely to have raveling when it experiences high annual ESALs (above 800,000). The interaction of age, average annual rainfall, and traffic indicates a combined effect for these variables, meaning that the probability of having raveling is very high for older sections under heavy traffic and high rainfall. The p-values of the Hosmer-Lemeshow statistics indicate an acceptable fit for the models with significant variables.

8.5 Wheelpath Crack Initiation

Since all the sections in this study consist of an asphalt overlay of existing asphalt or concrete pavement, the wheelpath cracks are expected to be the reflection of existing fatigue cracking from the underlying layer. It was expected that similar mechanisms would cause fatigue and reflection cracking, leading to wheelpath crack initiation. In the condition survey, all the cracks in the wheelpath were recorded as fatigue cracks, whether they were caused by reflection or not. No data is available to determine whether they were caused by reflection. However, the extent of wheelpath fatigue cracking prior to placement of the overlay cores was determined from historical Caltrans PMS data and included as an explanatory variable.

8.5.1 Descriptive Analysis

PCS 2000 evaluates fatigue cracking in terms of severity and extent. There are three severity levels of fatigue cracking: Alligator A, Alligator B, and Alligator C. Alligator A is characterized by a single longitudinal crack in the wheelpath, and its extent is recorded as the length of the crack in feet. Alligator B is characterized by interconnected cracks in the wheelpath that resemble the appearance of alligator skin. The extent of Alligator B is recorded as the length of the crack in feet. Alligator C is characterized by interconnected cracks outside the wheelpaths that resemble the appearance of alligator skin. The extent of Alligator C is recorded as greater or less than 25 percent of the section outside the wheelpaths for a 100-foot-long section. Since there are three areas outside the wheelpaths, the total length of the Alligator C cracking evaluated is 300 feet.

The PMS database contains fatigue cracking data collected annually. Although PCS 2000 specifies the evaluation of extent in terms of feet for Alligator A and Alligator B, the PMS data has the extent entered as "percent wheelpath cracked." The PMS data is available for the QP sections from the construction date of the section through 2004. The 2005, 2006, and 2007 condition surveys were conducted by UCPRC.

Wheelpath crack initiation was evaluated only for QP sections since there was no historical pavement condition data for ES sections. Alligator A and Alligator B cracking records were converted to percent cracking and summed to calculate the percent cracking in the wheelpath. The total number of sections evaluated was 59. Fourteen sections showed wheelpath cracking in the first year and 16 in the second year. Only 2 more sections showed wheelpath cracking after the second year. Eleven out of 32 sections showing fatigue cracking before the overlay showed wheelpath cracking in 2007, and 5 out of 27 previously uncracked sections showed wheelpath cracking in the overlay when surveyed in 2007. The presence of fatigue cracking in the underlying layer for QP-25 is not known. Out of 29 rubberized

sections, 6 showed wheelpath cracking, and out of 31 nonrubberized sections, 10 showed wheelpath cracking. Table 29 shows the number of sections that had wheelpath cracking before the overlay was placed and the number that currently have wheelpath cracking.

Table 29: Number of Previously and Currently Cracked Sections

Mix Type	Total Number of Sections	Total Number of Previously Cracked Sections	Total Number of Sections Currently Cracked
OGAC	15	6	3
RAC-O	18	8	3
RAC-G	11	7	3
DGAC	16	11	7

8.5.2 Survival Analysis

Survival analysis (or the duration model or hazard rate) was used to model the crack initiation. Survival analysis was originally developed for medical studies studying the factors affecting human life spans. Survival analysis studies the time to the occurrence of an event. It is called reliability analysis in engineering. Death or failure is called an event, which is the reason that survival analysis is also known as time-to-event analysis. Survival analysis was preferred over logistic regression for this study because survival analysis considers the time of failure rather than simply an indicator that failure has occurred in some time interval. Survival analysis is intended to explain the hazard (risk) function of event times (time-to-event distribution) and the associated survival functions, comparing the time-to-event times for different groups (treatment versus control) and the effects of predictors on the risk.

If time-to-event times are not observed completely, then these observations are called censored. Censoring usually occurs in pavement condition survey data, since it is impractical or impossible to observe the complete set of pavement lifetimes. There are various categories of censoring, such as right censoring, left censoring, and interval censoring. Right censoring occurs when follow-up is curtailed before the failure of one or more pavement sections.

The condition surveys are conducted annually, so it is known only that a cracked section *i* cracked within an interval of one year ($t_i - 1$, t_i), where t_i is the year the cracking was observed at section *i*. Sections that are not cracked at the time of the last condition survey are right censored. Thus the data in this study is either right censored or interval censored. The fact that there is censoring in this study does not provide any information, because the censoring is not related to the effects under investigation.

The likelihood function for both interval- and right-censored data can be constructed by multiplying the product of the differences between the survival functions at time t_i:

$$L = \prod_{i \varepsilon I} [S(t_i) - S(t_i - 1)] \prod_{i \varepsilon R} S(t_i) = \prod_{i=1}^{n} [S(t_i) - S(t_i - 1)]^{\delta i} [S(t_i)]^{1 - \delta i}$$

where

I = the interval-censored observations,

R = the right-censored observations, and

δi = whether the lifetime of the section has been observed (δi = 1) or not (δi = 0).

S(t) is the survival function that defines the probability of surviving longer than time t (110):

$$S(t) = P(T > t) = 1 - P(T \le t) = 1 - F(t)$$

$$0 \le S(t) \le 1; S(0) = 1, S(\infty) = 0$$

The parameters are estimated by maximizing the log likelihood function shown here (110).

$$l = \sum_{i=1}^{n} \{ \delta_i \log [S(t_i) - S(t_i - 1)] + (1 - \delta_i) \log[S(t_i)]\}$$

Cox Regression

It has been common practice to model pavement fatigue lives with survival models. Survival data can be modeled using parametric or semiparametric models. Parametric models use a parametric form for the hazard function, and semiparametric models do not specify the baseline hazard. When the data is more complex or has a less structured distribution, restrictions imposed by the parametric models may be inappropriate.

Semiparametric models assume a parametric form of the explanatory variables but allow an unspecified form for the underlying hazard function. The Cox model (proportional hazard model) is one of the most widely used semiparametric models. It is not based on any assumptions concerning the nature or shape of the underlying survival distribution. Different individuals have hazard functions proportional to one another. The Cox model is presented here. It does not make any assumption regarding the form of the baseline hazard function, $h_0(t)$.

$$\log h_i(t) = \log h_0(t) + \beta_1 x_{i1} + \ldots + \beta_k x_{ik}$$

where $h_0(t)$ = baseline or underlying hazard, and

$\beta_1 x_{i1} + \ldots + \beta_k x_{ik}$ = effect of covariates on baseline hazard.

A Cox regression model was developed using condition surveys from 59 sections. The event times were interval censored because of the annual frequency of the condition survey. However, the Cox model was developed using right-censored data, using only the left endpoint of the event times, to simplify the estimation of the parameters. The result of this approach is conservative survival times. The

dependent variable is the cumulative ESALs to failure. Failure is defined as 5 percent combined Alligator A and Alligator B cracking. The coefficients of the explanatory variables and the p-values as well as the p-value of Wald tests are shown in the Table 30. Wald statistics test the null hypothesis that all the regression coefficients are equal to zero. Wald statistics with p-values less than 0.05 indicate rejection of the null hypothesis that the coefficient is zero. The p-values less than 0.05 are shown in bold.

The presence of fatigue cracks below the surface layer prior to overlay and presence of transverse cracks on the surface of the overlay were found to be the significant variables affecting fatigue crack initiation. The presence of fatigue cracking below the surface layer reduces the overlay life, which confirms the assumption that wheelpath cracking is largely caused by the reflection of fatigue cracking from the underlying layers. The presence of transverse cracks on the pavement surface was found to affect the fatigue cracking. However, there is no causal relationship between the presence of transverse cracks on the surface and fatigue crack initiation. This variable was used in the analysis to check the reflection cracking assumption. Since the underlying mechanisms of fatigue and transverse cracking are different from each other, the high correlation between these variables may suggest that transverse and fatigue cracks are the reflection of the transverse cracks and fatigue cracks from the underlying layer, respectively. The final model for the wheelpath crack initiation is given in Equation (17).

Table 30: Single-Variable Cox Regression Model for Wheelpath Crack Initiation

Model Number	Explanatory Variable			Wald Test p-value
	Name	**Coefficient**	**p-value**	
1	Air-Void Content (%)	–0.025	0.57	0.57
2	Mix Type	–0.68	0.19	0.19
3	Rubber Inclusion	–0.47	0.36	0.36
4	Average Annual Rainfall (mm)	0.00010	0.87	0.87
5	Average Annual Wet Days	–0.004	0.55	0.55
6	Average Annual Maximum Daily Air Temp (°C)	–0.169	0.13	0.13
7	N.D. T > 30°C (yearly)	–0.0082	0.16	0.16
8	A.D.D > 30°C	–0.000225	0.17	0.17
9	Annual FT Cycles	–0.0024	0.89	0.89
10	A.A.T.H.M. (°C)	–0.070	0.18	0.18
11	PCC Below	0.41	0.49	0.49
12	Presence of Fatigue Cracking Below	1.39	**0.02**	0.02
13	Surface Thickness (mm)	0.00074	0.95	0.95
14	Total Pavement Thickness (mm)	–0.000040	0.99	0.99
15	Underlying Layer Thickness (mm)	–0.00011	0.97	0.97
16	Presence of Transverse Cracking	1.8	**0.00**	0.00

Fatigue Cracking Model

$H_0(t) = \exp(1.39 \times \text{Presence of fatigue cracking below})$ **(17)**

	Coef	exp(Coef)	SE(Coef)	Z	P
Presence of fatigue cracking	1.39	4.01	0.599	2.32	0.021

	exp(coef)	exp(–coef)	lower .95	upper .95
Presence of fatigue cracking	4.01	0.25	1.24	13

R-Sq = 0.1 (max possible = 0.814)

Likelihood ratio test = 6.22 on 1 df, p = 0.0126
Wald test = 5.36 on 1 df, p = 0.0206
Score (logrank) test = 6.17 on 1 df, p = 0.013

8.6 Summary of Findings

- Based on the analysis on the experimental design sections, only 5 sections out of 69 showed bleeding in the first year, and 9 sections showed bleeding in the second year. Therefore, there is limited bleeding for OGAC, RAC-O, DGAC, and RAC-G mixes. However, bleeding is a problem for F-mixes as 3 out of 5 F-mixes showed bleeding.
- Out of 69 experimental sections, only 6 showed rutting in the first year, and 9 sections showed rutting in the second year. None of the environmental test sections showed rutting. Therefore, rutting does not appear to be a major problem for any type of asphalt surface evaluated in this study.
- Regression analysis performed on the first year of data for the presence of transverse cracking confirmed the earlier findings that sections with higher air-void content and open gradation are less likely to have transverse cracking. Therefore, open-graded mixes are less likely to show transverse cracking compared to dense-graded mixes. Sections with greater rainfall and with PCC below the asphalt layer are more likely to have transverse cracking. The older mixes are more likely to have transverse cracking, which also supports the earlier findings. The second-year data, not included in the model, showed a marked increase in the presence of transverse cracking in the open-graded mixes, particularly those without rubber binders.

- Regression analysis of the presence of raveling confirmed the earlier findings that older sections and sections with greater rainfall and higher truck traffic are more likely to show raveling. The combined effects of rainfall, age, and traffic also increase the presence of raveling.
- All OGAC F-mixes showed a significant amount of raveling after eight years. Therefore, raveling is a problem for F-mixes without rubberized binders. After the second year of data collection, the oldest RAC-O F-mix (five years old) had raveled, while the two younger (two and four years old) RAC-O F-mixes had not.
- The regression model indicated that sections with fatigue cracking in the underlying layer prior to overlay are more likely to show wheelpath cracking.
- Based on the regression analysis, thickness was not found to be a significant variable affecting any cracking mechanism. A significant variable affecting the fatigue crack initiation was the presence of fatigue cracking prior to the overlay. It is likely that since most of the overlays were cracked before overlay that reflective cracking was the primary cracking mechanism.
- Based on the data in this study, mixes with rubber binder were not found to help reduce any distresses. However, this result may have been obtained because mixes with rubber binder tend to be placed on pavements with more extensive existing cracking than are nonrubberized mixes.
- The progression of distresses could not be evaluated because only a few sections showed distress in the second year of measurement.

9 ANALYSIS OF ACOUSTICAL PROPERTIES OF ASPHALT MIXES

Noise measurements were conducted on the test sections included in this study using the version of the on-board sound intensity method developed in California (OBSI-California). The results of the OBSI are given in terms of spectral content in one-third octave bands. The one-third octave band noise levels were summed to get the overall A-weighted sound intensity levels. The analysis of acoustical properties of different asphaltic mixes answers these questions:

- How much noise reduction do open-graded mixes provide both overall and in terms of frequency spectra?
- Do rubberized mixes provide noise reduction?
- How do the pavement characteristics and temperatures as well as the interaction of pavement characteristics affect the tire/pavement noise levels?
- Can the earlier models of the noise-generation mechanisms be verified?
- Is tire/pavement noise correlated with pavement absorption?

9.1 On-Board Sound Intensity Levels

9.1.1 Descriptive Analysis

Due to the road geometry, QP-48 and QP-49 were measured at 30 mph (50 km/h). Sound intensity measurements are highly dependent on speed, and currently there are no shift factors to convert 30-mph sound intensity measurements to equivalent values at 60 mph. These sections were therefore not included in the sound intensity analysis. An empirical equation was developed to convert the 35-mph measurements to 60 mph for frequency level analysis (see Appendix A). Therefore, the 35-mph measurements for these sections could be evaluated with the 60-mph measurements for the other sections. The QP-42 section had measurement errors in the first-year data collection; therefore, it was not included in the analysis.

After all the measurements were converted to their equivalent values at 60 mph, air-density corrections provided by the Transtec Group (111) were applied to sound intensity levels at each frequency. The air-density correction equation is provided in Appendix B. The noise measurements were conducted for two years. QP-9 was not included in the analysis since the middle of the section contains a patch that may affect the noise results. There was an error in the sound intensity measurements of QP-42; therefore, this section was not included in the sound intensity analysis either.

Figure 77 shows the sound intensity levels of the OGAC, RAC-O, RAC-G, and DGAC mixes. The figure shows that DGAC mixes have the highest sound intensity levels. OGAC and RAC-O mixes

have similar sound intensity levels and are quieter than the RAC-G and DGAC mixes. Sound intensity levels of RAC-G mixes are between those of open-graded mixes and DGAC mixes.

Figure 78 shows the sound intensity levels of OGAC, RAC-O, RAC-G, DGAC, and RAC-O F-mixes. OGAC F-mixes (QP-48 and QP-49) were not evaluated here since the sound intensity measurements were conducted at 30 mph on these sections. The figure shows that RAC-O F-mixes have the highest sound intensity levels.

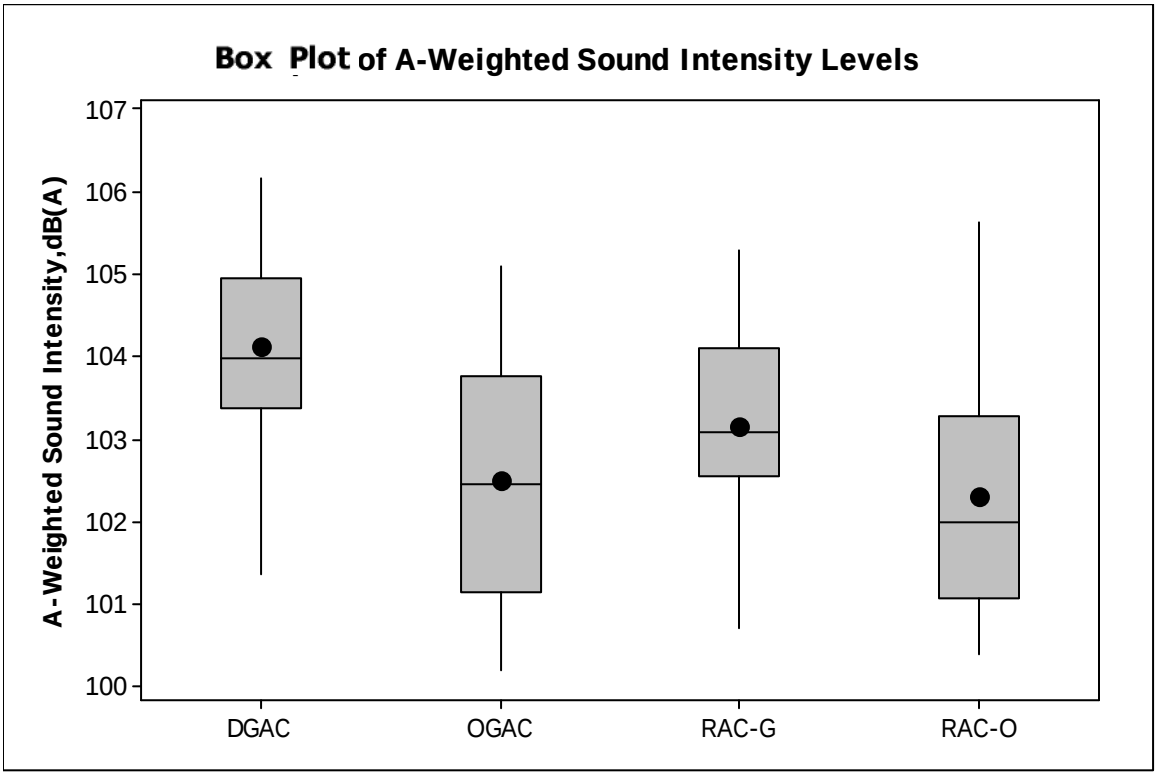

Figure 77: A-weighted sound intensity levels for different mix types.

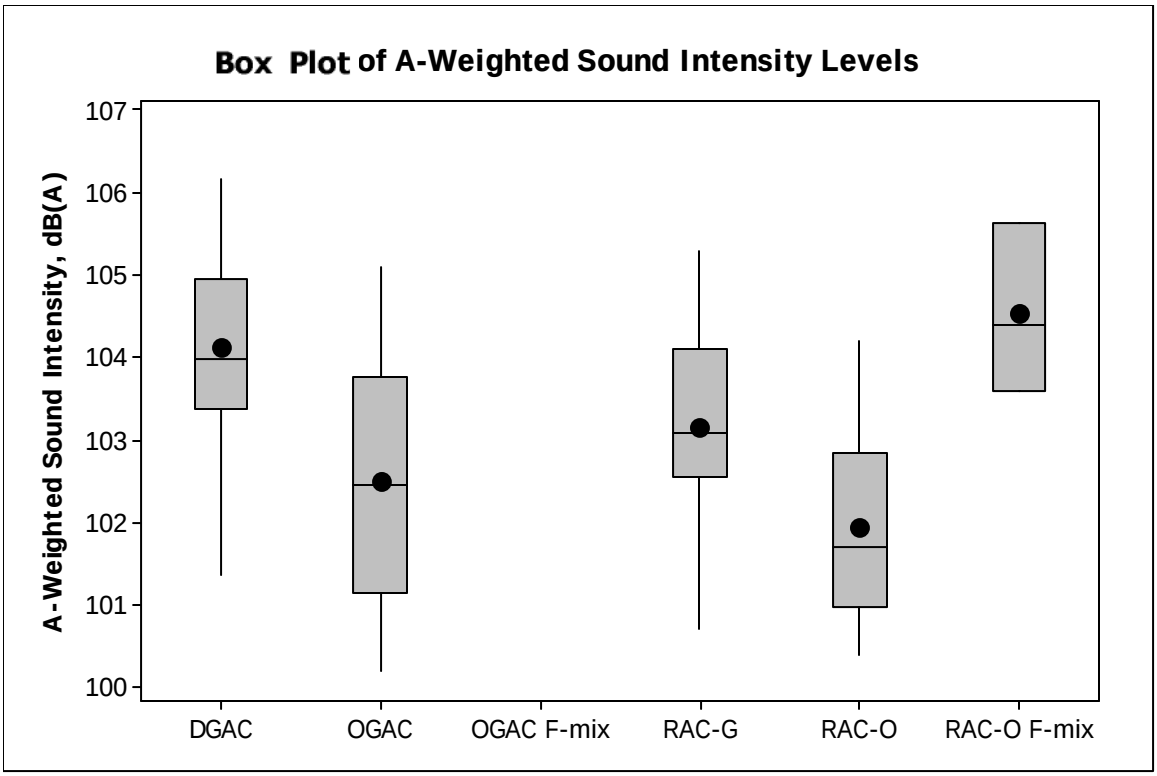

Figure 78: A-weighted sound intensity levels for different mix types with F-mixes separated.

Figure 79 shows the sound intensity levels for different mix types at different ages. The figure shows that sound intensity values generally increase with age. RAC-G mixes show the clearest trend of increasing sound intensity levels with age. The reason that one-to-four-year-old OGAC and RAC-O mixes are the quietest is that they have the lowest fineness modulus.

Based on the first-year data, the average noise levels of DGAC mixes is 103.7 dB (A) for those that are less than one year old, 104.5 dB (A) for those that are one to four years old, and 104.2 dB (A) for those that are more than four years old. In general, open-graded mixes are quieter than dense-graded mixes. There are five open-graded sections that have noise levels that are equal to or higher than the average noise levels of dense-graded mixes for a given age category. Two of these mixes are more than seven years old, two of them are F-mixes, and the other one is QP-20. The two older open-graded mixes have more severe distresses on the pavement surface than an average DGAC mix in their age category and hence have higher noise levels. F-mixes have a higher NMAS than the other open-graded mixes and hence very high texture depths, which increase the noise levels. They also show raveling, which may also increase the noise levels. The QP-20 section has very high air-void content, high texture depths, and a high IRI value. This section likely had some compaction problems because it is on a steep slope.

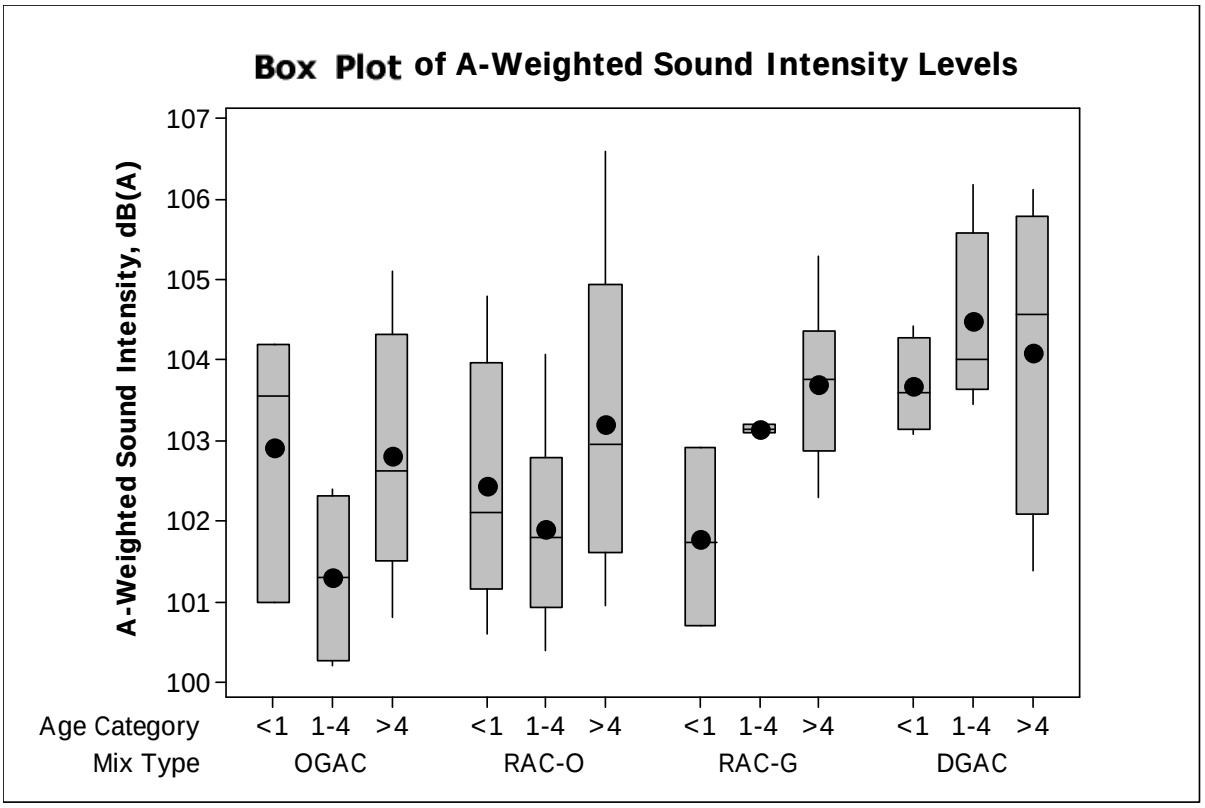

Figure 79: A-weighted sound intensity levels for different mix types at different ages.

Figure 80 shows the cumulative distribution function of reduction in noise levels for both OGAC and RAC-O types of open-graded mixes and RAC-G mixes compared to the average noise levels of DGAC mixes, which is 104 dB (A) across all ages. Since the noise levels of DGAC mixes do not change much for different age categories as shown in Figure 79, the overall average noise level of 104 dB (A) was used as a reference noise level for DGAC mixes. The F-mixes were not included in the plot since they have noise levels as high as dense-graded mixes even when they are new. A positive value indicates reduction in noise levels compared to the average DGAC mix noise level. The figure shows that the noise change is always between a 1 percent increase in noise and a reduction of 4 dB (A). At least a 3 dB (A) noise reduction is required for a surface to be considered a noise-reducing surface. Using on this criterion, only 25 percent of the open-graded mixes are noise-reducing surfaces across the eight-year range of ages. RAC-G mixes provide some noise reduction; however, the amount is almost never above 3 dB (A). The results in Figure 80 also show that over the entire population of sections, the RAC-O mixes are quieter than the OGAC mixes. At the 75th percentile of noise reduction, both open-graded mix types provide similar noise reduction. The difference between them increases at lower percentiles, to about 1 dB(A) at the 10th percentile. This finding may provide a preliminary indication that RAC-O mixes retain their

noise-reducing properties longer than OGAC mixes, since the lower percentiles of noise reduction are generally associated with older pavements.

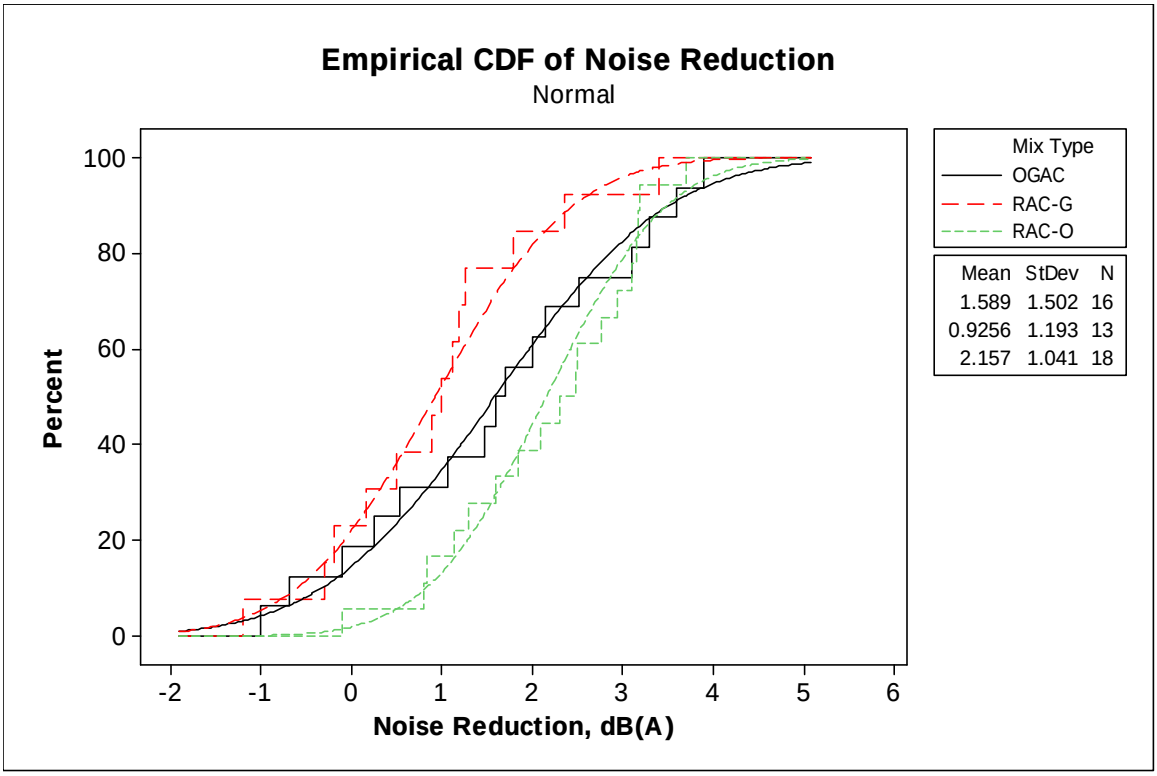

Figure 80: Cumulative distribution function of noise reduction of OGAC, RAC-O, and RAC-G mixes across an eight-year range of ages (positive value indicates a reduction in noise).

Figure 81 compares the first-year and second-year sound intensity levels for different mix types at different ages. The plot includes the sections that were measured in both the first and second years. The figure shows that the sound intensity levels increased in the second year for all mixes. However, this increase is less for mixes that are less than a year old. RAC-G mixes that are in the age category one to four years have the smallest variation, which is probably because that category contains the smallest number of mixes.

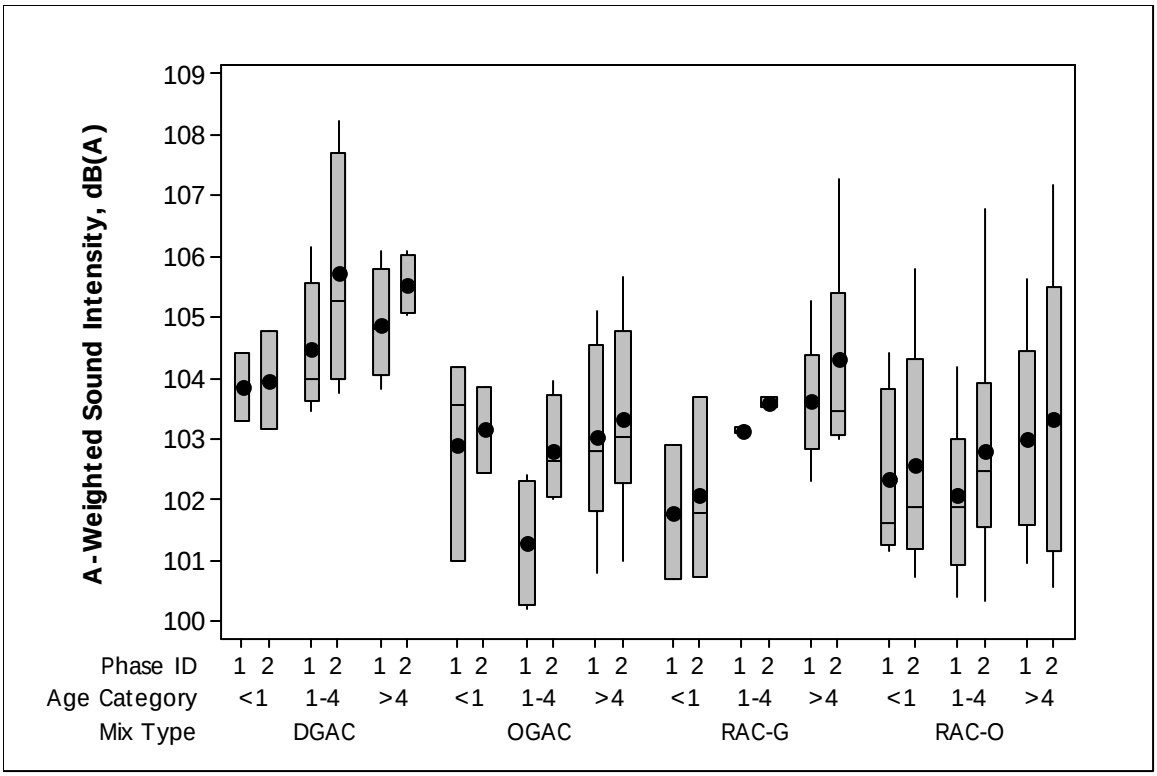

Figure 81: Comparison of A-weighted sound intensity levels for different mix types at different ages for first and second years.

Figure 82 shows the difference in sound intensity levels between the first year and the second year for different mixes at different ages. Since an increase in noise levels was expected, the noise levels in the first year were subtracted from the noise levels in the second year. The figure shows that the box plots for mixes that are less than a year old contain negative values. This finding indicates that the noise levels may stay the same or decrease within a year for mixes that are less than a year old, while for older mixes the noise levels usually increase. Except for RAC-G mixes, mixes one to four years old have the greatest increase in noise levels. It thus can be concluded that for this set of sections, the greatest increase in noise levels of asphalt mixes tended to be for mixes that were one to four years old.

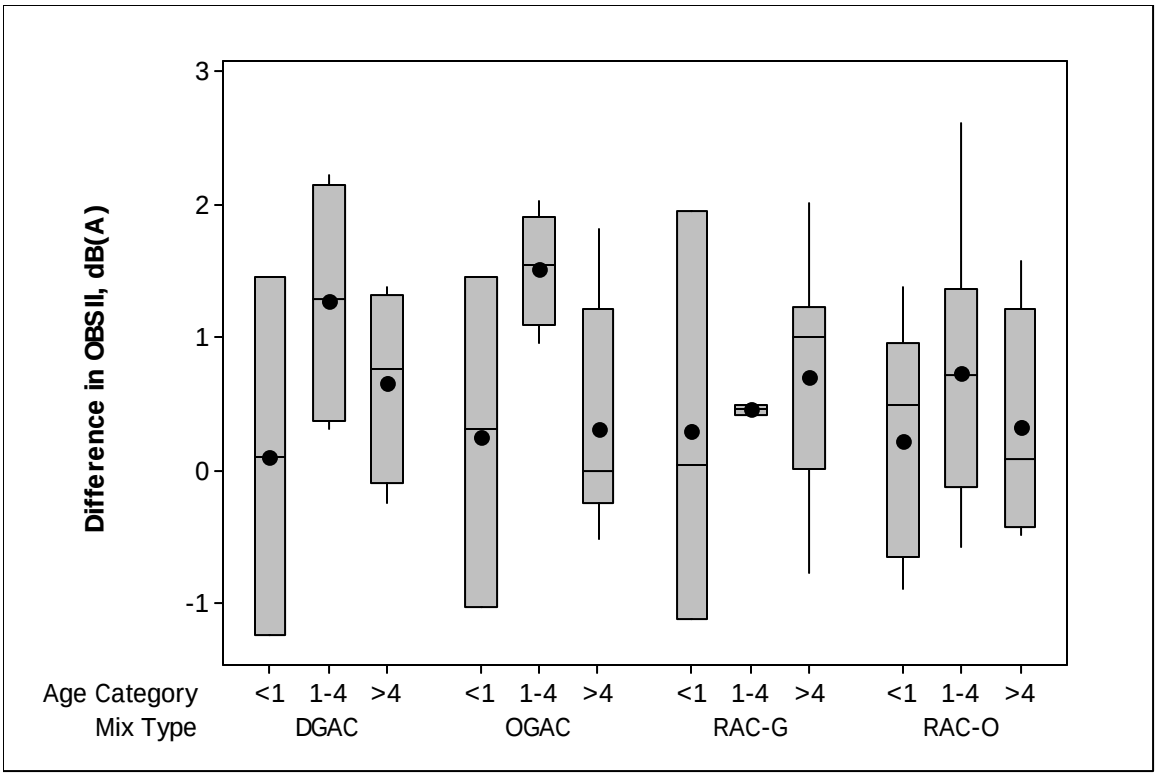

Figure 82: Difference in A-weighted sound intensity levels between first and second years for different mix types at different ages (positive value indicates an increase in noise).

9.1.2 Single-Variable Regression Analysis

Regression analysis was conducted to find the effects of surface properties, distresses, and acoustical absorption values on the sound intensity levels, Because the data set is small, one variable is used in each model. The coefficient of the explanatory variable and the constant term along with their p-values and the coefficient of determination (R^2) for each model are given in the Table 31. The p-values less than 0.05 are shown in bold.

Table 31: Regression Analysis of Single-Variable Models for Sound Intensity Levels

Model Number	Explanatory Variable			Constant Term	R^2 (%)
	Name	Coefficient	p-value		
1	Age (years)	0.15	**0.05**	102.43	5.8
2	Air-Void Content (%)	–0.11	**0.00**	104.30	12.8
3	Mix Type	–1.21	**0.00**	103.67	15.7
4	Fineness Modulus	–0.79	**0.05**	106.98	5.9
5	NMAS (mm)	0.15	**0.02**	101.07	8.4
6	C_u	0.04	**0.00**	102.19	15.0
7	Well-Gradedness	–0.005	0.99	103.08	0.0
8	Rubber Inclusion	–0.59	0.11	103.30	3.8
9	IRI (m/km)	0.86	**0.00**	101.78	12.4
10	MPD (microns)	0.00043	0.50	102.64	0.7
11	RMS	–0.0004	0.68	103.31	0.3
12	BPN	–0.0027	0.92	103.16	0.0
14	Surface Thickness (mm)	0.017	**0.04**	102.21	6.7
15	Presence of Fatigue Cracking	0.77	0.20	102.94	2.9
16	Presence of Raveling	1.26	**0.01**	102.83	9.9
17	Number of Transverse Cracks	0.025	0.48	103.01	0.8
18	Presence of Transverse Cracks	0.82	0.08	102.90	5.2
19	log (permeability) (cm/sec)	–0.27	**0.00**	101.62	21.5

Mix type, well-gradedness, rubber inclusion, and presence of raveling, fatigue cracking, and transverse cracking were used as categorical variables. The study found that age, air-void content, mix type, fineness modulus, NMAS, coefficient of uniformity, IRI, surface thickness, presence of raveling, and permeability are significant variables affecting the sound intensity results. Sound intensity increases as the pavement gets older. It decreases as the air-void content, permeability, and fineness modulus increase. Permeability better explains the variation in sound intensity levels than does the air-void content, probably because when the top part of the surface layer is clogged, the noise absorption and permeability decrease, while the air-void content, which is measured over the total volume of the mix, stays relatively constant.

Open-graded mixes have lower sound intensity levels compared to dense- and gap-graded mixes, which have denser gradation (a higher coefficient of uniformity). Sound intensity levels also increase with increasing thickness. However, note that air-void content is highly correlated with fineness modulus, C_u, and surface layer thickness. When the explanatory variables are highly correlated, the sample size should be increased to test the separate effects of each variable, and a factorial experiment including these variables should be conducted. However, increasing sample size and performing a full factorial experiment across all possible explanatory variables were not possible in this study, which included only

current practice. Therefore, at a given air-void content, the effects of fineness modulus, C_u, and surface layer thickness are not known.

This study also found that increasing IRI and the presence of raveling on the pavement surface increases the sound intensity levels. Note that these variables are highly correlated with age.

Figure 83 shows the sound intensity levels for different NMAS values. The figure shows that there is one point (QP-48), shown in a circle, that has the largest NMAS and highest noise levels and that shifts the regression curve for the open-graded mixes. Figure 84 shows the sound intensity levels for different NMAS values without QP-48. The figure shows that when QP-48 is excluded, there is no relationship between sound intensity and NMAS. A larger sample size is needed to further test the effects of NMAS. At this point, the effects of NMAS on sound intensity levels are inconclusive.

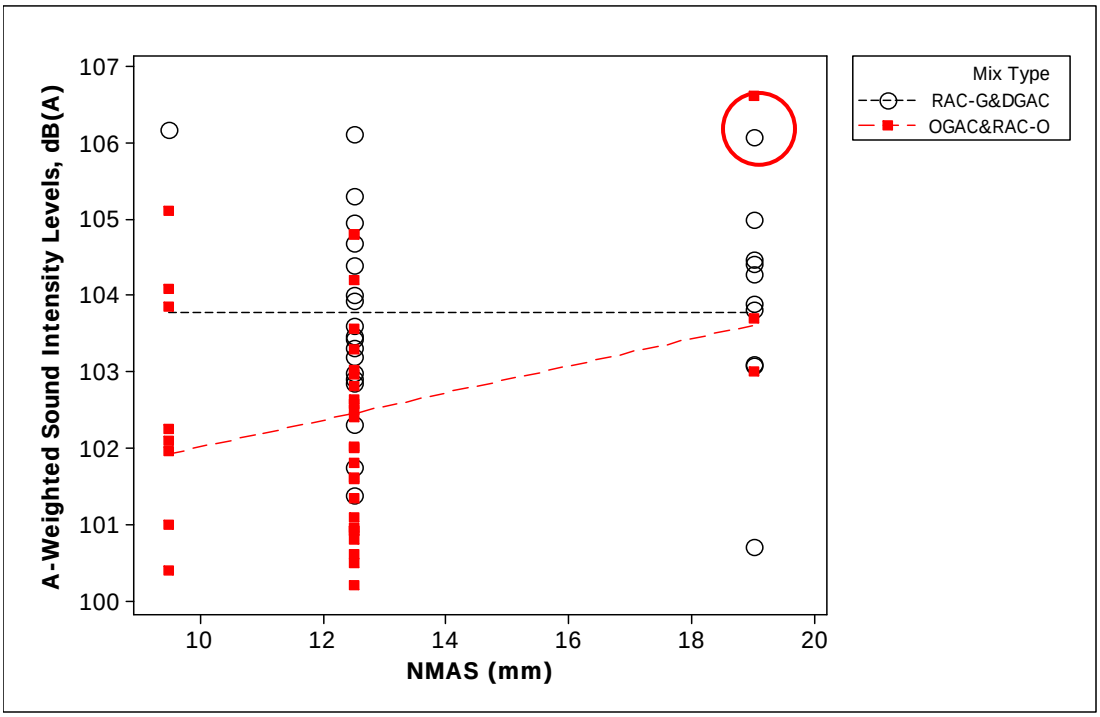

Figure 83: Scatter plot with a best-fit line of A-weighted sound intensity levels versus NMAS (mm).

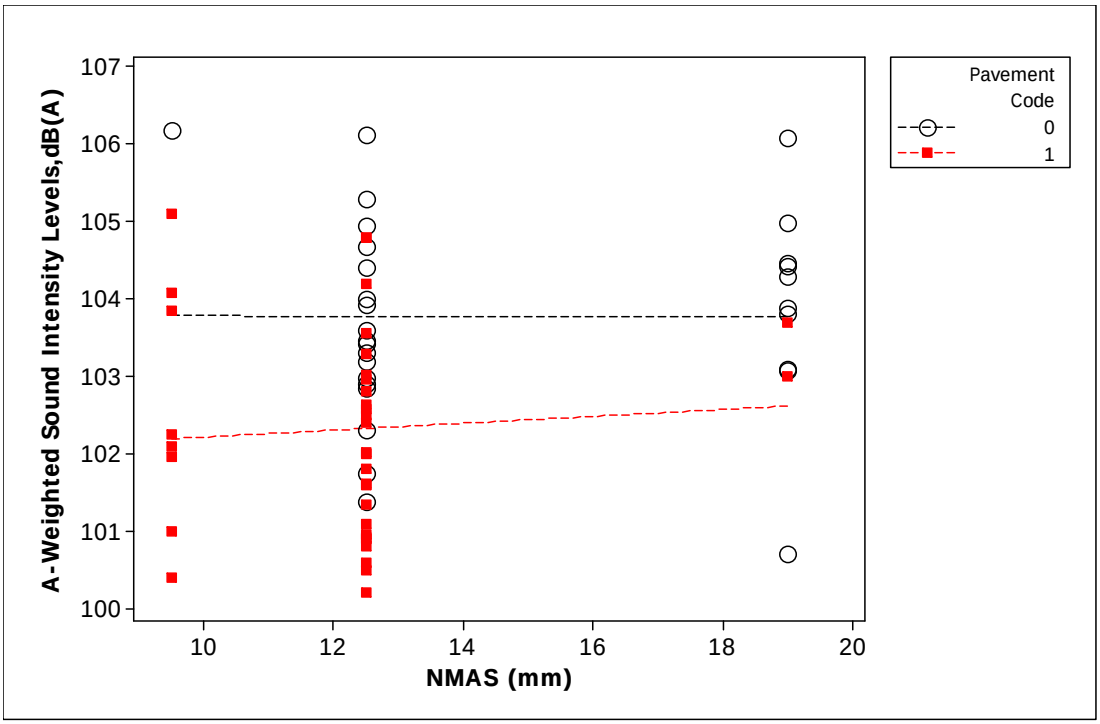

Figure 84: Scatter plot of A-weighted sound intensity levels versus NMAS (mm) without QP-48.

In the single-variable regression analysis with all the sections pooled together, macrotexture was not found to be significant. Figure 85 shows the sound intensity levels versus MPD values for different mix types. Looking at open-graded mixes alone, a correlation can be seen between the MPD values and the sound intensity for open-graded mixes. As MPD increases, the noise level increases. However, MPD has no significant effect on sound intensity levels for dense- and gap-graded mixes.

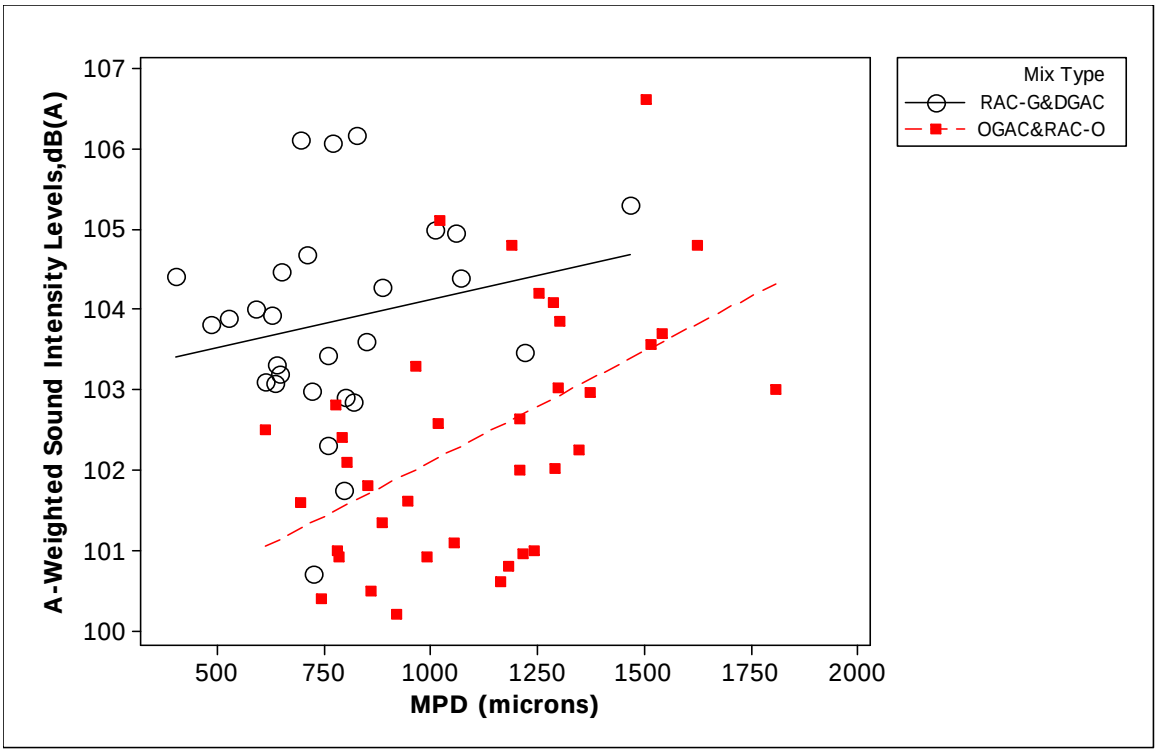

Figure 85: Scatter plot of sound intensity levels versus MPD for different mix types.

Figure 86 shows the sound intensity levels versus the air-void content for different mix types. The figure shows that noise levels decrease as the air-void content increases for dense- and gap-graded mixes. However, the noise levels do not change with the air-void content for open-graded mixes or for mixes that have air-void content above 15 percent. The figure also shows that open-graded mixes generally have lower noise levels than dense- and gap-graded mixes with the same air-void content in the range of 7.5 to 14 percent air voids.

Figure 87 shows the sound intensity levels versus the permeability values. The figure shows that the sound intensity values decrease with increasing permeability for dense- and gap-graded mixes since increasing air-void content reduces the noise levels for these mix types. However, there is no trend for open-graded mixes.

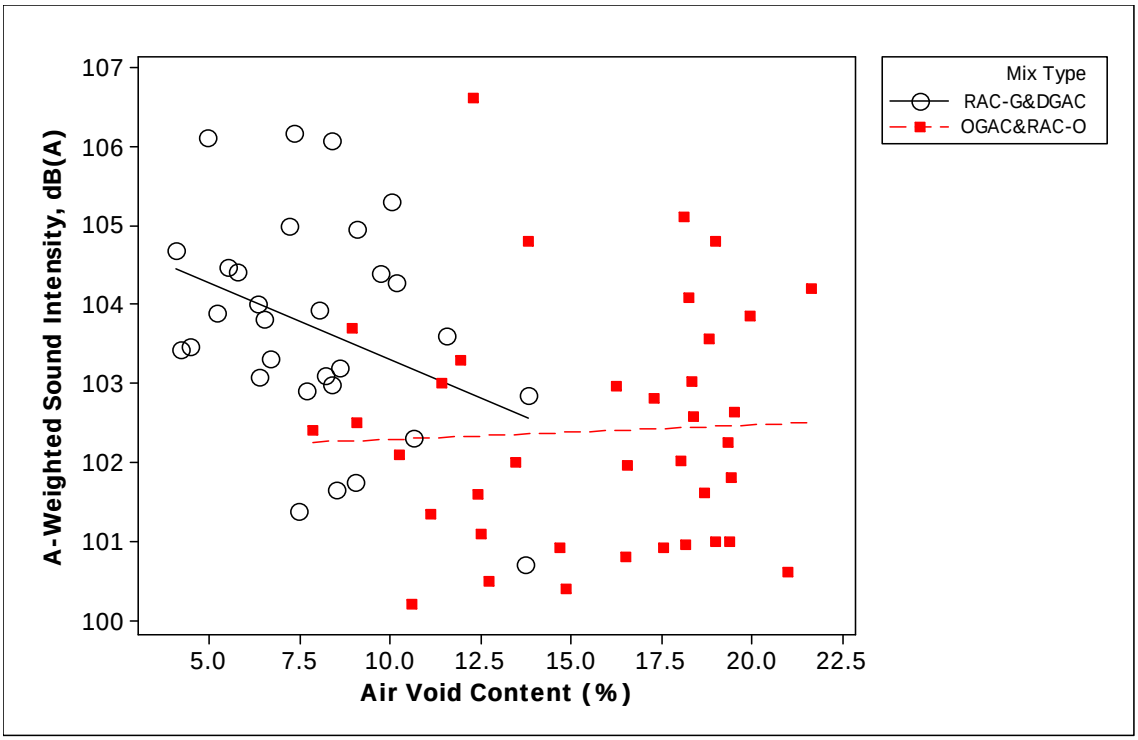

Figure 86: Scatter plot of A-weighted sound intensity levels versus air-void content for different mix types.

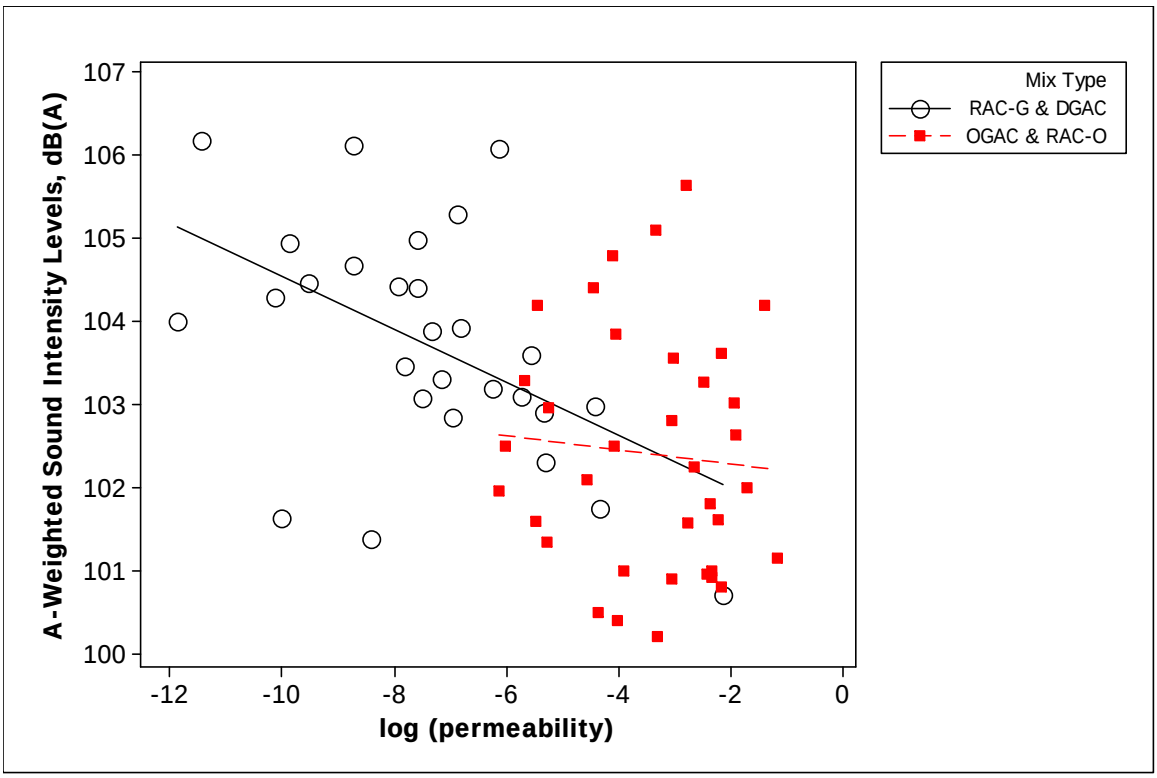

Figure 87: Scatter plot of A-weighted sound intensity levels versus log (permeability) for different mix types.

Figure 88 shows the sound intensity levels versus the fineness modulus. The figure shows that the sound intensity values decrease with increasing fineness modulus for dense- and gap-graded mixes; however, the sound intensity levels of open-graded mixes increase slightly with increasing fineness modulus, due to the eight sections, shown in the circle, that have fineness modulus values in the range of dense- and gap-graded mixes. Therefore, there is some indication that open-graded mixes with finer gradations may reduce the noise levels, although the data shown in the figure is not controlled for NMAS. The effect of fineness modulus for a given fixed NMAS cannot be seen here.

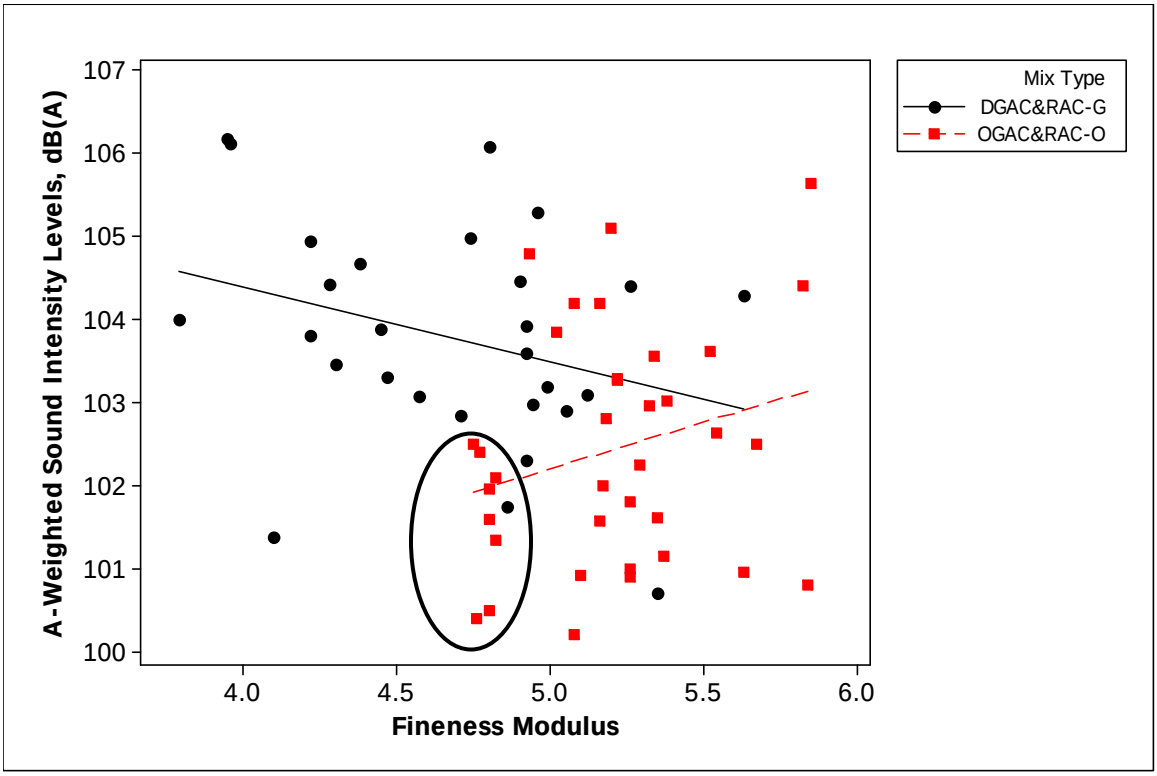

Figure 88: Scatter plot of A-weighted sound intensity levels versus fineness modulus for different mix types.

Figure 89 shows the sound intensity levels versus the surface layer thickness for different mix types. The figure shows that the noise levels of open-graded mixes decrease as the thickness increases, and the noise levels increase with increasing thicknesses for dense- and gap-graded mixes (dense- and gap-graded thicknesses are the thickness of the last overlay only).

The presence of a trend in the regression between the noise levels and thickness for open-graded mixes is due to the four square points shown in the circle, which have thick surface layers and lower noise levels. Without those points, the trend line would be flat. These results suggest that the thickness of open-graded mixes has little effect on noise reduction when the thickness is less than 50 mm, and that thicknesses greater than 50 mm may have a noise-reducing effect. Since the open-graded mixes are

usually placed as a 25- to 30-mm thick layer, there are not enough sections to draw a strong conclusion regarding the effect of thickness on the noise levels for open-graded mixes.

Figure 90 shows the relationship between air-void content and thickness. The figure shows that the air-void content decreases as the thickness increases, which explains the noise behavior of dense-graded mixes with increasing thickness: thicker lifts result in better compaction, decreasing air-void content.

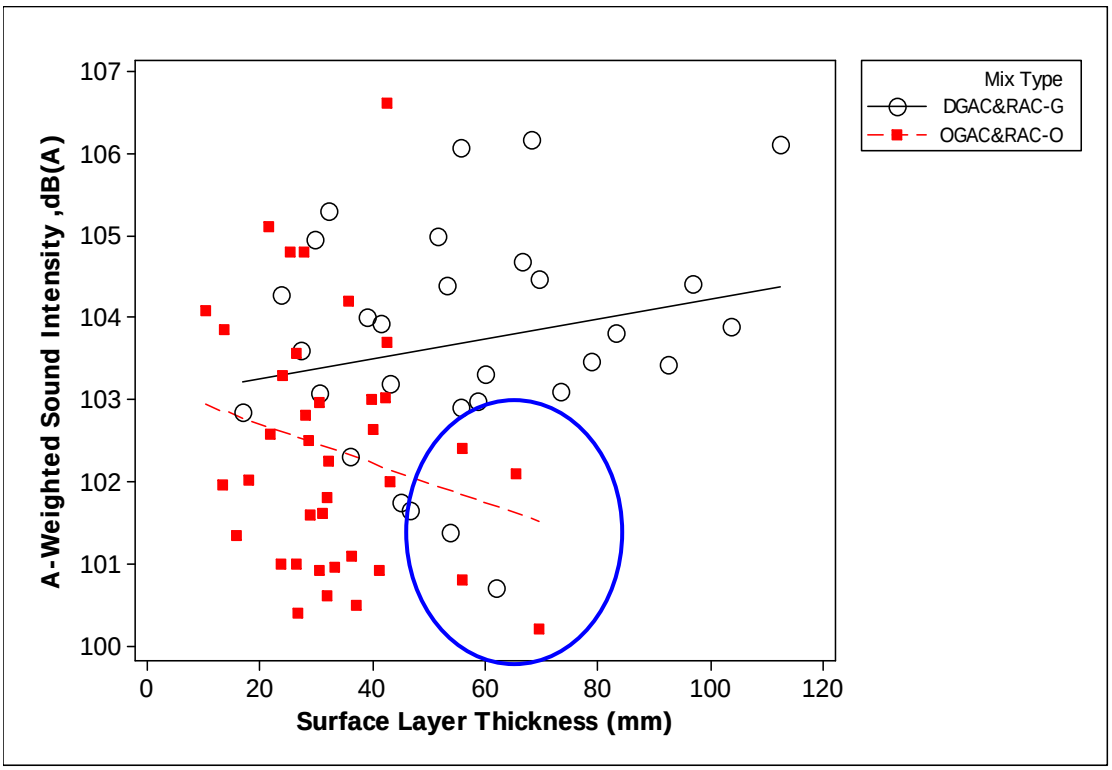

Figure 89: Scatter plot of A-weighted sound intensity levels versus surface layer thickness for different mix types.

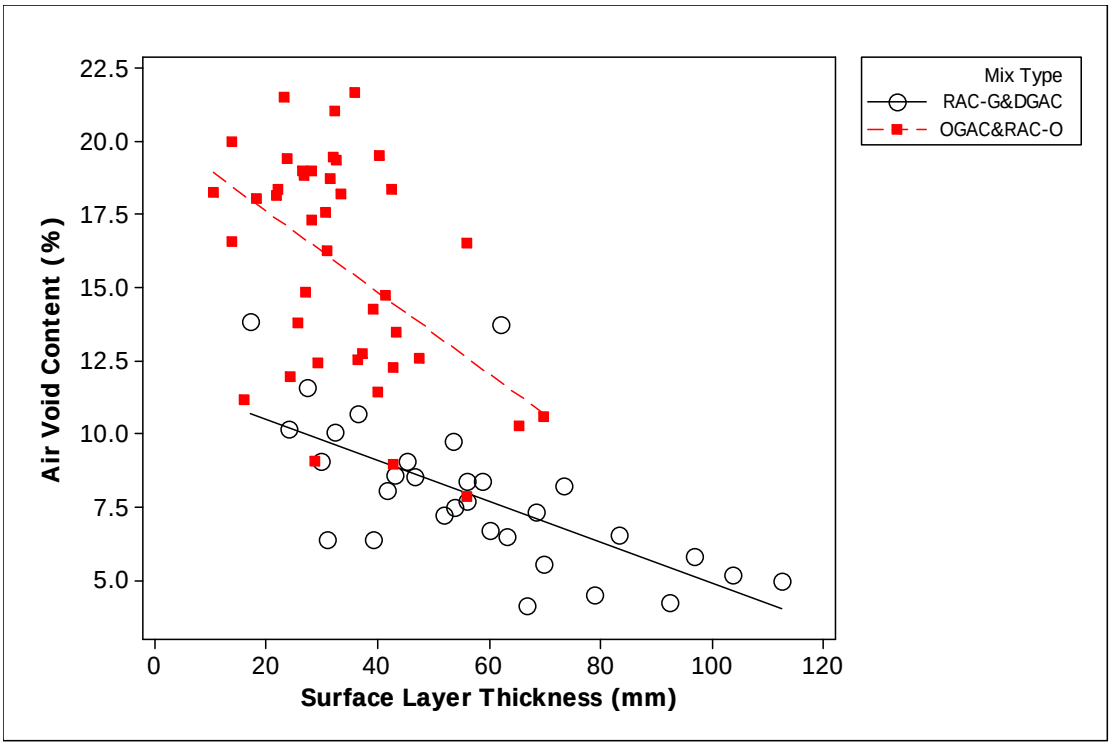

Figure 90: Scatter plot of air-void content versus surface thickness for different mix types.

Figure 91 shows the scatter sound intensity levels for rubberized and nonrubberized mixes and for different mix types. The figure shows that sound intensity levels of OGAC and RAC-O are the same, and that RAC-G mixes have lower noise levels than DGAC. The lower noise levels of RAC-G mixes are due to the higher air-void content of these mixes rather than rubber inclusion. Although rubberized mixes have almost half the stiffness of the nonrubberized mixes, there is no significant difference in the noise levels of RAC-O and OGAC mixes.

To further evaluate the effects of stiffness on noise levels, frequency sweep tests were conducted on the selected cores. Table 32 shows the shear modulus (G*), phase angle, and noise levels of four sections. Two of these sections are RAC-O, and the other two are RAC-G. The stiffness tests were conducted at 20°C. The results are given for 5- and 10-Hz frequencies. The stiffness tests at 10 Hz are intended to simulate the pavement behavior under traffic load. The table shows that ES-12 has almost twice the stiffness as the QP-33 section at both 5 and 10 Hz and the second highest phase angle, and that it is 2.5 dB (A) quieter than the QP-33 section. QP-12 and ES-21 have the same noise levels, and the stiffness of QP-12 is higher than that of the ES-21 section at 5 Hz. There was no stiffness measurement conducted at the 10-Hz frequency for the QP-12 section. Based on these few frequency sweep testing results, a preliminary conclusion is that stiffness does not have a clear effect on the noise levels.

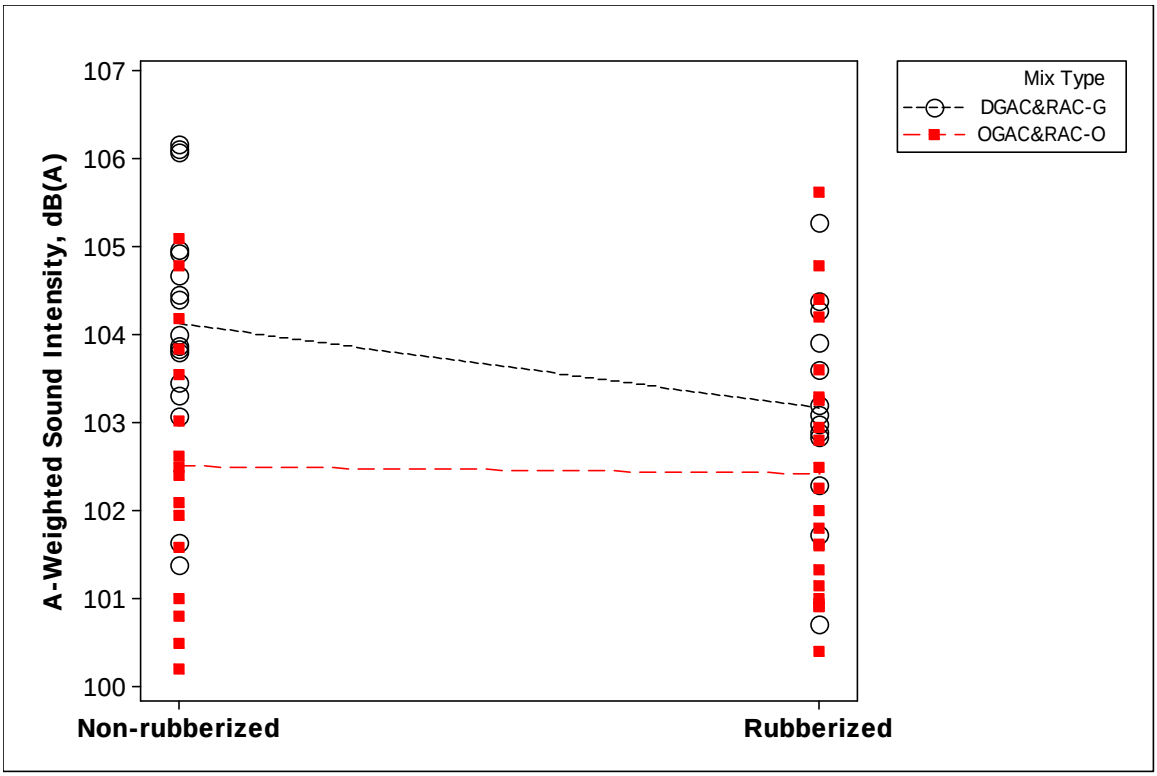

Figure 91: Scatter plot of sound intensity levels for rubberized and nonrubberized mixes.

Table 32: Comparison of Shear Modulus and A-Weighted Sound Intensity Levels for Selected Cores

Section ID	Frequency (5 Hz)		Frequency (10 Hz)		OBSI, dB (A)
	G* (shear modulus) (MPa)	Phase Angle	G* (shear modulus) (MPa)	Phase Angle	
QP-33: 60 mm RAC-G	1497.887	19.605	1796.299	16.272	100.7
ES-12 : 90 mm RAC-G	683.857	22.357	961.336	20.374	103.1
QP-12 :30 mm RAC-O	840.006	17.667	-	-	102.2
ES-21: 30 mm RAC-O	538.699	24.105	629.567	25.215	102.0

The literature review mentioned that pavement temperatures affect noise levels. To evaluate pavement temperature effects on noise levels, a separate study was conducted. Nine sections—three open graded, three gap graded, and three dense graded—which are subsets of the test sections, were selected, and OBSI measurements were taken at pavement temperatures of 15, 20, and 25°C.

Figure 92 shows the relationship plot for pavement temperatures and sound intensity levels. The figure shows that noise levels decrease with increasing temperature. However, the variation is very high, and the coefficient of determination (R^2) is very low (7.3 percent). At this point, a preliminary conclusion is that pavement temperatures do not significantly affect sound intensity levels. A larger data set is needed to fully evaluate the effects of pavement temperatures on noise levels.

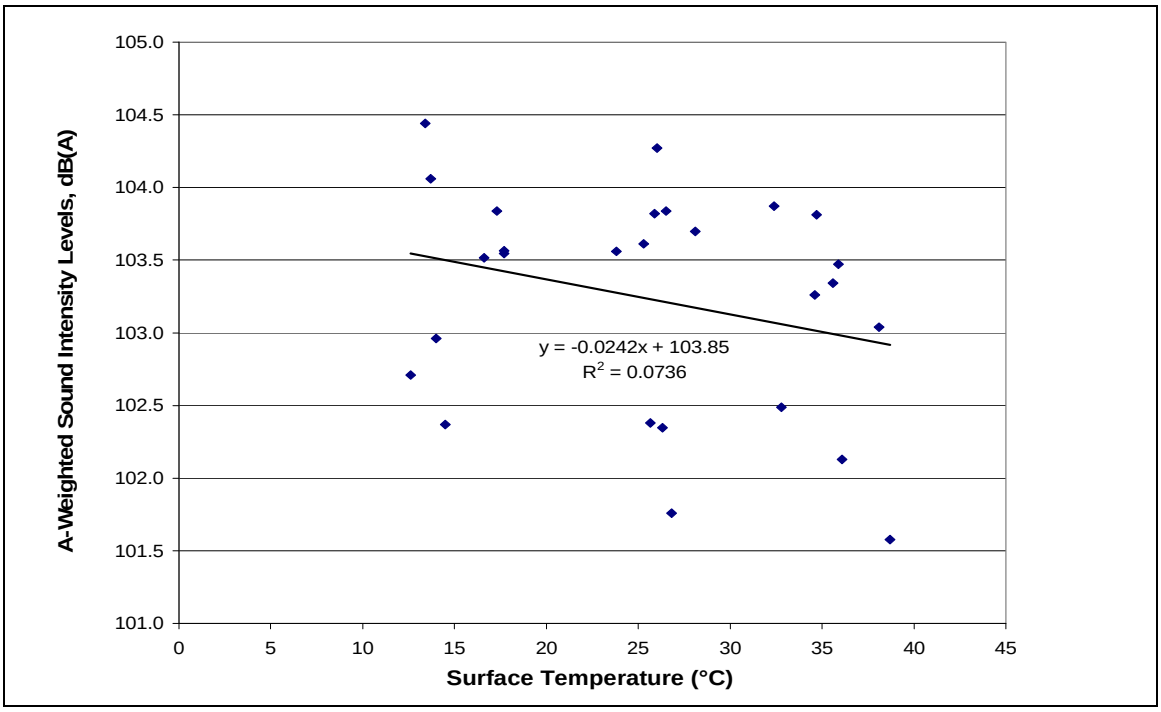

Figure 92: Relationship between A-weighted sound intensity levels and surface temperatures (ºC).

The final regression model explaining the sound intensity levels is presented here. Sound intensity levels were modeled using permeability, macrotexture, mix type, and presence of raveling. These variables can explain 73 percent of the variation in the sound intensity levels. QP-16 was not included in the sound intensity (OBSI) models since it was older than the other sections. The QP-20 and QP-32 sections were not included in the OBSI model either since QP-20 and QP-32 were identified as outliers in the regression. They may have been outliers because the OBSI levels of these two sections may have been over- or underestimated as they were measured at 35 mph and their equivalent values at 60 mph were used in the regression. Additionally, QP-9 was excluded from the analysis since the pavement surface includes patches that reduce the noise levels.

Model for Sound Intensity Levels

The regression equation, Equation (18), is

OBSI = 98.2 – 0.386 × log (permeability) + 0.00329 × MPD + 1.70 × Presence of raveling – 1.16 × Mix type **(18)**

Predictor	Coef	SE Coef	T	P
Constant	98.2389	0.6665	147.40	0.000
log (permeability)	–0.38649	0.06887	–5.61	0.000
Presence of raveling	1.6970	0.3192	5.32	0.000
MPD	0.0032884	0.0004739	6.94	0.000
Mix type	–1.1558	0.3916	–2.95	0.005

S = 0.859152 R-Sq = 73.1% R-Sq(adj) = 70.9%

Analysis of Variance

Source	DF	SS	MS	F	P
Regression	4	98.456	24.614	33.35	0.000
Residual error	49	36.169	0.738		
Total	53	134.625			

A total of 54 sections were used in the model. The permeability values range between 0.00001 and 0.3 cm/sec, and the MPD values range between 405 and 1,805 microns. The mix type and presence of raveling were used as categorical variables 0 and 1.

The sound intensity levels versus permeability values are shown for different mix types and for different macrotexture values in Figure 93. The MPD values were categorized as greater than 1,000 microns and less than 1,000 microns. The figure shows that at a given permeability, the open-graded mixes that have MPD values less than 1,000 microns have lower noise levels compared to the dense-graded mixes in the same MPD category. The lower noise levels for open-graded mixes are attributable to the circled points shown in the figure. These sections have lower fineness modulus than the other open-graded mixes as shown circled in Figure 93.

According to the OBSI equation [Equation (18)], at a constant MPD and permeability value, the presence of raveling on the pavement surface increases the noise levels approximately 1.7 dB (A). For a given surface condition and permeability, a 1,000-micron increase in MPD results in a 3.29 dB (A) increase in the sound intensity level. Open-graded mixes have lower noise levels compared to dense-graded mixes with the same surface condition, permeability, and MPD.

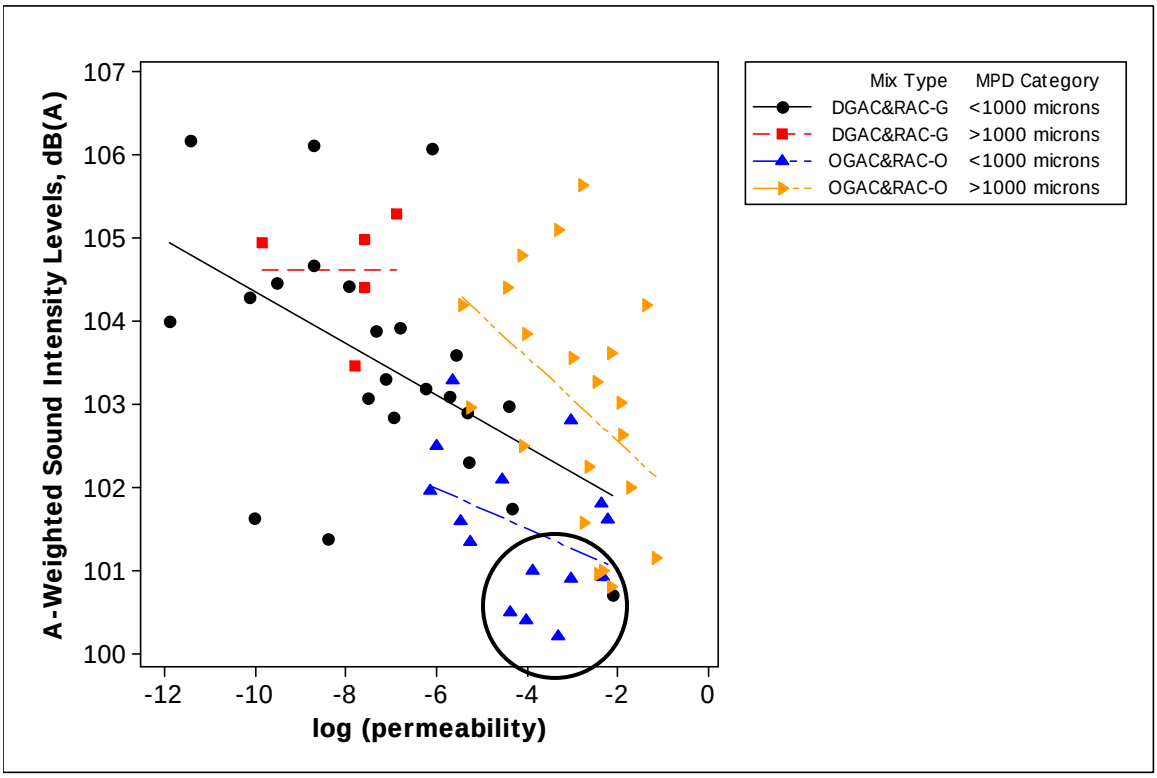

Figure 93: Scatter plot of A-weighted sound intensity levels versus log (permeability) for different mix types and for different MPD categories.

The effects of pavement characteristics on the difference in sound intensity levels in one year were also evaluated using regression analysis. Because the data set is small, one variable is used in each model. The dependent variable is the difference in sound intensity levels between second-year and first-year measurements. The independent variables are the air-void content change, IRI change, MPD change, and BPN change in one year and the mix type, fineness modulus, NMAS, C_u, and NMAS. The coefficient of the explanatory variable and the constant term along with their p-values and the coefficient of determination (R^2) for each model are given in the Table 33.

Table 33: Regression Analysis of Change in Sound Intensity Levels

Model Number	Explanatory Variable			Constant Term	R^2 (%)
	Name	Coefficient	p-value		
1	Change in AV Content (%)	0.0066	0.94	0.62	0.0
2	Mix Type	–0.24	0.37	0.665	1.4
3	Fineness Modulus	–0.43	0.13	2.71	3.8
4	NMAS (mm)	–0.018	0.72	0.77	0.2
5	C_u	0.017	0.06	0.17	6.0
6	Rubber Inclusion	–0.28	0.30	0.69	1.8
7	Change in IRI (m/km)	0.28	0.47	0.58	0.9
8	Change in MPD (microns)	–0.0014	0.10	0.62	4.5
9	Change in BPN	0.022	0.25	0.57	2.4

Regression analysis revealed that none of the variables evaluated affects the difference in noise levels between the first year and the second year. This result may have been obtained because one year may be too short to observe any difference in noise levels due to pavement characteristics.

9.1.3 Principal Components Regression

Multicollinearity is present if two predictor variables are highly correlated or if one predictor has a large multiple correlation with the other predictors. When the independent variables show multicollinearity, the ordinary least squares (OLS) regression leads to coefficient estimates that fluctuate largely in sign and magnitude due to a small change in the dependent or independent variables, and to large standard errors that are consequently insignificant.

Principal components regression (PCR) is one of the techniques used to handle the problem of multicollinearity. In this method, the original *k* variables are transformed into a new, smaller set of variables that are orthogonal (uncorrelated). These new, orthogonal variables are called principal components. This transformation ranks the components in order of importance: the first principal component covers the largest variation, the second component covers the largest remaining variation, and so on. Next, the least important components (components that have the least variation) are eliminated. A multiple linear regression analysis is then performed for the dependent variable against the reduced set of principal components using OLS. Since the principal components are independent of each other, it is appropriate to conduct OLS.

Table 34 shows the correlation of the significant variables for sound intensity levels. The table shows that air-void content, mix type, fineness modulus, C_u, and surface layer thickness; age, IRI, and presence of raveling; and age, air-void content, mix type, and fineness modulus are correlated. Although

the correlations between presence of raveling, IRI, and age are not strong, the small data set does not allow the use of correlated variables.

Principal components regression was conducted on the data to deal with the high correlation between the explanatory variables. In the analysis, two types of factoring were tried: principal components analysis and principal axis factoring (principal factor analysis). Figure 94 shows the scree plot of the principal components analysis. It shows the number of components on the X axis and the corresponding eigenvalues on the Y axis. The scree plot test is used to select the number of components, or factors. As the number of components increases, the eigenvalues decrease. It can be seen that the curve makes an elbow, and the slope of the curve decreases. The heuristic method is to drop the components after the one starting at the elbow. The scree plot in Figure 94 indicates that three principal components should be used.

Another method to select the number of components is to drop all the components with eigenvalues less than 1. Using this method, two principal components/factors were again selected by the SPSS software. Therefore, two components/factors were retained to make interpretation easier.

Table 34: Correlation Matrix of Significant Variables

		Age	Mix Type	AV (%)	IRI	Presence of Raveling	Fineness Modulus	C_u	Surface Layer Thickness
Correlation	**Age**	1.000	–0.015	–0.033	0.491	0.238	0.037	–0.101	–0.155
	Mix Type	–0.015	1.000	0.809	–0.080	0.078	0.651	–0.737	–0.582
	AV (%)	–0.033	0.809	1.000	–0.110	–0.073	0.641	–0.812	–0.691
	IRI	0.491	–0.080	–0.110	1.000	0.398	–0.046	0.096	0.089
	Presence of Raveling	0.238	0.078	–0.073	0.398	1.000	0.014	0.040	0.194
	Fineness Modulus	0.037	0.651	0.641	–0.046	0.014	1.000	–0.770	–0.532
	C_u	–0.101	–0.737	–0.812	0.096	0.040	–0.770	1.000	0.571
	Surface Layer Thickness	–0.155	–0.582	–0.691	0.089	0.194	–0.532	0.571	1.000

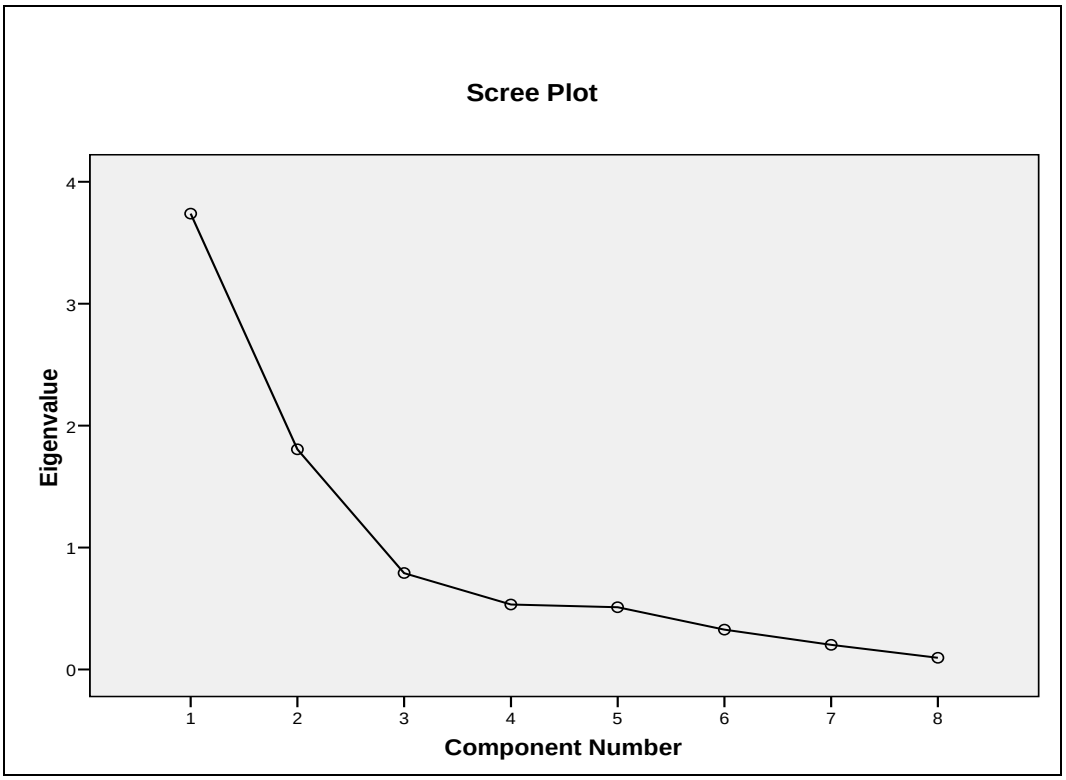

Figure 94: Scree plot for principal components analysis.

To make the output more understandable and to interpret the components/factors easily, the components/factors retained were rotated. Oblique rotation, which does not require the new axes to be orthogonal to each other, was used to rotate the factors. In oblique rotation, a pattern matrix and a structure matrix are obtained. The pattern matrix shows the correlation between the factors and variables uncontaminated by the factor overlap (unique contribution) and the structure matrix shows the correlation between the factors and variables. Table 35 shows the pattern matrix, and

Table 36 shows the structure matrix of the principal components analysis after the oblique rotation.

The pattern matrix was used in the interpretation of the components/factors. Only factor loadings exceeding 0.30 were reported in the pattern and structure matrices. As the tables show, AV, Cu, mix type, fineness modulus, and surface layer thickness are loaded on the first component; and presence of raveling, IRI, and age are loaded on the second component.

Table 37 shows the pattern matrix, and Table 38shows the structure matrix of the principal axis factoring (principal factor analysis) after the oblique rotation. As the tables show, AV, Cu, mix type, fineness modulus, and surface layer thickness are loaded on the first factor; and IRI, presence of raveling, and age are loaded on the second factor. The tables show that similar results were obtained from both analyses. The factor scores from principal component analysis were used in the regression analysis.

Table 35: Pattern Matrix Extracted by Principal Components Analysis

Explanatory Variable Name	**Component**	
	1	**2**
AV Content	0.919	
Cu	–0.913	
Mix Type	0.874	
Fineness Modulus	0.835	
Surface Layer Thickness	–0.760	
IRI		0.822
Presence of Raveling		0.787
Age		0.684

Table 36: Structure Matrix Extracted by Principal Components Analysis

Explanatory Variable Name	**Component**	
	1	**2**
AV Content	0.918	
Cu	–0.913	
Mix Type	0.874	
Fineness Modulus	0.836	
Surface Layer Thickness	–0.759	
IRI		0.822
Presence of Raveling		0.787
Age		0.685

Table 37: Pattern Matrix Extracted by Principal Axis Factoring

Explanatory Variable Name	Factor	
	1	2
AV Content	0.916	
Cu	–0.905	
Mix Type	0.839	
Fineness Modulus	0.784	
Surface Layer Thickness	–0.679	
IRI		0.761
Presence of Raveling		0.641
Age		0.477

Table 38: Structure Matrix Extracted by Principal Axis Factoring

Explanatory Variable Name	Factor	
	1	2
AV Content	0.914	
Cu	–0.905	
Mix Type	0.840	
Fineness Modulus	0.787	
Surface Layer Thickness	–0.677	
IRI		0.760
Presence of Raveling		0.640
Age		0.479

The next step in the principal components analysis is the interpretation of the components. The first component is positively and heavily loaded on air-void content. The rest of the variables loaded on this component are the variables that affect the air-void content; the first component was therefore named *flow variables*. Presence of raveling, IRI, and age are highly loaded on the second component; this factor was named *surface roughness*.

A regression analysis was conducted using the A-weighted sound intensity level as a dependent variable and factor scores as explanatory variables. Macrotexture was also included in the model since it affects the sound intensity levels of open-graded mixes [Equation (19)].

Model for Sound Intensity

OBSI = 100.6 – 1.30 × Flow variables + 0.62 × Surface roughness + 0.003 × MPD **(19)**

Predictor	Coef	SE Coef	T	P
Constant	100.561	0.702	145.86	0.000
Flow Variables	–1.3040	0.2245	–5.63	0.000
Surface Roughness	0.6180	0.1850	3.53	0.001
MPD	0.0030	0.0010	3.78	0.000

S = 1.12 R-Sq = 50.3% R-Sq(adj) = 47.1%

Analysis of Variance

Source	DF	SS	MS	F	P
Regression	3	67.712	22.57	17.85	0.000
Residual Error	53	66.976	1.264		
Total	56	134.687			

A total of 56 sections were used in the model. All the variables in the model were found to be significant at the 5 percent significance level, and they can explain 50 percent of the variation in sound intensity levels. According to the model, the sound intensity level decreases as the flow variables increase when the other variables are held constant, and the sound intensity increases as the surface roughness and macrotexture increase.

9.1.4 Summary of Findings

- Open-graded mixes have lower noise levels than dense- and gap-graded mixes—almost 2 dB (A) on average for all sections over the eight-year range of ages, which according to the literature is near the limit of what the human ear can discern. However, only 25 percent of the open-graded mixes provide noise reduction of more than 3 dB (A) relative to the average noise level of a DGAC mix, 104 dB (A) for the sections tested. Therefore, not all the open-graded mixes can be considered noise-reducing surfaces over the eight-year life span included in the study. Noise reductions between 2 and 6 dB (A) were reported in the literature for open-graded mixes placed on old distressed DGAC surfaces (112, 113). The results presented in this report are comparisons

between different surfaces of similar ages. Greater reductions of noise would be expected when new open-graded surfaces are placed on existing DGAC surfaces that have widespread and severe distresses than when comparing the noise levels of open-graded mixes with DGAC surfaces of similar age as was done in this study.

- RAC-G mixes have lower noise levels than DGAC mixes; however, the average noise reduction provided by RAC-G mixes is around 1.5 dB (A) relative to the average noise levels of DGAC mixes, 104 dB (A).
- The results show that over the entire population of sections, the RAC-O mixes are quieter than the OGAC mixes. Both provide similar levels of maximum noise reduction relative to average noise levels of DGAC mixes; however, the difference between them increases at lower percentiles, to about 1 dB(A) at the 10th percentile. This finding may provide a preliminary indication that RAC-O mixes retain their noise-reducing properties longer than OGAC mixes.
- Based on the very few frequency sweep results and comparison of the noise levels of rubberized mixes and nonrubberized mixes, a preliminary conclusion is that stiffness does not have a clear effect on noise levels.
- RAC-G is the quietest mix when it is less than one year old, compared to DGAC and open-graded mixes. However, it loses its noise-reducing properties in three to four years and become as noisy as dense-graded mixes. Therefore, a preliminary conclusion is that RAC-G mixes are not a good alternative to open-graded mixes.
- Single-variable regression analysis of the sound intensity levels confirmed the earlier findings that noise levels increase with increasing age and IRI and decrease with coarser gradation (as measured by fineness modulus and C_u) and with increasing air-void content and permeability. The presence of raveling on the pavement surface also increases the noise levels.
- The study showed that permeability can explain the variability of noise levels better than the other independent variables can, probably because permeability is affected by clogging, which usually takes place at the top part of the surface layer. When the surface air voids are clogged, noise absorption decreases, and therefore sound intensity levels increase.
- Further analysis of the effect of air-void content on noise levels revealed that the noise levels of mixes with air-void content above 15 percent are insensitive to air-void content. This result is due to increasing macrotexture, which increases the noise levels, surpassing the noise-reducing effects of air-void content. Therefore, air-void content does not affect the noise levels of open-graded mixes, especially those with air-void content above 15 percent.

- Open-graded mixes generally have lower noise levels than dense- and gap-graded mixes with air-void content in the range of 7.5 to 14 percent air voids. This result is probably due to the interconnected air voids of open-graded mixes, which help reduce noise.
- Sound intensity levels decrease with increasing thickness for open-graded mixes that are thicker than 50 mm. Sound intensity is insensitive to thickness changes for open-graded mixes that are thinner than 50 mm. Therefore, increasing thickness within 50 mm does not provide any additional noise reduction. Noise levels increase with thickness for dense- and gap-graded mixes because air-void content decreases with thickness.
- Increasing macrotexture increases the noise levels for open-graded mixes. Macrotexture has no effect on the noise levels for dense- and gap-graded mixes. The multiple regression analysis revealed that increasing MPD increases the noise levels at a constant permeability for a given surface condition, and the principal components regression revealed that increasing MPD increases the noise levels for a given gradation, thickness, age, and surface condition.
- Because macrotexture for open-graded mixes generally increases with increased NMAS, open-graded mixes with larger-size aggregates may be noisier. However, the effects of NMAS were inconclusive since most of the open-graded mixes have an NMAS of 12.5 mm. A larger sample size with different NMAS values is needed to further test the effects of NMAS
- Based on a very small study of the effects of pavement temperature on noise levels, a preliminary finding is that there is no relationship between pavement temperature and noise levels. However, the sample size was very small; therefore, a bigger sample size is needed to further test the effects of pavement temperatures.
- None of the pavement characteristics were found to affect the change in sound intensity levels between the first and second years of the study at a statistically significant level. One year may be too short a time to observe the change in pavement characteristics; hence, no effects on the noise levels were found.

9.2 One-Third Octave Band Analysis of Sound Intensity Levels

The results of the OBSI measurements were also analyzed in terms of spectral content in one-third octave bands. Figure 95 shows the one-third octave band spectra for a RAC-O section. The overall A-weighted sound intensity levels are calculated by summing sound intensity levels at each frequency using Equation (20):

$$\text{Overall average dB (A)} = 10 \times \log \sum_i 10^{f_i/10} \qquad \textbf{(20)}$$

where f_i is the A-weighted sound intensity level at each one-third octave frequency, dB (A).

The frequencies included in the analysis in this report are between 500 and 5,000 Hz. The frequencies below 500 Hz are contaminated by the effect of wind; therefore, they are excluded from the analysis.

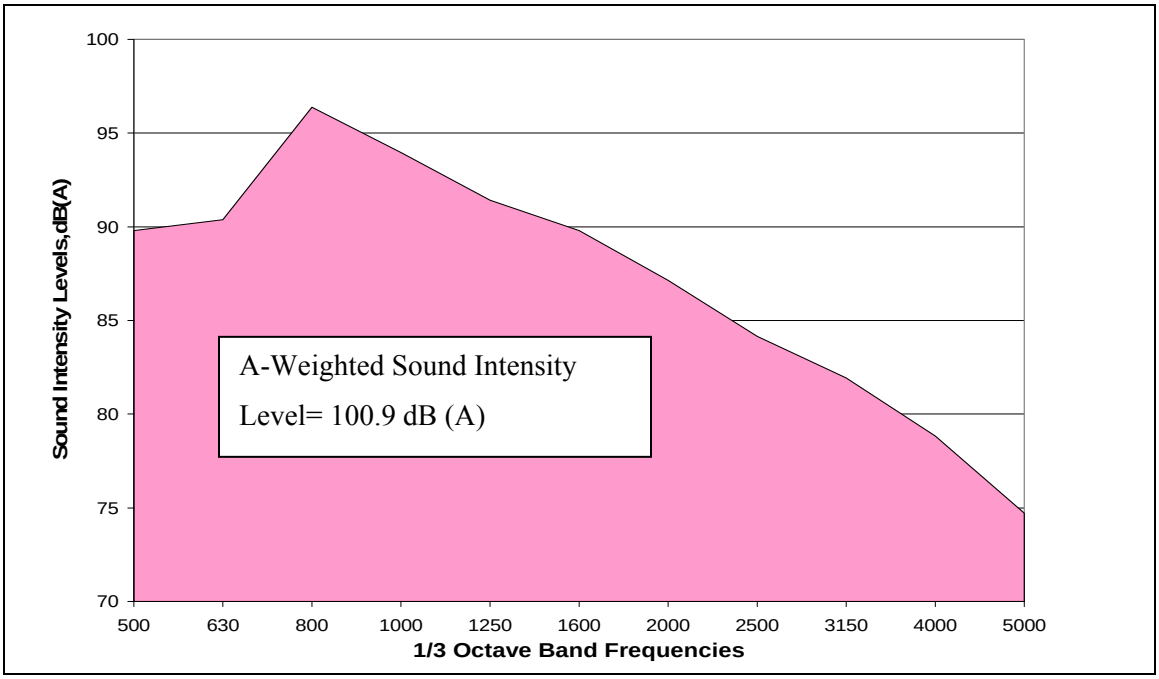

Figure 95: Example of one-third octave band spectrum of OBSI.

9.2.1 Evaluation of Pavement Surface Effects on the Spectral Content of Sound Intensity Levels

The literature survey mentioned that different pavement characteristics generate noise at different frequencies. Frequencies below 1,000 Hz are governed by impacts and shocks generated by macrotexture, friction, and tire tread, and frequencies above 1,000 Hz are controlled by air pumping generated by nonporous and smooth surfaces. Pavement temperatures also affect noise levels at the higher frequency ranges.

To find the effects of pavement characteristics on noise levels at different frequencies, regression analyses were conducted. The frequency analysis excludes some of the sections on which sound intensity measurements were conducted by Illingworth and Rodkin (01-N103, 01-N104, 01-N105, 01-N114, and 01-N121) because although there is a conversion factor for overall A-weighed sound intensity levels between UCPRC and Illingworth and Rodkin, no conversion factor between UCPRC and Illingworth and Rodkin measurements has been established for each one-third octave band frequency. QP-9 is also excluded from the analysis since it has a patch in the middle of the section that affects the noise levels.

Separate single-variable regressions were conducted for each frequency level (500 to 5,000 Hz). The coefficient of the explanatory variable and the constant term along with their p-values and the

coefficient of determination (R^2) for each model are given in Appendix C. Table 39 shows the significant variables affecting the sound intensity levels at the 5 percent significance level for each one-third octave band frequency and their signs.

The variables are shown in order from most significant (with the highest coefficient of determination) to least significant. Since QP-16 is older than the other sections, the age effects were evaluated with and without this section in the regression analysis. A plus sign (+) means increasing the value of the independent variable increases the noise levels at the given frequency. For the categorical variables, a plus sign indicates that the variable coded as 1 increases the noise levels compared to the variable coded as 0.

A total of 64 sections (including QP-16) were included in the regression analysis. The age of the sections included in the analysis ranges between 0.003 and 9 years (QP-16 excluded), air-void content ranges between 4 and 22 percent, fineness modulus ranges between 3.8 and 5.8, IRI ranges between 0.7 and 3.8 m/km, MPD ranges between 405 and 1807 microns, RMS ranges between 282 and 1122, NMAS ranges between 9.5 and 19 mm, C_u ranges between 3 and 58, and surface layer thickness ranges between 10 and 112 mm.

The variables affecting the one-third octave band frequencies were further evaluated, and multiple regression models were developed for each frequency. The variables in the regression models were selected to give the highest correlation coefficient. Since the flow variables and the surface roughness variables are highly correlated with each other, only one variable from each group was selected and used in the models.

Table 39: Pavement Characteristics Affecting Noise Levels at Different Frequencies

Significant Variables				
500	**630**	**800**	**1,000**	**1,250**
MPD (+)	MPD (+)	Mix Type (–)	Mix Type (–)	Air-Void Content (–)
RMS (+)	RMS (+)	Fineness Modulus (–)	Air-Void Content (–)	Mix Type (–)
Air-Void Content (+)	Air-Void Content (+)	C_u (+)	C_u (+)	C_u (+)
Fineness Modulus (+)	IRI (+)	Air-Void Content (–)	Fineness Modulus (–)	Age (+)
Mix Type (+)	Surface Thickness (-)	IRI (+)	Surface Thickness (+)	Fineness Modulus (–)
C_u (–)	C_u (–)	Rubber Inclusion (–)	NMAS (+)	NMAS (+)
IRI (+)	Mix Type (+)		IRI (+)	Presence of Transverse Cracking (+)
Surface Thickness (–)	Fineness Modulus (+)			IRI (+)
	Age (+)*			Presence of Fatigue Cracking (+)
				Surface Thickness (+)

Table 39: Pavement Characteristics Affecting Noise Levels at Different Frequencies *(continued)*

Significant Variables					
1,600	**2,000**	**2,500**	**3,150**	**4,000**	**5,000**
Air-Void Content (–)	Air-Void Content (–)	Air-Void Content (–)	Air-Void Content (–)	Air-Void Content (–)	Air-Void Content (–)
C_u (+)	Mix Type (–)	Mix Type (–)	RMS (–)	RMS (–)	RMS (–)
Mix Type (–)	C_u (+)	RMS (–)	MPD (–)	MPD (–)	Fineness Modulus (–)
Fineness Modulus (–)	Fineness Modulus (–)	C_u (+)	Fineness Modulus (–)	Fineness Modulus (–)	MPD (–)
Surface Thickness (+)	RMS (–)	Fineness Modulus (–)	C_u (+)	C_u (+)	C_u (+)
RMS (–)	Surface Thickness (+)	MPD (–)	Mix Type (–)	Mix Type (–)	Mix Type (–)
NMAS (+)	MPD (–)	Surface Thickness (+)	Surface Thickness (+)	Surface Thickness (+)	Surface Thickness (+)
MPD (–)	NMAS (+)	Presence of Transverse Cracking (+)	Presence of Transverse Cracking (+)	Presence of Transverse Cracking (+)	Presence of Transverse Cracking (+)
Age(+)	Presence of Transverse Cracking (+)	NMAS (+)		Age (+)	
Presence of Transverse Cracking (+)	Presence of Fatigue Cracking (+)				
Presence of Fatigue Cracking (+)	Age (+)*				

* QP-16 excluded

Note: Mix type was coded as 0 for dense- and gap-graded mixes and as 1 for open-graded mixes. Presence of fatigue cracking and of transverse cracking were both coded as 1.

500-Hz One-Third Octave Band

According to the single-variable regression analysis, increasing air-void content, fineness modulus, IRI, and texture increases the sound intensity levels, and increasing C_u and surface thickness reduces the noise levels for the 500-Hz one-third octave band. The analysis also found that open-graded mixes have higher noise levels than dense- and gap- graded mixes.

Figure 96 shows the MPD values versus the sound intensity levels for the 500-Hz band for different mix types. The figure shows that increasing MPD increases the noise levels for all mix types. The point circled is the oldest F-mix used in the analysis. The higher noise levels for this mix are due to its age and greater NMAS value and partially due to the error associated with conversion from 35 mph to 60 mph.

Figure 97 shows the air-void content versus the sound intensity levels for the 500-Hz band for different mix types. The figure shows that for open-graded mixes increasing air-void content increases the noise levels, while for dense- and gap graded mixes this trend is very weak. These results were obtained possibly because at lower frequencies higher air-void content excites the tire vibrations as well as MPD, or because MPD is not a good measure of texture in explaining tire vibrations. The effect of air-void content is more pronounced for higher air-void content and MPD values. The square points circled are the F-mixes, which have higher noise levels than the other mixes at a given air-void content.

The multiple regression model to predict 500-Hz band sound intensity levels is shown here. The MPD, air-void content, and IRI are used as independent variables in the model. Although air-void content was not significant at the 5 percent significance level, it was kept in the model. The model can predict 57 percent of the variation in noise levels. For a mix with a given air-void content and MPD, increasing IRI values increase the noise levels.

Model for 500-Hz One-Third Octave Band

The regression equation, Equation (21), is

500-Hz band = 83.5 + 0.00500 × MPD + 0.115 × Air-void content + 0.969 × IRI **(21)**

Predictor	Coef	SE Coef	T	P
Constant	83.5480	0.9378	89.09	0.000
MPD	0.0049954	0.0009934	5.03	0.000
AV content	0.11474	0.05874	1.95	0.056
IRI	0.9688	0.4630	2.09	0.041

S = 1.89346 R-Sq = 57.2% R-Sq(adj) = 54.9%

Analysis of Variance

Source	DF	SS	MS	F	P
Regression	3	277.454	92.485	25.80	0.000
Residual error	58	207.941	3.585		
Total	61	485.396			

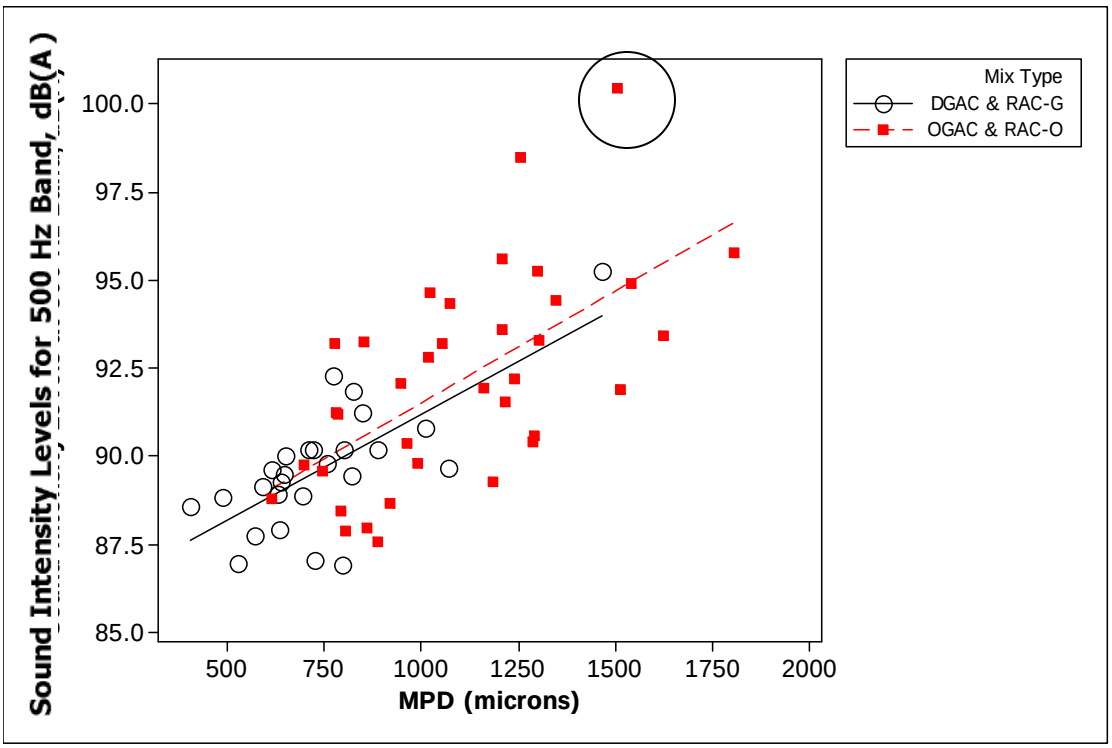

Figure 96: 500-Hz band sound intensity levels versus MPD.

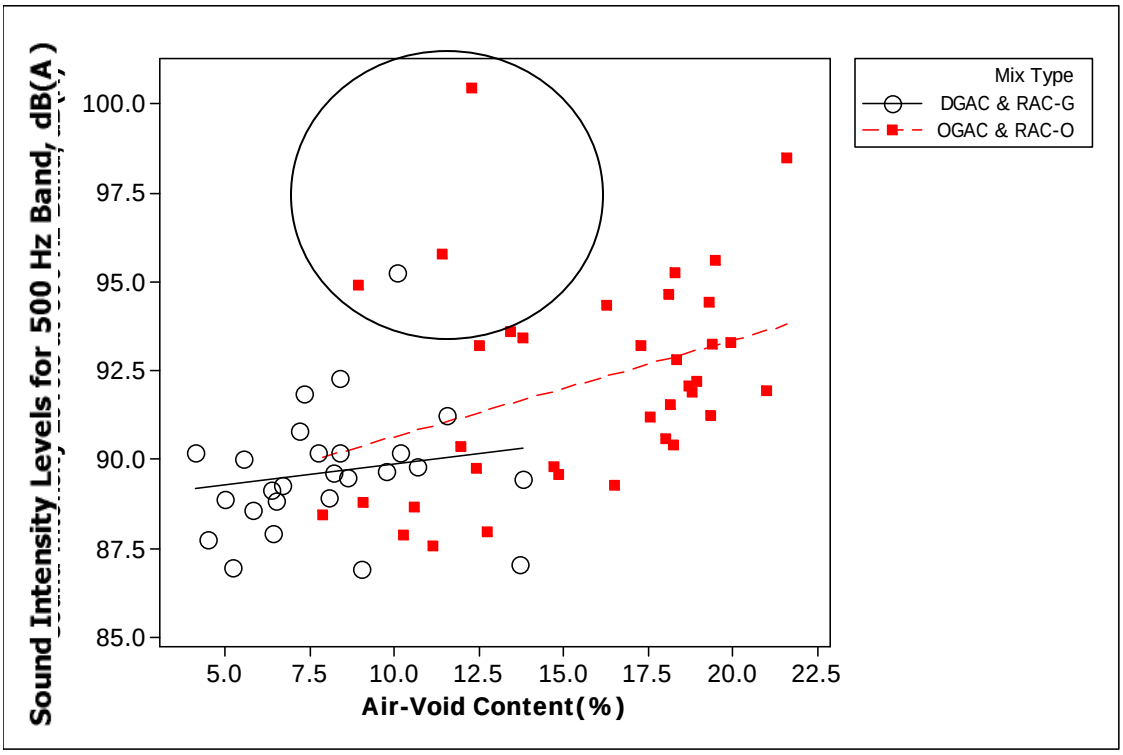

Figure 97: 500-Hz band sound intensity levels versus air-void content.

630-Hz One-Third Octave Band

The study found that noise levels for the 630-Hz band increase with increasing MPD, RMS, air-void content, IRI, fineness modulus, and age (with section QP-16 included). Noise levels decrease with increasing surface thickness and C_u. The study also found that open-graded mixes have higher noise levels than do gap- and dense-graded mixes.

The relationship between the sound intensity levels for the 630-Hz band and age is shown in Figure 98. Regression analysis revealed that age affects the noise levels only when QP-16 (circled in Figure 98), which is 14 years old, is included. This analysis indicates that age does not affect the noise levels for pavements less than 9 years old; however, it may increase the noise for the older mixes. Since there are no sections with ages between 9 and 13 years, the effect of age on noise levels is inconclusive for the 630-Hz band.

The model to predict the sound intensity levels for the 630-Hz band is given here. Only MPD was used in the model since air-void content and IRI were found to be insignificant when used with MPD. The model can explain 39 percent of the variation in the noise levels.

Model for 630-Hz One-Third Octave Band

The regression equation, Equation (22), is

630-Hz band = 88.0 + 0.0048 × MPD **(22)**

Predictor	Coef	SE Coef	T	P
Constant	87.9536	0.7800	112.76	0.000
MPD	0.0047985	0.0007812	6.14	0.000

S = 1.90003 R-Sq = 38.6% R-Sq(adj) = 37.6%

Analysis of Variance

Source	DF	SS	MS	F	P
Regression	1	136.21	136.21	37.73	0.000
Residual error	60	216.61	3.61		
Total	61	352.82			

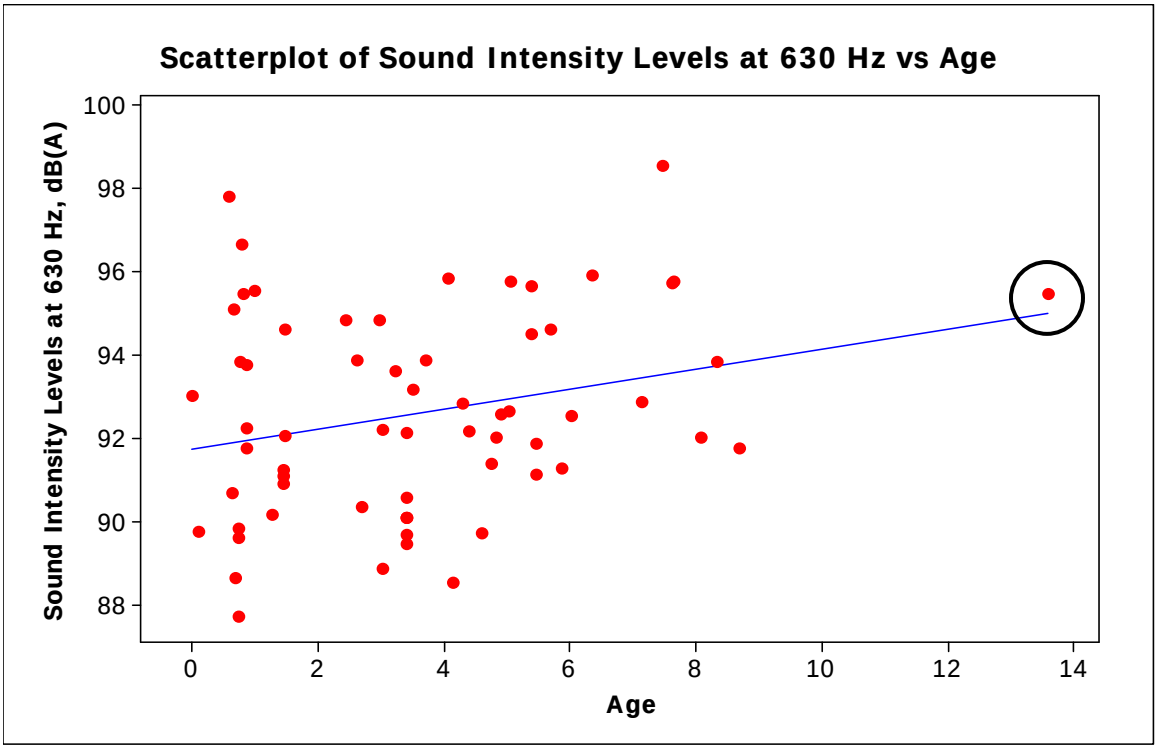

Figure 98: Sound intensity levels at 630-Hz band versus age.

800-Hz One-Third Octave Band

The single-variable regression analysis revealed that the 800-Hz band sound intensity decreases with increasing air-void content and fineness modulus, and that it increases with increasing C_u and IRI. Open-graded mixes have lower noise levels compared to dense- and gap-graded mixes for the 800-Hz band. The analysis found that rubber inclusion in the mix reduces the noise levels; however, this reduction occurs because RAC-G mixes have higher air-void content than DGAC mixes, not because of rubber inclusion, as explained earlier.

Figure 99 shows the relationship between sound intensity levels for the 800-Hz band and air-void content for different mixes. The figure shows that increasing air-void content reduces the noise for mixes with air-void content less than 15 percent. Figure 100 shows the relationship between noise levels for the 800-Hz band and MPD values for different mix types. In the single-variable regression analysis, MPD was not found to be significant. However, the figure shows that increasing MPD increases the noise levels for open-graded mixes. Therefore, it can be concluded that the noise-reducing benefits of air-void content are surpassed by the effects of texture for mixes with air-void content above 15 percent.

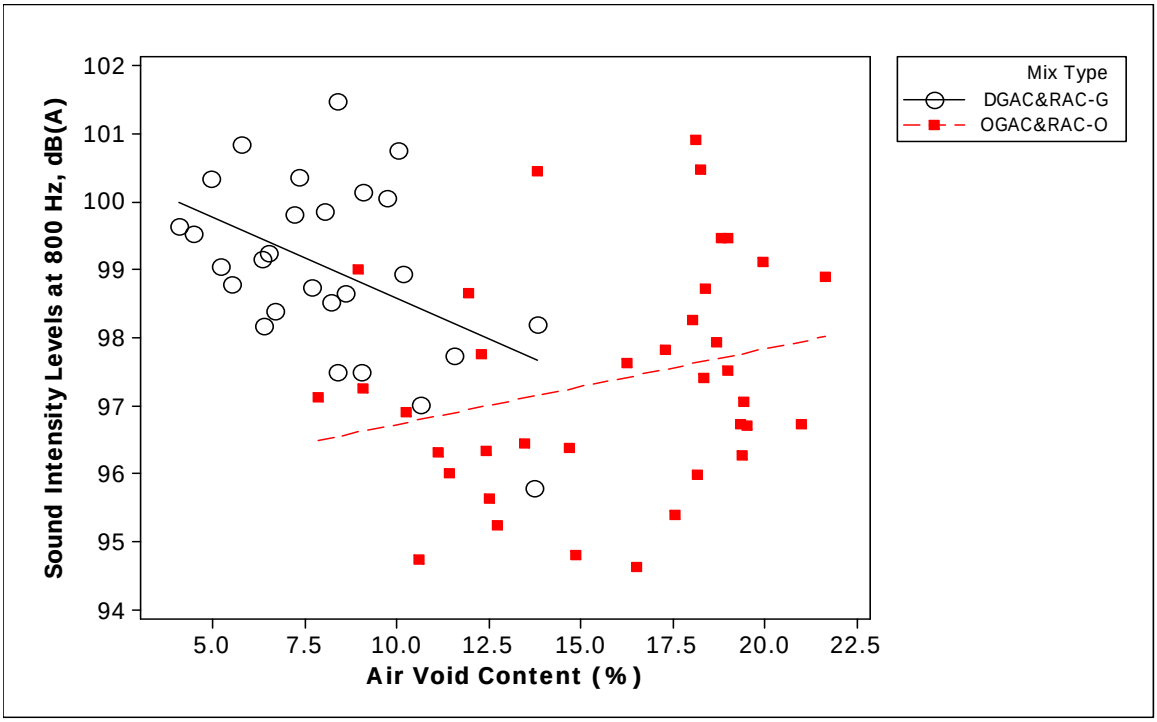

Figure 99: Sound intensity levels for 800 Hz versus air-void content for different mix types.

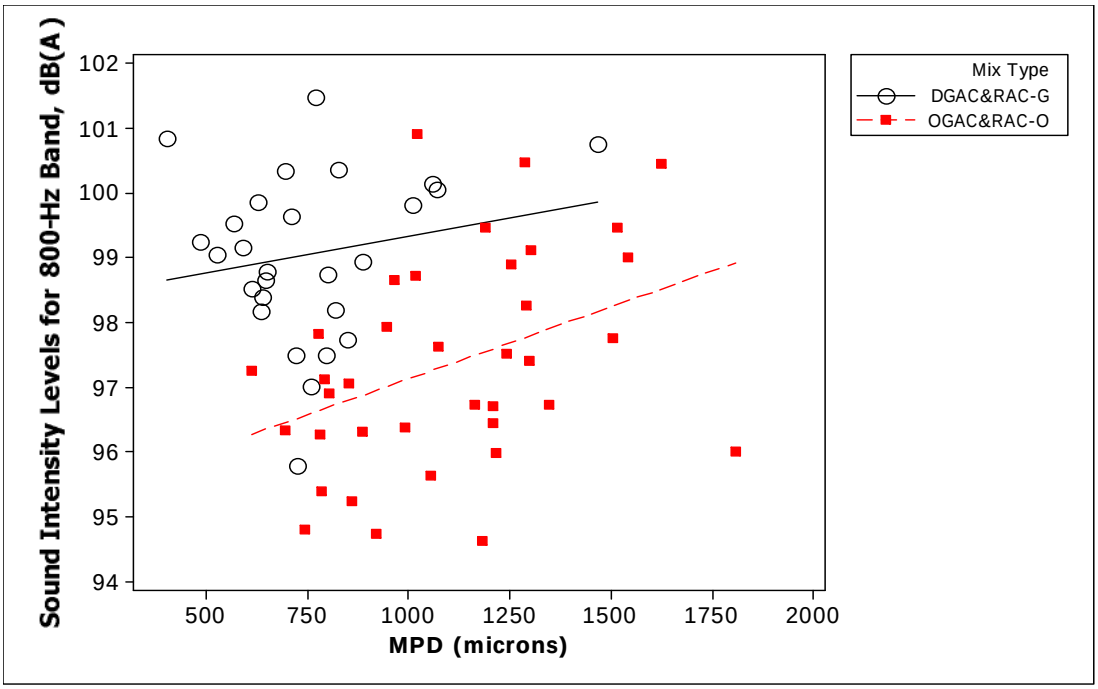

Figure 100: Sound intensity levels for 800 Hz versus MPD values for different mix types.

The model to predict the noise levels for the 800-Hz band is given here. Mix type, MPD, and fineness modulus were used as independent variables. This model can explain 39 percent of the variation in noise levels at this frequency.

Model for 800-Hz One-Third Octave Band

The regression equation, Equation (23), is

800-Hz band = 104 – 1.96 × Mix Type + 0.0029 × MPD – 1.53 × Fineness modulus **(23)**

Predictor	Coef	SE Coef	T	P
Constant	104.057	2.337	44.52	0.000
Fineness modulus	–1.5298	0.5432	–2.82	0.007
Mix type	–1.9556	0.4546	–4.30	0.000
MPD	0.0029005	0.0007970	3.64	0.001

S = 1.36426 R-Sq = 39.5% R-Sq(adj) = 36.3%

Analysis of Variance

Source	DF	SS	MS	F	P
Regression	3	69.127	23.042	12.38	0.000
Residual error	57	106.088	1.861		
Total	60	175.215			

Based on the equation, at a given MPD and fineness modulus, open-graded mixes have lower noise levels compared to dense- and gap-graded mixes. Figure 101 shows the relationship between air-void content and fineness modulus for different mix types. The figure shows that at a given fineness modulus, open-graded mixes have higher air-void content than do dense- and gap-graded mixes. The lower noise levels of open-graded mixes compared to dense- and gap-graded mixes at a given MPD and fineness modulus may be due to the higher air-void content of open-graded mixes, which may further reduce the noise levels. Air-void content could not be included in the regression analysis since it is highly correlated with fineness modulus.

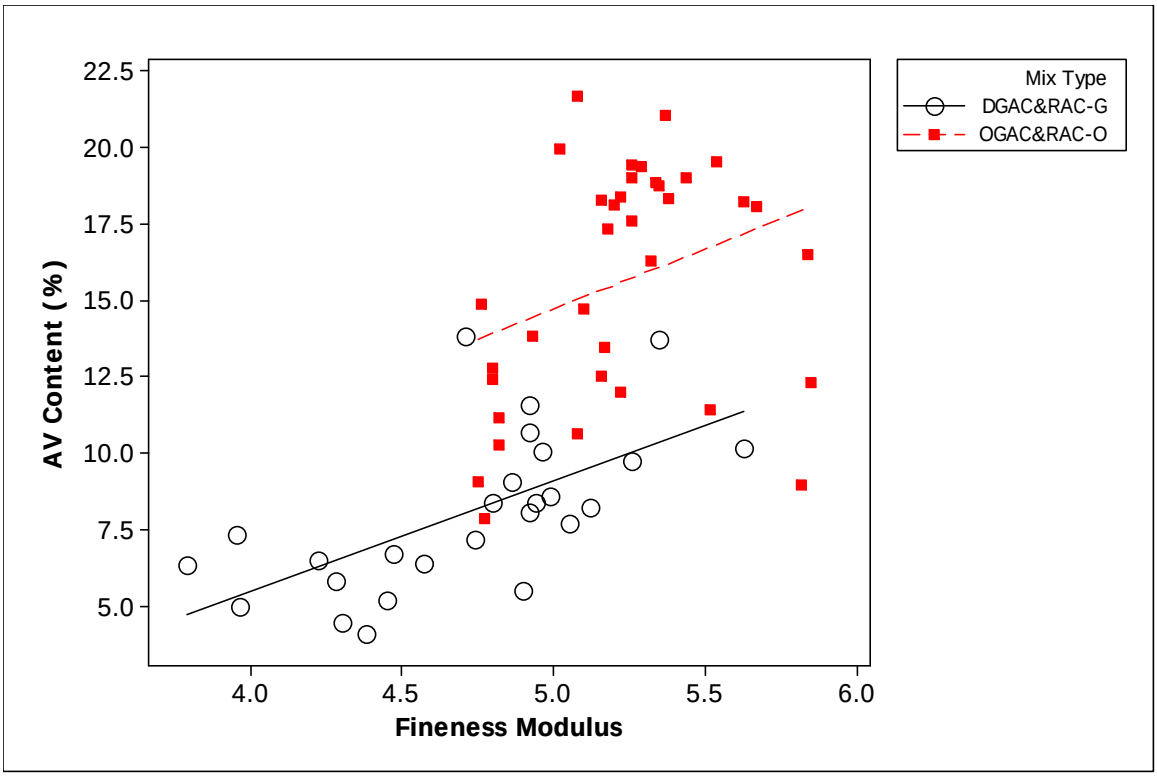

Figure 101: Air-void content versus fineness modulus for different mix types.

1,000-Hz One-Third Octave Band

According to the single-variable regression analysis, as air-void content and fineness modulus increase, noise levels decrease. Open-graded mixes have lower noise levels compared to dense- and gap-graded mixes. Increasing C_u, NMAS, and IRI increases the noise levels. Increasing surface thickness also increases the noise levels; however, this is because air-void content decreases as the surface thickness increases. There is no causal relationship between the surface thickness and noise levels; hence, its effects are not discussed further here in the frequency analysis.

Figure 102 shows the relationship between sound intensity levels for the 1,000-Hz band and air-void content. The figure shows that increasing air-void content reduces the noise levels of dense-and gap-graded mixes, while there is no trend for open-graded mixes. Figure 103 shows the relationship between sound intensity levels for the 1,000-Hz band and MPD values. The figure shows that increasing MPD increases the noise levels for open-graded mixes; however, there is no trend for dense-and gap-graded mixes. The figure also shows that open-graded mixes have lower noise levels than do dense-and gap-graded mixes at a given air-void content and MPD value.

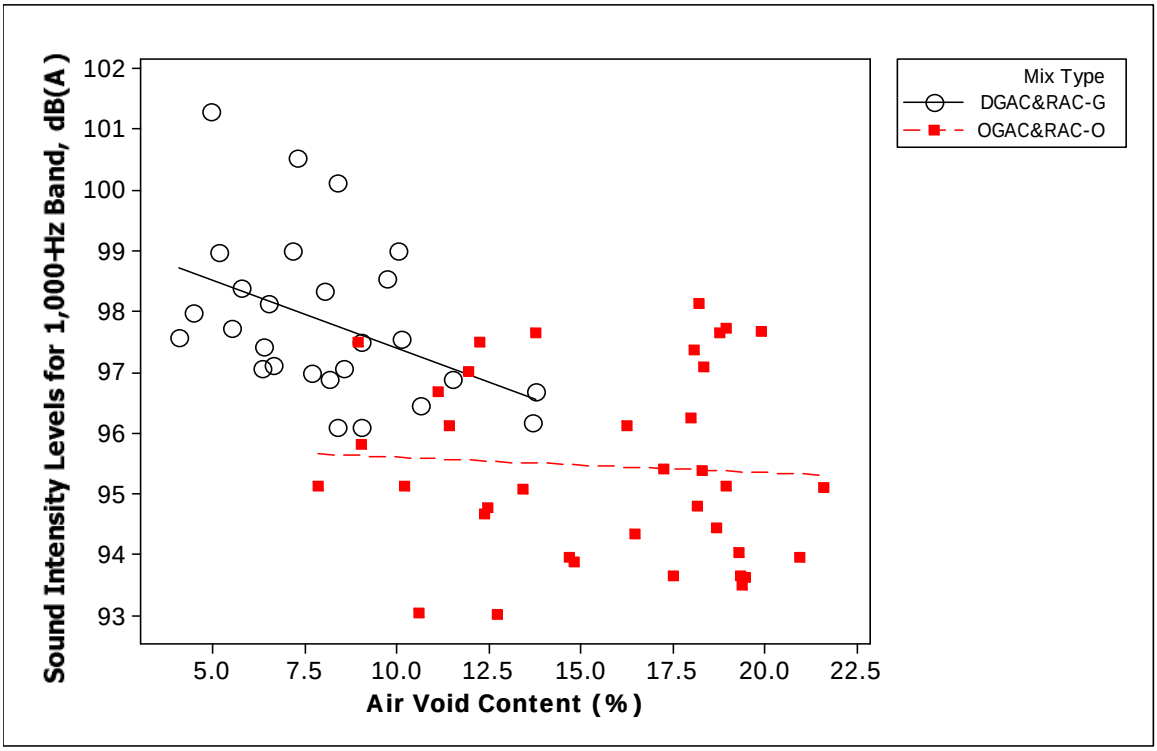

Figure 102: Sound intensity levels for 1,000-Hz band versus air-void content for different mix types.

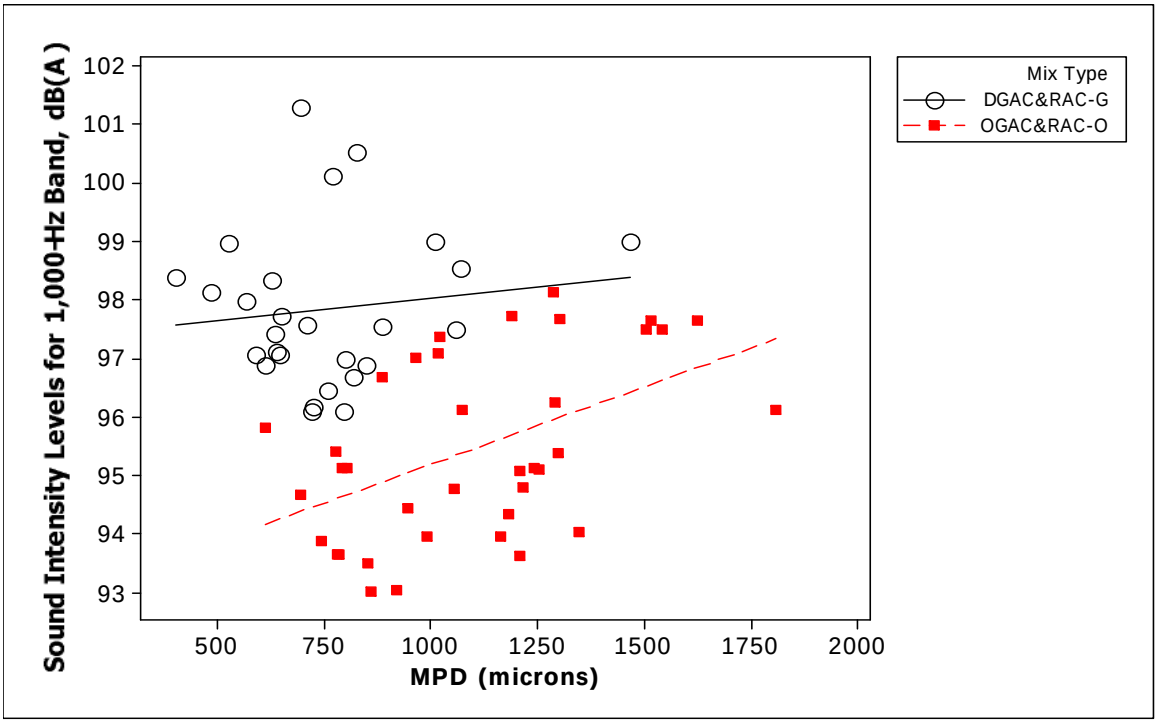

Figure 103: Sound intensity levels for 1,000-Hz band versus MPD values for different mix types.

The model to predict the noise levels for the 1,000-Hz band is given here. Mix type, MPD, and fineness modulus were used as independent variables. Mix type was included in the regression since open-graded mixes have higher air-void content at a given fineness modulus compared to the dense-graded mixes, as explained in the 800-Hz frequency band analysis. Air-void content could not be included in the model since it is highly correlated with the fineness modulus. The model for the 1,000-Hz frequency band can explain 57 percent of the variation in noise levels.

Model for 1,000-Hz One-Third Octave Band

The regression equation, Equation (24), is

1,000-Hz band = 103 + 0.00323 × MPD – 1.63 × Fineness modulus – 2.75 × Mix type **(24)**

Predictor	Coef	SE Coef	T	P
Constant	103.138	2.164	47.67	0.000
MPD	0.0032316	0.0007378	4.38	0.000
Fineness modulus	–1.6315	0.5029	–3.24	0.002
Mix type	–2.7546	0.4208	–6.55	0.000

S = 1.26294 R-Sq = 56.8% R-Sq(adj) = 54.5%

Analysis of Variance

Source	DF	SS	MS	F	P
Regression	3	19.445	39.815	24.96	0.000
Residual error	57	90.916	1.595		

1,250-Hz, 1,600-Hz, and 2,000-Hz One-Third Octave Bands

According to the single-variable regression analysis, noise levels for the 1,250-, 1,600-, and 2,000-Hz bands decrease as air-void content and fineness modulus increase, and noise levels increase as NMAS and C_u increase. Open-graded mixes have lower noise levels than dense- and gap-graded mixes. Noise levels also increase with increasing age; however, for noise levels for the 2,000-Hz band, the age effects are inconclusive since age is insignificant when QP-16 is excluded from the analysis. The presence of transverse and fatigue cracks on the pavement surface increases the noise levels. Noise levels decrease as texture (RMS and MPD) increases for the 1,600- and 2,000-Hz bands, which is the opposite of the trend found for the lower frequencies.

The models to predict the noise levels for the 1,250-, 1,600-, and 2,000-Hz bands are given here. The MPD was not found to be significant in the single-variable regression analysis for 1,250 Hz. However, MPD increases the noise levels when the mix types are analyzed separately, as shown in Figure 104. Therefore, MPD was included in the model for the 1,250-Hz band sound intensity levels. At a given age and MPD, increasing air-void content reduces the noise levels, and at a given age and air-void content, increasing MPD increases the noise levels for the 1,250-Hz band. The model can explain 72 percent of the variation in 1,250-Hz band sound intensity levels.

Air-void content and age were used as independent variables in the model for 1,600-Hz band sound intensity. The model can explain 76 percent of the variation in the noise levels. Air-void content and presence of transverse and fatigue cracking were used as independent variables in the model for 2,000-Hz band sound intensity levels. This model explained 77 percent of the variation in noise levels.

Based on the regression models for 1,250-Hz band noise levels, an open-graded mix with an air-void content of 15 percent and an MPD of 1,200 microns may provide approximately 2 dB (A) noise reduction compared to a dense-graded surface with an air-void content of 6.5 percent and an MPD of 500 microns. The same open-graded mix would provide approximately 3.5 dB (A) noise reduction for the 1,600-Hz band and 3.2 dB (A) for the 2,000-Hz band compared to a dense-graded mix with the given properties.

Model for 1,250-Hz One-Third Octave Band

The regression equation, Equation (25), is

1250 = 94.9 + 0.363 × Age – 0.421 × Air-void content + 0.00273 × MPD **(25)**

Predictor	Coef	SE Coef	T	P
Constant	94.8671	0.5797	163.65	0.000
Age	0.36330	0.07380	4.92	0.000
AV content	–0.42087	0.04038	–10.42	0.000
MPD	0.0027327	0.0006725	4.06	0.000

S = 1.31018 R-Sq = 71.9% R-Sq(adj) = 70.4%

Analysis of Variance

Source	DF	SS	MS	F	P
Regression	3	254.192	84.731	49.36	0.000
Residual error	58	99.560	1.717		
Total	61	353.752			

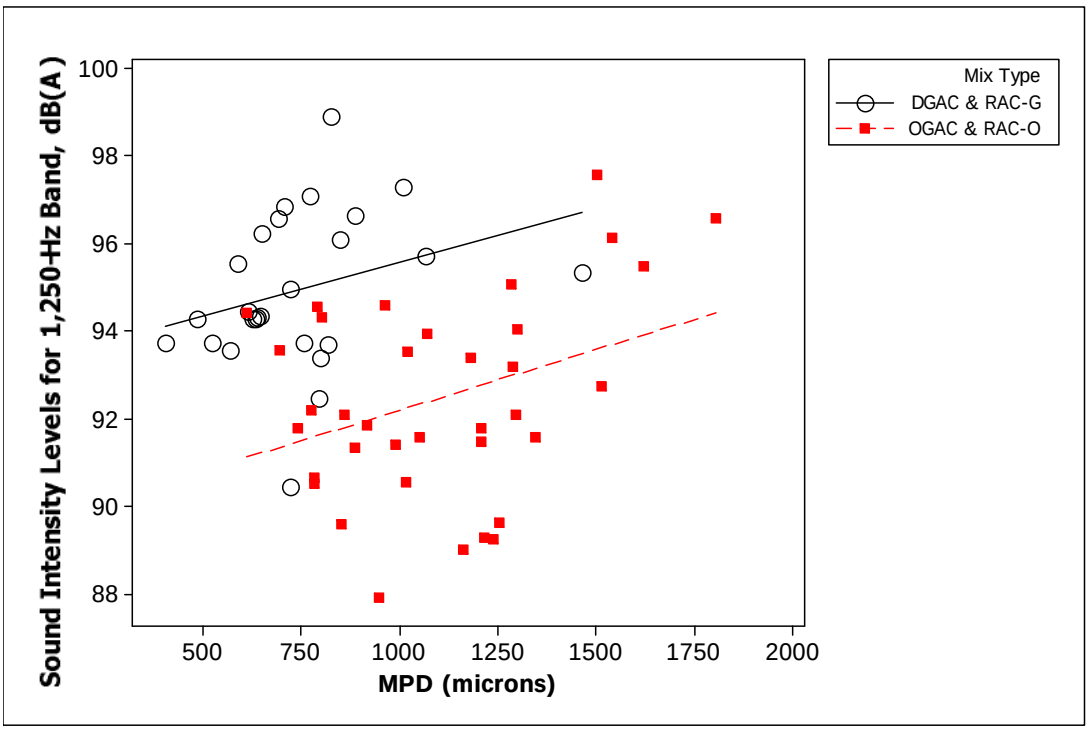

Figure 104: 1,250-Hz band sound intensity levels versus MPD for different mix types

Model for 1,600-Hz One-Third Octave Band

The regression equation, Equation (26), is

1,600-Hz band = 95.5 + 0.383 × Age – 0.433 × Air-void content **(26)**

Predictor	Coef	SE Coef	T	P
Constant	95.4868	0.5184	184.20	0.000
Age	0.38280	0.07338	5.22	0.000
AV content	–0.43349	0.03425	–12.66	0.000

S = 1.34904 R-Sq = 75.6% R-Sq (adj) = 74.8%

Analysis of Variance

Source	DF	SS	MS	F	P
Regression	2	333.47	166.73	91.62	0.000
Residual error	59	107.38	1.82		
Total	61	440.84			

Model for 2,000-Hz One-Third Octave Band

The regression equation, Equation (27), is

2,000-Hz band = 92.0 – 0.376 × Air-void content + 1.56 × Presence of fatigue cracking + 1.02 × Presence of transverse cracking **(27)**

Predictor	Coef	SE Coef	T	P
Constant	91.9647	0.4628	198.70	0.000
AV content	–0.37602	0.03218	–11.68	0.000
Presence of fatigue cracking	1.5637	0.5355	2.92	0.005
Presence of transverse cracking	1.0204	0.4098	2.49	0.016

S = 1.20090 R-Sq = 77.2% R-Sq(adj) = 75.8%

Analysis of Variance

Source	DF	SS	MS	F	P
Regression	3	244.255	81.418	56.46	0.000
Residual error	50	72.108	1.442		
Total	53	316.363			

2,500-Hz, 3,150-Hz, 4,000-Hz, and 5,000-Hz One-Third Octave Bands

Single-variable regression analysis revealed that noise levels for the 2,500-, 3,150-, 4,000-, and 5,000-Hz one-third octave bands decrease as air-void content, texture (MPD and RMS), and fineness modulus increase, and noise levels increase as C_u increases. Open-graded mixes have lower noise levels than dense- and gap-graded mixes. The presence of transverse cracks on the pavement surface increases the noise levels. Increasing NMAS increases the noise levels for the 2,500-Hz band, and increasing age increases the noise levels for the 4,000-Hz band. Figure 105 shows the sound intensity levels for the 4,000-Hz band versus the air-void content. The figure shows that increasing air-void content reduces the noise levels for all mix types.

Figure 106 shows the MPD versus the sound intensity levels for the 4,000-Hz band. The figure shows that increasing MPD reduces the noise levels of open-graded mixes; however, there is no trend for dense- and gap-graded mixes. Although it was not shown here, the same trends were found for MPD and air-void content at the 5,000-Hz band noise levels. The effect of MPD is more pronounced at higher MPD values or air-void content; therefore, the interaction between MPD and air-void content was evaluated in the multiple regression models for the 4,000- and 5,000-Hz bands.

The models to predict the sound intensity levels for the 2,500-, 3,150-, 4,000-, and 5,000-Hz bands are shown here. Air-void content, MPD, and age were used as independent variables in the models for the 2,500- and 3,150-Hz band sound intensity levels. The model can explain 60 percent of the variation in the 2,500-Hz band and 51 percent of the variation in the 3,150-Hz band sound intensity levels.

Age and the interaction of air-void content and MPD were used as independent variables in the 4,000- and 5,000-Hz band sound intensity levels. Although age was not found significant in the single-variable analysis, it turned out to be significant when included with MPD and air-void content. Therefore, it was kept in the model. The model explained 58 percent of the variation in the 4,000-Hz and 55 percent of the variation in the 5,000-Hz band noise levels.

Based on the regression models for 2,500-Hz band noise levels, an open-graded mix with an air-void content of 15 percent and an MPD of 1,200 microns may provide approximately 3.2 dB (A) noise reduction compared to a dense-graded surface with an air-void content of 6.5 percent and an MPD of 500 microns. The same open-graded mix may provide a noise reduction of 3 dB (A) for the 3,250-Hz band, 3.5 dB (A) for the 4,000-Hz band, and 3.2 dB (A) for the 5,000-Hz band compared to a dense-graded mix with the given properties.

Model for 2,500-Hz One-Third Octave Band

The regression equation, Equation (28), is

2,500-Hz band = 88.5 – 0.226 × Air-void content – 0.00185 × MPD + 0.267 × Age **(28)**

Predictor	Coef	SE Coef	T	P
Constant	88.5012	0.5908	149.80	0.000
Air-void content	–0.22591	0.04115	–5.49	0.000
MPD	–0.0018453	0.0006854	–2.69	0.009
Age	0.26672	0.07521	3.55	0.001

S = 1.33524 R-Sq = 60.0% R-Sq(adj) = 57.9%

Analysis of Variance

Source	DF	SS	MS	F	P
Regression	3	154.936	51.645	28.97	0.000
Residual error	58	103.406	1.783		
Total	61	258.342			

Model for 3,150-Hz One-Third Octave Band

The regression equation, Equation (29), is

3,150-Hz band = 86.5 – 0.194 × Air-void content – 0.00200 × MPD + 0.264 × Age **(29)**

Predictor	Coef	SE Coef	T	P
Constant	86.4828	0.6548	132.08	0.000
AV content	–0.19353	0.04561	–4.24	0.000
MPD	–0.0020005	0.0007597	–2.63	0.011
Age	0.26390	0.08336	3.17	0.002

S = 1.47991 R-Sq = 51.2% R-Sq(adj) = 48.7%

Analysis of Variance

Source	DF	SS	MS	F	P
Regression	3	133.376	44.459	20.30	0.000
Residual error	58	127.028	2.190		
Total	61	260.404			

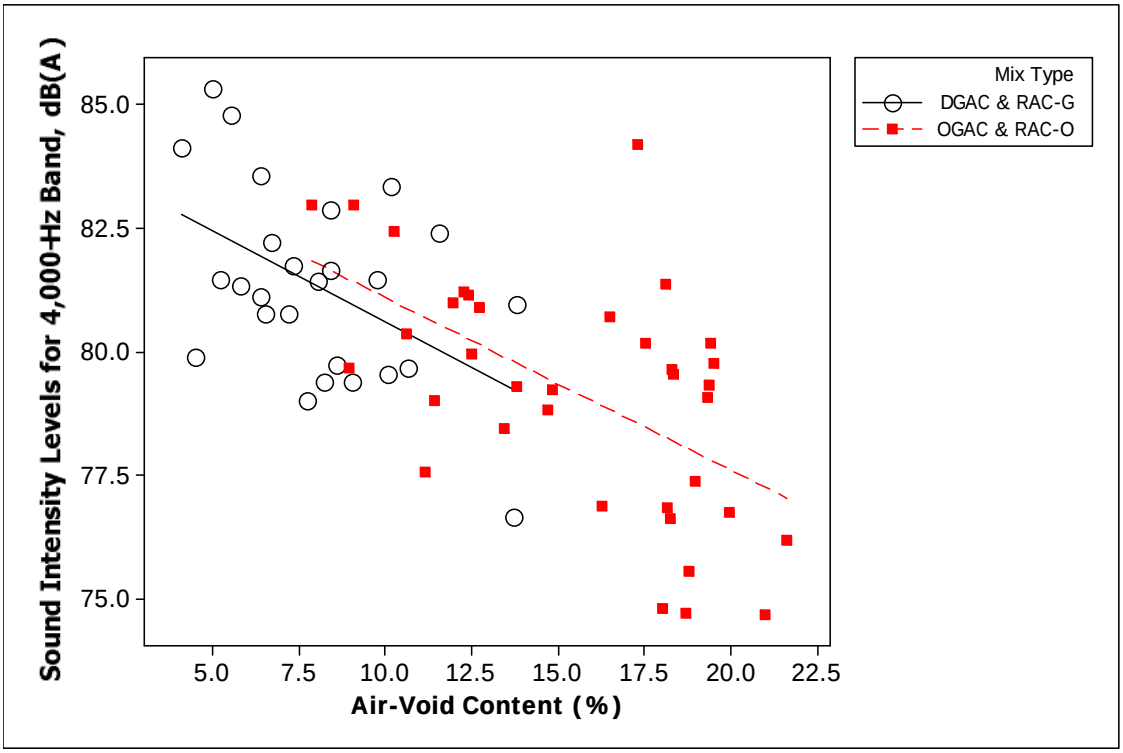

Figure 105: 4,000-Hz band sound intensity levels versus air-void content for different mix types.

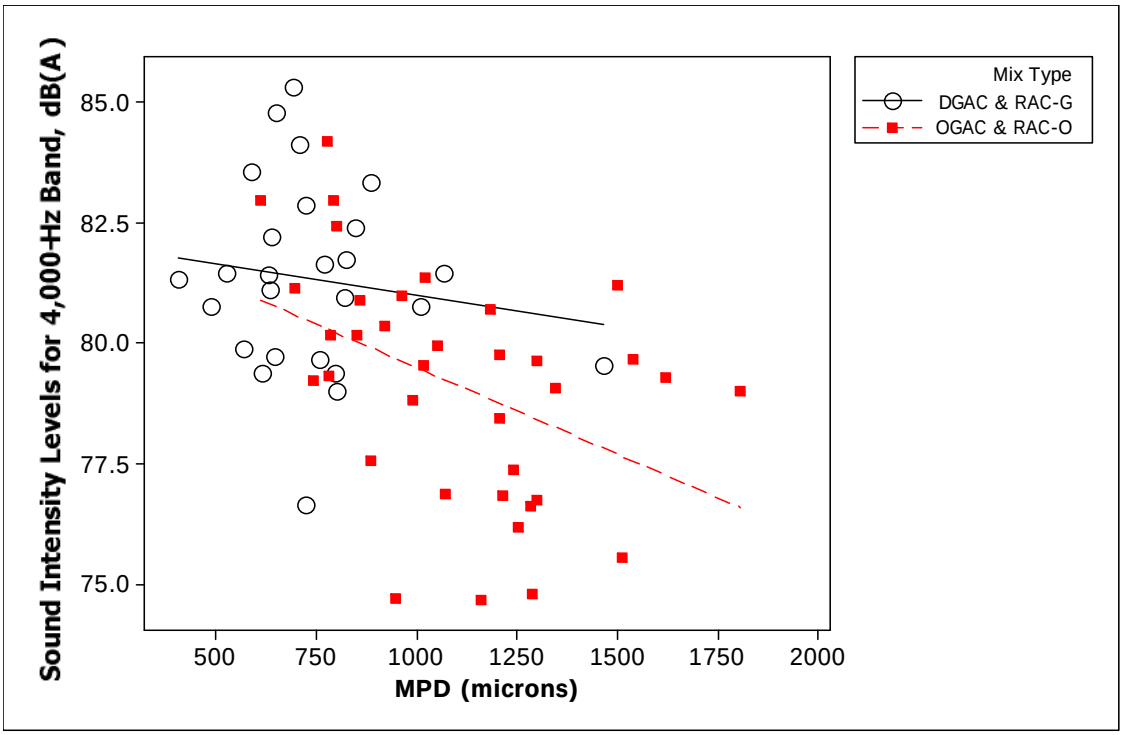

Figure 106. 4,000-Hz band sound intensity levels versus MPD for different mix types.

Model for 4,000-Hz One-Third Octave Band

The regression equation, Equation (30), is

4,000-Hz band = 81.8 – 0.000235 × Air-void content × MPD + 0.363 × Age **(30)**

Predictor	Coef	SE Coef	T	P
Constant	81.7740	0.4827	169.40	0.000
AV content × MPD	–0.00023507	0.00002751	–8.55	0.000
Age	0.36325	0.08874	4.09	0.000

S = 1.61989 R-Sq = 58.3% R-Sq(adj) = 56.9%

Analysis of Variance

Source	DF	SS	MS	F	P
Regression	2	216.33	108.17	41.22	0.000
Residual error	59	154.82	2.62		
Total	61	371.15			

Model for 5,000-Hz One-Third Octave Band

The regression equation, Equation (31), is

5,000-Hz band = 77.4 – 0.000215 × Air-void content × MPD + 0.272 × Age **(31)**

Predictor	Coef	SE Coef	T	P
Constant	77.4114	0.4611	167.88	0.000
AV content × MPD	–0.00021468	0.00002628	–8.17	0.000
Age	0.27162	0.08477	3.20	0.002

S = 1.54740 R-Sq = 54.8% R-Sq(adj) = 53.3%

Analysis of Variance

Source	DF	SS	MS	F	P
Regression	2	171.614	85.807	35.84	0.000
Residual error	59	141.273	2.394		
Total	61	312.887			

9.2.2 Evaluation of Pavement Temperature Effects on the Frequency Content of Sound Intensity Levels

In addition to the pavement properties, pavement temperature effects on the one-third octave band frequency levels were evaluated as explained in Section 9.1.2. OBSI was measured on nine sections at pavement temperatures of 15, 20, and 25°C. Figure 107 through Figure 117 show the pavement temperature effects on the one-third octave band sound intensity levels obtained from the study. The figures show that there is no trend between sound intensity levels and pavement temperatures.

The sample size used in this study was small. To evaluate the pavement temperature effects on different mix types, a larger sample is needed. The data points shown in the circles in Figure 107 and Figure 110 belong to QP-3, which has higher air-void content and higher MPD values than other mixes, which results in much higher noise levels for the 500-Hz band and much lower noise levels for the 1,000-Hz band.

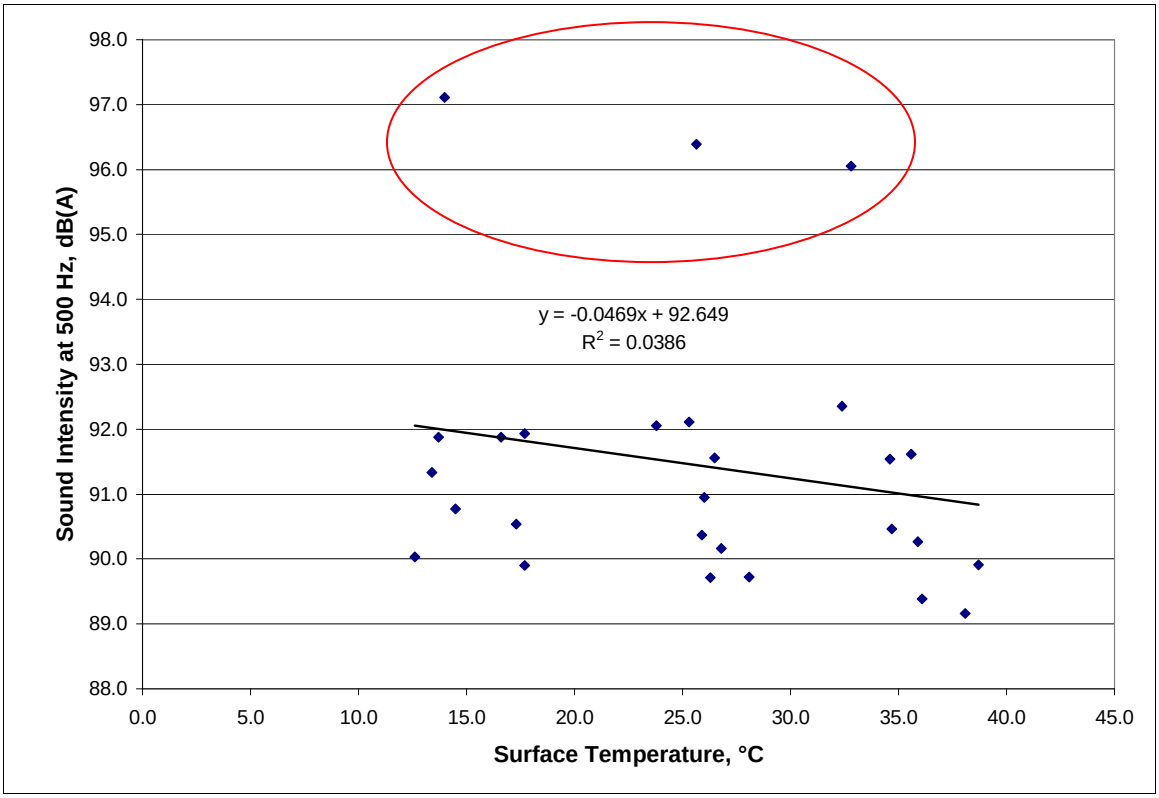

Figure 107: Relationship between sound intensity at 500 Hz and surface temperatures (ºC).

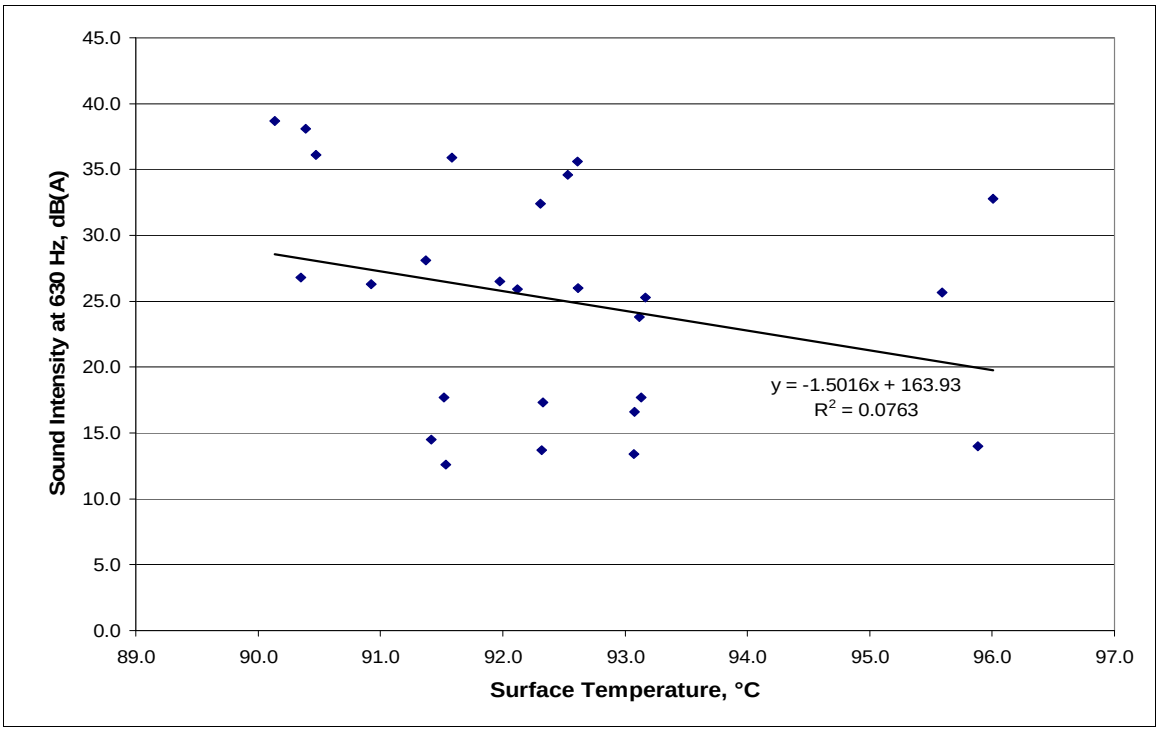

Figure 108: Relationship between sound intensity at 630 Hz and surface temperatures (ºC).

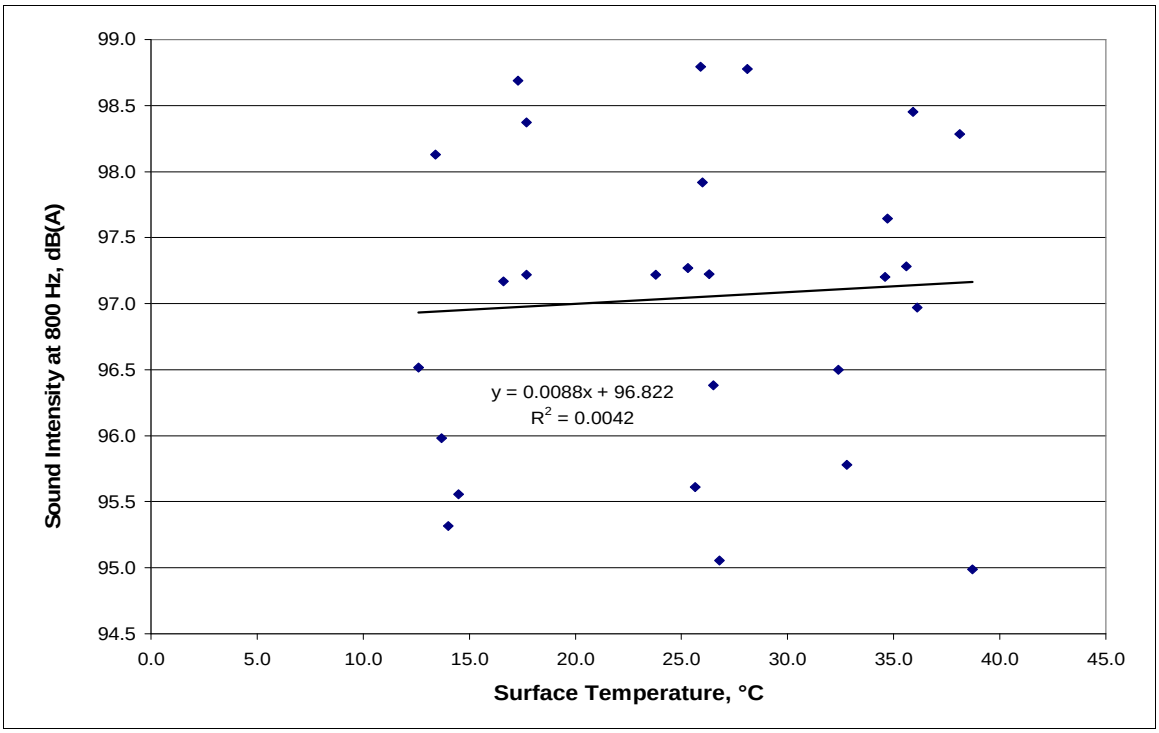

Figure 109: Relationship between sound intensity at 800 Hz and surface temperatures (ºC).

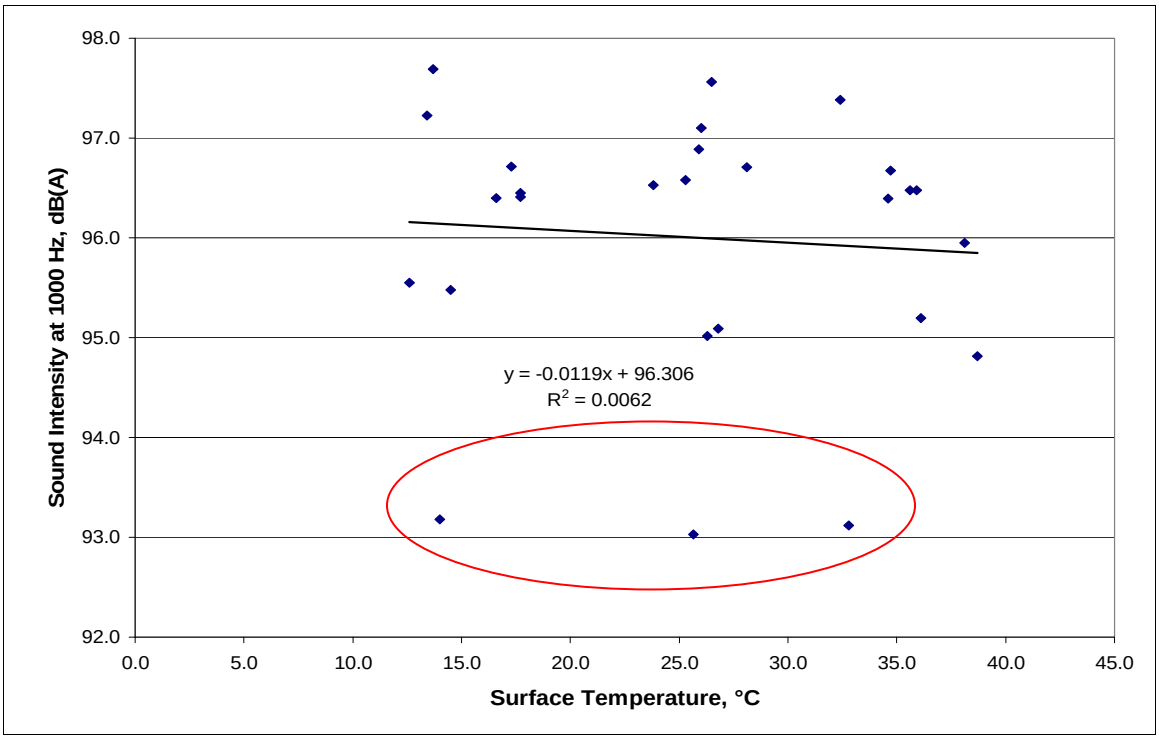

Figure 110: Relationship between sound intensity at 1,000 Hz and surface temperatures (ºC).

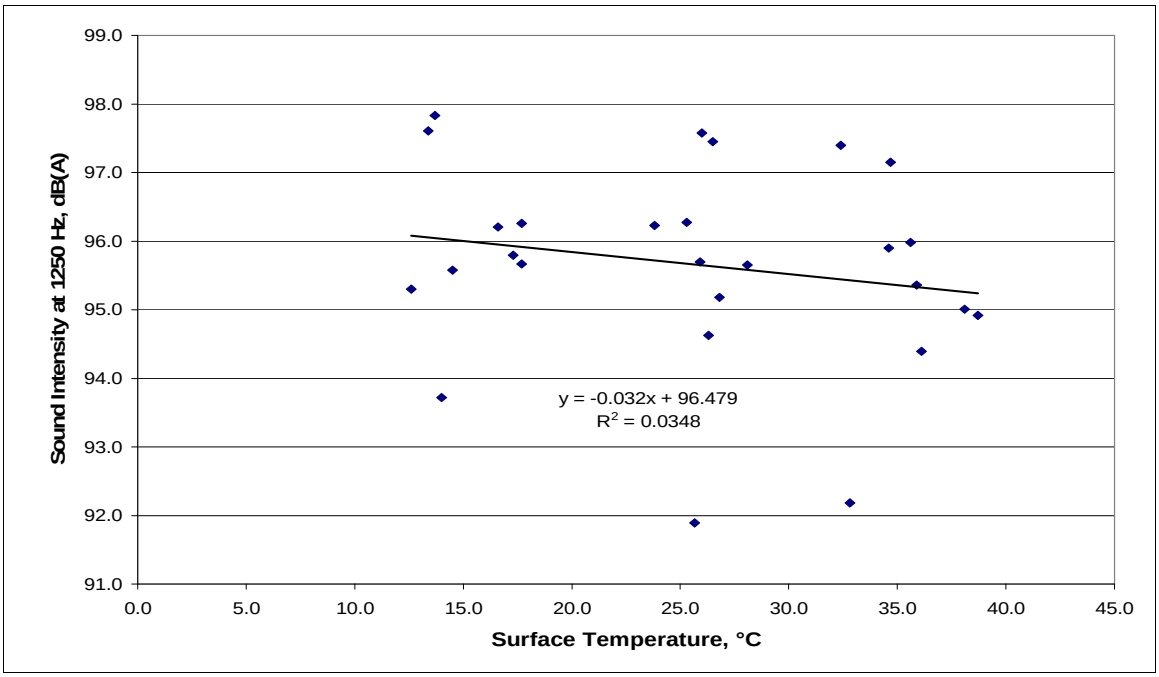

Figure 111: Relationship between sound intensity at 1,250 Hz and surface temperatures (ºC).

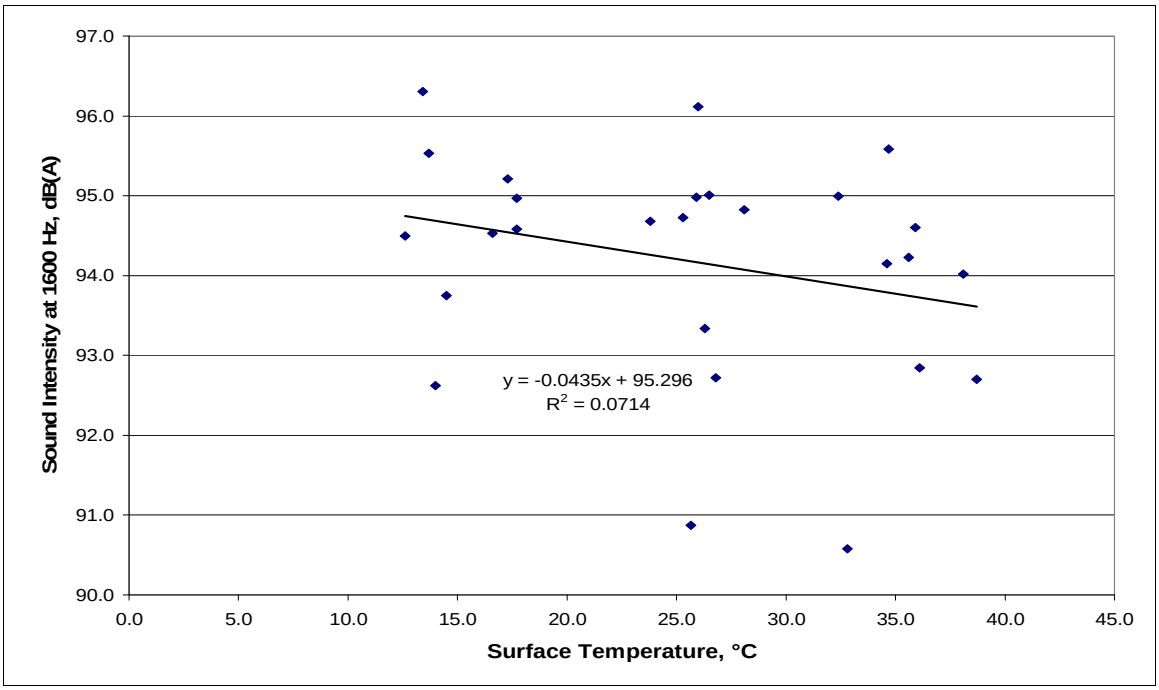

Figure 112: Relationship between sound intensity at 1,600 Hz and surface temperatures (ºC).

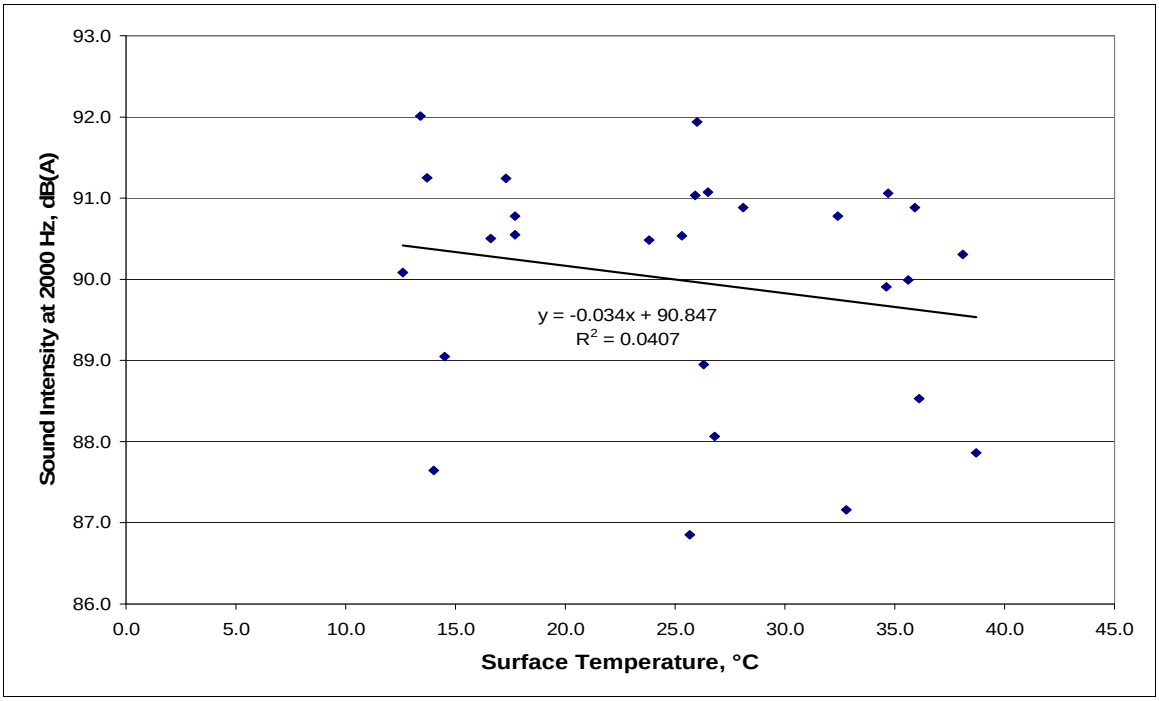

Figure 113: Relationship between sound intensity at 2,000 Hz and surface temperatures (ºC).

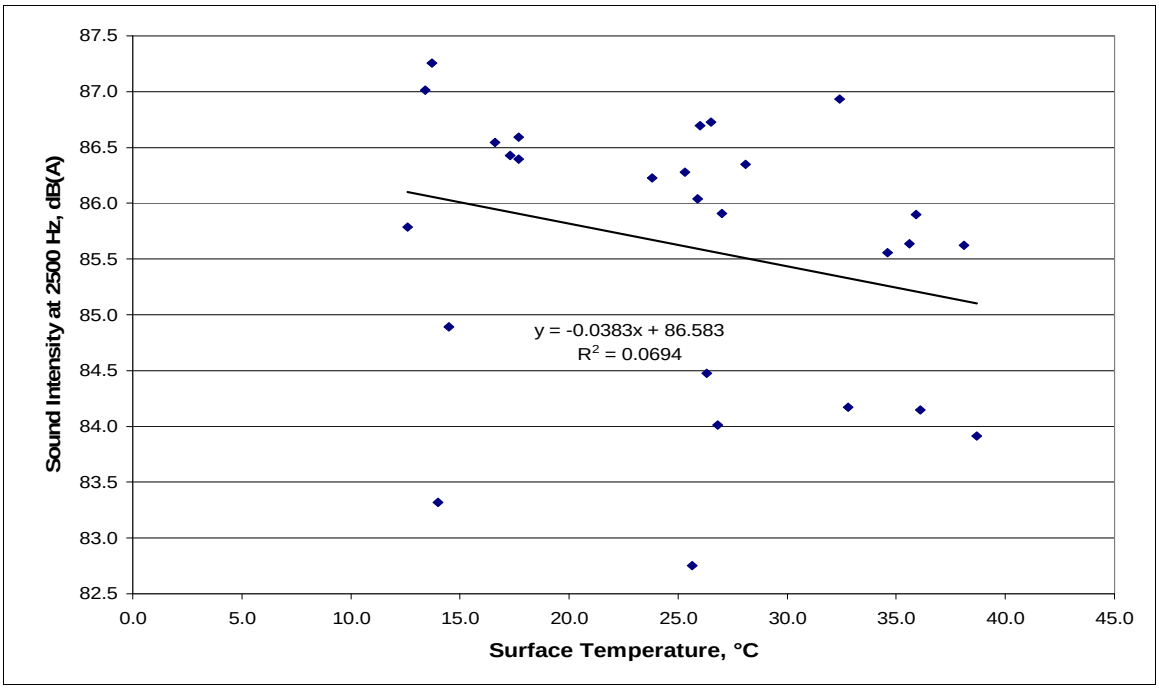

Figure 114: Relationship between sound intensity at 2,500 Hz and surface temperatures (ºC).

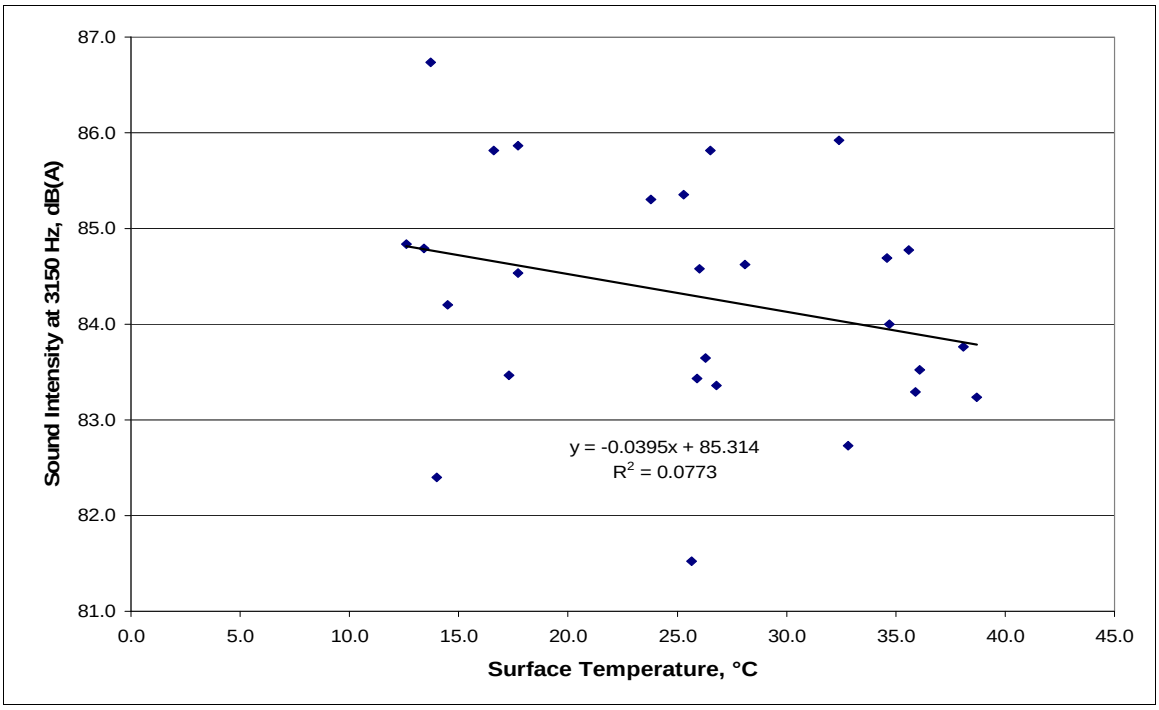

Figure 115: Relationship between sound intensity at 3,150 Hz and surface temperatures (ºC).

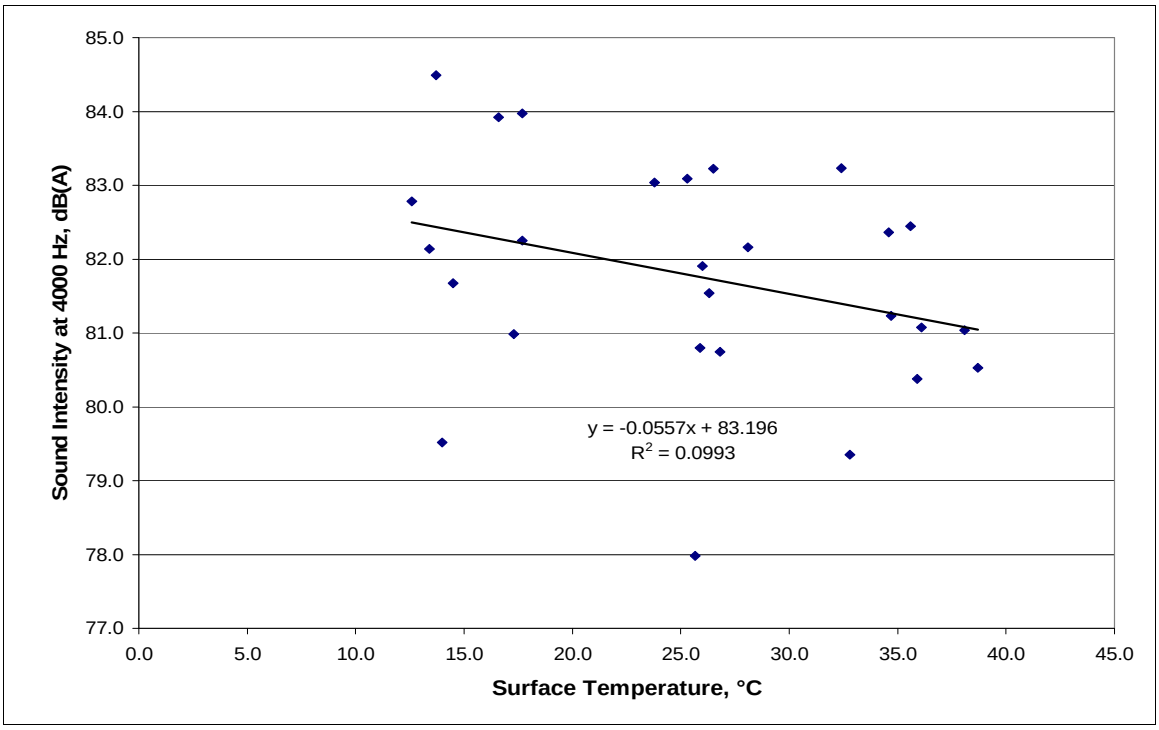

Figure 116: Relationship between sound intensity at 4,000 Hz and surface temperatures (ºC).

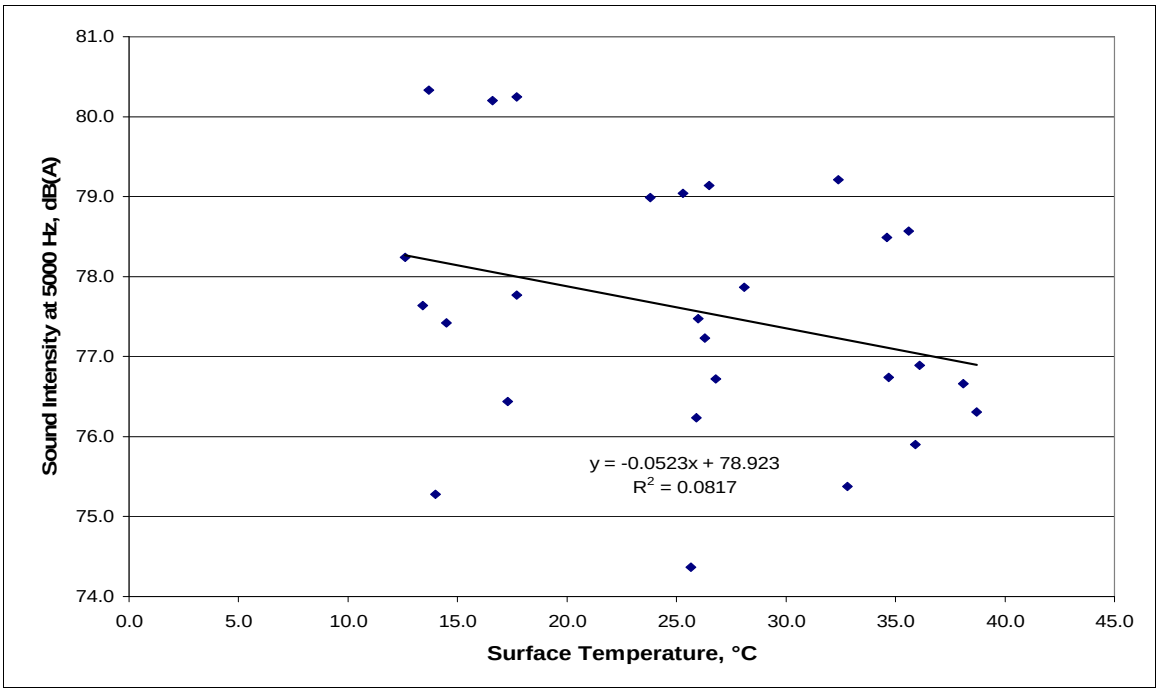

Figure 117: Relationship between sound intensity at 5,000 Hz and surface temperatures (ºC).

9.2.3 Summary of Findings

Figure 118 compares the one-third octave band sound intensity levels for open-graded (OGAC and RAC-O mixes) and non-open-graded mixes (DGAC and RAC-G mixes) at different ages. The figure shows that open-graded mixes have higher sound intensity levels at frequencies lower than 800 Hz, which can be explained by the greater macrotexture values and air-void content of open-graded mixes. The open-graded mixes have lower noise levels than the dense-graded mixes in the upper frequencies. Older pavements have higher noise levels than younger ones with the same mix type.

At high frequencies (above 2,500 Hz), all the mixes except the new open-graded and oldest dense-graded mixes have the same noise levels. The new open-graded mix (QP-41) has the lowest noise levels, and the old DGAC mix (QP-11) has the highest noise levels. These results may be due to the presence of distresses on the surfaces of the old DGAC mix, which affect the sound intensity at high frequencies, as well as the high air-void content of the new RAC-O mix, which reduces the noise levels at higher frequencies.

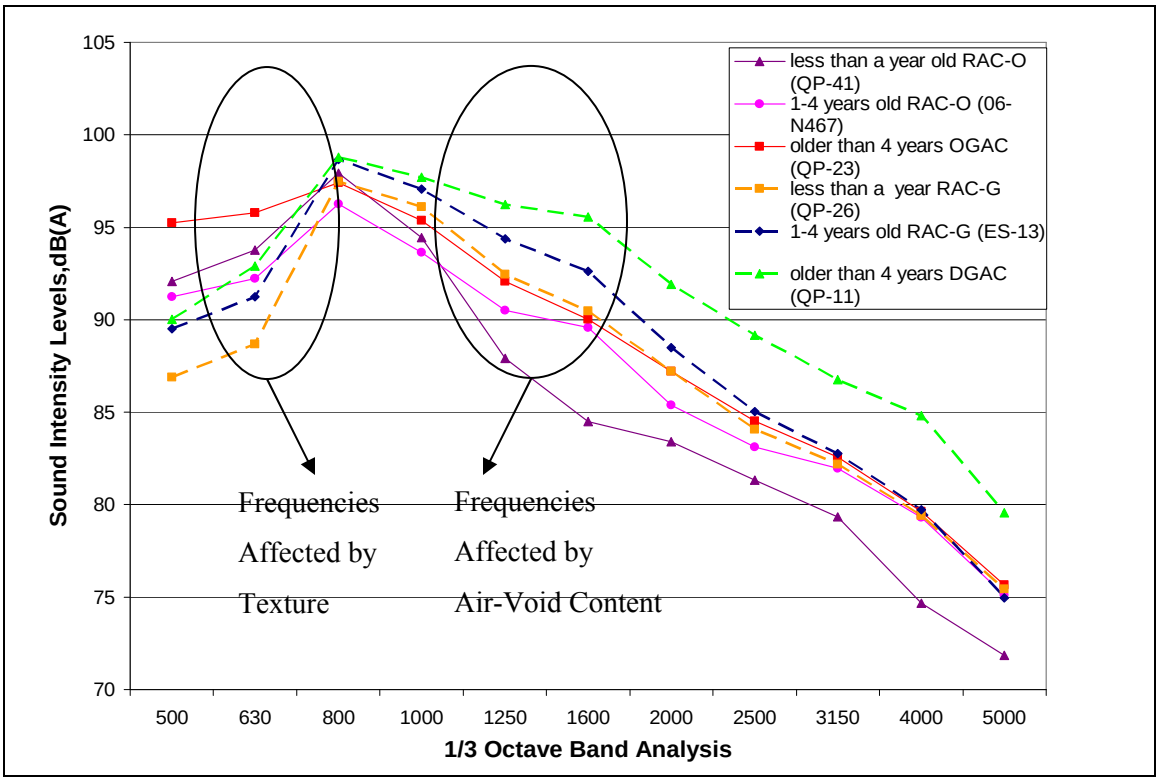

Figure 118: Example of one-third octave band sound intensity levels for different mix types at different ages.

Although the presence of raveling was found to be a significant variable affecting the overall A-weighted sound intensity levels, it was not found to be significant in the frequency analysis, probably due

to the exclusion of sections 01-N103 (OGAC), 01-N104 (OGAC), 01-N105 (OGAC), 01-N114 (DGAC), and 01-N121 (DGAC) from the frequency analysis. The overall A-weighted sound intensities from these sections measured by Illingworth and Rodkin were converted to the equivalent values as measured by UCPRC; however, the offset between the two measurements for different frequencies is not known. Therefore, these sections were excluded from the frequency analysis

- The results of the frequency analysis validated the noise-generation mechanisms from the earlier theoretical and statistical models:
    - This study confirmed the results of Sandberg et al. (75) that the texture affects the impact and shock mechanisms, and that increasing texture increases the noise levels at lower frequencies (less than 1,000 Hz). The study also confirmed that higher macrotexture at higher frequencies reduces the noise related to air pumping as it increases the air paths on the pavement surface. This study also showed that the frequency range in which the texture has negative correlation with the noise levels is above 2,000 Hz.
    - The results confirmed that in the middle frequency range, between 800 and 1,250 Hz, there is a mix effect of increased tire vibrations and reduced air-pumping noise for increasing texture.
    - Increasing air-void content was found to reduce the noise levels in the higher frequency range that are due to the dissipation of air-pumping noise through the air voids, confirming the earlier findings of Sandberg et al. (75). The air-pumping noise governs the noise level frequencies above 1,250 Hz.
- In this study, air-void content was also found to increase the noise levels around 500 Hz at a given texture depth, especially for open-graded mixes. Increasing air-void content is associated with the aggregate spacing as well as the texture depth. For high air-void content and hence high texture depths, air-void content may affect the shape of the tire, and the tire surface may not be taking the shape of the exact pavement surface profile, which may result in higher contact pressures and hence greater tire vibrations and higher noise levels. This effect may be more pronounced at higher air-void content values, above 15 percent.
- The study found that open-graded mixes may provide noise reduction of up to 3.5 dB (A) at higher frequencies compared to dense-graded mixes. It is known that the human ear is more sensitive to high-frequency noise; therefore, open-graded mixes may be perceived as quieter even though the overall A-weighted noise levels are not significantly different from those of dense-graded mixes. The noise reduction at higher frequencies should be matched with the human perception of the noise reduction to evaluate the effects of the open-graded mixes.

- The tire/pavement noise is dominant at frequencies between 800 and 1,250 Hz. Therefore, these frequencies affect the overall A-weighted noise levels. Since these middle frequency ranges are affected by both tire vibrations and air-pumping effects, no clear effects of air-void content and macrotexture can be seen in the overall A-weighted noise levels. Additionally, the macrotexture has both negative and positive effects on the spectral content of tire/pavement noise. Therefore, macrotexture was not found to be significant when evaluated by itself in the regression analysis.
- Age was found to increase the noise levels at around 1,250, 1,600, and 4,000 Hz in single-variable analyses. However, age was significant for all frequencies above 1,000 Hz when included with other variables. The presence of distresses on the pavement surface was found to increase the noise levels at higher frequencies (greater than 1,250 Hz).
- IRI was found to affect the noise levels at frequencies less than 1,600 Hz.
- Microtexture and pavement temperature were not found to affect the noise levels. A bigger sample size is needed to further test the effects of pavement temperatures on noise levels.

9.3 Evaluation of Acoustical Absorption Values

The acoustical absorption values of the test sections were evaluated to determine the differences in the absorption values for different mixes and to predict the highway noise levels from the absorption values measured in the laboratory. In this study, acoustical properties of the test sections were evaluated to compare absorption values for different mixes and to compare acoustical absorption with noise levels.

Acoustical absorption measurements were taken on two cores from each section, one in the wheelpath and one between the wheelpaths, using an impedance tube. The impedance tube provided the acoustical absorption values for frequencies up to 1,700 Hz with a resolution of 3.125 Hz. Due to erroneous measurements below 200 Hz, these frequencies were not included in the analysis. The absorption values presented in this study are averages of absorption values between 200 and 1,700 Hz. Absorption values range between 0 and 1. An absorption value of 0 indicates that there is no absorption, and an absorption value of 1 indicates that all the noise striking the surface is absorbed and there is no reflected sound.

9.3.1 Descriptive Analysis

Figure 119 shows the variation in wheelpath absorption values for different mix types. The figure shows that open-graded mixes have higher absorption values than gap-and dense-graded mixes. RAC-G mixes have slightly higher absorption values than dense-graded mixes.

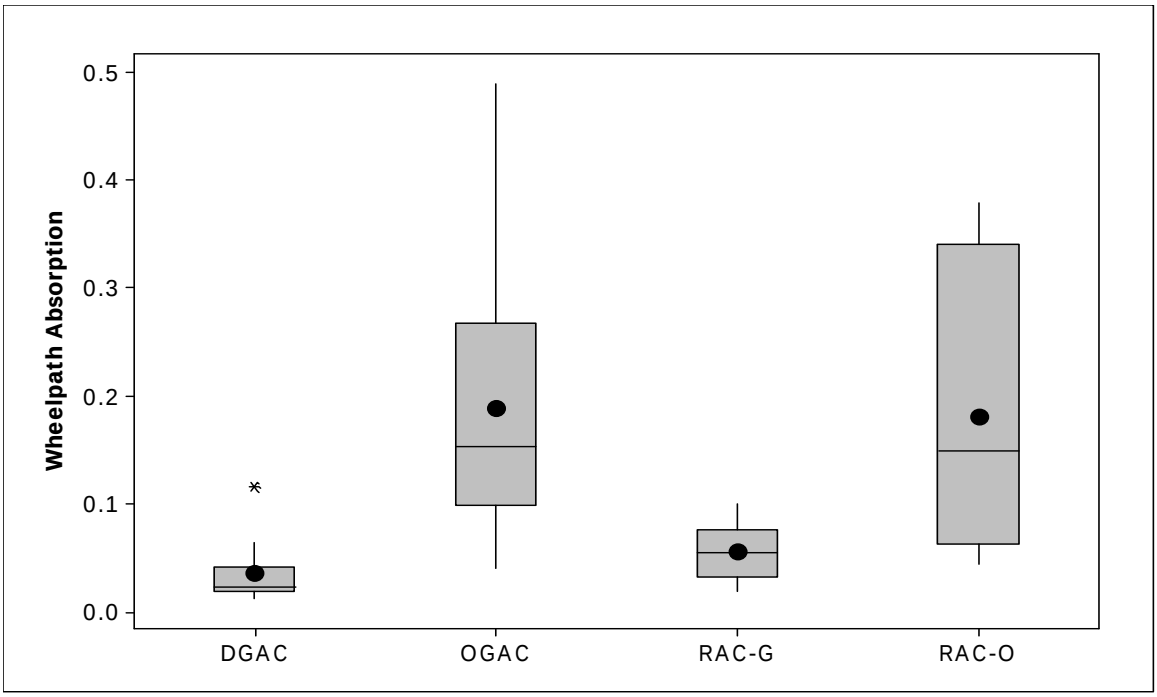

Figure 119: Box plots of absorption values for different mix types.

Figure 120 shows the variation in wheelpath absorption values for different mix types at different ages. The figure shows that the change in absorption values over time follows the same trend as permeability, shown earlier in Figure 37, which suggests that absorption is highly correlated with permeability. The absorption values of RAC-O mixes decreased with age. For other mix types, the absorption values were greater for the mixes that were one to four years old compared with the mixes that were less than one year old, and less for the mixes older than four years compared with the mixes that were one to four years old. The reduction in absorption values between mixes less than a year old and those greater than a year old could be due to compaction of the mix under traffic and clogging, which reduces the air-void content and therefore reduces absorption. Note that different sections are evaluated in the different age groups; therefore, the apparent increase over time in the absorption values of OGAC and RAC-G mixes may be heavily influenced by the absorption of these sections when they were originally built.

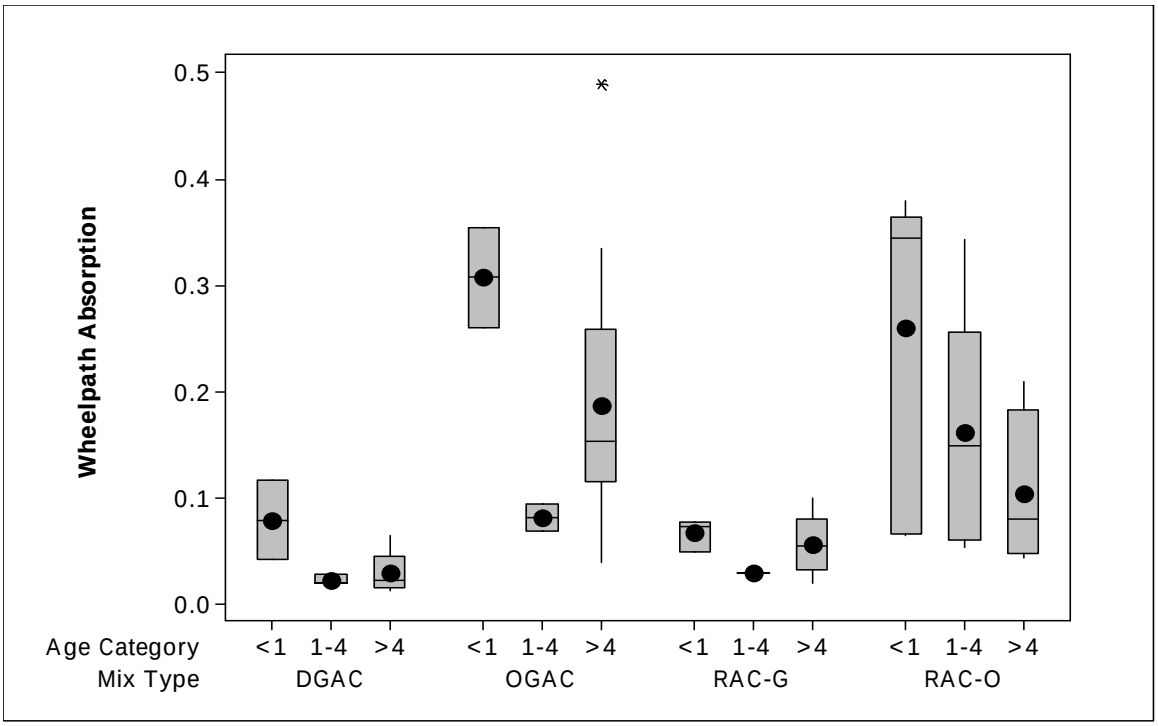

Figure 120: Comparison of wheelpath absorption values for different mix types at different ages.

9.3.2 Correlation of Acoustical Absorption Values with Air-Void Content and Surface Thickness

The literature review mentioned that the absorption values are affected by the air-void content and thickness of the surface layer. Figure 121 shows the correlation of the natural logarithm of absorption values with air-void content. There is a linear trend between the natural logarithm of absorption values and the air-void content. Increasing air-void content increases the average absorption values. Air-void content explains 63 percent of the variation in the absorption values.

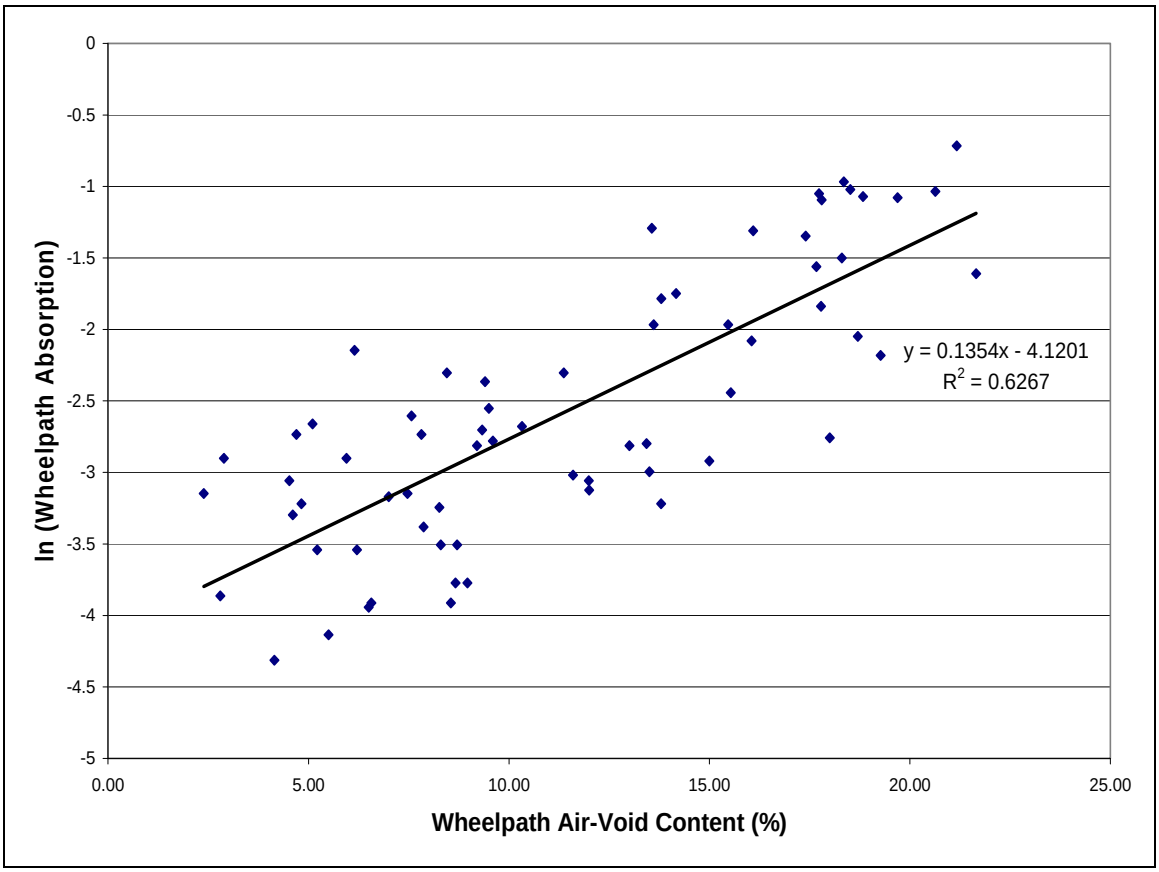

Figure 121: Correlation of absorption values with air-void content for all mixes pooled together.

Figure 122 shows the correlation of absorption values with the surface layer thicknesses for different mix types. The figure shows that increasing thickness does not appear to have a significant effect on the absorption values for any of the mix types.

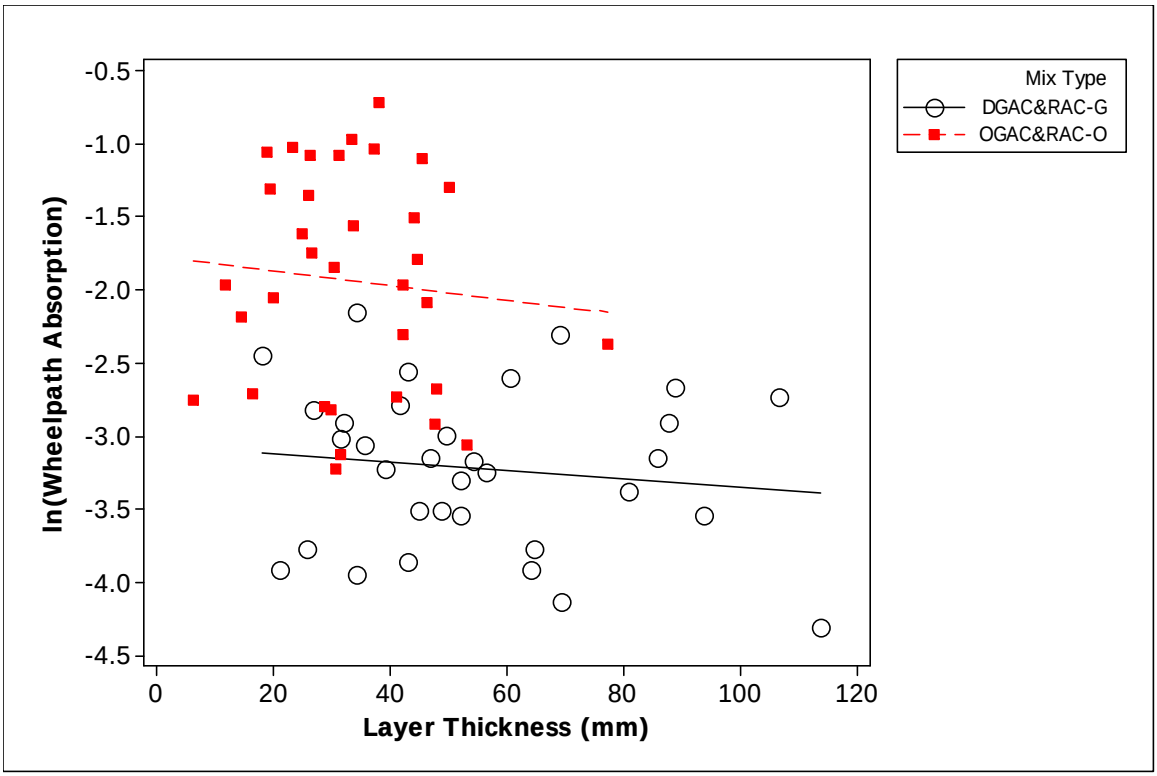

Figure 122: Correlation of absorption values with surface layer thickness for different mix types.

9.3.3 Correlation of Absorption Values with A-Weighted Sound Intensity Levels

In the correlation analysis of sound intensity levels, overall and for the one-third octave band, with the sound absorption values, the new type of mixes—RUMAC-GG, Type D-MB, Type G-MB, and BWC—were analyzed with the OGAC, RAC-O, RAC-G, and DGAC mixes. Therefore, in this section and in Section 9.3.4, the gap-graded mixes include RAC-G, RUMAC-GG, BWC, and Type G-MB, and the dense-graded mixes include DGAC and Type D-MB mixes.

Figure 123 shows the relationship of sound intensity levels versus the absorption values for different mix types. The figure shows that increasing absorption values reduces the sound intensity levels for dense- and gap-graded mixes. However, the noise levels do not change with the absorption values for open-graded mixes, probably because open-graded mixes have greater macrotexture, which increases the noise levels and overrides the noise-absorbing benefits of the high air-void content. A similar relationship between sound intensity and air-void content can be seen in Figure 86 earlier in this report since acoustical absorption is highly correlated with air-void content.

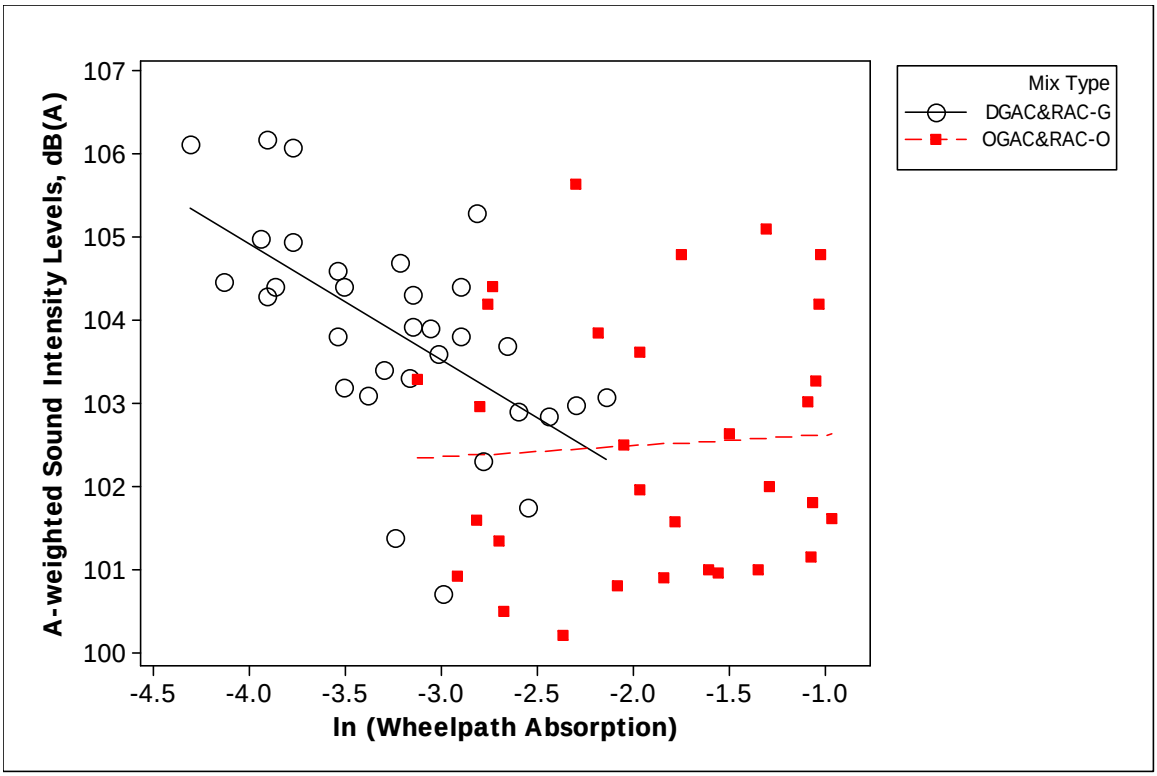

Figure 123: A-weighted sound intensity levels versus absorption values for different mix types.

Since the absorption values and mix type are highly correlated, they cannot be used in the same regression. Therefore, separate analyses were conducted for different mix types to evaluate the relationship between A-weighted sound intensity levels and absorption values. Figure 124 and Figure 125 show the relationship between sound intensity levels and dense- and gap-graded mixes and open-graded mixes, respectively. The figures show that there is no correlation between sound intensity and absorption values for open-graded mixes.

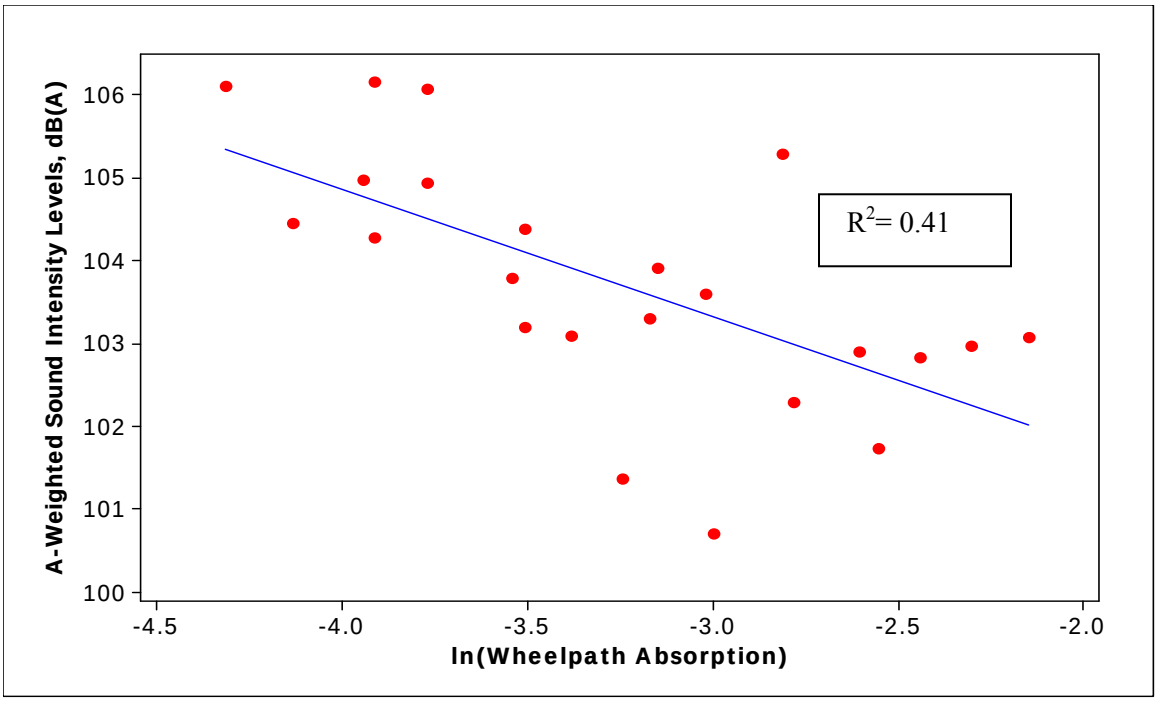

Figure 124: Correlation of sound intensity levels with wheelpath absorption for dense- and gap-graded mixes.

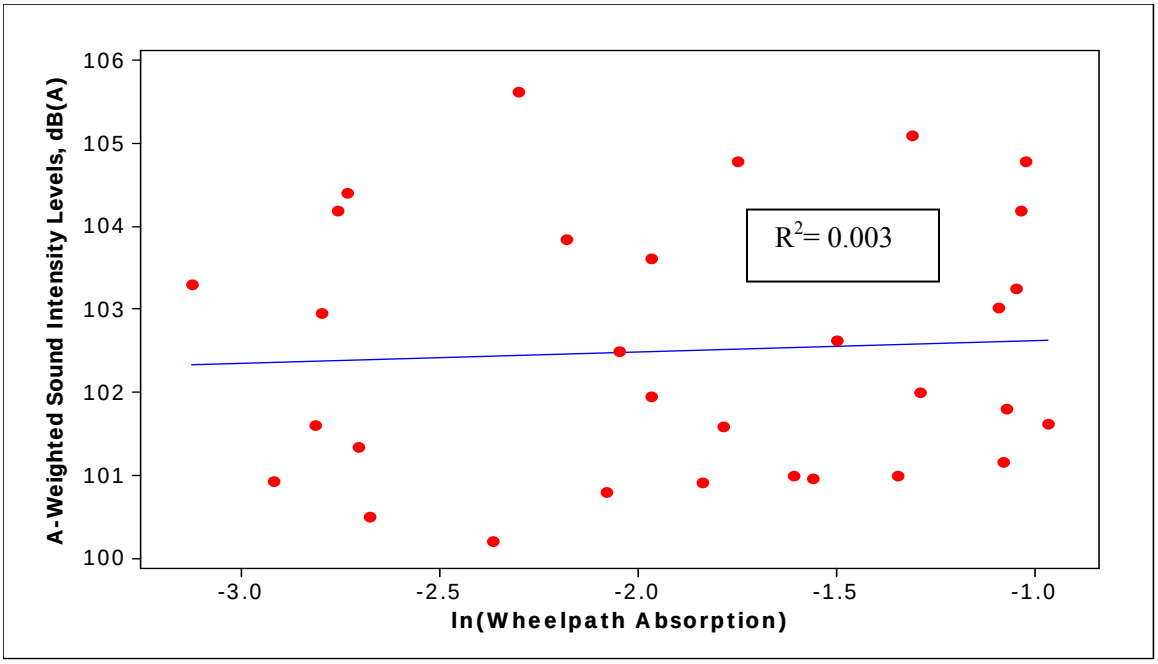

Figure 125: Correlation of sound intensity levels with wheelpath absorption for open-graded mixes.

9.3.4 Correlation of Sound Absorption Values with One-Third Octave Band Frequency Sound Intensity Levels

No correlation was found between the overall sound intensity levels and absorption values for open-graded mixes. However, the study found that open-graded mixes have higher absorption values and lower noise levels than gap- and dense-graded mixes. The spectral contents of the sound intensity levels were evaluated to fully understand the absorption effects on the noise levels**.** Since the OBSI levels were given in one-third octave bands for frequencies between 500 and 5,000 Hz, and the absorption values were obtained for frequencies between 200 and 1,700 Hz with a resolution of 3.125 Hz, the average absorption was correlated with each one-third octave band center frequency within the range of impedance tube frequencies.

9.3.4.1 Sound Intensity Levels for 500-Hz One-Third Octave Band

Figure 126 shows the sound intensity levels for the 500-Hz band versus the absorption values. The figure shows that increasing absorption values reduces the sound intensity levels for dense- and gap-graded mixes, and increasing absorption values increases the sound intensity levels for open-graded mixes. Absorption was found to be correlated with sound intensity levels at around 500 Hz for open-graded mixes because it is highly correlated with air-void content, and increasing air-void content increases the noise levels at lower frequencies for open-graded mixes. Therefore, the study concluded that that there is no casual relationship between absorption values and sound intensity levels at 500 Hz for open-graded mixes.

Regression analysis was conducted to determine the effects of acoustical absorption and mix type on sound intensity levels for the 500-Hz band only for dense- and gap-graded mixes since the relationship between sound intensity levels for the 500-Hz band and absorption is not causal.

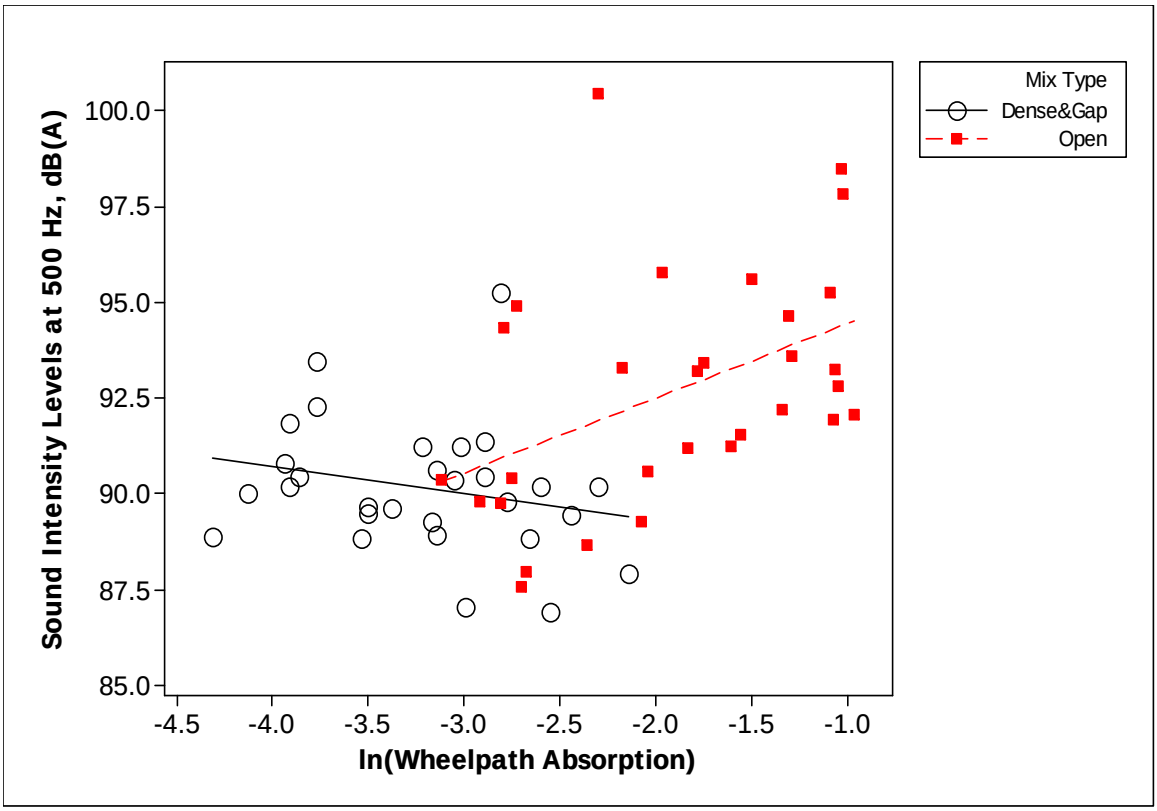

Figure 126: Sound intensity levels for 500-Hz band versus absorption values.

The relationship between the 500-Hz band sound intensity levels and absorption is given here. From the regression analysis, absorption was found to be insignificant for dense- and gap-graded mixes. It can be concluded that at 500 Hz, absorption has no effect on noise levels because the lower-frequency noise levels are governed by tire vibrations caused by surface texture.

Gap- and Dense-Graded Mixes

The regression equation, Equation (32), is

500-Hz band = 87.9 – 0.694 × ln(Wheelpath absorption) **(32)**

Predictor	Coef	SE Coef	T	P
Constant	87.930	1.839	47.82	0.000
ln(Wheelpath absorption)	–0.6937	0.5623	–1.23	0.228

S = 1.71152 R-Sq = 5.3% R-Sq(adj) = 1.8%

9.3.4.2 Sound Intensity Levels for 630-Hz One-Third Octave Band

Figure 127 shows the sound intensity levels for the 630-Hz band versus the absorption values. The figure shows that increasing absorption values reduce the sound intensity levels for dense and gap-graded mixes, while increasing absorption values increase the sound intensity levels for open-graded mixes, as in the case of the 500-Hz band frequency levels. Noise increases with increasing absorption because increasing air-void content increases the noise levels at lower frequencies. Since the relationship between 630-Hz band sound intensity levels and absorption is not causal for open-graded mixes, regression analyses were conducted only for dense- and gap-graded mixes.

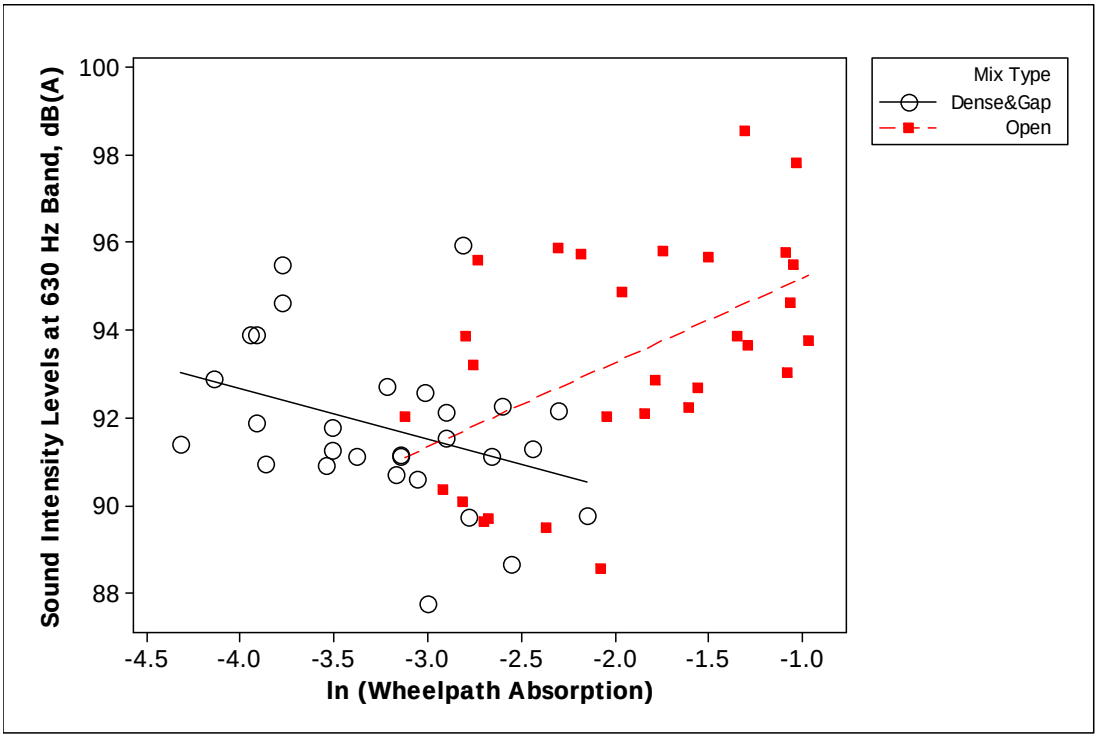

Figure 127: Sound intensity levels for 630-Hz band versus absorption values.

The relationship between 630-Hz band sound intensity levels and absorption is given here. Increasing absorption reduces the noise levels for dense- and gap-graded mixes. The absorption values can explain only 14 percent of the variation in noise levels. It can be concluded that the noise levels at frequencies around 630 Hz are still governed by tire vibrations.

For Gap- and Dense-Graded Mixes

The regression equation, Equation (33), is

630-Hz band = 88.0 – 1.17 × ln(Wheelpath absorption) **(33)**

Predictor	Coef	SE Coef	T	P
Constant	88.015	1.846	47.69	0.000
ln(Wheelpath absorption)	–1.1671	0.5643	–2.07	0.048

S = 1.71772 R-Sq = 13.7% R-Sq(adj) = 10.5%

9.3.4.3 Sound Intensity Levels for 800-Hz One-Third Octave Band

Figure 128 shows the sound intensity levels for the 800-Hz band versus the absorption values. The figure shows that increasing absorption values reduce the sound intensity levels for dense- and gap-graded mixes. However, there is no correlation between sound intensity levels and absorption values for open-graded mixes for the 800-Hz band. Therefore, regression analysis was conducted to determine the effects of acoustical absorption on sound intensity levels for the 800-Hz band only for dense- and gap-graded mixes.

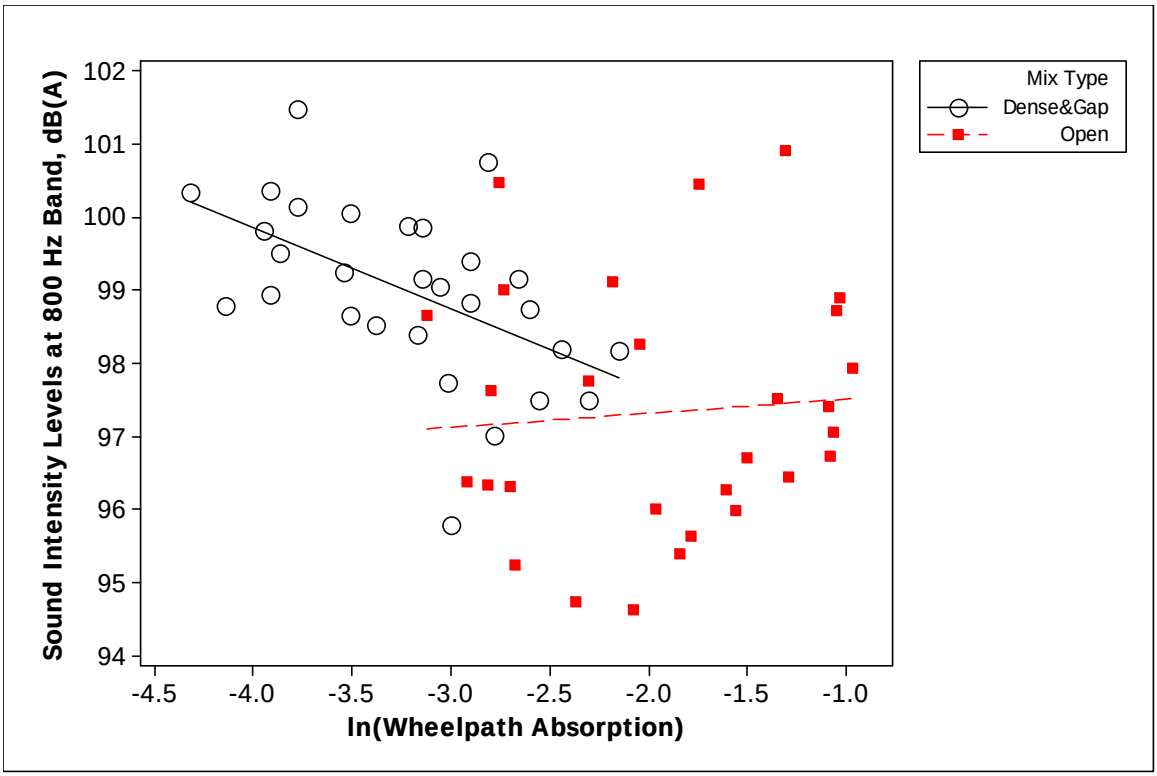

Figure 128: Sound intensity levels for 800-Hz band versus absorption values.

The relationship between 800-Hz band sound intensity levels and absorption is given here for gap- and dense-graded mixes. Increasing absorption reduces the noise levels. The absorption values can explain 28 percent of the variation in noise levels. There is no trend for open-graded mixes because increasing air-void content increases the MPD, and increasing the MPD increases the noise levels at lower frequencies; therefore, the noise-absorbing benefits of open-graded mixes are surpassed by their greater MPD values at lower frequencies. It can be concluded that at frequencies of around 800 Hz, the tire vibrations increase the noise levels only for high macrotexture values.

For Gap- and Dense-Graded Mixes

The regression equation, Equation (34), is

800-Hz band = 95.4 – 1.11 × ln(Wheelpath absorption) **(34)**

Predictor	Coef	SE Coef	T	P
Constant	95.417	1.118	85.36	0.000
ln(Wheelpath absorption)	–1.1129	0.3418	–3.26	0.003

S = 1.04034 R-Sq = 28.2% R-Sq(adj) = 25.5%

9.3.4.4 Sound Intensity Levels for 1,000-Hz One-Third Octave Band

Figure 129 shows the sound intensity levels for the 1,000-Hz band versus the absorption values. The figure shows that increasing absorption values reduce the sound intensity levels for dense- and gap-graded mixes. There is no clear trend for open-graded mixes because of the four points circled in Figure 129, which have much lower noise levels than the other mixes at a given absorption value. The circled mixes have higher permeability compared to the dense- and gap-graded mixes with the same absorption values; they are younger than the open-graded mixes with the same absorption values. The higher permeability of the circled mixes may indicate that the absorption capacity of the whole section is higher than indicated by the values obtained from the impedance tube in this study since the absorption values are based on one core from the wheelpath.

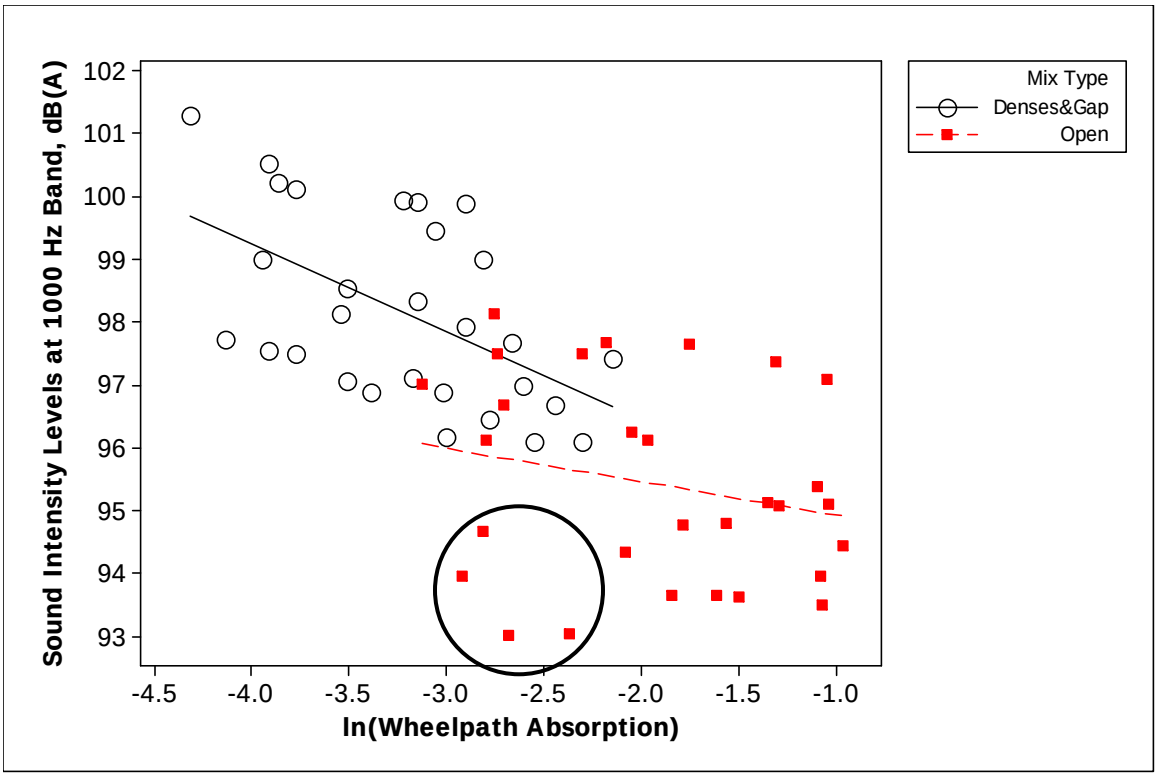

Figure 129: Sound intensity levels for 1,000-Hz band versus absorption values.

Figure 130 shows the sound intensity values versus the absorption values for different mix types and different macrotexture values. The figure shows that open-graded mixes with MPD values greater than 1,000 microns have higher noise levels compared to those with MPD values less than 1,000 microns at a given absorption. This difference is the result of the increased vibrations due to the high texture depths. Regression analysis was conducted to determine the effects of acoustical absorption and mix type on sound intensity levels for the 1,000-Hz band.

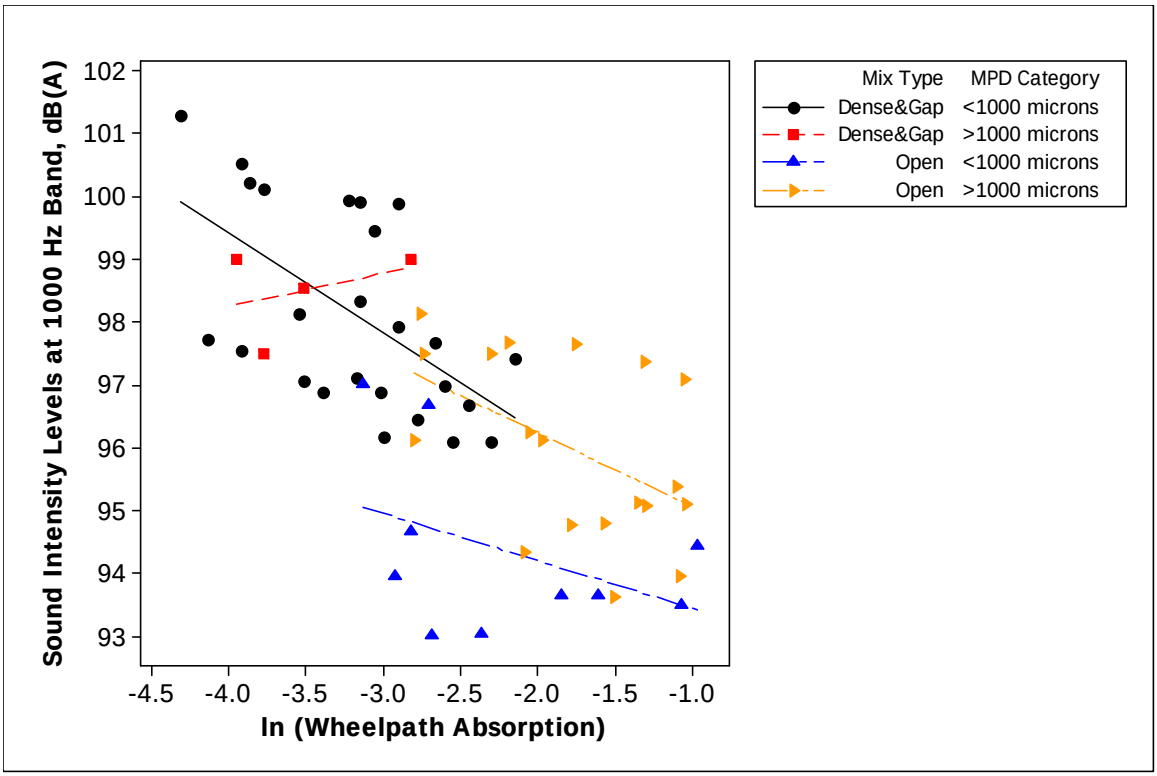

Figure 130: Sound intensity levels for 1,000-Hz band versus absorption values for different mix types and different macrotexture values.

For All Mix Types

The regression equation, Equation (35), is

1,000-Hz band = 92.9 – 1.53 × ln(Wheelpath absorption) **(35)**

Predictor	Coef	SE Coef	T	P
Constant	92.8607	0.6137	151.31	0.000
ln Wheelpath absorption	–1.5289	0.2253	–6.79	0.000

S = 1.54190 R-Sq = 45.1% R-Sq(adj) = 44.2%

Analysis of Variance

Source	DF	SS	MS	F	P
Regression	1	109.51	109.51	46.06	0.000
Residual error	56	133.14	2.38		
Total	57	242.65			

The model can explain 45 percent of the variation in the sound intensity levels for the 1,000-Hz band. It can be concluded that air pumping starts to govern the noise generation at frequencies around 1,000 Hz. However, the tire vibrations may cause significant noise levels for mixes with high macrotexture values.

9.3.4.5 Sound Intensity Levels for 1,250-Hz One-Third Octave Band

Figure 131 shows the sound intensity levels for the 1,250-Hz band versus the absorption values. The figure shows that increasing absorption values reduce the sound intensity levels for all types of mixes. Regression analysis was conducted to determine the effects of acoustical absorption on sound intensity levels for the 1,250 Hz band.

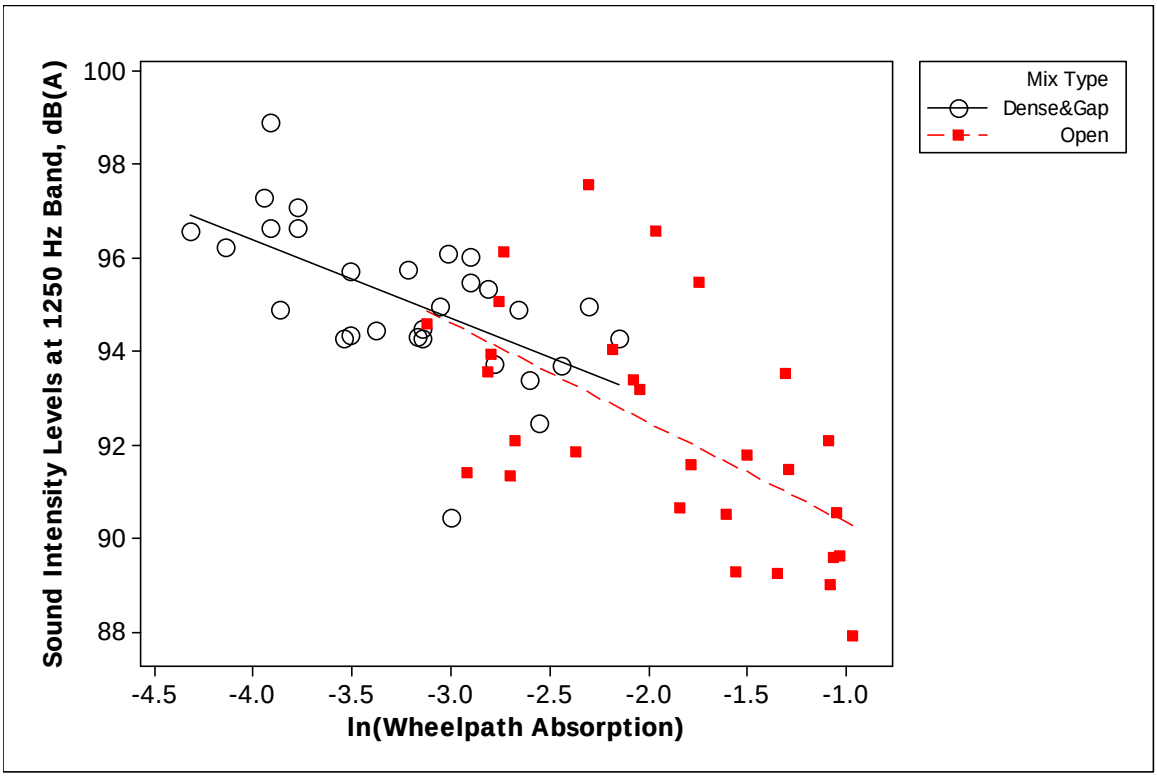

Figure 131: Sound intensity levels for 1,250-Hz band versus absorption values.

For All Mix Types

The regression equation, Equation (36), is

1,250-Hz band = 88.6 – 1.99 × ln(Wheelpath absorption) **(36)**

Predictor	Coef	SE Coef	T	P
Constant	88.6237	0.6519	135.94	0.000
ln(Wheelpath absorption)	–1.9901	0.2411	–8.26	0.000

S = 1.69106 R-Sq = 54.5% R-Sq(adj) = 53.7%

Analysis of Variance

Source	DF	SS	MS	F	P
Regression	1	194.89	194.89	68.15	0.000
Residual error	57	163.00	2.86		
Total	58	357.89			

Regression analysis revealed that absorption is a significant variable affecting the sound intensity levels for the 1,250-Hz band. The regression analysis shows that increasing absorption reduces the sound intensity levels. The model can explain 54 percent of the variation in the sound intensity levels for the 1,250-Hz band.

9.3.4.6 Sound Intensity Levels for 1,600-Hz One-Third Octave Band

Figure 132 shows the sound intensity levels for the 1,600-Hz band versus the absorption values. The figure shows that increasing absorption values reduce the sound intensity levels for all types of mixes, as was the case for the 1,250-Hz frequency band. Regression analysis was conducted to determine the effects of acoustical absorption on sound intensity levels for the 1,600-Hz band.

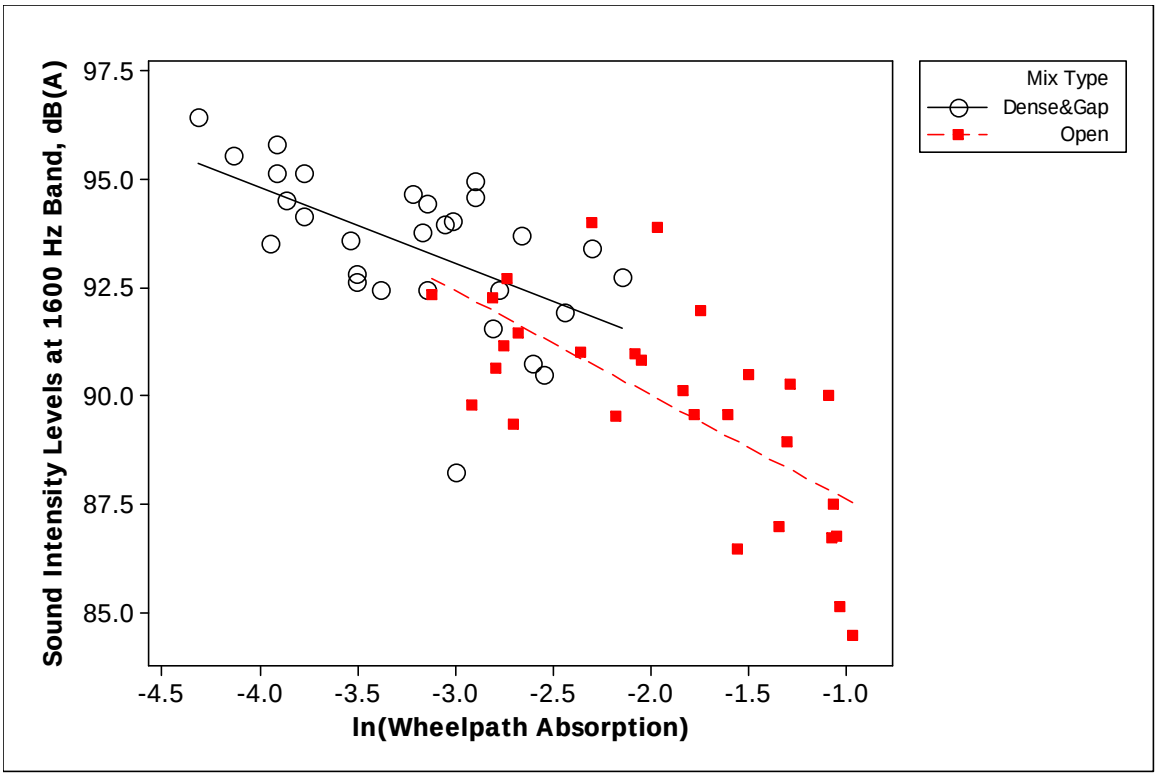

Figure 132: Sound intensity levels for 1,600-Hz band versus absorption values.

For All Mix Types

The regression equation, Equation (37), is

1,600-Hz band = 85.3 – 2.39 × ln(Wheelpath absorption) **(37)**

Predictor	Coef	SE Coef	T	P
Constant	85.3182	0.6396	133.40	0.000
ln(Wheelpath absorption)	–2.3886	0.2436	–9.81	0.000

S = 1.63376 R-Sq = 66.2% R-Sq(adj) = 65.6%

Analysis of Variance

Source	DF	SS	MS	F	P
Regression	1	256.66	256.66	96.16	0.000
Residual error	49	130.79	2.67		
Total	50	387.45			

The regression analysis showed that absorption is a significant variable affecting the sound intensity levels for the 1,600-Hz band. Increasing absorption reduces the sound intensity levels according to the regression. The model can explain 66 percent of the variation in the sound intensity levels for the 1,600-Hz band.

9.3.5 Summary of Findings

- The noise levels of dense- and gap-graded mixes decrease with increasing absorption. However, no correlation was found between the overall A-weighted sound intensity and absorption for open-graded mixes. There is no correlation because open-graded mixes are insensitive to air-void content. Since noise is absorbed when it is propagating away from the tire/pavement contact patch to the side of the road rather than at the tire/pavement contact patch, absorption values may be better correlated with way-side noise levels measured next to highways.
- The noise levels around the 500-Hz frequency are governed by tire vibrations; therefore, absorption has no effect on the noise levels.
- At frequencies above 630 Hz, absorption reduces the noise levels caused by air pumping for dense- and gap-graded mixes.

- Tire vibrations may cause significant noise levels for open-graded mixes with high macrotexture values at lower frequencies (less than 1,000 Hz), and there is no trend between noise and absorption.
- The noise-reducing effect of absorption can be seen at 1,000 Hz for open-graded mixes, if macrotexture is also considered.
- The noise-reducing effects of absorption can be clearly seen at frequencies above 1,000 Hz for open-graded mixes.
- Air-pumping noise governs noise generation at frequencies above 1,000 Hz, confirming the earlier findings, as increasing absorption reduces the noise levels regardless of the macrotexture values. This trend is stronger for higher frequencies, which are considered more annoying to humans.
- Open-graded mixes have higher absorption values than dense- and gap-graded mixes. Dense- and gap-graded mixes have very low absorption values (usually less than 0.1). OGAC and RAC-O mixes have similar absorption values, which range between 0.1 and 0.5.
- Absorption values generally decrease with time. Absorption change over time follows the same trend as permeability change rather than air-void content change. This finding confirms that clogging occurs at the top part of the surface layer, reducing permeability and acoustical absorption, while the change in air-void content is small.
- No correlation was found between surface layer thickness and absorption. There may be no correlation because all the open-graded mixes evaluated are placed in thin lifts, usually less than 30 mm.

10 ANALYSIS OF ENVIRONMENTAL NOISE MONITORING SITE SECTIONS

The environmental noise monitoring site sections include 23 test sections from six sites as shown earlier in this report in Table 5. These 23 environmental test sections (labeled ES in this study) were built by Caltrans to test pavement noise, durability, permeability, and friction performance trends for new types of surface mixes. They include asphalt mixes that are not widely used in California, such as Type-G MB, Type-D MB, RUMAC-GG, and EU gap-graded mixes, as well as commonly used mixes such as OGAC, RAC-O, DGAC, and RAC-G, included in the test sections as controls. These mixes are described in Chapter 3. The climate information for the ES sections is given in Table 6, and the traffic levels are given in Table 7. The test sections of Fresno 33 and LA 138 include different mix types placed next to each other. Since these mixes experience the same traffic and climate, they allow direct comparison of performance of different mix types as well as of the same mixes with different thicknesses. This information will help in the development of specifications for quieter and more durable mix designs. In addition to OBSI measurements, the pass-by measurement, which is a way-side noise measurement, was conducted for the LA 138 mixes. Comparison of way-side measurements with noise measurements at the source (OBSI) reveals the effects of absorption on noise levels for sound traveling along the road surface.

The same data collection procedure was conducted on the environmental test sections as on the experimental design sections (QP sections). The environmental test sections with OGAC, RAC-O, RAC-G, and DGAC surfaces were used along with the experimental design sections in developing the models for performance variables. All the environmental test sections were evaluated for each performance variable for two years. This portion of this report presents an analysis of the performance trends of the different mixes at each site.

10.1 Fresno 33 Sections

The Fresno 33 site consists of nine test sections with five different surfacing mixes—RAC-G, Type-G MB, Type-D MB, RUMAC-GG, and DGAC—in the northbound direction of State Route 33. The layout of the test sections is given in Figure 133. Except for the DGAC control surface, all the sections were placed with both 45- and 90-mm thicknesses to evaluate the thickness effects on the pavement performance. All sections have an NMAS of 19 mm. The test sections were one year old during the first-year measurements.

The MB mixes generally have lower stiffness values than the other mix types, and the DGAC mix has the highest stiffness value at 20°C. This detail also provides an indication of effect of stiffness on noise for dense- and gap-graded mixes. All the rubberized mixes have the same aggregate gradations; the DGAC mix has slightly finer gradation than the Type D-MB mix.

The following analysis demonstrates the permeability, friction, roughness, noise, and surface condition for different mixes over two years and compares them for different thicknesses and different mixes. It answers these questions:

- How does the performance of dry- (RUMAC-GG) and terminal-process rubber (MB) compare to wet-process asphalt rubber (RAC-G) and dense-graded asphalt concrete (DGAC) under the same traffic and climate with respect to noise, friction, roughness, and distress?
- How does increased thickness affect the cracking performance of rubberized mixes?

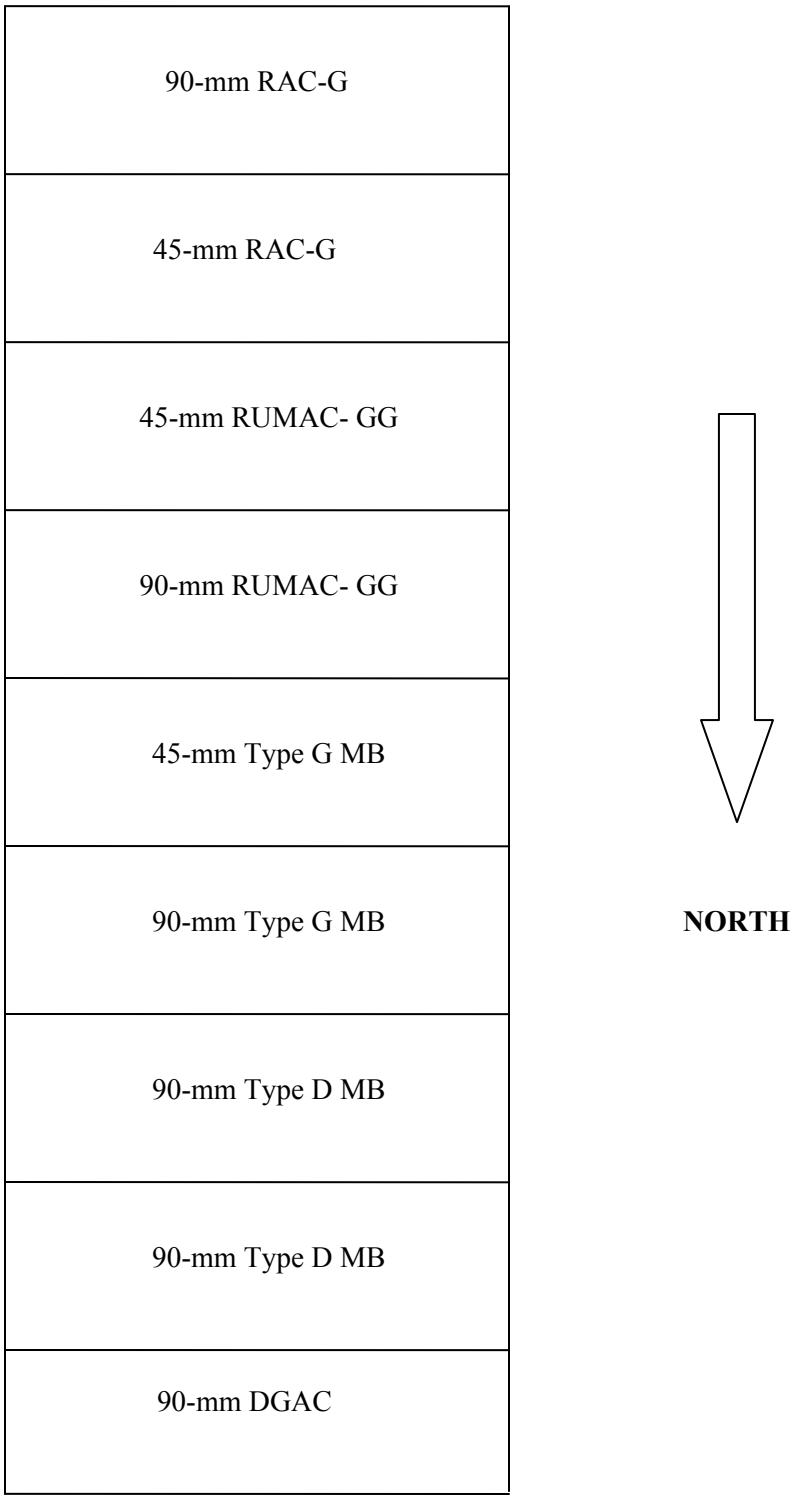

Figure 133: Layout of Fresno 33 sections.

Figure 134 and Figure 135 show the first-year and second-year center and wheelpath air-void content and permeabilities for the Fresno 33 sections. According to the figures, the RAC-G mixes are undercompacted and hence have higher air-void content and permeability values than the other gap-graded mix types and dense-graded mixes. Their permeabilities in the second-year measurements, when they were two years old, are reduced significantly, showing the same trend as the RAC-G mixes in the QP sections. The RUMAC-GG, Type G-MB, Type D-MB, and DGAC mixes have very low permeabilites, with permeabilities very close to zero.

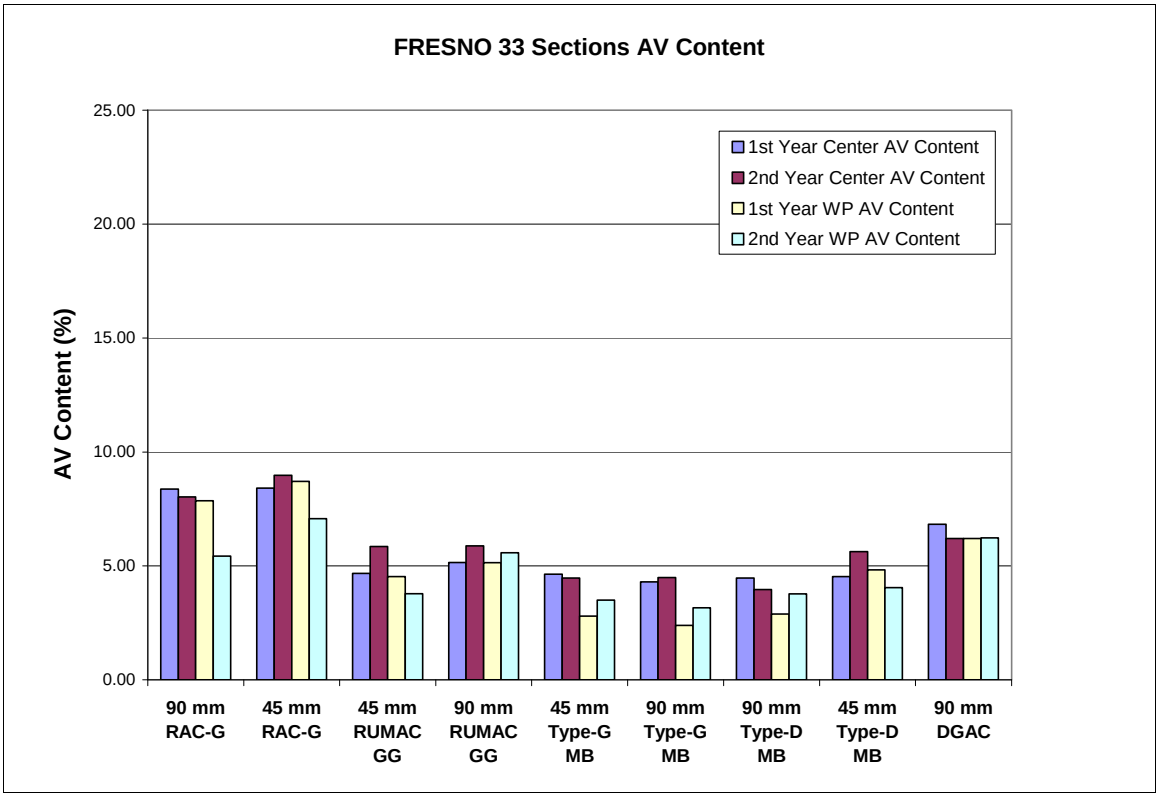

Figure 134: First-year and second-year air-void content for Fresno 33 sections.

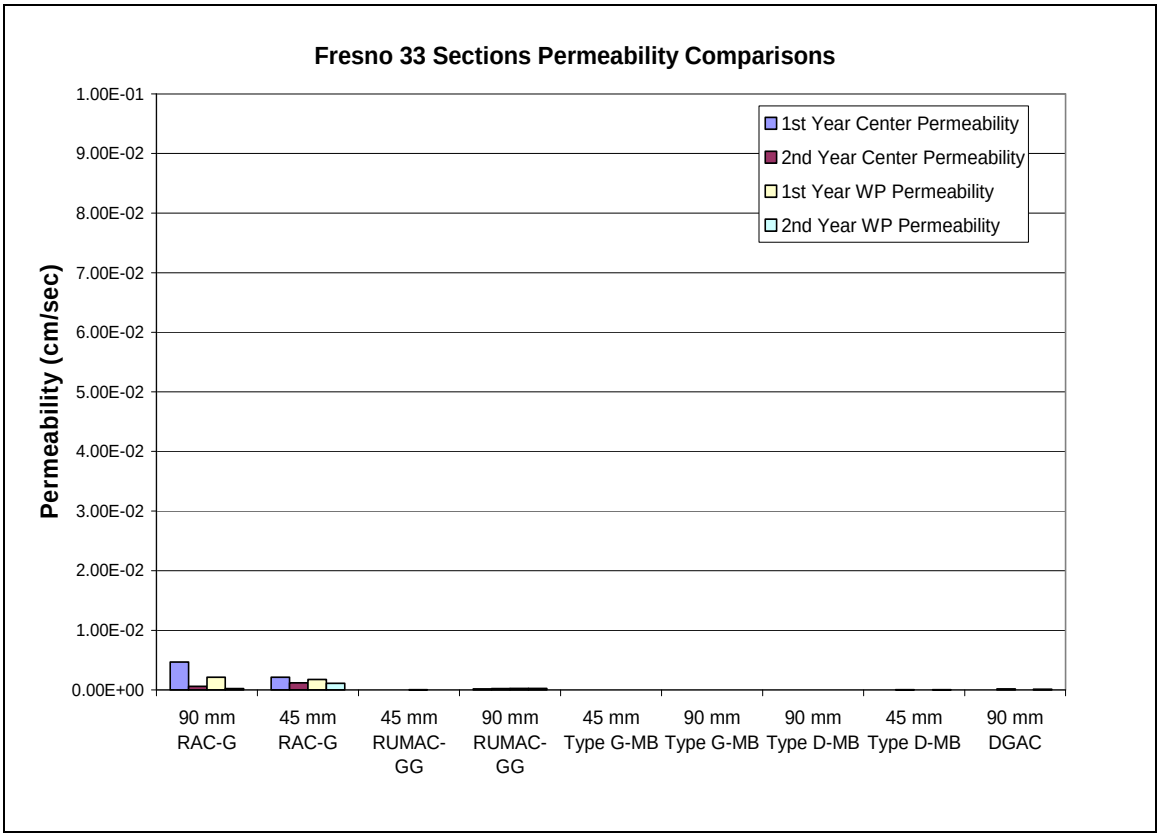

Figure 135: First-year and second-year permeability values for Fresno 33 sections. (Note: The scale for permeability was selected for comparison of permeability values across different ES sections).

The first-year and second-year center and wheelpath BPN and the IRI values for the Fresno 33 sections were also evaluated; however, they are not shown in this report. All the sections were found to have similar BPN and IRI values. The BPN values in both the first and second years are above 50, indicating that the Fresno 33 sections still provide satisfactory friction according to a criterion discussed in a Caltrans research document (15) believed to have been written in the 1960s. Since all the IRI values in both the first and second year are less than 1.5 m/km, all sections have good ride quality based on FHWA criteria. The thicker sections generally had higher IRI values than the thinner sections.

Figure 136 shows the first-year and second-year MPD values for the Fresno 33 sections. The figure shows that the RAC-G mixes have higher MPD values than the RUMAC-GG and Type G-MB mixes and that the MPD values of Type D-MB and DGAC mixes are close to each other. All sections show an increase in macrotexture values from year one to year two, confirming the findings from the experimental design sections. This increase is probably due to an increase in distresses from the first year to the second year.

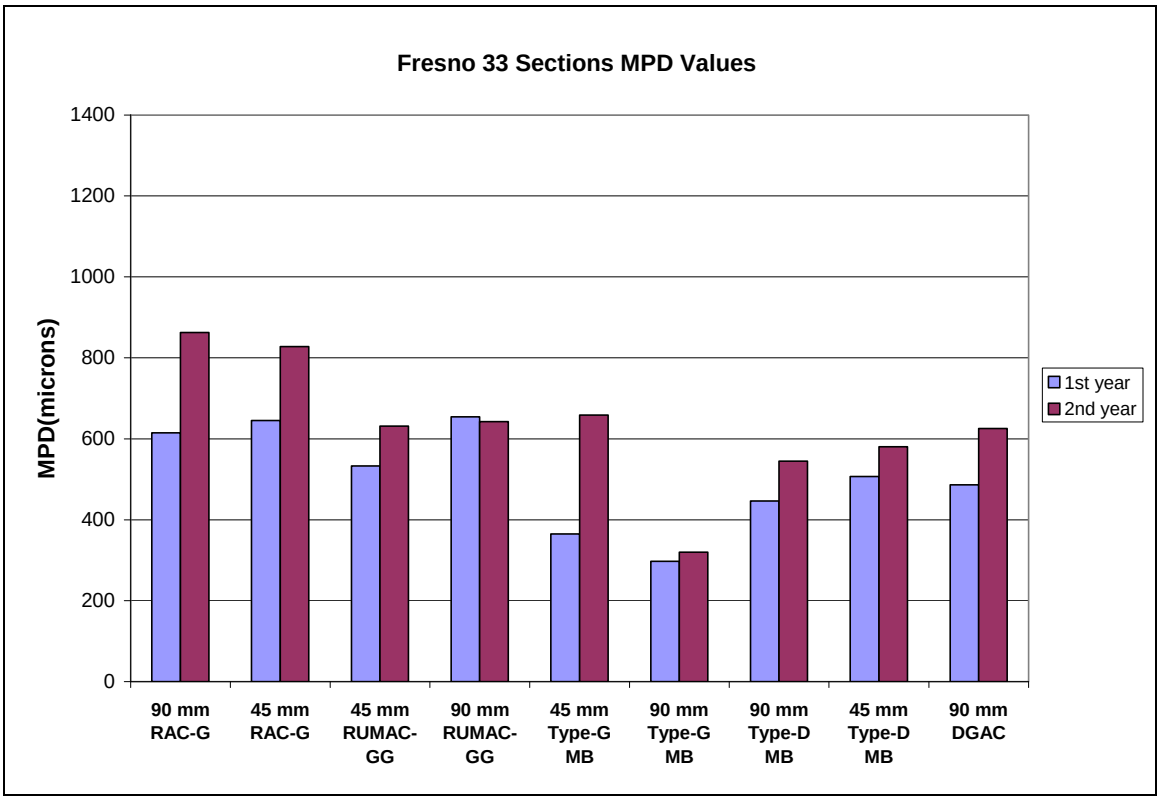

Figure 136: First-year and second-year MPD values for Fresno 33 section.

Figure 137 shows the first-year and second-year sound intensity levels for the Fresno 33 sections. The figure shows that the RAC-G mixes have the lowest noise levels, probably due to their higher air-void content. However, the noise difference between the RAC-G mixes and the DGAC mixes is less than 2 dB (A).

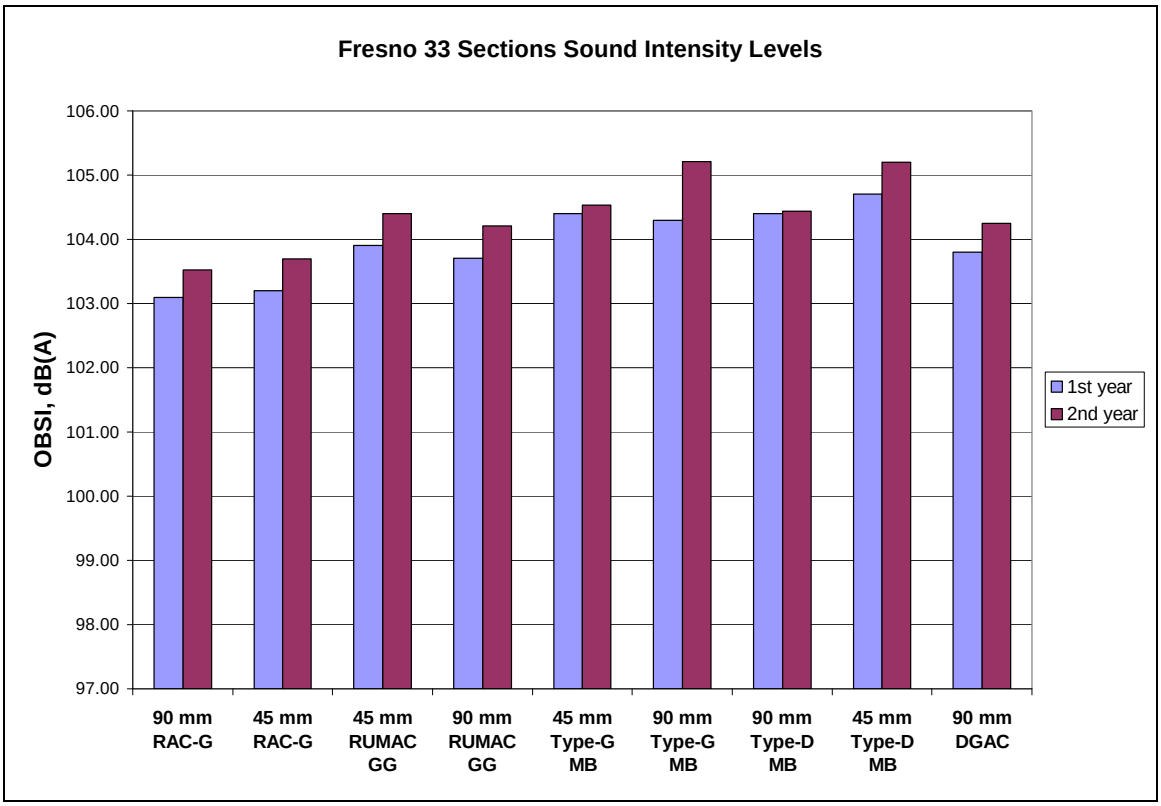

Figure 137: First-year and second-year sound intensity levels for Fresno 33 sections.

Based on the sound intensity analysis, the new mixes, Type G-MB and RUMAC-GG, do not perform as well as the RAC-G mixes. They have similar BPN values but lower MPD values than RAC-G mixes. The Type-D MB mixes have friction values and noise levels similar to those of DGAC mixes.

In addition to permeability, friction, and noise measurements, condition surveys were conducted at each test section. The distresses were recorded for two years and are shown in Appendix D.

After serving for two years, all the mixes except the DGAC mix show a high amount of bleeding, with a bleed area of more than 150 m^2, although the as-built binder contents match the design binder contents. Bleeding of the 45-mm Type G-MB mix is shown in Figure 138. The figure shows that bleeding occurs in both wheelpaths for the whole section. Although all the mixes except the DGAC mix show extensive bleeding, they still provide acceptable friction. All the mixes except Type G-MB show raveling. Among all mixes, the 90-mm RUMAC-GG and Type D-MB mixes perform the best as they show only bleeding, while all the other mixes have cracking, and most show raveling.

Figure 138: Bleeding for 45-mm Type G-MB mix

Increasing thickness may help reduce the cracking for RUMAC-GG and Type D-MB since 45-mm RUMAC-GG and Type D-MB sections show cracking, while 90-mm RUMAC-GG and Type D-MB sections show no cracking. The 90-mm RUMAC-GG mix is more resistant to cracking compared to 90-mm Type G-MB. All rubberized mixes (RAC-G, RUMAC-GG, Type G-MB, and Type D-MB) show bleeding, with RUMAC-GG and MB mixes showing the highest amount, while DGAC has no bleeding problems. Therefore, bleeding is a problem for the new rubberized mixes: RUMAC-GG and MB.

10.2 Sacramento 5 and San Mateo 280 Sections

Sacramento 5 and San Mateo 280 sites consist of thin RAC-O overlays of cracked PCC. The Sacramento 5 sections have thicknesses around 30 mm, and the San Mateo 280 section has a thickness of 40 mm. The Sacramento 5 site was evaluated for both the northbound (NB) and southbound (SB) directions, while San Mateo 280 was evaluated only for the northbound direction. PCC pavements generally tend to be noisier than AC pavements; therefore, overlaying PCC with an open-graded mix reduces the noise levels and also increases the service life of the pavement. The Sacramento 5 sections

were one year old and the San Mateo section was three years old during the first-year measurements. Both sites have an NMAS of 12.5 mm. The following analysis demonstrates the air-void content, permeability, friction, roughness, noise, and surface condition for RAC-O mixes and compares the performance variables for the northbound and southbound directions for the Sacramento 5 sections. It answers these questions:

- How does the performance of the Sacramento 5 and San Mateo 280 sections, which are overlays of PCC, compare to the performance of other open-graded mixes that are placed over AC?

Are there any differences between the performance in the northbound and southbound directions for the Sacramento 5 section and if so, why?

Figure 139 and Figure 140 show the first-year and second-year center and wheelpath air-void content and permeabilities of the Sacramento 5 sections, and Figure 141 and Figure 142 show the first-year and second-year center and wheelpath air-void content and permeabilities of the San Mateo 280 section. According to Figure 139, the air-void content in the southbound direction ranges between 15 and 20 percent, and the air-void content in the northbound direction ranges between 18 and 22 percent for the Sacramento 5 sections. According to Figure 140, the permeability in the northbound direction is greater than in the southbound direction, a result due to the higher air-void content in the northbound direction.

The San Mateo 280 section has lower air-void content, just below 15 percent; however, it has much higher permeability values than the Sacramento 5 sections. The wheelpath permeability of the San Mateo 280 section is almost twice that of the center and also twice that of the wheelpath permeability of the Sacramento 5 sections. This finding may indicate some cleaning effect of traffic since San Mateo 280 is the only section where the wheelpath permeability is greater than that of the center, and the permeability of the wheelpath increased in one year while the center stayed almost the same. These results may be the combined effect of the heavy traffic and high rainfall that the section experiences; the traffic level and rainfall amount for the San Mateo 280 section are much higher than the average values for the QP sections.

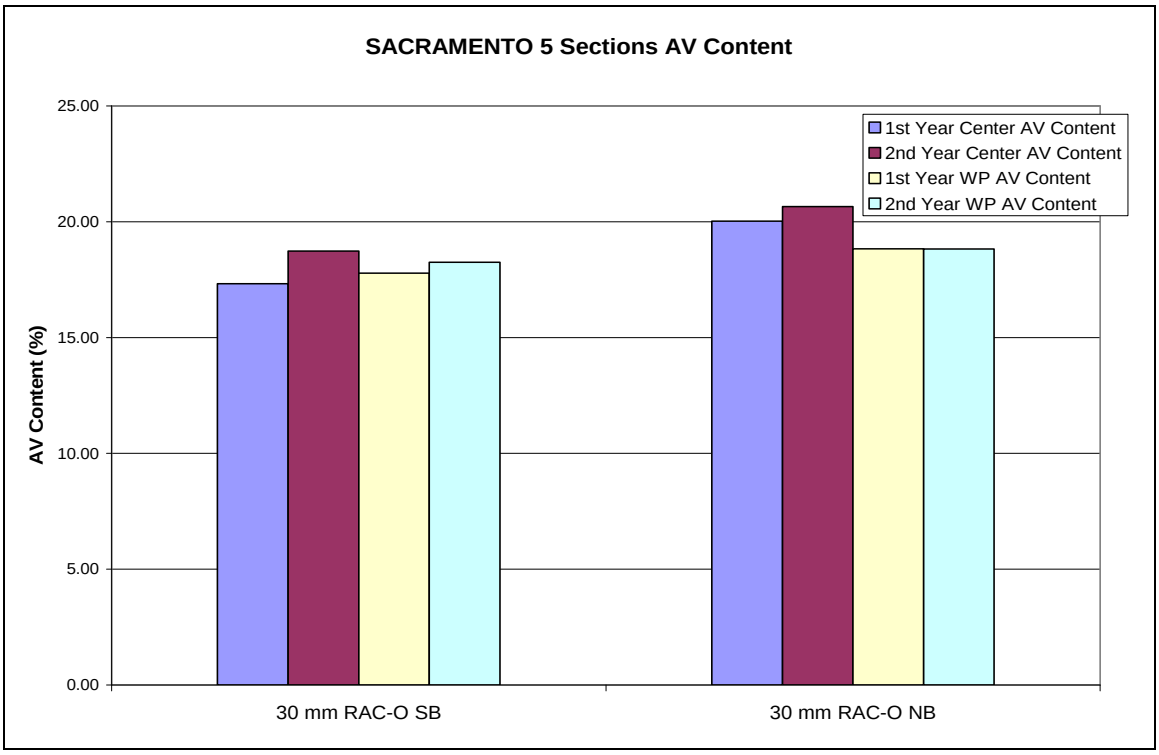

Figure 139: First-year and second-year air-void content for Sacramento 5 sections.

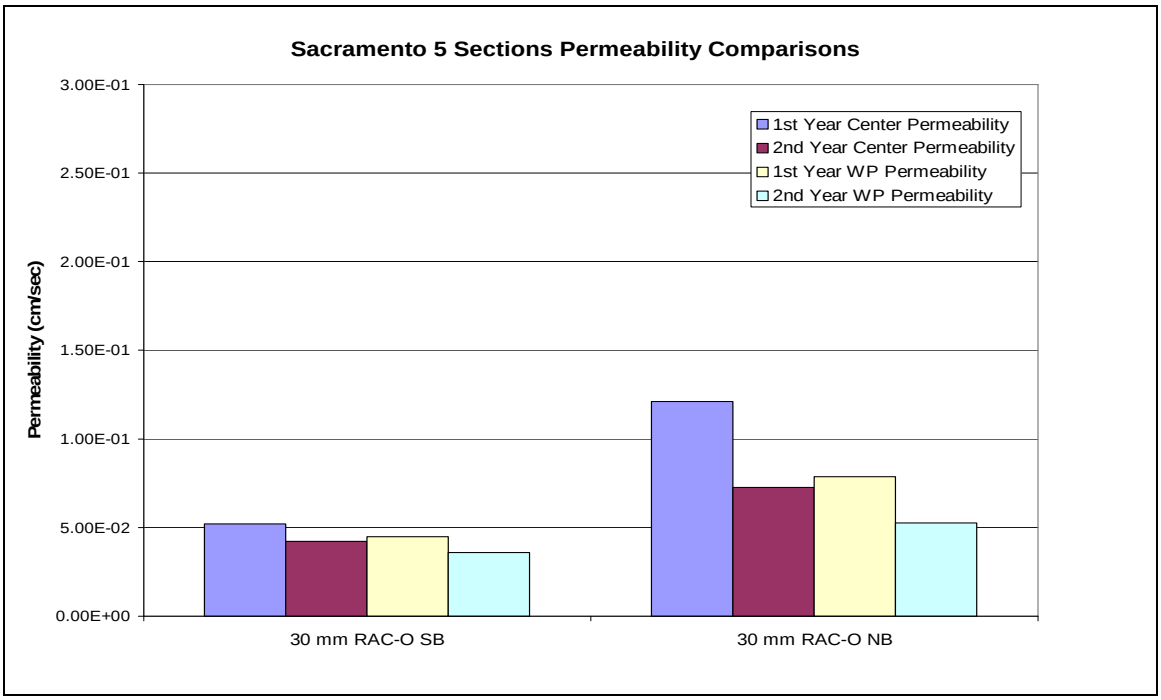

Figure 140: First-year and second-year permeability values for Sacramento 5 sections.

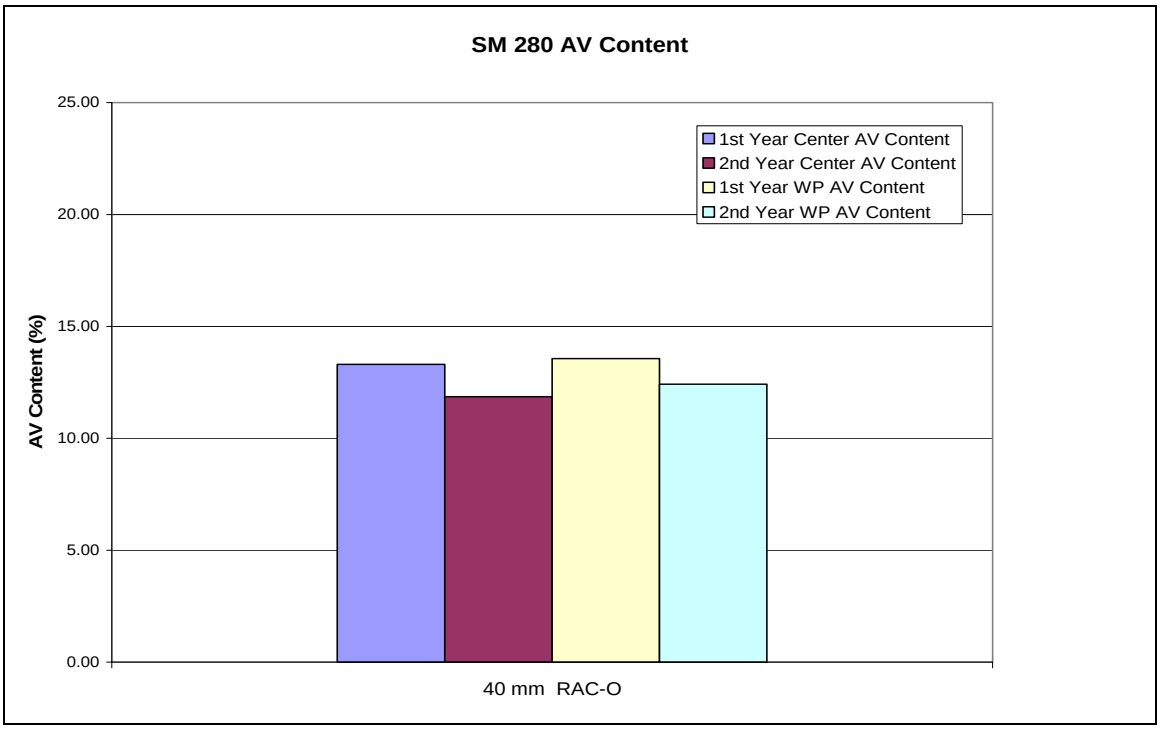

Figure 141: First-year and second-year air-void content for San Mateo 280 section.

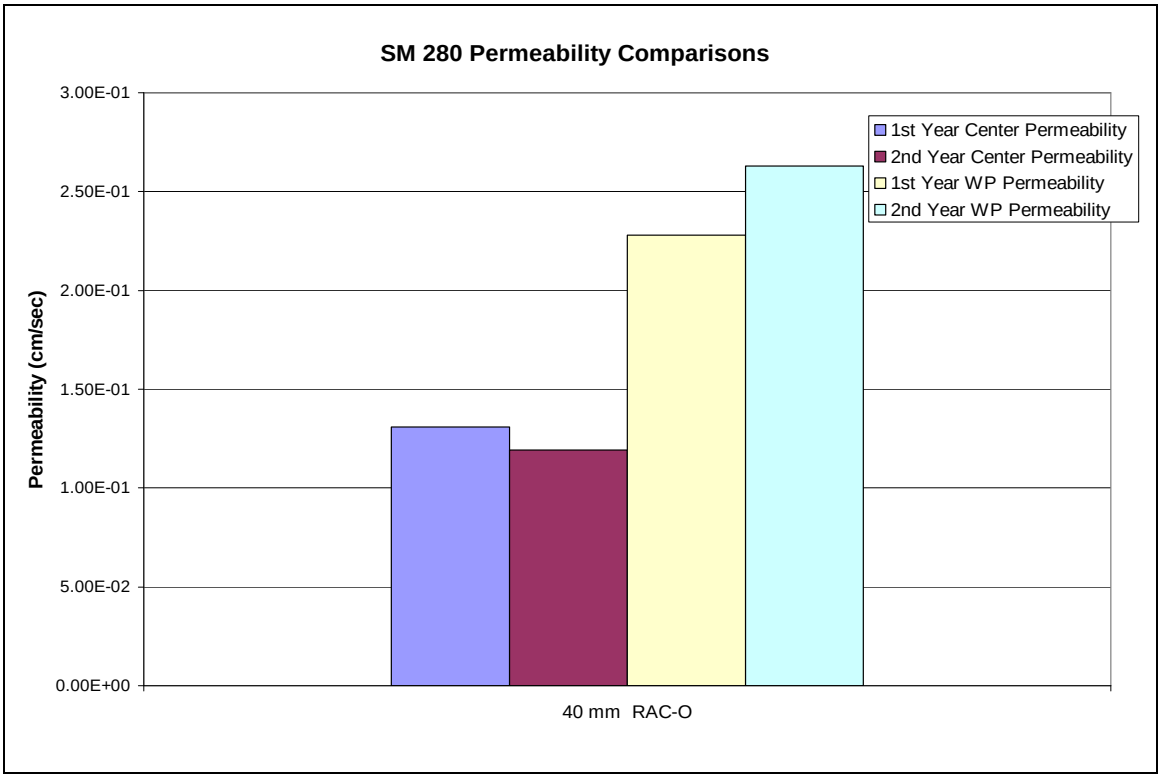

Figure 142: First-year and second-year permeability values for San Mateo 280 section.

The first-year and second-year center and wheelpath BPNs for the Sacramento 5 and San Mateo 280 sections were also evaluated; however, they are not shown in this report. The BPNs in both the first and second year are above 50, indicating that the Sacramento 5 and San Mateo 280 sites still provide satisfactory friction according to a criterion discussed in a Caltrans (15) research document believed to have been written in the 1960s.

Figure 143 and Figure 144 show the first-year and second-year left and right IRI values for the Sacramento 5 and San Mateo 280 sites, respectively. Both sites provide only "acceptable" ride quality based on FHWA criteria. The figures show that the right IRI value for the San Mateo 280 section is almost twice the left IRI value; however, the reason for this difference is unknown. The IRI of RAC-O mixes for the QP sections ranges between 0.8 and 1.25 m/km, with an average of 1.10 m/km, and the IRI of RAC-O mixes that are one to four years old ranges between 0.7 and 1.70 m/km, with an average of 1.25 m/km, as can be seen earlier in Figure 67. Both the Sacramento 5 and San Mateo 280 sites have higher IRI values than the majority of the QP sections, probably due to the cracked PCC underneath, which has a high IRI value. These findings may suggest that the IRI of thin overlays are affected by the IRI of the underlying PCC.

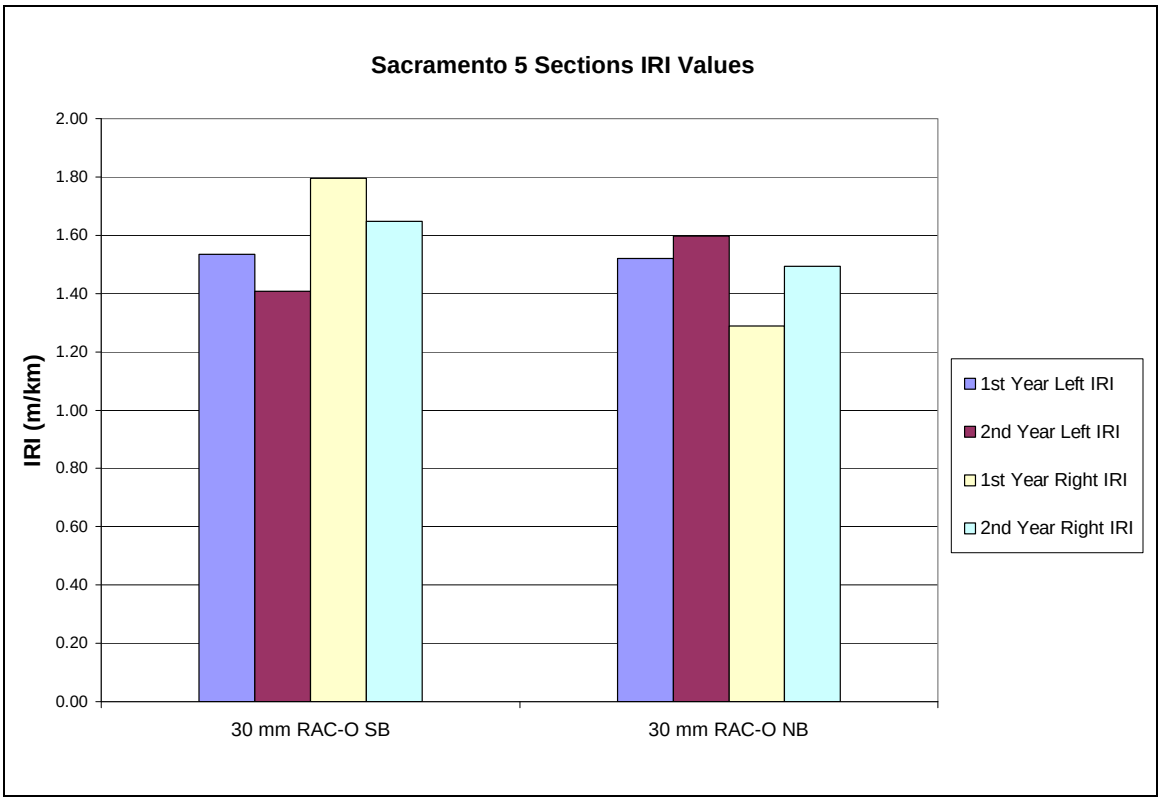

Figure 143: First-year and second-year IRI values for Sacramento 5 sections.

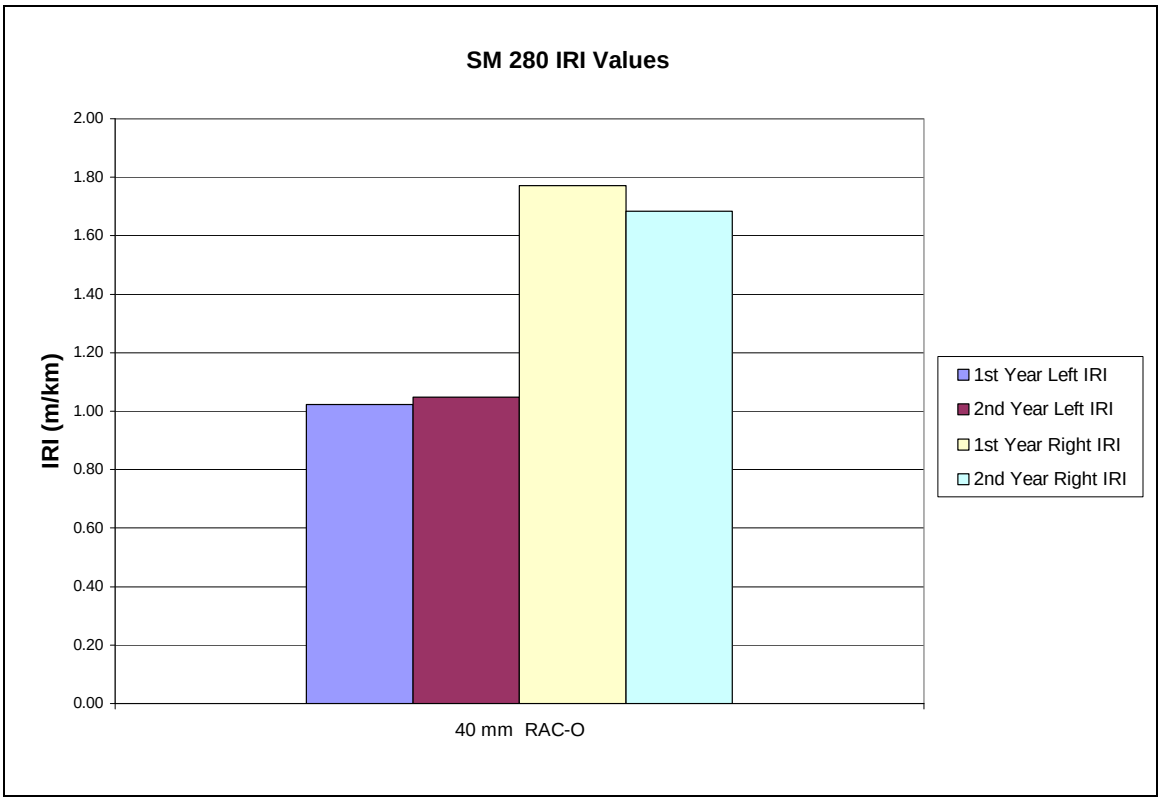

Figure 144: First-year and second-year IRI values for San Mateo 280 section.

Figure 145 and Figure 146 compare the first-year and second-year MPD values for the Sacramento 5 and San Mateo sites, respectively. The figures show that the MPD values in the northbound direction are much higher than in the southbound direction in the second year for the Sacramento 5 sections. The greater increase in the northbound direction is probably due to higher air-void content and more distresses.

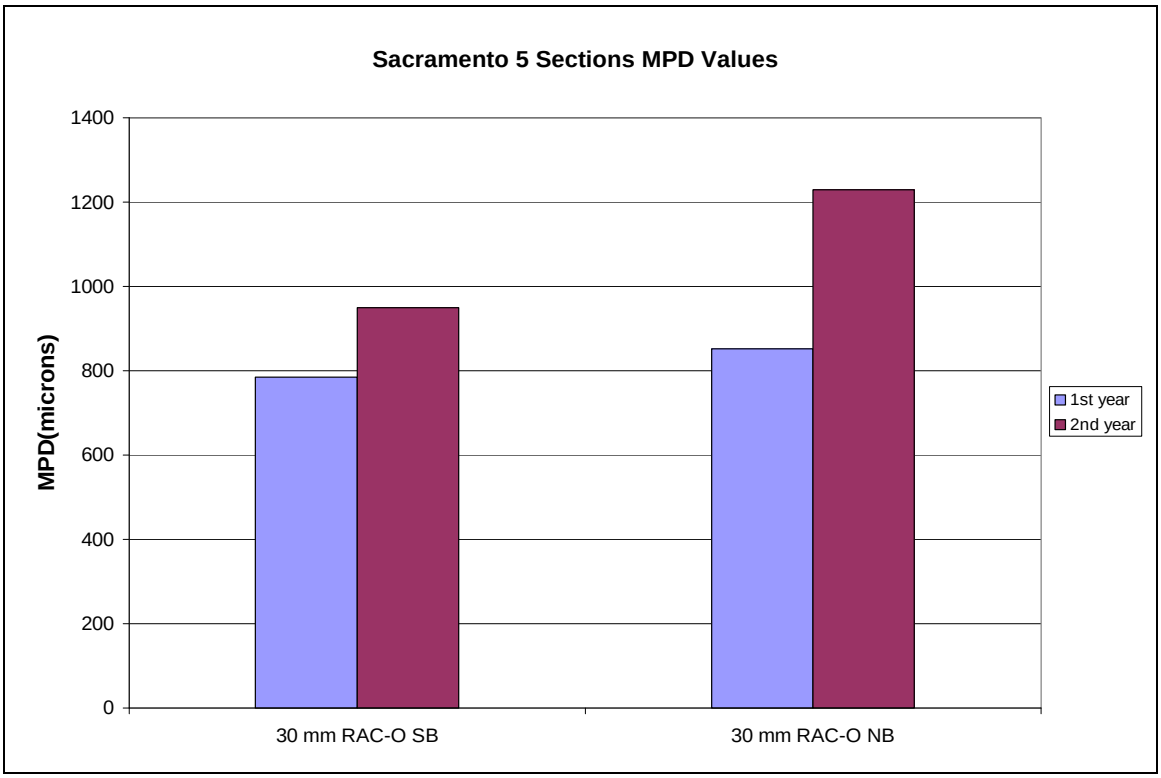

Figure 145: First-year and second-year MPD values for Sacramento 5 sections.

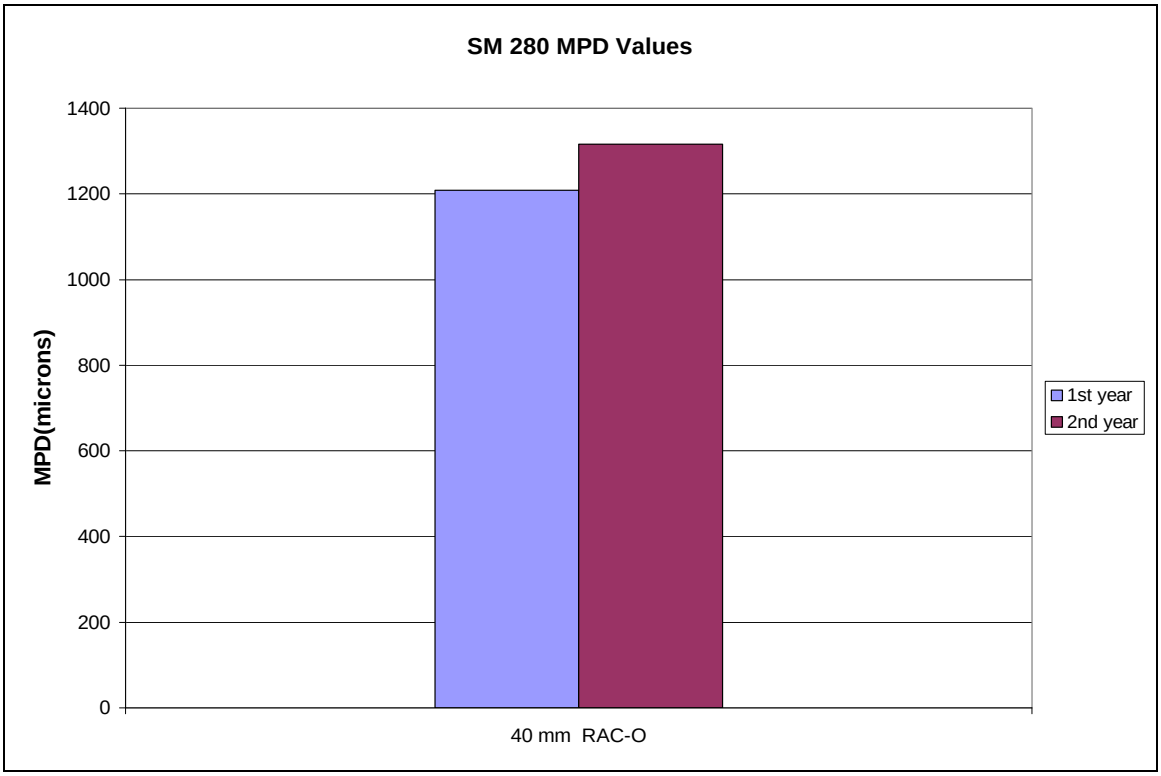

Figure 146: First-year and second-year MPD values for San Mateo 280 section.

Figure 147 and Figure 148 show the first-and second-year sound intensity levels for the Sacramento 5 and San Mateo 280 sites, respectively. According to the figure, the northbound section of the Sacramento 5 site has slightly higher noise levels than the southbound section; however, the difference is less than 1 dB (A). The results presented in Chapter 9 showed that increasing air-void content does not reduce the noise levels for mixes with air-void content above 15 percent; therefore, the higher noise levels for the northbound section are most likely due to the higher MPD values and distresses. The noise levels of the Sacramento 5 sections increased almost 1 dB (A) from the first year to the second year; there was a slight reduction in the noise levels of the San Mateo 280 section, but this finding is likely due to a measurement error.

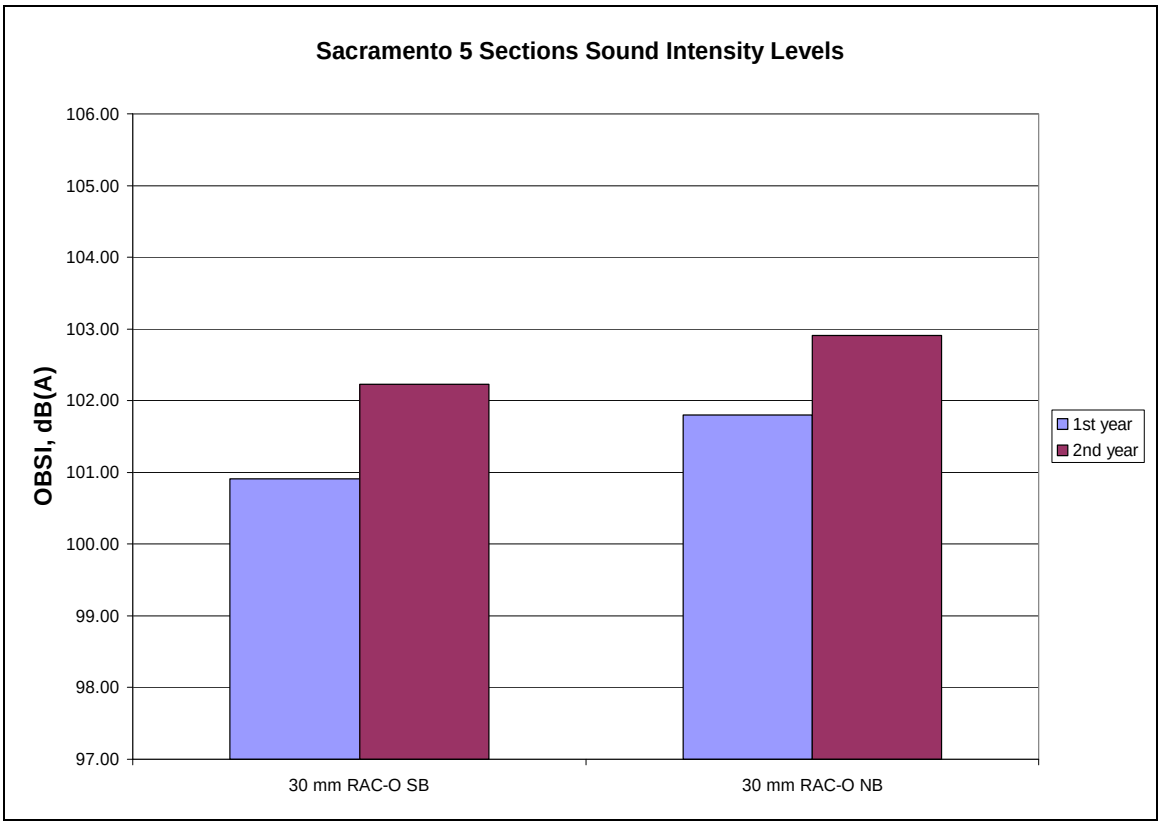

Figure 147: First-year and second-year sound intensity levels for Sacramento 5 sections.

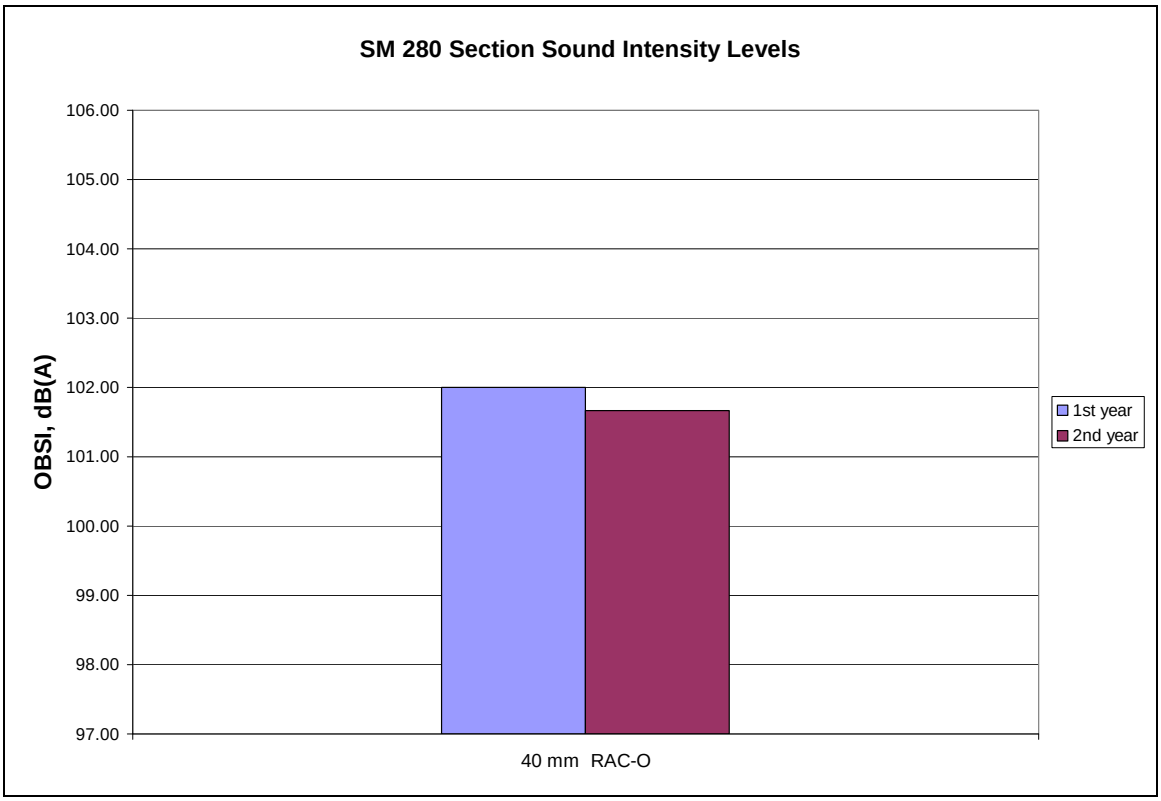

Figure 148: First-year and second-year sound intensity levels for San Mateo 280 section.

In addition to permeability, friction, and noise measurements, condition surveys were conducted at each test section. The distresses were recorded for two years and are shown in Appendix D.

According to the condition surveys, both directions of Sacramento 5 site showed cracking and raveling in the first year, while in the second year they showed only cracking; however, this difference can probably be accounted for by the difference in surveyors from year to year, and their perception of raveling. All cracks were reflective cracks from the underlying PCC, and the amount of cracking increased from the first year to the second year. For the San Mateo 280 site, no distresses were recorded for the first year, and in the second year the section showed minor raveling, with an approximate area of 0.1 m^2.

In summary, the northbound direction of the Sacramento 5 site has higher permeability and higher friction (higher MPD and similar BPN); however, it has slightly higher noise levels and more distresses compared to the southbound direction. The higher permeability, friction, and amount of distresses in the northbound direction is due to the higher air-void content, and the higher noise levels are probably due to the higher macrotexture.

The IRI values of the Sacramento 5 and San Mateo 280 sites are higher than those of the RAC-O mixes that are overlays of AC. Other than the IRI values, the performance of the RAC-O mixes used on

the Sacramento 5 and San Mateo 280 sections is not different from that of the RAC-O mixes of the experimental design sections that are primarily placed on asphalt pavements.

10.3 LA 138 Sections

The LA 138 site includes three mix types—OGAC, RAC-O, BWC, and DGAC—which were placed in both the eastbound and westbound lanes. Measurements were taken on the nine test sections: eastbound (EB) and westbound (WB) directions for the OGAC, RAC-O, and BWC sections and the westbound direction for the DGAC mix. The layout of the test sections is given in Figure 149. All the mixes have an NMAS of 12.5 mm. The test sections were three years old during the first-year measurements.

The noise levels were also measured for Caltrans by the Volpe National Transportation Systems Center using the pass-by method. This measurement allowed evaluation of the effect of absorption on the noise levels next to highways and of the relationship between OBSI and pass-by measurements.

OGAC was placed in 75- and 30-mm thicknesses in different sections to determine the effect of thickness on noise reduction and distress development. The DGAC section was placed as a control section, and BWC was placed to compare its performance with that of open-graded mixes since it is being considered as an alternative to open-graded mixes to reduce hydroplaning and spray and splash. The following analysis shows the air-void content, permeability, friction, roughness, noise, and surface condition for the different mixes over two years and compares the performance variables for different thicknesses and different mixes. The analysis helps answer these questions:

- How does absorption affect the noise levels next to highways?
- How do the OBSI measurements compare to the pass-by measurements?
- Does thickness affect noise reduction and distress development?
- How does the performance of open-graded and BWC mixes compare to the performance of the DGAC mix on the control section?
- How does the performance of the BWC mix compare to that of the open-graded mixes?
- Do OGAC and RAC-O perform similarly under the same traffic and climatic conditions?

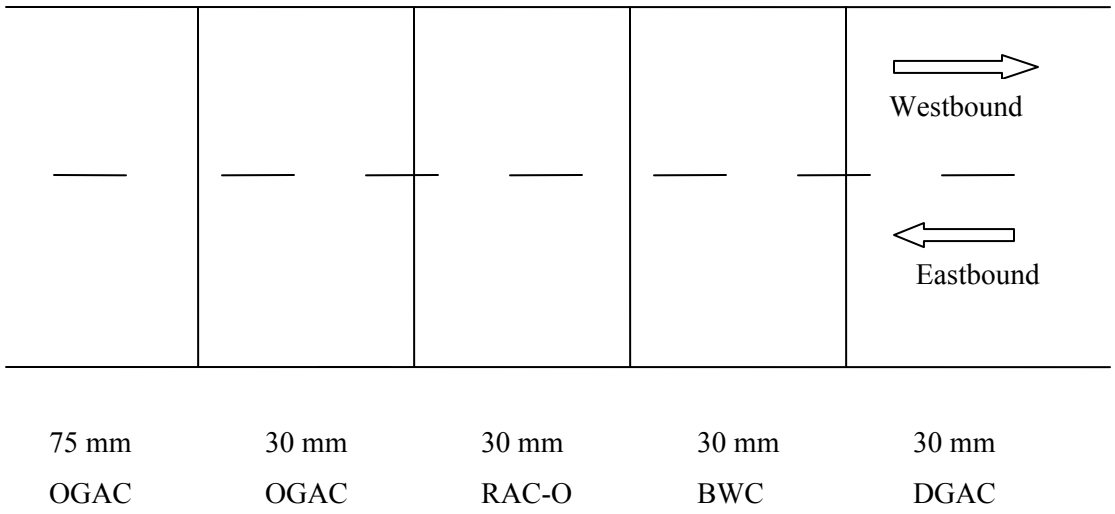

Figure 149: Layout of the test sections.

Figure 150 and Figure 151 show the first-year and second-year center and wheelpath air-void content and permeability values, respectively, for the LA 138 sections. As expected, open-graded mixes have the highest air-void content. Based on the findings from the QP sections, the average air-void content of the open-graded mixes is around 15 percent. However, most of the LA 138 open-graded mixes have much lower air-void content than is typical. The permeability of the OGAC and RAC-O mixes is also lower than the average permeability of OGAC and RAC-O mixes in the same age category. The figures show that the eastbound sections have higher air-void content and permeability values than the westbound sections. This may be due to compaction differences during construction as well as the difference in truck traffic volumes in the two directions.

The 75-mm OGAC has the highest permeability, although it does not have the highest air-void content. CT scan results showed that the top part of the surface layer of the 75-mm OGAC eastbound section was not clogged. The higher permeability of this section confirms the CT scan findings. The DGAC mixes have permeabilities: close to zero.

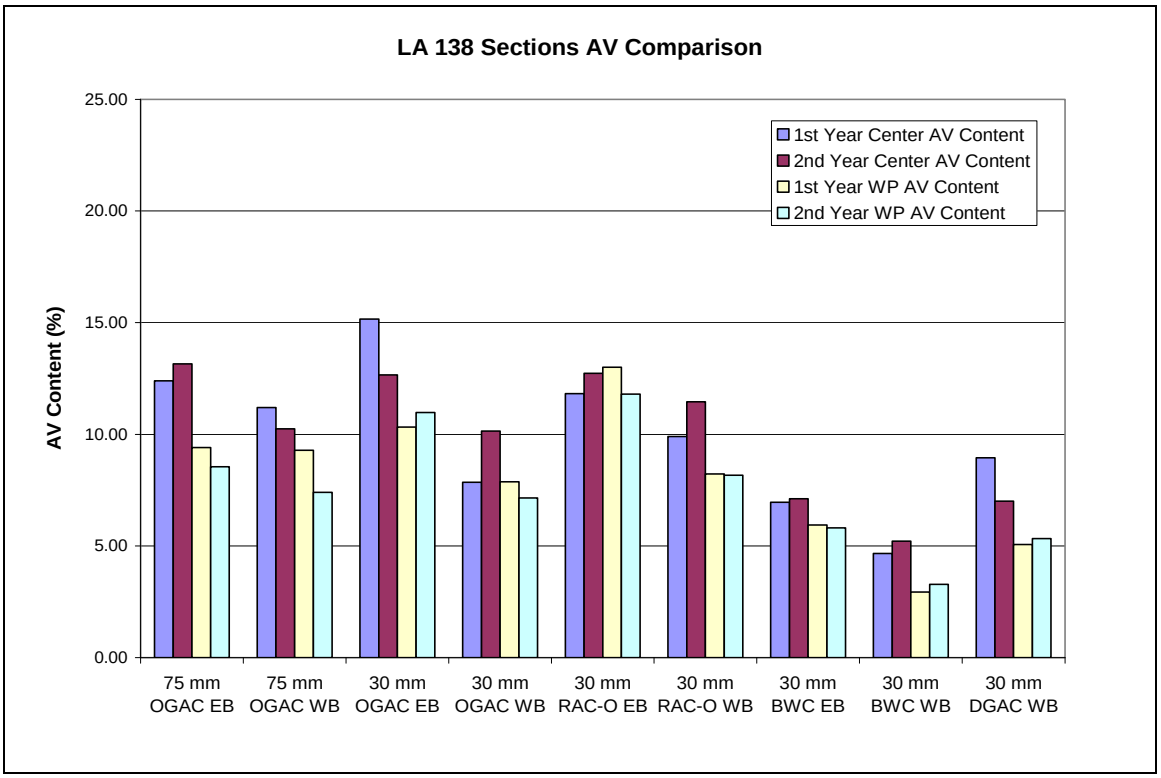

Figure 150: Comparison of first-year and second-year air-void content for LA 138 sections.

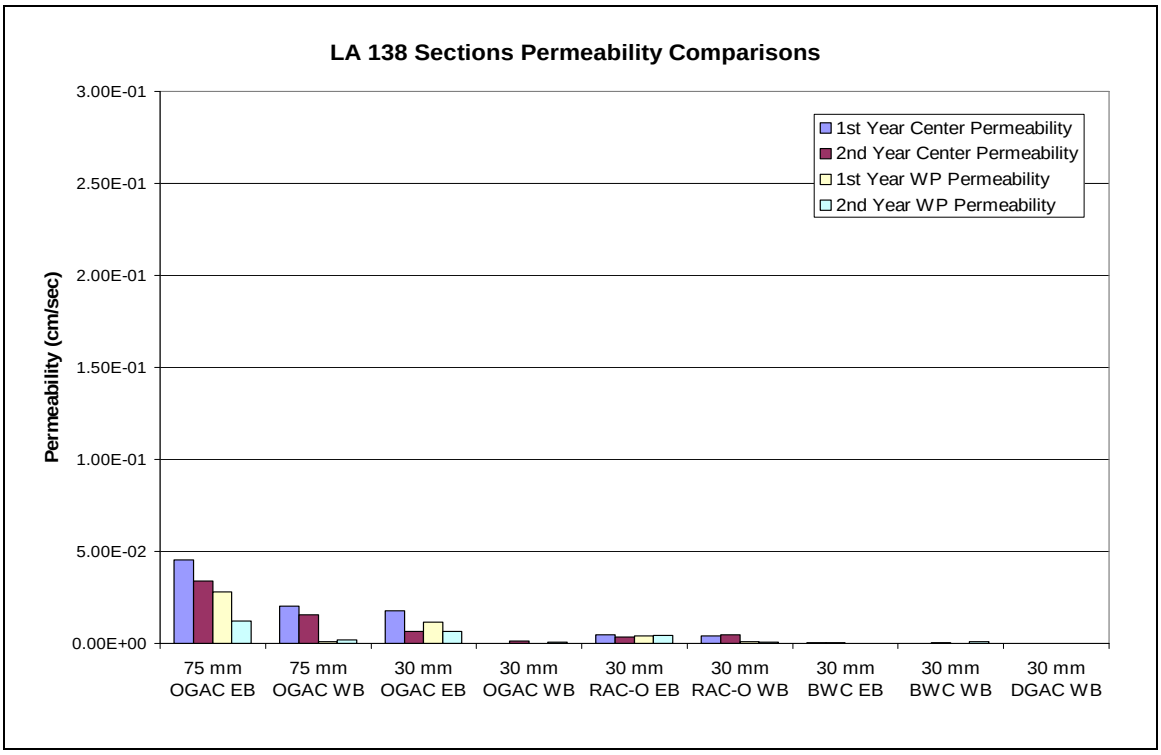

Figure 151: Comparison of first-year and second-year permeability values for LA 138 sections.

The first-year and second-year center and wheelpath BPNs were also evaluated; however, they are not shown in this report. The BPNs in both the first and second years are above 50, indicating that the LA 138 sections still provide satisfactory friction according to a criterion discussed in a Caltrans (15) research document believed to have been written in the 1960s.

Figure 152 shows the first-year and second-year left and right wheelpath IRI values for the LA 138 sections. According to the figure, RAC-O mixes have the lowest IRI values. The LA 138 RAC-O mixes have lower IRI values compared to those of the QP sections. In the first year of measurements, all sections provide "good" ride according to the FHWA criteria.

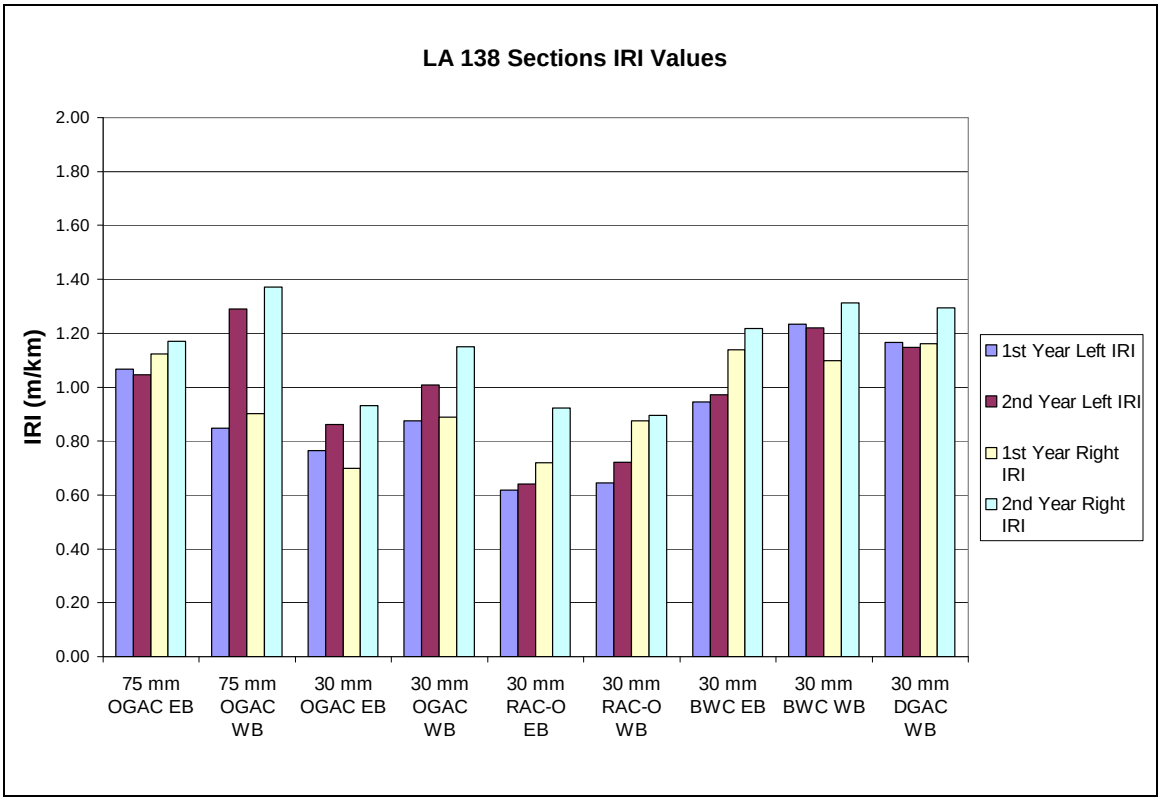

Figure 152: First-year and second-year IRI values for LA 138 sections.

Figure 153 shows the first-year and second-year MPD values for the LA 138 sections. The figure shows that open-graded mixes have higher MPD values than the BWC and dense-graded mixes. RAC-O mixes have the smallest MPD values among open-graded mixes. The findings from the QP sections showed that the MPD of open-graded mixes is usually above 1,000 microns. However, LA 138 open-graded sections usually have MPD values less than 1,000 microns, which may be due to their lower air-void content. BWC mixes have MPD values similar to those of RAC-O and DGAC mixes. There is some increase in MPD values in the second year, which may be due to an increase in distresses, roughening the

surface. However, no condition survey was conducted on these sections in the first year; therefore, no comparisons could be made.

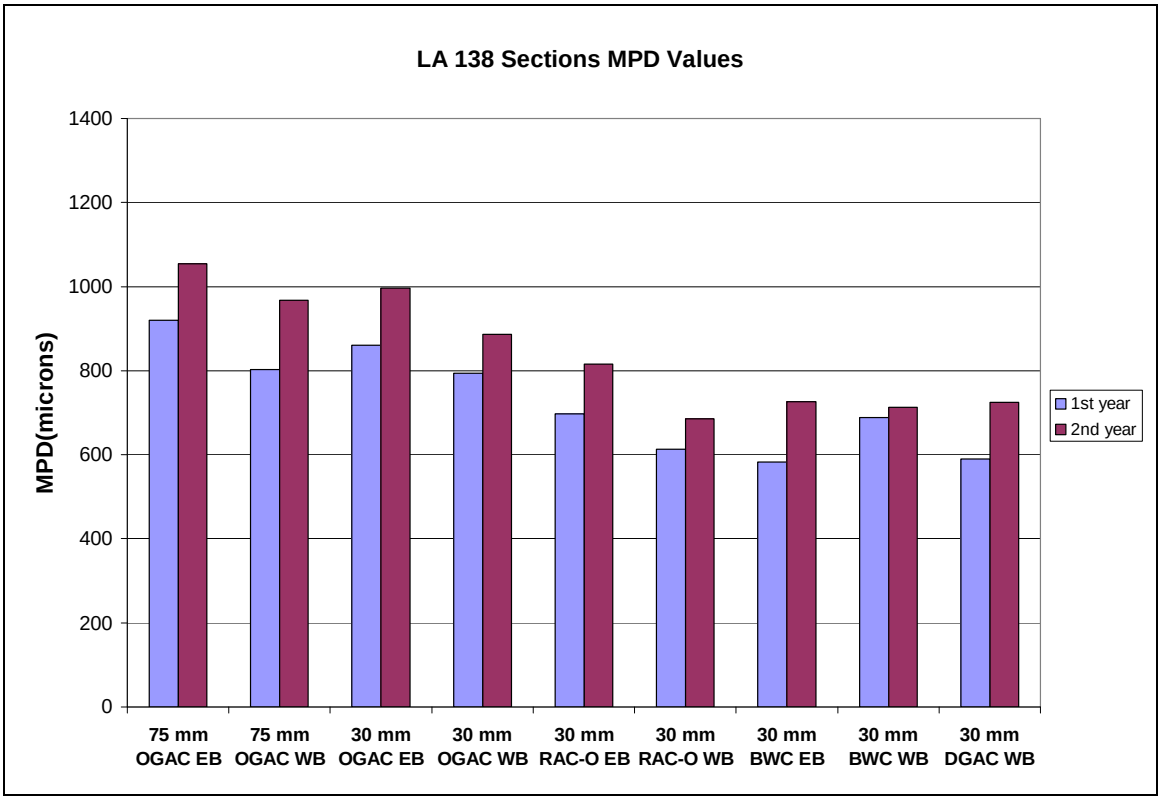

Figure 153: First-year and second-year MPD values for LA 138 sections.

Figure 154 shows the first-and second-year sound intensity levels for the LA 138 sections. The figure shows that the westbound open-graded mixes have higher noise levels than the eastbound mixes. As these mixes have air-void content of less than 15 percent, the lower noise levels of the eastbound sections can be explained by the higher air-void content of these mixes compared to those of the westbound sections.

DGAC mixes have the highest noise levels. The open-graded mixes can provide up to 4 dB (A) more noise reduction than the DGAC mix. The 75-mm OGAC does not provide any additional noise reduction. Based on the analysis of the QP sections, the average sound intensity level of open-graded mixes is around 102 dB (A). The eastbound OGAC sections in the first-year measurements have lower noise levels than the average. This distinction may be due to the lower MPD values of the LA 138 open-graded mixes. LA 138 open-graded mixes also have finer gradations than those of the QP sections, as shown circled in Figure 88 earlier in this report. The lower noise levels of these sections may be due to their finer gradations since there is some indication that open-graded mixes with finer gradations may generate less noise than those with coarser gradations, as shown in Figure 88.

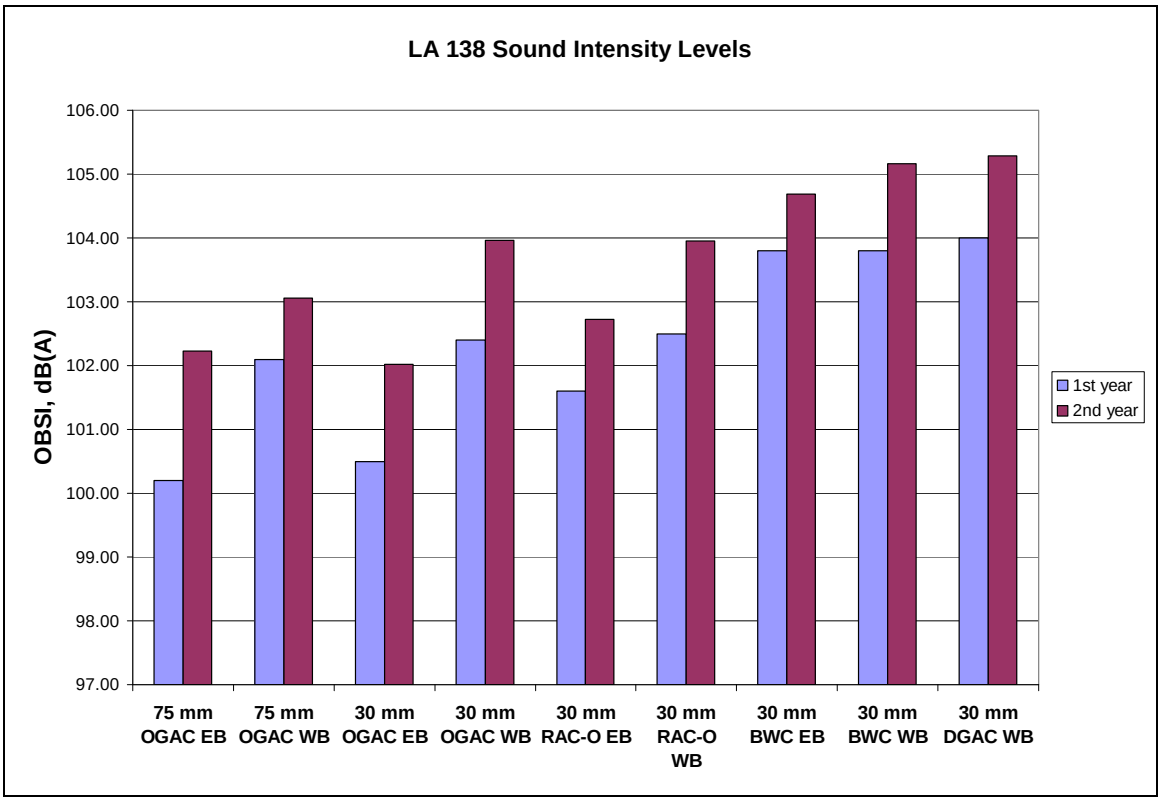

Figure 154: Comparison of sound intensity levels for LA 138 sections.

Figure 155 shows the noise reduction provided by OGAC, RAC-O, and BWC mixes compared to the DGAC section up to 52 months after construction using the pass-by method. There are no pass-by measurements for BWC mixes after 16 months. The first-year data collection by UCPRC corresponds to the age of 40 months.

Figure 155 shows that 30-mm OGAC has the highest noise levels and that the 75-mm OGAC has the lowest noise levels. The 75-mm OGAC can reduce noise levels by up to 4 dB (A) more than the DGAC section. Note that the reference DGAC mix used in the pass-by measurements is located at the east end of the test sections, and the reference DGAC used in the OBSI measurement is located at the west end of the test sections. Although the two reference DGAC mixes are different for the two measurement methods, the noise levels of the mixes should not be much different. Despite the possible difference between the noise levels of the DGAC mixes, a relative comparison of the noise reduction of open-graded mixes can still be made.

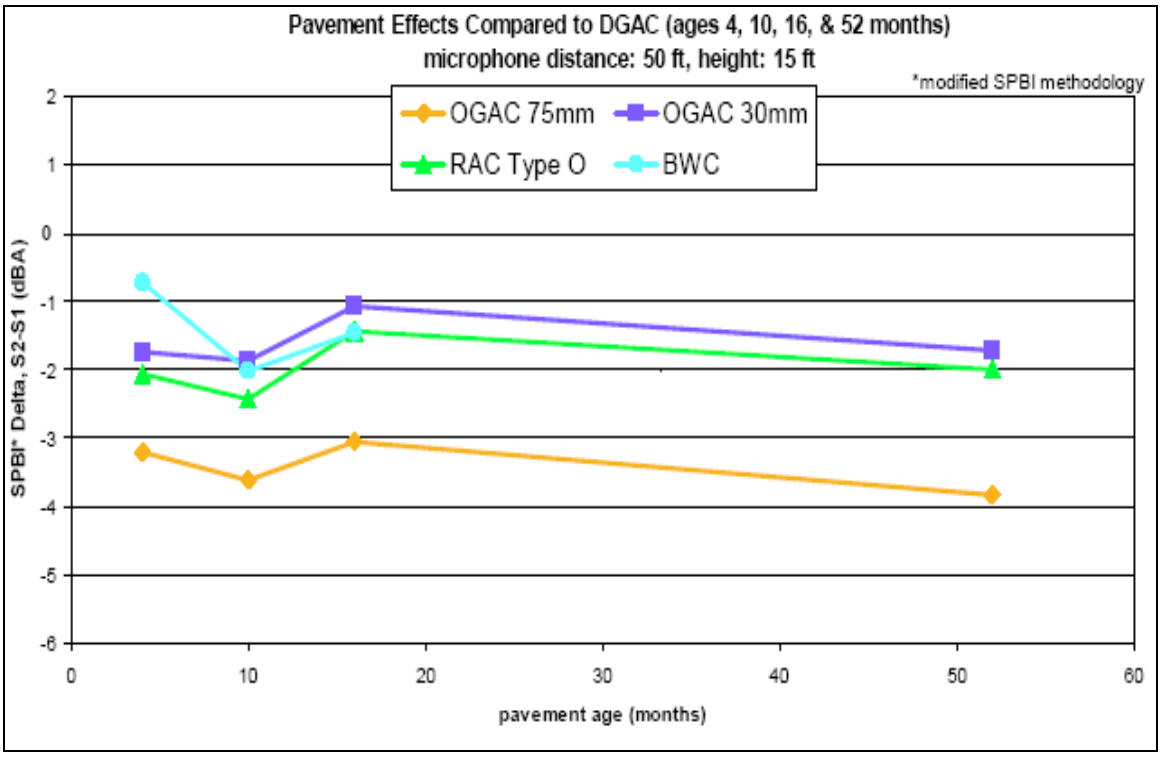

Figure 155: Noise reduction from pass-by measurements by Volpe National Transportation Systems Center for LA 138 mixes.

Table 40 shows the absorption values of center and wheelpath cores of OGAC, RAC-O, and BWC mixes as well as the noise reduction of these mixes compared to the DGAC mix using OBSI and pass-by measurements. The noise reduction using the OBSI method is the average of the eastbound and westbound measurements. The 75-mm OGAC provides the greatest noise reduction and hence is the quietest mix based on both the OBSI and pass-by measurements. The noise reduction is greater using the pass-by measurements than the OBSI measurements.

The 75-mm OGAC and 30-mm OGAC have almost the same noise levels when measured using the OBSI method; the 75-mm OGAC provides greater noise reduction than the 30-mm OGAC when measured using the pass-by method. The additional noise reduction for the 75-mm OGAC found using the pass-by method may be due to its higher center lane absorption values. The 75-mm OGAC center lane core has a resonance frequency at 750 Hz, which is close to the frequencies where the tire/pavement noise is dominant; therefore, it may provide additional noise reduction since noise levels at peak frequencies are reduced.

The 30-mm RAC-O mix is quieter than the 30-mm OGAC mix when the pass-by noise levels are compared; however, the 30-mm OGAC mix is quieter than the 30-mm RAC-O mix when the OBSI levels are compared. The difference in noise levels between the two measurement methods is approximately 1 dB (A). This difference cannot be explained by absorption values, since the absorption values for these

two sections are not significantly different from each other. The measurements were taken on a 150-m segment of the road with the OBSI method and on the whole section with the pass-by method; therefore, the difference between the pass-by and OBSI results may be due to the differences in the noise levels of different segments of the road since the noise levels may vary within the same section.

Table 40: Absorption Values and Noise Reduction of LA 138 Open-Graded and BWC Sections

Mix Type	Wheelpath Average Absorption	Wheelpath Maximum Absorption	Wheelpath Resonance Frequency	Center Average Absorption	Center Maximum Absorption	Center Resonance Frequency	OBSI Average Noise Reduction for Both Directions	Pass-by Noise Reduction(40 months)
75-mm OGAC	0.094	0.13	1700	0.185	0.25/0.29	300/750	2.85	3.5
30-mm OGAC	0.0687	0.12	300	0.096	0.18	320	2.55	1.5
30-mm RAC-O	0.06	0.1	450	0.133	0.17	500	1.95	1.8
30-mm BWC	0.055	0.18	450	0.045	0.06	1570	0.20	N/A

In addition to permeability, friction, and noise measurements, condition surveys were conducted at the test sections. The first-year condition survey was conducted on the DGAC section and the eastbound sections for open-graded and BWC mixes. In the second year, a condition survey was conducted on both the eastbound and westbound sections. The distresses for each section are given in Appendix D.

The eastbound open-graded mixes show only transverse cracking, while the westbound RAC-O, BWC, and DGAC sections also show fatigue cracking. In the second-year condition survey, no raveling was recorded; however, this finding can probably be accounted for by the difference in surveyors from year to year, with their different perceptions of raveling, as raveling is a distress that can be difficult to assess visually unless it is severe. The number and length of the cracks increased for all sections, except for the 30-mm RAC-O EB section. It can thus be concluded that the RAC-O mix has had the slowest distress progression.

In summary, increased thickness was not found to increase durability or provide any additional noise reduction when noise is measured at the source (OBSI method). However, 75-mm OGAC has significantly lower noise levels when the noise is measured using the pass-by method. These lower noise levels may be due to the higher absorption values of the 75-mm OGAC. The surface layer of the 75-mm OGAC eastbound section has higher permeability, which indicates that it is less clogged on the surface compared to the other sections. Therefore, the higher noise absorption values may be due to the presence of surface air voids as well as increased thickness.

The pass-by and OBSI methods yielded similar results for the 75-mm OGAC section. However, there is almost a 1 dB (A) difference in the noise levels predicted by the two methods for the 30-mm OGAC and RAC-O sections, although there is no significant difference in the absorption values of the two sections. Therefore, the pass-by and OBSI measurements did not match well for thinner mixes.

Open-graded mixes have the highest permeabilities and macrotexture and the lowest noise levels among all mix types. BWC mixes perform more similarly to DGAC mixes than to open-graded mixes; they have lower permeabilities and macrotexture and higher noise levels than open-graded mixes. Therefore, BWC cannot be considered as an alternative to open-graded mixes in reducing hydroplaning. Except for some raveling that appeared on the open-graded mixes, all mixes performed similarly in terms of distresses. RAC-O mixes have lower IRI values, confirming the findings from the QP sections that the IRI progression is slower in rubberized mixes. Also, rubberized mixes may have slower distress propagation, as the severity and amount of distresses stayed relatively constant for the eastbound RAC-O mix compared to the other mix types.

10.4 LA 19 Section

The LA 19 section has a European gap-graded (EU-GG) mix as a surface layer. It was less than a year old when the first-year measurements were conducted. This section was placed to compare its performance with the gap-graded mixes used in California. The following analysis evaluates the air-void content, permeability, friction, roughness, noise, and surface condition for the EU-GG mix. The analysis answers these questions:

- How does the performance of the EU-GG mix compare to that of the gap-graded mixes (RAC-G) used in California in terms of permeability, texture, noise, and distresses?
- Do the results yield any recommendations for changes to RAC-G mixes to improve their performance?

Figure 156 compares the gradation of the EU-GG mix with the RAC-G specification in California. The figure shows that the EU-GG mix has a gradation within the range of California RAC-G mixes.

Figure 157 and Figure 158 show the first-year and second-year center and wheelpath air-void content and permeability values for the LA 19 section. The air-void content of California rubberized gap-graded mixes ranges between 8 and 12.5 percent. The figures show that the air-void content of the EU-GG mix is around 12 percent, which is in the range for California gap-graded mixes (RAC-G) in their first year. The average permeability of California gap-graded mixes that are less than a year old is 0.05 cm/sec. The EU-GG mix has permeability values of around 0.05 cm/sec when it is one year and two years old. This value is within the range for RAC-G mixes in their first year; however, it is much higher than for RAC-G mixes that are older than one year. This finding may indicate that EU-GG does not compact under traffic like RAC-G mixes and hence does not lose its permeability within a few years after construction.

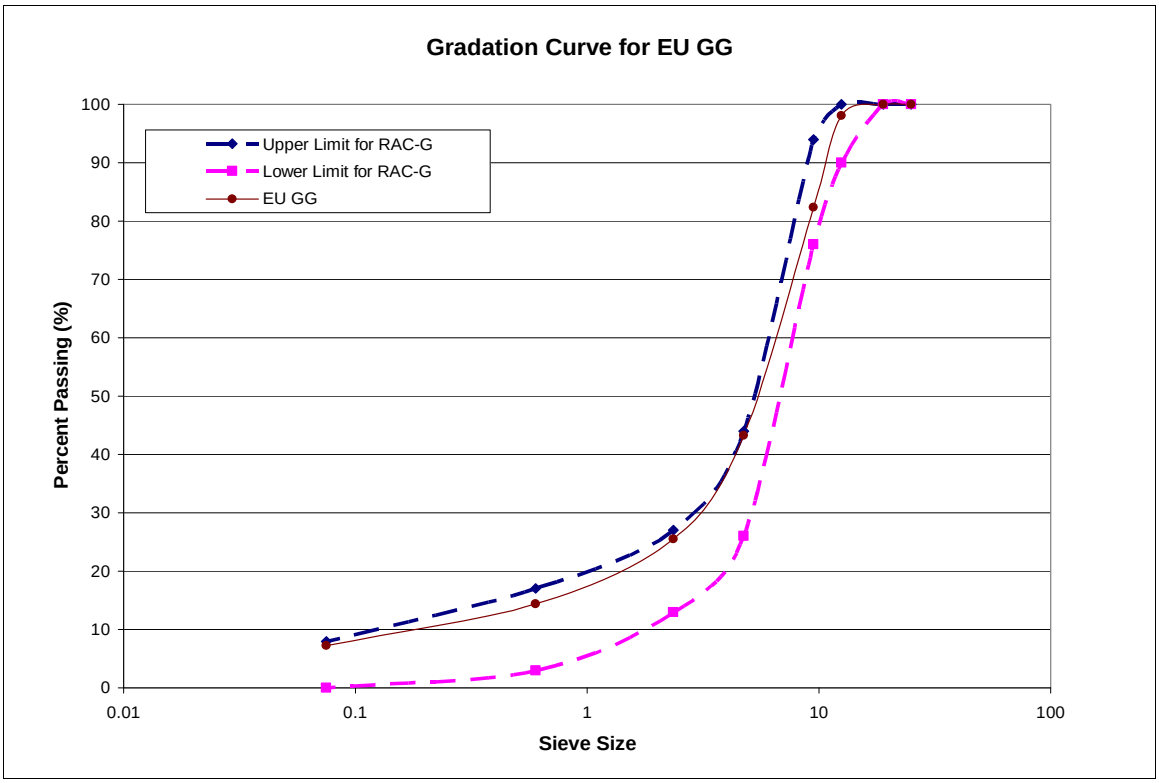

Figure 156: Comparison of gradation of LA 19 section with RAC-G gradation.

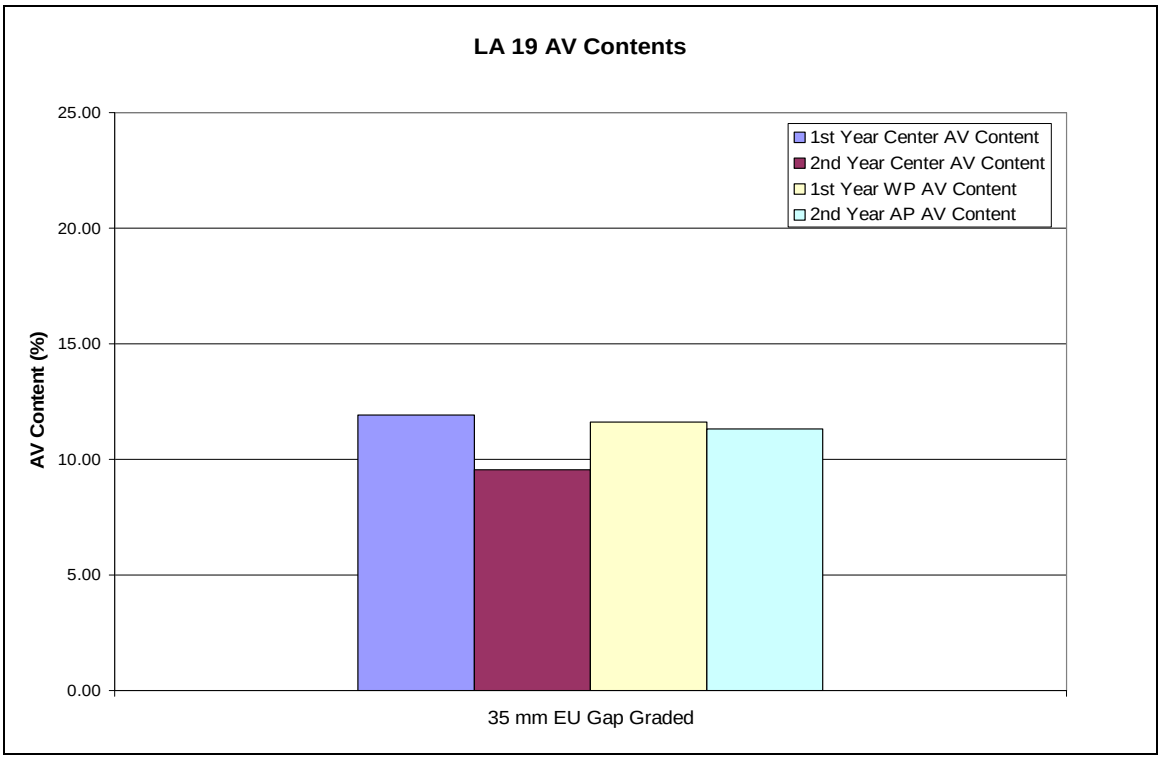

Figure 157: First-year and second-year air-void content for LA 19 section.

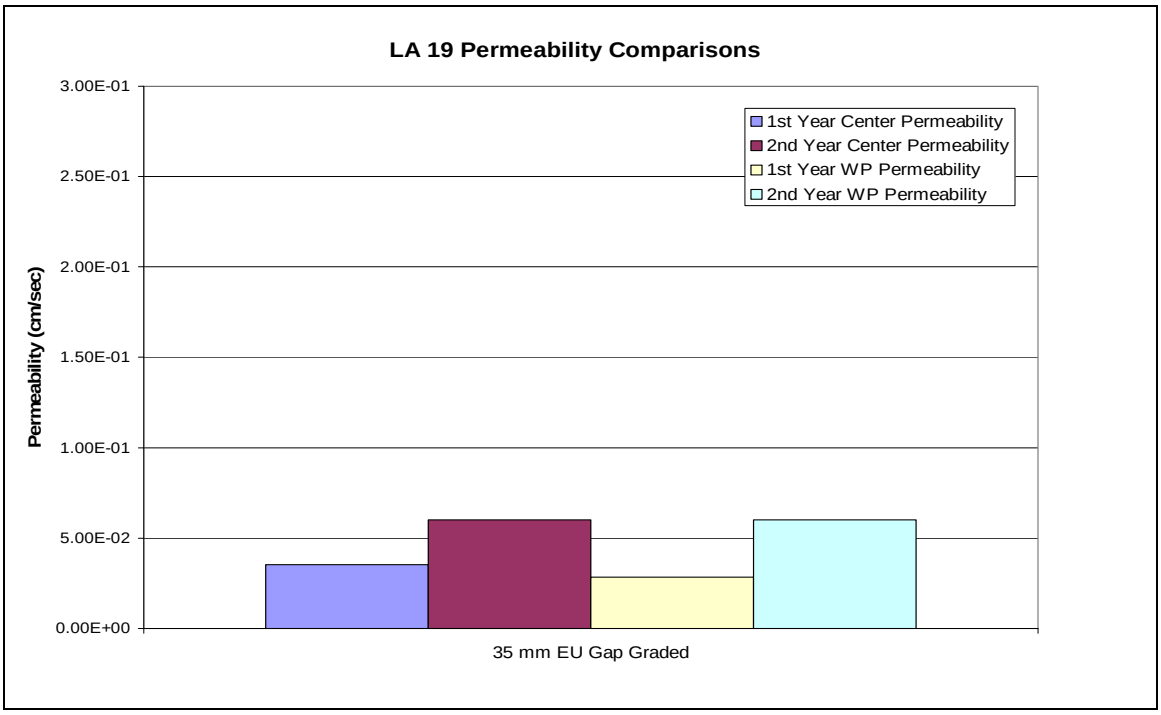

Figure 158: Comparison of first-year and second-year permeability values for LA 19 section.

The first-year and second-year center and wheelpath BPN and the IRI values for the LA 19 section were also evaluated; however, they are not shown in this report. The BPNs in both the first and second years are above 50, indicating that the LA 19 section provides satisfactory friction according to a criterion discussed in a Caltrans (15) research document believed to have been written in the 1960s. Since all the IRI values in both the first and second years are less than 1.5 m/km, this section has "good" ride quality according to FHWA criteria.

Figure 159 shows the first-year and second-year MPD values for the LA 19 section. The figure shows that the MPD value is 800 microns in the first year and 1,000 microns in the second year. The MPD values for RAC-G mixes range between 600 and 1,000 microns; thus, the EU-GG mix has MPD values within the range of those for RAC-G mixes.

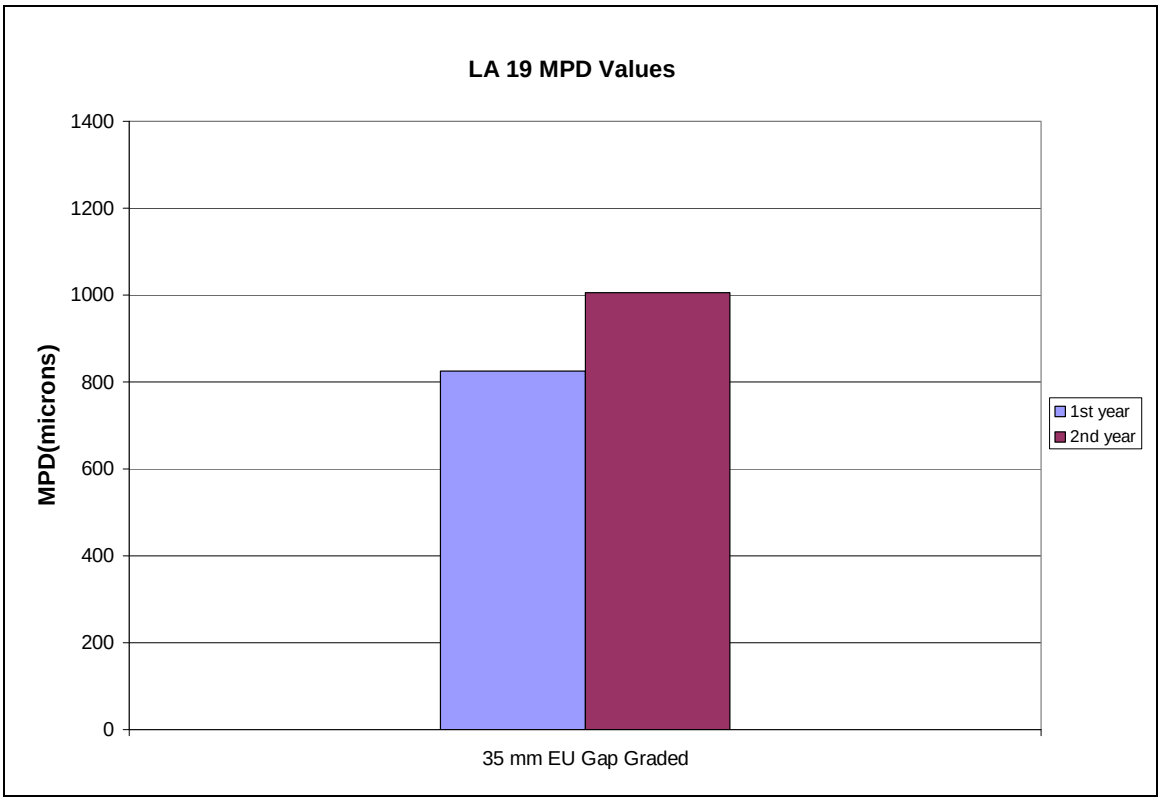

Figure 159: First-year and second-year MPD values for LA 19 section.

Figure 160 shows the first-and second-year sound intensity levels for LA 19. The noise levels ranges from around 101 to 102 dB (A). The average sound intensity level of RAC-G mixes is 101.5 dB (A); thus, the EU-GG mix has noise levels close to those of RAC-G mixes.

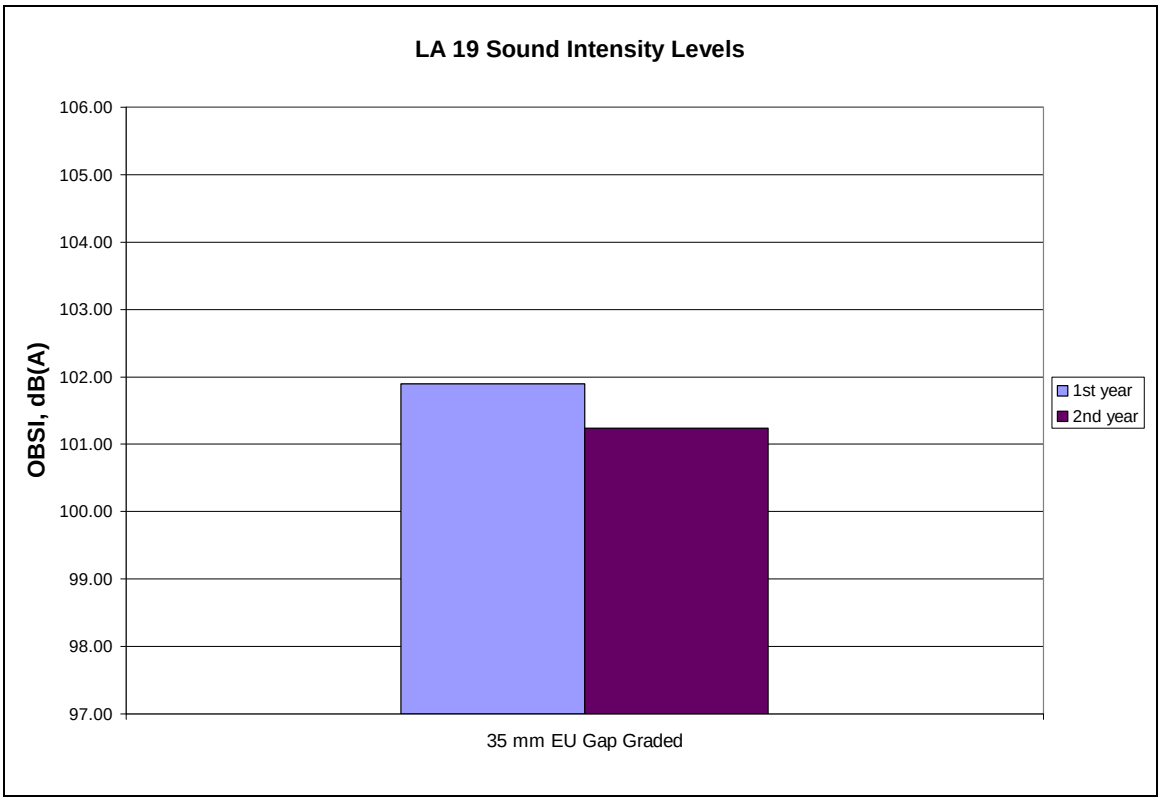

Figure 160: First-year and second-year sound intensity levels for LA 19 section.

In addition to measurement of permeability, friction, roughness, and noise, a condition survey was conducted on the LA 19 section. It showed no distresses in the first year and showed bleeding, with an approximate bleed area of 150 m^2, in the second year.

The sound intensity of the LA 19 section appears to have decreased, despite the small measured increase in MPD. This finding may be due to the measured increase in permeability.

It can be concluded that, compared to the RAC-G mixes used in California, the EU-GG mix performs similarly in terms of friction, durability, and noise levels; however, based on two years of performance data, it can also be concluded that it may compact less under traffic than RAC-G mixes.

10.5 Yolo 80 Section

The Yolo 80 section has OGAC as a surface layer. It was seven years old in the first year of measurements and is one of the oldest open-graded mixes in California. It was placed to evaluate the noise-reducing properties of open-graded mixes. Noise measurements have been taken annually by Caltrans to evaluate the change in acoustical properties over time. The following analysis evaluates the air-void content, permeability, friction, roughness, noise, and surface condition for the Yolo 80 section. The analysis answers these questions:

- How does age affect the performance of open-graded mixes?
- Why does the Yolo 80 section have the highest noise levels among all the open-graded mixes?

Figure 161 and Figure 162 show the first-year and second-year center and wheelpath air-void content and permeability values for the Yolo 80 section. The figures show that this section has high air-void content, above 15 percent, which is the average air-void content of open-graded mixes. The average permeability of OGAC mixes that are older than four years is 0.05 cm/sec based on the analysis of the experimental design (QP) sections; however, the Yolo 80 section has lower permeability than the average, probably due to clogging at the surface.

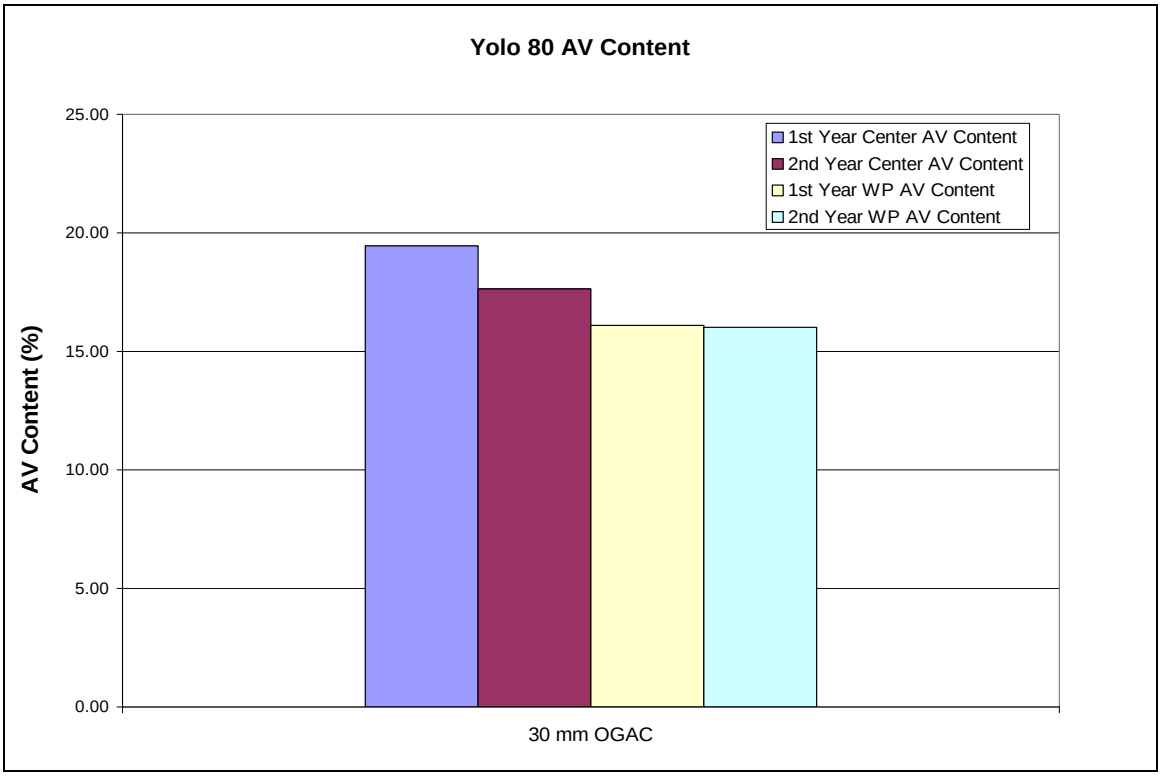

Figure 161: First-year and second-year air-void content for Yolo 80 section.

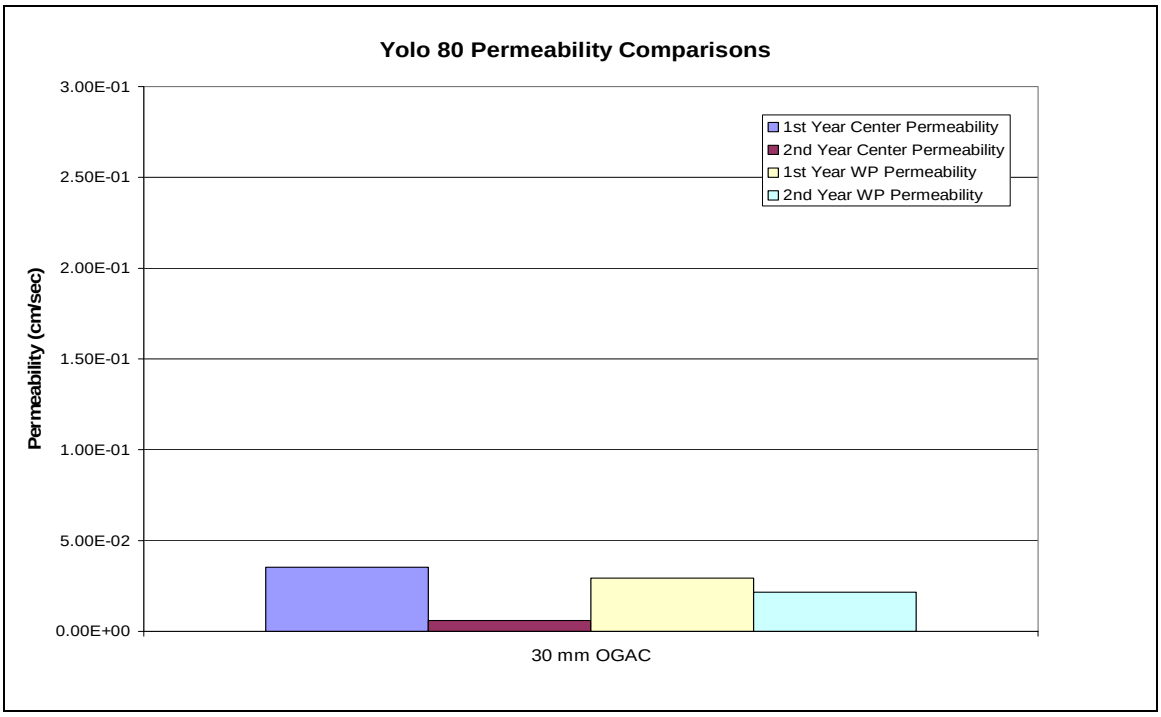

Figure 162: First- year and second-year permeability values for Yolo 80 section.

The first-year and second-year center and wheelpath BPN and the IRI values for the Yolo 80 section were also evaluated. The BPNs in both the first and second years are above 50, indicating that the Yolo 80 section still provides satisfactory friction according to a criterion discussed in a Caltrans (15) research document believed to have been written in the 1960s. Since all the IRI values in both the first and second year are less than 1.20 m/km, this section has "good" ride quality according to FHWA criteria.

Figure 163 shows the first-year and second-year MPD values for the Yolo 80 section. The figure shows that the MPD value is 1,000 microns in the first year and 1,350 microns in the second year. The average MPD of open-graded mixes is around 1,100 based on the findings from the experimental design (QP) sections; therefore, the Yolo 80 section has higher MPD values in the second year than the average. The increase in the MPD values is probably due to the appearance of raveling on the pavement surface.

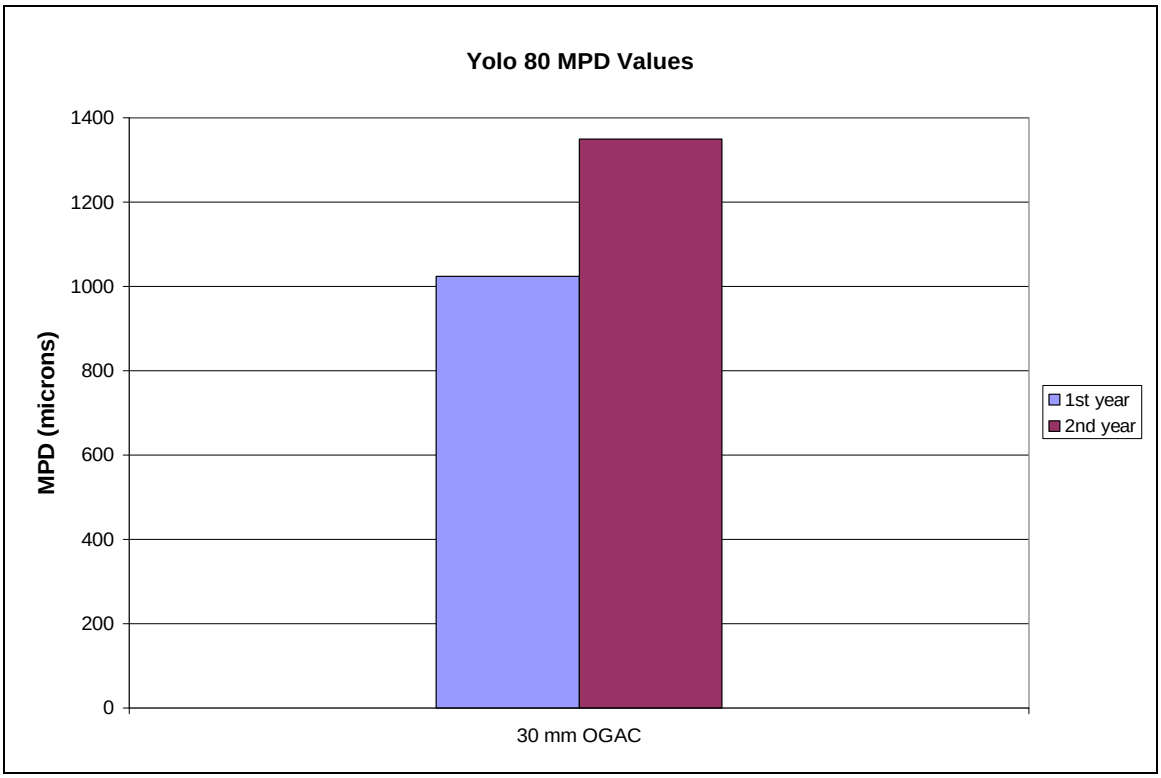

Figure 163: First-year and second-year MPD values for Yolo 80 section.

Figure 164 shows the first-and second-year sound intensity levels for Yolo 80. The Yolo 80 section has the highest noise levels among all the open-graded mixes tested. Compared to other open-graded mixes, the Yolo 80 section still has high air-void content and permeability values. Therefore, the higher noise levels are not due to clogging. Based on the multiple regression equation [Equation (18)] for OBSI levels given in Section 9.1.2, the OBSI of Yolo 80 is predicted to be 102.6 dB (A); thus, the higher noise levels of this section cannot be explained by the proposed model.

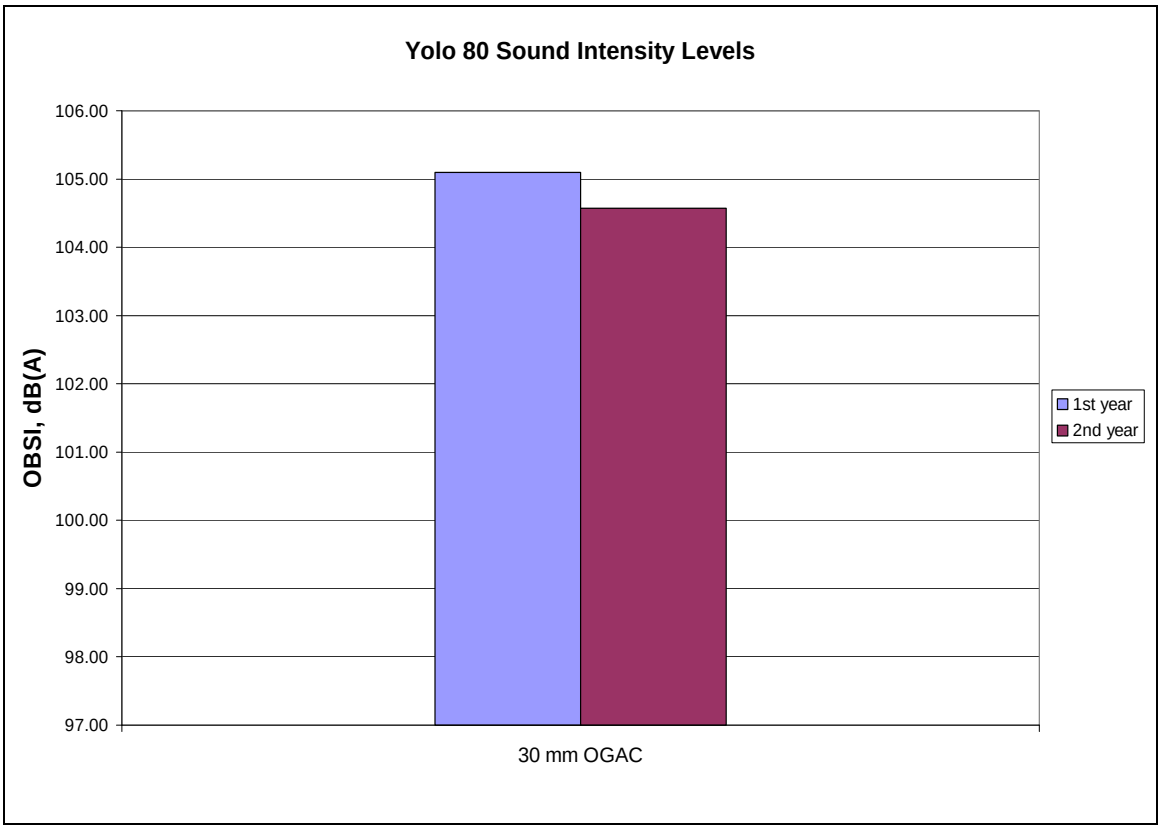

Figure 164: First-year and second-year sound intensity levels for Yolo 80 section.

In addition to measurement of permeability, friction, roughness, and noise, a condition survey was conducted on the Yolo 80 section. It showed raveling, with an approximate ravel area of 60 m^2, in the first year; and it showed raveling, with an approximate ravel area of 300 m^2, and bleeding, with a bleed area of 300 m^2, in the second year.

It can be concluded that Yolo 80 still provides sufficient friction and acceptable ride quality and has higher permeability than the gap- and dense-graded mixes. However, it has very high noise levels.

10.6 Summary of Environmental Noise Monitoring Site Sections Analysis

Data was collected on the test sections for two years. The following list summarizes the findings from the environmental noise monitoring site (ES) test sections.

- The results of the analysis of environmental test sections confirmed the findings from the experimental design (QP) sections.
- Higher absorption values may help reduce the noise levels next to highways since, compared to the 30-mm OGAC, the 75-mm OGAC provides additional noise reduction when the noise levels are measured using the pass-by method.

- Increasing thickness does not provide any additional benefits when the noise is measured at the source (OBSI) since 75-mm OGAC and 30-mm OGAC on the eastbound lanes have the same noise levels. However, increasing thickness may reduce the noise levels when the noise is measured next to the highway (pass-by method). The 75-mm OGAC section may have lower noise levels not due to its thickness but because it is less clogged on the surface.
- The 75-mm OGAC mix has the lowest noise levels in both pass-by and OBSI measurements. However, there is approximately 1 dB (A) difference in the noise levels of 30-mm OGAC and RAC-O mixes when measured by the two methods. The noise levels vary within different segments of the same section; therefore, the difference between the measurements using the two methods may be because the OBSI measurements were conducted on only a 150-m segment of the section, while the pass-by method measured the noise levels of the whole section.
- The new rubberized mixes of the Fresno 33 section do not enhance safety or reduce noise levels compared to the alternative mixes currently in use, RAC-G and DGAC, according to the measurements taken as part of this study. The Fresno 33 mixes are also more prone to bleeding. The BWC on Fresno 33 cannot be considered as an alternative to open-graded mixes as it has lower permeability and friction (macrotexture) and higher noise levels.
- The European gap-graded mix on LA 19 performs similarly to RAC-G mixes in California in terms of friction, noise, and distresses. However, two years of data showed that the European gap-graded mix may not compact under traffic as much as RAC-G mixes do.
- Increasing thickness may help improve cracking resistance for RUMAC-GG and Type D-MB mixes. When they are placed in thicker lifts (90 mm), RUMAC-GG and Type D-MB have better crack resistance than the other mixes. The thicker open-graded mixes have higher permeabilities than the thinner ones, confirming the CT scan results that thicker mixes are less prone to clogging.
- The AC overlays of PCC have higher IRI values compared to the AC overlays of AC.
- The OGAC mixes perform similarly to RAC-O mixes except for the IRI progression; the rubberized mixes have lower IRI values compared to the nonrubberized mixes. There is also some indication that the rubberized mixes may have slower progression of distresses compared to nonrubberized mixes under the same traffic and climatic conditions.
- After eight years of service, the Yolo 80 section still provides acceptable friction (according to a criterion from an old Caltrans research report, not an official standard) and good ride quality and has high permeabilities compared to dense- and gap-mixes. However, although it has permeability and MPD values close to those of the other open-graded mixes, it has very high noise levels.

- Two years' data was not enough to see any changes in the performance of the asphalt mixes. The second-year data was used mostly as a control for the first-year data.
- Raveling was recorded in the first year but not in the second year in the condition surveys for the Sacramento 5 and LA 138 sections, probably due to different surveyors in the two years; raveling is a difficult distress to evaluate visually, and assessment is subjective. Except in a few condition surveys, the data collected both years has been consistent, with similar values from year to year.

11 EVALUATION OF PERFORMANCE MODELS AND PREDICTION OF LIFETIME FOR DIFFERENT ASPHALT MIX TYPES

One of the objectives of this study is to estimate how long the open-graded mixes last in terms of the performance variables of permeability, friction, roughness, durability, and noise level. Open-graded mixes have higher permeability, higher texture, and lower noise levels than dense- and gap-graded mixes; however, estimation of how long they retain these properties is needed to compare the life-cycle costs of open-graded mixes with the costs of other mix types. Open-graded mixes lose their benefits when they become impermeable and then have noise levels as high as those of dense-graded mixes. These mixes fail when distresses, friction, and roughness reach unacceptable levels, as explained in Section 1.4.

Chapters 5 to 9 compare the performance of different mixes using descriptive statistics and regression analyses. This chapter evaluates the effectiveness of proposed regression models to predict the performance variables and also estimates the time to failure for different mixes under different climate and traffic conditions using the respective models.

This chapter answers these questions:

- Can the proposed models be used to predict the performance variables? Can they be used to predict the lifetime of different mix types?
- How long do the open-graded mixes last in terms of permeability and noise-reducing properties?
- How long do the open-graded mixes last in terms of noise reduction?
- How long do the asphaltic mixes last in terms of friction and roughness?
- What is the variable that limits the lifetime of asphaltic mixes?

11.1 Evaluation of Permeability and Clogging Models

Open-graded and gap-graded mixes have higher air-void content and hence greater permeability than dense-graded mixes when first built. However, they lose their permeability over time due to clogging. Permeability is important for safety as well as noise reduction. When the top part of the asphalt layer is clogged, the air-void content remains relatively constant; however, permeability and sound absorption decrease. Therefore, loss of permeability not only reduces safety but also decreases noise reduction. Since the RAC-G mixes are not placed to improve drainage, retaining permeability is important only for its noise reduction effect for these mixes.

The multiple regression model for permeability developed in Chapter 5, Equation (8), is shown here. Permeability is affected by age, mix type, air-void content, and fineness modulus.

Equation 8

log (permeability) = –6.49 – 0.118 Age + 0.552 Mix type + 0.0804 Air-void content + 0.682 Fineness modulus

R-Sq = 72.1%

Using the model for permeability given here, the time it takes for open- and gap-graded mixes to reach permeabilites close to those of dense-graded mixes can be predicted. The average permeability content of dense-graded mixes is 0.00065 cm/sec, and this value does not change much over the lifetimes of these mixes. The average initial permeability of a new open-graded mix is 0.12 cm/sec, and the average initial permeability of a new RAC-G mix is 0.05 cm/sec. The average air-void content of new open-graded mixes is 17.5 percent, the average air-void content of new RAC-G mixes is around 10 percent, and the average air-void content of new dense-graded mixes is around 6.5 percent. The fineness modulus of open-graded and RAC-G mixes is similar and ranges between 4.5 and 6.0.

For a new typical RAC-G mix, with air-void content of 10 percent and fineness modulus of 5.2, the model predicts that the mix will take around 9 years to become as impermeable as dense-graded mixes. For a new typical open-graded mix, with air-void content of 17.5 percent and fineness modulus of 5.2, the mix will takes around 19 years to become as impermeable as dense-graded mixes.

For comparison, only two open-graded and two RAC-G mixes out of 56 sections that are less than nine years old have permeabilities as low as the average for dense-graded mixes. Those four mixes have lower initial air-void content and finer gradations than most of the other open-graded and RAC-G mixes. There is one RAC-G section that is nine years old and has a permeability value as low as the average for dense-graded mixes. Based on these evaluations and the coefficient of determination (R^2) of the equation, it can be concluded that this equation gives good estimates of permeability values within the given range of variables. However, it predicts the permeability of a new dense-graded mix with zero air-void content as 0.0006 cm/sec, although a mix would not be permeable at all if it does not contain any air voids. This erroneous prediction occurs because the lowest air-void content in the study data set was 4.1 percent (Table 11). The equation should not be used for air-void content values outside the range in the data set.

Open-graded mixes retain their permeabilities over a longer time compared to RAC-G mixes with the same air-void content because the initial permeability of open-graded mixes is higher. Therefore, RAC-G mixes may lose their noise-reducing properties in a shorter time than do open-graded mixes.

11.2 Evaluation of Microtexture Models

The multiple regression model for microtexture developed in Chapter 6, Equation (13), is shown here. The BPN is affected by AADTT and cumulative number of temperatures over 25°C. BPN is mainly affected by aggregate properties; therefore, the BPNs of different mix types are similar to each other.

Equation (13)

$\log BPN = 1.79 - 0.0398\ AADTT - 0.00140\ (Age \times N.D.\ T > 25)^{0.5}$

R-Sq = 12.3%

Despite the extremely low R^2 value for this equation, it was used to provide an indication of the BPNs of the mix types included in this study. These results provide only an indication of expected results.

The average BPN of a new section is around 60. For a section under high truck traffic (AADTT > 1,750) and high annual temperatures (200 days in a year with temperatures above 25°C), the model indicates that it would take on the order of 24 years for the BPN to decrease to 45 BPN, which is the minimum criterion used for comparison purposes in this project, and it would take on the order of 48 years for the same section with low truck traffic (AADTT < 1,750) to attain the same BPN. For a section with low annual temperatures (50 days in a year with temperatures above 25°C) and high truck traffic (AADTT > 1,750), the model predicts that it would take 96 years for the BPN to decrease to 45 BPN, and it would take 191 years for the same section with low truck traffic (AADTT < 1,750) to attain the same BPN.

Table 41 shows the predicted lifetime of the mixes. The table shows that the proposed equation overestimates the polishing time since 4 out of 72 sections have BPN values below 45, and they are less than 14 years old. This overestimation occurs because the coefficient of determination (R^2) is low. Characterization of aggregate type was outside the scope of this project and is most likely the missing explanatory variable. Note that predicted lifetimes beyond 9 years rely on extrapolation since no sections older than 9 years were evaluated in this study.

The difference in BPN from year to year was also evaluated using single regression analysis. A positive difference in BPN indicates reduction in the BPN. Based on this analysis, age difference affects the change in BPN values, although it can be seen that there is almost no correlation; the equation was used to provide an indication of change in BPN. The single regression model for the difference in BPN values is shown as Equation (A).

Equation (A)

Difference in BPN= –14.65 + 15.14 Age difference

R-Sq = 8.8%

Based on Equation (A), a reduction of 15 BPN, which is the difference between the average initial BPN (60) and the minimum BPN for satisfactory friction (45), is obtained in two years. Table 41 shows the predicted lifetime of the mixes using Equation (A). This equation overestimates the reduction in BPN. Since the age difference used in Equation (A) ranges between 0 and 1.5 years, it cannot predict changes in the BPN values in the long term.

The single-variable analysis also indicated that increasing rainfall reduces the BPN values, as shown earlier in Table 21. The single regression model for the effect of rainfall on the difference in BPN values is shown here as Equation (B).

Equation (B)

Difference in BPN = –4.50 + 0.007 Amount of rainfall

R-Sq = 15.4%

Based on Equation (B), a reduction of 15 BPN, which is the difference between the average initial BPN (60) and the minimum BPN that provides acceptable friction (45), can be seen in four years. Table 41 shows the predicted lifetime of the mixes using Equation (B). This equation also seems to overestimate the reduction in BPN values since there are no sections that are less than four years old with BPN values less than 45. Therefore, it cannot be used to predict the change in BPN values in the long term.

Table 41: Predicted Lifetime of Different Mix Types for BPN Values

Equation	Initial BPN	Failure for BPN (unsatisfactory)	AADTT	N.D. T > 25°C	Average Annual Rainfall (mm)	Predicted Lifetime (years)
13	60	45	>1,750	200	-	**24**
13	60	45	>1,750	50	-	**96**
13	60	45	<1750	200	-	**48**
13	60	45	<1,750	50	-	**191**
A	60	45	-	-	-	**2**
B	60	45	-	-	800	**4**

The multiple regression model, Equation (13), indicated that BPN decreases with increasing number of high temperatures experienced by the section, and the single regression model, Equation (B), indicated that increasing rainfall reduces the BPN. There is a negative correlation between the amount of rainfall and the number of high temperatures; therefore, the sections with high rainfall usually have low temperatures. Since rainfall and temperature have opposite effects on friction, their effects may cancel out each other in the long term. Also, the rainfall effect may be only a short-term effect since the time difference between two measurements is less than 1.5 years. Based on the findings, more polish-resistant aggregates would be preferred for sections with high truck traffic, high temperatures, and high rainfall; however, friction was not found to be a problem for the California mixes evaluated.

11.3 Evaluation of Roughness Models

Two roughness (IRI) models were developed in Chapter 7. Equation (15) explains the IRI values using rubber inclusion and climatic variables. It is known that the IRI values are highly affected by the as-built IRI. Therefore, inclusion of as-built IRI values would help clarify the unexplained variance in the IRI at a given age. However, the as-built IRI values of the test sections are unknown.

Based on Equation (15), for a rubberized section with moderate temperatures (60 days in a year with temperatures above 30°C) and high rainfall (average annual rainfall of 800 mm), it would take 11 years to attain IRI values of 2.65 m/km (170 in/mi), which is the maximum acceptable value according to the FHWA, and the same section with low rainfall (average annual rainfall of 200 mm) would attain the same value in 45 years. For a nonrubberized section, a section with moderate temperatures (60 days in a year with temperatures above 30°C) and high rainfall (average annual rainfall of 800 mm) would take 9 years to attain IRI values of 2.65 m/km, which is the maximum acceptable value according to the FHWA, and the same section with low rainfall (average annual rainfall of 200 mm) would attain the same value in 35 years. It can be seen that rainfall has a big effect on the change in IRI values. Note that no sections have a combination of very high temperatures (with temperatures above 30°C) and high rainfall. Therefore, only moderate temperatures were evaluated. Since cumulative rainfall was used in the model, there was no correlation between rainfall and temperature variables.

Equation (15)

$1/\sqrt{IRI}$ = 0.815 + 0.0700 Rubber inclusion – 0.000038 Age × Average annual rainfall + 0.00115 Number of temperatures > 30°C

R-Sq = 46.0%

Among all the sections evaluated in this study, seven sections do not satisfy the "acceptable ride" criterion. Two of them are rubberized mixes, and three of them are open-graded mixes. One of the seven sections is less than a year old, which means that the higher IRI value is associated with the as-built IRI rather than climate. The other sections are older than six years and usually have high rainfall. Therefore, it can be concluded that Equation (15) may give reasonable estimates of the lifetime of the pavement in terms of roughness. Note that predicted lifetimes beyond nine years rely on extrapolation since no sections older than nine years were evaluated in this study.

The second roughness model, Equation (16), explained in Chapter 7, is shown here. It explains the IRI values using age and surface distresses. Based on this equation, for a section with no surface distresses (Presence of rutting = 0 and Presence of raveling = 0), it would take 21 years to attain IRI values meeting the "acceptable ride" criterion, and for a section with both rutting and raveling (Presence of rutting = 1 and Presence of raveling = 1), it would take 4 years to attain the same IRI values. Only two sections show both raveling and rutting; however, both of them are older than 5 years; therefore, the equation may underestimate the time it takes to attain "unacceptable" ride. The equation does not separate out the effects of severity and extent of rutting and raveling as the distress variables were used as categorical variables (0 or 1). Therefore, if the sections used in the modeling of the IRI included more sections with high-distress extents, the equation would likely predict a lower lifetime for a section with less distresses.

Equation (16)

IRI = 1.14 + 0.072 Age + 0.662 Presence of rutting + 0.540 Presence of raveling

R-Sq = 39.7%

The seven sections that do not satisfy the "acceptable ride" criterion have either rutting or raveling present on the surfaces. In addition to the variables age, rainfall, rubber inclusion, and temperature from the earlier model, the presence of distresses is likely contributing to the IRI and reducing the lifetime of the pavements. However, due to the small sample size, climate and distress variables could not be used in the same equation.

11.4 Evaluation of On-Board Sound Intensity Model

Two sound intensity (OBSI) models were developed in Chapter 9. The multiple regression model, Equation (18), is shown here. Permeability, MPD, mix type, and presence of raveling were used as explanatory variables in the model as shown here. Permeability is preferred over the air-void content variable in the model, since it takes into account the unclogged air voids at the top part of the surface layer and the connectivity of the air voids, which help reduce noise levels.

Equation (18)

OBSI = 98.2– 0.386 × log (permeability) + 0.00329 × MPD + 1.70 × Presence of raveling – 1.16 × Mix type

R-Sq = 73.1%

The permeability and MPD values at a given age were estimated using Equation (8) and Equation (14), respectively. Equation (18) was used to estimate the time it takes for open-graded and RAC-G mixes to attain noise levels as high as those of dense-graded mixes. In estimating the lifetimes, it was assumed that the air-void content of all mixes and the permeability of the DGAC mixes stay constant over time, and that all mixes have an NMAS of 12.5 mm. The effect of raveling was not evaluated in the comparison of OBSI levels of different mix types since the failure time in terms of raveling was not identified in this study.

Based on Equation (18), for an open-graded mix with an air-void content of 15 percent and fineness modulus of 5.2 and with high rainfall (average annual rainfall of 800 mm), it takes seven years to attain noise levels as high as those of dense-graded mixes, and for the same mix under low rainfall (average annual rainfall of 200 mm), it takes eight years to attain the same noise levels as those of dense-graded mixes. For a RAC-G mix with air-void content of 10 percent and a fineness modulus of 5.0, the model predicts that it takes less than one year for these mixes to lose their noise reduction effects and to attain noise levels as high as those of dense-graded mixes.

Based on Equation (18), open-graded mixes may provide noise reduction for up to eight years. The average noise level of dense-graded mixes that are four to eight years old is approximately 104 dB (A). Thirty percent of the open-graded mixes have noise levels higher than the average noise levels for dense-graded mixes, 104 dB (A). Therefore, it can be concluded that Equation (18) may provide close estimates of the time it takes for open-graded mixes to lose their noise-reducing properties. However, RAC-G mixes have lower noise levels than DGAC mixes when they are new and lose their noise-reducing properties after four to five years. Therefore, Equation (18) overestimates the noise levels of

RAC-G mixes. This overestimation occurs because the permeability model, Equation (8), underestimates the permeability values of new RAC-G mixes.

11.5 Prediction of Lifetime for Different Asphalt Mix Types

The performance models were evaluated for their effectiveness in estimating the performance variables and were used to estimate the lifetime of the different mix with respect to the performance criteria: permeability, roughness (IRI), friction (BPN), and noise (OBSI).

It can be concluded that the permeability model can give reasonable estimates of the lifetime of open-graded mixes. The permeability model was not used to calculate the lifetime of gap-graded and dense-graded mixes because they are intended to be impermeable. The models for BPN and the one-year change in BPN do not provide good estimates of the lifetimes of the mixes in terms of BPN. This inability to provide good estimates is due to the missing variable, aggregate type, which is expected to affect the BPN values. The IRI model can give moderately reasonable estimates of the lifetime before the section no longer provides "acceptable" ride quality, here based on the FHWA criterion of 2.65 m/km (170 in/mi). The minimum lifetime predicted by the IRI model is nine years. However, some sections that are less than nine years old do not provide "acceptable" ride quality; therefore, the mixes may last less than the time estimated by the model. The reason for the difference between the actual and predicted IRI values is that the IRI of the overlay later in its life is highly affected by the as-built IRI, which was not included in the analysis. The OBSI model can give reasonable estimates of the lifetime of the open-graded mixes; however, it underestimates the lifetime of the RAC-G mixes because the permeability model, Equation (8), underestimates the permeability values of new RAC-G mixes.

The best estimate of the time to failure of asphalt mixes in terms of permeability, friction (BPN), roughness, and noise reduction is given in Table 42. Since the regions with higher rainfall are associated with low temperatures, high rainfall and low temperatures are shown in the same cell. High rainfall is given as 800 mm and low rainfall is given as 200 mm in the models. Therefore, the actual lifetimes would be shorter than the predicted values for mixes that receive annual rainfall greater than 800 mm. Dense-graded mix performance was evaluated only for friction (BPN) and roughness (IRI); therefore, the DGAC (nonrubberized and non-open-graded mix) cells do not show any values for permeability, macrotexture, and OBSI. Permeability was not evaluated for RAC-G mixes since they are intended to be impermeable, although permeability is predicted for RAC-G mixes for use in the OBSI equation. The equations used to predict the failure time were given along with the performance variables in earlier chapters of this report.

Predicted lives greater than 9 years but less than 19 years are shown as >9 in Table 42. Predicted lives greater than 19 years, where the extrapolation indicates very long lives, are shown as >>9. This

approach was used because nearly all the sections in the data set used for the regressions are 9 years old or less.

It can be seen that OBSI controls the lifetime of the open- and gap-graded mixes. For open-graded mixes that are under high rainfall, the predicted lifetime is around seven years, and for those that are under low rainfall, the predicted lifetime is around eight years. Since open-graded mixes lose their noise-reducing properties before they lose their frictional properties and ride quality, the rubber inclusion does not provide any benefit according to the models. If the open-graded mixes are placed in low-rainfall and low-trafficked areas, the increase in MPD values would be less and the distress progression would be slower; however, under low rainfall, clogging may be greater, and the mixes would lose their permeability faster.

For RAC-G mixes, the predicted lifetime based on the OBSI model is less than one year. However, the descriptive statistics in Chapter 9 showed that it usually takes more than four years for RAC-G mixes to lose their noise-reducing properties. Therefore, the OBSI model underestimates the failure time for RAC-G mixes. The RAC-G mixes have MPD values close to those of DGAC mixes; therefore, they have the same noise levels as dense-graded mixes when their permeability is reduced to a level similar to those of DGAC mixes. It can be concluded that the estimated lifetime of the RAC-G mixes is less than one year if they are intended as a noise-reducing layer based on the OBSI model, and about four years when based on the descriptive statistics for the number of years before their noise levels are similar to those of DGAC mixes.

Roughness is the performance variable that controls the lifetime of dense-graded mixes that are under high rainfall. The predicted failure time for dense-graded mixes is nine years when they are under high rainfall. When they are under low rainfall, the failure time is 24 years for mixes that are under high truck traffic and 35 years for those that are under low truck traffic. It can be concluded that climate greatly affects the performance of all types of asphalt mixes. Note that all the sections in this study are less than nine years old, and therefore predicted lifetimes beyond nine years are extrapolated.

Table 42: Predicted Lifetime of Different Asphalt Mix Types with Respect to Performance Variables

Performance Variables	High Traffic								Low Traffic							
	High Rainfall/Low Temperature				Low Rainfall/High Temperature				High Rainfall/Low Temperature				Low Rainfall/High Temperature			
	Rubberized		Non-rubberized		Rubberized		Non-rubberized		Rubberized		Non-rubberized		Rubberized		Non-rubberized	
	Open Graded	RAC-G	Open Graded	DGAC	Open Graded	RAC-G	Open Graded	DGAC	Open Graded	RAC-G	Open Graded	DGAC	Open Graded	RAC-G	Open Graded	DGAC
Permeability (Eq. 8)	>9	–	>9	–	>9	–	>9	–	>9	–	>9	–	>9	–	>9	–
BPN (Eq. 13)	>>9	>>9	>>9	>>9	>>9	>>9	>9	>>9	>>9	>>9	>>9	>>9	>>9	>>9	>9	>>9
IRI (Eq.15)	>9	>9	9	9	>>9	>>9	>>9	>>9	>9	>9	9	9	>>9	>>9	>>9	>>9
OBSI (Eq. 18)	7	4*	7	–	8	4*	8	–	7	4*	7	–	8	4*	8	–
Minimum Lifetime	**7**	**4***	**7**	**9**	**8**	**4***	**8**	**>>9**	**7**	**4***	**7**	**9**	**8**	**4***	**8**	**>>9**

* Predicted by descriptive statistics assuming that RAC-G is intended as a noise-reducing overlay; OBSI model underpredicts noise performance and indicates less than one year of noise-reducing performance. See discussion in text.

Note: >9 indicates extrapolated life of 10 to 19 years; >>9 indicates extrapolated life greater than 19 years.

12 CONCLUSIONS, RECOMMENDATIONS, AND RECOMMENDATIONS FOR FURTHER WORK

12.1 Conclusions

In this report, the performance of open-graded mixes as well as of other asphaltic mixes used in California was evaluated in terms of safety, noise, and durability. Data was collected on the OGAC, RAC-O, RAC-G, and DGAC mixes as well as on some new mixes such as bonded wearing course (BWC), gap-graded asphalt rubber (RUMAC-GG), gap-graded rubber modified asphalt (Type G-MB), and dense-graded rubber modified asphalt (Type D-MB). The objectives of this study were to:

- Evaluate the durability and effectiveness of open-graded mixes in increasing safety and reducing noise compared to other asphalt surfaces
- Determine the pavement characteristics that affect tire/pavement noise
- Correlate sound absorption with tire/pavement noise
- Evaluate the performance of new mixes compared to the asphaltic mixes currently used in California

12.1.1 Performance of Open-Graded Mixes

The results showed that current open-graded mixes reduced tire/pavement noise compared to the dense-graded mixes included in the study by almost 2 dB (A) on average for all sections over the eight-year range of ages, which according to the literature is near the limit of what the human ear can discern. Twenty-five percent of the open-graded mixes provided noise reduction above 3 dB (A) compared to the average noise level of a DGAC mix, which is 104 dB (A) for the sections tested. Over the entire set of sections including all ages, the open-graded mix noise levels were between 1 dB (A) greater and 4 dB (A) less than the average DGAC noise level. The noise levels of the DGAC mixes in the study were similar across all ages of pavement.

Noise reductions between 2 dB (A) and 6 dB (A) were reported in the literature for open-graded mixes (112, 113). The results presented in this report are from comparisons between different surfaces of similar ages. Greater noise reductions would be expected when new open-graded surfaces are placed on existing DGAC surfaces that have widespread and severe distresses than when comparing the noise levels of open-graded mixes with those of DGAC surfaces of similar ages as was done in this study.

Also note that noise levels above 1,000 Hz are generally considered more annoying, and that increasing air-void content and increasing macrotexture reduce the noise levels at higher frequencies. Since open-graded mixes have higher air-void content and macrotexture, they may reduce the noise levels at higher frequencies and so may be perceived by the human ear as quieter and the noise as less annoying

than dense-graded mixes, even though the overall A-weighted noise levels are not significantly different from each other.

Open-graded mixes have higher permeability and friction than dense-graded and RAC-G mixes; therefore, they can reduce hydroplaning and spray and splash and hence improve safety. Based on the results of the conditions surveys for pavements less than nine years old included in this study, they also may be less prone to transverse cracking. However, although it could not be revealed statistically in this study, it is expected that open-graded mixes would be more prone to raveling since their high permeability would be expected to increase the oxidation rate of the binder, in comparison to the less permeable DGAC and RAC-G mixes.

Open-graded mixes lose their noise-reducing properties with time mainly due to clogging and also due to the presence of distresses on the pavement surface. The work in this study predicts their noise levels to reach those of dense-graded mixes within seven years. Clogging occurs at the top part of the surface layer and reduces its permeability. There is also some indication that thicker mixes, above 50 mm, may be less clogged and hence have higher permeabilities than thinner mixes. The longevity of benefits provided by open-graded mixes varies with mix properties, rainfall, and presence of raveling.

From this small sample of pavements in California, there does not appear to be a major difference in performance between RAC-O and OGAC mixes with respect to noise and permeability benefits across the age ranges. However, the rate of increase in IRI is slower for rubberized mixes. Although the data was not statistically significant in this study, rubberized mixes tended to have better cracking performance, which would be expected to slow the rate of noise in later years.

12.1.2 Performance of RAC-G Mixes

It appears from the data that RAC-G mixes provide some noise benefit compared to DGAC mixes. Most of the noise benefits from RAC-G appear to come from the fact that they have higher air-void content than DGAC mixes when they are built (compaction of RAC-G is by method specification, where the compaction method is specified and the relative density is not specified, rather than by an end-result specification where the relative density is specified and the contractor chooses the compaction method.). However, they lose their permeability faster than the open-graded mixes, and hence their noise-reducing properties. Based on the descriptive statistics, the noise levels from RAC-G mixes appear to approach those of DGAC within four years. The sound intensity model overpredicts the noise levels of RAC-G mixes; therefore, this model cannot be used to estimate the lifetime of RAC-G mixes in terms of noise reduction.

12.1.3 Variables Affecting Tire/Pavement Noise

The study showed that tire/pavement noise is greatly influenced by pavement surface characteristics such as gradation, macrotexture, age, and presence of distresses. Coarser gradation and increasing air-void content reduce the overall noise levels, and the presence of distresses and increasing macrotexture and age increase the overall noise levels, confirming the previous findings of other researchers. However, this study found that the overall A-weighted noise levels are insensitive to changes in air-void content for open-graded mixes with air-void content above 15 percent. This insensitivity occurs because air-void content above 15 percent is usually associated with higher macrotexture (MPD) values, and for large texture depths, increasing air-void content does not reduce the overall noise levels, and its effects are surpassed by those of increased tire vibrations.

Since California mixes are placed in thin layers (around 30 mm), thickness was not found to affect the noise levels of the sections studied. However, there is some indication that increasing thickness may lower the noise levels for thicknesses above 50 mm (2 inches).

The pavement temperature was not found to significantly affect the noise levels.

The use of rubber asphalt binders was also not found to significantly affect the noise levels, although the noise levels of RAC-O mixes were somewhat less than those of OGAC mixes.

The low frequencies of tire/pavement noise were found to be governed by tire vibrations due to high macrotexture, and the higher frequencies were found to be governed by air-pumping mechanisms that can be reduced by the presence of air voids on the pavement surface, confirming the findings of previous researchers on the noise-generation mechanisms. However, increasing air-void content was found to increase the noise levels at a given macrotexture at lower frequencies, probably due to increased tire vibrations.

At frequencies around 800 to 1,000 Hz, where the tire/pavement noise is highest, the air-pumping cannot be reduced by increasing air-void content above 15 percent, and tire vibrations govern the noise generation for mixes with high air-void content and high macrotexture values. This trend can also be seen in the overall noise levels.

At frequencies above 1,000 Hz, higher air-void content and higher macrotexture values reduce the air-pumping noise. Therefore, open-graded mixes have significantly lower noise levels at frequencies above 1,000 Hz.

12.1.4 Correlation of Absorption Values with Noise Levels

The noise levels of dense- and gap-graded mixes decrease with increasing absorption. However, no correlation was found between the overall A-weighted sound intensity and absorption for open-graded mixes. Correlations between sound intensity (noise) measured in the field and laboratory absorption

values depended on frequency. Noise levels around 500 Hz are governed by tire vibrations; therefore, absorption has no effect on the noise levels for any mix type. At frequencies above 630 Hz, absorption reduces the noise levels caused by air pumping for dense- and gap-graded mixes, and there are clear trends relating noise to absorption.

Tire vibrations may cause significant noise levels for open-graded mixes with high macrotexture values at lower frequencies (less than 1,000 Hz), and there is no trend between noise and absorption. The noise-reducing effect of absorption can be seen at 1,000 Hz for open-graded mixes, if macrotexture is also considered. The noise-reducing effects of absorption can be clearly seen at frequencies above 1,000 Hz for open-graded mixes. Air-pumping noise governs noise generation at frequencies above 1,000 Hz, confirming the earlier findings, as increasing absorption reduces the noise levels regardless of the macrotexture values. This trend is stronger for higher frequencies, which are considered more annoying to humans.

12.1.5 Performance of New Mixes

The bituminous wearing course (BWC) mix placed on the LA 138 sections has lower permeability and friction, higher noise levels, and almost the same distress development as current Caltrans open-graded mixes in the LA 138 section study.

Based on the Fresno 33 (Firebaugh) sections, the RUMAC-GG and Type G-MB mixes did not perform as well the RAC-G mix when placed in thin lifts (45 mm); the RUMAC-GG and Type G-MB mixes have higher noise levels and are more susceptible to bleeding. However, RUMAC-GG was more crack resistant when placed in thick layers (90 mm). Type D-MB, which may be a candidate as an alternative to dense-graded mixes after further investigation, has performance characteristics very similar to those of DGAC mixes, and it may provide better crack resistance; however, it was more susceptible to bleeding.

The European gap-graded (EU-GG) mix placed on LA 19 has performance characteristics very similar to those of gap-graded mixes (RAC-G) used in California.

F-mixes have been used only in a wet environment on the north coast. Indications are that they do not perform as well as OGAC and RAC-O with regard to noise, probably because of their large NMAS values and raveling.

12.1.6 Other Conclusions

Note that the conclusions presented here are valid within the range of the air-void content, thickness, age, and gradation properties of the mixes used in this study and under California climate and traffic conditions. The OBSI measurements were conducted using an Aquatread 3 tire and a passenger car. The

conclusions may differ for trucks and vehicles with different tires as noise-generation mechanisms are highly dependent on the vehicle and tire type. Also note that the OBSI method is a near-source measurement; therefore, it captures only the tire/pavement noise. Since the noise levels next to highways are also affected by noise propagation and noise absorption under propagation, the greater absorption values measured as part of this project may indicate that the open-graded mixes provide higher levels of noise reduction at the side of the highway than these results may show.

The comparison of pass-by measurements made by Volpe (unverified by UCPRC with regard to wind speeds and other factors) with OBSI measurements indicated that absorption may provide additional noise reduction next to highways since 75-mm OGAC shows higher noise reduction than dense-graded mixes when measured using the pass-by method. However, the pass-by measurements found no additional noise reduction for the 30-mm OGAC and RAC-O sections.

The effects of NMAS and thickness could not be fully evaluated as these variables have different specifications for different mix types. Open-graded mixes have NMAS values of 9.5 and 12.5 mm, and dense- and gap-graded mixes have NMAS values of 12.5 and 19 mm. F-mixes are the only open-graded mixes with an NMAS value of 19 mm. Open-graded mixes are placed in thin layers, while RAC-G and DGAC mixes are usually placed in a thicker lift. RAC-G mixes are usually placed at half the thickness of DGAC mixes as the rubber content allows for reduced thickness, providing structural and reflection crack retardation equivalency. Therefore, NMAS and thickness effects were identified only within each mix type. Also, rubberized mixes are usually overlays of pavements with more extensive cracking than the pavements on which DGAC mixes are placed. Therefore, the effects of rubber on crack retardation could not be fully evaluated.

The effects of stiffness on noise levels were evaluated by comparing the noise levels of rubberized and nonrubberized mixes as well as by comparing shear modulus values with overall tire/pavement noise levels. The study's preliminary conclusion is that stiffness does not play a major role in determining overall tire/pavement noise levels for mixes of the types included in this study. The effects of stiffness on different frequencies and sound absorption were not evaluated.

12.2 Recommendations

Based on the findings, none of the other asphalt mix types evaluated in this study can provide an alternative to current Caltrans open-graded mixes in terms of noise reduction and safety. However, durability of open-graded mixes compared to other mix types depends on the climatic conditions and traffic.

The results indicate that the current recommendation for the best approach to noise reduction is to use thin layers of open-graded mixes with nominal maximum aggregate sizes of 12.5 or 9.5 mm. The smaller

aggregate sizes will somewhat reduce air-void content and permeability; however, open-graded mixes with smaller aggregate sizes will likely have greater durability because of their lower air-void content and will likely cost less than open-graded mixes with larger aggregate sizes because they can be constructed as thinner lifts. The results indicated that the desired air-void content for open-graded mixes for noise reduction could be limited to a maximum of 15 percent since higher air-void content does not provide any additional noise reduction and reduces durability. Mixes with lower air-void content would also be more resistant to clogging.

There do not appear to be noise-reduction benefits from increasing the thickness of open-graded mixes for thicknesses less than 50 mm. However, the results gave some indication that thicknesses greater than 50 mm (2 inches) reduce noise. Placing open-graded mixes in thicker lifts would also help reduce the IRI value and increase cracking resistance for overlays of PCC. The results also gave some indication that thicker lifts may be less susceptible to clogging.

Open-graded mixes have longer lives in terms of noise and permeability with low levels of truck traffic and rainfall. High truck traffic increases clogging, and mixes under low rainfall are also more susceptible to clogging, although they are less likely to show raveling and polishing. When placing open-graded mixes, the air-void content and thickness will need to be balanced with the permeability requirements needed to reduce hydroplaning for a given site.

Overall preliminary recommendations for open-graded mix design based on the results of this study are shown in Table 43. These recommendations are also the basis for recommendations for further work to improve the performance of open-graded mixes, discussed in the next section of this report (Section 12.3).

Table 43: Preliminary Recommendation for Open-Graded Mix and Thickness Design to Achieve Performance Goals

	Performance Criteria (relevant section of report)				
Mix and Thickness Design Variables	**Noise (Sections 9.1.4 and 9.2.3)**	**Permeability (Section 5.4)**	**Durability** (Section 8.6)*** **	**Ride Quality (Section 7.3)**	**Friction (Section 6.7)**
Air-Void Content	15 percent or less	Maximize*	Minimize		Maximize
Nominal Max Aggregate Size	Minimize	12.5 mm instead of 9.5 mm			Maximize
Gradation	Greater fineness modulus (coarser gradation)	Greater fineness modulus (coarser gradation)			Greater fineness modulus (coarser gradation)
Binder Type			Rubberized	Rubberized	
Overlay Thickness	Greater than 50 mm may help				

* Permeability recommendations should be based on expected rainfall events for a particular project location. Development of these criteria are outside the scope of this project.
** Durability is defined as resistance to distress development.
*** Few sections had significant distresses, and results were not statistically significant. Recommendations regarding durability are based on judgment as well as the results of this study.

12.3 Recommendations for Further Work

In this study, pavement characteristics and noise were observed for two years. However, two years is a short time to observe any trends. Therefore, permeability, friction, IRI, and sound intensity measurements and condition surveys should be conducted on the given sections for at least two or three years to develop better time histories and to see more sections reach failure. As of this writing funding has been committed by Caltrans for two more years of measurement on the asphalt mix sections and updating of the models and performance predictions based on the four years of results. A similar study, funded for two years, will be performed on concrete surfaces.

Open-graded mixes have lower noise levels than dense- and gap-graded mixes at higher frequency levels, which may be a benefit that A-weighted measurements do not capture well in terms of annoyance rather than audibility. Since the human ear is most sensitive at frequencies between 1,000 and 4,000 Hz, the open-graded mixes may be perceived as quieter than dense-graded mixes with the same overall noise levels. The noise levels should be correlated with the human perception of annoyance to better evaluate noise-mitigation strategies.

Since the reason for placing open-graded mixes is to reduce the noise levels next to highways, the way-side measurements should be better correlated with OBSI levels than was possible in this study to understand the actual noise reduction provided by open-graded mixes.

At 500 Hz, increasing air-void content was found to increase noise levels along with macrotexture; however, the noise-generation mechanism is unknown. The further effects of air-void content on noise levels at lower frequencies should be evaluated. In addition, a new parameter that correlates better with the sound intensity levels should be developed. This parameter can be a combination of MPD, RMS, and air-void content as well as a new measure of macrotexture.

The results gave some indication that open-graded mixes with finer gradations (lower fineness modulus) may provide lower noise levels, particularly at higher frequencies of noise. In this study, only a few open-graded mixes had fine gradations. The effects of fineness modulus on the noise levels should be further evaluated, particularly for mixes with the same NMAS.

This study could not fully evaluate the effects of NMAS and thickness on pavement performance. Therefore, a laboratory study should be performed to consider the durability, sound absorption (correlated with high-frequency noise), and permeability for a full factorial experiment considering these variables. Some optimization of the mixes based on initial results should also be performed. Since the presence of polymer-modified binders could not be identified for the OGAC sections in this study because of a lack of reliable as-built records for many sections, polymer and conventional binders, as well as rubberized binders used by Caltrans, should also be included in the factorial. Macrotexture should also be measured, since the results indicate that absorption and macrotexture provide an indication of noise at 1,000 Hz.

The results of the laboratory study will provide a basis for designing a factorial for field-test sections to verify the laboratory results regarding the effects of thickness, NMAS, fineness modulus, and binder type on clogging, cracking, and noise levels. Permeability and noise measurements as well as condition surveys should be conducted on these test sections. The air-void content should also be measured using CT scans with a higher resolution than used in this study. A resolution around 15 microns (based on the results of this study) would be enough to see fine particles clogging the mix. The effects of pavement temperature on noise levels were evaluated measuring nine sections at three temperatures. No correlation was found between pavement temperatures and noise levels. A larger data set, with open-, gap-, and dense-graded mixes, should be obtained, and measurements should be conducted using a wider range of pavement temperatures. It would be useful to analyze the effects of pavement temperature on noise levels separately for each mix type.

REFERENCES

1. California Department of Transportation (Caltrans). Quieter Pavements Road Map and Work Plan. 2005.
2. University of California Pavement Research Center. Work Plan for: "Investigation of Noise, Durability, Permeability and Friction Performance Trends for Asphaltic Pavement Surface Types," PPRC Strategic Plan Item 4.16. June 2005. UCPRC-WP-2005-01 (downloadable at www.its.berkeley.edu/pavementresearch)
3. Norton. M. P. Fundamentals of Noise and Vibration Analysis for Engineers. Cambridge University Press, Cambridge, England, 1989.
4. World Health Organization Regional Office for Europe. Noise and Health. www.euro.who.int/noise/. Accessed March 2005.
5. Berglund. B., T. Lindvall, and D. H. Schwela. Guidelines for Community Noise. World Organization, Geneva, Switzerland, 2000. www.who.int/docstore/peh/noise/guidelines2.html. Accessed March 2005.
6. Swiss Agency for the Environment, Forests and Landscape (SAEFL). Monetisation of the Health Impact Due to Traffic Noise. Environmental Documentation No.166, Noise, Berne, Switzerland, 2003.
7. Van Blokland, G. Understanding and Handling Road Surface Acoustics. websrv2.tekes.fi/ opencms/opencms/OhjelmaPortaali/Kaynnissa/Infra/fi/Dokumenttiarkisto/Viestinta_ja_aktivointi/ Seminaarit/Hiljaseminaari/pptpresentationMxPFinland.pdf. Accessed Feb. 2005.
8. FHWA. Indiana Department of Transportation Highway Noise Policy. 1997. www.fhwa.dot.gov/ indiv/noisplcy.htm. Accessed Feb. 2005.
9. Van den Berg, M. The Ultimate Goal of Noise Control at the Source. www.xs4all.nl/~rigolett/ ENGELS/ultimate-goal.pdf. Accessed Feb. 2006.
10. Sandberg, U., and J. A. Ejsmont. Tyre/Road Noise Reference Book. Informex, Kisa, Sweden, 2002.
11. CALM. Coordination of European Research for Advanced Transport Noise Mitigation. www.calm-network.com/index_start.htm. Accessed Feb. 2006.
12. Nelson, P. M., and S. M. Phillips. Quieter Road Surfaces. *TRL Annual Review,* Transportation Research Laboratories, United Kingdom, 1997.
13. Sandberg, U. Tyre/Road Noise Myths and Realities. Proc., Inter-Noise 2001, The Hague, Netherlands, Aug. 2001.

14. McDaniel, R. S., and W. D. Thorton. Field Evaluation of a Porous Friction Course for Noise Control. Presented at 2005 Annual Meeting of the Transportation Research Board, Washington, D.C., Jan. 2005.
15. California Department of Transportation (Caltrans). *Skid Resistance.* Undated. This is a research document from the development of CT Method 342, likely in the 1960s.
16. FHWA. FY 2002 Performance Plan and FY 2000 Performance Report. 2002. www.fhwa.dot.gov/reports/2002plan/index.htm. Accessed Feb. 2006.
17. California Department of Transportation (Caltrans). Thin Maintenance Overlays. Oct. 2003. www.dot.ca.gov/hq/maint/mtag/ch8_maint_overlays.pdf. Accessed Feb. 2006.
18. WSDOT Pavement Guide. hotmix.ce.washington.edu/wsdot_web
19. Kanitpong, K., C. H. Benson, and H. U. Bahia. Hydraulic Conductivity (Permeability) of Laboratory Compacted Asphalt Mixtures. In Transportation Research Record 1767, TRB, National Research Council, Washington, D.C., 2001, pp. 25–32.
20. Brown, E. R., M. R. Hainin, A. Cooley, and G. Hurley. NCHRP Report 531: Relationship of Air Voids, Lift Thickness, and Permeability in Hot Mix Asphalt Pavements. TRB, Washington, D.C., 2004.
21. Mallick, R. B., et al. An Evaluation of Factors Affecting Permeability of Superpave Designed Pavements. NCAT Report 03-02. Auburn, Ala., June 2003. www.eng.auburn.edu/center/ncat/reports/rep03-02.pdf. Accessed Feb. 2007.
22. Choubane, B., G. C. Page, and J. A. Musselman. Investigation of Water Permeability of Coarse Graded Superpave Pavements. Research Report FL/DOT/SMO/97-41. July 1997.
23. Cooley, Jr., L. A., B. D. Prowell, and E. R. Brown. Issues Pertaining to the Permeability Characteristics of Coarse-Graded Superpave Mixes. NCAT Report 02-06. Auburn, Ala., July 2002. www.eng.auburn.edu/center/ncat/reports/rep02-06.pdf. Accessed Feb. 2007.
24. Wisconsin Department of Transportation. Effect of Pavement Thickness on Superpave Mix Permeability and Density. WisDOT Highway Research Study 0092-02-14, Sept. 2004. www.dot.wisconsin.gov/library/research/docs/finalreports/0214cpermeability.pdf. Accessed Feb. 2007.
25. prEN 13108-7:2005 – Bituminous mixtures – Material specification – Part 7: Porous Asphalt. European Committee for Standards, Brussels, Belgium. National standards comforming to the European Standard may be accessed at http://www.cen.eu/esearch/ (last accessed 24 June, 2008).
26. Poulikakos, L., R. Gubler, M. N. Partl, et al. Current State of Porous Asphalt in Switzerland. Proceedings, 10th International Conference on Asphalt Pavements ISAP, Québec City, Quebec, Canada, Aug. 12–17, 2006.

27. Isenring, T., H. Koster, and I. Scazziga. Experiences with Porous Asphalt in Switzerland. In Transportation Research Record 1265, TRB, National Research Council, Washington, D.C., 1990, pp. 41–53.
28. Personal communication with Larry Scofield, May 2008.
29. Bendtsen, H. Presentation of Research Program on Clogging. October 2005. www.innovatieprogrammageluid.nl/English/index.html. Accessed Feb. 2006.
30. Bendtsen, H., et al. Report 120: Clogging of Porous Bituminous Surfacing: An Investigation in Copenhagen. Danish Road Institute, 2002.
31. Kragh, J. Danish-Dutch Cooperation on Noise Reducing Surfaces. Personal communication, Jan. 2007. Kuijpers, A. Further Analysis of the Sperenberg Data. M+ P.MVM 99.3.1. The Hague, Netherlands, Nov. 2001.
32. Morgan. P. A., P. M. Nelson, and H. Steven. Integrated Assessment of Noise Reduction Measures in the Road Transport Sector. TRL Project Report PR SE/ 652/03, Wokingham, Berkshire, England, United Kingdom, Nov. 2003.
33. Van Heystraeten, G., and C. Moraux. Ten Years' Experience of Porous Asphalt in Belgium. In Transportation Research Record 1265, TRB, National Research Council, Washington, D.C., 1990, pp. 34–40.
34. Jayawickrama, P. W., and B. Thomas. Correction of Field Skid Measurements for Seasonal Variations in Texas. In Transportation Research Record 1639, TRB, National Research Council, Washington, D.C., 1997, pp. 155–161.
35. World Road Association (PIARC). Report of the Committee on Surface Characteristics. XVIII World Road Congress, Brussels, Belgium, 1987.
36. Lavin, P. Asphalt Pavements: A Practical Guide to Design, Production and Maintenance for Engineers and Architects. Taylor and Francis, New York, 2003.
37. McGhee, K., and G. W. Flintsch. High-Speed Texture Measurements of Pavements. Virginia Transportation Research Council Report, Charlottesville, Va., 2003.
38. ASTM E 1960, Standard Practice for Calculating International Friction Index of a Pavement Surface. ASTM Annual Book of Standards, Vol. 04.03. Conshohocken, Penn., 2003.
39. Luo, Y. Effect of Pavement Temperature on Frictional Properties of Hot-Mix-Asphalt Surfaces at the Virginia Smart Road. Ph.D. dissertation. Virginia Polytechnic Institute and State University, 2003.
40. Asi, I. M. Evaluating Skid Resistance of Different Asphalt Concrete Mixes. Building and Environment, 42, 2005, pp. 325–329.

41. Hill B. J., and J. J. Henry. Mechanistic Model for Predicting Seasonal Variations in Skid Resistance. In Transportation Research Record 946, TRB, National Research Council, Washington. D.C., 1982, pp. 29–37.
42. Skerritt, W. H. Aggregate Type and Traffic Volume as Controlling Factors in Bituminous Pavement Friction. In Transportation Research Record No. 1418, Transportation Research Board, National Research Council, Washington, D.C., pp. 22–29.
43. Crouch L. K., J. D. Gothard, G. Head, and W. A. Goodwin. Evaluation of Textural Retention of Pavement Surface Aggregates. In Transportation Research Record 1486, TRB, 1995, pp. 124–129.Descornet. G. A Criterion for Optimizing Surface Characteristics. In Transportation Research Record 1215, TRB, National Research Council, Washington, D.C., 1989, pp. 173–177.
44. Smith, B. J., and R. G. Pollock. Textural and Mineralogical Characterization of Kansas Limestone Aggregates in Relation to Physical Test Results. FHWA-KS- 97/4, Final Report, 1997.
45. Bazlamit S., and F. Reza. Changes in Asphalt Pavement Friction Components and Adjustment of Skid Number for Temperature. Journal of Transportation Engineering, ASCE, 131(6), 2005, pp. 470–476.
46. Croney, D., and P. Croney. Design and Performance of Road Pavements, 3rd ed. McGraw-Hill, New York, 1998, pp. 471–472.
47. Hill B. J., and J. J. Henry. Short-Term, Weather-Related Skid Resistance Variation. In Transportation Research Record 836, TRB, National Research Council, Washington. D.C., 1978, pp. 76–81.
48. Oliver, J. W. H. Seasonal Variation of Skid Resistance in Australia. Australia Road Research Board, Special Report No. 37, 1989.
49. Fwa T., Y. Choo, and Y. Liu. Effect of Aggregate Spacing on Skid Resistance of Asphalt Pavement. Journal of Transportation Engineering, ASCE, 129(4), 2003, 420–426.
50. Page, G. C. Open-Graded Friction Courses: Florida's Experience. In Transportation Research Record 1427, TRB, National Research Council, Washington, D.C., 1993, pp. 1–4.
51. Huddleston. I. J., H. Zhou, and R. G. Hicks. Evaluation of Open-Graded Asphalt Concrete Mixtures Used in Oregon. In *Transportation Research Record 1427,* TRB, National Research Council, Washington, D.C., 1993, pp. 5–12.
52. Stroup-Gardiner, M., and E. R. Brown. *NCHRP Report 441: Segregation of Hot-Mix Asphalt Pavements.* TRB, National Research Council, Washington, D.C., 2000.
53. Flintsch, G., E. Leon, K. K. McGhee, and I. L. Al-Qadi. Pavement Surface Macrotexture Measurement and Application. Transportation Research Board Annual Meeting, Washington, D.C., 2003.

54. *WAPA Asphalt Pavement Guide.*Published on interactivecompact disk by the Washington Asphalt Pavement Association. www.asphaltwa.com/wapa_web/modules/08_evaluation/ 08_categories.htm. Accessed Feb. 2007.

55. Sayers, M. W., T. D. Gillepsie, and C. A. V. Queiroz. The International Road Roughness Experiment: Establishing Correlation and Calibration Standard for Measurements. World Bank Technical Paper 45, World Bank, Washington, D.C., 1986.

56. Lee, D. G., and J. S. Russell. Panel Data Analysis of Factors Affecting As-Built Roughness of Asphaltic Concrete Pavements. Journal of Transportation Engineering, Vol. 130, No. 4, July 1, 2004.
57. Perera, R. W., and S. D. Kohn. NCHRP 40: LTTP Data Analysis: Factors Affecting Pavement Smoothness. Transportation Research Board. National Research Council, Washington, D.C., Aug. 2001.
58. Mantravadi, K. K. LTPP-Distress Due to Environment. Center for Transportation Research and Education, Iowa State University, 2000. www.ctre.iastate.edu/mtc/papers/mant.pdf. Accessed Feb. 2006.
59. Simpson, A. L., E. Owusu-Antwi, O. J. Pendleton, and Y. Lee. Sensitivity Analysis for Selected Pavement Distresses. Strategic Highway Research Program, National Research Council, Washington, D.C., 1994.
60. Rauhut, B., H. L. Von Quintus, and A. Eltahan. Performance of Rehabilitated Asphalt Concrete Pavement in LTTP Experiments (Data Collected Through February 1997). Publication No. FHWA-RD-00-029, June 2000.
61. Lu, Q., et al. Truck Traffic Analysis Using Weigh-in-Motion (WIM) Data in California. University of California Pavement Research Center, Davis, Berkeley, June 2002. (UCPRC-TM-2008-08)
62. Gokhale S., et al. Rut Initiation Mechanisms in Asphalt Mixtures as Generated Under Accelerated Pavement Testing. In *Transportation Research Record 1940*, TRB, National Research Council, Washington, D.C., 1990, pp. 136–145.
63. Fromm, H. J., and Phang, W. A. A Study of Transverse Cracking of Bituminous Pavements. *Proc., Association of Asphalt Paving Technologists*, Vol. 41, 1972, pp. 383–423.
64. Haas, R., Meyer, F., Assaf, G., and Lee, H. A Comprehensive Study of Cold Climate Airport Pavement Cracking. *Proc., Association of Asphalt Paving Technologists*, Vol. 56, 1987, pp. 198–245.

65. Lytton, R. L., et al. (1993). *Development and Validation of Performance Prediction Models and Specifications for Asphalt Binders and Paving Mixes.* Report No.SHRP-A-357. Strategic Highway Research Program, National Research Council, Washington, D.C.
66. Wolters, R. O. *Raveling of Hot-Mix Asphalt.* Minnesota Asphalt Pavement Association, Oct. 2003. www.asphaltisbest.com/PDFs/Raveling_of_HMA_Oct03.pdf. Accessed Feb. 2007.
67. Harvey, J. T., et al. Fatigue Performance of Asphalt Concrete Mixes and Its Relationship to Asphalt Concrete Pavement Performance in California. University of California Pavement Research Center, Berkeley, Jan. 1996.
68. Finn, F. N., and J. A. Epps. *Pavement Failure Analysis with Guidelines for Rehabilitation of Flexible Pavements.* Research Report 214-17. Texas Transportation Institute, Texas A&M University System, College Station, Tex., 1980.
69. Pell, P.S. and Cooper, K.E., The effect of testing and mix variables on the fatigue performance of bituminous materials, Annual Meeting of Association of Asphalt Paving Technologists, Phoenix, Arizona (1975).
70. Lister, N. W., and W. D. Powell. Design Practice for Bituminous Pavement in the United Kingdom. *Proc., 6th International Conference on the Structural Design of Asphalt Pavement*, Vol. 1, Ann Arbor, Mich., 1987, pp. 220–231.
71. Tangella, R., et al. *Summary Response on Fatigue Response of Asphalt Mixtures.* Prepared for Strategic Highway Research Program Project A-003-A, TM-UCB-A-003A-89-3, Institute of Transportation Studies, University of California, Berkeley, Feb. 1990.
72. Von Quintus, H. L., A. L. Simpson, and A. A. Eltahan. *Rehabilitation of Asphalt Concrete Pavements: Initial Evaluation of the SPS5 Experiment Final Report.* Research Report FHWA-RD-01-168. Long-Term Pavement Performance Program, Federal Highway Administration, Washington, D.C., Oct. 2000.
73. Madanat, S., Z. Nakat, and N. Sathaye. *Development of Empirical-Mechanistic Pavement Performance Models Using Data from the Washington State PMS Database.* University of California Pavement Research Center, Davis, Berkeley, 2005. (UCPRC-RR-2005-05)
74. Wang, Y., K. C. Mahboub, and D. E. Hancher. Survival Analysis of Fatigue Cracking for Flexible Pavements Based on Long-Term Pavement Performance Data. *Journal of Transportation Engineering*, Vol. 131, Issue 8, Aug. 2005.
75. Sandberg, U., and G. Descornet. Road Surface Influence on Tire/Road Noise: Part 1. *Proc., Inter-Noise 80,* Miami, Fla., 1980.
76. Kuijpers, A. *Further Analysis of the Sperenberg Data.* M+ P.MVM 99.3.1. The Hague, Netherlands, Nov. 2001.

77. Domenichini, L., et al. Relationship Between Road Surface Characteristics and Noise Emission. *Proc., TINO First International Colloquium on Vehicle Tyre Road Interaction,* Rome, Italy, 1999.
78. Van Keulen, W., and M . Duškov. *Inventory Study on Basic Knowledge on Tire/Road Noise.* Road and Hydraulic Engineering Division of Rijkswaterstaat, Delft, Netherlands, Oct. 2005.
79. Hayden, R. E. Roadside Noise from the Interaction of a Rolling Tire with Road Surface. *Proc., Purdue Noise Conference,* West Lafayette, Ind., 1971, pp. 62–67.
80. Landstrom, U., A. Kjellberg, M. Tesarz, and E. Akerlund. Exposure Levels, Tonal Components, and Noise Annoyance in the Working Environment. *Environment International,* 21, 1995, pp. 265–275.
81. *Sound Quality Metrics.* Undated. www. acoustics.salford.ac.uk. Accessed March 2007.
82. Bray, J., P. Cragg, A. Macknigh, and R. Mills. *Lecture Notes on Human Physiology,* 4th ed. Blackwell Science, Boston, 1998.
83. Ishiyama, T., and T. Hashimato. The Impact of Sound Quality on Annoyance Caused by Road Traffic Noise: An Influence on Frequency Spectra on Annoyance. *JSAE Review,* 21, 2000, pp. 225–230.
84. American Concrete Pavement Association (ACPA). *Concrete Pavement Progress.* 2006. www.pavement.com/CPP/2006/CPP-6b-06.htm. Accessed Sept. 2007.
85. Oshino, Y., T. Mikami, and H. Tachibana. Study of Road Surface Indices for the Assessment of Tire/Toad Noise. *Proc., Inter-Noise 2001,* The Hague, Netherlands, August 2001.
86. Descornet, G., and S. Ulf. Road Surface Influence on Tire/Road Noise: Part 2. *Proc., Inter-Noise 80,* Miami, Fla., 1980.
87. Descornet. G. A Criterion for Optimizing Surface Characteristics. In *Transportation Research Record 1215,* TRB, National Research Council, Washington, D.C., 1989, pp. 173–177.
88. Wayson, R. *Relationship Between Pavement Surface Texture and Highway Traffic Noise.* National Cooperative Highway Research Program, Synthesis of Highway Practice 268, National Academy Press, Washington, D,C., 1998.
89. Nelson, P. M. Designing Porous Road Surfaces to Reduce Traffic Noise. *TRL Annual Review,* Transportation Research Laboratories, Wokingham, Berkshire, England, United Kingdom, 1994.
90. Berengier, M. C., M. R. Stinson, G. A. Daigle, and J. F. Hamet. Porous Road Pavements: Acoustical Characterization and Propagation Effects. *Journal of Acoustical Society of America*, Vol. 101 (1), Jan. 1997, pp. 155–162.

91. Berengier. M. C., J. F. Hamet, and P. Bar. Acoustical Properties of Porous Asphalts: Theoretical and Environmental Aspects. In *Transportation Research Record 1265,* TRB, National Research Council, Washington, D.C., 1990, pp. 9–24.
92. Meiarashi, S., et al. Noise Reduction Properties of Porous Elastic Road Surfaces. *Applied Acoustics,* Vol. 47, No. 3, pp. 239–250, 1996.
93. Meiarashi, S., et al. Noise Reduction Effect of Equivalent Continuous A-Weighted Sound Pressure Levels by Porous Elastic Road Surface and Drainage Asphalt Pavement. Presented at 2006 Annual Meeting of the Transportation Research Board, Washington, D.C., Jan. 2006. Meiarashi, S., et al. Noise Reduction Properties of Porous Elastic Road Surfaces. *Applied Acoustics,* Vol. 47, No. 3, pp. 239–250, 1996.
94. Hanson D. I., and R. S. James. *Colorado DOT Tire/pavement Noise Study.* Colorado Department of Transportation Research Report No. CDOT-DTD-R-2004-5. April 2004.
95. Nelson, P. M., and P. G. Abott. Acoustical Performance of Pervious Macadam for High-Speed Roads. In *Transportation Research Record 1265,* TRB, National Research Council, Washington, D.C., 1990, pp. 25–33.
96. Sandberg, U. State-of-the-Art of Low-Noise Pavements. Presented at SILVIA Final Seminar, Brussels, Belgium, Aug. 2005. 217.118.140.155/Silvia/Final%20Seminar/ Presentation_6_State_Of_The_Art_Low_Noise_Surfaces.pdf. Accessed Feb. 2006.
97. Anfosso-Le´de´e, F., and Y. Pichaud. Temperature Effect on Tyre–Road Noise. *Applied Acoustics,* No. 68, 2007, pp. 1–16.
98. Kuijpers, A. *Memo on Temperature Effects on Tyre/Road Noise and on Tyre Stiffness.* M + P.WG27/2002/2/akreport, 2002. www.silentroads.nl. Accessed Feb. 2007.
99. Sandberg, U. *The Multi-Coincidence Peak Around 1000 Hz in Tyre/Road Noise Spectra.* Euronoise, Naples, Italy, 2003.
100. California Department of Transportation (Caltrans). *Caltrans Traffic and Vehicle Data Systems.* 2005[a]. www.dot.ca.gov/hq/traffops/saferesr/trafdata/. Accessed Feb. 2007.
101. Climate Database for Integrated Model (CDIM), Version 1.0. PaveSys, Bethesda, Md., 2004.
102. California Department of Transportation (Caltrans). Office Manual: Guide to the Investigation and Remediation of Distress in Flexible Pavements. Dec. 2002.
103. California Department of Transportation (Caltrans). *Pavement Evaluation Manual: Pavement Condition Survey (PCS).* 2000, p. 114.
104. Cooley, Jr., L. A., E. R. Brown, and S. Maghsoodloo. *Development of Critical Field Permeability and Pavement Density Values for Coarse-Graded Superpave Pavements.* NCAT Report No. 01-03. National Center for Asphalt Technology, Sept. 2001.

105. Donovan, P., and B. Rymer. Quantification of Tire/Pavement Noise: Application of the Sound Intensity Method. Proceedings, 33rd International Congress and Exposition on Noise Control Engineering, Prague, Czech Republic, August 22–25, 2004.
106. Industrial Computed Tomography. www.bioimaging.com/ Industrial_Computed_Tomography.asp. Accessed Feb. 2006.
107. California Department of Transportation (Caltrans). *Open-Graded Friction Course Usage Guide.* Feb. 2006. www.dot.ca.gov/hq/esc/Translab/fpmlab/Open%20Graded%20Friction%20Course%20Usage%20Guide.pdf. Accessed Sept. 2007.
108. Steven, B. *Friction Test of Pavement Preservation Treatments: Operator/Machine Variability and Temperature Corrections.* University of California Pavement Research Center, Berkeley and Davis, 2007.
109. Lee, C., W. Nokes, and J. Harvey. *Performance of Pavement Preservation Treatments.* University of California Pavement Research Center, Davis and Berkeley, 2007.
110. Klein, J., and M. Moeschberger. *Survival Analysis: Techniques for Censored and Truncated Data,* 2nd ed. Springer, New York, 2003.
111. Transtec Group. Personal communication, 2005.
112. Voskuilen, J. *Experiences with Porous Asphalt in the Netherlands.* EPFL Journee de Lavoc, Lausanne, Switzerland, 2005.
113. *Silent Roads.* Undated. www.silentroads.nl/. Accessed Sept. 2007.

APPENDICES

APPENDIX A: CORRECTION OF OBSI VALUES FOR SPEED (FROM 35 MPH TO 60 MPH)

Speed corrections were applied at each frequency:

500 Hz: $OBSI_{60} = 1.99 * OBSI_{35} – 78.4$

630 Hz: $OBSI_{60} = 1.12 * OBSI_{35} – 2.68$

800 Hz: $OBSI_{60} = 0.889 * OBSI_{35} + 18.5$

1,000 Hz: $OBSI_{60} = 1.06 * OBSI_{35} + 2.89$

1,250 Hz: $OBSI_{60} = 1.14 * OBSI_{35} – 3.96$

1,600 Hz: $OBSI_{60} = 0.932 * OBSI_{35} + 14.2$

2,000 Hz: $OBSI_{60} = 0.959 * OBSI_{35} + 11.9$

2,500 Hz: $OBSI_{60} = 1.03 * OBSI_{35} + 6.18$

3,150 Hz: $OBSI_{60} = 1.04 * OBSI_{35} + 5.51$

4,000 Hz: $OBSI_{60} = 1.03 * OBSI_{35} + 6.76$

5,000 Hz: $OBSI_{60} = 0.945 * OBSI_{35} + 12.3$

$OBSI_{35}$ = OBSI measurement at 35 mph

$OBSI_{60}$ = Equivalent OBSI values at 60 mph

APPENDIX B: AIR-DENSITY CORRECTION

Air-density corrections were applied at each frequency level. Following are the equations for air-density corrections:

Mskg = 3.884266 × 10 ^ ((7.5 × Tc)/(237.7 + Tc))

Mkg = Mskg × Humidity%/100

Tvc = ((1 + 1.609 × Mkg)/(1 + Mkg)) × Tc

Baro = Bmb × exp(–Am/7000)

AirDensity = (Baro × 100)/((Tvc + 273) × 287))

OBSICorrection = 10 × (Log_{10}(ReferenceAirDensity) – Log_{10}(AirDensity))

where

Mskg = factor to use in humidity correction,

Tc = temperature (°C),

Mkg = adjustment for humidity,

Baro = adjustment of pressure for altitude,

Bmb = calculation of pressure in mbars,

Am = calculation of altitude in meters,

Tvc = application of correction to temperature using the humidity adjustment, and

ReferenceAirDensity = 1.21.

APPENDIX C: REGRESSION ANALYSIS FOR EACH FREQUENCY LEVEL

Table C1 through Table C11 show the regression analysis for each frequency level.

Table C1: Regression Analysis for 500 Hz

Model Number	Explanatory Variable				Constant Term		R^2 (%)
	Name		Coefficient	p-value	Coefficient	p-value	
1	Age	with QP-16	0.21	0.11	90.45	0.00	4.0
		without QP-16	0.21	0.16	90.46	0.00	3.1
2	Air-Void Content		0.30	0.00	87.47	0.00	27.5
3	Surface Type		2.54	0.00	89.77	0.00	18.8
4	Fineness Modulus		3.08	0.00	75.84	0.00	23.2
5	NMAS		–0.05	0.66	91.98	0.00	0.3
6	C_u		0.0019	0.00	0.102	0.00	17.9
7	Well-Gradedness		–0.99	0.18	91.67	0.00	2.9
8	Rubber Inclusion		0.59	0.42	90.92	0.00	1.0
9	IRI		1.55	0.00	88.96	0.00	11.0
10	log (MPD)*		–0.0083	0.00	0.129	0.00	50.3
11	log (RMS)*		–0.0078	0.00	0.126	0.00	40.6
12	BPN		–0.018	0.72	92.39	0.00	0.2
13	Pavement Temperature		0.005	0.82	90.74	0.00	0.1
14	log (Surface Thickness)*		–4.04	0.01	97.64	0.00	8.7
15	Presence of Fatigue Cracking		1.00	0.39	91.44	0.00	1.3
16	Presence of Raveling		1.28	0.20	91.19	0.00	2.8
17	Number of Transverse Cracks		0.025	0.61	91.40	0.00	0.5
18	Presence of Transverse Cracks		–0.42	0.64	91.60	0.00	0.4

*Dependent variable is $(1/OBSI500)^{0.5}$.

Table C2: Regression Analysis for 630 Hz

Model Number	Explanatory Variable				Constant Term		R^2 (%)
	Name		Coefficient	p-value	Coefficient	p-value	
1	Age	with QP-16	0.24	0.03	91.75	0.00	6.9
		without QP-16	0.22	0.08	91.79	0.00	4.8
2	Air-Void Content		0.215	0.00	89.92	0.00	19.8
3	Surface Type		1.47	0.01	91.76	0.00	9.0
4	Fineness Modulus		1.53	0.02	84.93	0.00	8.2
5	NMAS		–0.080	0.44	93.70	0.00	1.0
6	C_u		–0.053	0.01	93.73	0.00	9.7
7	Well-Gradedness		–0.33	0.59	92.77	0.00	0.5
8	Rubber Inclusion		–0.369	0.55	92.82	0.00	0.6
9	IRI		1.39	0.00	90.57	0.00	12.6
10	MPD		0.0049	0.00	87.88	0.00	38.9
11	RMS		0.0068	0.00	88.16	0.00	28.9
12	BPN		–0.014	0.73	93.54	0.00	0.2
13	Pavement Temperature		0.013	0.53	91.95	0.00	0.7
14	log (Surface Thickness)*		0.0020	0.01	0.100	0.00	9.8
15	Presence of Fatigue Cracking		1.06	0.28	92.75	0.00	2.1
16	Presence of Raveling		1.35	0.11	92.52	0.00	4.4
17	Number of Transverse Cracks		0.04	0.34	92.66	0.00	1.6
18	Presence of Transverse Cracks		0.078	0.91	92.80	0.00	0.0

*Dependent variable is $(1/OBSI630)^{0.5}$.

Table C3: Regression Analysis for 800 Hz

Model Number	Explanatory Variable				Constant Term		R^2 (%)
	Name		Coefficient	p-value	Coefficient	p-value	
1	Age	with QP-16	0.153	0.05	97.51	0.00	5.7
		without QP-16	0.138	0.13	97.56	0.00	3.6
2	Air-Void Content		–0.11	0.00	99.48	0.00	11.2
3	Surface Type		–1.68	0.00	99.04	0.00	24.1
4	Fineness Modulus		–1.40	0.00	105.12	0.00	14.3
5	NMAS		0.083	0.24	96.97	0.00	2.2
6	C_u		0.042	0.00	97.20	0.00	13.3
7	Well-Gradedness		0.30	0.49	97.96	0.00	0.8
8	Rubber Inclusion		–0.88	0.03	98.55	0.00	6.7
9	IRI		0.90	0.00	96.74	0.00	10.8
10	MPD		–0.00022	0.75	98.28	0.00	0.2
11	RMS		–0.0015	0.18	99.04	0.00	2.9
12	BPN		0.083	0.24	96.97	0.00	2.2
13	Pavement Temperature		0.045	0.00	96.43	0.00	15.9
14	log (Surface Thickness)		0.65	0.52	97.03	0.00	0.7
15	Presence of Fatigue Cracking		0.74	0.28	98.11	0.00	2.1
16	Presence of Raveling		0.98	0.09	98.00	0.00	4.7
17	Number of Transverse Cracks		0.02	0.34	98.10	0.00	1.6
18	Presence of Transverse Cracks		0.73	0.15	98.03	0.00	3.6

Table C4: Regression Analysis for 1,000 Hz

Model Number	Explanatory Variable				Constant Term		R^2 (%)
	Name		Coefficient	p-value	Coefficient	p-value	
1	Age	with QP-16	0.125	0.15	96.01	0.00	3.2
		without QP-16	0.132	0.19	95.99	0.00	2.8
2	Air-Void Content		–0.207	0.00	99.05	0.00	31.4
3	Surface Type		–2.38	0.00	97.84	0.00	40.1
4	Fineness Modulus		–1.76	0.00	105.34	0.00	19.2
5	NMAS		0.196	0.01	93.87	0.00	10.2
6	C_u		0.071	0.00	95.02	0.00	31.1
7	Well-Gradedness		0.07	0.88	96.47	0.00	0.0
8	Rubber Inclusion		–0.80	0.08	96.90	0.00	4.6
9	IRI		0.86	0.02	95.19	0.00	8.3
10	MPD		–0.0007	0.35	97.15	0.00	1.4
11	RMS		–0.0023	0.05	98.00	0.00	5.9
12	BPN		0.0020	0.95	96.36	0.00	0.0
13	Pavement Temperature		0.067	0.00	94.00	0.00	28.9
14	Surface Thickness		0.030	0.00	95.13	0.00	12.9
15	Presence of Fatigue Cracking		0.69	0.35	96.53	0.00	1.5
16	Presence of Raveling		0.96	0.13	96.43	0.00	3.8
17	Number of Transverse Cracks		0.0079	0.80	96.62	0.00	0.1
18	Presence of Transverse Cracks		0.804	0.15	96.45	0.00	3.6

Table C5: Regression Analysis for 1,250 Hz

Model Number	Explanatory Variable				Constant Term		R^2 (%)
	Name		Coefficient	p-value	Coefficient	p-value	
1	Age	with QP-16	0.39	0.00	92.11	0.00	18.9
		without QP-16	0.41	0.00	92.04	0.00	16.9
2	Air-Void Content		–0.32	0.00	97.53	0.00	45.4
3	Surface Type		–2.52	0.00	94.99	0.00	27.4
4	Fineness Modulus		–1.87	0.00	102.97	0.00	13.0
5	NMAS		0.254	0.01	90.15	0.00	10.3
6	C_u		0.082	0.00	91.86	0.00	24.9
7	Well-Gradedness		–0.31	0.61	93.71	0.00	0.4
8	Rubber Inclusion		–1.02	0.08	94.09	0.00	4.6
9	IRI		1.09	0.02	91.93	0.00	8.0
10	MPD		–0.00041	0.67	93.93	0.00	0.3
11	RMS		–0.0020	0.20	94.84	0.00	2.6
12	BPN		–0.033	0.43	95.52	0.00	1.0
13	Pavement Temperature		0.014	0.47	92.96	0.00	0.9
14	log (Surface Thickness)		2.92	0.03	88.89	0.00	6.7
15	Presence of Fatigue Cracking		2.08	0.03	93.23	0.00	7.6
16	Presence of Raveling		1.12	0.19	93.34	0.00	2.9
17	Number of Transverse Cracks		0.068	0.11	93.26	0.00	4.4
18	Presence of Transverse Cracks		1.70	0.02	93.11	0.00	8.7

Table C6: Regression Analysis for 1,600 Hz

Model Number	Explanatory Variable				Constant Term		R^2 (%)
	Name		Coefficient	p-value	Coefficient	p-value	
1	Age	with QP-16	0.34	0.00	90.17	0.00	11.8
		without QP-16	0.36	0.00	90.11	0.00	10.5
2	Air-Void Content		–0.43	0.00	96.81	0.00	65.4
3	Surface Type		–3.19	0.00	93.27	0.00	34.8
4	Fineness Modulus		–3.04	0.00	106.68	0.00	26.7
5	NMAS		0.312	0.00	87.25	0.00	12.1
6	C_u		0.11	0.00	89.14	0.00	35.3
7	Well-Gradedness		0.46	0.50	91.26	0.00	0.7
8	Rubber Inclusion		–1.24	0.06	92.11	0.00	5.4
9	IRI		0.45	0.41	90.76	0.00	1.1
10	MPD		–0.0030	0.00	94.32	0.00	12.0
11	RMS		–0.0058	0.00	95.23	0.00	17.4
12	BPN		–0.019	0.68	92.55	0.00	0.3
13	Pavement Temperature		–0.018	0.43	92.11	0.00	1.1
14	log (Surface Thickness)		5.54	0.00	82.65	0.00	19.2
15	Presence of Fatigue Cracking		2.30	0.03	90.96	0.00	7.6
16	Presence of Raveling		1.02	0.28	91.16	0.00	2.0
17	Number of Transverse Cracks		0.074	0.12	90.99	0.00	4.3
18	Presence of Transverse Cracks		2.03	0.01	90.78	0.00	10.1

Table C7: Regression Analysis for 2,000 Hz

Model Number	Explanatory Variable				Constant Term		R^2 (%)
	Name		Coefficient	p-value	Coefficient	p-value	
1	Age	with QP-16	0.21	0.04	86.85	0.00	6.3
		without QP-16	0.21	0.08	86.86	0.00	4.8
2	Air-Void Content		–0.37	0.00	92.29	0.00	65.8
3	Surface Type		–3.22	0.00	89.50	0.00	47.7
4	Fineness Modulus		–3.02	0.00	102.78	0.00	35.8
5	NMAS		0.279	0.00	83.91	0.00	13.2
6	C_u		0.105	0.00	85.48	0.00	43.2
7	Well-Gradedness		0.82	0.16	87.32	0.00	3.2
8	Rubber Inclusion		–1.12	0.05	88.25	0.00	6.0
9	IRI		0.54	0.24	86.84	0.00	2.1
10	MPD		–0.0032	0.00	90.78	0.00	19.1
11	RMS		–0.0066	0.00	91.95	0.00	30.2
12	BPN		0.011	0.78	86.96	0.00	0.1
13	Pavement Temperature		0.009	0.64	87.33	0.00	0.4
14	log (Surface Thickness)		5.88	0.00	78.32	0.00	29.2
15	Presence of Fatigue Cracking		2.01	0.03	87.34	0.00	7.7
16	Presence of Raveling		1.24	0.13	87.40	0.00	3.8
17	Number of Transverse Cracks		0.064	0.12	87.34	0.00	4.3
18	Presence of Transverse Cracks		2.01	0.00	87.09	0.00	13.2

Table C8: Regression Analysis for 2,500 Hz

Model Number	Explanatory Variable				Constant Term		R^2 (%)
	Name		Coefficient	p-value	Coefficient	p-value	
1	Age	with QP-16	0.18	0.06	84.20	0.00	5.5
		without QP-16	0.20	0.06	84.12	0.00	5.6
2	Air-Void Content		–0.28	0.00	88.42	0.00	50.0
3	Surface Type		–2.41	0.00	86.24	0.00	34.5
4	Fineness Modulus		–2.42	0.00	97.00	0.00	29.5
5	NMAS		0.169	0.04	82.60	0.00	6.2
6	C_u		0.078	0.00	83.23	0.00	31.1
7	Well-Gradedness		0.79	0.13	84.54	0.00	3.7
8	Rubber Inclusion		–0.94	0.06	85.37	0.00	5.4
9	IRI		0.15	0.70	84.62	0.00	0.2
10	MPD		–0.0034	0.00	88.14	0.00	27.0
11	RMS		–0.0061	0.00	88.87	0.00	33.7
12	BPN		0.0086	0.81	84.31	0.00	0.1
13	Pavement Temperature		–0.022	0.20	85.77	0.00	2.8
14	log (Surface Thickness)		4.86	0.00	77.15	0.00	25.6
15	Presence of Fatigue Cracking		1.37	0.10	84.57	0.00	4.7
16	Presence of Raveling		1.12	0.12	84.55	0.00	4.2
17	Number of Transverse Cracks		0.059	0.09	84.47	0.00	4.9
18	Presence of Transverse Cracks		1.95	0.00	84.22	0.00	16.8

Table C9: Regression Analysis for 3,150 Hz

Model Number	Explanatory Variable				Constant Term		R^2 (%)
	Name		Coefficient	p-value	Coefficient	p-value	
1	Age	with QP-16	0.16	0.08	82.46	0.00	4.6
		without QP-16	0.20	0.06	82.34	0.00	5.4
2	Air-Void Content		–0.26	0.00	86.32	0.00	41.0
3	Surface Type		–1.90	0.00	84.16	0.00	21.1
4	Fineness Modulus		–2.13	0.00	93.75	0.00	22.4
5	NMAS		0.139	0.11	81.20	0.00	4.1
6	C_u		0.066	0.00	81.69	0.00	21.6
7	Well-Gradedness		0.822	0.12	82.72	0.00	3.9
8	Rubber Inclusion		–0.87	0.08	83.54	0.00	4.6
9	IRI		–0.11	0.79	83.22	0.00	0.1
10	MPD		–0.0033	0.00	86.26	0.00	25.1
11	RMS		–0.0056	0.00	86.74	0.00	27.9
12	BPN		0.0062	0.86	82.65	0.00	0.0
13	Pavement Temperature		–0.046	0.00	84.81	0.00	11.6
14	log (Surface Thickness)		4.39	0.00	76.10	0.00	20.7
15	Presence of Fatigue Cracking		1.02	0.22	82.77	0.00	2.6
16	Presence of Raveling		1.20	0.08	82.67	0.00	5.1
17	Number of Transverse Cracks		0.046	0.18	82.63	0.00	3.2
18	Presence of Transverse Cracks		1.75	0.00	82.38	0.00	14.4

Table C10: Regression Analysis for 4,000 Hz

Model Number	Explanatory Variable				Constant Term		R^2 (%)
	Name		Coefficient	p-value	Coefficient	p-value	
1	Age	with QP-16	0.27	0.02	79.04	0.00	8.4
		without QP-16	0.29	0.02	78.96	0.00	7.9
2	Air-Void Content		–0.32	0.00	84.12	0.00	44.1
3	Surface Type		–2.30	0.00	81.35	0.00	21.0
4	Fineness Modulus		–2.73	0.00	93.72	0.00	25.0
5	NMAS		0.15	0.14	77.95	0.00	3.4
6	C_u		0.082	0.00	78.30	0.00	22.7
7	Well-Gradedness		0.87	0.17	79.66	0.00	3.0
8	Rubber Inclusion		–1.13	0.07	80.64	0.00	5.2
9	IRI		–0.003	0.99	80.02	0.00	0.0
10	MPD		–0.0041	0.00	83.94	0.00	25.6
11	RMS		–0.0068	0.00	84.50	0.00	28.1
12	BPN		–0.0095	0.82	80.55	0.00	0.1
13	Pavement Temperature		–0.056	0.00	82.22	0.00	12.4
14	log (Surface Thickness)		5.13	0.00	71.89	0.00	19.2
15	Presence of Fatigue Cracking		1.66	0.10	79.601	0.00	4.8
16	Presence of Raveling		1.43	0.09	79.55	0.00	4.9
17	Number of Transverse Cracks		0.067	0.11	79.45	0.00	4.6
18	Presence of Transverse Cracks		2.07	0.00	79.21	0.00	13.6

Table C11: Regression Analysis for 5,000 Hz

Model Number	Explanatory Variable				Constant Term		R^2 (%)
	Name		Coefficient	p-value	Coefficient	p-value	
1	Age	with QP-16	0.20	0.06	74.87	0.00	5.4
		without QP-16	0.21	0.08	74.83	0.00	4.8
2	Air-Void Content		–0.29	0.00	79.30	0.00	42.8
3	Surface Type		–2.05	0.00	76.78	0.00	19.8
4	Fineness Modulus		–2.59	0.00	88.57	0.00	26.5
5	NMAS		0.15	0.12	73.57	0.00	3.9
6	C_u		0.075	0.00	74.02	0.00	22.6
7	Well-Gradedness		0.76	0.19	75.27	0.00	2.7
8	Rubber Inclusion		–0.96	0.09	76.12	0.00	4.4
9	IRI		–0.06	0.89	75.69	0.00	0.0
10	MPD		–0.0038	0.00	79.25	0.00	26.3
11	RMS		–0.0064	0.00	79.77	0.00	28.9
12	BPN		–0.0026	0.94	75.72	0.00	0.0
13	Pavement Temperature		–0.043	0.03	77.25	0.00	8.2
14	log (Surface Thickness)		4.70	0.00	68.14	0.00	19.1
15	Presence of Fatigue Cracking		1.31	0.16	75.27	0.00	3.5
16	Presence of Raveling		1.49	0.05	75.14	0.00	6.3
17	Number of Transverse Cracks		0.057	0.14	75.12	0.00	3.9
18	Presence of Transverse Cracks		1.88	0.00	74.88	0.00	13.2

APPENDIX D: CONDITION SURVEY OF ENVIRONMENTAL NOISE MONITORING SITE SECTIONS FOR TWO YEARS

Site Name	Mix Types	First-Year Condition Survey	Second-Year Condition Survey
Los Angeles 138 (LA 138)	OGAC, 75 mm Eastbound	1 low-severity transverse crack with a length of 0.6 m; 0.5 m^2 raveling	2 low-severity transverse cracks with a length of 5.4 m
	OGAC, 30 mm Eastbound	No distresses	6 low-severity transverse cracks with a length of 7 m
	RAC-O, 30 mm Eastbound	10 low-severity transverse cracks with a length of 36 m; 0.5 m^2 raveling	10 low-severity transverse cracks with a length of 38 m
	BWC, 30 mm Eastbound	8 low-severity transverse cracks with a length of 27 m; 9 medium-severity transverse cracks with a length of 33 m	13 medium-severity transverse cracks with a length of 48 m
	DGAC, 30 mm Westbound	1 low-severity transverse crack with a length of 3 m	14 medium-severity transverse cracks with a length of 45.4 m; 5.4-m low-severity and 2.5 m^2 medium-severity fatigue cracking
Los Angeles 19 (LA 19)	European Gap-Graded Mix, 30 mm	No distresses	150 m^2 bleeding
Yolo 80	OGAC, 20 mm	60 m^2 raveling	300 m^2 raveling; 300 m^2 bleeding
Fresno 33 (Fre 33)	RAC-G, 45 mm	1.3-m longitudinal crack; 10 low-severity transverse cracks with a total length of 20 m.	47-m longitudinal cracking; 9-m low-severity and 15 m^2 medium-severity fatigue cracking; 51 low-severity transverse cracks with a total length of 136 m; 170 m^2 raveling; 170 m^2 bleeding
	RAC-G, 90 mm	11 low-severity transverse cracks with a total length of 24 m; 6 medium-severity transverse cracks with a total length of 15 m; 0.04 m^2 raveling	150-m low-severity and 5 m^2 medium-severity fatigue cracking; 33 medium-severity transverse cracks with a total length of 65 m; 150 m^2 raveling; 160 m^2 bleeding

	RUMAC-GG, 45 mm	39 low-severity transverse cracks with a total length of 111 m; one medium-severity transverse crack with a length of 3.35 m	150-m medium-severity longitudinal cracking; 45 medium-severity transverse cracks with a total length of 135 m; 180 m^2 raveling; 180 m^2 bleeding
	RUMAC-GG, 90 mm	No distresses	150 m^2 bleeding
	Type-G MB, 45 mm	210 m^2 bleeding	3-m low-severity and 15 m^2 medium-severity fatigue cracking; 210 m^2 bleeding
	Type-G MB, 90 mm	154 m^2 bleeding	12.5 m^2 fatigue cracking; 245 m^2 bleeding
	Type-D MB, 45 mm	40 m^2 bleeding	1-m low-severity and 8 m^2 medium-severity fatigue cracking; 32 m^2 raveling; 345 m^2 bleeding
	Type-D MB, 90 mm	2 m^2 bleeding	300 m^2 bleeding
	DGAC, 90 mm	No distresses	No distresses
San Mateo 280 (SM 280)	RAC-O, 45 mm	No distresses	0.1 m^2 raveling
Sacramento 5 (Sac 5)	OGAC, 30 mm Northbound	18 low-severity reflective cracks with a total length of 51 m; 3 medium-severity reflective cracks with a total length of 13 m	6 low-severity reflective cracks with a total length of 21.6 m; 7 medium-severity reflective cracks with a total length of 22.5 m; 8 high-severity reflective cracks with a total length of 28.8 m
	OGAC, 30 mm Southbound	18 low-severity reflective cracks with a total length of 44 m; 60 m^2 raveling	17 low-severity reflective cracks with a total length of 63.2 m; 1 medium-severity reflective crack with a total length of 3.7 m